Towards Fast Converging Lattice Sums

A thesis presented in partial fulfilment of the
requirements for the degree of

Doctor of Philosophy
in
Physics

at
Massey University, Albany
New Zealand

Antony Burrows

2022

Abstract

In the field of solid state physics there are many open questions surrounding the best configuration of packing spheres to calculating binding energies to J/mol accuracy. Many of these problems have attracted attention from individuals in many faculties from mathematics, physics and chemistry over the course of the last four centuries. A significant amount of work has been done modernizing interaction potentials from the early twentieth century by the use of modern computers and quantum chemical software programs extending versions of the most common two-body potential. The historical survey of the methods leading up until the late nineteen eighties serves as the basis for where we step off for much of the analytic techniques for evaluating lattice sums and their use in answering these open questions. Investigations in to the stability of certain packing configurations compared to others in the solid state can be made with the use of fast techniques to evaluate the properties of such systems, many of which are developed here and used throughout the work in the various projects seen below.

The aim of this work is to show that the evaluation of lattice constants and the formulae to calculate them can be given in a concise and efficient form with the use of mathematical and numerical methods. Analytical expressions can be found that are given in terms of real exponents and these expressions can be evaluated to arbitrary precision within a satisfactory amount of computer time. In contrast to the infinite structure that forms the lattice in the physical world, the techniques to calculate its sum have evolved from an infinite direct summation to methods that treat the sum associated with the quadratic form of the lattice re-expressing it as a sum of simple functions using number theoretic techniques and treating sums in terms of fast converging series or sums of hyperbolic functions.

The results of this investigation are multiple new formulae for the cubic lattice systems, including expressions for the simple cubic lattice and famous Madelung constant in N–dimensions. A new expression was found for the hexagonal close packed structure that is computationally elegant and allowed the examination of the behaviour of the two-body Lennard–Jones potential in terms of the lattice parameters. A single parameter sum was found for the simple cubic system that was used to investigate the effect of pressure on body centered cubic system compared to the face centered cubic system.

Acknowledgements

At this point in my life with the closing of what has probably been one of the largest chapters, I express my sincere gratitude to all the people who have given their time and been generous with their resources to help me get to where I am today. From the start of the journey coming back to tertiary education, thankyou to Emilie and the Mendez family for their generosity and support in the first years. Moving into science I would like to thank those from the chemistry department; Marie-Anne, John, Al and Joyce for giving me a chance at chemistry and science, for the additional work over summer school and during the semester, it was really a great help - you all have been very kind with your knowledge and time, and the times in the laboratory and amongst you all have been very memorable, thankyou. Elke thankyou for your time to sit down with me at the start. Vesna, thankyou for keeping us all glued together and assisting with all the administrative matters, I'm sure the group would not be here without you. To Shaun, truly thankyou for the countless hours you gave teaching me mathematics and being patient with me. As a co-supervisor you have been invaluable in the role but also as a solid sounding board for discussion on many topics from mathematics to running and life, thankyou for always having the time for me. Peter, I can not thankyou enough. You have been there not only for me, but for the entire research group over what can arguably be said to be one of the hardest times the world has been in the last half century. To keep us all on track and have the time for each of us, no matter what was going on was really the coolest experience I've had with a supervisor, I couldn't have asked for a better one! To everyone at the NZIAS that has been on this journey at the same time; Odile for your conversation and help over the years. Lukas for your help with computer related issues. Morten for being an awesome office mate, thanks for the endless help with programming and linux related queries. Ray for being the worst card game partner but the best team mate overall, and Sarthak your natural void will never be forgotten. To Mum & Dad thankyou for your continued support over many years, I can not thank you enough. To Alex, thankyou for making the last year a very special one, through thick and thin for living it with me and for all of the ways you have supported me throughout, It has been truly an unforgettable feeling to have had you there.

Contents

List of Publications

The results presented in this thesis have been released previously in the following publications:

[1] A. Burrows, S. Cooper, E. Pahl, and P. Schwerdtfeger, "Analytical methods for fast converging lattice sums for cubic and hexagonal close-packed structures", Journal of Mathematical Physics **61**, 10.1063/5.0021159 (2020).

[2] P. Schwerdtfeger, A. Burrows, and O. R. Smits, "The Lennard-Jones Potential Revisited: Analytical Expressions for Vibrational Effects in Cubic and Hexagonal Close-Packed Lattices", J. Phys. Chem. A **125**, 3037 (2021).

[3] A. Burrows, S. Cooper, and P. Schwerdtfeger, *The cuboidal lattices and their lattice sums*, 2021.

[4] A. Burrows, S. Cooper, and P. Schwerdtfeger, "Instability of the body-centered cubic lattice within the sticky hard sphere and lennard-jones model obtained from exact lattice summations", Phys. Rev. E **104**, 035306 (2021).

[5] P. Schwerdtfeger and A. Burrows, "Cuboidal bcc to fcc transformation of lennard-jones phases under high pressure derived from exact lattice summations", The Journal of Physical Chemistry C, 10.1021/acs.jpcc.2c01255 (2022).

[6] A. Burrows, S. Cooper, and P. Schwerdtfeger, "The madelung constant in N dimensions", (2022).

[7] P. Schwerdtfeger, S. Cooper, and A. Burrows, "The lattice sum for a hexagonal close packed structure and its dependence on the c/a ratio of the hexagonal cell parameters.", unpublished (2022).

List of Acronyms

RGS	rare gas solid
ELJ	extended Lennard-Jones
sc	simple cubic
bcc	body-centered cubic
fcc	face-centered cubic
GN	Gregory-Newton
hcp	hexagonal-closed packed
acc	axial centred cuboidal
mcc	mean centred-cuboidal
LJ	Lennard-Jones
IEEE	IEEE Electrical and Electronics Engineers

List of Figures

List of Tables

1 Introduction

1.1 Historical Review of Lattice Sums

Lattice sums have a long history in solid-state physics and discrete mathematics [1]. They connect lattices to observables such as the equation of state for a bulk system using interacting potentials between the lattice points in bulk atomic or molecular solids in three-dimensional space [2–5]. The central idea here is to account for all dispersive, ionic or covalent interactions in a bulk system using analytically expressed two-body potentials between the atoms in a lattice, which leads to convergent infinite series expressions by summing over all two-body interactions. If one is lucky, such series lead to analytical expressions in terms of standard functions such as the Riemann or Hurwitz zeta function.

Work on interaction potentials from the early twentieth century was carried out by researchers such as Lennard-Jones (LJ), Fürth, Born, Grüneisen etc., and most notable cases for such interactions are the Lennard-Jones [6] for dispersive type of interactions and the Coulomb potential for ionic interactions, leading in the latter case, for example, to the famous Madelung constant derived as early as in 1918 [7]. For such potentials the corresponding lattice sums become functions of quadratic forms associated with the lattice $\mathscr{L}$[8]. Over the past century much work has contributed to the mathematical analysis of lattice sums, and the evaluation of conditionally convergent series required new thinking and more elaborate mathematical techniques [1].

The first occurrence of what is generally considered a lattice sum was by Appell in 1884, where he produced an analytical expression derived for a single one-dimensional set of point charges [9]. At the turn of the twentieth century Epstein introduced what is now called the Epstein-zeta function, a more general version of the Riemann and Hurwitz zeta functions that belongs to the class of Dirichlet functions, given in terms of a real positive-definite $(N \times N)$ matrix. The equation by Epstein sums over any positive definite N-dimensional integer lattice and served as a basis for future work on lattice sums to come. X-ray studies carried out particularly by Bragg contributed the knowledge that salt crystals consisted of interpenetrating lattices of the corresponding ions and the numerical evaluation of lattices became an important topic for Born and his students (particularly Emersleben) who

studied lattice vibrations and crystal binding energies [10–12] Just before the end of the 1910's saw the first accurate numerical result for sodium chloride (rock salt) produced by Madelung in 1919 [13]. The summation method used by Madelung was similar to that of Appell, however the method for calculating the potential due to a line of alternating charges was complicated by geometric considerations needed to decompose more complex lattice structures. Thus the need for a more flexible summation formula was met by Ewald which was based on the Appell–Epstein approach and was formulated for cubic systems in terms of ordinary theta functions [14].

At this point in the chronology of the historical perspective on lattice sums story, we shall pause to mention the simultaneous development on interaction potentials. Leading up to the early 1920's, before the mathematics of lattice sums were combined with interaction potentials in solid-state studies, the discussion on interaction potentials started as early as in 1903 with Mie suggesting an equation of state containing a volume dependent term of the form $(AV^{-1} - BV^{-\nu/3})$ with $\nu > 3$ [15]. Following this, in 1912 Grüneisen[3] published the exact formula for what became later the well known (n,m) LJ potential,

$$\phi_{\mathrm{LJ}}^{(n,m)}(r) = \frac{nm}{n-m}\,\varepsilon\left[\frac{1}{n}\left(\frac{r_e}{r}\right)^n - \frac{1}{m}\left(\frac{r_e}{r}\right)^m\right], \tag{1.1.1}$$

with $n > m$ ($n,m \in \mathbb{R}$ and $n,m > 3$). Here ε is the dissociation energy and r_e the equilibrium bond distance. The LJ potential is the most widely used interaction potential in quantum chemistry and physics and is of central importance for this thesis. A few selected LJ curves are shown in Figure 1.1.

In 1920 Kratzer also introduced a less general (2,1) potential which went unnoticed [16]. The Grüneisen (n,m) potential was modified by Born and Landé[17] in 1918 for ionic crystal and the same year Madelung introduced the lattice sum for ionic crystals today known as the Madelung constant as mentioned above [7]. It was not until 1924 after Lennard-Jones solved the equation of state analytically to derive the parameters based on experimental results, that the LJ (n,m) potential gained notoriety [18]. However the physical relevance of the r^{-6} long-rang dispersive interaction term came much later in 1930 by London [19]. What is curious about the time line is that Simon and Simpson used the Grüneisen potential in 1924 giving it a proper citation, and Lennard-Jones in his second paper also cited Simon and Simpson's paper in 1924 within a series of papers, but Grüneisen's paper was ignored.

Emersleben summarized the results of his work on the Grundpotential in two papers in 1923, which subsequently was the topic of his thesis. In the first

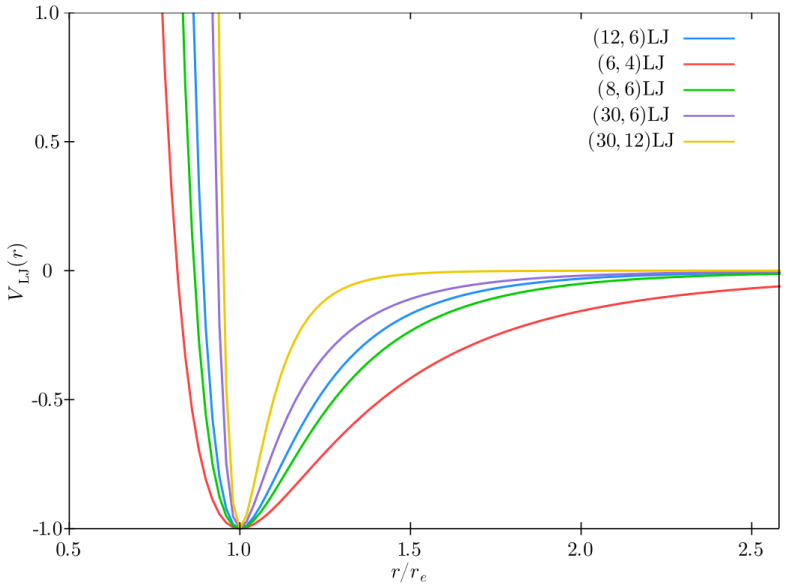

Figure 1.1 Lennard-Jones potentials for a selection of parameters (n,m).

paper Emersleben extended the Grundpotential idea to an arbitrary Bravais lattice and to the case of a general inverse power law [20, 21]. Only one year later in 1924 Lennard-Jones produced his work on lattices sums for cubic crystal systems which serves as the first attempt to calculate the corresponding lattice sums to sufficient accuracy for these types of solid-state crystal systems [22, 23]. Much of the work performed throughout Project 1 of this thesis starts from Lennard-Jones's work on the calculation of crystal potentials or lattice sums for the cubic crystal systems. The three methods from Ewald, Emersleben and Jones all had their advantages and disadvantages, however throughout the 1930's to 1940's the field of lattice sums did not see much progress. The lattice summation for the hexagonal-closed packed (hcp) structure was explored early by Kane and Goeppert-Mayer in 1940, but has never been evaluated to high precision except for some special cases such as noble gas solids [24–26]. In the 1950's work by Mackenzie, Schreiber, Hoff, Benson et al. was produced dealing with the practical evaluation of electrostatic sums, which were reduced to fast converging series of modified Bessel or exponential functions [27–30].

In the late 1960's Emersleben elaborated on number theoretical techniques suggested by Jones and Ingham [31]. Theta functions were used by Appell and Ewald in the numerical evaluation of lattice sums earlier, however the Mellin transform of theta function was not used until 1972 when Glasser

produced a series of papers using analytic techniques including the theta function transform and number theoretical methods to evaluate lattice sums [32–35]. The mid 1970's saw a large amount of work published using number theoretical techniques and function theory of such sums, e.g., Pathria and Chaba developed a method, based on the application of Poisson's summation formula, for the analytic evaluation of a specific class of two-dimensional lattice sums involving modified Bessel functions [36–38]. Around the same time Zucker and Robertson evaluated binary quadratic forms from a number theoretical perspective using Dirichlet L-functions and following this into the 1980's [39]. Terras published work using a Bessel function expansion and subsequent reduction of positive definite quadratic forms, but went relatively unnoticed. Terras' method is used in the work contained in Project 1 [40]. Hautot used Schlomilch series with a Hankel transform to obtain results that were similar to that of Van der Hoff–Benson in the evaluation of slowly convergent series.[41] Comprehensive reviews on lattice sums can be found by Borwein and co-workers in [1] and work on the Madelung constant by Crandall in [42].

1.2 Crystal Lattices and Systems

The term "lattice" used in its strict mathematical sense means a regular periodic array of points. The term is now generally accepted in the literature on the properties of crystalline solids as referring to the arrangement of the atoms, molecules or ions making up the crystal. When we therefore refer to a "crystal lattice" we mean the lattice which would determine the mean position of the atoms, molecules or ions making up the crystal. In a general sense when we discuss a set of points to which a *basis* is attached, we call this a lattice. Consequently, the position vector $\vec{r}$ of the lattice points in a three dimensional lattice is given in terms of three translation vectors $\vec{b}_1, \vec{b}_2, \vec{b}_3$ by

$$\vec{r}_{ijk} = \vec{a} + i\vec{b}_1 + j\vec{b}_2 + k\vec{b}_3\,, \tag{1.2.1}$$

where i, j, k are integers and $\vec{a}$ is a constant. If the origin is a lattice point then we may take

$$\vec{r}_{ijk} = i\vec{b}_1 + j\vec{b}_2 + k\vec{b}_3\,. \tag{1.2.2}$$

The parallelepiped formed by the use of three basic vectors is called the *unit cell*. Other vectors of the lattice may be used as basic vectors but unless they satisfy certain conditions they will not define the lattice without the use of additional bases. If no additional basis is required then the basic vectors are called *primitive* vectors. Here we must distinguish between a true lattice with a basis which cannot be reduced to a simple lattice, and a lattice represented

by using basic "coordinate" vectors $\vec{b}_1, \vec{b}_2, \vec{b}_3$ and an additional basis vector $\vec{a}$. In the case of a simple lattice we would always be able to find three new vectors $\vec{b}'_1, \vec{b}'_2, \vec{b}'_3$ by means in which the lattice can be represented without an additional basis vector $\vec{a}$, i.e., by *primitive* vectors.

In a similar fashion the distinction between a *primitive cell* applies only to a lattice defined by *primitive vectors*, while a *unit cell* is a parallelepiped in three dimensions derived from any three 'coordinate' vectors[a]. The *primitive cell* corresponds to the volume of space associated with a single lattice point. On the other hand, the *unit cell* will have volume associated with s lattice points if there are $(s-1)$ additional basis vectors.

In crystallography the state of appearing unchanged in orientation following displacement is called self-coincidence, and it is evident that a crystal lattice can only be brought into self-coincidence in a finite number of ways and therefore the symmetry operations of a crystal form a finite group. Such a group can only possess symmetry operations about a fixed point O, which leave the the point O unmoved. Finite groups whose operations all leave one point unmoved are called *point groups*. A space group is a group of transformations and may be considered to be made up of two parts, a pattern unit and a repeat mechanism. The analogy here is like the repeating pattern of victorian style wallpaper. A lattice system is a group of lattices with the same set of lattice point groups which are subgroups of the space group. Within the set of lattice systems there are 14 different types of lattices named after the French physicist Auguste Bravais. Bravais lattices are categorized by their relationships to lengths a, b, c of the sides of the unit cell, and angles between each side given by α, β, γ. As an example the Bravais lattices with orthorhombic systems obey the following equations:

$$a \neq b \neq c \text{ and } \alpha = \beta = \gamma = 90\,.$$

In Figure 1.2 four Bravais lattices are shown, the primitive cell also known as simple cubic (sc), body-centered cubic (bcc) and face-centered cubic (fcc) from the Cubic system and additionally base centered cubic from the Orthorhombic system.

In the work that follows, crystal systems from the Orthorhombic, Tetragonal and Hexagonal systems are focused on, those being simple, body centered, mean centered, axial centred, face centered cubic and hexagonal close packed structures.

[a] Coxeter calls the generalization of a parallelepiped in higher dimensions a parallelotope [43].

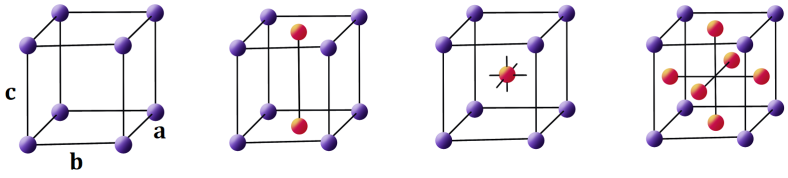

Figure 1.2 simple cubic, base centered cubic, body-centered cubic and face-centered cubic lattices.

1.3 Rare Gas Solids

Kepler studied the densities of sphere packing almost four centuries ago resulting in his famous conjecture that no arrangement of equally sized spheres has a greater packing density than fcc and hcp arrangements. The field of packing convex bodies in N-dimensional space is still an intensively researched and debated topic in mathematics. Concerning the coordination number of an atom in a solid, Gregory and Newton discussed the kissing numbers of spheres and proposed what is known as the Gregory-Newton (GN) problem of 12 kissing spheres. Following this, these problems and related ones have attracted the attention of many prominent mathematicians. As the work on sphere packing problems has progressed many new results have been published on this topic. This has led to many interesting connections with other fields of mathematics, such as graph theory, and solid-state physics.

Elemental rare-gas clusters are known to be typical examples of Lennard-Jones (LJ) systems.[44, 45] When considered in the solid state the periodic crystal is predicted to have a hexagonal close-packed structure [46], while the experimentally determined structures for the Ne, Ar and Kr crystals are all face centered cubic. This discrepancy, known as the rare gas solid (RGS) problem has led to an intense debate about the growth process of such clusters, as well as on the effects accounting for the difference in the predicted energies of the fcc and hcp lattices.[47] This difference is actually much smaller than originally anticipated, being only a few J/mol. This leads to the interesting question as to why only fcc structures are found under normal pressure. This puzzle has stimulated much theoretical research on the interactions between rare-gas atoms themselves and the computation of the cohesive energies.

With the development of many interaction potentials coming out of the early to mid twentieth century, much work has been done on calculating accurate binding energies for solid-state systems. More recently, the LJ potential was extended to a more general form of an inverse power series, namely the extended

Lennard-Jones (ELJ) potential,

$$\phi_{\mathrm{ELJ}}(r) = \sum_{n>3} c_n r^{-n} \tag{1.3.1}$$

with the right boundary condition for the coefficients c_n such that $\phi_{\mathrm{ELJ}}(r_e) = -\varepsilon$ at the equilibrium distance r_e of the potential energy curve. In the ELJ form, the 2-body potential curve is constructed from accurate point wise data obtained from highly accurate quantum-chemical 2-body calculations.[48] For a range of internuclear distances this data is fitted to the inverse power series (7.1.2) with up to any number of ELJ coefficients c_n instead of just two. An advantage of the ELJ form is that for certain crystal types an analytical form for the cohesive energy per atom can be obtained by making use of lattice sums L_n (Lennard-Jones-Ingham coefficients). The importance of the cohesive energy curve is that it is the ground state energy of a solid, and whether it is stable or not depends on the critical points along some coordinate. Lattice sums can be applied to calculate basic solid-state properties like the pressure or the bulk modulus as volume derivatives of the cohesive energy, and for lattice energy minimization including zero-point vibrational and temperature effects.[48–54]

To illustrate this the total cohesive energy per atom, $E_{\mathrm{coh}}(V)$ is divided into static $E_{\mathrm{coh}}^{\mathrm{stat}}(V)$ and dynamic $E_{\mathrm{coh}}^{\mathrm{dyn}}(V)$ contributions, the latter resulting from zero-point vibrational motion:

$$E_{\mathrm{coh}}(V) = E_{\mathrm{coh}}^{\mathrm{stat}}(V) + E_{\mathrm{coh}}^{\mathrm{dyn}}(V)\,.$$

The total static contribution can be approximated within the many-body ansatz including two and higher body contributions in the solid if the many-body expansion is converging fast.[55] Translational symmetry is used to evaluate the most important two-body contribution through an ELJ potential and corresponding lattice sums, $E_{\mathrm{coh}}^{\mathrm{stat}}(V) \cong E_{\mathrm{ELJ}}(V)$, and the dynamic part is given by

$$E_{\mathrm{coh}}^{\mathrm{dyn}}(V) \cong E_{\mathrm{ELJ}}^{\mathrm{ZPVE}}(V) + E_{\mathrm{ELJ}}^{\mathrm{AZPVE}}(V)\,,$$

where $E_{ELJ}^{ZPVE}(V)$ is the volume dependent zero-point vibrational energy (ZPVE) contribution within the harmonic oscillator approximation, and $E_{ELJ}^{AZPVE}(V)$ is the corresponding anharmonicity correction (AZPVE), further details are given in Section 7.2. Throughout the work on lattice sums the stability of cubic lattices are studied along transition paths where a single parameter lattice sum is derived and where pressure is applied to the lattice. The evaluation of these physical properties is achieved by the use of fast

converging lattice sums. The methods in which these sums are constructed are a large topic of the work seen below.

1.4 Outline

In this thesis, seven projects are presented which will be briefly outlined in the following.

- In the Project 1, lattice sums are evaluated in three dimensions to computer precision for the simple, body centered and face-centered cubic lattices and, for the first time the hexagonal close-packed structure. The work reports on re-expressing the slow converging lattice sums as rapidly converging series by using a number of different mathematical tools such as Terras and Van der Hoff-Benson expansions in terms of Bessel functions enabling results to high computer precision. The work discusses the slow converging nature of lattice sums especially at lower exponential values. The project explores and explains what can be done with direct summation techniques and makes use of number theoretical tools to reduce double sums into combinations of well known standard functions. The Terras method is used to treat lattice sums in terms of a decomposition of the Epstein zeta function and reduction of dimension of the pure quadratic form. This results in a decrease in the computer time required to evaluate lattice sums for lower exponential values. The project looks at the Van der Hoff-Benson expansion, which is just another technique to convert lattice sums into fast converging series of Bessel functions. Some work on analytical formulae in terms of hyperbolic functions are shown for even values of exponents in the four lattice types discussed, which are derived for the special case of exponent $s = 4$. Numerical results for lattice sums to computer precision are presented, and also an interesting comparison between fcc and hcp lattice sums for non integer values. In the last section of this project suggestions for future avenues of research and applications of high precision, fast converging lattice sums are given. These avenues are later explored and reported on in the following projects. The Mellin transformation and theta function methods are discussed in the appendix as well as the use of Kronecker symbols which connect two dimensional sums back to number theoretical techniques.

- In the Project 2, analytical formulae are derived for the zero-point vibrational energy and anharmonicity corrections of the cohesive energy and the mode Grüneisen parameter within the Einstein model

for the cubic lattices (sc, bcc and fcc) and for the hexagonal close-packed structure. This extends the work done by Lennard-Jones and Ingham in 1924, Corner in 1939 and Wallace in 1965. The formulae are based on the description of two-body energy contributions by an inverse power expansion (the extended Lennard-Jones potential). These make use of fast converging three-dimensional lattice sums which are applied to the rare gas solids and discuss associated critical points. The derived formulae give qualitative but nevertheless deep insight into vibrational effects in solids from the lightest (helium) to the heaviest rare gas element (oganesson), both presenting special cases because of strong quantum effects for the former and strong relativistic effects for the latter.

- Project 3 explores lattice sums of cuboidal lattices, which connect the face-centered with the mean-centered and the body-centered cubic lattices through parameter dependent lattice vectors. The work presents the characteristics of cuboidal lattices $\mathscr{L}(A)$ dependent on a single parameter A. The method which is employed is to decompose the sum into two separate lattice sums related to a scaled cubic lattice and a scaled Madelung constant. Using the theta transformation method, fast converging series in terms of Bessel functions are derived and the packing density for four specific cuboidal lattices along the A parameter pathway $1/3 \leq A \leq 1$ are discussed. The lattice sum smoothly connects the fcc, mean centred-cuboidal (mcc), bcc and axial centred cuboidal (acc) lattices. Analytical continuations of these lattice sums are discussed in detail.

- In Project 4, the single parameter lattice sum from the previous project is used to explore the rearrangement from body-centered cubic to the face-centered lattice. Analytical expressions for the cohesive energy in terms of lattice sums are obtained and the transformation between the bcc and fcc phases and their relative stabilities, which have been the subject of many discussions, are explored. The common belief is that strong repulsive forces favor close-packed arrangements such as fcc or hcp, whereas soft repulsion favors less dense packed structures such as bcc. By making use of a single parameter lattice sum, that transitions the acc lattice through to fcc, cohesive energy differences for each structure are obtained. This leads to an interesting result which shows that the bcc lattice is not a stable lattice compared to fcc for a (a,b) Lennard-Jones potential. The results show that bcc only has a small range of exponents (a,b) along the potential energy curve where it is metastable before the structure moves toward a more stable fcc phase.

- Project 5, investigates the effects of pressure on the body centered cuboidal lattice. The stability of the body-centered cubic (bcc) compared to the face-centered cubic (fcc) phase at finite pressures is investigated through exact lattice summations using a general (a,b) Lennard-Jones potential ($a > b > 3$). The work exposes the metastability of the bcc lattice at lower values of a and b, where use of such low values in the Lennard-Jones two-body potential lead to a potential curve of unphysical nature. The bcc phase decreases in stability with increasing pressure. The high pressure limit is found at exponent $a = 7.6603891$ for the repulsive wall. The work shows that the acc and mcc lattices are not stable in terms of a $(12,6)$ Lennard-Jones potential and that, in order to stabilze crystal structures of this type one requires other bonding conditions that can not be simply described by a two-body potential such as the Lennard-Jones potential.

- Project 6 looks at a convergent series expansion for the N-dimensional Madelung constant $M_N(s)$, where s is the exponent of the Madelung series (usually chosen as $s = 1/2$). The series expansion incorporated the number of representations of N-squares $r_N(m)$ which are produced by a recursive formula. Values for $M_N(s)$ for $s = \frac{1}{2}, \frac{3}{2}, 3$ and 6 for dimension up to $N = 20$ are presented as well as values for $M_N(1/2)$ up to $N = 100$. This work extends Zucker's original analysis on N-dimensional Madelung constants for even dimensions up to $N = 8$.[56] In this work the analytic continuation of the sum is explored and the behaviour at even values of N is shown.

- In Project 7, the work by Lennard-Jones and Ingham, and later by Kane and Goeppert-Mayer is continued by presenting a general lattice sum formula for the hexagonal close packed structure with different c/a ratios for the two parameters a and c of the hexagonal unit cell. The lattice sum is expressed in terms of fast converging series of Bessel functions. Having a function that is analytic, allows the examination of the behaviour of a Lennard-Jones potential as a function of the c/a ratio with lower kissing number, in contrast to the hard-sphere model, where the ideal ratio is $c/a = \sqrt{8/3}$ with 12 kissing spheres around a central atom. An occurrence of a slight symmetry breaking effect and the appearance of a second metastable minimum for the (12,6) Lennard-Jones potential is observed. It is also shown that analytical continuation of the (n,m) Lennard-Jones potential to the domain

$n, m < 3$ such as the Kratzer potential ($n = 2, m = 1$) gives unphysical results.

Part I

Theoretical Background

2 Lattice Sums

2.1 Lattices

For any basis of $\mathbb{R}^n$, the subgroup of all linear combinations with integer coefficients of the basis vectors defines a lattice $\mathscr{L}$. That is, a lattice in $\mathbb{R}^n$ is a set of points p_m at positions

$$\vec{r}_m = m_1\vec{b}_1 + \cdots + m_n\vec{b}_n \tag{2.1.1}$$

from a chosen origin (the subscript m in $\vec{r}_m$ stands for all the m_i used), where $m_1,\ldots,m_n$ run over all integers and $\vec{b}_1,\ldots,\vec{b}_n$ is a fixed set of n lattice vectors which span $\mathbb{R}^n$, commonly referred to as basis vectors. In the below equation, a lattice $\mathscr{L}$ is defined to be a discrete subgroup of $\mathbb{R}^n$ as a set of linear combinations of basis vectors

$$\mathscr{L} = \left\{ \vec{r}_m \;\middle|\; \vec{r}_m = \sum_{i=1}^{n} m_i\vec{b}_i \;,\; m_i \in \mathbb{Z} \text{ for } i = 1,2,3,\ldots,n \right\}. \tag{2.1.2}$$

Where $d \leq n$ refers to the dimension of the lattice $\mathscr{L}$, and each $\vec{b}_i$ is a $(1\times n)$ vector with entries in $\mathbb{R}$ for all i. The set $\left\{\vec{b}_i\right\}_{i=1}^{d}$, where $d = \dim(\mathscr{L})$ is linearly independent over $\mathbb{R}$ and called a *basis* for $\mathscr{L}$, and we can say that the lattice is generated by the vectors $\vec{b}_1,\ldots,\vec{b}_d$. Let B be a $n\times m$ matrix where $m \geq n$, and $\left\{\vec{b}_i\right\}_{i=1}^{n}$ form a basis for the lattice $\mathscr{L}$ for all i.

$$B = \left[\vec{b}_1\,\vec{b}_2\,\vec{b}_3\,\ldots\,\vec{b}_n\right]^{\top}$$

Then B is called a generator matrix for the lattice. The lattice consists of all linear combination of the basis vectors $\vec{b}_i$ for all i. Rewriting equation (2.1.2), the definition of $\mathscr{L}$ can be written as

$$\mathscr{L} = \left\{ \vec{m}B \middle| \vec{m}^{\top} = (m_1,m_2,m_3,\ldots,m_d), \vec{m} \in \mathbb{Z} \right\}. \tag{2.1.3}$$

2.1.1 Quadratic Form of the lattice

Any $(n\times n)$ real symmetric matrix A determines the quadratic form q_A in n variables by the equation

$$q_A(x_1,\ldots,x_n)=\sum_{i=1}^{n}\sum_{j=1}^{n}a_{ij}x_ix_j=\vec{x}^{\top}A\vec{x}. \tag{2.1.4}$$

The matrix A for q is given as

$$A=\begin{pmatrix} a_{11} & a_{12} & a_{13} & \ldots & a_{1n}\\ a_{21} & a_{22} & a_{23} & \ldots & a_{2n}\\ a_{31} & a_{32} & a_{33} & \ldots & a_{3n}\\ \vdots & \vdots & \vdots & \vdots & \vdots\\ a_{n1} & a_{n2} & a_{n3} & \ldots & a_{nn}\end{pmatrix}. \tag{2.1.5}$$

Except for the so-called Madelung constant we restrict ourselves to three dimensions where the relationship to q_A with the symmetric (3×3) matrix A and integer entries for $\vec{x}$ is

$$q_A(i,j,k)=\begin{pmatrix} i & j & k\end{pmatrix}A\begin{pmatrix} i\\ j\\ k\end{pmatrix} \tag{2.1.6}$$

or equivalently

$$q_A(i,j,k)=\vec{x}^{\top}A\vec{x}\quad\text{where}\quad\vec{x}=\begin{pmatrix} i\\ j\\ k\end{pmatrix}. \tag{2.1.7}$$

2.1.2 The Gram Matrix

As basis vectors $\vec{b}_1,\vec{b}_2,\ldots,\vec{b}_n$ generate the lattice $\mathscr{L}$, then let G be a $n\times n$ symmetric matrix, whose (i,j) entry is the scalar product $\vec{b}_i\cdot\vec{b}_j$. G is called the *Gram matrix*, and is defined by its basis vectors $\{\vec{b}_i\}$ with $i=1,2,\ldots,n$, through

$$G=BB^{\top}=\begin{pmatrix} \vec{b}_1\cdot\vec{b}_1 & \vec{b}_1\cdot\vec{b}_2 & \vec{b}_1\cdot\vec{b}_3 & \ldots & \vec{b}_1\cdot\vec{b}_n\\ \vec{b}_2\cdot\vec{b}_1 & \vec{b}_2\cdot\vec{b}_2 & \vec{b}_2\cdot\vec{b}_3 & \ldots & \vec{b}_2\cdot\vec{b}_n\\ \vec{b}_3\cdot\vec{b}_1 & \vec{b}_3\cdot\vec{b}_2 & \vec{b}_3\cdot\vec{b}_3 & \ldots & \vec{b}_3\cdot\vec{b}_n\\ \vdots & \vdots & \vdots & \vdots & \vdots\\ \vec{b}_n\cdot\vec{b}_1 & \vec{b}_n\cdot\vec{b}_2 & \vec{b}_n\cdot\vec{b}_3 & \ldots & \vec{b}_n\cdot\vec{b}_n\end{pmatrix}. \tag{2.1.8}$$

In three dimensions, the distance to any point in the lattice is given by

$$|\vec{r}|^2 = (i,j,k)G(i,j,k)^\top = (i,j,k)\begin{pmatrix} \vec{b}_1\cdot\vec{b}_1 & \vec{b}_1\cdot\vec{b}_2 & \vec{b}_1\cdot\vec{b}_3 \\ \vec{b}_2\cdot\vec{b}_1 & \vec{b}_2\cdot\vec{b}_2 & \vec{b}_2\cdot\vec{b}_3 \\ \vec{b}_3\cdot\vec{b}_1 & \vec{b}_3\cdot\vec{b}_2 & \vec{b}_3\cdot\vec{b}_3 \end{pmatrix}\begin{pmatrix} i \\ j \\ k \end{pmatrix}$$

$$\begin{aligned} &= i^2\vec{b}_1\cdot\vec{b}_1 + ij\vec{b}_1\cdot\vec{b}_2 + ik\vec{b}_1\cdot\vec{b}_3 \\ &+ ij\vec{b}_2\cdot\vec{b}_1 + j^2\vec{b}_2\cdot\vec{b}_2 + jk\vec{b}_2\cdot\vec{b}_3 \\ &+ ik\vec{b}_3\cdot\vec{b}_1 + jk\vec{b}_3\cdot\vec{b}_2 + k^2\vec{b}_3\cdot\vec{b}_3\,. \end{aligned}$$

Which is the quadratic form needed for work dealing with a lattice $\mathscr{L}$.

There are a few important definitions used within Chapter 8 that should be highlighted when dealing with the Gram matrix [57]. Two generator matrices B_1 and B_2 are equivalent if $B_2 = cUB_1\mathscr{O}$, where c a non-zero real number describing scaling, $\mathscr{O}$ a real orthogonal matrix ($\mathscr{O}\mathscr{O}^\top = 1$) with $\det(\mathscr{O}) = \pm 1$ describing rotation and reflection of the lattice, and U a matrix containing integers with $\det(U) = 1$ describing a change of basis matrix. An example of the above is given by the vectors

$$\vec{v_1} = \begin{pmatrix} 2 \\ 1 \end{pmatrix}, \vec{v_2} = \begin{pmatrix} 1 \\ 1 \end{pmatrix} \text{ and } \vec{u_1} = \begin{pmatrix} 1 \\ -3 \end{pmatrix}, \vec{u_2} = \begin{pmatrix} -2 \\ 7 \end{pmatrix}, \tag{2.1.9}$$

which are different descriptions of the same lattice. The generator matrices B_1, B_2 respectively are

$$B_1 = \begin{pmatrix} 2 & 1 \\ 1 & 1 \end{pmatrix}, B_2 = \begin{pmatrix} 1 & -3 \\ -2 & 7 \end{pmatrix}. \tag{2.1.10}$$

If $c = 1$ and there is no rotation or reflection by O, then $U = B_2 B_1^{-1}$. By (2.1.10)

$$U = \begin{pmatrix} 4 & -7 \\ -9 & 16 \end{pmatrix} \tag{2.1.11}$$

with $\det(U) = 1$. Using the generator matrices from (2.1.10) and U from (2.1.11), $G_2 = B_2 B_2^\top = U G_1 U^\top$ is shown by

$$G_1 = B_1 B_1^\top = \begin{pmatrix} 5 & 3 \\ 3 & 2 \end{pmatrix} \text{ and } G_2 = B_2 B_2^\top = \begin{pmatrix} 10 & -23 \\ -23 & 53 \end{pmatrix}. \tag{2.1.12}$$

Which results in

$$
\begin{aligned}
UG_1U^\top &= \begin{pmatrix} 4 & -7 \\ -9 & 16 \end{pmatrix} \begin{pmatrix} 5 & 3 \\ 3 & 2 \end{pmatrix} \begin{pmatrix} 4 & -9 \\ -7 & 16 \end{pmatrix} \\
&= \begin{pmatrix} -1 & -2 \\ 3 & 5 \end{pmatrix} \begin{pmatrix} 4 & -9 \\ -7 & 16 \end{pmatrix} \\
&= \begin{pmatrix} 10 & -23 \\ -23 & 53 \end{pmatrix} \\
&= G_2 \,.
\end{aligned} \tag{2.1.13}
$$

Therefore given two equivalent generator matrices B_1 and B_2, the corresponding Gram matrices are related by

$$G_2 = B_2B_2^\top = cUB_1\mathscr{O}\left(cUB_1\mathscr{O}\right)^\top = c^2UB_1\mathscr{O}\mathscr{O}^\top B_1^\top U^\top = c^2UG_1U^\top .$$

The minimum distance $d_{\min}$ in a lattice L can be obtained from the Gram matrix

$$d_{\min} = \min\left\{+\sqrt{\vec{m}G\vec{m}^\top} \mid \vec{m} \in \mathbb{Z}^3\backslash(0,0,0)^\top\right\}. \tag{2.1.14}$$

The volume of the parallelotope spanned by the lattice vectors $\vec{b}_i$ can similarly be expressed in terms of the Gram matrix,

$$V = \det(B) = \sqrt{\det(G)}\,. \tag{2.1.15}$$

2.2 Lattice Sums

In this section a general definition of the term *lattice sum* is given. From a historical perspective, and in much of the current literature, a strict definition for a lattice sum has somehow been avoided. However, lattice sums (at least the ones we are mostly concerned here) generally are functions of quadratic forms $\vec{x}^\top G\vec{x}$ with $\vec{x} \in \mathbb{Z}^n$, i.e., the expression $\vec{x}^\top G\vec{x}$ is the quadratic form including the Gram matrix which is associated with the lattice $\mathscr{L}$ (or simply, the associated quadratic form) [58, 59]. For so-called multi-lattices, like the hexagonal close packed structure, one needs to extend the definition here, which will be discussed further below.

As mentioned earlier in Section 2.1 from equation (2.1.1), a lattice is generated by a linear combination of basis vectors with integer coefficients. In three-dimensional space ($n = 3$), a specific lattice is spanned by the basis vectors $\vec{b}_1, \vec{b}_2, \vec{b}_3$,

$$\vec{r}_m = m_1\vec{b}_1 + m_2\vec{b}_2 + m_3\vec{b}_3\,. \tag{2.2.1}$$

A method for evaluating lattice sums involves accumulating the functional con-

tributions $f(\vec{r}_i)$ at each lattice point $\vec{r}_i$ in some sequential order with respect to one arbitrary point located at $\vec{p}_0$ (placed at the origin). For this the set of distances $r_i = |\vec{p}_i - \vec{p}_0|$ from the origin to all lattice points are used, and the corresponding values $f(r_i)$ ($r_i = |\vec{r}_i|$ if not dependent on the direction), which defines the lattice sum. For example, a function representing an inverse power potential $\phi(r) = \lambda r^{-s}$ of strength λ, we accumulate the reciprocal of these values raised to an exponent s. We will be interested in lattice sums of the form,

$$L_d(G,s) = \sum_{\vec{m}\in\mathbb{Z}^d}{}' [\vec{m}^\top G\vec{m} + c]^{-s} \tag{2.2.2}$$

where $\vec{m}^\top G\vec{m}$ refer to a positive definite quadratic form $q(\vec{m})$ of dimension d, similar to (2.1.4), G is the corresponding (symmetric) Gram matrix and c is a real number called the inhomogeneity. As Lennard-Jones and others pointed out in their original work on lattice sums, the Epstein zeta function uses positive definite real quadratic forms,

$$Z_d(A,s) = \frac{1}{2}\sum_{\vec{m}\in\mathbb{Z}^d}{}' (\vec{m}^\top A\vec{m})^{-s} \tag{2.2.3}$$

with s being in general a complex variable $\mathrm{Re}(s) > d/2$ [60]. The sum is over all column vectors with integer coefficients and excluding the origin denoted by the prime. It is evident from comparing the two formulae, that for $c = 0$ (which is the case for Bravais lattices) with real positive definite quadratic forms the lattice sum $L_d(G,s)$ belongs to the class of Epstein zeta functions. Epstein zeta functions therefore often serve as the starting point for treating lattice sums. A mention here is that the inhomogeneity c arises for multi-lattices such as hcp and often creates problems in dealing with lattice sums. The Epstein zeta function is a generalization of the Riemann zeta function,

$$\zeta(s) = \sum_{n=1}^{\infty} n^{-s}, \tag{2.2.4}$$

which converges for $\mathrm{Re}(s) > 1$. We can find another expression for the Riemann zeta function by using the gamma function defined by

$$\Gamma(s) = \int_0^\infty t^{s-1}e^{-t}\,dt\,. \tag{2.2.5}$$

Under the change of variable $t = bx$ this becomes

$$b^{-s} = \frac{1}{\Gamma(s)}\int_0^\infty x^{s-1}e^{-bx}\,\mathrm{d}x\,. \tag{2.2.6}$$

Rewriting (2.2.4) using (2.2.6) gives

$$\zeta(s) = \sum_{n=1}^{\infty} n^{-s} = \frac{1}{\Gamma(s)} \sum_{n=1}^{\infty} \int_0^{\infty} t^{s-1} e^{-nt}\, dt\,. \tag{2.2.7}$$

As the summation index is over n, then $\sum_{n=1}^{\infty} e^{-nt}$ in (2.2.7) can be resolved as a geometric series giving

$$\zeta(s) = \frac{1}{\Gamma(s)} \int_0^{\infty} t^{s-1} \frac{e^{-t}}{1-e^{-t}}\, dt\,. \tag{2.2.8}$$

Multiplying the numerator and denominator by e^t gives the integral representation of the Riemann zeta function

$$\zeta(s) = \frac{1}{\Gamma(s)} \int_0^{\infty} \frac{t^{s-1}}{e^t - 1}\, dt\,. \tag{2.2.9}$$

The Mellin transformation $M\{f\}(s)$ of a function $f(t)$ is defined by

$$M\{f\}(s) = \int_0^{\infty} t^{s-1} f(t)\, dt\,. \tag{2.2.10}$$

Therefore by (2.2.5) the Mellin transformation of the negative exponential e^{-t} is just the gamma function,

$$M\left\{e^{-t}\right\}(s) = \int_0^{\infty} t^{s-1} e^{-t}\, dt\, = \Gamma(s)\,, \tag{2.2.11}$$

and

$$M\left\{\frac{1}{e^t - 1}\right\}(s) = \Gamma(s)\zeta(s)\,. \tag{2.2.12}$$

The Mellin transformation along with the integral representation of the gamma function are used extensively throughout the treatment of lattice sums as shown by the prototype,

$$\sum_{\vec{x}\in\mathbb{Z}^d} [q_A(x_1,\ldots,x_d)]^{-s} = \frac{1}{\Gamma(s)} \sum_{\vec{x}\in\mathbb{Z}^d} \int_0^{\infty} t^{s-1} e^{-[q_A(x_1,\ldots,x_d)]t}\, dt \tag{2.2.13}$$

which is then re-expressed in terms of fast converging Bessel functions.[26, 61] In Section 4.3.1 the methodology used in the treatment of lattice sums using the Mellin transformation is shown in detail, and it will become clear that in many cases this integral transformation serves as the starting point for lattice sums. In Chapter 4 other mathematical methods for the fast evaluation of lattice sums are given. These methods ultimately have been used in the publication that resulted from the project in Chapters 6–8.

2.3 Cubic Lattice Sums

In simple cubic, body centered cubic and face centered cubic lattices the derivation of the lattice sum follows the ideas of Reference [48]. The lattice vectors $\vec{b}_i$ (for $i,j,k \in \mathbb{Z}$) for the sc, bc and fcc lattices in three dimensions are introduced, such that the position $\vec{r}_m$ of any atom in the lattice can be written as ($m = (ijk)$):

$$\vec{r}_{ijk} = i\vec{b}_1 + j\vec{b}_2 + k\vec{b}_3 \quad \text{with} \quad i,j,k \in \mathbb{Z} \tag{2.3.1}$$

The lattice vectors for the different lattices are:

$$\vec{b}_1^{\,\mathrm{sc}} = a\,(1,0,0)^\top \quad , \quad \vec{b}_2^{\,\mathrm{sc}} = a\,(0,1,0)^\top \quad , \quad \vec{b}_3^{\,\mathrm{sc}} = a\,(0,0,1)^\top \tag{2.3.2}$$

$$\vec{b}_1^{\,\mathrm{bcc}} = \frac{a}{2}\,(1,1,-1)^\top \quad , \quad \vec{b}_2^{\,\mathrm{bcc}} = \frac{a}{2}\,(-1,1,1)^\top \quad , \quad \vec{b}_3^{\,\mathrm{bcc}} = \frac{a}{2}\,(1,-1,1)^\top \tag{2.3.3}$$

$$\vec{b}_1^{\,\mathrm{fcc}} = \frac{a}{2}\,(1,1,0)^\top \quad , \quad \vec{b}_2^{\,\mathrm{fcc}} = \frac{a}{2}\,(0,1,1)^\top \quad , \quad \vec{b}_3^{\,\mathrm{fcc}} = \frac{a}{2}\,(1,0,1)^\top \tag{2.3.4}$$

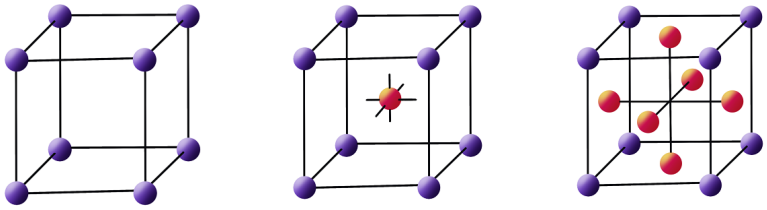

Figure 2.1 From the left to right: The simple cubic (sc), body-centred cubic (bcc), face-centred cubic (fcc) lattices.

For the simple cubic case, the corresponding vector to any point in the lattice with $i,j,k \in \mathbb{Z}$

$$\begin{aligned} \vec{r_{ijk}}/a &= i\vec{b}_1^{\,\mathrm{sc}} + j\vec{b}_2^{\,\mathrm{sc}} + k\vec{b}_3^{\,\mathrm{sc}} \\ &= i\,(1,0,0)^\top + j\,(0,1,0)^\top + k\,(0,0,1)^\top = (i,j,k)^\top \\ |r_{ijk}|/a &= \sqrt{(i^2+j^2+k^2)} \end{aligned} \tag{2.3.5}$$

Here we set conveniently the lattice parameter to one, $a = 1$, that is the distances are given in units of a. This implies that the nearest neighbor

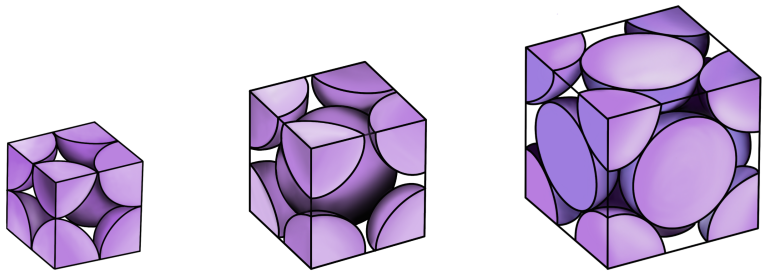

Figure 2.2 The cubic lattices (sc, bcc, fcc) shown in their relative packing configuration, note the difference in size of the unit cell.

distance r_s in the simple cubic lattice $r_s^{\mathrm{sc}} = a$ becomes $r_s = 1$, and for the body centered cubic lattice we have $r_s^{\mathrm{bcc}} = \frac{\sqrt{3}}{2}$ whereas for face centered cubic lattice we have $r_s^{\mathrm{fcc}} = \frac{1}{\sqrt{2}}$.

In the case of an inverse power potential, the lattice sum for the simple cubic lattice, (L_s^{sc}), then becomes the summation of all distances from a chosen lattice point at the origin to every point in the lattice,

$$L_s^{\mathrm{sc}} = {\sum_{i,j,k\in\mathbb{Z}}}' \frac{1}{|r_{ijk}|^s} = {\sum_{i,j,k\in\mathbb{Z}}}' \frac{1}{(i^2+j^2+k^2)^{\frac{s}{2}}} . \tag{2.3.6}$$

For the distances $r_m = |\vec{r}_m|$ from an arbitrarily chosen atom at the origin to all other atoms in the lattice the following equations apply

$$\begin{aligned} r_{ijk}^{\mathrm{sc}}/a &= r_s^{\mathrm{sc}} \left(i^2+j^2+k^2\right)^{\frac{1}{2}} = \left(i^2+j^2+k^2\right)^{\frac{1}{2}} \\ r_{ijk}^{\mathrm{bcc}}/a &= r_s^{\mathrm{bcc}} \left[i^2+j^2+k^2-\tfrac{2}{3}\left(ij+ik+jk\right)\right]^{\frac{1}{2}} \\ &= \frac{1}{2}\left(3i^2+3j^2+3k^2-2ij-2ik-2jk\right)^{\frac{1}{2}} \\ r_{ijk}^{\mathrm{fcc}}/a &= r_s^{\mathrm{fcc}} \left(i^2+j^2+k^2+ij+ik+jk\right)^{\frac{1}{2}} \\ &= \frac{1}{\sqrt{2}}\left(i^2+j^2+k^2+ij+ik+jk\right)^{\frac{1}{2}} . \end{aligned}$$

The corresponding quadratic forms for sc, bcc and fcc depend only on the underlying crystal structure

$$S_{ijk}^{\mathrm{sc}} = i^2 + j^2 + k^2 \tag{2.3.9a}$$

$$S_{ijk}^{\mathrm{bcc}} = i^2 + j^2 + k^2 - \tfrac{2}{3}(ij + ik + jk) \tag{2.3.9b}$$

$$S_{ijk}^{\mathrm{fcc}} = i^2 + j^2 + k^2 + ij + ik + jk \tag{2.3.9c}$$

$$= \frac{1}{2}\left[(i+j)^2 + (i+k)^2 + (j+k)^2\right].$$

With the corresponding crystal potential of $\phi(r) = r^{-s}$ the lattice sum L_s for each lattice are obtained:

$$L_s^{\mathrm{sc}} = \sum_{i,j,k\in\mathbb{Z}\setminus(0,0,0)} \left(i^2 + j^2 + k^2\right)^{-s} \tag{2.3.10}$$

$$L_s^{\mathrm{bcc}} = \left(\frac{\sqrt{3}}{2}\right)^s \left(L_s^{\mathrm{sc}} + \sum_{i,j,k\in\mathbb{Z}} \left(\left(i+\tfrac{1}{2}\right)^2 + \left(j+\tfrac{1}{2}\right)^2 + \left(k+\tfrac{1}{2}\right)^2\right)^{-s}\right) \tag{2.3.11}$$

$$L_n^{\mathrm{fcc}} = 3 \sum_{i,j,k\in\mathbb{Z}\setminus(0,0,0)} \left(2i^2 + j^2 + k^2\right)^{-s} + 2^{1-s} L_n^{\mathrm{sc}}. \tag{2.3.12}$$

Equations (2.3.10)-(2.3.12) were first derived by Lennard-Jones for the cubic cases [6]. Alternative decompositions are obtained by combinations of sub-lattices or by direct manipulation of the lattice sums as shown in Section 4.

2.3.1 Alternating Cubic Lattices

In a simple ionic solid, the Madelung constant depends of the crystal type through its Coulomb interactions between the charged atoms taken as partial point charges. To calculate the Madelung constant for a crystal lattice in three dimensions the summations starts from a central atom and moves radially in successively alternating shells until all nearest neighbours of the same electric charge are summed for any particular shell. For a simple cubic lattice with alternating charges in the crystal structure (as in NaCl) the Madelung constant (or function) $M(s) \equiv M_{\mathrm{sc}}(s)$ is given by the 3D alternating lattice sum

$$M(s) = {\sum_{i,j,k\in\mathbb{Z}}}' \frac{(-1)^{i+j+k}}{(i^2 + j^2 + k^2)^s} \quad , \tag{2.3.13}$$

where the summation is over all integer values, the prime behind the sum indi-

cates that $i = j = k = 0$ is omitted, $s \in \mathbb{R}$, and $s = \frac{1}{2}$ is chosen (as mentioned below) for a Coulomb-type of interaction. The sum $M(s)$ is absolutely convergent for $s > \frac{3}{2}$, but only conditionally convergent for smaller s-values [62, 63]. The most common equation for the Madelung Constant is often expressed in the literature with $s = 1/2$, and is given by

$$\sum_{i,j,k\in\mathbb{Z}}{}' \frac{(-1)^{i+j+k}}{\sqrt{i^2+j^2+k^2}}. \tag{2.3.14}$$

The resulting sum for $M(\frac{1}{2}) = -1.747\ 564\ 594\ 633\ 182\ \ldots$ where the summation is performed over expanding 3-dimensional cubes and not spheres [64].The Riemann Series Theorem states that one can converge to any desired value or even diverge by a suitable rearrangement of the terms in such a series, this then poses a problem for conditionally convergent series. This problem is well known for the Madelung constant ($s = \frac{1}{2}$) and has been documented and analyzed in great detail by Borwein et al [26, 63, 65] and Crandall et al [42, 64]. The more popular method of summing over expanding spheres is often found in much of the literature on solid state physics concerning the Madelung constant, however this method produces a divergent series as shown by Emersleben [66]. The sum over expanding cubes agrees with the value (for $s = {}^1/_2$ and was shown by Borwein et al [67]. The valve of $M(s)$ for other s values is defined as being the value of the function obtained by the process of analytic continuation.

There are many expansions available leading to an accurate determination of the Madelung constant [64]. Perhaps the most prominent formulas are the ones by Benson-Mackenzie [27, 68]

$$M\left(\tfrac{1}{2}\right) = -12\pi \sum_{i,j\in\mathbb{N}} \operatorname{sech}^2\left[\frac{\pi}{2}\sqrt{(2i-1)^2+(2j-1)^2}\right] \tag{2.3.15}$$

and by Hautot [64, 69]

$$M\left(\tfrac{1}{2}\right) = -\frac{\pi}{2} + 3\sum_{i,j\in\mathbb{Z}}{}' \quad \frac{(-1)^i \operatorname{cosech}\left(\pi\sqrt{i^2+j^2}\right)}{\sqrt{i^2+j^2}}. \tag{2.3.16}$$

The Madelung sum can also be extended to a N dimensional series where $N \geq 1$, again the prime on the sum indicates that the term corresponding to $i_1 = \cdots = i_N = 0$ is not included,

$$M_N(s) = \sum_{i_1,\ldots,i_N\in\mathbb{Z}}{}' \frac{(-1)^{i_1+\cdots+i_N}}{(i_1^2+i_2^2+\cdots+i_N^2)^s} = \sum_{\vec{i}\in\mathbb{Z}^N\setminus\{\vec{0}\}} \frac{(-1)^{\vec{i}\cdot\vec{1}}}{|\vec{i}|^{2s}} \quad . \tag{2.3.17}$$

As with the 3D lattice, the N-dimensional lattice can be constructed from its N linearly independent basis lattice vectors. In Section 5.2 the general formula for the N-dimensional Madelung sum is introduced, as shown in (2.3.17). We derive a formula for $M_N(s)$ in terms of fast converging Bessel function expansions.

2.4 The Hexagonal Close Packed Multi-Lattice

The hexagonal close-packed structure (hcp) contains two atoms in its primitive unit cell and is therefore is not a lattice in the sense of (2.1.1), rather the hcp structure is the union of two sets: one of which is a lattice, the other is a translation of a lattice. The hcp structure is sometimes termed a multi-lattice and constructed from two shifted hexagonal Bravais lattices. This complicates the treatment of the corresponding lattice sum as an inhomogeneity parameter c is introduced into the quadratic form. However, the distance to any point in the hcp lattice can be still be reached resulting in two different lattice sums. In order to show this we introduce the hexagonal lattice first spanned by the following lattice vectors,

$$\vec{b}_1^{\,\mathrm{hex}} = a\,(1,0,0)^\top \quad , \quad \vec{b}_2^{\,\mathrm{hex}} = a\left(\frac{1}{2},\frac{\sqrt{3}}{2},0\right)^\top \quad , \quad \vec{b}_3^{\,\mathrm{hex}} = c\,(0,0,1)^\top , \tag{2.4.1}$$

with the corresponding lattice constants a and c. The distance to any point in the hexagonal structure can be found by

$$r_{ijk}^{\mathrm{hex}} = |i\vec{b}_1^{\,\mathrm{hex}} + j\vec{b}_2^{\,\mathrm{hex}} + k\vec{b}_3^{\,\mathrm{hex}}| \tag{2.4.2}$$

$$= a\left(i^2 + ij + j^2 + \frac{c^2}{a^2}k^2\right)^{\frac{1}{2}} \tag{2.4.3}$$

with the minimum distance of $r_s = \min\{a,c\}$. The corresponding quadratic form for the hexagonal lattice is,

$$S_{ijk}^{\mathrm{hex}} = i^2 + ij + j^2 + \frac{c^2}{a^2}k^2 \tag{2.4.4}$$

Now we need to introduce the middle hexagonal B layer into the hexagonal lattice to obtain the hcp structure with the ABAB... sequence. This can be done by shifting the lattice points by $\vec{v}_s^{\,\top} = \left(\frac{a}{2},\frac{a}{2\sqrt{3}},\frac{c}{2}\right)$ above the centroid of the triangle of three neighboring lattice points in the A layer, which defines the distances between a lattice point in the A layer to all lattice points in the B

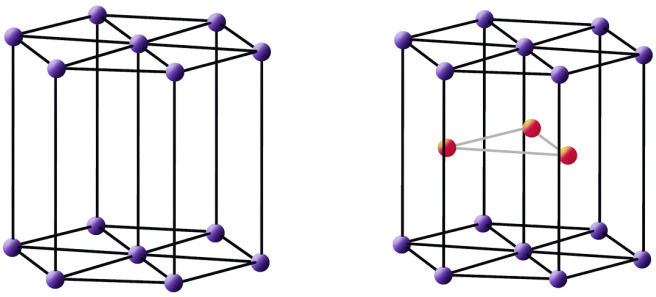

Figure 2.3 Hexagonal lattice (hex) and hexagonal closed packed (hcp) structure. Note for the hexagonal lattice (left) the middle layer is missing.

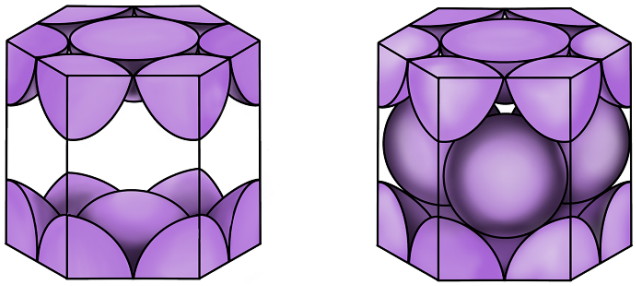

Figure 2.4 The hexagonal closed packed structure (right) in the packed configuration and hexagonal lattice (left) missing centre layer compared to hcp for illustration.

layer,

$$\vec{r}^{\,\mathrm{B}}_{ijk} = i\vec{b}_1^{\,\mathrm{hex}} + j\vec{b}_2^{\,\mathrm{hex}} + k\vec{b}_3^{\,\mathrm{hex}} + \vec{v}_s\,. \tag{2.4.5}$$

When treated in this way one obtains a lattice sum containing the part from the original hexagonal lattice and the one containing an inhomogeneous quadratic form

$$L_s^{\mathrm{hcp}} = {\sum_{i,j,k\in\mathbb{Z}}}' \left(S_{ijk}^{\mathrm{hex}}\right)^{-s} + \sum_{i,j,k\in\mathbb{Z}} \left(S_{ijk}^{\mathrm{B}}\right)^{-s} \tag{2.4.6}$$

with

$$S_{ijk}^{hex} = i^2 + j^2 + ij + \frac{c^2}{a^2}k^2 \tag{2.4.7}$$

and

$$S^{\mathrm{B}}_{ijk} = \left(i+\tfrac{1}{3}\right)^2 + \left(j+\tfrac{1}{3}\right)^2 + \left(i+\tfrac{1}{3}\right)\left(j+\tfrac{1}{3}\right) + \frac{c^2}{a^2}\left(k+\tfrac{1}{2}\right)^2 \tag{2.4.8}$$

$$= i(i+1) + j(j+1) + ij + \frac{c^2}{a^2}k(k+1) + 1. \tag{2.4.9}$$

The equation in (2.4.8) was first used by Kane and Goeppert-Mayer [24] but not explicitly stated (see Bell and Zucker for details [70].) This inhomogeneous form can complicate the evaluation of the triple sum and also makes the direct summation expensive for small values of the exponents s. Fortunately, one can derive a formula in terms of pure quadratic forms, for example, Stein decomposed the hcp structure into four interpenetrating orthorhombic lattices for the special case of $\frac{c}{a} = \sqrt{\frac{8}{3}}$, which represents the ideal hcp lattice. With reference to Project 1, it is easy to show that [71]

$$L^{hcp}_n = \sum_{m=1}^{4} {\sum_{i,j,k\in\mathbb{Z}}}' a_m \left(S^{hcp}_{ijk}(\alpha_i)\right)^{-s}, \tag{2.4.10}$$

with $a_1 = \frac{3}{2}, a_2 = 3^{\frac{n}{2}}/2, a_3 = -3^{\frac{n}{2}}/2, a_4 = -\frac{1}{2}$ and $\alpha_1 = \frac{8}{3}, \alpha_2 = 2, \alpha_3 = 8, \alpha_4 = \frac{2}{3}$. In this case, the ideal hcp structure has the same number of nearest neighbors and thus the same limit as the fcc lattice, i.e., $L^{hcp}_\infty = 12$.

Methods for evaluating the lattice sums for the hcp structure through direct summation techniques and via more elaborate methods are shown in Sections 4.2.4 and 4.5. In Project 7 we show that both sums in (2.4.6) can be evaluated by a very similar technique using only two sums compared to four in (2.4.10), nevertheless providing a useful computational check.

2.5 Kronecker & Legendre notation

For this thesis a few important mathematical functions and definitions need to be introduced. The Kronecker symbol, written as $(\frac{a}{n})$ or $(a|n)$, is a generalization of the Jacobi symbol to all integers n, and is used extensively in this thesis. Two integers a, b whose difference is divisible by n are said to be congruent modulo n and is written $a \equiv b \pmod{n}$. An integer q is called a quadratic residue modulo n if it is congruent to a perfect square modulo n; i.e., if there exists an integer x such that:

$$x^2 \equiv q \pmod{n}, \tag{2.5.1}$$

and noting that $1 \leq q \leq n-1$. The Legendre symbol defined as

$$\left(\frac{a}{p}\right) = \begin{cases} 1 & \text{if } a \text{ is a quadratic residue modulo } p \text{ and } a \not\equiv 0 (\text{mod } p), \\ 0 & \text{if } a \equiv 0 (\text{mod } p), \\ -1 & \text{otherwise .} \end{cases} \tag{2.5.2}$$

For an integer a and any positive integer n, the Kronecker symbol is defined by

$$\left(\frac{a}{n}\right) = \left(\frac{a}{p_1}\right)^{e_1} \left(\frac{a}{p_2}\right)^{e_2} \ldots \left(\frac{a}{p_k}\right)^{e_k}, \tag{2.5.3}$$

with $n = {p_1}^{e_1} {p_2}^{e_2} \ldots {p_k}^{e_k}$ being the prime factorization for n. The terms of the right of (2.5.3) are Legendere symbols. If $k > 1$ is an integer, then a function $\chi(n)$ is called a Dirichlet character (mod k) if it is completely multiplicative, periodic with period k, and vanishes when $(n,k) > 1$. In terms of the Kronecker symbol, let $\chi_k = (\frac{d}{m})$ be the Kronecker symbol. Then its elementary Dirichlet L-series (modulo k) associated with the *character* χ is a function of the form

$$L_k(s,\chi) = \sum_{n=1}^{\infty} \frac{\chi_k(n)}{n^s}, \tag{2.5.4}$$

where χ_k is a Dirichlet character and k will be referred to as the period or order of the L-series. As an example the Riemann zeta function is represented by

$$L_1(s,1) = \sum_{n=1}^{\infty} \frac{\chi_1(n)}{n^s} = 1^{-s} + 2^{-s} + 3^{-s} + \cdots = \zeta(s) . \tag{2.5.5}$$

Dirichlet series involving Kronecker symbols of the form $\sum_{n=1}^{\infty} \left(\frac{a}{n}\right) n^{-s}$ for various values of a are used in Sections 4.2, 6 and Project 1, Appendix B to evaluate single and double sums.

2.6 Dirichlet Series

Dirichlet has shown that the number of times an integer n is represented by a quadratic form with discriminant d is

$$r_N(n) = \sum_{e|n}^{\infty} \left(\frac{d}{e}\right) . \tag{2.6.1}$$

The above equation is valid when n has no divisor in common with d and the sum is over all the divisors of n. With $r_N(n)$ being the number of solutions to the sum of squares $m_1^2 + m_2^2 + \cdots + m_N^2 = n$ then the corresponding Dirichlet

L-series corresponding to $r_N(n)$ is shown by

$$L_N(s) = \sum_{n=1}^{\infty} r_N(n) n^{-s}. \tag{2.6.2}$$

Closed forms are available via the Mellin transform for $L_N(s)$ for certain values of N namely $N = 2,4,6$ and 8 from the explicit formula known for $r_N(n)$, the corresponding q-series were known to Jacobi. Dirichlet series are related to two-dimensional sums of the form,

$$\sum_{x_1,x_2=-\infty}^{\infty}{}' [q(x_1,x_2)]^{-s} \tag{2.6.3}$$

where $q(x_1,x_2) = a{x_1}^2 + bx_1x_2 + c{x_2}^2$ is an integer quadratic form with the discriminant of $d = b^2 - 4ac$. For example for the binary quadratic form $q = a^2 + b^2$ with corresponding sum

$$S_q = \sum_{-\infty}^{+\infty}{}' \left(a^2 + b^2\right)^{-s} \text{ and determinant } d = -4, \tag{2.6.4}$$

when n is odd it can have no factor in common with $d = -4$ then, by Dirichlet's formula,

$$r_q(n) = 4 \sum_{a|n} \left(\frac{-4}{a}\right).$$

Taking $n = ax$ and summing over the odd values of a and x, then

$$\begin{aligned} S_q &= 4\left(1-2^{-s}\right)^{-1} \sum_{a=1,\text{odd}}^{\infty} \frac{\chi_{-4}(a)}{a^s} \sum_{x=1,\text{odd}}^{\infty} \frac{1}{x^s} \\ &= 4\left(1-2^{-s}\right)^{-1} L_{-4}(s) L_1(s) \left(1-2^{-s}\right) \\ &= 4L_{-4}(s) L_1(s) \\ &= 4\beta(s)\zeta(s). \end{aligned} \tag{2.6.5}$$

The above result is referenced extensively throughout the work on lattice sums. In fact an alternate route to evaluating lattice sums is by reducing N-dimensional sums to an ordinary Dirichlet series. For this the sums over the S_N are rearranged as,

$$L_s = \sum_{\vec{x}\in\mathbb{Z}^d} [q(x_1,\ldots,x_d)]^{-s} = l^s \sum_{n\in\mathbb{N}} \frac{r_d^{\mathscr{L}}(n)}{n^s} \tag{2.6.6}$$

with $r_d^{\mathscr{L}}(n)$ being the number of different representations fulfilling the equation $lS_{n_d} = n$,[72, 73] with l being the smallest integer such that $n \in \mathbb{N}$ for all combinations of $n_d \in \mathbb{Z}$ in the S_N expressions ($l^{\text{sc}} = 1, l^{\text{bcc}} = 3, l^{\text{fcc}} = 1, l^{\text{hcp}} = 3$).

The number $r_d^{\mathscr{L}}(n)$ represents the number of points in the lattice $\mathscr{L}$ at distance r_n from a selected central lattice point. It should be noted that the lattice sum for hcp can be written as as a single Dirichlet sum even though two atoms are in the unit cell. The work presented in Section 6 primarily focuses on lattice sums in three-dimensions, and therefore the representations $r_3^{\mathscr{L}}(n)$ are listed in Table A.1. Larger sequences of $r_3^{\mathscr{L}}(n)$ numbers can be found in the Sloane tables but often is is convenient to populate local tables when (computationally efficient) for sums of squares when doing a lattice sum evaluation [74, 75]. For this, the representations of the sum of squares is obtained from the recursive formula,

$$r_{N+1}(m) = r_N(m) + 2 \sum_{\substack{i\in\mathbb{N} \\ m-i^2\geq 0}} r_N(m-i^2) \tag{2.6.7}$$

keeping in mind that $r_N(0) = 1$. The above formula is used in Section 11 to produce large in memory or tabulated $r_N(n)$ tables in the evaluation of the Madelung constant in N-dimensions.

The problem for the slow converging Dirichlet series with small exponents s is that, in contrast to the even dimensional quadratic forms, there is not much known for the $r_d(n)$ values for the odd dimensional sum of squares ($D = 2m+1, m \in \mathbb{N}$). One of the exceptions is the simple cubic case in three dimensions where a (rather cumbersome) formula for $r_3(n)$ has been provided by Bateman [76]. The values of the coefficients $r_3(n)$ are unbounded, e.g., $r_3(n^2) = 6(n+1-(-1)^{(n-1)/2})$ for any odd prime n [77]. The series converges slowly due to the fact that n^{-s} does not decay fast enough, Therefore the use of the Dirichlet series in the evaluation of lattice sums is most convenient for larger values of the exponent s. Nevertheless, the series expansion is particularly useful when incorporating the Bessel function method as computer precision can be reached only after a few terms in the expansion. This is shown in Section 4.3.

2.7 Theta Functions

Euler introduced the following theta function as a tool in the study of the number of representation of integers as sums of squares The classical theta function is given by

$$\theta(\tau) = \sum_{n=-\infty}^{\infty} e^{\pi i n^2 \tau} = 1 + 2\sum_{n=1}^{\infty} e^{\pi i n^2 \tau}. \tag{2.7.1}$$

Observe that

$$\theta^2(\tau) = \sum_{n=-\infty}^{\infty} e^{\pi i n^2 \tau} \sum_{m=-\infty}^{\infty} e^{\pi i m^2 \tau}$$
$$= \sum_{k=0}^{\infty} r_2(k) e^{\pi i k \tau}, \tag{2.7.2}$$

where $r_2(k)$ is the integer number of ways in which k can be written as a sum of two squares $k = n^2 + m^2$. Or shown by the following q-series [78]

$$\left(\sum_{m=-\infty}^{\infty} q^{m^2} \right)^2 = \sum_{m=-\infty}^{\infty} \sum_{n=-\infty}^{\infty} q^{m^2+n^2} = \sum_{N=0}^{\infty} r_2(k) q^k . \tag{2.7.3}$$

A Jacobi theta function is a function defined for a complex variable z and a parameter τ given by the equation

$$\theta(z,\tau) = \sum_{n=-\infty}^{\infty} e^{2\pi i n z + \pi n^2 \tau}, \tag{2.7.4}$$

for $\mathrm{Im}(\tau) > 0$. Theta functions may be expressed in terms q, denoted $\theta_n(z,q)$ or the half period theta function as $\theta_n(z,q\tau)$ where $|q| < 1$ and τ (the half-period ratio) are related by $q \equiv e^{i\pi\tau}$. The Jacobi theta functions for a complex argument z are

$$\theta_1(z,q) = \sum_{n=-\infty}^{\infty} (-1)^{n-1/2} q^{(n+1/2)^2} e^{(2n+1)iz} \tag{2.7.5}$$

$$\theta_2(z,q) = \sum_{n=-\infty}^{\infty} q^{(n+1/2)^2} e^{(2n+1)iz} \tag{2.7.6}$$

$$\theta_3(z,q) = \sum_{n=-\infty}^{\infty} q^{n^2} e^{2niz} \tag{2.7.7}$$

$$\theta_4(z,q) = \sum_{n=-\infty}^{\infty} (-1)^n q^{n^2} e^{2niz} . \tag{2.7.8}$$

In lattice sums our interest lies in the case where $z = 0$, therefore

$$\theta_1(q) = \sum_{n=-\infty}^{\infty} (-1)^{n-1/2} q^{(n+1/2)^2} = 2q^{1/4}(1-3q^2+5q^6-\dots) \tag{2.7.9}$$

$$\theta_2(q) = \sum_{n=-\infty}^{\infty} q^{(n+1/2)^2} = 2q^{1/4}(1+q^2+q^6+\dots) \tag{2.7.10}$$

$$\theta_3(q) = \sum_{n=-\infty}^{\infty} q^{n^2} = 1+2q+2q^4+\dots \tag{2.7.11}$$

$$\theta_4(q) = \sum_{n=-\infty}^{\infty} (-1)^n q^{n^2} = 1-2q+2q^4-2q^9+\dots . \tag{2.7.12}$$

Theta functions have been used in the numerical evaluation of lattice sums since Appell and Ewald [9, 14], however Mellin transformations of theta functions were not used until the work of Glasser [32–35] in the mid nineteen seventies. Throughout the work on lattice sums in this thesis and the projects accompanying it, we make use of theta functions and the transformation formula seen in the next section. For more information some properties are shown in Appendix B.

2.7.1 Theta function transformation

The transformation formula for theta functions displays one of their most useful properties in application, and throughout the application to lattice sums this property is leveraged. The transformation formula for theta functions is [79, 80]:

$$\sum_{n=-\infty}^{\infty} e^{-\pi n^2 t + 2\pi i n a} = \frac{1}{\sqrt{t}} \sum_{n=-\infty}^{\infty} e^{-\pi (n+a)^2/t}, \quad \text{assuming } \mathrm{Re}(t) > 0. \tag{2.7.13}$$

2.7.2 The cubic theta function

The analogue of the sum of two squares result is

$$\sum_{m=-\infty}^{\infty} \sum_{n=-\infty}^{\infty} q^{m^2+mn+n^2} = \sum_{k=0}^{\infty} u_2(k) q^k \tag{2.7.14}$$

where

$$u_2(k) = \#\left\{m^2+mn+n^2 = k\right\} = \begin{cases} 1 & \text{if } k = 0, \\ 6\sum_{d|k} \chi_{-3}(d) & \text{if } k \geq 1, \end{cases} \tag{2.7.15}$$

where the sum is again over the positive divisors d of k.[78]

2.8 Lennard-Jones Potential

The (n,m) Lennard-Jones (LJ) potential beside the Morse potential is the most widely used interaction potential for diatomic systems in the physical and biological sciences [18, 81–90]. The LJ potential introduced in 1924 by Lennard-Jones is dependent on the variable r, which is the distance between two atoms and has the following form

$$\phi_{LJ}(r) = \frac{\lambda_n}{r^n} - \frac{\lambda_m}{r^m} \quad , \quad m < n \,, \tag{2.8.1}$$

$$\tag{2.8.2}$$

where λ_m and λ_n are parameters derived from experimental results, however at the time when Lennard-Jones introduced this potential, m and n were not fixed. The function in equation (2.8.1) produces a potential curve such that there is a minimum at some equilibrium distance r. During the early 20th century as discussed in the previous chapter, the LJ potential (not commonly known at the time by that name) combines attractive and repulsive terms to describe the overall interaction. The shape of the curve is manipulated by different values of m and n, and as such, for distances smaller than the equilibrium distance the potential curve goes to positive infinity, whereas for larger values of r the potential approaches zero.

The viral equations of state are functions that describe the pressure–volume–temperature behavior of pure substances or mixtures in the gas state. Lennard-Jones used this potential to solve the integral expression in the second viral coefficient B in the equation of state analytically to derive the parameters λ_m and λ_n based on experimental results. Therefore, the more common definition of the LJ potential is given below in terms of a parameter for the potential well depth ε and the equilibrium distance r_e that can be determined by the size and interaction strength of the atoms

$$\phi_{LJ}(r) = \frac{nm}{n-m}\varepsilon \left[\frac{1}{n}\left(\frac{r_e}{r}\right)^n - \frac{1}{m}\left(\frac{r_e}{r}\right)^m \right] . \tag{2.8.3}$$

The two parameters m and n attribute to the long range behaviour and short range behaviours respectively. Lennard-Jones used lattice parameters and heats of sublimation from experimental data to fit the potential to produce a suitable value for the short-range parameter as it cannot be derived from the equation of state [23, 91, 92]. Despite attempts at deriving the long range behaviour, it was not until the 1930 that the correct physical description of the

long-rang dispersive term came by London [19]. Lennard-Jones eventually settled for the values of $m = 6$ and $n = 12$, the latter to fit experimental data, giving rise to what is now days most commonly referred to as the (12,6) Lennard-Jones potential [93]. Figure 2.5 shows the potential in equation (2.8.3) with varying values of the well depth ε and the equilibrium distance r_e.

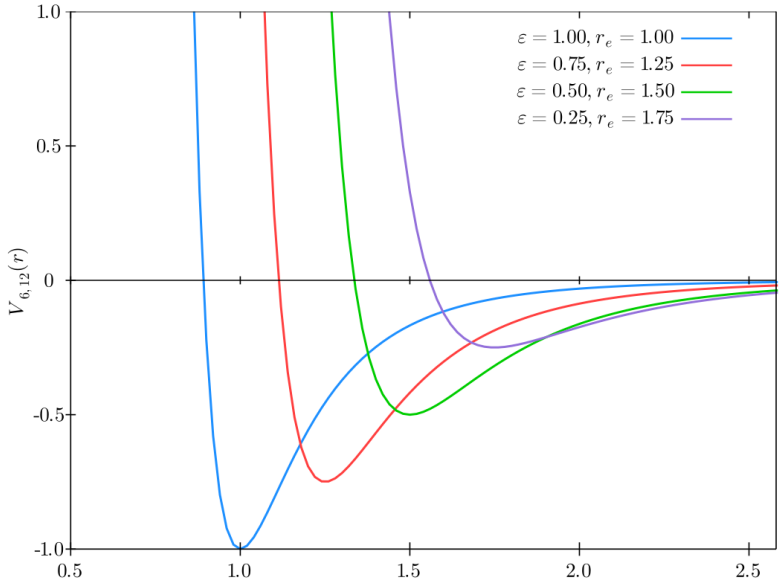

Figure 2.5 Lennard-Jones potential curves for the (6,12)-LJ potential with various values of ε and r_e.

2.8.1 Extended Lennard-Jones Potential

The problem with the LJ potential is that is lacks flexibility, any change in the exponents m and n restricts the accuracy of the two body potential. Thus extending the potential to a more general extended Lennard-Jones (ELJ) potential, originally introduced for integer exponents by Born in 1940 is shown below [94],

$$\phi_{\mathrm{ELJ}}(r) = \sum_{n=1}^{n_{\max}} c_n r^{-s_n} . \tag{2.8.4}$$

Here the s_n are fixed real numbers. The coefficients c_n have to be chosen such that $\phi_{\mathrm{ELJ}}(r)$ has a minimum at $r = r_e$ and $\phi_{\mathrm{ELJ}}(r_e) = -\varepsilon$. r_e is the equilibrium distance on the potential energy curve [48]. The number of exponents $n = 1$ to n_{max} has to be determined based on the system being studied. The coefficients c_n are determined by a fitting procedure based on accurate dissociation curves for the two-body system calculated for example by relativistic

coupled-cluster theory. It was shown that (7.1.2) only converges for $s_n > 3$ in the infinite three-dimensional solid, although this is directly related to the convergence of lattice sums studied much earlier [26, 48]. The ELJ potential is more accurate than the simple LJ potential, and has the advantage of being computationally very efficient when compared to other more elaborate analytical forms treating the short- and long-range behaviour separately.[95–97]

2.9 Cohesive Energy

An important advantage of the ELJ form is that for certain crystals analytical forms for solid-state properties can be found in terms of lattice sums, for example to describe the cohesive energy per atom $E_{\mathrm{ELJ}}^{\mathrm{coh}}$. The required distances for these sums, $r_m = |\vec{r}_m|$, from an arbitrarily chosen atom at the origin to all other atoms in the lattice are summarized below (m denotes (ijk))

$$\begin{aligned} r_m^{\mathrm{sc}} &= r_s \left(i^2+j^2+k^2\right)^{\frac{1}{2}} \\ &= a \left(i^2+j^2+k^2\right)^{\frac{1}{2}} && \text{(2.9.1a)} \\ r_m^{\mathrm{bcc}} &= r_s^{\mathrm{bcc}} \left[i^2+j^2+k^2-\tfrac{2}{3}\left(ij+ik+jk\right)\right]^{\frac{1}{2}} \\ &= \frac{a}{2}\left(3i^2+3j^2+3k^2-2ij-2ik-2jk\right)^{\frac{1}{2}} && \text{(2.9.1b)} \\ r_m^{\mathrm{fcc}} &= r_s^{\mathrm{fcc}} \left(i^2+j^2+k^2+ij+ik+jk\right)^{\frac{1}{2}} \\ &= \frac{a}{\sqrt{2}}\left(i^2+j^2+k^2+ij+ik+jk\right)^{\frac{1}{2}} && \text{(2.9.1c)} \\ r_m^{\mathrm{hex}} &= a\left(i^2-ij+j^2+\tfrac{c^2}{a^2}k^2\right)^{\frac{1}{2}} && \text{(2.9.1d)} \\ r_m^{\mathrm{B}} &= \left(i+\tfrac{1}{3}\right)^2+\left(j+\tfrac{1}{3}\right)^2+\left(i+\tfrac{1}{3}\right)\left(j+\tfrac{1}{3}\right)+\frac{c^2}{a^2}\left(k+\tfrac{1}{2}\right)^2 \\ & && \text{(2.9.1e)} \end{aligned}$$

Note that for the general hcp lattice a union of a hexagonal (hex) lattice and shifted hexagonal lattice (B) are taken. The minimum distance for the hcp lattice depends on the choice of c/a, i.e.

$$r_s = \min\left\{a, c, \sqrt{\frac{a^2}{3}+\frac{c^2}{4}}\right\} = a \min\left\{1, \gamma, \sqrt{\frac{1}{3}+\frac{1}{4}\gamma^2}\right\}, \qquad \text{(2.9.2)}$$

for which $r_s = a$ and $\gamma = \frac{c}{a} = \sqrt{\frac{8}{3}}$ which leads to the ideal hcp lattice with 12 kissing spheres around the central atom. Using the these distances, the two-body contribution to the cohesive energy per atom can be evaluated for each

crystal system by summing over all atoms in the lattice. Integrating this into the ELJ potential from equation (6.1.3) the following equation for the cohesive energy of the solid ($E^{\text{coh}}_{\text{ELJ}}$) can be derived

$$\begin{aligned} E^{\text{coh}}_{\text{ELJ}}(a) &= \frac{1}{2} \sum_{m \in \text{ lattice}} \phi_{\text{ELJ}}(r_m) \\ &= \frac{1}{2} \sum_{m \in \text{ lattice}} \sum_{n>3} c_n r_m^{-n} \\ &= \frac{1}{2} \sum_{n>3} c_n \left(\sum_{i,j,k \in \mathbb{Z} \setminus (0,0,0)} S_{ijk}^{-\frac{n}{2}} \right) r_s^{-n} \\ &= \frac{1}{2} \sum_{n>3} c_n L_n r_s^{-n} . \end{aligned} \tag{2.9.3}$$

In the above, $\phi_{\text{ELJ}}(r_m)$ is the potential at distance r_m, which is re-expressed in ELJ form [6, 22, 48]. The sum $\sum_{m \in \text{ lattice}}$ is replaced by a lattice coefficient (lattice sum at the exponent s, L_{s_n}) for the particular lattice type and the final cohesive energy for an entire solid can be expressed as

$$E^{\text{coh}}_{\text{ELJ}}(r_0) = \frac{1}{2} \sum_{n=1}^{n_{\max}} c_n L_{s_n} r_s^{-s_n} , \tag{2.9.4}$$

where r_s is the nearest neighbour distance of the solid.[48, 98, 99] A note here is that the lattice sums L_n only depend on the lattice structure, while system-specific information is exclusively contained in the nearest neighbour distance r_s and the potential coefficients c_n. The overall advantage of the form in (6.1.3) is that, as the lattice coefficients and the coefficients c_n only need to be calculated once, leads to fast cohesive energy calculations.

3 Computational Aspects

3.1 Computational

In Section I the lattice sum is described as a sum of an inverse power law (see equation 2.2.2). When dealing with lattice sums whether by direct summation or in terms of standard functions or fast converging Bessel functions also, such small floating point values present a problem for traditional methods of representing and carrying out floating point arithmetic while preserving precision. Since the first electronic computers were developed the speed at which rounding errors can potentially accumulate in a disastrous way is a challenge for the programmer to overcome or to deal with the limitation of floating point arithmetic-logic unit. Most often, instability is caused not by the accumulation of millions of rounding errors, but by the insidious growth of just a few rounding errors. In the case of direct summation over $i, j, k \in \mathbb{N}$ the accumulation of rounding errors needs to be confined to a region of floating point value where there is no impact on the requested accuracy of the result or eliminated entirely. Consistency of numerical precision throughout the algorithm is also a precondition that must be satisfied.

3.1.1 Floating Point Format

The Institute of IEEE (IEEE) Standard for Floating-Point Arithmetic (IEEE-754) is a technical standard for floating-point computation established in 1985 [100]. The standard addressed many problems found in the diverse floating point implementations that made them difficult to use reliably and portability. Many hardware floating point units now use the IEEE 754 standard.

Figure (3.1) shows IEEE 754 floating point single 32-bit (top) and double 64-bit (bottom) precision representations. With reference to the single precision format; the most significant bit (bit 31) represents the sign denoting a positive or negative value being stored and also is the sign of the mantissa (or significand). The exponent (bits 30-23) is either an 8-bit signed integer from −128 to 127 (2's complement) or an 8-bit unsigned integer from 0 to 255. An exponent in the range −126 .. +127 is biased by adding 127 to get a value in the range 1 .. 254. Exponents range from −126 to +127 because exponents of −127 (all 0's) and +128 (all 1's) are reserved for special numbers. The true signif-

icand includes 23 fraction bits to the right of the binary point and an implicit leading bit (bits 22-0) (to the left of the binary point) with value 1, unless the exponent is stored with all zeros. Thus only 23 fraction bits of the significand appear in the memory format, but the total precision is 24 bits (equivalent to $\log_{10} 2^{24} \approx 7.225$ decimal digits). For double precision the equivalent precision is $\log_{10} 2^{53} \approx 15.955$ decimal digits and quadruple precision (not shown below) the equivalent precision is $\log_{10} 2^{113} \approx 34.016$ decimal digits.

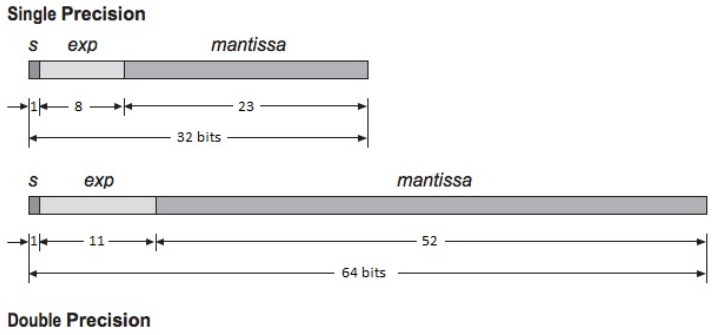

Figure 3.1 IEEE 754 single & double precision floating point format; in memory the bits are laid out most significant bit (b_{31} for single, b_{63} for double) to the left).

Thus the real value assumed by a given 32-bit binary32 data with a given biased sign, exponent e (the 8-bit unsigned integer), and a 23-bit fraction is

$$(-1)^{b_{31}} \times (1.b_{22}b_{21}...b_0)_2 \times 2^{(b_{30}b_{29}...b_{23})_2 - 127} \tag{3.1.1}$$

which in decimal yields

$$value = (-1)^{sign} \times \left(\sum_{i=1}^{23} b_{23-i} 2^{-i} \times 2^{e-127} \right). \tag{3.1.2}$$

In the C programming language the header file "float.h" describes the characteristics of floating types for the specific system and compiler implementation used. These constants (described in "float.h") are proposed by ANSI C allowing programs to be made more portable. There are three *floating types*. designated as `float`, `double` and `long double`. The set of values of the type `float` is a subset of the set of values of the type `double`. The set of values of the type `double` is a subset of the set of values of the type `long double`.

The `long double` type was present in the original 1989 C standard, [101] support was improved by the 1999 revision of the C standard, or C99, which extended the standard library to include functions operating on long doubles.

<cfloat>(float.h)			
name	value	stands for	expresses
FLT_EPSILON DBL_EPSILON LDBL_EPSILON	1E-5 or smaller 1E-9 or smaller 1E-9 or smaller	EPSILON	Difference between 1 and the least value greater than 1 that is representable.
FLT_DIG DBL_DIG LDBL_DIG	6 or greater 10 or greater 10 or greater	DIGits	Number of decimal digits that can be rounded into a floating-point and back without change in the number of decimal digits.

Table 3.1 Machine epsilon defined in float.h

Unlike types `float` and `double`, Most C compilers implement `long double` as an 80-bit extended precision type supported by x86 hardware, the non-IEEE "double-double" (to maintain data structure alignment) or in IEEE 754 quadruple-precision floating-point format if a higher precision format is provided. Table (3.1) shows the C programming floating point specification (defined in float.h) the `long double` floating-point types' properties are no different from `double` thus making the default precision the same as `long double`. Machine epsilon (ε) is defined to be the smallest positive number which, when added to 1, gives a number different from 1. To achieve greater precision in calculations for lattice constants moving outside the realm of the standard C floating point data types is necessary.

3.1.2 Floating Point Precision & Rounding

To illustrate the difference in precision of floating point data types a single point sample calculation with reference to equation (2.3.10) for the lattice constant (L_n) in the simple cubic lattice located at $i = 12, j = 13, k = 14$ for $s = 5$ is shown below. The reference value was calculated using Wolfram Alpha to 500 decimal places:

$$\begin{aligned}\left(12^2+13^2+14^2\right)^{-5} = 2.&92692159097690550848261371131827933\\&11099995542447868485529782353147948\\&40009742013803964865724289227150881\\&11237240867270959344135283537519162\\&54981435616997300439022526413370340\\&6407102470...\times 10^{-14}.\end{aligned} \tag{3.1.3}$$

Results are shown below for the sample calculation in (3.1.3) using various C floating point data types; "**`float`**" (32-bit), "**`double`**" (64-bit) and "**`long double`**" (80 to 128-bit), "**`mpfr_t`**" precision = 128-bit (equivalent IEEE754 quadruple), "**`mpfr_t`**" 256-bit and "**`mpfr_t`**" 512-bit, with comparison to the real value (3.1.3).

Digits in pink show where precision deviates from the real value (3.1.3).

$$
\begin{aligned}
\text{C 32-bit} &= 2.926921\mathbf{6}\cdots\times 10^{-14}\\
\text{C 64-bit} &= 2.9269215909769054\cdots\times 10^{-14}\\
\text{C 128-bit} &= 2.9269215909769054\cdots\times 10^{-14}\\
\text{MPFR 256-bit} &= 2.92692159097690550848261371131827933110999955424478684855297823531479\\
&\quad 4840095\cdots\times 10^{-14}\\
\text{MPFR 512-bit} &= 2.92692159097690550848261371131827933110999955424478684855297823531479\\
&\quad 48400974201380396486572428922715088111237240867270959344135283537519\\
&\quad 16254981435616988\cdots\times 10^{-14}
\end{aligned}
$$

It can be seen that the C-single precision result deviates from the real value (3.1.3) at the 7^{th} digit after the decimal point. C-double precision loses accuracy 16 digits after the decimal point, C-(psudo)quadruple precision shows the same accuracy as C-double. "**`mpfr_t`**" 512-bit has the greatest (as expected) however it was determined that "**`mpfr_t`**" 256-bit would be used as the minimum precision used throughout the programs, an equivalent precision is $\log_{10} 2^{257} \approx 77.365$ decimal digits.

An Infinite Sum

The evaluation of lattice sums by direct summation and/or with use of some series expansions results in an infinite sum. From a computational perspective the problem can be understood by the simple example below. It is well known that

$$\sum_{k=1}^{\infty}\frac{1}{k^2}=\frac{\pi^2}{6}=1.644934066848\ldots$$

Suppose one was not aware of this identity and wished to approximate the sum numerically. The most obvious strategy is to evaluate the sum for increasing k until the computed sum does not change. In single precision this yields the value 1.64472532, which is first attained at $k = 4096$. This agrees with the exact infinite sum to just four significant digits out of a possible nine. The explanation for the poor accuracy is due to summing the numbers from largest to smallest, and the small numbers are unable to contribute to the sum. For $k = 4096$ constructs $s + 4096^{-2} = s + 2^{-24}$, where $s \approx 1.6$. Single precision corresponds to a 24-bit significand, so the term that is being adding to s "drops off the end" of the computer word, as do all successive terms. The simplest cure for this inaccuracy is to sum in the opposite order: from smallest to largest. Unfortunately, this requires knowledge of how many terms to take before the summation begins. Taking the first 100 terms, the difference between the computed sum and the exact sum can be estimated by an integral

$$\begin{aligned} |\text{exact - approximation}| &= \left[\sum_{k=1}^{\infty} \frac{1}{k^2}\right] - \left[\sum_{k=1}^{101} \frac{1}{k^2}\right] = \sum_{k=102}^{\infty} \frac{1}{k^2} \\ &\simeq \int_{102}^{\infty} \frac{1}{x^2}\, dx = \left[-\frac{1}{x}\right]_{102}^{\infty} = \frac{1}{102} \simeq 0.01\,. \end{aligned}$$

Summing over the first 100 values produces an error in the 2nd decimal place. To achieve high accuracy using direct summation proves to be hopeless as one would require an order of 10^{10} terms for an error of 10^{-10} which is impractical. When dealing with lattice sums that can be expressed as simple functions, in most cases there are tried and tested algorithms that can evaluate special functions to desirable precision with the use of arbitrary precision floating point libraries. In the case of sums that involve sums of Bessel function expansions, one can acheive the desired accuracy after less than 500 terms. The contribution of the terms containing Bessel functions to the total lattice sum is very low however. When using simple direct summation arbitrary floating point arithmetic is desirable but ultimately futile unless an extremely large value of bit precision is used and only suitable for sums involving large values of s.

3.2 Program Package Lattice Sums

To achieve an accuracy of greater than double precision floating point (≈ 15.955 decimal digits) in the calculation of the lattice sums for each crystal system, a suitable arbitrary-precision arithmetic software library had to be chosen based on its compatibility with the C-programming language, which was the language of choice for programs to be written in, and to be

compatible with the compiler/design suite used to create and debug the program. A program "lattice sums" was written in the programming language C++ for the evaluation of lattice constants to arbitrary precision using the numerical libraries MPFR and Arb which is a C library for rigorous real and complex arithmetic with arbitrary precision [102]. Arb tracks numerical errors automatically using ball arithmetic, a form of interval arithmetic based on a midpoint-radius representation. The functionality that Arb provides is extensive and makes it a great bolt on candidate for a software library, it includes polynomials, power series, matrices, integration, root-finding, and many transcendental functions.

Part II

Methods

4 Mathematical Methods

4.1 Methods for the Evaluation of Lattice Sums

In this chapter methods for the fast evaluation of lattice sums are briefly discussed based on some of the theory described in Part I. The easiest method to be applied is using symmetry within the lattice to reduce the summation to a smaller section of the lattice and to achieve faster convergence. Lennard-Jones in his 1925 paper used direct summation for the cubic lattices except for small exponents $s \in \mathbb{N}$ where convergence becomes problematic [6]. However, using symmetry still results in a sum that may converge rather slowly, and it is evident that this method is futile if one requires high precision for low values of the exponent s. Direct summation is explored in Section 4.2.

Throughout the treatment of lattice sums a procedure to express lattice sums in terms of fast converging functions or expressed as a product of simple sums is advantageous. Number theoretical techniques are employed in an effort to express lattice sums as sums of simple functions, e.g., as sums of simple zeta and Bessel functions. One then looks to express a lattice sum as sums over modified Bessel functions of the second kind or in terms of theta functions of argument $q = e^{-t}$ that can be re-expressed by other simple functions [26, 61]. The method in both cases follows a similar route, firstly the sum is written as a Mellin transform, then the modular transformation for theta functions is applied to the transformed sum, or it is written as a q-series. The sum then is re-written taking into account particular cases of the summation index and expressed in the form of Hobson's integral to obtain a series of fast converging Bessel functions or simple functions. In the sections below, various methods are shown for the treatment of lattice sums. Many of which are used throughout this work and given in the results section of this thesis.

4.2 Direct Lattice Summation using Symmetry

Lennard-Jones used direct summation of the lattice sums L_s of cubic lattices except for small exponents $s \in \mathbb{N}$ [6]. However, restricting the sums to $i, j, k \leq N_{\max}$ the computational effort scales $O(N_{\max}^3)$ and yield accuracy proportional to $\frac{1}{N^{s-3}}$ with N^3 terms. In this section symmetry from the origin in $\mathbb{Z}^3$ space within the lattice is utilized to save computational effort and time.

While this ultimately does not change the overall scaling law, it reduces the prefactor substantially, and makes the sums computationally more attractive for larger exponents of $s \geq 8$. For example, Stein introduced a parallel algorithm and exploited the symmetry by partitioning the crystal into octants of $\mathbb{Z}^3$ [99].

The importance of the simple cubic lattice sum lies in the fact it is the most efficient to evaluate. It is therefore advantageous to evaluate the simple cubic sub-lattice first for the later treatment of other lattices. A partitioning of the bcc and fcc lattice points in the summations was already explored by Lennard-Jones, and it is one of the techniques we used to reduce the complexity of the bcc and fcc lattice sums as shown below.[22] For direct summations, it is convenient to choose expressions for the lattice sum with the symmetric matrix S of the quadratic form $\vec{i}^{\top}\mathbf{A}\vec{i}$ $(\vec{i} \in \mathbb{Z}^3)$ being diagonal, as the resulting double sums can all be expressed in terms of well-known Hurwitz zeta functions. For the following lattice sums, a table of results for the exponent $s \in \mathbb{R}, s > {}^3/_2$, is show in Table A.4 in the Appendix. Some related notation to the decompositons seen in sections below is introduced.

The Hurwitz zeta function is defined for $s > 1$ by

$$\zeta(s,x) = \sum_{i=0}^{\infty} (i+x)^{-s} . \tag{4.2.1}$$

The Hurwitz zeta function is a generalization of the Riemann ζ-function with $\zeta(s,1) = \zeta(s)$ and used extensively in this work. For the following it is convenient to define the linear combination of Hurwitz zeta functions by

$$\zeta(s;c_1,\ldots,c_n;d_1,\ldots,d_m) = \sum_{i=1}^{n} \zeta(s,c_i) - \sum_{i=1}^{m} \zeta(s,d_i) . \tag{4.2.2}$$

In this notation $\zeta(s) = \zeta(s;1;-)$ and $\zeta(s,x) = \zeta(s;x;-)$, where a dash indicates an empty parameter list and the last semicolon may be removed if no values are provided. A simple example is the Dirichlet beta function given by

$$\beta(s) = \sum_{i=0}^{\infty} (-1)^i (2i+1)^{-s}, \tag{4.2.3}$$

with $\lim_{s\to\infty} \beta(s) = 1$. Which can be expressed in terms of the Hurwitz zeta functions by

$$\begin{aligned}\beta(s) &= \frac{1}{1^s} - \frac{1}{3^s} + \frac{1}{5^s} - \dots \\ &= \left(\frac{1}{1^s} + \frac{1}{5^s} + \frac{1}{9^s} + \dots\right) - \left(\frac{1}{3^s} + \frac{1}{7^s} + \frac{1}{11^s} + \dots\right) \\ &= \frac{1}{4^s}\left(\frac{1}{(\frac{1}{4})^s} + \frac{1}{(\frac{5}{4})^s} + \frac{1}{(\frac{9}{4})^s} + \dots\right) - \left(\frac{1}{(\frac{3}{4})^s} + \frac{1}{(\frac{7}{4})^s} + \frac{1}{(\frac{11}{4})^s} + \dots\right) \\ &= \frac{1}{4^s}\left(\zeta(s,\tfrac{1}{4}) - \zeta(s,\tfrac{3}{4})\right) \\ &= 4^{-s}\zeta\left(s;\tfrac{1}{4}\,;\,\tfrac{3}{4}\right). \end{aligned} \tag{4.2.4}$$

4.2.1 Simple cubic lattice

The most straight forward way to use symmetry within the simple cubic lattice is to separate the three-dimensional space into octants (factor of 8) and each octant into 6 sectors giving equal contributions due to the symmetry within each octant, this equates to a factor of 48 in the triple sum. One can then take the two-dimensional planes in the lattice when $i = 0$ or $j = 0$ or $k = 0$ and separate these into double sums. The cases where $i = j$, $j = k$ or $i = k$, these become single sums for which the Riemann zeta function $\zeta(s)$ defined by (2.2.4) with $\lim_{s\to\infty}\zeta(s) = 1$ is used. The resulting equation for the simple cublic lattice sum is given by

$$\begin{aligned}L_s^{\mathrm{sc}} = {\sum_{i,j,k\in\mathbb{Z}}}' \left(i^2+j^2+k^2\right)^{-s} &= -\left(9+6\times 2^{-s}+8\times 3^{-s}\right){\sum_{i\in\mathbb{Z}}}' i^{-s} \\ &+ 3{\sum_{i,j\in\mathbb{Z}}}' \left(i^2+j^2\right)^{-s} + 6{\sum_{i,j\in\mathbb{Z}}}' \left(2i^2+j^2\right)^{-s} + 48\sum_{1\le i<j<k} \left(i^2+j^2+k^2\right)^{-s}. \end{aligned} \tag{4.2.5}$$

The first double sum in (4.2.5) can be expressed as a product of the Dirichlet beta and Riemann zeta functions known as the Lorenz–Hardy-sum,[103, 104]

$${\sum_{i,j\in\mathbb{Z}}}' \left(i^2+j^2\right)^{-s} = 4\beta(s)\zeta(s), \tag{4.2.6}$$

with the Dirichlet beta function given by (4.2.3). Finally, the second double sum has been evaluated by Zucker,[105]

$$Z_1(s) = {\sum_{i,j\in\mathbb{Z}}}' \left(2i^2+j^2\right)^{-s} = 2^{-3s+1}\zeta(s)\zeta\left(s;\tfrac{1}{8},\tfrac{3}{8}\,;\,\tfrac{5}{8},\tfrac{7}{8}\right), \tag{4.2.7}$$

with

$$\zeta\left(s;\tfrac{1}{8},\tfrac{3}{8}\,;\,\tfrac{5}{8},\tfrac{7}{8}\right)=\zeta\left(s,\tfrac{1}{8}\right)+\zeta\left(s,\tfrac{3}{8}\right)-\zeta\left(s,\tfrac{5}{8}\right)-\zeta\left(s,\tfrac{7}{8}\right). \tag{4.2.8}$$

We obtain the lattice sum for simple cubic as

$$\begin{aligned}L_s^{\mathrm{sc}}=12\zeta(s)\beta(s)-2\left(9+6\times 2^{-s}+8\times 3^{-s}\right)\zeta(s)\\ +6Z_1(s)+48\sum_{1\le i<j<k}\left(i^2+j^2+k^2\right)^{-s},\end{aligned} \tag{4.2.9}$$

reducing the summation to the octant of positive values. The standard Riemann zeta, Hurwitz zeta and Dirichlet beta functions can easily be evaluated to computer precision by using the Euler-Maclaurin summation formula.[106] Even though there is a saving by a factor of 48 in computer time for the remaining triple sum, the sum remains slowly converging for small values of s. Restricting the summation to $(i^2+j^2+k^2)\le N_{\max}^2$ and choosing $N_{\max}$ sufficiently large, this direct summation technique is accurate and fast enough for evaluation of lattice sums for exponents $s\ge 8$. For $s=8$ ($s=7$) with $N_{\max}=1500$ (3000), the sum is accurate to within 10^{-14}. Here the triple sum contributes only to 0.028% (0.115%) to the total value.

4.2.2 Body centered cubic lattice

The bcc lattice is described by the formula below, similar to (2.3.11), which separates the sum into sublattices [22]

$$L_s^{\mathrm{bcc}}=\left(\frac{3}{4}\right)^s L_s^{\mathrm{sc}}+3^s\sum_{i,j,k\in\mathbb{Z}}\left[(2i+1)^2+(2j+1)^2+(2k+1)^2\right]^{-s}. \tag{4.2.10}$$

Using symmetry between positive and negative integers we obtain,

$$L_s^{\mathrm{bcc}}=\left(\frac{3}{4}\right)^s L_s^{\mathrm{sc}}+8\times 3^s\sum_{i,j,k\in\mathbb{N}}\left\{(2i-1)^2+(2j-1)^2+(2k-1)^2\right\}^{-s}. \tag{4.2.11}$$

Separating out the cases for $i=j$, $i=k$ and $j=k$ we arrive at

$$L_s^{\mathrm{bcc}} = \left(\frac{3}{4}\right)^s L_s^{\mathrm{sc}} - 2^{-s+4}\zeta\left(s,\tfrac{1}{2}\right) + 24\times 3^s \sum_{i,j\in\mathbb{N}} \left\{2(2i-1)^2+(2j-1)^2\right\}^{-s} + 16\times 3^{s+1} \sum_{1\le i<j<k} \left\{(2i-1)^2+(2j-1)^2+(2k-1)^2\right\}^{-s}. \tag{4.2.12}$$

Using the Hurwitz zeta function with argument $\frac{1}{2}$ we have the relation to the Riemann zeta function,

$$\zeta\left(s,\tfrac{1}{2}\right) = (2^s-1)\,\zeta(s). \tag{4.2.13}$$

The double sum appearing in (4.2.12) can be reformulated (as shown in 4.2),

$$\sum_{i,j\in\mathbb{N}} \left\{2(2i-1)^2+(2j-1)^2\right\}^{-s} = \tfrac{1}{4}\left(1-2^{-s}+2^{-s}\right)Z_1(s) - \tfrac{1}{4}Z_3(s), \tag{4.2.14}$$

with the factor of $\frac{1}{4}$ coming from the fact that we only sum over natural numbers on the left hand side. Zucker's sum Z_1 has been defined in (4.2.7) and Z_3 is defined by

$$Z_3(s) = 2^{-3s}\left[\left(1-2^{-s}+2^{1-2s}\right)\zeta(s)\zeta\left(s;\tfrac{1}{8},\tfrac{3}{8};\tfrac{5}{8},\tfrac{7}{8}\right) + \beta(s)\zeta\left(s;\tfrac{1}{8},\tfrac{7}{8};\tfrac{3}{8},\tfrac{5}{8}\right)\right], \tag{4.2.15}$$

using decompositions methods outlined in Section 6 Appendix B and the compact notation for sums of Hurwitz zeta functions given by (4.2.2). Taking all terms together including (4.2.9), we obtain

$$\begin{aligned} L_s^{\mathrm{bcc}} = {} & 3^{s+1}\,2^{-s+2}\beta(s)\zeta(s) - \left(16+3^{s+2}\,2^{1-s}+3^{s+1}\,2^{-3s+2}\right)\zeta(s) \\ & + 3^{s+1}\,2^{-3s+1}\left[\left(1-2^{-s}+2^{1-s}\right)\zeta(s)\zeta\left(s;\tfrac{1}{8},\tfrac{3}{8}\,;\,\tfrac{5}{8},\tfrac{7}{8}\right)\right. \\ & \left. -\beta(s)\zeta\left(s;\tfrac{1}{8},\tfrac{7}{8};\tfrac{3}{8},\tfrac{5}{8}\right)\right] \\ & + 3^{s+1}\,2^{-s+4} \sum_{\substack{1\le i<j<k \\ m\in\{0,1\}}} \left\{\left(i-\tfrac{m}{2}\right)^2+\left(j-\tfrac{m}{2}\right)^2+\left(k-\tfrac{m}{2}\right)^2\right\}^{-s}. \end{aligned} \tag{4.2.16}$$

4.2.3 Face centered cubic lattice

For the face centered cubic lattice a decomposition is started from splitting the lattice sum in in sub-lattices (as described above). A note here is that (2.3.12) is not taken as it leads to difficulties. Instead we take the most symmetric

formula with respect to the three summation indices alternating sum given by Zucker, [61]

$$\begin{aligned} L_s^{\mathrm{fcc}} &= 2^{s-1} {\sum_{i,j,k\in\mathbb{Z}}}' \left[1+(-1)^{i+j+k}\right] \left(i^2+j^2+k^2\right)^{-s} \\ &= 2^{s-1} L_s^{\mathrm{sc}} + 2^{s-1} {\sum_{i,j,k\in\mathbb{Z}}}' (-1)^{i+j+k} \left(i^2+j^2+k^2\right)^{-s} . \end{aligned} \tag{4.2.17}$$

In analogy to the sc case, we start with the case $i=0$, $j=0$ or $k=0$ and get

$$\begin{aligned} L_s^{\mathrm{fcc}} = 2^{s-1} L_s^{\mathrm{sc}} - 3\times 2^{s-1} {\sum_{i\in\mathbb{Z}}}' (-1)^i i^{-s} + 3\times 2^{s-1} {\sum_{i,j\in\mathbb{Z}}}' (-1)^{i+j} \left(i^2+j^2\right)^{-s} \\ + 2^{s+2} \sum_{i,j,k\in\mathbb{N}} (-1)^{i+j+k} \left(i^2+j^2+k^2\right)^{-s} . \end{aligned} \tag{4.2.18}$$

The single sum represents the Dirichlet eta function $\eta(s)$ which can be rewritten in terms of the Riemann zeta function,

$$\eta(s) = \sum_{i=1}^{\infty} (-1)^{i-1} i^{-s} = \left(1-2^{1-s}\right) \zeta(s) . \tag{4.2.19}$$

The double sum in (4.2.18) has been evaluated by Zucker in 1974,[107]

$$Z_2(s) = {\sum_{i,j\in\mathbb{Z}}}' (-1)^{i+j} \left(i^2+j^2\right)^{-s} = -4\beta(s)\eta(s) , \tag{4.2.20}$$

Therefore obtaining

$$\begin{aligned} L_s^{\mathrm{fcc}} = 2^{s-1} L_s^{\mathrm{sc}} - 3\times 2^{s+1} \left(1-2^{1-s}\right) \beta(s)\zeta(s) + 3\times 2^s \left(1-2^{1-s}\right) \zeta(s) \\ + 2^{s+2} \sum_{i,j,k\in\mathbb{N}} (-1)^{i+j+k} \left(i^2+j^2+k^2\right)^{-s} . \end{aligned} \tag{4.2.21}$$

The triple sum is decomposed further as we did for the simple cubic case by taking the diagonal sums with $i=j$ or $j=k$ or $i=k$ out,

$$\begin{aligned} L_s^{\mathrm{fcc}} = 2^{s-1} L_s^{\mathrm{sc}} - 3\times 2^{s+1} \left(1-2^{1-s}\right) \beta(s)\zeta(s) \\ + \left(3\times 2^s + 3^{-s} 2^{s+3}\right) \left(1-2^{1-s}\right) \zeta(s) \\ + 3\times 2^{s+2} \sum_{i,j\in\mathbb{N}} (-1)^j \left(2i^2+j^2\right)^{-s} \\ + 3\times 2^{s+3} \sum_{1\le i<j<k} (-1)^{i+j+k} \left(i^2+j^2+k^2\right)^{-s} . \end{aligned} \tag{4.2.22}$$

The double sum in (4.2.22) has been decomposed in terms of Dirichlet L-series

and shown in Section 6 Appendix B, [105]

$$\begin{aligned}
&\sum_{i,j\in\mathbb{Z}}{}' (-1)^j \left(2i^2+j^2\right)^{-s} = \sum_{\substack{i,j\in\mathbb{Z}\\ j \text{ even}}}{}' \left(2i^2+j^2\right)^{-s} - \sum_{\substack{i,j\in\mathbb{Z}\\ j \text{ odd}}} \left(2i^2+j^2\right)^{-s} \\
&= 2\sum_{\substack{i,j\in\mathbb{Z}\\ j \text{ even}}}{}' \left(2i^2+j^2\right)^{-s} - \sum_{i,j\in\mathbb{Z}}{}' \left(2i^2+j^2\right)^{-s} = 2\sum_{i,j\in\mathbb{Z}}{}' \left(2i^2+(2j)^2\right)^{-s} - Z_1(s) \\
&= \left(2^{1-s}-1\right) Z_1(s)\,.
\end{aligned} \tag{4.2.23}$$

Taking all terms together we obtain a formula similar in nature to the simple cubic case,

$$\begin{aligned}
L_s^{\text{fcc}} &= 12\beta(s)\zeta(s) - 2\left(6+9\times 2^{-s}+3^{-s}2^{-s+3}\right)\zeta(n) + 6Z_1(s) \\
&\quad + 3\times 2^{s+3} \sum_{1\le i<j<k} \left[1+(-1)^{i+j+k}\right] \left(i^2+j^2+k^2\right)^{-s}\,.
\end{aligned} \tag{4.2.24}$$

4.2.4 The Hexagonal Close-Packed Structure

The hexagonal close-packed structure contains two atoms in its primitive unit cell. The first lattice sum used for the hcp structure by Kane and Goeppert-Meyer treated the sub-lattices corresponding to these two atoms separately, unfortunately the lattice sum was never given in their publication. However a lattice sum for hcp with an inhomogeneous quadratic form is shown by [24]

$$L_s^{hcp} = \sum_{i,j,k\in\mathbb{Z}}{}' \left(S_{ijk}^{hex}\right)^{-s} + \sum_{i,j,k\in\mathbb{Z}} \left(S_{ijk}^{\text{B}}\right)^{-s} \tag{4.2.25}$$

with

$$S_{ijk}^{hex} = i^2+j^2+ij+\tfrac{c^2}{a^2}k^2 \tag{4.2.26}$$

and

$$\begin{aligned}
S_{ijk}^{\text{B}} &= \left(i+\tfrac{1}{3}\right)^2 + \left(j+\tfrac{1}{3}\right)^2 + \left(i+\tfrac{1}{3}\right)\left(j+\tfrac{1}{3}\right) + \tfrac{c^2}{a^2}\left(k+\tfrac{1}{2}\right)^2 \\
&= i(i+1)+j(j+1)+ij+\tfrac{c^2}{a^2}k(k+1)+1.
\end{aligned} \tag{4.2.27}$$

With the hcp lattice parameters c and a being set to $\frac{c}{a} = \sqrt{\frac{8}{3}} = \alpha$. For the direct summation we consider the general quadratic form in the sum appearing in (4.2.26), reduce the summation again to the positive integers by consideration of $i=0$, $j=0$ or $k=0$, and have a change in variable for the lattice parameter

γ to α, the sum for the hexagonal lattice then becomes

$$\begin{aligned}\sum_{i,j,k\in\mathbb{Z}}{}' \left[S_{ijk}^{\text{hex}}(\alpha)\right]^{-s} &= \sum_{i,j,k\in\mathbb{Z}}{}' (i^2+j^2+ij+\alpha k^2)^{-s} \\ &= 4\sum_{\substack{i,j,k\in\mathbb{N}\\ m\in\{-1,1\}}} (i^2+j^2+mij+\alpha k^2)^{-s} + \sum_{i,j\in\mathbb{Z}}{}' (i^2+j^2+ij)^{-s} \\ &\quad + 2\sum_{i,k\in\mathbb{Z}}{}' (i^2+\alpha k^2)^{-s} - 2\left(2+\alpha^{-s}\right)\zeta(s)\,.\end{aligned} \tag{4.2.28}$$

The first double sum has been treated by Fletcher et al.[108] and later by Zucker [105]

$$\sum_{i,j\in\mathbb{Z}}{}' (i^2+j^2+ij)^{-s} = 3^{1-s}2\zeta(s)\zeta(s;\tfrac{1}{3}\,;\,\tfrac{2}{3})\,. \tag{4.2.29}$$

If we use permutation symmetry between the two indices i and j we finally get

$$\begin{aligned}\sum_{i,j,k\in\mathbb{Z}}{}' \left[S_{ijk}^{\text{hex}}(\alpha)\right]^{-s} &= 8\sum_{\substack{i,j,k\in\mathbb{N},i<j\\ m\in\{-1,1\}}} (i^2+j^2+mij+\alpha k^2)^{-s} + 2\times 3^{1-s}\zeta(s)\zeta(s;\tfrac{1}{3}\,;\,\tfrac{2}{3}) \\ &\quad + 2S_2(s,\alpha) + 4\sum_{i,k\in\mathbb{N}} \left(i^2+\alpha k^2\right)^{-s} + 4\sum_{i,k\in\mathbb{N}} \left(3i^2+\alpha k^2\right)^{-s} - 2\left(2+\alpha^{-s}\right)\zeta(s) \\ &= 8\sum_{\substack{1\le i<j,k\in\mathbb{N}\\ m\in\{-1,1\}}} (i^2+j^2+mij+\alpha k^2)^{-s} + 2\times 3^{1-s}\zeta(s)\zeta(s;\tfrac{1}{3}\,;\,\tfrac{2}{3}) \\ &\quad + 3S_2(s,\alpha) + 3^{-s}S_2(s,\tfrac{\alpha}{3}) - 6\left(1+3^{-s-1}+\alpha^{-s}\right)\zeta(s)\,.\end{aligned} \tag{4.2.30}$$

The remaining double sum of the form

$$S_2(s,\alpha) = \sum_{i,j\in\mathbb{Z}}{}' \left(i^2+\alpha j^2\right)^{-s} \tag{4.2.31}$$

is left to be evaluated, for which there are six different values of $\alpha = \left\{2, 8, {}^8\!/_3, {}^2\!/_3, {}^8\!/_9, {}^2\!/_9\right\}$. $S_2(s,2) = Z_1(s)$ is defined by (4.2.7). The sum with $\alpha = \frac{2}{3}$ has been evaluated by Zucker as,[105]

$$\begin{aligned}S_2(s,\tfrac{2}{3}) &= 3^s \sum_{i,j\in\mathbb{Z}}{}' (3i^2+2j^2)^{-s} \\ &= 2^{-3s}\left[\zeta(s)\zeta(s;\tfrac{1}{24},\tfrac{5}{24},\tfrac{7}{24},\tfrac{11}{24}\,;\,\tfrac{13}{24},\tfrac{17}{24},\tfrac{19}{24},\tfrac{23}{24})\right. \\ &\quad \left. - \zeta(s;\tfrac{1}{8},\tfrac{7}{8}\,;\,\tfrac{3}{8},\tfrac{5}{8})\zeta(s;\tfrac{1}{3}\,;\,\tfrac{2}{3})\right]\,.\end{aligned} \tag{4.2.32}$$

This leaves three double sums $S_2(s,\frac{2}{9}), S_2(s,\frac{8}{9})$ and $S_2(s,\frac{8}{3})$ in (4.2.30) that needed to be analyzed in this thesis. For this a decomposition in terms of

Hurwitz zeta functions and a method outlined in Sections 4.3.1 and 4.3.2 is used along with the results of Chan and Toh.[109] As the results for these double sums are rather lengthy, Section 6.11 should be seen for the expression in terms of Hurwitz zeta functions. The complete expression for the hcp lattice sum with the coefficients a_i and α_i defined in (2.4.10) is then given by,

$$L_s^{\text{hex}} = \sum_{n\in\{1,2,3,4\}} a_n \Bigg\{ 8 \sum_{\substack{i,j,k\in\mathbb{N}, i<j \\ m\in\{-1,1\}}} (i^2+j^2+mij+\alpha_n k^2)^{-s} + 3S_2(s,\alpha_n) + 3^{-s} S_2(s,\tfrac{\alpha_n}{3}) \Bigg\} + 2\times 3^{1-s}\zeta(s)[\zeta(s;\tfrac{1}{3}\,;\,\tfrac{2}{3}) - 6\left[1+3^{-s-1}+\left(\frac{3}{8}\right)^s\right]\zeta(s)\,. \tag{4.2.33}$$

The evaluation of L_s^{B} is complicated by the homogeneity parameter for which we turn to the Terras or van der Hoff–Benson method, as can be seen in Project 1. Overall the hcp formula above requires more time to evaluate and alternative methods are explored in the following sections of this chapter, these are shown in detail in Section 6. A alternate method of evaluating the hcp lattice without using direct summation is the subject to Project 7.

4.3 Theta Function and Bessel Function Method

In this section two worked examples are shown. In the first example, a simple sum is written as a q-series which then is rewritten in terms of as simple functions that can be evaluated exactly. Secondly, the three dimensional simple cubic lattice sum is expressed as a combination of simple functions and a sum of Bessel sums in Section 4.3.2. The general procedure makes use of an integral transformation such as the Mellin transformation defined in (2.2.10) and the integral representation of the gamma function. The resulting expression for the overall lattice sum is broken up into sums which are able to be evaluated by Hobson's integral and thus written in terms of fast converging Bessel functions. Where possible the factor in each sum is written using Dirichlet's sum of squares theorem to reduce the computational effort.

4.3.1 Theta function method via Mellin transformation

As a basic example, let us now consider the double sum

$$S(s) = {\sum_{m,n\in\mathbb{Z}}}' \left(am^2+bn^2\right)^{-s}, \tag{4.3.1}$$

where the sum is over all integer values of m and n with the term $(m,n) = (0,0)$ omitted. Using the definition of the Mellin transform in (2.2.10) and the prototype from (2.2.11) with the function $f(t) = e^{-(am^2+bn^2)t}$ we obtain

$$\begin{aligned} S(s) &= {\sum_{m,n\in\mathbb{Z}}}' \frac{1}{\Gamma(s)} \int_0^\infty t^{s-1} e^{-(am^2+bn^2)t}\, dt \\ &= \frac{1}{\Gamma(s)} \int_0^\infty t^{s-1} {\sum_{m,n\in\mathbb{Z}}}' e^{-(am^2+bn^2)t}\, dt\,. \end{aligned} \tag{4.3.2}$$

Consider the sum in (4.3.2), and set $q = e^{-u}$. For many values of a and b the theta series can be written in the form

$${\sum_{m,n\in\mathbb{Z}}}' q^{am^2+bn^2} = \sum_{k,n\in\mathbb{N}} f_1(k)\, f_2(n)\, q^{kn} \tag{4.3.3}$$

for some functions $f_1(k)$ and $f_2(n)$. Using (4.3.3) in (4.3.2) we deduce

$$\begin{aligned} S(s) &= \frac{1}{\Gamma(s)} \int_0^\infty t^{s-1} \sum_{k,n\in\mathbb{N}} f_1(k)\, f_2(n)\, e^{-knt}\, dt \\ &= \sum_{m,n\in\mathbb{N}} \frac{f_1(k)\, f_2(n)}{(kn)^s} = \left(\sum_{k=1}^{\infty} \frac{f_1(k)}{k^s} \right) \left(\sum_{n=1}^{\infty} \frac{f_2(n)}{n^s} \right). \end{aligned} \tag{4.3.4}$$

For example when $a = b = 1$ for (4.3.3) we have by Jacobi's sum of two squares theorem [Ref.[78], p.177]

$${\sum_{m,n\in\mathbb{Z}}}' q^{m^2+n^2} = 4 \sum_{k,n\in\mathbb{N}} \sin\frac{\pi n}{2}\, q^{kn}\,, \tag{4.3.5}$$

and so $f_1(k) = 1$ and $f_2(n) = 4\sin\frac{\pi n}{2}$. It follows that

$${\sum_{m,n\in\mathbb{Z}}}' \left(m^2+n^2\right)^{-s} = 4 \left(\sum_{k\in\mathbb{N}} \frac{1}{k^s} \right) \left(\sum_{n\in\mathbb{N}} \frac{\sin\frac{\pi n}{2}}{n^s} \right) \quad = 4\,\zeta(s)\,\beta(s)\,, \tag{4.3.6}$$

which was mentioned in (4.2.6). For other values of a and b, formulas of the type (4.3.3) can be found in the literature.[107]

4.3.2 Application of the integral transformation to Bessel function

In this section a the three dimensional lattice sum for the simple cubic lattice $L_3^{\mathrm{SC}}(s)$ is expressed as sums of fast converging Bessel functions. This method is used extensively throughout the published work in the following sections and particularly in Section 5 where N-dimensional lattice sums are investigated. We start from the lattice sum for a simple cubic is defined by

$$L_3^{\mathrm{SC}}(s) = {\sum_{i,j,k}}' \frac{1}{(i^2+j^2+k^2)^s} \tag{4.3.7}$$

where the summation is over all integer values of i, j, k, and the prime on the summation sign denotes that the term corresponding to $i = j = k = 0$ is omitted. The series converges for $s > 3/2$.

Following the method outlined in Section 5.1, the expression in (4.3.7) is separated into the sum over i and j and a sum over k

$$L_3^{\mathrm{SC}}(s) = \left(\sum_{k=1}^{\infty} \frac{1}{(k^2)^s}\right)\left(\sum_{i,j}^{\infty} \frac{1}{(i^2+j^2)^s}\right). \tag{4.3.8}$$

By way of (2.2.6) in a similar fashion, the Mellin transformation of (4.3.8) results in

$$L_3^{\mathrm{SC}}(s) = \frac{\pi^s}{\Gamma(s)} \int_0^{\infty} t^{s-1} \left(\sum_{k=1}^{\infty} e^{-\pi k^2 t}\right)\left(\sum_{i,j=-\infty}^{\infty} e^{-\pi(i^2+j^2)t}\right) \mathrm{d}t\,. \tag{4.3.9}$$

By using the modular transformation of theta functions, the sum can be rewritten as

$$L_3^{\mathrm{SC}}(s) = \frac{\sqrt{\pi}}{\Gamma(s)} \int_0^{\infty} t^{s-1} \left(\sum_{k=1}^{\infty} e^{-\pi k^2 t}\right)\left(\frac{1}{\sqrt{t}} \sum_{i,j=-\infty}^{\infty} e^{-\pi(i^2+j^2)/t}\right) \mathrm{d}t\,. \tag{4.3.10}$$

Using the gamma function relation in (2.2.6) and a special case of Jacobi's imaginary transformation for theta function defined by

$$\sum_{p=-\infty}^{\infty} e^{-pt} = \left(\frac{\pi}{t}\right)^{1/2} \sum_{q=-\infty}^{\infty} e^{-q^2\pi/t}\,. \tag{4.3.11}$$

The first sum in (4.3.10) is the Riemann zeta function and the integral can be evaluated by the integral representation of the gamma function and expressed in terms of the modified Bessel function $K_\nu(x)$ by using the formula, e.g., [79] or [110],

$$\int_0^{\infty} t^{\nu-1} e^{-at-b/t} dt = 2\left(\frac{b}{a}\right)^{\nu/2} K_\nu(2\sqrt{ab})\,, \tag{4.3.12}$$

which is valid for Re (p) and Re $(q) > 0$. Thus (4.3.10) can be rewritten as,

$$L_3^{\mathrm{SC}}(s) = \zeta(2s) + \sqrt{\pi}\frac{\Gamma(s-\frac{1}{2})}{\Gamma(s)} \sum_{i,j=-\infty}^{\infty}{}' \left(i^2+j^2\right)^{-s} \tag{4.3.13}$$
$$+ \frac{4\pi^s}{\Gamma(s)} \sum_{k=1}^{\infty} \sum_{i,j=-\infty}^{\infty}{}' \left(\frac{k}{\sqrt{i^2+j^2}}\right)^{s-\frac{1}{2}} K_{s-\frac{1}{2}}\left(2\pi k\sqrt{i^2+j^2}\right).$$

The first double sum can be evaluated by (4.3.6). The factor in front of the Bessel function can be be re-expressed as the number of representations of the sum of two squares. That is, the terms are being sorted according to the value of i^2+j^2, with the number of such terms being equal to the number of solutions in integers to

$$m = i^2 + j^2,$$

which is given as $r_2(m)$, see Section 2.6 for more details. Therefore the lattice sum for a simple cubic lattice in three dimensions is

$$L_3^{\mathrm{SC}}(s) = \zeta(2s) + \sqrt{\pi}\frac{\Gamma(s-\frac{1}{2})}{\Gamma(s)} 4\zeta(s)\beta(s) \tag{4.3.14}$$
$$+ \frac{4\pi^s}{\Gamma(s)} \sum_{k=1}^{\infty} \sum_{m=1}^{\infty} r_2(m) \left(\frac{k}{\sqrt{m}}\right)^{s-\frac{1}{2}} K_{s-\frac{1}{2}}\left(2\pi k\sqrt{m}\right).$$

4.4 van der Hoff–Benson Expansion

Van der Hoff and Benson derived a number of interesting expansions for lattice sums that are very useful for the lattices considered here.[111] Here a more general expansion than that presented in the original paper is presented

$$\sum_{i\in\mathbb{Z}} \left[(i+a)^2+x^2\right]^{-s} = \pi^{\frac{1}{2}} \frac{\Gamma\left(s-\frac{1}{2}\right)}{\Gamma(s)} |x|^{1-2s}$$
$$+ 4\pi^s \Gamma(s)^{-1} \sum_{m\in\mathbb{N}} \left(\frac{m}{|x|}\right)^{s-\frac{1}{2}} \cos(2\pi m a)\, K_{s-\frac{1}{2}}\left(2\pi m|x|\right), \tag{4.4.1}$$

with $a \in [0,1)$. The expansion does not reduce the number of summations for the triple sums we are seeking, but the expression on the right hand side contains a series of fast converging Bessel sums. What is useful about this expansion, is that it can be used not only for the cubic lattices but also for the hcp structure. The Van der Hoff–Benson expansion is computationally as efficient as the one used for the Terras decomposition of the Epstein zeta function.[112]

4.5 Terras Decomposition

Emersleben [20, 113–116] and later Lennard-Jones and Ingham[6] pointed out that the sums over the inverse powers of the S_{ijk} terms are special cases of Epstein's generalized zeta functions defined in (2.2.3) [117]. The N-dimensional generalized Epstein zeta function $Z(A_N, c)$ containing an inhomogeneity is defined by

$$Z_{A_N}(c;\vec{u},\vec{v}) = {\sum_{\vec{z}\in\mathbb{Z}^N}}' e^{2\pi i\vec{u}\cdot(A_N\vec{z})} \left|A_N\vec{z}-\vec{v}\right|^{-c}, \tag{4.5.1}$$

with $c \in \mathbb{C}$, $\vec{u},\vec{v} \in \mathbb{R}^N$, N is the dimension, and A_N is a $N \times N$ real positive definite matrix. If $\vec{v} = 0$ or $\vec{v} =$ a lattice point in (4.5.1) then the prime means the term $\vec{z} = \vec{0}$ is ommited from the sums, otherwise sum over all $\vec{z}$. The relation between the generalized Epstein zeta function and our lattice sums is,

$${\sum_{i,j,k\in\mathbb{Z}}}' S_{ijk}^{-s} = Z_{A_3}(s;\vec{0}_3,\vec{0}_3), \tag{4.5.2}$$

where $\vec{0}_3$ is the zero vector in 3D-space and the inhomogeneity parameter $\vec{v}$ in (4.5.1) is zero. For the smallest integer exponent $s = 2$, Lennard-Jones used an expansion of the Epstein function in terms of Bessel functions for the cubic lattices. In fact, for quadratic forms where $\vec{v} = \vec{0}$ the Epstein zeta function can be reduced successively in dimension down to the remaining Riemann zeta function $\zeta(x)$ of dimension N=1. A detailed description with all the required proofs can be found in Terras' seminal paper or in Project 1 [112]. In order to achieve the reduction in dimension for the cubic lattices the expression for a quadratic form is used,

$$\left|A_N\vec{z}\right|^2 = \vec{z}^{\top}\left(A_N^{\top}A_N\right)\vec{z} = \vec{z}^{\top}S_N\vec{z} \quad \text{with} \quad S_N = A_N^{\top}A_N, \tag{4.5.3}$$

where S_N is an $N \times N$ positive definite and symmetric matrix according to (4.5.3). In fact, for lattice sums S_N is the Gram matrix and A the generator matrix consisting of the lattice vectors in N-dimensional space.

The expansion method introduced by Terras is briefly outlined using the following relation for dimension N=3,[112]

$$Z_{S_3}(s) = \frac{1}{2}Z_{A_3}(2s;\vec{0}_3,\vec{0}_3) = \frac{1}{2}{\sum_{\vec{k}\in\mathbb{Z}^3}}' \left(\vec{k}^{\top}S_3\vec{k}\right)^{-s}, \tag{4.5.4}$$

with $s > \frac{3}{2}$. The reduction to dimension N=2 and then to N=1 by an expansion in terms of Bessel functions, which is similar to the procedure followed in (4.3.13) proceeds as follows,

$$Z_{S_3}(s) = Z_{S_2}(s) + \pi \frac{\Gamma(s-1)}{\Gamma(s)} \det(S_2)^{-\frac{1}{2}} Z_t(s-1) + \frac{\pi^s}{\Gamma(s)} H_{1,2}(S_3, s)\,, \quad (4.5.5)$$

with

$$Z_x(s) = x^{-s}\zeta(2s)\,. \quad (4.5.6)$$

Here we start the block decomposition, we are looking to find $\vec{q}_2$ and t with the 2×2 sub-matrix S_2 being defined by

$$S_2 = \begin{pmatrix} \sigma_{11} & \sigma_{12} \\ \sigma_{12} & \sigma_{22} \end{pmatrix}. \quad (4.5.7)$$

The block-diagonalization of the 3×3 matrix S_3 to obtain S_2 sub matrix is given by

$$S_3 = \begin{pmatrix} a & \vec{b}_2^{\top} \\ \vec{b}_2 & S_2 \end{pmatrix} = \begin{pmatrix} 1 & \vec{q}_2^{\top} \\ \vec{0}_2 & I_2 \end{pmatrix} \begin{pmatrix} t & \vec{0}_2^{\top} \\ \vec{0}_2 & S_2 \end{pmatrix} \begin{pmatrix} 1 & \vec{0}_2^{\top} \\ \vec{q}_2 & I_2 \end{pmatrix}. \quad (4.5.8)$$

The subscript for the matrix elements denotes the dimension of the corresponding matrix/vector, e.g. $\vec{b}_2$, $\vec{q}_2$ are vectors in $\mathbb{R}^2$. This gives the relations,

$$\vec{b}_2 = S_2\vec{q}_2 \quad \Longrightarrow \quad \vec{q}_2 = S_2^{-1}\vec{b}_2 \quad (4.5.9)$$

and

$$a = t + \vec{q}_2^{\top} S_2 \vec{q}_2 \quad \Longrightarrow \quad t = a - \vec{b}_2^{\top} S_2^{-1} \vec{b}_2 \quad (4.5.10)$$

with $t \neq 0$.
The expansion in terms of Bessel functions is as follows[118, 119]

$$\begin{aligned} Z_{S_2}(s) = {} & \sigma_{22}^{-\frac{1}{2}} p^{\frac{1}{2}-s} \pi^{\frac{1}{2}} \Gamma\left(s-\tfrac{1}{2}\right) \Gamma(s)^{-1} \zeta(2s-1) + \sigma_{22}^{-s}\zeta(2s) \quad (4.5.11) \\ & + 4\pi^s \Gamma(s)^{-1} \sigma_{22}^{-\frac{1}{2}} \sum_{i,j\in\mathbb{N}} \left[\left(i^2 j^{-2} p \sigma_{22}\right)^{\frac{1}{4}-s} \cos(2\pi\sigma_{12}\sigma_{22}^{-1} ij) \right. \\ & \left. K_{\frac{1}{2}-s}\left(2\pi p^{\frac{1}{2}} \sigma_{22}^{-\frac{1}{2}} ij\right) \right], \end{aligned}$$

with S_2 and the different parameters and functions being defined by,

$$p = \sigma_{11} - \frac{\sigma_{12}^2}{\sigma_{22}}\,, \quad (4.5.12)$$

$$H_{1,2}(S_3,s) = \det(S_2)^{-\frac{1}{2}} \sum_{j\in\mathbb{Z}\setminus\{0\};\vec{k}\in\mathbb{Z}^2\setminus\{\vec{0}_2\}} \left(j^2 t\right)^{\frac{1}{2}(1-s)} \left(\vec{k}^\top S_2^{-1}\vec{k}\right)^{\frac{1}{2}(s-1)} \times \cos\left(2\pi j\vec{k}^\top\vec{q}_2\right) K_{1-s}\left(2\pi\left[j^2 t\vec{k}^\top S_2^{-1}\vec{k}\right]^{\frac{1}{2}}\right). \tag{4.5.13}$$

Combining all the equations the lattice sum in terms of this expansion is

$$\begin{aligned} Z_{S_3}(s) &= \pi\Gamma(s-1)\Gamma(s)^{-1}\det(S_2)^{-\frac{1}{2}} t^{1-s}\zeta(s-2) \\ &+ \sigma_{22}^{-\frac{1}{2}} p^{\frac{1}{2}(1-s)}\pi^{\frac{1}{2}}\Gamma\left(\tfrac{1}{2}(s-1)\right)\Gamma(s)^{-1}\zeta(s-1) + \sigma_{22}^{-s}\zeta(s) \\ &+ 4\pi^s\Gamma(s)^{-1}\sigma_{22}^{-\frac{1}{4}(1+s)} p^{\frac{1}{4}(1-s)} \sum_{i,j\in\mathbb{N}} \left[\left(i^{-1}j\right)^{\frac{1}{2}(s-1)} \cos(2\pi\sigma_{12}\sigma_{22}^{-1}ij)\right. \\ &\quad \left. K_{\frac{1}{2}(1-s)}\left(2\pi p^{\frac{1}{2}}\sigma_{22}^{-\frac{1}{2}}ij\right)\right] \\ &+ \frac{2t^{\frac{1}{2}(1-s)}\pi^s}{\Gamma(s)}\det(S_2)^{-\frac{1}{2}} \sum_{j\in\mathbb{N};\vec{k}\in\mathbb{Z}^2\setminus\{\vec{0}_2\}} \left[\cos\left(2\pi j\vec{k}^\top\vec{q}_2\right)\right. \\ &\quad \left. j^{(1-s)}\left(\vec{k}^\top S_2^{-1}\vec{k}\right)^{\frac{1}{2}(s-1)} K_{1-s}\left(2\pi j\left[t\vec{k}^\top S_2^{-1}\vec{k}\right]^{\frac{1}{2}}\right)\right]. \end{aligned} \tag{4.5.14}$$

For the case that $\vec{k}^\top\vec{q}_2 \in \mathbb{Z}$ the last cosine term becomes unity (which will be used for the sc and fcc case discussed below) and we can substitute the last sum over $\vec{k}\in\mathbb{Z}^2\setminus\{\vec{0}_2\}$ by its Dirichlet series,

$$\begin{aligned} Z_{S_3}(s) &= \frac{2\pi t^{1-s}}{s-2}\det(S_2)^{-\frac{1}{2}}\zeta(s-2) + \sigma_{22}^{-\frac{1}{2}} p^{\frac{1}{2}(1-s)}\pi^{\frac{1}{2}}\Gamma\left(\tfrac{1}{2}(s-1)\right) \\ &\quad \Gamma(s)^{-1}\zeta(s-1) + \sigma_{22}^{-s}\zeta(s) \\ &\quad + 4\pi^s\Gamma(s)^{-1}\sigma_{22}^{-\frac{1}{4}(1+s)} p^{\frac{1}{4}(1-s)} \sum_{i,j\in\mathbb{N}} \left[\left(i^{-1}j\right)^{\frac{1}{2}(s-1)}\right. \\ &\quad \left. \cos(2\pi\sigma_{12}\sigma_{22}^{-1}ij) K_{\frac{1}{2}(s-1)}\left(2\pi p^{\frac{1}{2}}\sigma_{22}^{-\frac{1}{2}}ij\right)\right] \\ &\quad + \frac{2(\alpha t)^{\frac{1}{2}(1-s)}\pi^s}{\Gamma(s)}\det(S_2)^{-\frac{1}{2}} \sum_{j,k\in\mathbb{N}} \left[j^{(1-s)}k^{\frac{1}{2}(s-1)}\right. \\ &\quad \left. r_2^{\alpha S_2^{-1}}(k)\, K_{s-1}\left(2\pi j\left(t\alpha^{-1}k\right)^{\frac{1}{2}}\right)\right]. \end{aligned} \tag{4.5.15}$$

In the above, $r_2^{\alpha S_2^{-1}}(k)$ is the integer number of different representations fulfilling the equation

$$\vec{j}^{\top}\alpha S_2^{-1}\vec{j} = k \quad \text{with} \quad \vec{j} \in \mathbb{Z}^2 \setminus \{\vec{0}_2\}, \tag{4.5.16}$$

where α is the prefactor in front of the S_2^{-1} matrix such that only integers in the resulting 2D quadratic form remain, i.e., $aj_1^2 + bj_2^2 + cj_1j_2$ with $a,b,c \in \mathbb{Z}$. The relationship between Bessel functions $K_\nu(x) = K_{-\nu}(x)$ is used,[120] and the gamma function relation

$$\Gamma(x+1) = x\Gamma(x). \tag{4.5.17}$$

Higher order Bessel functions can be successively reduced to lower order Bessel functions by

$$K_\nu(x) = \frac{2(\nu-1)}{x}K_{\nu-1}(x) + K_{\nu-2}(x). \tag{4.5.18}$$

What remains to be evaluated in (6.6.16) are the Bessel functions K_1, K_0 and $K_{\frac{1}{2}}$. For which half-integer orders of the Bessel function can be expressed by the equation

$$K_{\frac{1}{2}}(x) = K_{-\frac{1}{2}}(x) = \sqrt{\frac{\pi}{2x}}e^{-x}. \tag{4.5.19}$$

The $r_2(k)$ values have been discussed in Chapter 2.6 and can be calculated by the method shown in Section (11.5) equation (11.A.10). Most of the value for $Z_{S_3}(s)$ for small exponents s is contained in the first three terms in (6.6.16), while at large exponents s the Bessel sums dominate. Derivations of the Epstein expansion for the three cubic and the hexagonal close-packed structures using the Terras method are shown in Section 6.6.

We note that Crandall introduced an algorithm for the general numerical treatment of Epstein zeta functions [121], which should be considered in future work.

4.6 Single Parameter Cuboidal Lattice Formula

Throughout the study of the cubic lattice sums, we primarily focus on sc, bcc and fcc lattices. However, an expression in terms of single parameter would be useful in the study of packing densities, and the overall physical stability of the lattice under varying lattice parameters. In Project 3 from chapter 4.6.1 we search for formulas that are both simple and computationally efficient. The formulas shown in this section and subsequently from Project 3 and were used to show that the single parameter A lattice sum $L(A;s)$ can be

analytically continued to complex values of s, with a simple pole at $s = 3/2$ and no other singularities.

Here we introduce the axial centered-cuboidal lattice, and along with Conway and Sloane, introduce the mean centered-cuboidal lattice (mcc), which are just other, but perhaps not so well known, cubic lattices characterised on the path between fcc and acc through bcc. We then consider the lattice generated by the vectors $(\pm u, \pm v, 0)^\top$ and $(0, \pm v, \pm v)^\top$, where u and v are non-zero real numbers.[122] To make it specific, take the basis vectors

$$\vec{b}_1 = (u, v, 0)^\top, \quad \vec{b}_2 = (u, 0, v)^\top, \quad \vec{b}_3 = (0, v, v)^\top. \tag{4.6.1}$$

Then the generator matrix B is given by

$$B = \begin{pmatrix} u & v & 0 \\ u & 0 & v \\ 0 & v & v \end{pmatrix}$$

which has determinant $-2uv^2$. The Gram matrix is

$$G = BB^\top = \begin{pmatrix} u^2+v^2 & u^2 & v^2 \\ u^2 & u^2+v^2 & v^2 \\ v^2 & v^2 & 2v^2 \end{pmatrix} = v^2 \begin{pmatrix} 1+A & A & 1 \\ A & 1+A & 1 \\ 1 & 1 & 2 \end{pmatrix} \tag{4.6.2}$$

where $A = u^2/v^2$ and G is positive definite for $A > 0$. Conway and Sloane use $\sigma = u/v$, so $A = \sigma^2$.[123] The most important cases, in decreasing numerical order, are:

1. $A = 1$: the face-centred cubic (fcc) lattice;
2. $A = 1/\sqrt{2}$: the mean centred-cuboidal (mcc) lattice;
3. $A = 1/2$: the body-centred cubic (bcc) lattice;
4. $A = 1/3$: the axial centred-cuboidal (acc) lattice.

The fcc and bcc lattices are well known. The corresponding Gram matrices for the fcc and bcc lattices are identical to the ones shown in our previous paper on lattice sums, see Project 1. The mcc and acc lattices occur in [122] and [123]. The mcc lattice is the densest isodual lattice in three-dimensional space.
The quadratic form associated with the A-lattice is

$$\begin{aligned} g(i,j,k) &= (i,j,k)\, G(i,j,k)^\top \\ &= (u^2+v^2)i^2 + (u^2+v^2)j^2 + 2v^2k^2 + 2u^2ij + 2v^2ik + 2v^2jk \\ &= u^2(i^2+j^2) + v^2(j+k)^2 + v^2(i+k)^2 \\ &= v^2\left(A(i+j)^2 + (j+k)^2 + (i+k)^2\right). \end{aligned} \tag{4.6.3}$$

In Project 3 the minimum distance of the quadratic form with parameter A is discussed and re-scaled to make the minimum distance 1 (see Section (8.2). Specifically in Project 5 this expression of the quadratic form is used to discuss the stability of the body-centered and face-centered cubic lattices. The following quadratic form in terms of a single parameter A is therefore defined as

$$g(A;i,j,k) = \frac{1}{A+1}\left(A(i+j)^2 + (j+k)^2 + (i+k)^2\right), \tag{4.6.4}$$

corresponding to the rescaled Gram matrix

$$G(A) := \frac{1}{(d_{\min})^2}\, G = \frac{1}{A+1}\begin{pmatrix} 1+A & A & 1 \\ A & 1+A & 1 \\ 1 & 1 & 2 \end{pmatrix}. \tag{4.6.5}$$

The following lattice sum is introduced and is important in solid state theory,[1]

$$L(A;s) = \sum_{i,j,k}{}' \left(\frac{1}{g(A;i,j,k)}\right)^s = \sum_{i,j,k}{}' \left(\frac{A+1}{A(i+j)^2 + (j+k)^2 + (i+k)^2}\right)^s \tag{4.6.6}$$

where $1/3 \leq A \leq 1$. The prime on the summation symbol will denote that the sum ranges over all integer values except for the zero vector as discussed before. This lattice sum smoothly connects the four different cuboidal lattices, i.e., when $A = 1$, $1/\sqrt{2}$, $1/2$ or $1/3$ we obtain the expressions for the lattices fcc, mcc, bcc and acc respectively (face-centred cubic, mean centred-cuboidal, body-centred cubic, and axial centred cuboidal). In these cases, we also write

$$\begin{aligned} L_3^{\mathrm{fcc}}(s) &= L(1;s), \\ L_3^{\mathrm{mcc}}(s) &= L(1/\sqrt{2};s), \\ L_3^{\mathrm{bcc}}(s) &= L(1/2;s), \\ \text{and} \quad L_3^{\mathrm{acc}}(s) &= L(1/3;s). \end{aligned}$$

4.6.1 Evaluation of the sum $L(A;s)$

One method of evaluating the sum $L(A;s)$ is to use the Terras decomposition (discussed in Section 4.5). This was done for fcc and bcc in Section Project 1 and can in principle also be used for $L(A;s)$ [8]. What follows in this subsection is a condensed description of an easier method that also works with the whole parameter range $1/3 \leq A \leq 1$ and hence gives the lattice sum for all four lattices fcc, mcc, bcc and acc. In fact, the advantage here is that we obtain two formulas which not only can be used as numerical checks, but also

contain different information about their analytic continuation. We begin by writing the lattice sum in the form

$$\begin{aligned} L(A;s) &= \sum_{i,j,k}{}' \left(\frac{A+1}{A(i+j)^2+(j+k)^2+(i+k)^2} \right)^s \\ &= \sum_{\substack{I,J,K \\ I+J+K \text{ even}}}{}' \left(\frac{A+1}{AI^2+J^2+K^2} \right)^s \\ &= \frac{(A+1)^s}{2} \sum_{i,j,k}{}' \frac{1+(-1)^{i+j+k}}{(Ai^2+j^2+k^2)^s}. \end{aligned} \tag{4.6.7}$$

Therefore, we evaluate the sums

$$T_1(A;A;s) := \sum_{i,j,k}{}' \frac{1}{(Ai^2+j^2+k^2)^s} \tag{4.6.8}$$

and

$$T_2(A;s) := \sum_{i,j,k}{}' \frac{(-1)^{i+j+k}}{(Ai^2+j^2+k^2)^s}. \tag{4.6.9}$$

By (4.6.7), (4.6.8) and (4.6.9), the required lattice sum is given by

$$L(A;s) = \frac{(A+1)^s}{2} \left(T_1(A;s) + T_2(A;s) \right). \tag{4.6.10}$$

4.6.2 The sum $T_1(A;s)$

A first relation for $T_1(A;s)$

We shall consider two ways for handling the sum in (4.6.8). The first is to separate the terms according to whether $i = 0$ or $i \neq 0$, which gives rise to

$$T_1(A;s) = f(s) + 2F(s) \tag{4.6.11}$$

where

$$f(s) = \sum_{j,k}{}' \frac{1}{(j^2+k^2)^s}$$

and

$$F(s) = \sum_{i=1}^{\infty} \sum_{j=-\infty}^{\infty} \sum_{k=-\infty}^{\infty} \frac{1}{(Ai^2+j^2+k^2)^s}.$$

This is the starting point of the approach taken by Selberg and Chowla [124,

Section 7]. Another way is to separate the terms according to whether $(j,k) = (0,0)$ or $(j,k) \neq (0,0)$ and write

$$T_1(A;s) = 2g(s) + G(s) \tag{4.6.12}$$

where

$$g(s) = \sum_{i=1}^{\infty} \frac{1}{(Ai^2)^s}$$

and

$$G(s) = \sum_{j,k}{}' \sum_{i=-\infty}^{\infty} \frac{1}{(Ai^2+j^2+k^2)^s}.$$

The series $F(s)$, $g(s)$ and $G(s)$ also depend on A. For simplicity we omit the parameter A from the notation and just write $F(s)$, $g(s)$ and $G(s)$ in place of $F(A;s)$, $g(A;s)$ and $G(A;s)$, respectively. We will now analyse (4.6.11); for

$$f(s) = \sum_{j,k}{}' \frac{1}{(j^2+k^2)^s} = 4\zeta(s)\beta(s)$$

the expression is well known and is the result of (4.3.6). For the evaluation of $F(s)$, by the integral formula for the gamma function (2.2.5) the procedure proceeds in a similar fashion to what is outlined in Section 4.3.2, the full process for $F(s)$ can be see in the published work in Project 3. The result is

$$\pi^{-s}\Gamma(s)F(s) = \sum_{i=1}^{\infty} \int_0^{\infty} x^{s-2} e^{-\pi A x i^2} \, \mathrm{d}x + \sum_{i=1}^{\infty} \sum_{N=1}^{\infty} r_2(N) \int_0^{\infty} x^{s-2} e^{-\pi A x i^2 - \pi N/x} \, \mathrm{d}x \tag{4.6.13}$$

$$= \frac{\Gamma(s-1)\zeta(2s-2)}{A^{s-1}\pi^{s-1}} + 2\sum_{i=1}^{\infty} \sum_{N=1}^{\infty} \left[r_2(N) \left(\frac{N}{Ai^2} \right)^{(s-1)/2} K_{s-1}\left(2\pi i\sqrt{AN}\right) \right]. \tag{4.6.14}$$

On using all of the above back in (4.6.11) we obtain

$$\sum_{i,j,k}{}' \frac{1}{(Ai^2+j^2+k^2)^s} = 4\zeta(s)L_{-4}(s) + \frac{2\pi}{(s-1)} \frac{\zeta(2s-2)}{A^{s-1}} + \frac{4\pi^s}{\Gamma(s)} A^{(1-s)/2} \sum_{i=1}^{\infty} \sum_{N=1}^{\infty} r_2(N) \left(\frac{N}{i^2} \right)^{(s-1)/2} K_{s-1}\left(2\pi i\sqrt{AN}\right). \tag{4.6.15}$$

This is essentially Selberg and Chowla's formula [124, p. 45]. They write it in a slightly different form in terms of a sum over the divisors of N to minimise the number of Bessel function evaluations. We will leave it as it is for simplicity.

A second formula for the sum $T_1(A;s)$

This time the sum is split into terms according to (4.6.12). The procedure resulting from the integral formula for the gamma function, then modular transformation for the theta function results in

$$\begin{aligned}
&\sum_{i,j,k}{}' \frac{1}{(Ai^2+j^2+k^2)^s} \\
&= 2A^{-s}\zeta(2s) + 4\sqrt{\frac{\pi}{A}}\frac{\Gamma\left(s-\frac{1}{2}\right)}{\Gamma(s)}\zeta\left(s-\frac{1}{2}\right)L_{-4}\left(s-\frac{1}{2}\right) \\
&\quad + \frac{4}{A^{s+\frac{1}{4}}}\frac{\pi^s}{\Gamma(s)}\sum_{N=1}^{\infty}\sum_{i=1}^{\infty} r_2(N)\left(\frac{i}{\sqrt{N}}\right)^{s-\frac{1}{2}} K_{s-\frac{1}{2}}\left(2\pi i\sqrt{\frac{N}{A}}\right). \qquad (4.6.16)
\end{aligned}$$

The terms in (4.6.15) involve K_{s-1} Bessel functions whereas $K_{s-1/2}$ Bessel functions occur in (4.6.16). That is because each application of the theta function transformation formula lowers the subscript in the resulting Bessel function by $1/2$, due to the creation of a $x^{-1/2}$ factor in the integral. The theta function transformation formula is used twice (i.e., the formula is squared) in the derivation of (4.6.15) and only once in the derivation of (4.6.16). For full details see Section 8. Each of (4.6.15) and (4.6.16) turns out to have its own advantages, as will be seen in Project 3, Sections VI C and VI D.

4.6.3 The alternating sum $T_2(A;s)$

The analysis in the previous sections can be modified to handle the alternating series (4.6.9) which has the term $(-1)^{i+j+k}$ in the numerator, as follows. Separating the terms according to whether $i=0$ or $i\neq 0$ gives

$$T_2(A;s) = h(s) + 2H(S) \qquad (4.6.17)$$

where

$$h(s) = \sum_{j,k}{}' \frac{(-1)^{j+k}}{(j^2+k^2)^s}$$

and

$$H(s)=\sum_{i=1}^{\infty}\sum_{j=-\infty}^{\infty}\sum_{k=-\infty}^{\infty}\frac{(-1)^{i+j+k}}{(Ai^2+j^2+k^2)^s}.$$

By a known result shown in Appendix B equation (B.0.2), we have

$$h(s)=-4(1-2^{1-s})\zeta(s)L_{-4}(s).$$

By the integral formula for the gamma function and the modular transformation for theta functions using the formula from Section 8, Appendix 8.A, (8.8.A.14), $H(s)$ can be expressed as

$$\begin{aligned}\pi^{-s}\Gamma(s)H(s)&=\int_0^{\infty}x^{s-2}\sum_{i=1}^{\infty}(-1)^i e^{-\pi Axi^2}\sum_{N=0}^{\infty}r_2(4N+1)e^{-\pi(4N+1)/2x}\ \mathrm{d}x\\&=\sum_{i=1}^{\infty}\sum_{N=0}^{\infty}(-1)^i r_2(4N+1)\int_0^{\infty}x^{s-2}e^{-\pi Axi^2-\pi(4N+1)/2x}\ \mathrm{d}x.\end{aligned}$$

The integral can be expressed in terms of Bessel functions to give

$$\pi^{-s}\Gamma(s)H(s)=2\sum_{i=1}^{\infty}\sum_{N=0}^{\infty}(-1)^i r_2(4N+1)\left(\frac{2N+\frac{1}{2}}{Ai^2}\right)^{(s-1)/2}K_{s-1}\left(2\pi i\sqrt{A(2N+\frac{1}{2})}\right).$$

On using all of the above back in (8.C.10) we obtain

$$\begin{aligned}&\sum_{i,j,k}{}'\ \frac{(-1)^{i+j+k}}{(Ai^2+j^2+k^2)^s}\\&=-4(1-2^{1-s})\zeta(s)L_{-4}(s)\\&+\frac{4\pi^s}{\Gamma(s)}A^{(1-s)/2}\sum_{i=1}^{\infty}\sum_{N=0}^{\infty}(-1)^i r_2(4N+1)\left(\frac{2N+\frac{1}{2}}{i^2}\right)^{(s-1)/2}K_{s-1}\left(2\pi i\sqrt{A(2N+\frac{1}{2})}\right).\end{aligned}\tag{4.6.18}$$

4.6.4 A second formula for the alternating sum $T_2(A;s)$

This time we separate the terms according to whether $(j,k)=(0,0)$ or $(j,k)\neq(0,0)$ and write

$$T_2(A;s)=2\sum_{i=1}^{\infty}\frac{(-1)^i}{(Ai^2)^s}+J(s)\tag{4.6.19}$$

where

$$J(s)=\sum_{j,k}{}'\sum_{i=-\infty}^{\infty}\frac{(-1)^{i+j+k}}{(Ai^2+j^2+k^2)^s}.$$

Again in a similar way, an alternate expression for $T_2(A;s)$ is obtained as

$$\begin{aligned}
&\sum_{i,j,k}{}' \ \frac{(-1)^{i+j+k}}{(Ai^2+j^2+k^2)^s} \\
&= -2A^{-s}(1-2^{1-2s})\zeta(2s) \\
&\quad + \frac{4}{A^{s+\frac{1}{4}}}\frac{\pi^s}{\Gamma(s)}\sum_{N=1}^{\infty}\sum_{i=1}^{\infty}(-1)^N r_2(N)\left(\frac{i-\frac{1}{2}}{\sqrt{N}}\right)^{s-\frac{1}{2}} K_{s-\frac{1}{2}}\left(2\pi(i-\frac{1}{2})\sqrt{\frac{N}{A}}\right).
\end{aligned} \tag{4.6.20}$$

4.6.5 Two formulas for $L(A;s)$

As discussed at the start of this section, formulas (4.6.21) and (4.6.22) can be used as numerical checks against each other. Further, each formula offers different information about special values of the lattice sum, as will be seen in when the sums are analytically continued. On substituting the results of (4.6.15) and (4.6.18) back into (4.6.10) we obtain a formula for $L(A;s)$ in terms of K_{s-1} Bessel functions:

$$\begin{aligned}
L(A;s) = 4\left(\frac{A+1}{2}\right)^s \zeta(s)L_{-4}(s) + \frac{\pi A}{s-1}\left(1+\frac{1}{A}\right)^s \zeta(2s-2) \\
+ \frac{2\pi^s\sqrt{A}}{\Gamma(s)}\left(\sqrt{A}+\frac{1}{\sqrt{A}}\right)^s \sum_{i=1}^{\infty}\sum_{N=1}^{\infty}\left[r_2(N)\left(\frac{N}{i^2}\right)^{(s-1)/2}\right. \\
\left. K_{s-1}\left(2\pi i\sqrt{AN}\right)\right] \\
+ \frac{2\pi^s\sqrt{A}}{\Gamma(s)}\left(\sqrt{A}+\frac{1}{\sqrt{A}}\right)^s \sum_{i=1}^{\infty}\sum_{N=0}^{\infty}(-1)^i r_2(4N+1) \\
\times\left(\frac{2N+\frac{1}{2}}{i^2}\right)^{(s-1)/2} K_{s-1}\left(2\pi i\sqrt{A(2N+\frac{1}{2})}\right).
\end{aligned} \tag{4.6.21}$$

An alternative formula uses the results of (4.6.16) and 4.6.20 in (4.6.10), to obtain the formula involving $K_{s-1/2}$ Bessel functions:

$$L(A;s) = 2\left(\frac{A+1}{4A}\right)^s \zeta(2s) + 2\sqrt{\frac{\pi}{A}}\,(A+1)^s \frac{\Gamma\left(s-\frac{1}{2}\right)}{\Gamma(s)}\,\zeta\left(s-\frac{1}{2}\right) L_{-4}\left(s-\frac{1}{2}\right)$$
$$+ \frac{2}{A^{1/4}}\left(\sqrt{A}+\frac{1}{\sqrt{A}}\right)^s \frac{\pi^s}{\Gamma(s)} \sum_{N=1}^{\infty}\sum_{i=1}^{\infty} N^{(1-2s)/4}\, r_2(N)$$
$$\times\left\{ i^{s-\frac{1}{2}} K_{s-\frac{1}{2}}\left(2\pi i\sqrt{\frac{N}{A}}\right) + (-1)^N \left(i-\frac{1}{2}\right)^{s-\frac{1}{2}} \right.$$
$$\left. K_{s-\frac{1}{2}}\left(2\pi(i-\frac{1}{2})\sqrt{\frac{N}{A}}\right)\right\}. \qquad (4.6.22)$$

4.6.6 Analytic continuation of the lattice sum $L(A;s)$

The lattice sums $L(A;s)$ can be continued analytically to the whole s-plane, and what is shown in Section 8.6 and briefly below is the resulting functions have a single simple pole at $s = 3/2$ and no other singularities.

Behaviour of the lattice sums at $s = 3/2$

We start by showing that $L(A;s)$ has a simple pole at $s = 3/2$ and determine the residue. In the formula (4.6.21), all of the terms are analytic at $s = 3/2$ except for the term involving $\zeta(2s-2)$. It follows that

$$\begin{aligned}
\lim_{s\to 3/2}(s-3/2)L(A;s) &= \lim_{s\to 3/2}(s-3/2)\frac{\pi A}{s-1}\left(1+\frac{1}{A}\right)^s \zeta(2s-2) \\
&= 2\pi A\left(1+\frac{1}{A}\right)^{3/2} \lim_{s\to 3/2}(s-3/2)\zeta(2s-2) \\
&= \frac{2\pi}{\sqrt{A}}\,(A+1)^{3/2} \times \frac{1}{2}\lim_{u\to 1}(u-1)\zeta(u) \\
&= \frac{\pi}{\sqrt{A}}\,(A+1)^{3/2}
\end{aligned}$$

where (12.A.19) was used in the last step of the calculation. It follows further that $L(A;s)$ has a simple pole at $s = 3/2$ and the residue is given by

$$\mathrm{Res}(L(A;s),3/2) = \frac{\pi}{\sqrt{A}}\,(A+1)^{3/2}.$$

By (8..8) this is just 12 times the packing density, i.e.,

$$\mathrm{Res}(L(A;s),3/2) = 12\Delta_{\mathscr{L}}.$$

For example, taking $A = 1$ gives

$$\mathrm{Res}(L_3^{\mathrm{FCC}}(s), 3/2) = 2\sqrt{2}\,\pi \tag{4.6.23}$$

while taking $A = 1/2$ gives

$$\mathrm{Res}(L_3^{\mathrm{BCC}}(s), 3/2) = 3\sqrt{3}\,\pi/2.$$

Laurent's theorem implies there is an expansion of the form

$$L(A;s) = \frac{c_{-1}}{s-3/2} + c_0 + \sum_{n=1}^{\infty} c_n (s-3/2)^n \tag{4.6.24}$$

where

$$c_{-1} = \mathrm{Res}(L(A;s), 3/2) = \frac{\pi}{\sqrt{A}}\,(A+1)^{3/2}$$

and the coefficients c_0, c_1, $c_2, \ldots$ depend on A but not on s. To calculate c_0, start with the fact that

$$\begin{aligned}
&\lim_{s\to 3/2}\left(\frac{\pi A}{s-1}\left(1+\frac{1}{A}\right)^s \zeta(2s-2) - \frac{c_{-1}}{s-3/2}\right) \\
&\quad = \frac{\pi}{\sqrt{A}}\,(A+1)^{3/2}\left(2\gamma - 2 + \log\left(1+\frac{1}{A}\right)\right)
\end{aligned}$$

where $\gamma = 0.57721566490153286060\cdots$ is Euler's constant. Then use (4.6.21) and (4.5.11) to deduce

$$\begin{aligned}
c_0 &= \lim_{s\to 3/2}\left(L(A;s) - \frac{c_{-1}}{s-3/2}\right) \\
&= \sqrt{2}\,(A+1)^{3/2}\,\zeta\left(\frac{3}{2}\right) L_{-4}\left(\frac{3}{2}\right) \\
&\quad + \frac{\pi}{\sqrt{A}}\,(A+1)^{3/2}\left(2\gamma - 2 + \log\left(1+\frac{1}{A}\right)\right) \\
&\quad + \frac{2\pi}{\sqrt{A}}\,(A+1)^{3/2}\sum_{k=1}^{\infty}\sum_{N=1}^{\infty}\frac{1}{k}\,r_2(N)\exp\left(-2\pi k\sqrt{AN}\right) \\
&\quad + \frac{2\pi}{\sqrt{A}}\,(A+1)^{3/2}\sum_{k=1}^{\infty}\sum_{N=0}^{\infty}\frac{(-1)^k}{k}\,r_2(4N+1)\exp\left(-2\pi k\sqrt{A\left(2N+\frac{1}{2}\right)}\right).
\end{aligned}$$

Interchanging the order of summation and evaluating the sum over k gives

$$\begin{aligned} c_0 &= \sqrt{2}\,(A+1)^{3/2}\,\zeta\left(\frac{3}{2}\right) L_{-4}\left(\frac{3}{2}\right) \\ &\quad + \frac{\pi}{\sqrt{A}}\,(A+1)^{3/2}\left(2\gamma - 2 + \log\left(1+\frac{1}{A}\right)\right) \\ &\quad - \frac{2\pi}{\sqrt{A}}\,(A+1)^{3/2}\sum_{N=1}^{\infty} r_2(N)\log\left(1-e^{-2\pi\sqrt{AN}}\right) \\ &\quad - \frac{2\pi}{\sqrt{A}}\,(A+1)^{3/2}\sum_{N=0}^{\infty} r_2(4N+1)\log\left(1+e^{-\pi\sqrt{2A(4N+1)}}\right). \end{aligned}$$

Numerical evaluation in the case $A = 1$ gives

$$c_0|_{A=1} = 6.98405\,25503\,22247\,93406\cdots. \tag{4.6.25}$$

The formulas (4.6.21), (4.6.22) have been used to produce the graphs of $y = L_3^{\mathrm{FCC}}(s)$ on the intervals $-10 < s < 10$ in Figure 8.3 shown in Project 3.

5 N-dimensional Lattice Sums

In this section lattice sums in N dimensions are introduced. The general procedure is to extend the quadratic form for lattices to the N^{th} dimension through N lattice vectors resulting in a positive definite $N \times N$ Gram matrix. Only two simple examples of cubic lattices are given below, other important lattices in N-dimensions can be found in the data base at Ref[125]. The procedure to treat such high dimensional lattice sums is to either reduce the dimension from N to $(N-1)$ obtaining a recursive formula, or to derive directly a fast converging series that generally holds for all dimensions. This can be done by various techniques such as the Terras decomposition [40] or by applying the Mellin transformation for theta functions as described in Section 4.3. These methods result in fast converging series involving modified Bessel $K_\nu(x)$ as shown in (4.3.12). The procedure described below is also presented in Project 7 for the specific case of the Madelung constant.

5.1 N-dimensional Simple Cubic

The simple cubic lattice in three dimensions is given by

$$L_3^{\text{SC}}(s) = \sum_{i_1,i_3,i_3}{}' \frac{1}{\left(i_1^2+i_2^2+i_3^2\right)^s},$$

where the subscript 3 of $L_3^{\text{SC}}(s)$ denotes the dimension $N=3$. To extend the lattice sum to any positive integer dimension N, we consider the lattice sum defined by

$$L_N^{\text{SC}}(s) = \sum_{i_1,\ldots,i_N}{}' \frac{1}{(i_1^2+i_2^2+\cdots+i_N^2)^s}$$

where the summation is over all integer values of i_1, i_2, …, i_N, and the prime on the summation sign denotes that the term corresponding to $i_1 = i_2 = \cdots = i_N = 0$ is omitted. The series converges for $s > N/2$.

5.1.1 first recurrence relation

To find a recurrence relation in terms of the dimension N, consider

$$L_{N+1}^{\text{SC}}(s) = \sum_{i_1,\ldots,i_N,i_{N+1}}{}' \frac{1}{(i_1^2+i_2^2+\cdots+i_N^2+i_{N+1}^2)^s}.$$

Replace the last summation index i_{N+1} with k and separate the sum into the two cases $k = 0$ and $k \neq 0$ to get

$$L_{N+1}^{\mathrm{SC}}(s) = L_N^{\mathrm{SC}}(s) + 2F(s) \tag{5.1.1}$$

where

$$F(s) = \sum_{k=1}^{\infty} \left(\sum_{i_1,\ldots,i_N} \frac{1}{(i_1^2 + i_2^2 + \cdots + i_N^2 + k^2)^s} \right). \tag{5.1.2}$$

The sum in is over positive integer values of k, and over all integer values of $i_1, i_2, \ldots, i_N$.
By the gamma function integral in the form shown in (2.2.5) and the method outlined in Section 4.3.2 we have

$$\begin{aligned} \pi^{-s}\Gamma(s)F(s) &= \int_0^{\infty} t^{s-1} \left(\sum_{k=1}^{\infty} e^{-\pi k^2 t} \right) \left(\sum_{i_1,\ldots,i_N} e^{-\pi(i_1^2+\cdots+i_N^2)t} \right) \mathrm{d}t \\ &= \int_0^{\infty} t^{s-1} \left(\sum_{k=1}^{\infty} e^{-\pi k^2 t} \right) \left(\sum_{j=-\infty}^{\infty} e^{-\pi j^2 t} \right)^N \mathrm{d}t. \end{aligned}$$

By using the modular transformation for the theta function, this can be written as

$$\pi^{-s}\Gamma(s)F(s) = \int_0^{\infty} t^{s-1} \left(\sum_{k=1}^{\infty} e^{-\pi k^2 t} \right) \left(\frac{1}{\sqrt{t}} \sum_{j=-\infty}^{\infty} e^{-\pi j^2/t} \right)^N \mathrm{d}t.$$

This can be rearranged further to give

$$\pi^{-s}\Gamma(s)F(s) = \int_0^{\infty} t^{s-1-\frac{N}{2}} \left(\sum_{k=1}^{\infty} e^{-\pi k^2 t} \right) \left(\sum_{m=0}^{\infty} r_N(m)\, e^{-\pi m/t} \right) \mathrm{d}t$$

where $r_N(m)$ is the number of representations of m as a sum of N squares, shown earlier in Section 2.6. Separating out the $m = 0$ term using $r_N(0) = 1$ gives

$$\begin{aligned} \pi^{-s}\Gamma(s)F(s) = &\sum_{k=1}^{\infty} \left(\int_0^{\infty} t^{s-1-\frac{N}{2}} e^{-\pi k^2 t}\, \mathrm{d}t \right) \\ &+ \int_0^{\infty} t^{s-1-\frac{N}{2}} \left(\sum_{k=1}^{\infty} e^{-\pi k^2 t} \right) \left(\sum_{m=1}^{\infty} r_N(m)\, e^{-\pi m/t} \right) \mathrm{d}t. \end{aligned}$$

The first integral can be evaluated using (2.2.5). Therefore we obtain

$$\begin{aligned}
&\pi^{-s}\Gamma(s)F(s)\\
&=\Gamma\left(s-\frac{N}{2}\right)\sum_{k=1}^{\infty}\frac{1}{(\pi k^2)^{s-\frac{N}{2}}}+\sum_{k=1}^{\infty}\sum_{m=1}^{\infty}r_N(m)\int_0^{\infty}t^{s-1-\frac{N}{2}}\,e^{-\pi k^2 t-\pi m/t}\,\mathrm{d}t\\
&=\frac{\Gamma(s-\frac{N}{2})}{\pi^{s-\frac{N}{2}}}\,\zeta(2s-N)+2\sum_{k=1}^{\infty}\sum_{m=1}^{\infty}r_N(m)\left(\frac{\sqrt{m}}{k}\right)^{s-\frac{N}{2}}K_{s-\frac{N}{2}}\left(2\pi k\sqrt{m}\right)
\end{aligned}$$

where $K_\nu(x)$ is the modified Bessel function which we have arrived at by using the formula in (4.3.12) above. To reduce the number of Bessel function evaluations we put $r=k^2m$ so that

$$\begin{aligned}
\pi^{-s}\Gamma(s)F(s)=\frac{\Gamma(s-\frac{N}{2})}{\pi^{s-\frac{N}{2}}}\,\zeta(2s-N)\\
+2\sum_{r=1}^{\infty}\sum_{k^2|r}\left(\frac{\sqrt{r}}{k^2}\right)^{s-\frac{N}{2}}r_N\left(\frac{r}{k^2}\right)K_{s-\frac{N}{2}}\left(2\pi\sqrt{r}\right).
\end{aligned}$$

Multiply by $2\pi^s/\Gamma(s)$ to get $2F(s)$, and use this in (5.1.1) and (5.1.2) to get the reduction formula

$$L^{\mathrm{SC}}_{N+1}(s)=L^{\mathrm{SC}}_N(s)+2\pi^{N/2}\frac{\Gamma(s-\frac{N}{2})}{\Gamma(s)}\zeta(2s-N)+\frac{4\pi^s}{\Gamma(s)}\sum_{r=1}^{\infty}c(N,r)K_{s-\frac{N}{2}}\left(2\pi\sqrt{r}\right) \tag{5.1.3}$$

where

$$c(N,r)=\sum_{k^2|r}\left(\frac{\sqrt{r}}{k^2}\right)^{s-\frac{N}{2}}r_N\left(\frac{r}{k^2}\right). \tag{5.1.4}$$

When $N=2$, this agrees with Selberg and Chowla's formula [124, (45)].

5.1.2 Second recurrence relation

We again separate the sum for $L^{\mathrm{SC}}_{N+1}(s)$ into two cases, this time according to whether $i_1=i_2=\cdots=i_N=0$ or $i_1, i_2, \ldots, i_N$ are not all zero, to get

$$L^{\mathrm{SC}}_{N+1}(s)=2\zeta(2s)+G(s) \tag{5.1.5}$$

where $\zeta(s)$ is the Riemann zeta function, and

$$G(s) = \sum_{k=-\infty}^{\infty} \left(\sum_{i_1,\dots,i_N}{}' \frac{1}{(i_1^2+i_2^2+\cdots+i_N^2+k^2)^s} \right).$$

Now proceed as in the previous section and apply the integral formula for the gamma function and then the modular transformation for the theta function to obtain

$$\begin{aligned}\pi^{-s}\Gamma(s)G(s) &= \int_0^\infty t^{s-1} \sum_{i_1,\dots,i_N}{}' e^{-\pi(i_1^2+\cdots+i_N^2)t} \sum_{k=-\infty}^{\infty} e^{-\pi k^2 t}\,\mathrm{d}t \\ &= \int_0^\infty t^{s-3/2} \sum_{i_1,\dots,i_N}{}' e^{-\pi(i_1^2+\cdots+i_N^2)t} \sum_{k=-\infty}^{\infty} e^{-\pi k^2/t}\,\mathrm{d}t.\end{aligned}$$

Separate the $k=0$ term, to get

$$\begin{aligned}\pi^{-s}\Gamma(s)G(s) &= \int_0^\infty t^{s-3/2} \sum_{i_1,\dots,i_N}{}' e^{-\pi(i_1^2+\cdots+i_N^2)t}\,\mathrm{d}t \\ &\quad + 2\int_0^\infty t^{s-3/2} \sum_{i_1,\dots,i_N}{}' e^{-\pi(i_1^2+\cdots+i_N^2)t} \sum_{k=1}^{\infty} e^{-\pi k^2/t}\,\mathrm{d}t.\end{aligned}$$

The first integral can be evaluated by the gamma function integral, while the second integral can be expressed in terms of the modified Bessel function by (4.3.12). The result is

$$\begin{aligned}\pi^{-s}\Gamma(s)G(s) &= \pi^{-(s-\frac{1}{2})}\Gamma\left(s-\frac{1}{2}\right) \sum_{i_1,\dots,i_N}{}' \frac{1}{(i_1^2+i_2^2+\cdots+i_N^2)^{s-\frac{1}{2}}} \\ &\quad + 4 \sum_{i_1,\dots,i_N}{}' \sum_{k=1}^{\infty} \left(\frac{k}{\sqrt{i_1^2+\cdots+i_N^2}} \right)^{s-\frac{1}{2}} K_{s-\frac{1}{2}}\left(2\pi k\sqrt{i_1^2+\cdots+i_N^2}\right) \\ &= \pi^{-(s-\frac{1}{2})}\Gamma\left(s-\frac{1}{2}\right) L_N^{\mathrm{SC}}\left(s-\frac{1}{2}\right) \\ &\quad + 4\sum_{m=1}^{\infty}\sum_{k=1}^{\infty} r_N(m) \left(\frac{k}{\sqrt{m}}\right)^{s-\frac{1}{2}} K_{s-\frac{1}{2}}\left(2\pi k\sqrt{m}\right).\end{aligned}$$

On using this formula for $G(s)$ back in (5.1.5) we obtain

$$L_{N+1}^{\mathrm{SC}}(s) = 2\zeta(2s) + \sqrt{\pi}\,\frac{\Gamma(s-\frac{1}{2})}{\Gamma(s)}\,L_N^{\mathrm{SC}}\left(s-\frac{1}{2}\right) + \frac{4\pi^s}{\Gamma(s)}\sum_{m=1}^{\infty}\sum_{k=1}^{\infty} r_N(m)\left(\frac{k}{\sqrt{m}}\right)^{s-\frac{1}{2}} K_{s-\frac{1}{2}}\left(2\pi k\sqrt{m}\right). \tag{5.1.6}$$

On putting $r = k^2 m$ this may be written in a form more efficient for computation, as

$$L_{N+1}^{\mathrm{SC}}(s) = 2\zeta(2s) + \sqrt{\pi}\,\frac{\Gamma(s-\frac{1}{2})}{\Gamma(s)}\,L_N^{\mathrm{SC}}\left(s-\frac{1}{2}\right) + \frac{4\pi^s}{\Gamma(s)}\sum_{r=1}^{\infty} d(N,r)K_{s-\frac{1}{2}}\left(2\pi\sqrt{r}\right) \tag{5.1.7}$$

where

$$d(N,r) = \sum_{k^2|r}\left(\frac{k^2}{\sqrt{r}}\right)^{s-\frac{1}{2}} r_N\left(\frac{r}{k^2}\right). \tag{5.1.8}$$

If we take $N = 2$ in (5.1.6) and use the result

$$L_2^{\mathrm{SC}}(s) = 4\zeta(s)\beta(s)$$

where

$$\zeta(s) = \sum_{j=1}^{\infty}\frac{1}{j^s}$$

is the Riemann zeta function, and

$$\beta(s) = \sum_{j=0}^{\infty}\frac{(-1)^j}{(2j+1)^s},$$

then we obtain

$$L_3^{\mathrm{SC}}(s) = 2\zeta(2s) + 4\sqrt{\pi}\,\frac{\Gamma(s-\frac{1}{2})}{\Gamma(s)}\,\zeta(s-\frac{1}{2})\beta(s-\frac{1}{2}) + \frac{4\pi^s}{\Gamma(s)}\sum_{m=1}^{\infty}\sum_{k=1}^{\infty} r_2(m)\left(\frac{k}{\sqrt{m}}\right)^{s-\frac{1}{2}} K_{s-\frac{1}{2}}\left(2\pi k\sqrt{m}\right). \tag{5.1.9}$$

This is consistent with [1, (6.4.3)].

Figure 5.1 shows the evaluation of 5.1.6 for dimension $N = 3, 4,$ and 3 and Figure 5.2 the evaluation of 5.1.6 for dimension $N = 10, 11, \ldots, 16$

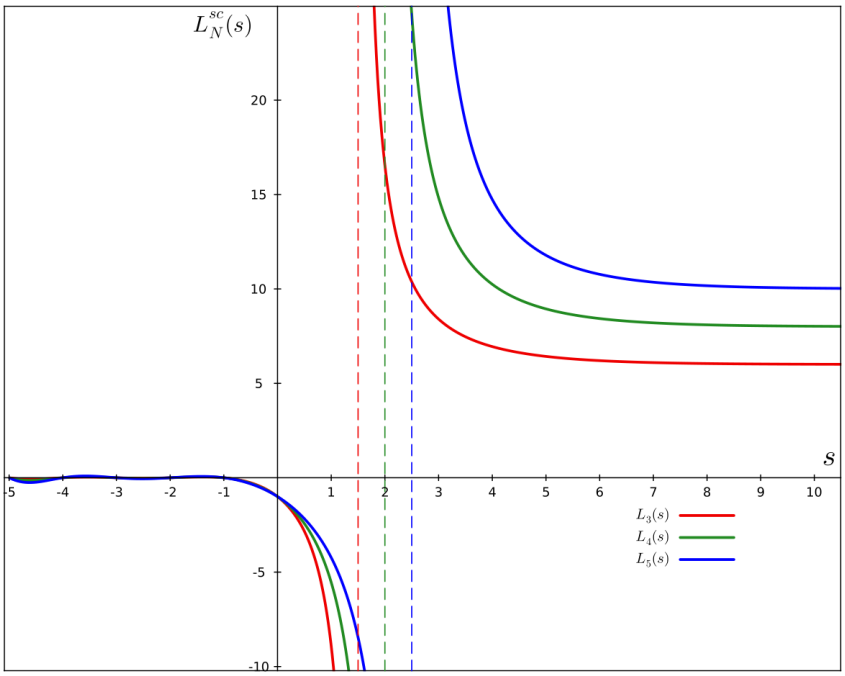

Figure 5.1 Simple cubic N-dimensional lattice sums for $N = 3, 4,$ and 9.

5.1.3 Convergence

The formulas (5.1.3) and (5.1.6) provide two different ways to compute $L_{N+1}^{\mathrm{SC}}(s)$, and therefore provide a check. It is not necessary to iterate all the way down to the value $N = 1$. That's because exact values of $L_N^{\mathrm{SC}}(s)$ in terms of L-functions exist in the cases $N = 2$, 4 and 8:

$$\begin{aligned} L_2^{\mathrm{SC}}(s) &= 4\zeta(s)\beta(s), \\ L_4^{\mathrm{SC}}(s) &= 8(1-2^{2-2s}\zeta(s)\zeta(s-1), \\ L_8^{\mathrm{SC}}(s) &= 16(1-2^{1-s}+2^{4-2s})\zeta(s)\zeta(s-3). \end{aligned}$$

These formulas are equivalent to Jacobi's sum of two, four and eight squares theorems, e.g., see [78, Section 3.8] and Glasser and Zucker's 1980 paper.
The infinite series of modified Bessel functions in (5.1.3) converges fast because of the asymptotic formula

$$K_\nu(z) \sim \sqrt{\frac{\pi}{2z}}e^{-z} \quad \text{as } z \to \infty.$$

The coefficients $c(N,r)$ and $d(N,r)$ in (5.1.4) and (5.1.7) can be efficiently cal-

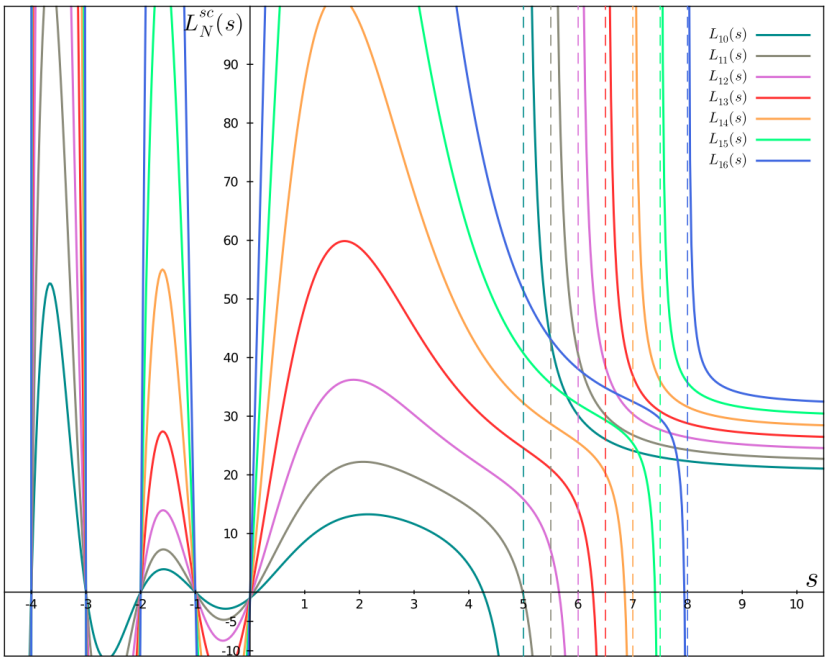

Figure 5.2 Simple cubic N-dimensional lattice sums for $N = 10, \ldots, 16$.

culated from a table of values of $r_N(m)$. Thus, the formulas (5.1.3) and (5.1.6) allow one to compute the $(N+1)$-dimensional lattice sum $L_{N+1}^{\mathrm{SC}}(s)$ from the N-dimensional sum $L_N^{\mathrm{SC}}(s)$ together with some other terms that can be calculated efficiently.

In the three dimensional case, one way of calculating $L_3^{\mathrm{SC}}(s)$ is to use (5.1.3) with $N = 2$ together with the value of $L_2^{\mathrm{SC}}(s)$ given above. Another way, that could be used as a computational check, is to use (5.1.3) with $N = 3$ together with the value of $L_4^{\mathrm{SC}}(s)$.

5.2 N-dimensional Madelung Constant

In section 2.3.1 the three dimensional alternating sum is discussed and the formula (2.3.14) is used to calculate the Madelung constant. In this section we derive two useful expansions for the N-dimensional Madelung constant using a similar method to the simple cubic in the previous section. Consider $M_{N+1}(s)$ and change the last summation index to k, and write

$$M_{N+1}(s) = {\sum_{\substack{i_1,\ldots,i_N\in\mathbb{Z}\\ k\in\mathbb{Z}}}}' \frac{(-1)^{i_1+\cdots+i_N+k}}{(i_1^2+i_2^2+\cdots+i_N^2+k^2)^s}. \tag{5.2.1}$$

Now separate the sum into the two cases $k = 0$ and $k \neq 0$ to get

$$M_{N+1}(s) = M_N(s) + 2F(s) \tag{5.2.2}$$

where

$$F(s) = \sum_{k\in\mathbb{N}} \left(\sum_{i_1,\ldots,i_N\in\mathbb{Z}} \frac{(-1)^{i_1+\cdots+i_N+k}}{(i_1^2+i_2^2+\cdots+i_N^2+k^2)^s} \right). \tag{5.2.3}$$

By the gamma function integral in the form ($\mathbb{R}_+ = \{x \in \mathbb{R} \mid x \geq 0\}$)

$$\frac{1}{z^s} = \frac{1}{\Gamma(s)} \int_{\mathbb{R}_+} t^{s-1} e^{-zt}\, \mathrm{d}t \tag{5.2.4}$$

we have

$$\begin{aligned} &\pi^{-s}\Gamma(s)F(s) = \\ &\quad \int_{\mathbb{R}_+} t^{s-1} \left(\sum_{k\in\mathbb{N}} (-1)^k e^{-\pi k^2 t} \right) \left(\sum_{i_1,\ldots,i_N\in\mathbb{Z}} (-1)^{i_1+\cdots+i_N} e^{-\pi(i_1^2+\cdots+i_N^2)t} \right) \mathrm{d}t \\ &= \int_{\mathbb{R}_+} t^{s-1} \left(\sum_{k\in\mathbb{N}} (-1)^k e^{-\pi k^2 t} \right) \left(\sum_{j\in\mathbb{Z}} (-1)^j e^{-\pi j^2 t} \right)^N \mathrm{d}t. \end{aligned} \tag{5.2.5}$$

By using the modular transformation for the theta function [79],

$$\sum_{n\in\mathbb{Z}} e^{-\pi n^2 t + 2\pi i n a} = \frac{1}{\sqrt{t}} \sum_{n\in\mathbb{Z}} e^{-\pi(n+a)^2/t} \tag{5.2.6}$$

we get

$$\pi^{-s}\Gamma(s)F(s) = \int_{\mathbb{R}_+} t^{s-1} \left(\sum_{k\in\mathbb{N}} (-1)^k e^{-\pi k^2 t} \right) \left(\frac{1}{\sqrt{t}} \sum_{j\in\mathbb{Z}} e^{-\pi(j+\frac{1}{2})^2/t} \right)^N \mathrm{d}t. \tag{5.2.7}$$

This can be rearranged further to give

$$\begin{aligned} \pi^{-s}\Gamma(s)F(s) = \int_{\mathbb{R}_+} \Big\{ & t^{s-1-\frac{N}{2}} \left(\sum_{k\in\mathbb{N}} (-1)^k e^{-\pi k^2 t} \right) \\ & \left(\sum_{m\in\mathbb{N}_0} r_N^{\mathrm{odd}}(8m+N)\, e^{-\pi(8m+N)/4t} \right) dt \Big\} \end{aligned} \tag{5.2.8}$$

where $\mathbb{N}_0$ denotes the natural numbers including zero, and $r_N^{\mathrm{odd}}(m)$ is the num-

ber of representations of m as a sum of N odd squares. That is, $r_N^{\text{odd}}(m)$ is the number of solutions of

$$(2j_1+1)^2+(2j_2+1)^2+\cdots+(2j_N+1)^2=m \tag{5.2.9}$$

in integers. The integral in (5.2.8) can be evaluated in terms of Bessel functions by means of the formula (4.3.12) to give

$$\pi^{-s}\Gamma(s)F(s)=2\sum_{k\in\mathbb{N}}\sum_{m\in\mathbb{N}_0}\left\{(-1)^k r_N^{\text{odd}}(8m+N)\left(\frac{8m+N}{4k^2}\right)^{(2s-N)/4}\right. \\ \left.\times K_{s-N/2}\left(\pi k\sqrt{8m+N}\right)\right\}. \tag{5.2.10}$$

On using this result back in (5.2.1) we obtain the recursion relation for the Madelung constant in terms of the dimension N,

$$\begin{aligned} M_{N+1}(s) &= M_N(s)+\frac{4\pi^s}{\Gamma(s)}\sum_{k\in\mathbb{N}}\sum_{m\in\mathbb{N}_0}\left\{(-1)^k r_N^{\text{odd}}(8m+N)\right. \\ &\qquad\left.\times\left(\frac{8m+N}{4k^2}\right)^{(2s-N)/4}K_{s-N/2}\left(\pi k\sqrt{8m+N}\right)\right\} \\ &= M_N(s)+\sum_{m\in\mathbb{N}_0} r_N^{\text{odd}}(8m+N)c_{s,N}(m) \end{aligned} \tag{5.2.11}$$

with

$$c_{s,N}(m)=\frac{4\pi^s}{\Gamma(s)}\sum_{k\in\mathbb{N}}(-1)^k\left(\frac{8m+N}{4k^2}\right)^{(2s-N)/4}K_{s-N/2}\left(\pi k\sqrt{8m+N}\right). \tag{5.2.12}$$

For fixed N, the term $r_N^{\text{odd}}(8m+N)$ can become very large for larger m and N values, but is more than compensated by the exponentially decreasing Bessel function. The $r_N^{\text{odd}}(m)$ values can be determined recursively which is described in Project 6, Appendix (Section 11.5).

While the recursion relation (5.2.11) is useful if the Madelung constant of lower dimension is known, we seek for a second formula where the recursion relation has been resolved. Here, we proceed as above and separate the sum for $M_{N+1}(s)$ into two cases according to whether $i_1=i_2=\cdots=i_N=0$ or $i_1, i_2, \ldots, i_N$ are not all zero. This gives

$$M_{N+1}(s) = 2\sum_{k\in\mathbb{N}} \frac{(-1)^k}{k^{2s}} + g(s) \tag{5.2.13}$$

where

$$g(s) = \sum_{k\in\mathbb{Z}} \left({\sum_{i_1,\dots,i_N\in\mathbb{Z}}}' \frac{(-1)^{i_1+\cdots+i_N+k}}{(i_1^2+i_2^2+\cdots+i_N^2+k^2)^s} \right).$$

Applying the integral formula for the gamma function and then the modular transformation for the theta function we obtain

$$\begin{aligned}
\pi^{-s}\Gamma(s)g(s) &= \int_{\mathbb{R}_+} t^{s-1} {\sum_{i_1,\dots,i_N\in\mathbb{Z}}}' (-1)^{i_1+\cdots+i_N} e^{-\pi(i_1^2+\cdots+i_N^2)t} \sum_{k\in\mathbb{Z}} (-1)^k e^{-\pi k^2 t}\,\mathrm{d}t \qquad (5.2.14)\\
&= \int_{\mathbb{R}_+} t^{s-3/2} {\sum_{i_1,\dots,i_N\in\mathbb{Z}}}' (-1)^{i_1+\cdots+i_N} e^{-\pi(i_1^2+\cdots+i_N^2)t} \sum_{k\in\mathbb{Z}} e^{-\pi(k+\frac{1}{2})^2/t}\,\mathrm{d}t\\
&= 2\int_{\mathbb{R}_+} t^{s-3/2} {\sum_{i_1,\dots,i_N\in\mathbb{Z}}}' (-1)^{i_1+\cdots+i_N} e^{-\pi(i_1^2+\cdots+i_N^2)t} \sum_{k\in\mathbb{N}} e^{-\pi(k-\frac{1}{2})^2/t}\,\mathrm{d}t,
\end{aligned}$$

where the last step follows by noting

$$\sum_{k\in\mathbb{Z}} e^{-\pi(k+\frac{1}{2})^2/t} = 2\sum_{k\in\mathbb{N}_0} e^{-\pi(k+\frac{1}{2})^2/t} = 2\sum_{k\in\mathbb{N}} e^{-\pi(k-\frac{1}{2})^2/t}. \tag{5.2.15}$$

In terms of the modified Bessel function this becomes, by (4.3.12),

$$\begin{aligned}
\pi^{-s}\Gamma(s)g(s) &= 4 {\sum_{i_1,\dots,i_N\in\mathbb{Z}}}' \sum_{k\in\mathbb{N}} \left\{ (-1)^{i_1+\cdots+i_N} \left(\frac{k-\frac{1}{2}}{\sqrt{i_1^2+\cdots+i_N^2}} \right)^{s-\frac{1}{2}} \right.\\
&\qquad \left. K_{s-\frac{1}{2}}\left(2\pi(k-\frac{1}{2})\sqrt{i_1^2+\cdots+i_N^2} \right) \right\} \qquad (5.2.16)\\
&= 4\sum_{m\in\mathbb{N}} \sum_{k\in\mathbb{N}} (-1)^m r_N(m) \left(\frac{k-\frac{1}{2}}{\sqrt{m}} \right)^{s-\frac{1}{2}} K_{s-\frac{1}{2}}\left(2\pi(k-\frac{1}{2})\sqrt{m} \right).
\end{aligned}$$

On using this back in (5.2.13) we obtain

$$\begin{aligned}
M_{N+1}(s) = -2\eta(2s) + \frac{4\pi^s}{\Gamma(s)} \sum_{m\in\mathbb{N}} (-1)^m r_N(m) \sum_{k\in\mathbb{N}} \left(\frac{k-\frac{1}{2}}{\sqrt{m}} \right)^{s-\frac{1}{2}}\\
K_{s-\frac{1}{2}}\left(\pi(2k-1)\sqrt{m} \right). \qquad (5.2.17)
\end{aligned}$$

The method above is also presented in Section 12 where the N-dimensional lattice sum for the Madelung constant is given. Figure 5.3 shows the evaluation of 5.2.17 for $M_1(s), M_2(s), M_3(s), M_4(s), M_6(s)$ and $M_8(s)$. With reference to Figure 5.3, the famous value of the Madelung constant $M(\frac{1}{2}) = -1.747\,564\,594\,633\,182\,\ldots$ can be seen on the line for $M_3(s)$. Other values of the Madelung constant, for which the original formula does not converge absolutely are achieved by analytic continuation shown by Figure 5.3.

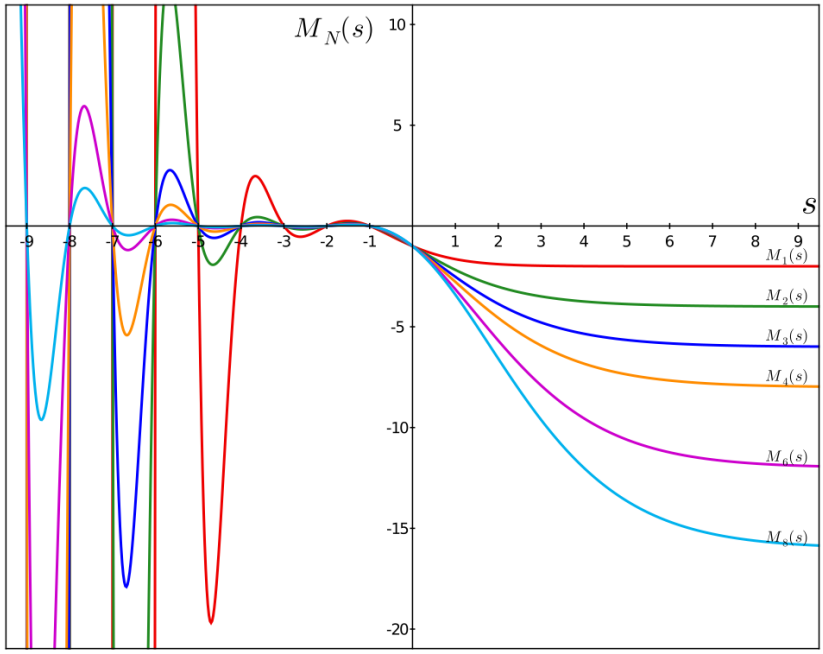

Figure 5.3 The Madelung constant $M_1(s), M_2(s), M_3(s), M_4(s), M_6(s)$ and $M_8(s)$ for $s \in [-9, 9]$.

Part III

Results

6 Project 1 - Analytical methods for fast converging lattice sums for cubic and hexagonal close-packed lattices[a]

6.1 Introduction

Introduced in 1924, the (n,m) Lennard-Jones (LJ) potential[18, 81, 83] has become (besides the Morse potential) the most widely used two-body potential in the simulation of weakly interacting systems in the solid, liquid or the gas phase.[45] Its enormous success in treating inter-atomic and inter-molecular interactions has been attributed to the rather simple analytical form,

$$V_{\mathrm{LJ}}(r) = \frac{nm}{n-m}\varepsilon\left[\frac{1}{n}\left(\frac{r_e}{r}\right)^n - \frac{1}{m}\left(\frac{r_e}{r}\right)^m\right] \quad \underset{m=6}{\overset{n=12}{=}} \quad \varepsilon\left[\left(\frac{r_e}{r}\right)^{12} - 2\left(\frac{r_e}{r}\right)^6\right]. \tag{6.1.1}$$

The LJ potential has only two parameters: r_e, the interatomic distance; and ε the binding energy between two atoms (taken as a positive value). Observe, $V_{\mathrm{LJ}}(r)$ is symmetric in m and n, also $V_{\mathrm{LJ}}(r)$ has a minimum at $r = r_e$. Without loss of generality these two parameters may be set to unity, however this restricts the accuracy of the diatomic potential. Therefore we consider the more general extended Lennard-Jones (ELJ) potential originally introduced for integer exponents by Born in 1940,[94]

$$V_{\mathrm{ELJ}}(r) = \sum_{n=1}^{n_{max}} c_n r^{-s_n}. \tag{6.1.2}$$

Here the s_n are fixed real numbers. The coefficients c_n have to be chosen such that $V_{\mathrm{ELJ}}(r)$ has a minimum at $r = r_e$ and $V_{\mathrm{ELJ}}(r_e) = -\varepsilon$. r_e is the equilibrium distance on the potential energy curve.[48] It was shown that the above expression converges only for $s_n > 3$ for the infinite 3D solid[48] (the Kratzer potential,[16] $\phi(r) = c_1 r^{-1} + c_2 r^{-2}$, can therefore not be used for solids), although this is directly related to the convergence of lattice sums studied much

[a]This chapter is composed of sections previously published in the article "Analytical methods for fast converging lattice sums for cubic and hexagonal close-packed structures"[58] and is reprinted by permission from the publisher ©2022 American Institute of Physics. Some sections may have been modified to fit the style of this thesis.

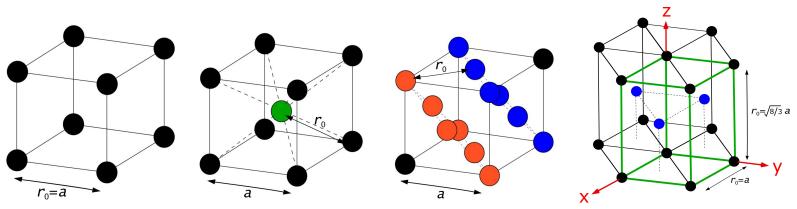

Figure 6.1 From the left to right: The simple cubic (sc), body-centered cubic (bcc) and face-centered cubic (fcc) lattices and the hexagonal close-packed (hcp) structure with corresponding lattice constants. We have the following relationships between the the nearest neighbor distance r_0 and the lattice constants a,c: sc $r_0 = a$, bcc $r_0 = \sqrt{3}a/2$, fcc $r_0 = \sqrt{2}a/2$, and hcp $c/a = c/r_0 = \sqrt{8/3}$.

earlier.[26] The ELJ potential is more accurate than the simple LJ potential, and has the advantage of being computationally very efficient when compared to other more elaborate analytical forms treating the short- and long-range behaviour separately.[95–97]

Another important advantage of the ELJ form is that for certain crystals one can find an analytical form for the cohesive energy per atom E_{ELJ}^{coh} because of the homogeneity of $r \mapsto r^{-s}$,[6, 22, 48]

$$E_{\mathrm{ELJ}}^{coh}(r_0) = \frac{1}{2}\sum_{n=1}^{n_{max}} c_n L_{s_n} r_0^{-s_n}. \tag{6.1.3}$$

Here the L_{s_n} are called lattice sums or Lennard-Jones–Ingham (LJI) coefficients,[6] and r_0 is the nearest neighbour distance of the solid. LJI coefficients for the simple cubic (sc), body-centered cubic (bcc), face-centered cubic (fcc) and hexagonal close-packed (hcp) structures as shown in Figure 6.1 have been obtained for integer values of s_n to reasonable accuracy.[48, 98, 99]

Let us define a N-dimensional lattice $\mathscr{L}$ of rank $n \leq N$ as the set of all (lattice) points $\{p_i\}$ generated by all integer combinations of n linearly independent (lattice) vectors $\vec{b}_1,...,\vec{b}_n \in \mathbb{R}^N$, which form a basis of $\mathscr{L}$,[126] i.e. a Bravais lattice in three dimensions. We also regard a union of lattices $\mathscr{L} = \cup\mathscr{L}_i$ as a lattice in $\mathbb{R}^N$ as long as it contains a unit cell that, by definition, gives rise to translational symmetry. In this sense, the hexagonal close-packed structure is a lattice, but not a Bravais lattice. However, we note that Conway and Sloane[127] refer to hcp as a non-lattice packing, and we will therefore use the term hcp structure for the following.

If we assign certain values (real or complex) to these lattice points through a given function ϕ and sum over all values generated by ϕ we obtain what is called a lattice sum, i.e., $S_{\mathscr{L}} = \sum_{p\in\mathscr{L}} \phi(p)$. For the special case of a $\phi(r) = r^{-s}$ type of potential and a lattice of rank N used in this work, lattice sums take the

form:

$$L_s(N;\mathbf{S},a,f) = {\sum_{\vec{i}\in\mathbb{Z}^N}}' f(\vec{i}) \left|\vec{i}^{\top}\mathbf{S}\vec{i}+a\right|^{-s/2}. \tag{6.1.4}$$

Here we introduce an inhomogeneity parameter $a \in \mathbb{R}$, $\mathbf{S}$ is a positive definite symmetric $N \times N$ matrix defining the quadratic form (QF), and the summation runs over all N-tuples $\vec{i}$ with integer components. The prime at the sum indicates that terms leading to singularities are avoided in the summation. The function $f(\vec{i})$ takes care of possible prefactors, e.g. for alternating series. For example, the famous Madelung constant M_N for an ionic crystal of alternating charges (Coulomb lattice with $\phi(r) = r^{-1}$) is defined by the series

$$M_N = L_1(N;\mathbf{I},0,f) = {\sum_{\vec{i}\in\mathbb{Z}^N}}' (-1)^{i_1+i_2+\ldots+i_N} |\vec{i}|^{-1}, \tag{6.1.5}$$

where $\mathbf{S}$ is the identity matrix $\mathbf{I}$ in this special case. Note that the Madelung series is conditionally convergent and care has to be taken in the order of the summation.[65]

The matrix $\mathbf{S}$ and the inhomogeneity parameter a differ for different lattices in N-dimensional space. Hund's extension of Born's Grundpotential[128–130] is contained in such inhomogeneous quadratic forms. Equation (6.1.4) has been further generalized to the complex plane by Epstein.[117] The evaluation of these lattice sums (analytic continuation, convergence behavior, integral forms, reduction in dimension, lattice isomorphisms, etc.) has a long history in mathematics.[26, 131, 132]

Exact expressions of lattice sums in terms of standard functions such as the Dirichlet L-functions are known for many lattices in two or higher even dimensions,[61, 105, 107, 133, 134] but are rare for the odd dimensional case.[26] For example, the lattice sum for the Madelung constant in three dimensions can be reduced to a two-dimensional sum (Benson's formula),[135] and for the simple cubic case in three dimensions Bateman provided an expression in terms of a Dirichlet series with a number-theoretical solution for the number of representations of a sum of three squares, $r_3(n)$.[76] However, for small exponents s in (6.1.4) these series are very slowly converging and one requires different techniques to obtain accurate numbers for lattice sums.

A detailed historical survey on lattice sums has been given recently by Borwein et al.[26] For the 3D crystal lattices considered here, i.e., the sc, bcc, and fcc lattices, the first attempt to calculate the corresponding lattice sums to sufficient accuracy was by Lennard-Jones and Ingham, who used expansions in terms of Bessel functions.[6, 22] In order to efficiently calculate such lattice sums they used for the first time number-theoretical tools. In 1953 Van der Hoff and Benson introduced an expansion in terms of Bessel functions for lattice sums,[111] (see also the work by Hautot[69, 136]) which we will use extensively in this work. In 1973, Terras introduced an expansion

of quadratic forms in terms of Bessel functions to successively reduce the dimension N in the Epstein zeta function by block-diagonalizing the matrix $\mathbf{S}$ of the quadratic form.[112] This work has however gone relatively unnoticed. Further improvement came from the work by Zucker in 1975 who evaluated lattice sums and Madelung constants for cubic and tetragonal lattices to 10 significant digits by using a Mellin transformation in conjunction with Jacobian θ-functions.[61] Interestingly, the lattice sum for the hexagonal close-packed structure was given early by Kane and Goeppert-Mayer in 1940,[24] but has never been evaluated to high precision except for some special cases.[25, 26] For ionic lattices we refer to a review article in 1964 by Tosi.[137]

In this article we evaluate lattice sums in three dimensions to computer (double) precision for the sc, bcc, fcc and, for the first time, for the hexagonal close-packed structure. Re-expressing the slow converging lattice sums as rapidly converging series by using a number of different mathematical tools such as Terras and Van der Hoff-Benson expansions in terms of Bessel functions allows us to achieve the high computer precision needed. The present paper can be seen as a continuation of Zucker's seminal work in this field. [61, 105, 107] Once the lattice sums are known they can be applied to calculate basic solid state properties like the pressure or the bulk modulus as volume derivatives of the cohesive energy, and for lattice energy minimization including zero-point vibrational and temperature effects.[48–52, 54, 138] We notice that the crystallization conjecture which states that under certain conditions particles always place themselves into periodic configurations still remains unsolved, even for well known interaction potentials.[139] We note however that for Lennard-Jones potentials progress on the local optimality of cubic lattices has been made recently by Bétermin.[140]

In the next section (12.2) we introduce lattice sums for the above-mentioned lattice types and give formulae that connect back to the ELJ potential. Section 6.3 briefly discusses the slow converging nature of such sums, especially at lower values of s_n. Section 6.4 explains what can be done with direct summation techniques. This is particularly useful for large exponents where a simple direct summation can be done in a relatively short amount of time to computer precision. Section 6.5 reformulates the lattice sums as Dirichlet series and highlights some number-theoretical problems, this method again is preferred for higher values of s_n. We then show in Section 6.6 an effective treatment of lattice sums in terms of the Terras decomposition of the Epstein zeta function using pure quadratic forms.[112, 141] By reducing the problem in dimension this speeds up the convergence of the sum by a significant factor. Section 6.7 shows another technique to convert lattice sums into fast convergent series, the Van der Hoff-Benson expansion. This technique offers yet another pathway in which to speed up the calculation of three dimensional lattice sums using fast converging Bessel functions. Finally, in Section 6.8 analytic formulae in terms of hyperbolic functions are shown for even values of exponents in the

four lattice types discussed, which we derive for the special case of exponent $s = 4$. Numerical results for lattice sums to computer precision are discussed in Section 6.9, as well as an interesting comparison between fcc and hcp lattice sums for non integer values. Section 6.10 sums up the body of work in this paper and suggests avenues for further research and applications of high precision, fast converging lattice sums. The appendices help the reader with short discussions and examples of some of the methodology used in formulas from previous sections. The Mellin transformation and theta function method are discussed in Appendix 6.A. Appendix 6.B discusses methods used in the evaluation of doubles sums. Appendix 6.C gives definitions of some Kronecker symbols and Appendix D shows expressions for half integer Bessel functions.

6.2 Lattice Sums for Cubic and Hexagonal Lattices in Three Dimensions

Choosing one arbitrary lattice point located at $\vec{p}_0$, we obtain the set of distances $r_m = |\vec{p}_i - \vec{p}_0|$ to all other lattice points with $\vec{r}_m = i\vec{b}_1 + j\vec{b}_2 + k\vec{b}_3 \quad with \quad i,j,k \in \mathbb{Z}$, where $\vec{b}_i$ are the basis vectors for a specific lattice. By summing over all lattice points in the lattice $\mathscr{L}$ using the underlying lattice symmetry and the corresponding lattice vectors, we can write the cohesive energy (6.1.3) as:

$$\begin{aligned} E_{\mathrm{ELJ}}^{coh}(r_0) &= \frac{1}{2}\sum_{\{r_m\}}\sum_{n=1}^{n_{max}} c_n r_m^{-s_n} \\ &= \frac{1}{2}\sum_{n=1}^{n_{max}} c_n \left(\sum_{i,j,k\in\mathbb{Z}\setminus(0,0,0)} S_{ijk}^{-\frac{s_n}{2}} \right) r_0^{-s_n} \\ &= \frac{1}{2}\sum_{n=1}^{n_{max}} c_n L_{s_n} r_0^{-s_n}. \end{aligned} \tag{6.2.1}$$

The last formula only depends on the ELJ potential coefficients c_n, the next-neighbour distance in the lattice $r_0 = min\{r_m\}$, and the LJI coefficients L_{s_n}. The latter only depend on the crystal symmetry and the strength of the potential term s_n. In the following we only consider $s_n > 3$ for the 3D case and disregard analytical continuations. We further generalize our considerations here by lifting the restriction for s_n to integer values, i.e., $s_n \in \mathbb{R}$. We can now discuss the lattice sums for the cubic lattices and the hexagonal close-packed structure as shown in Fig. 6.1.

6.2.1 Cubic Lattices

The primitive unit cell of each cubic lattice only contains one atom (lattice point), therefore spanning the entire lattice from any arbitrary point is rather

trivial using the corresponding lattice vectors for the unit cell. If we introduce the basis vectors for the three cubic lattices with the lattice constants shown in Figure 6.1,

$$\begin{aligned}
\vec{b}_1^{\mathrm{sc}^\top} &= a\,(1,0,0) \quad , \quad \vec{b}_2^{\mathrm{sc}^\top} = a\,(0,1,0) \quad , \quad \vec{b}_3^{\mathrm{sc}^\top} = a\,(0,0,1) \\
\vec{b}_1^{\mathrm{bcc}^\top} &= \frac{a}{2}\,(1,1,-1) \quad , \quad \vec{b}_2^{\mathrm{bcc}^\top} = \frac{a}{2}\,(-1,1,1) \quad , \quad \vec{b}_3^{\mathrm{bcc}^\top} = \frac{a}{2}\,(1,-1,1) \\
\vec{b}_1^{\mathrm{fcc}^\top} &= \frac{a}{2}\,(1,1,0) \quad , \quad \vec{b}_2^{\mathrm{fcc}^\top} = \frac{a}{2}\,(0,1,1) \quad , \quad \vec{b}_3^{\mathrm{fcc}^\top} = \frac{a}{2}\,(1,0,1)
\end{aligned} \tag{6.2.2}$$

one finds for the LJI coefficients for the simple cubic (sc), body-centered cubic (bcc) and face-centered cubic (fcc) lattice sums using the lattice vectors the following quadratic forms:

$$S_{ijk}^{\mathrm{sc}} = i^2 + j^2 + k^2\,, \tag{6.2.3a}$$

$$S_{ijk}^{\mathrm{bcc}} = i^2 + j^2 + k^2 - \tfrac{2}{3}\,(ij + ik + jk)\,, \tag{6.2.3b}$$

$$\begin{aligned}
S_{ijk}^{\mathrm{fcc}} &= i^2 + j^2 + k^2 + ij + ik + jk \\
&= \frac{1}{2}\left[(i+j)^2 + (i+k)^2 + (j+k)^2\right]\,.
\end{aligned} \tag{6.2.3c}$$

The formula for the sc lattice (sum of three squares), (6.2.3a) is exactly the equation Lennard-Jones obtained in 1924.[22] The importance of the simple cubic LJI coefficients lies in the fact that they are the most efficient to evaluate and it is thus always computationally advantageous to re-discover simple cubic sub-lattices for the evaluation of the other cubic lattices. This partitioning of the bcc and fcc lattice points in the summations was already introduced by Lennard-Jones, i.e., for the fcc lattice, we get[22]

$$L_{s_n}^{\mathrm{fcc}} = 3 \sum_{i,j,k\in\mathbb{Z}}{}' \left(2i^2 + j^2 + k^2\right)^{-\frac{s_n}{2}} - 2^{1-\frac{s_n}{2}} L_{s_n}^{sc}\,. \tag{6.2.4}$$

Here and for the following, the notation $\sum'$ implies that singularities in the sum are avoided, i.e., the index triple $(i,j,k) = (0,0,0)$ is excluded. Alternative decompositions are easily obtained by combinations of sub-lattices or by direct manipulation of the lattice sums:

$$L_{s_n}^{\mathrm{fcc}} = 3 \times 2^{\frac{s_n}{2}} \sum_{i,j,k\in\mathbb{Z}} \left[(2i+1)^2 + (2j+1)^2 + 4k^2\right]^{-\frac{s_n}{2}} + 2^{-\frac{s_n}{2}} L_{s_n}^{\mathrm{sc}}\,, \tag{6.2.5}$$

or the decomposition given by Zucker,[61]:

$$\begin{aligned} L_{s_n}^{fcc} &= 2^{\frac{s_n}{2}-1} {\sum_{i,j,k\in\mathbb{Z}}}' \left[1+(-1)^{i+j+k}\right] \left(i^2+j^2+k^2\right)^{-\frac{s_n}{2}} \\ &= 2^{\frac{s_n}{2}-1} L_{s_n}^{sc} + 2^{\frac{s_n}{2}-1} {\sum_{i,j,k\in\mathbb{Z}}}' (-1)^{i+j+k} \left(i^2+j^2+k^2\right)^{-\frac{s_n}{2}} . \end{aligned} \tag{6.2.6}$$

For the bcc lattice the following formulae can easily be found in that way [22]:

$$L_{s_n}^{bcc} = \left(\frac{3}{4}\right)^{\frac{s_n}{2}} L_{s_n}^{sc} + 3^{\frac{s_n}{2}} \sum_{i,j,k\in\mathbb{Z}} \left[(2i+1)^2+(2j+1)^2+(2k+1)^2\right]^{-\frac{s_n}{2}} . \tag{6.2.7}$$

and

$$L_{s_n}^{bcc} = \frac{1}{2} 3^{\frac{s_n}{2}} {\sum_{i,j,k\in\mathbb{Z}}}' \left[1+(-1)^{i+j+k}\right] \left(2i^2+2j^2+k^2\right)^{-\frac{s_n}{2}} . \tag{6.2.8}$$

For all formulae, we find that the lattice sums converge to the number of nearest neighbors in the limit as $s_n \to \infty$, so $L_\infty^{sc} = 6$, $L_\infty^{fcc} = 12$, and $L_\infty^{bcc} = 8$ as one expects for strongly decaying interactions.

6.2.2 Hexagonal Close-Packed Structure

The hexagonal close-packed structure contains two atoms in its primitive unit cell. The first lattice sum derived for the hcp structure by Kane and Goeppert-Meyer [24] treated the sub-lattices corresponding to these two atoms separately and therefore arrived at a lattice sum with an inhomogeneous quadratic form

$$L_{s_n}^{hcp} = {\sum_{i,j,k\in\mathbb{Z}}}' \left(S_{ijk}^{hcp1}\right)^{-\frac{s_n}{2}} + \sum_{i,j,k\in\mathbb{Z}} \left(S_{ijk}^{hcp2}\right)^{-\frac{s_n}{2}} \tag{6.2.9}$$

with

$$S_{ijk}^{hcp1} = i^2+j^2+ij+\tfrac{8}{3}k^2 \tag{6.2.10}$$

and

$$\begin{aligned} S_{ijk}^{hcp2} &= \left(i+\tfrac{1}{3}\right)^2 + \left(j+\tfrac{1}{3}\right)^2 + \left(i+\tfrac{1}{3}\right)\left(j+\tfrac{1}{3}\right) + \tfrac{8}{3}\left(k+\tfrac{1}{2}\right)^2 \\ &= i(i+1)+j(j+1)+ij+\frac{8}{3}k(k+1)+1. \end{aligned} \tag{6.2.11}$$

This can complicate the evaluation of the triple sum and makes the direct summation very expensive, in particular for low values of s_n. Fortunately, one can derive a simpler formula, for example, Stein decomposed the hcp structure into four interpenetrating orthorhombic lattices. It is easy to show that from a linear

combination of sub-lattices we get[142]

$$L_{s_n}^{hcp} = \sum_{i,j,k\in\mathbb{Z}}{}' \left(S_{ijk}^{hcp}(\tfrac{8}{3})\right)^{-\frac{s_n}{2}} + \frac{3^{\frac{s_n}{2}}}{2} \sum_{\substack{i,j,k\in\mathbb{Z} \\ k\equiv 1 \pmod 2}} \left(S_{ijk}^{hcp}(2)\right)^{-\frac{s_n}{2}} - \frac{1}{2} \sum_{\substack{i,j,k\in\mathbb{Z} \\ k\equiv 1 \pmod 2}} \left(S_{ijk}^{hcp}(\tfrac{2}{3})\right)^{-\frac{s_n}{2}} \tag{6.2.12}$$

with

$$S_{ijk}^{hcp}(c) = i^2 + j^2 + ij + ck^2. \tag{6.2.13}$$

By adding terms with even k to the last two sums and subtracting them again we obtain lattice sums which are sums of pure quadratic forms without any restrictions on the indices i, j and k. Nevertheless, it is possible to partition the summation over the lattice points in such a way that all quadratic forms involved are homogeneous

$$L_{s_n}^{hcp} = \sum_{m=1}^{4} \sum_{i,j,k\in\mathbb{Z}}{}' a_m \left(S_{ijk}^{hcp}(c_i)\right)^{-\frac{s_n}{2}}, \tag{6.2.14}$$

with $a_1 = \frac{3}{2}, a_2 = 3^{\frac{s}{2}}/2, a_3 = -3^{\frac{s}{2}}/2, a_4 = -\frac{1}{2}$ and $c_1 = \frac{8}{3}, c_2 = 2, c_3 = 8, c_4 = \frac{2}{3}$. The hcp structure has the same number of nearest neighbors and thus the same limit as the fcc lattice, i.e., $L_{\infty}^{hcp} = 12$.

6.3 Lattice Sum Convergence

The lattice sums considered here are slowly convergent series for small exponents of s_n, and the question naturally arises how far we have to sum to achieve a given accuracy, i.e., we search for N_{max} such that the remainder of the triple sum is smaller than a given ε,

$$|\Delta L_{s_n}(N_{max})| = |L_{s_n} - L_{s_n}(N_{max})| = |L_{s_n} - \sum_{\substack{i,j,k\in\mathbb{Z} \\ |i|,|j|,|k|\le N_{max}}} (S_{ijk})^{-\frac{s_n}{2}}| \le \varepsilon\,, \tag{6.3.1}$$

where L_{s_n} is the exact LJI coefficient. Using Epstein's zeta functions, which will be described further below, Lennard-Jones and Ingham were able to calculate these coefficients for the sc, bcc and fcc lattices to an accuracy of $\varepsilon \sim 10^{-4}$ for small exponents of s_n.[6] For the cubic lattices, Zucker improved these summations by using the Mellin transform to about $\varepsilon = 10^{-8}$. It is, however, desirable to achieve at least computer precision for these lattice sums, i.e., $\varepsilon = 10^{-14}$ for double precision. As one can see from Figure 11.5, convergence

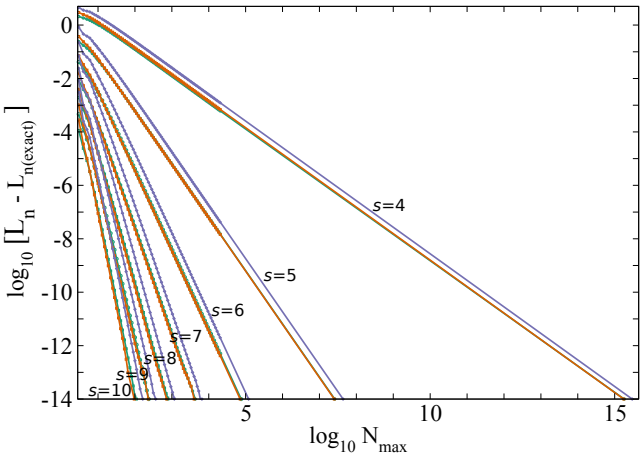

Figure 6.2 Convergence behaviour of the Lennard-Jones–Ingham coefficients $\Delta L_n(N_{max}) = L_n(exact) - L_n(N_{max})$ with increasing expansion value N_{max} for the sc (green line), bcc (red line) and fcc (purple line) lattices and for different exponents of $n \in \mathbb{N}$ on a double logarithmic scale, calculated from the lattice sums and extrapolated to large N_{max} values. The values L_n for the sc, bcc, fcc and hcp structures are found in Section 6.9.

can be very slow, especially for the smallest exponents $s_n = 4$ and $s_n = 5$ where N_{max} has to be about 10^8 and 10^{16} (extrapolated), respectively. This is computationally not feasible. Even for $s_n = 6$ we need $N_{max} = 10^5$ which for a triple sum becomes computationally demanding. It was already recognized[48, 99] that direct summations lead to rather inaccurate LJI coefficients for small exponents s.

One can get lower and upper limits for $\Delta L_{s_n}(N_{max})$ by using the Cauchy integral test if the function $S_{i,j,k}$ is monotonically decreasing in the variables i, j and k. To show the slow convergence behavior, we take the simple cubic lattice as an example for the Cauchy estimate of the remaining sum and restrict the triple sum to $i^2 + j^2 + k^2 \leq N_{max}^2$. We conveniently transform this lattice sum into spherical coordinates and integrate over the angular part to obtain an error estimate,

$$\Delta L_{s_n}(N_{max}) \approx 4\pi \int_{N_{max}}^{\infty} dr\, r^{-s_n+2} = \frac{4\pi}{s_n - 3} N_{max}^{-s_n+3}. \qquad (6.3.2)$$

We immediately see the problem with the convergence behaviour for small exponents s_n, e.g., for an accuracy of $< 10^{-14}$ in the lattice sum one requires $N_{max} \approx 10^{16}$ for $s_n = 4$. Testing just for the next summation values beyond

N_{max} in the sum,

$$\Delta L_{s_n}(N_{max}) - \Delta L_{s_n}(N_{max}+1) = 4\pi N_{max}^{-s_n+2}, \tag{6.3.3}$$

is not sufficient as we go down by one order of magnitude in N_{max}, i.e., small contributions at large integer values i, j, k sum up to sizeable amounts for small exponents s_n. We therefore require other summation techniques to achieve faster convergence, which is the subject of the following sections.

6.4 Direct Summation through Symmetry Considerations

Lennard-Jones used direct summation of the lattice sums L_{s_n} for the cubic lattices except for small exponents $s_n \in \mathbb{N}$,[6] however, restricting the sums to $i, j, k \leq N_{max}$ the computational effort scales $O(N_{max}^3)$. We can save computer time by utilising both permutation and inversion symmetry at the origin in $\mathbb{Z}^3$ space. This does not change the overall scaling law but reduces the prefactor substantially, and makes the sums computationally more attractive for larger exponents of $s_n \geq 8$. For example, most recently Stein introduced a parallel algorithm and exploited the symmetry by partitioning the crystal into octants.[99]

For direct summations, it is convenient to choose expressions for the lattice sums with the symmetric matrix S of the quadratic form $\vec{i}^{\top}\mathbf{S}\vec{i}$ $(\vec{i} \in \mathbb{Z}^3)$ being diagonal, as the resulting double sums can all be expressed in terms of well-known Hurwitz zeta functions. For simplicity, we drop the index for the exponent and use $s \equiv s_n \in \mathbb{R}, s > 3$, for the following.

6.4.1 The Simple Cubic Case

Separating the sums into parts containing either $i = 0$, $j = 0$ or $k = 0$, as well as $i = j$, $j = k$ or $i = k$ using inversion symmetry in i, j and k for the remainder we get

$$\begin{aligned} L_s^{sc} = {\sum_{i,j,k\in\mathbb{Z}}}' \left(i^2+j^2+k^2\right)^{-\frac{s}{2}} = -\left(9+6\times 2^{-\frac{s}{2}}+8\times 3^{-\frac{s}{2}}\right){\sum_{i\in\mathbb{Z}}}' i^{-s} \\ +3{\sum_{i,j\in\mathbb{Z}}}' \left(i^2+j^2\right)^{-\frac{s}{2}} + 6{\sum_{i,j\in\mathbb{Z}}}' \left(2i^2+j^2\right)^{-\frac{s}{2}} + 48\sum_{1\leq i<j<k} \left(i^2+j^2+k^2\right)^{-\frac{s}{2}}. \end{aligned} \tag{6.4.1}$$

The factor of 48 in the last term comes from subdividing the three dimensional space first into octants (factor of 8) and each octant into 6 sectors giving equal contributions due to permutation symmetry.

In the single sum we have the Riemann zeta function $\zeta(s)$ defined as,

$$\zeta(s) = \sum_{i=1}^{\infty} i^{-s}, \tag{6.4.2}$$

with $\lim_{s\to\infty}\zeta(s) = 1$. Further, the first double sum in (6.4.1) can be expressed as a product of the Dirichlet beta and Riemann zeta functions known as the Lorenz–Hardy-sum,[103, 104]

$$\sum_{i,j\in\mathbb{Z}}{}' \left(i^2 + j^2\right)^{-s} = 4\beta(s)\zeta(s). \tag{6.4.3}$$

The Dirichlet beta function is given by

$$\beta(s) = \sum_{i=0}^{\infty}(-1)^i(2i+1)^{-s}, \tag{6.4.4}$$

with $\lim_{s\to\infty}\beta(s) = 1$. Finally, the second double sum has been evaluated by Zucker,[105]

$$Z_1(s) = \sum_{i,j\in\mathbb{Z}}{}' \left(2i^2 + j^2\right)^{-s} = 2^{-3s+1}\zeta(s)\zeta\left(s; \tfrac{1}{8}, \tfrac{3}{8}\ ;\ \tfrac{5}{8}, \tfrac{7}{8}\right), \tag{6.4.5}$$

with

$$\zeta\left(s; \tfrac{1}{8}, \tfrac{3}{8}\ ;\ \tfrac{5}{8}, \tfrac{7}{8}\right) = \zeta\left(s, \tfrac{1}{8}\right) + \zeta\left(s, \tfrac{3}{8}\right) - \zeta\left(s, \tfrac{5}{8}\right) - \zeta\left(s, \tfrac{7}{8}\right), \tag{6.4.6}$$

and the Hurwitz zeta function defined as

$$\zeta(s,x) = \sum_{i=0}^{\infty}(i+x)^{-s}. \tag{6.4.7}$$

The Hurwitz zeta function is a generalization of the Riemann ζ-function with $\zeta(s,1) = \zeta(s)$. For the following it is convenient to define the sum of Hurwitz zeta functions as

$$\zeta(s; c_1, \ldots, c_n; d_1, \ldots, d_m) = \sum_{i=1}^{n}\zeta(s, c_i) - \sum_{i=1}^{m}\zeta(s, d_i). \tag{6.4.8}$$

In this notation $\zeta(s) = \zeta(s;1;-)$ and $\zeta(s,x) = \zeta(s;x;-)$, where a dash indicates an empty parameter list and the last semicolon may be removed if no values are provided. The Dirichlet beta function can be expressed in terms of the Hurwitz zeta function by,

$$\beta(s) = 4^{-s}\zeta\left(s; \tfrac{1}{4}\ ;\ \tfrac{3}{4}\right). \tag{6.4.9}$$

We finally obtain

$$L_s^{sc} = 12\zeta(\tfrac{s}{2})\beta(\tfrac{s}{2}) - 2\left(9 + 6\times 2^{-\frac{s}{2}} + 8\times 3^{-\frac{s}{2}}\right)\zeta(s) + 6Z_1\left(\tfrac{s}{2}\right) + 48\sum_{1\le i<j<k}\left(i^2+j^2+k^2\right)^{-\frac{s}{2}}, \qquad (6.4.10)$$

reducing the summation to the octant of positive values. The standard Riemann zeta, Hurwitz zeta and Dirichlet beta functions can easily be evaluated to computer precision by using the Euler-Maclaurin summation formula.[106] We save a factor 48 in computer time for the remaining triple sum, however, the sum remains slowly converging for small values of s. Restricting the summation to $(i^2+j^2+k^2) \le N_{max}^2$ and choosing N_{max} sufficiently large, this direct summation technique is accurate and fast enough for evaluation of lattice sums for exponents $s \ge 8$. For $s = 8$ ($s = 7$) with $N_{max} = 1500$ (3000), the sum is accurate to within 10^{-14}. Here the triple sum contributes only to 0.028% (0.115%) to the total value.

6.4.2 The Body-Centered Cubic Case

Here we conveniently use the quadratic form (6.2.7). Using again symmetry between positive and negative integers we get,

$$L_s^{bcc} = \left(\frac{3}{4}\right)^{\frac{s}{2}} L_s^{sc} + 8\times 3^{\frac{s}{2}}\sum_{i,j,k\in\mathbb{N}}\left\{(2i-1)^2+(2j-1)^2+(2k-1)^2\right\}^{-\frac{s}{2}}, \qquad (6.4.11)$$

and with permutation symmetry (separating out the cases for $i=j$, $i=k$ and $j=k$) we arrive at

$$L_s^{bcc} = \left(\frac{3}{4}\right)^{\frac{s}{2}} L_s^{sc} - 2^{-s+4}\zeta\left(s,\tfrac{1}{2}\right) + 24\times 3^{\frac{s}{2}}\sum_{i,j\in\mathbb{N}}\left\{2(2i-1)^2+(2j-1)^2\right\}^{-\frac{s}{2}} + 16\times 3^{\frac{s}{2}+1}\sum_{1\le i<j<k}\left\{(2i-1)^2+(2j-1)^2+(2k-1)^2\right\}^{-\frac{s}{2}}. \qquad (6.4.12)$$

For the Hurwitz zeta function with argument $\frac{1}{2}$ we have the relation to the Riemann zeta function,

$$\zeta\left(s,\tfrac{1}{2}\right) = (2^s-1)\,\zeta(s). \qquad (6.4.13)$$

The double sum appearing in (6.4.12) can be reformulated (for details see Ap-

pendix 6.B),

$$\sum_{i,j\in\mathbb{N}} \left\{2(2i-1)^2+(2j-1)^2\right\}^{-\frac{s}{2}} = \tfrac{1}{4}\left(1-2^{-\frac{s}{2}}+2^{-s}\right)Z_1(\tfrac{s}{2}) - \tfrac{1}{4}Z_3(\tfrac{s}{2}), \tag{6.4.14}$$

with the factor of $\frac{1}{4}$ coming from the fact that we only sum over natural numbers on the left hand side. Zucker's sum Z_1 has been defined in (6.4.5) and Z_3 is defined by

$$Z_3(s) = 2^{-1}\left(1-2^{-s}+2^{1-2s}\right)Z_1(s) + 2^{-3s}\beta(s)\zeta\left(s;\tfrac{1}{8},\tfrac{7}{8}\,;\,\tfrac{3}{8},\tfrac{5}{8}\right). \tag{6.4.15}$$

Taking all terms together including (6.4.10), we finally get

$$\begin{aligned} L_s^{bcc} &= 3^{\frac{s}{2}+1}\,2^{-s+2}\beta(\tfrac{s}{2})\zeta(\tfrac{s}{2}) - \left(16+3^{\frac{s}{2}+2}\,2^{1-s}+3^{\frac{s}{2}+1}\,2^{-\frac{3s}{2}+2}\right)\zeta(s) \\ &\quad + 3^{\frac{s}{2}+1}\,2^{-\frac{3s}{2}+1}\left[\left(1-2^{-\frac{s}{2}}+2^{1-s}\right)\zeta(\tfrac{s}{2})\zeta\left(\tfrac{s}{2};\tfrac{1}{8},\tfrac{3}{8}\,;\,\tfrac{5}{8},\tfrac{7}{8}\right)\right. \\ &\qquad \left. -\beta(\tfrac{s}{2})\zeta\left(\tfrac{s}{2};\tfrac{1}{8},\tfrac{7}{8}\,;\,\tfrac{3}{8},\tfrac{5}{8}\right)\right] \\ &\quad + 3^{\frac{s}{2}+1}\,2^{-s+4}\sum_{\substack{1\le i<j<k\\ m\in\{0,1\}}}\left\{\left(i-\tfrac{m}{2}\right)^2+\left(j-\tfrac{m}{2}\right)^2+\left(k-\tfrac{m}{2}\right)^2\right\}^{-\frac{s}{2}}. \end{aligned} \tag{6.4.16}$$

Restricting the summation to $(i^2+j^2+k^2)\le N_{max}^2$ with $N_{max}=1500$ (3000) as in the simple cubic case, for $s=8$ ($s=7$) the sum is accurate to 10^{-14}. Here the triple sums contribute only to 0.038% (0.14%) to the total value. Note that for large exponents s, (6.4.16) needs to be rearranged because of large compensating sums in the expression containing the sum of Hurwitz zeta functions defined in (6.4.8).

6.4.3 The Face-Centered Cubic Case

We could take (6.2.4) for decomposing the sums, but this leads to difficulties in treating the resulting triple sum efficiently. Instead, we take the most symmetric formula with respect to the three summation indices, the alternating sum in (6.2.6). In analogy to the sc case, we start with the case $i=0$, $j=0$ or $k=0$ and get

$$\begin{aligned} L_s^{fcc} &= 2^{\frac{s}{2}-1}L_s^{sc} - 3\times 2^{\frac{s}{2}-1}{\sum_{i\in\mathbb{Z}}}'(-1)^i i^{-s} + 3\times 2^{\frac{s}{2}-1}{\sum_{i,j\in\mathbb{Z}}}'(-1)^{i+j}\left(i^2+j^2\right)^{-\frac{s}{2}} \\ &\quad + 2^{\frac{s}{2}+2}\sum_{i,j,k\in\mathbb{N}}(-1)^{i+j+k}\left(i^2+j^2+k^2\right)^{-\frac{s}{2}}. \end{aligned} \tag{6.4.17}$$

The single sum represents the Dirichlet eta function $\eta(s)$ which can be rewritten in terms of the Riemann zeta function,

$$\eta(s) = \sum_{i=1}^{\infty} (-1)^{i-1} i^{-s} = \left(1 - 2^{1-s}\right) \zeta(s) . \tag{6.4.18}$$

The double sum has been evaluated by Zucker in 1974,[107]

$$Z_2(s) = {\sum_{i,j\in\mathbb{Z}}}' (-1)^{i+j} \left(i^2 + j^2\right)^{-s} = -4\beta(s)\eta(s) , \tag{6.4.19}$$

and we get

$$\begin{aligned} L_s^{fcc} = {} & 2^{\frac{s}{2}-1} L_s^{sc} - 3 \times 2^{\frac{s}{2}+1} \left(1 - 2^{1-\frac{s}{2}}\right) \beta(\tfrac{s}{2}) \zeta(\tfrac{s}{2}) + 3 \times 2^{\frac{s}{2}} \left(1 - 2^{1-s}\right) \zeta(s) \\ & + 2^{\frac{s}{2}+2} \sum_{i,j,k\in\mathbb{N}} (-1)^{i+j+k} \left(i^2 + j^2 + k^2\right)^{-\frac{s}{2}} . \end{aligned} \tag{6.4.20}$$

We decompose the triple sum further as we did for the simple cubic case by taking the diagonal sums with $i = j$ or $j = k$ or $i = k$ out,

$$\begin{aligned} L_s^{fcc} = {} & 2^{\frac{s}{2}-1} L_s^{sc} - 3 \times 2^{\frac{s}{2}+1} \left(1 - 2^{1-\frac{s}{2}}\right) \beta(\tfrac{s}{2}) \zeta(\tfrac{s}{2}) \\ & + \left(3 \times 2^{\frac{s}{2}} + 3^{-\frac{s}{2}} 2^{\frac{s}{2}+3}\right) \left(1 - 2^{1-s}\right) \zeta(s) \\ & + 3 \times 2^{\frac{s}{2}+2} \sum_{i,j\in\mathbb{N}} (-1)^{j} \left(2i^2 + j^2\right)^{-\frac{s}{2}} \\ & + 3 \times 2^{\frac{s}{2}+3} \sum_{1\le i<j<k} (-1)^{i+j+k} \left(i^2 + j^2 + k^2\right)^{-\frac{s}{2}} . \end{aligned} \tag{6.4.21}$$

The double sum in (6.4.21) has been evaluated by Zucker in terms of Dirichlet L-functions,[105] and is related to the simpler double sum (6.4.5) (for details see Appendix 6.B),

$$\sum_{i,j\in\mathbb{N}} (-1)^{j} \left(2i^2 + j^2\right)^{-s} = \tfrac{1}{2} \left(2^{1-s} - 1\right) \left[\tfrac{1}{2} Z_1(s) - \left(1 + 2^{-s}\right) \zeta(s)\right] . \tag{6.4.22}$$

Taking all terms together we obtain a formula similar in nature to the simple cubic case,

$$\begin{aligned} L_s^{fcc} = {} & 12\beta(\tfrac{s}{2}) \zeta(\tfrac{s}{2}) - 2 \left(6 + 9 \times 2^{-\frac{s}{2}} + 3^{-\frac{s}{2}} 2^{-\frac{s}{2}+3}\right) \zeta(n) + 6 Z_1(\tfrac{s}{2}) \\ & + 3 \times 2^{\frac{s}{2}+3} \sum_{1\le i<j<k} \left[1 + (-1)^{i+j+k}\right] \left(i^2 + j^2 + k^2\right)^{-\frac{s}{2}} . \end{aligned} \tag{6.4.23}$$

Restricting the summation again to $(i^2 + j^2 + k^2) \le N_{max}^2$ with $N_{max} = 1500$ (3000), for $s = 8$ ($s = 7$) the sum is accurate to 10^{-14}. Here the

triple sum contributes only to 0.19% (0.53%) of the total value.

6.4.4 The Hexagonal Close-Packed Case

We consider the general form of the sum appearing in (6.2.9) reduce the summation again to the positive integers by consideration of $i = 0$, $j = 0$ or $k = 0$,

$$\begin{aligned}
&\sum_{i,j,k\in\mathbb{Z}}{}' \left[S_{ijk}^{hcp}(c)\right]^{-\frac{s}{2}} = \sum_{i,j,k\in\mathbb{Z}}{}' (i^2+j^2+ij+ck^2)^{-\frac{s}{2}} \\
&= 4 \sum_{\substack{i,j,k\in\mathbb{N} \\ m\in\{-1,1\}}} (i^2+j^2+mij+ck^2)^{-\frac{s}{2}} \\
&+ \sum_{i,j\in\mathbb{Z}}{}' (i^2+j^2+ij)^{-\frac{s}{2}} + 2\sum_{i,k\in\mathbb{Z}}{}' (i^2+ck^2)^{-\frac{s}{2}} - 2\left(2+c^{-\frac{s}{2}}\right)\zeta(s). \quad (6.4.24)
\end{aligned}$$

The first double sum has been treated by Fletcher et al.[108] and later by Zucker[105]

$$\sum_{i,j\in\mathbb{Z}}{}' (i^2+j^2+ij)^{-s} = 3^{1-s}2\zeta(s)\zeta(s;\tfrac{1}{3}\ ;\ \tfrac{2}{3}). \quad (6.4.25)$$

If we use permutation symmetry between the two indices i and j we finally get

$$\begin{aligned}
\sum_{i,j,k\in\mathbb{Z}}{}' \left[S_{ijk}^{hcp}(c)\right]^{-\frac{s}{2}} &= 8 \sum_{\substack{i,j,k\in\mathbb{N},i<j \\ m\in\{-1,1\}}} (i^2+j^2+mij+ck^2)^{-\frac{s}{2}} \\
&+ 2\times 3^{1-\frac{s}{2}}\zeta(\tfrac{s}{2})\zeta(\tfrac{s}{2};\tfrac{1}{3}\ ;\ \tfrac{2}{3}) \\
&+ 2S_2(\tfrac{s}{2},c) + 4\sum_{i,k\in\mathbb{N}} \left(i^2+ck^2\right)^{-\frac{s}{2}} \\
&+ 4\sum_{i,k\in\mathbb{N}} \left(3i^2+ck^2\right)^{-\frac{s}{2}} - 2\left(2+c^{-\frac{s}{2}}\right)\zeta(s) \\
= 8 \sum_{\substack{1\le i<j,k\in\mathbb{N} \\ m\in\{-1,1\}}} &(i^2+j^2+mij+ck^2)^{-\frac{s}{2}} + 2\times 3^{1-\frac{s}{2}}\zeta(\tfrac{s}{2})\zeta(\tfrac{s}{2};\tfrac{1}{3}\ ;\ \tfrac{2}{3}) \\
&+ 3S_2(\tfrac{s}{2},c) + 3^{-\frac{s}{2}}S_2(\tfrac{s}{2},\tfrac{c}{3}) - 6\left(1+3^{-\frac{s}{2}-1}+c^{-\frac{s}{2}}\right)\zeta(s). \quad (6.4.26)
\end{aligned}$$

The remaining double sums

$$S_2(s,c) = \sum_{i,j\in\mathbb{Z}}{}' \left(i^2+cj^2\right)^{-s} \quad (6.4.27)$$

dependent on the rational constant $c \in \mathbb{Q}$ need to be treated separately.

Observe that $S_2(s,2) = Z_1(s)$ is defined in (6.4.5), and $S_2(s,8) = Z_3(s)$ is given in (6.B.20) in Appendix 6.B. For $c = \frac{2}{3}$ the sum has been evaluated by Zucker[105]

$$\begin{aligned} S_2(s,\tfrac{2}{3}) &= 3^s {\sum_{i,j\in\mathbb{Z}}}' (3i^2+2j^2)^{-s} \\ &= 2^{-3s}\left[\zeta(s)\zeta(s;\tfrac{1}{24},\tfrac{5}{24},\tfrac{7}{24},\tfrac{11}{24}\ ;\ \tfrac{13}{24},\tfrac{17}{24},\tfrac{19}{24},\tfrac{23}{24})\right. \\ &\qquad \left. -\zeta(s;\tfrac{1}{8},\tfrac{7}{8}\ ;\ \tfrac{3}{8},\tfrac{5}{8})\zeta(s;\tfrac{1}{3}\ ;\ \tfrac{2}{3})\right]. \end{aligned} \tag{6.4.28}$$

There are in total three double sums $S_2(s,\frac{2}{9}), S_2(s,\frac{8}{9})$ and $S_2(s,\frac{8}{3})$ in (6.4.26) to be further analyzed. Fortunately, these can be be decomposed into (rather lengthy) expressions in terms of Hurwitz zeta functions given in Appendix 6.B. We can now give the complete expression for the hcp lattice sum with the coefficients a_i and c_i defined in (6.2.14),

$$\begin{aligned} L_s^{hcp} = \sum_{n\in\{1,2,3,4\}} a_n \Bigg\{ & 8 \sum_{\substack{i,j,k\in\mathbb{N}, i<j \\ m\in\{-1,1\}}} (i^2+j^2+mij+c_n k^2)^{-\frac{s}{2}} + 3S_2(\tfrac{s}{2},c_n) \\ & + 3^{-\frac{s}{2}} S_2(\tfrac{s}{2},\tfrac{c_n}{3}) \Bigg\} \\ + 2\times 3^{1-\frac{s}{2}} \zeta(\tfrac{s}{2}) & [\zeta(\tfrac{s}{2};\tfrac{1}{3}\ ;\ \tfrac{2}{3}) - 6\left[1+3^{-\frac{s}{2}-1}+\left(\frac{3}{8}\right)^{\frac{s}{2}}\right]\zeta(s). \end{aligned} \tag{6.4.29}$$

This formula requires more computer time compared to the other three lattices. Hence for the hcp structure it is perhaps more convenient to take the Dirichlet series for large exponents s, and the Terras decomposition for small exponents s, which will be discussed further below. Nevertheless, restricting the summation to $i < j \le N_{max}$ and $k \le N_{max}$ with $N_{max} = 3000$, for $s = 8$ ($s = 7$) the sum is accurate to within 10^{-14}. Here the triple sum contributes to 5.46% (7.69%) of the total value.

6.5 Dirichlet Series

A second route to evaluate lattice sums is by reducing the triple sums to an ordinary Dirichlet series. For this we rearrange the sums over the S_{ijk} as follows,

$$L_s = {\sum_{i,j,k\in\mathbb{Z}}}' S_{ijk}^{-\frac{s}{2}} = l^{\frac{s}{2}} \sum_{n\in\mathbb{N}} r_3^{\mathscr{L}}(n) n^{-\frac{s}{2}}, \tag{6.5.1}$$

with $r_3^{\mathscr{L}}(n)$ being the number of different representations fulfilling the equation $lS_{ijk} = n$,[72, 73] with l being the smallest integer such that $n \in \mathbb{N}$ for all combinations of $i,j,k \in \mathbb{Z}$ in the S_{ijk} expressions ($l^{sc} = 1, l^{bcc} = 3, l^{fcc} = 1, l^{hcp} = 3$).

The representations $r_3^{\mathscr{L}}(n)$ are listed in Table A.1. Larger sequences of $r_3^{\mathscr{L}}(n)$ numbers can be found in the Sloane tables (some sequences are known to up to n=10,000).[74, 75] The number $r_3^{\mathscr{L}}(n)$ represents the number of points in the lattice $\mathscr{L}$ at distance r_n from a selected central lattice point. Note that the lattice sum for hcp can be written as as a single Dirichlet sum even though two atoms are in the unit cell. The use of the Dirichlet series to obtain the LJI coefficients L_s is most convenient for larger values of s.

The problem for the slow converging Dirichlet series with small exponents s is that, in contrast to the even dimensional quadratic forms, there is not much known for the $r_D(n)$ values for the odd dimensional sum of squares ($D = 2m+1, m \in \mathbb{N}$). One of the exceptions is the simple cubic case in three dimensions where a (rather cumbersome) formula for $r_3(n)$ has been provided by Bateman.[76]

For the sc case ($S_{ijk}^{sc} = i^2 + j^2 + k^2$) we have zeros appearing in Table A.1 because of Legendre's three-square theorem ($n \in \mathbb{N}$ can be represented as a sum of three squares if and only if $n \neq 2^{2k}(8l+7), k, l \in \mathbb{N}_0$). It is also known that $r_3^{sc}(4^k n) = r_3^{sc}(n)$ for all $k \in \mathbb{N}$. Further, $r_3^{fcc}(n) = r_3^{sc}(2n)$ and therefore Legendre's three-square theorem also applies for the fcc lattice sum ($n \neq 2^{2k+1}(8l+7), k, l \in \mathbb{N}_0$), and we have $r_3^{fcc}(4^k(2n)) = r_3^{fcc}(2n)$.[133] Moreover, we observe from Table A.1 that $r_3^{bcc}(n) = r_3^{sc}(n)$ iff $r_3^{bcc}(n) \neq 0$. This can easily be proven by regarding the bcc lattice as a sub-lattice of the sc lattice with half the lattice constant a and the required lattice points removed. Furthermore, the same procedure can be used for the relation between the sc and fcc lattices. Again we regard the fcc lattice as a sub-lattice of sc with half the lattice constant and remove every point from an sc lattice with $1/2a$ where the sum of the indices $(i+j+k)$ is odd. Therefore, we get $r_3^{fcc}(n) = r_3^{sc}(2n)$.

The values of the coefficients $r_3(n)$ are unbounded, e.g., $r_3(n^2) = 6(n+1-(-1)^{(n-1)/2})$ for any odd prime n[77]. The series converges slowly due to n^{-s} not decaying fast enough.

Nevertheless, this series expansion is particularly useful for the fast converging LJI coefficients at larger exponents s as all LJI coefficients can be computed fast from a database of $r_3(n)$ values. However, for example, to reach computer accuracy for a lattice sum with exponent $s = 8$ one has to sum to values of $N_{max} > 10^7$.

This is perhaps not surprising as we can view the Dirichlet series for such lattice sums as a space filling curve in $\mathbb{Z}^D$ compressed for the cases where different combinations of $(i, j, k, \dots)$ have the same value of $r_D(n)$. For small values of s the sum still requires approximately $n_{max} \sim N_{max}^D$ terms in the Dirichlet series (N_{max}^3 in our case), therefore making it also slow converging.

Efficient algorithms can be developed to obtain the $r_3(n)$ values, however large storage arrays are required. Nevertheless, this is the method of choice for the LJI coefficients L_s with $s \geq 8$. For this we produced 5×10^7 $r_3(n)$ integer values for the sc, bcc, fcc and hcp structures, which are available online on our

Table 6.1 Number of presentations $r_3^{\mathscr{L}}(n)$ for the sc, bcc, fcc and hcp structures (sequences A005875, A004013, A004015 and A004012 in Sloane's database[75]).

n	$r_3^{\mathrm{sc}}(n)$	$r_3^{\mathrm{bcc}}(n)$	$r_3^{\mathrm{fcc}}(n)$	$r_3^{\mathrm{hcp}}(n)$
0	1	1	1	1
1	6	0	12	0
2	12	0	6	0
3	8	8	24	12
4	6	6	12	0
5	24	0	24	0
6	24	0	8	6
7	0	0	48	0
8	12	12	6	2
9	30	0	36	18
10	24	0	24	0
11	24	24	24	12
12	8	8	24	6
13	24	0	72	0
14	48	0	0	0
15	0	0	48	12
16	6	6	12	0
17	48	0	48	12
18	36	0	30	6
19	24	24	72	6
20	24	24	24	12
21	48	0	48	24
22	24	0	24	6
23	0	0	48	0
24	24	24	8	0
25	30	0	84	12
26	72	0	24	0
27	32	32	96	12
28	0	0	48	0
29	72	0	24	24
30	48	0	0	12
31	0	0	96	12
32	12	12	6	2
33	48	0	96	12
34	48	0	48	6
35	48	48	48	24
36	30	30	36	6
37	24	0	120	12
38	72	0	24	0
39	0	0	48	24
40	24	24	24	0
41	96	0	48	12
42	48	0	48	0

CTCP webpage for download.[143]

6.6 Terras' Decomposition of the Epstein Zeta Function

Emersleben[20, 113–116] and later Lennard-Jones and Ingham[6] pointed out that the sums over the inverse powers of the S_{ijk} terms are special cases of Epstein's generalized zeta functions.[117] The N-dimensional generalized Epstein zeta function ($\mathscr{Z}$-function for short) is defined as,

$$\mathscr{Z}_{A_N}(c;\vec{u},\vec{v}) = {\sum_{\vec{z}\in\mathbb{Z}^N}}' e^{2\pi i\vec{u}\cdot(A_N\vec{z})}\,|A_N\vec{z}-\vec{v}|^{-c}\,, \tag{6.6.1}$$

with $c\in\mathbb{C}$, $\vec{u},\vec{v}\in\mathbb{R}^N$, N is the dimension, and A_N is a $N\times N$ real positive definite matrix. Some well-known functions like the Riemann or Hurwitz zeta functions are included in this class of $\mathscr{Z}$-functions. The relation between the $\mathscr{Z}$-function and our sums in the LJI coefficients is obvious,

$${\sum_{i,j,k\in\mathbb{Z}}}' S_{ijk}^{-\frac{s}{2}} = \mathscr{Z}_{A_3}(s;\vec{0}_3,\vec{0}_3)\,, \tag{6.6.2}$$

where $\vec{0}_3$ is the zero vector in 3D-space and the inhomogeneity parameter a in (6.1.4) is zero.

For the smallest integer exponent $s=4$, Lennard-Jones used an expansion of the Epstein function in terms of Bessel functions for the cubic lattices. In fact, for quadratic forms where $\vec{v}=\vec{0}$ the $\mathscr{Z}$-function can be reduced successively in dimension (in our case from dimension N=3) down to the remaining Riemann zeta function $\zeta(x)$ of dimension N=1. A detailed description with all the required proofs can be found in Terras' seminal paper from 1973.[112] In order to achieve this for the cubic lattices we use the expression for a quadratic form,

$$|A_N\vec{z}|^2 = \vec{z}^{\top}\left(A_N^{\top}A_N\right)\vec{z} = \vec{z}^{\top}S_N\vec{z} \quad with \quad S_N = A_N^{\top}A_N\,, \tag{6.6.3}$$

and S_N is an $N\times N$ positive definite and symmetric matrix according to (6.6.3). We briefly outline the expansion method introduced by Terras[112] using the following relation for dimension N=3 (we introduce the factor of $1/2$ to be in line with Terras' definition),

$$Z_{S_3}(s) = \frac{1}{2}\mathscr{Z}_{A_3}(2s;\vec{0}_3,\vec{0}_3) = \frac{1}{2}{\sum_{\vec{k}\in\mathbb{Z}^3}}'\left(\vec{k}^{\top}S_3\vec{k}\right)^{-s}, \tag{6.6.4}$$

with $s>\frac{3}{2}$. The reduction to dimension N=2 and then to N=1 by an expansion

in terms of Bessel functions proceeds as follows,

$$Z_{S_3}(s) = Z_{S_2}(s) + \pi \frac{\Gamma(s-1)}{\Gamma(s)} \det(S_2)^{-\frac{1}{2}} Z_t(s-1) + \frac{\pi^s}{\Gamma(s)} H_{1,2}(S_3, s)\,, \quad (6.6.5)$$

with

$$Z_x(s) = x^{-s}\zeta(2s)\,, \quad (6.6.6)$$

Here we block-diagonalized the 3×3 matrix S_3 to obtain the 2×2 symmetric sub-matrix S_2,

$$S_3 = \begin{pmatrix} a & \vec{b}_2^{\top} \\ \vec{b}_2 & S_2 \end{pmatrix} = \begin{pmatrix} 1 & \vec{q}_2^{\top} \\ \vec{0}_2 & I_2 \end{pmatrix} \begin{pmatrix} t & \vec{0}_2^{\top} \\ \vec{0}_2 & S_2 \end{pmatrix} \begin{pmatrix} 1 & \vec{0}_2^{\top} \\ \vec{q}_2 & I_2 \end{pmatrix}. \quad (6.6.7)$$

The subscript for the matrix elements denotes the dimension of the corresponding matrix/vector, e.g. $\vec{b}_2$, $\vec{q}_2$ are vectors in $\mathbb{R}^2$. This gives the relations,

$$\vec{b}_2 = S_2\vec{q}_2 \quad \Longrightarrow \quad \vec{q}_2 = S_2^{-1}\vec{b}_2 \quad (6.6.8)$$

and

$$a = t + \vec{q}_2^{\top} S_2 \vec{q}_2 \quad \Longrightarrow \quad t = a - \vec{b}_2^{\top} S_2^{-1} \vec{b}_2 \quad (6.6.9)$$

with $t \neq 0$ and

$$S_2^{-1} = \det(S_2)^{-1} \begin{pmatrix} \sigma_{22} & -\sigma_{12} \\ -\sigma_{12} & \sigma_{11} \end{pmatrix}. \quad (6.6.10)$$

The expansion in terms of Bessel functions is as follows for a real valued function,[118, 119]

$$\begin{aligned} Z_{S_2}(s) = {} & \sigma_{22}^{-\frac{1}{2}} p^{\frac{1}{2}-s} \pi^{\frac{1}{2}} \Gamma\left(s-\tfrac{1}{2}\right) \Gamma(s)^{-1} \zeta(2s-1) + \sigma_{22}^{-s}\zeta(2s) \\ & + 4\pi^s \Gamma(s)^{-1} \sigma_{22}^{-\frac{1}{2}} \sum_{i,j\in\mathbb{N}} \left(i^2 j^{-2} p \sigma_{22}\right)^{\frac{1}{4}-\frac{s}{2}} cos(2\pi\sigma_{12}\sigma_{22}^{-1} ij) \\ & \times K_{\frac{1}{2}-s}\left(2\pi p^{\frac{1}{2}} \sigma_{22}^{-\frac{1}{2}} ij\right), \end{aligned} \quad (6.6.11)$$

with $S_2 = (\sigma_{ij})$ and the different parameters and functions are defined as follows,

$$p = \sigma_{11} - \frac{\sigma_{12}^2}{\sigma_{22}}\,, \quad (6.6.12)$$

$$H_{1,2}(S_3,s) = det(S_2)^{-\frac{1}{2}} \sum_{j\in\mathbb{Z}\setminus\{0\};\vec{k}\in\mathbb{Z}^2\setminus\{\vec{0}_2\}} \left(j^2 t\right)^{\frac{1}{2}(1-s)} \left(\vec{k}^\top S_2^{-1}\vec{k}\right)^{\frac{1}{2}(s-1)} \times cos\left(2\pi j\vec{k}^\top\vec{q}_2\right) K_{1-s}\left(2\pi\left[j^2 t\vec{k}^\top S_2^{-1}\vec{k}\right]^{\frac{1}{2}}\right) \tag{6.6.13}$$

and K_ν is the modified Bessel function of the second kind defined by

$$K_\nu(x) = \frac{1}{2}\int_0^\infty u^{\nu-1} exp\left\{-x\left(u+u^{-1}\right)/2\right\} du \quad for \quad |arg(x)| < \tfrac{1}{2}\pi, \tag{6.6.14}$$

where we consider only the real part of the function. We combine all equations and use the usual power of $\frac{s}{2}$ for our lattice sums,

$$\begin{aligned}
Z_{S_3}\left(\tfrac{s}{2}\right) &= \pi\Gamma\left(\tfrac{s}{2}-1\right)\Gamma\left(\tfrac{s}{2}\right)^{-1} det\,(S_2)^{-\frac{1}{2}} t^{1-\frac{s}{2}}\zeta(s-2) \\
&+ \sigma_{22}^{-\frac{1}{2}} p^{\frac{1}{2}(1-s)}\pi^{\frac{1}{2}}\Gamma\left(\tfrac{1}{2}(s-1)\right)\Gamma\left(\tfrac{s}{2}\right)^{-1}\zeta(s-1) + \sigma_{22}^{-\frac{s}{2}}\zeta(s) \\
&+ 4\pi^{\frac{s}{2}}\Gamma\left(\tfrac{s}{2}\right)^{-1}\sigma_{22}^{-\frac{1}{4}(1+s)} p^{\frac{1}{4}(1-s)} \sum_{i,j\in\mathbb{N}} \left(i^{-1}j\right)^{\frac{1}{2}(s-1)} cos(2\pi\sigma_{12}\sigma_{22}^{-1}ij) \\
&\qquad \times K_{\frac{1}{2}(1-s)}\left(2\pi p^{\frac{1}{2}}\sigma_{22}^{-\frac{1}{2}} ij\right) \\
&+ \frac{2t^{\frac{1}{2}(1-\frac{s}{2})}\pi^{\frac{s}{2}}}{\Gamma\left(\frac{s}{2}\right)} det(S_2)^{-\frac{1}{2}} \sum_{j\in\mathbb{N};\vec{k}\in\mathbb{Z}^2\setminus\{\vec{0}_2\}} cos\left(2\pi j\vec{k}^\top\vec{q}_2\right) j^{(1-\frac{s}{2})} \\
&\qquad \times \left(\vec{k}^\top S_2^{-1}\vec{k}\right)^{\frac{1}{2}(\frac{s}{2}-1)} K_{1-\frac{s}{2}}\left(2\pi j\left[t\vec{k}^\top S_2^{-1}\vec{k}\right]^{\frac{1}{2}}\right).
\end{aligned} \tag{6.6.15}$$

For the case that $\vec{k}^\top\vec{q}_2 \in \mathbb{Z}$ the last cosine term becomes unity (which will be used for the sc and fcc case discussed below) and we can substitute the last

sum over $\vec{k} \in \mathbb{Z}^2 \setminus \{\vec{0}_2\}$ by its Dirichlet series,

$$
\begin{aligned}
Z_{S_3}\left(\tfrac{s}{2}\right) &= \frac{2\pi t^{1-\frac{s}{2}}}{s-2} det\left(S_2\right)^{-\frac{1}{2}} \zeta(s-2) \\
&+ \sigma_{22}^{-\frac{1}{2}} p^{\frac{1}{2}(1-s)} \pi^{\frac{1}{2}} \Gamma\left(\tfrac{1}{2}(s-1)\right) \Gamma\left(\tfrac{s}{2}\right)^{-1} \zeta(s-1) + \sigma_{22}^{-\frac{s}{2}} \zeta(s) \\
&+ 4\pi^{\frac{s}{2}} \Gamma\left(\tfrac{s}{2}\right)^{-1} \sigma_{22}^{-\frac{1}{4}(1+s)} p^{\frac{1}{4}(1-s)} \sum_{i,j\in\mathbb{N}} \left(i^{-1} j\right)^{\frac{1}{2}(s-1)} cos(2\pi\sigma_{12}\sigma_{22}^{-1} ij) \\
&\qquad \times K_{\frac{1}{2}(s-1)}\left(2\pi p^{\frac{1}{2}} \sigma_{22}^{-\frac{1}{2}} ij\right) \\
&+ \frac{2\left(\alpha t\right)^{\frac{1}{2}(1-\frac{s}{2})} \pi^{\frac{s}{2}}}{\Gamma\left(\frac{s}{2}\right)} det(S_2)^{-\frac{1}{2}} \sum_{j,k\in\mathbb{N}} j^{(1-\frac{s}{2})} k^{\frac{1}{2}(\frac{s}{2}-1)} \, r_2^{\alpha S_2^{-1}}(k) \\
&\qquad \times K_{\frac{s}{2}-1}\left(2\pi j \left(t\alpha^{-1}k\right)^{\frac{1}{2}}\right), \qquad (6.6.16)
\end{aligned}
$$

with $r_2^{\alpha S_2^{-1}}(k)$ the number of different representations fulfilling the equation

$$\vec{j}^{\top} \alpha S_2^{-1} \vec{j} = k \quad with \quad \vec{j} \in \mathbb{Z}^2 \setminus \{\vec{0}_2\}, \qquad (6.6.17)$$

where α is the prefactor in front of the S_2^{-1} matrix such that we only have integers in the resulting 2D quadratic form, i.e., $aj_1^2 + bj_2^2 + cj_1j_2$ with $a,b,c \in \mathbb{Z}$. Here we used the fact that $K_\nu(x) = K_{-\nu}(x)$,[120] and the relation for the gamma function

$$\Gamma(x+1) = x\Gamma(x). \qquad (6.6.18)$$

The higher order Bessel functions can be successively reduced to lower order Bessel functions by

$$K_\nu(x) = \frac{2(\nu-1)}{x} K_{\nu-1}(x) + K_{\nu-2}(x), \qquad (6.6.19)$$

and all what remains to be evaluated in (6.6.16) are the Bessel functions K_1, K_0 and $K_{\frac{1}{2}}$. Further, for half-integer orders of the Bessel function we can use the equation

$$K_{\frac{1}{2}}(x) = K_{-\frac{1}{2}}(x) = \sqrt{\frac{\pi}{2x}} e^{-x}. \qquad (6.6.20)$$

The $r_2(k)$ values are known to sufficient order and can be tabulated. Most of the value for $Z_{S_3}\left(\frac{s}{2}\right)$ for small exponents s is contained in the first three terms in (6.6.16), while at large exponents s the Bessel sums dominate. We now derive the Epstein expansion for the three cubic and the hexagonal close-packed structures.

6.6.1 The Simple Cubic Case

Here we have

$$\sum_{i,j,k\in\mathbb{Z}}{}' (S^{sc}_{ijk})^{-\frac{s}{2}} = \mathscr{Z}_{I_3}(s;0_3,0_3)\,, \tag{6.6.21}$$

where I_3 is the 3×3 identity matrix. This case is particularly easy as we have $\vec{b}_2 = \vec{0}_2$ (and the cosine term in the second Bessel sum vanishes), $S_3 = I_3$ and $S_2 = S_2^{-1} = I_2$ being identity matrices. From this we get $\alpha = 1$, σ_{12}=0, σ_{22}=1, p=1, t=1, and d$et(S_2) = 1$. Equation (6.6.16) therefore simplifies to

$$\begin{aligned} Z^{sc}_{S_3}\left(\tfrac{s}{2}\right) &= \frac{2\pi}{s-2}\zeta(s-2) + \pi^{\frac{1}{2}}\Gamma\left(\tfrac{s}{2}-\tfrac{1}{2}\right)\Gamma\left(\tfrac{s}{2}\right)^{-1}\zeta(s-1) + \zeta(s) \\ &+ 4\pi^{\frac{s}{2}}\Gamma\left(\tfrac{s}{2}\right)^{-1}\sum_{i,j\in\mathbb{N}}\left(i^{-1}j\right)^{\frac{1}{2}(s-1)} K_{\frac{s}{2}-\frac{1}{2}}(2\pi ij) \\ &+ 2\pi^{\frac{s}{2}}\Gamma\left(\tfrac{s}{2}\right)^{-1}\sum_{j,k\in\mathbb{N}} j^{(1-\frac{s}{2})}k^{\frac{1}{2}(\frac{s}{2}-1)}\, r_2^{I_2}(k)\, K_{\frac{s}{2}-1}\left(2\pi jk^{\frac{1}{2}}\right). \end{aligned} \tag{6.6.22}$$

For the special case $s = 4$ we obtain by using (11.A.9) and (6.6.20), as well as $\zeta(4) = \pi^4/90$ and $\zeta(2) = \pi^2/6$

$$\begin{aligned} Z^{sc}_{S_3}(2) &= \frac{\pi^3}{6} + \frac{\pi^4}{90} + \frac{\pi}{2}\zeta(3) + \pi\sum_{i,j\in\mathbb{N}}\left(2\pi i^{-2}j + i^{-3}\right)e^{-2\pi ij} \\ &+ 2\pi^2\sum_{j,k\in\mathbb{N}} j^{-1}k^{\frac{1}{2}}\, r_2^{I_2}(k)\, K_1\left(2\pi jk^{\frac{1}{2}}\right), \end{aligned} \tag{6.6.23}$$

identical to the original formula of Lennard-Jones[22] (except for a factor of 2 because of equation (6.6.4)).[b]

6.6.2 The Body-Centered Cubic Case

In this case we have the symmetric matrix for the quadratic form

$$\sum_{i,j,k\in\mathbb{Z}}{}' (S^{bcc}_{ijk})^{-\frac{s}{2}} = \mathscr{Z}_{A_3^{bcc}}(s;0_3,0_3) \quad , \quad A_3^{bcc} = \frac{1}{\sqrt{3}}\begin{pmatrix} 1 & -1 & -1 \\ -1 & 1 & -1 \\ -1 & -1 & 1 \end{pmatrix} \tag{6.6.24}$$

$$\left(A_3^{bcc\top}A_3^{bcc}\right) = \frac{1}{3}\begin{pmatrix} 3 & -1 & -1 \\ -1 & 3 & -1 \\ -1 & -1 & 3 \end{pmatrix} \quad , \quad S_2^{bcc} = \frac{1}{3}\begin{pmatrix} 3 & -1 \\ -1 & 3 \end{pmatrix} \tag{6.6.25}$$

$$, \qquad \left(S_2^{bcc}\right)^{-1} = \frac{3}{8}\begin{pmatrix} 3 & 1 \\ 1 & 3 \end{pmatrix},$$

[b] In the paper by Lennard-Jones[22] the exponential expression in the 4th term in eq. (6.6.23) appears as a power rather than a multiplicative factor which is a misprint.

and we have $\alpha = \frac{8}{3}$, σ_{22}=1, $\sigma_{12} = -\frac{1}{3}$, $p = \frac{8}{9}$, $t = \frac{2}{3}$, a=1, $\vec{b}_2^{\top} = \frac{1}{3}(-1,-1)$ and $det(S_2) = \frac{8}{9}$. Unfortunately we have $\vec{k}^{\top}\vec{q}_2 = -\frac{1}{2}(k_1+k_2)$ and the cosine term in (6.6.15) does not vanish. This was, probably, realized early on by Lennard-Jones as in his original 1924 paper he only evaluated the sc and the fcc lattices using the Epstein zeta function, but not bcc.[22] We can, however, simplify (6.6.15). Using the $\vec{k}^{\top}\vec{q}_2$ expression we get for (6.6.15),

$$
\begin{aligned}
Z_{S_3}\left(\tfrac{s}{2}\right) &= \frac{3^{\frac{s}{2}}\pi}{2^{\frac{s}{2}-\frac{1}{2}}(s-2)}\zeta(s-2) + \frac{2^{\frac{3}{2}(s-1)}\pi^{\frac{1}{2}}\Gamma\left(\frac{1}{2}(s-1)\right)}{3^{s-1}\Gamma\left(\frac{s}{2}\right)}\zeta(s-1)+\zeta(s) \\
&+ \frac{4\times 3^{\frac{1}{2}(s-1)}\pi^{\frac{s}{2}}}{8^{\frac{1}{4}(s-1)}\Gamma\left(\frac{s}{2}\right)}\sum_{i,j\in\mathbb{N}}\left(i^{-1}j\right)^{\frac{1}{2}(s-1)}cos\left(\frac{2\pi}{3}ij\right)\ K_{\frac{1}{2}(1-s)}\left(\frac{4\sqrt{2}\pi}{3}ij\right) \\
&+ \frac{3^{\frac{1}{2}(1-\frac{s}{2})}\pi^{\frac{s}{2}}}{2^{\frac{s}{4}}\Gamma\left(\frac{s}{2}\right)}\sum_{j\in\mathbb{N};\vec{k}\in\mathbb{Z}^2\setminus\{\vec{0}_2\}}\left\{(-1)^{j(k_1+k_2)}j^{(1-\frac{s}{2})}\left(\vec{k}^{\top}S_2^{-1}\vec{k}\right)^{\frac{1}{2}(\frac{s}{2}-1)}\right. \\
&\qquad \left. K_{1-\frac{s}{2}}\left(\left(\tfrac{8}{3}\right)^{\frac{1}{2}}\pi j\left[\vec{k}^{\top}S_2^{-1}\vec{k}\right]^{\frac{1}{2}}\right)\right\}.
\end{aligned}
\tag{6.6.26}
$$

The quadratic form here is $\frac{8}{3}\vec{k}^{\top}S_2^{-1}\vec{k} = 3k_1^2+3k_2^2+2k_1k_2 = m$ and has the following property: m is even iff (k_1+k_2) is even and odd iff (k_1+k_2) is odd. We can therefore use (6.6.16) with a slight modification in the second Bessel sum,

$$
\begin{aligned}
Z_{S_3}\left(\tfrac{s}{2}\right) &= \frac{3^{\frac{s}{2}}\pi}{2^{\frac{s}{2}-\frac{1}{2}}(s-2)}\zeta(s-2) + \frac{2^{\frac{3}{2}(s-1)}\pi^{\frac{1}{2}}\Gamma\left(\frac{1}{2}(s-1)\right)}{3^{s-1}\Gamma\left(\frac{s}{2}\right)}\zeta(s-1)+\zeta(s) \\
&+ \frac{4\times 3^{\frac{1}{2}(s-1)}\pi^{\frac{s}{2}}}{8^{\frac{1}{4}(s-1)}\Gamma\left(\frac{s}{2}\right)}\sum_{i,j\in\mathbb{N}}\left(i^{-1}j\right)^{\frac{1}{2}(s-1)}cos\left(\frac{2\pi}{3}ij\right)\ K_{\frac{1}{2}(1-s)}\left(\frac{4\sqrt{2}\pi}{3}ij\right) \\
&+ \frac{3^{\frac{s}{2}}\pi^{\frac{s}{2}}}{2^{s-\frac{3}{2}}\Gamma\left(\frac{s}{2}\right)}\sum_{j,m\in\mathbb{N}}(-1)^{jm}j^{(1-\frac{s}{2})}m^{\frac{1}{2}(\frac{s}{2}-1)}\ r_2^{\alpha S_2^{-1}}(m)\ K_{\frac{s}{2}-1}\left(\pi j\sqrt{m}\right).
\end{aligned}
\tag{6.6.27}
$$

This formula is ideal for low values of the exponent s. For large values of s, the second sum containing Bessel functions and the first term containing the Riemann $\zeta(s-2)$ function become infinitely large but opposite in sign with $s\to\infty$. This can in principle be rectified by taking the problematic terms out of the summation, but is not required here as we can use the Dirichlet series for large s values.

6.6.3 The Face-Centered Cubic Case

For this case we get for the symmetric matrix of our quadratic form,

$$\sum_{i,j,k\in\mathbb{Z}}{}' (S_{ijk}^{\text{fcc}})^{-\frac{s}{2}} = \mathscr{Z}_{A_3^{\text{fcc}}}(s;0_3,0_3) \quad , \quad A_3^{\text{fcc}} = \frac{1}{\sqrt{2}}\begin{pmatrix}1&1&0\\0&1&1\\1&0&1\end{pmatrix} \tag{6.6.28}$$

$$\left(A_3^{\text{fcc}\top}A_3^{\text{fcc}}\right) = S_3^{\text{fcc}} = \frac{1}{2}\begin{pmatrix}2&1&1\\1&2&1\\1&1&2\end{pmatrix} \quad , \quad S_2^{\text{fcc}} = \frac{1}{2}\begin{pmatrix}2&1\\1&2\end{pmatrix}, \tag{6.6.29}$$

$$\left(S_2^{\text{fcc}}\right)^{-1} = \frac{2}{3}\begin{pmatrix}2&-1\\-1&2\end{pmatrix},$$

which leads to $\vec{b}_2^{\top} = \frac{1}{2}(1,1)$ and $\vec{k}^{\top}\vec{q}_2 = \frac{1}{2}(k_1+k_2)$ like in the bcc case. Unlike the bcc case however we can use (6.2.4) with the matrix,

$$\left(A_3^{\text{fcc}\top}A_3^{\text{fcc}}\right) = S_3^{\text{fcc}} = \frac{1}{2}\begin{pmatrix}2&0&0\\0&1&0\\0&0&1\end{pmatrix}, \tag{6.6.30}$$

with $S_2 = S_2^{-1} = I_2$, $\vec{b}_2 = \vec{0}_2$, $\alpha = 1$, σ_{12}=0, σ_{22}=1, p=1, t=2, and $\det(S_2) = 1$. This is similar to the simple cubic case except for the t-factor appearing for example in the second Bessel sum, i.e., using (6.6.16) we get

$$\begin{aligned} Z_{S_3} &= \frac{2^{2-\frac{s}{2}}\pi}{s-2}\zeta(s-2) + \pi^{\frac{1}{2}}\Gamma\left(\tfrac{1}{2}(s-1)\right)\Gamma\left(\tfrac{s}{2}\right)^{-1}\zeta(s-1) + \zeta(s) \\ &+ 4\pi^{\frac{s}{2}}\Gamma\left(\tfrac{s}{2}\right)^{-1}\sum_{i,j\in\mathbb{N}}\left(i^{-1}j\right)^{\frac{1}{2}(s-1)}K_{\frac{1}{2}(s-1)}(2\pi ij) \\ &+ \frac{2^{\frac{3}{2}-\frac{s}{4}}\pi^{\frac{s}{2}}}{\Gamma\left(\frac{s}{2}\right)}\sum_{j,k\in\mathbb{N}} j^{(1-\frac{s}{2})}k^{\frac{1}{2}(\frac{s}{2}-1)}\, r_2^{S_2^{-1}}(k)\, K_{\frac{s}{2}-1}\left(2\sqrt{2}\pi jk^{\frac{1}{2}}\right). \end{aligned} \tag{6.6.31}$$

6.6.4 The hexagonal close-packed case

If we take the original lattice sum for hcp introduced by Kane and Goeppert-Mayer in 1940,[24] we get

$$\sum_{i,j,k\in\mathbb{Z}}{}' (S_{ijk}^{\mathrm{hcp1}})^{-\frac{s}{2}} = \mathscr{Z}_{A_3^{\mathrm{hcp}}}(s;0_3,0_3) \quad with \quad A_3^{\mathrm{hcp}} = \frac{1}{2}\begin{pmatrix} \sqrt{2+\sqrt{3}} & \sqrt{2-\sqrt{3}} & 0 \\ \sqrt{2-\sqrt{3}} & \sqrt{2+\sqrt{3}} & 0 \\ 0 & 0 & \sqrt{\frac{32}{3}} \end{pmatrix} \tag{6.6.32}$$

$$\sum_{i,j,k\in\mathbb{Z}}{}' (S_{ijk}^{\mathrm{hcp2}})^{-\frac{s}{2}} = \mathscr{Z}_{A_3^{\mathrm{hcp}}}(s;0_3,\vec{v}) \quad with \quad \vec{v} = \frac{1}{\sqrt{6}}(1,1,2)^{\top}. \tag{6.6.33}$$

However, the Terras decomposition is available for pure quadratic forms only and it is not clear if it can be extended for the more general Epstein zeta function (6.6.1). We therefore consider instead the matrices derived from (6.2.14),

$$\left(A_3^{\mathrm{hcp1}\top} A_3^{\mathrm{hcp1}}\right) = S_3^{\mathrm{hcp1}} = \begin{pmatrix} c & 0 & 0 \\ 0 & 1 & \frac{1}{2} \\ 0 & \frac{1}{2} & 1 \end{pmatrix}, \quad S_2^{\mathrm{hcp1}} = \begin{pmatrix} 1 & \frac{1}{2} \\ \frac{1}{2} & 1 \end{pmatrix} \tag{6.6.34}$$

$$, \quad \left(S_2^{\mathrm{hcp1}}\right)^{-1} = \frac{4}{3}\begin{pmatrix} 1 & -\frac{1}{2} \\ -\frac{1}{2} & 1 \end{pmatrix}$$

with $c \in \{\frac{2}{3}, 2, \frac{8}{3}, 8\}$, σ_{22}=1, $\sigma_{12} = \frac{1}{2}$, $p = \frac{3}{4}$, $a = t = c$, $\vec{b}_2^{\top} = \vec{q}_2^{\top} = (0,0)$ and $det(S_2) = \frac{3}{4}$. From this we obtain

$$\begin{aligned} Z_{S_3}\left(\tfrac{s}{2},c\right) &= \pi\left(\tfrac{3}{4}\right)^{-\frac{1}{2}} c^{1-\frac{s}{2}} \Gamma\left(\tfrac{s}{2}-1\right)\Gamma\left(\tfrac{s}{2}\right)^{-1}\zeta(s-2) \\ &+ \left(\tfrac{3}{4}\right)^{\frac{1}{2}(1-s)} \pi^{\frac{1}{2}} \Gamma\left(\tfrac{1}{2}(s-1)\right)\Gamma\left(\tfrac{s}{2}\right)^{-1}\zeta(s-1) + \zeta(s) \\ &+ 4\pi^{\frac{s}{2}}\left(\tfrac{3}{4}\right)^{\frac{1}{4}(1-s)} \Gamma\left(\tfrac{s}{2}\right)^{-1} \sum_{i,j\in\mathbb{N}} (-1)^{ij}\left(i^{-1}j\right)^{\frac{1}{2}(s-1)} K_{\frac{1}{2}(1-s)}\left(\sqrt{3}\pi ij\right) \\ &+ \frac{2\left(\frac{3}{4}\right)^{-\frac{1}{2}} c^{\frac{1}{2}(1-\frac{s}{2})}\pi^{\frac{s}{2}}}{\Gamma\left(\frac{s}{2}\right)} \sum_{j\in\mathbb{N};\vec{k}\in\mathbb{Z}^2\setminus\{\vec{0}_2\}} \left\{ j^{(1-\frac{s}{2})}\left(\vec{k}^{\top} S_2^{-1}\vec{k}\right)^{\frac{1}{2}(\frac{s}{2}-1)} \right. \\ &\qquad \left. K_{1-\frac{s}{2}}\left(2\pi j\left[c\vec{k}^{\top} S_2^{-1}\vec{k}\right]^{\frac{1}{2}}\right)\right\}. \end{aligned} \tag{6.6.35}$$

Adding the individual terms together in (6.2.14) with the different prefactors and c-values, and using our number-theoretical tool as before, we get

$$
\begin{aligned}
Z_{S_3}\left(\tfrac{s}{2}\right) &= \frac{3}{2}Z_{S_3}\left(\tfrac{s}{2},\tfrac{8}{3}\right)+\frac{3^{\frac{s}{2}}}{2}Z_{S_3}\left(\tfrac{s}{2},2\right)-\frac{3^{\frac{s}{2}}}{2}Z_{S_3}\left(\tfrac{s}{2},8\right)-\frac{1}{2}Z_{S_3}\left(\tfrac{s}{2},\tfrac{2}{3}\right)\\
&= \frac{2\sqrt{2}}{s-2}\left(\tfrac{3}{2}\right)^{\frac{s-3}{2}}\pi\zeta(s-2)\\
&+\left(\tfrac{3}{4}\right)^{\frac{1}{2}(1-s)}\pi^{\frac{1}{2}}\Gamma\left(\tfrac{1}{2}(s-1)\right)\Gamma\left(\tfrac{s}{2}\right)^{-1}\zeta(s-1)+\zeta(s)\\
&+4\left(\tfrac{3}{4}\right)^{\frac{1}{4}(1-s)}\pi^{\frac{s}{2}}\Gamma\left(\tfrac{s}{2}\right)^{-1}\sum_{j,k\in\mathbb{N}}\left\{(-1)^{jk}\left(jk^{-1}\right)^{\frac{1}{2}(1-s)}\right.\\
&\qquad\left.K_{\frac{1}{2}(1-s)}\left(\sqrt{3}\pi jk\right)\right\}\\
&+2^{\frac{1}{4}(6-s)}\sqrt{3}\pi^{\frac{s}{2}}\Gamma\left(\tfrac{s}{2}\right)^{-1}\sum_{j,k\in\mathbb{N}}\left\{j^{(1-\frac{s}{2})}k^{\frac{1}{2}(\frac{s}{2}-1)}\,r_2^{\alpha S_2^{-1}}(k)\right.\\
&\qquad\left.K_{1-\frac{s}{2}}\left(\tfrac{8}{3}\sqrt{2}\pi jk^{\frac{1}{2}}\right)\right\}\\
&+2^{\frac{1}{4}(s+2)}3^{\frac{s}{4}}\pi^{\frac{s}{2}}\Gamma\left(\tfrac{s}{2}\right)^{-1}\sum_{j,k\in\mathbb{N}}\left\{j^{(1-\frac{s}{2})}k^{\frac{1}{2}(\frac{s}{2}-1)}\,r_2^{\alpha S_2^{-1}}(k)\right.\\
&\qquad\left.K_{1-\frac{s}{2}}\left(4\sqrt{\tfrac{2}{3}}\pi jk^{\frac{1}{2}}\right)\right\}\\
&-\left(\tfrac{3}{2}\right)^{\frac{s}{4}}2^{\frac{3}{2}}\pi^{\frac{s}{2}}\Gamma\left(\tfrac{s}{2}\right)^{-1}\sum_{j,k\in\mathbb{N}}\left\{j^{(1-\frac{s}{2})}k^{\frac{1}{2}(\frac{s}{2}-1)}\,r_2^{\alpha S_2^{-1}}(k)\right.\\
&\qquad\left.K_{1-\frac{s}{2}}\left(8\sqrt{\tfrac{2}{3}}\pi jk^{\frac{1}{2}}\right)\right\}\\
&-2^{\frac{1}{4}(s+2)}3^{-\frac{1}{2}}\pi^{\frac{s}{2}}\Gamma\left(\tfrac{s}{2}\right)^{-1}\sum_{j,k\in\mathbb{N}}\left\{j^{(1-\frac{s}{2})}k^{\frac{1}{2}(\frac{s}{2}-1)}\,r_2^{\alpha S_2^{-1}}(k)\right.\\
&\qquad\left.K_{1-\frac{s}{2}}\left(\tfrac{4}{3}\sqrt{2}\pi jk^{\frac{1}{2}}\right)\right\}
\end{aligned}
\tag{6.6.36}
$$

with $\alpha=\frac{3}{4}$.

We finally note that the sums containing the Bessel functions are fast converging because of their asymptotic behavior, e.g. $K_{1/2}(x)\sim(\pi/2x)^{\frac{1}{2}}e^{-x}$. The expansion in terms of Bessel functions is particularly useful for the L_s coefficients with low exponent s. For large s values the Dirichlet series is numerically far more stable as already mentioned, the Epstein Bessel function expansion can contain large compensating terms with increasing exponent s.

6.7 The Van der Hoff–Benson Expansion

Van der Hoff and Benson derived a number of interesting expansions for lattice sums that are very useful for the lattices considered here.[111] We start with a more general expansion than that presented in the original paper,

$$\begin{aligned}\sum_{i\in\mathbb{Z}}\left[(i+a)^2+x^2\right]^{-s} &= \pi^{\frac{1}{2}}\frac{\Gamma\left(s-\frac{1}{2}\right)}{\Gamma(s)}|x|^{1-2s} \\ &+4\pi^s\Gamma(s)^{-1}\sum_{m\in\mathbb{N}}\left(\frac{m}{|x|}\right)^{s-\frac{1}{2}}cos(2\pi ma)\,K_{s-\frac{1}{2}}(2\pi m|x|)\end{aligned} \tag{6.7.1}$$

with $a\in[0,1)$. The proof can be found in the Appendix 6.A. The expansion does not reduce the number of summations for the triple sums we are seeking, but the expression on the right hand side contains a series of fast converging Bessel sums as discussed in the previous section. More important here is that these expansions can be used not only for the cubic lattices but also for the hcp structure as we shall see. The Van der Hoff–Benson expansion is computationally as efficient as the one used for the Epstein zeta function introduced in the previous section.[112] The resulting equations are perhaps related to the one from the Epstein decomposition, which we do not explore further here.

6.7.1 The simple cubic case

We use $a=0$ for (6.7.1) and get

$$\sum_{i\in\mathbb{Z}}\left(i^2+x^2\right)^{-s}=\frac{\pi^{1/2}\Gamma\left(s-\frac{1}{2}\right)}{|x|^{2s-1}\Gamma(s)}+\frac{4\pi^s}{|x|^{s-\frac{1}{2}}\Gamma(s)}\sum_{m\in\mathbb{N}}m^{s-\frac{1}{2}}K_{s-\frac{1}{2}}(2\pi m|x|) \tag{6.7.2}$$

with $x\neq 0$. To proceed we replace s with $\frac{s}{2}$ and put $x=(j^2+k^2)^{1/2}$ for our lattice sum, and remember that the case $x\neq 0$ was excluded. In order to correct for this we introduce an extra sum from the original summation over the index i in (6.2.1). Finally we sum over the remaining two indices i,j of the lattice sum,

$$\begin{aligned}L_s^{sc} &= {\sum_{i\in\mathbb{Z}}}' i^{-s}+\frac{\pi^{1/2}\Gamma\left(\frac{s-1}{2}\right)}{\Gamma\left(\frac{s}{2}\right)}{\sum_{j,k\in\mathbb{Z}}}'\left(j^2+k^2\right)^{\frac{1-s}{2}} \\ &+\frac{4\pi^{\frac{s}{2}}}{\Gamma\left(\frac{s}{2}\right)}{\sum_{j,k\in\mathbb{Z}}}'\sum_{m\in\mathbb{N}}\left(\frac{m}{(j^2+k^2)^{\frac{1}{2}}}\right)^{\frac{s-1}{2}}K_{\frac{s-1}{2}}\left(2\pi m\left(j^2+k^2\right)^{\frac{1}{2}}\right).\end{aligned} \tag{6.7.3}$$

Using the definitions (11.A.1) and (6.4.3) and taking special cases $k=0$ or $j=0$ out of the sum to use symmetry in both summation indices we get

$$L_s^{sc} = 2\zeta(s) + \frac{4\pi^{1/2}\Gamma\left(\frac{s-1}{2}\right)}{\Gamma\left(\frac{s}{2}\right)}\zeta(\tfrac{s-1}{2})\beta(\tfrac{s-1}{2}) + \frac{16\pi^{\frac{s}{2}}}{\Gamma\left(\frac{s}{2}\right)}\sum_{k,m\in\mathbb{N}}\left(\frac{m}{k}\right)^{\frac{s-1}{2}} K_{\frac{s-1}{2}}(2\pi mk) + \frac{16\pi^{\frac{s}{2}}}{\Gamma\left(\frac{s}{2}\right)}\sum_{j,k,m\in\mathbb{N}}\left(\frac{m}{(j^2+k^2)^{\frac{1}{2}}}\right)^{\frac{s-1}{2}} K_{\frac{s-1}{2}}\left(2\pi m\left(j^2+k^2\right)^{\frac{1}{2}}\right). \quad (6.7.4)$$

We could use again the Dirichlet L-series in the last sum as we did for the Epstein zeta function. However, we can also take care of the special case $(j=k)$ and simplify further by using permutation symmetry of j,k,

$$L_s^{sc} = 2\zeta(s) + \frac{4\pi^{1/2}\Gamma\left(\frac{s-1}{2}\right)}{\Gamma\left(\frac{s}{2}\right)}\zeta(\tfrac{s-1}{2})\beta(\tfrac{s-1}{2}) + \frac{16\pi^{\frac{s}{2}}}{\Gamma\left(\frac{s}{2}\right)}\sum_{k,m\in\mathbb{N}}\left(\frac{m}{k}\right)^{\frac{s-1}{2}}\left\{K_{\frac{s-1}{2}}(2\pi mk) + 2^{\frac{1-s}{4}}K_{\frac{s-1}{2}}\left(2\sqrt{2}\pi mk\right)\right\} + \frac{32\pi^{\frac{s}{2}}}{\Gamma\left(\frac{s}{2}\right)}\sum_{m,j<k\in\mathbb{N}}\left(\frac{m}{(j^2+k^2)^{\frac{1}{2}}}\right)^{\frac{s-1}{2}} K_{\frac{s-1}{2}}\left(2\pi m\left(j^2+k^2\right)^{\frac{1}{2}}\right). \quad (6.7.5)$$

6.7.2 The body-centered cubic case

We choose $a=\frac{1}{2}$ for (6.7.1),

$$\sum_{i\in\mathbb{Z}}\left((2i+1)^2+x^2\right)^{-s} = \frac{\pi^{1/2}\Gamma\left(s-\frac{1}{2}\right)}{2|x|^{2s-1}\Gamma(s)} + \frac{2^{\frac{3}{2}-s}\pi^s}{|x|^{s-\frac{1}{2}}\Gamma(s)}\sum_{m\in\mathbb{N}}(-1)^m m^{s-\frac{1}{2}}K_{s-\frac{1}{2}}(\pi m|x|), \quad (6.7.6)$$

and consider the second term in (6.2.7) together with (6.7.6) and $x \equiv x_{jk}^2 =$

$(2j+1)^2+(2k+1)^2,$

$$L_s^{\mathrm{bcc}} = \sum_{i,j,k\in\mathbb{Z}} \left[(2i+1)^2+(2j+1)^2+(2k+1)^2\right]^{-\frac{s}{2}} = \frac{\pi^{1/2}\Gamma\left(\frac{s-1}{2}\right)}{2\Gamma\left(\frac{s}{2}\right)} {\sum_{j,k\in\mathbb{Z}}}' |x_{jk}|^{1-s} + \frac{2^{\frac{3-s}{2}}\pi^{\frac{s}{2}}}{\Gamma\left(\frac{s}{2}\right)} {\sum_{j,k\in\mathbb{Z}}}' |x_{jk}|^{\frac{1-s}{2}} \sum_{m\in\mathbb{N}} (-1)^m m^{\frac{s-1}{2}} K_{\frac{s-1}{2}}\left(\pi m|x_{jk}|\right). \tag{6.7.7}$$

We came across the double sum on the left hand side of this equation before in (6.4.12). Now we further expand this sum by using (6.7.6) again and obtain,

$$\begin{aligned} L_s^{\mathrm{bcc}} = {} & \frac{\pi\Gamma\left(\frac{s}{2}-1\right)}{4\Gamma\left(\frac{s}{2}\right)} \sum_{k\ odd,\ k\in\mathbb{Z}} |k|^{2-s} \\ & + \frac{2^{1-\frac{s}{2}}\pi^{\frac{s}{2}}}{\Gamma\left(\frac{s}{2}\right)} \sum_{k\ odd,\ k\in\mathbb{Z}} |k|^{1-\frac{s}{2}} \sum_{m\in\mathbb{N}} (-1)^m m^{\frac{s}{2}-1} K_{\frac{s}{2}-1}\left(\pi m|k|\right) \\ & + \frac{2^{\frac{3-s}{2}}\pi^{\frac{s}{2}}}{\Gamma\left(\frac{s}{2}\right)} \sum_{j,k\in\mathbb{Z}} |x_{jk}|^{\frac{1-s}{2}} \sum_{m\in\mathbb{N}} (-1)^m m^{\frac{s-1}{2}} K_{\frac{s-1}{2}}\left(\pi m|x_{jk}|\right). \end{aligned} \tag{6.7.8}$$

Using (6.6.18) and (6.4.13) and considering again symmetry and the special case $j=k$ we get

$$\begin{aligned} L_s^{\mathrm{bcc}} = {} & \frac{\pi}{(s-2)}\left(1-2^{2-s}\right)\zeta(s-2) \\ & + \frac{2^{2-\frac{s}{2}}\pi^{\frac{s}{2}}}{\Gamma\left(\frac{s}{2}\right)} \sum_{k\ odd,\ k\in\mathbb{N}} \sum_{m\in\mathbb{N}} (-1)^m \left(\frac{m}{k}\right)^{\frac{s}{2}-1} K_{\frac{s}{2}-1}\left(\pi mk\right) \\ & + \frac{2^{\frac{3}{4}(5-s)}\pi^{\frac{s}{2}}}{\Gamma\left(\frac{s}{2}\right)} \sum_{k\ odd,\ k\in\mathbb{N}} \sum_{m\in\mathbb{N}} (-1)^m \left(\frac{m}{k}\right)^{\frac{s-1}{2}} K_{\frac{s-1}{2}}\left(\sqrt{2}\pi mk\right) \\ & + \frac{2^{\frac{9-s}{2}}\pi^{\frac{s}{2}}}{\Gamma\left(\frac{s}{2}\right)} \sum_{j\wedge k\ odd,\ j<k\in\mathbb{N}} \sum_{m\in\mathbb{N}} (-1)^m \left(\frac{m}{(j^2+k^2)^{\frac{1}{2}}}\right)^{\frac{s-1}{2}} \\ & \qquad \times K_{\frac{s-1}{2}}\left(\pi m\left(j^2+k^2\right)^{\frac{1}{2}}\right). \end{aligned} \tag{6.7.9}$$

We note that as in the case of the Epstein zeta function we have large compensating terms here which requires further attention for large exponents s, e.g. one has to use quadruple precision for the accurate calculation of the lattice sums or take care of these large terms. Nevertheless, adding the sc and bcc terms from (6.2.7), (6.7.5) and (6.7.8) we finally get,

$$
\begin{aligned}
L_s^{bcc} &= 2\left(\frac{3}{4}\right)^{\frac{s}{2}}\zeta(s)+\frac{3^{\frac{s}{2}}\pi}{(s-2)}\left(1-2^{2-s}\right)\zeta(s-2)\\
&+4\left(\frac{3}{4}\right)^{\frac{s}{2}}\frac{\pi^{1/2}\Gamma\left(\frac{s-1}{2}\right)}{\Gamma\left(\frac{s}{2}\right)}\zeta(\tfrac{s-1}{2})\beta(\tfrac{s-1}{2})\\
&+\left(\frac{3}{4}\right)^{\frac{s}{2}}\frac{16\pi^{\frac{s}{2}}}{\Gamma\left(\frac{s}{2}\right)}\sum_{k,m\in\mathbb{N}}\left(\frac{m}{k}\right)^{\frac{s-1}{2}}\left\{K_{\frac{s-1}{2}}(2\pi mk)+2^{\frac{1-s}{4}}K_{\frac{s-1}{2}}\left(2\sqrt{2}\pi mk\right)\right\}\\
&+\frac{3^{\frac{s}{2}}2^{2-\frac{s}{2}}\pi^{\frac{s}{2}}}{\Gamma\left(\frac{s}{2}\right)}\sum_{k\ odd,\ k\in\mathbb{N}}\sum_{m\in\mathbb{N}}(-1)^m\left(\frac{m}{k}\right)^{\frac{s}{2}-1}K_{\frac{s}{2}-1}(\pi mk)\\
&+\frac{3^{\frac{s}{2}}2^{\frac{3}{4}(5-s)}\pi^{\frac{s}{2}}}{\Gamma\left(\frac{s}{2}\right)}\sum_{k\ odd,\ k\in\mathbb{N}}\sum_{m\in\mathbb{N}}(-1)^m\left(\frac{m}{k}\right)^{\frac{s-1}{2}}K_{\frac{s-1}{2}}\left(\sqrt{2}\pi mk\right)\\
&+32\left(\frac{3}{4}\right)^{\frac{s}{2}}\frac{\pi^{\frac{s}{2}}}{\Gamma\left(\frac{s}{2}\right)}\sum_{m,j<k\in\mathbb{N}}\left(\frac{m}{(j^2+k^2)^{\frac{1}{2}}}\right)^{\frac{s-1}{2}}K_{\frac{s-1}{2}}\left(2\pi m\left(j^2+k^2\right)^{\frac{1}{2}}\right)\\
&+\frac{3^{\frac{s}{2}}2^{\frac{9-s}{2}}\pi^{\frac{s}{2}}}{\Gamma\left(\frac{s}{2}\right)}\sum_{j\wedge k\ odd,\ j<k\in\mathbb{N}}\sum_{m\in\mathbb{N}}(-1)^m\left(\frac{m}{(j^2+k^2)^{\frac{1}{2}}}\right)^{\frac{s-1}{2}}\\
&\qquad\times K_{\frac{s-1}{2}}\left(\pi m\left(j^2+k^2\right)^{\frac{1}{2}}\right).
\end{aligned}
\tag{6.7.10}
$$

We can, for example, make further simplifications by combining the Bessel function sums containing the $\sqrt{2}$ in the argument,

$$
\begin{aligned}
L_s^{bcc} &= 2\left(\frac{3}{4}\right)^{\frac{s}{2}}\zeta(s)+\frac{3^{\frac{s}{2}}\pi}{(s-2)}\left(1-2^{2-s}\right)\zeta(s-2)\\
&+4\left(\frac{3}{4}\right)^{\frac{s}{2}}\frac{\pi^{1/2}\Gamma\left(\frac{s-1}{2}\right)}{\Gamma\left(\frac{s}{2}\right)}\zeta(\tfrac{s-1}{2})\beta(\tfrac{s-1}{2})\\
&+\left(\frac{3}{4}\right)^{\frac{s}{2}}\frac{16\pi^{\frac{s}{2}}}{\Gamma\left(\frac{s}{2}\right)}\sum_{k,m\in\mathbb{N}}\left(\frac{m}{k}\right)^{\frac{s-1}{2}}K_{\frac{s-1}{2}}(2\pi mk)\\
&+\frac{3^{\frac{s}{2}}2^{2-\frac{s}{2}}\pi^{\frac{s}{2}}}{\Gamma\left(\frac{s}{2}\right)}\sum_{k\ odd,\ k\in\mathbb{N}}\sum_{m\in\mathbb{N}}(-1)^m\left(\frac{m}{k}\right)^{\frac{s}{2}-1}K_{\frac{s}{2}-1}(\pi mk)\\
&+\frac{3^{\frac{s}{2}}2^{\frac{3}{4}(5-s)}\pi^{\frac{s}{2}}}{\Gamma\left(\frac{s}{2}\right)}\sum_{k,m\in\mathbb{N}}(-1)^{mk}\left(\frac{m}{k}\right)^{\frac{s-1}{2}}K_{\frac{s-1}{2}}\left(\sqrt{2}\pi mk\right)\\
&+32\left(\frac{3}{4}\right)^{\frac{s}{2}}\frac{\pi^{\frac{s}{2}}}{\Gamma\left(\frac{s}{2}\right)}\sum_{m,j<k\in\mathbb{N}}\left(\frac{m}{(j^2+k^2)^{\frac{1}{2}}}\right)^{\frac{s-1}{2}}K_{\frac{s-1}{2}}\left(2\pi m\left(j^2+k^2\right)^{\frac{1}{2}}\right)\\
&+\frac{3^{\frac{s}{2}}2^{\frac{9-s}{2}}\pi^{\frac{s}{2}}}{\Gamma\left(\frac{s}{2}\right)}\sum_{j\wedge k\ odd,\ j<k\in\mathbb{N}}\sum_{m\in\mathbb{N}}(-1)^m\left(\frac{m}{(j^2+k^2)^{\frac{1}{2}}}\right)^{\frac{s-1}{2}}\\
&\qquad\times K_{\frac{s-1}{2}}\left(\pi m\left(j^2+k^2\right)^{\frac{1}{2}}\right).
\end{aligned}
\tag{6.7.11}
$$

6.7.3 The face-centered cubic case

For the fcc case we proceed in a similar fashion using $x^2 = \left(j^2+k^2\right)/2$ for (6.2.4) in the Van der Hoff-Benson Expansion expansion (6.7.2),

$$L_s^{fcc} = 3\times 2^{-\frac{s}{2}} L_s^{fcc1} - 2^{1-\frac{s}{2}} L_s^{sc} = 3\times 2^{-\frac{s}{2}} {\sum_{i,j,k\in\mathbb{Z}}}' \left(i^2+\frac{j^2+k^2}{2}\right)^{-\frac{s}{2}} - 2^{1-\frac{s}{2}} L_s^{sc}. \tag{6.7.12}$$

We treated the sc lattice before and only consider the first part in this equation. This sum, however, is similar to the sc case, i.e., we only have to substitute $j \to j/\sqrt{2}$ and $k \to k/\sqrt{2}$ and get

$$\begin{aligned} L_s^{fcc} = {\sum_{i,j,k\in\mathbb{Z}}}' \left(i^2+\frac{j^2+k^2}{2}\right)^{-\frac{s}{2}} &= 2\zeta(s) + \frac{2^{\frac{s+3}{2}}\pi^{1/2}\Gamma\left(\frac{s-1}{2}\right)}{\Gamma\left(\frac{s}{2}\right)}\zeta(\tfrac{s-1}{2})\beta(\tfrac{s-1}{2}) \\ &+ \frac{16\pi^{\frac{s}{2}}}{\Gamma\left(\frac{s}{2}\right)} \sum_{k,m\in\mathbb{N}} \left(\frac{m}{k}\right)^{\frac{s-1}{2}} \left\{ 2^{\frac{s-1}{4}} K_{\frac{s-1}{2}}\left(\sqrt{2}\pi mk\right) + K_{\frac{s-1}{2}}\left(2\pi mk\right)\right\} \\ &+ 32\frac{2^{\frac{s-1}{4}}\pi^{\frac{s}{2}}}{\Gamma\left(\frac{s}{2}\right)} \sum_{m,j<k\in\mathbb{N}} \left(\frac{m}{\left(j^2+k^2\right)^{\frac{1}{2}}}\right)^{\frac{s-1}{2}} K_{\frac{s-1}{2}}\left(\sqrt{2}\pi m\left(j^2+k^2\right)^{\frac{1}{2}}\right). \end{aligned} \tag{6.7.13}$$

6.7.4 The hexagonal close-packed case

As already mentioned the hcp structure is the most difficult case to be treated for lower exponents s. For the Terras decomposition of the Epstein zeta function one has an additional $\vec{v}$-vector in (6.6.33), and the method only applies for pure quadratic forms which requires a minimum of four terms. However, for both sums in (6.2.9) and (6.2.12) we can apply the Van der Hoff-Benson expansion and, in addition, may apply Terras' decomposition for the remaining double sum. We consider the two different decompositions here.

Case 1

We rewrite (6.2.9) as

$$\begin{aligned} L_s^{hcp} = &\left(\frac{3}{8}\right)^{\frac{s}{2}} {\sum_{i,j,k\in\mathbb{Z}}}' \left[i^2+\tfrac{3}{8}\left(j^2+k^2+jk\right)\right]^{-\frac{s}{2}} \\ &+ \left(\frac{3}{2}\right)^{\frac{s}{2}} \sum_{i,j,k\in\mathbb{Z}} \left[(2i+1)^2+\tfrac{3}{2}\left\{\left(j+\tfrac{1}{3}\right)^2+\left(k+\tfrac{1}{3}\right)^2+\left(j+\tfrac{1}{3}\right)\left(k+\tfrac{1}{3}\right)\right\}\right]^{-\frac{s}{2}}. \end{aligned} \tag{6.7.14}$$

Now we can use both expansions (6.7.2) and (6.7.6) and remember that the case $x \neq 0$ was excluded in (6.7.2),

$$\begin{aligned} L_s^{hcp} &= 2\left(\tfrac{3}{8}\right)^{\frac{s}{2}}\zeta(s) + \frac{\left(\frac{3}{8}\right)^{\frac{1}{2}}\pi^{1/2}\Gamma\left(\frac{s-1}{2}\right)}{\Gamma\left(\frac{s}{2}\right)} \sum_{j,k\in\mathbb{Z}} \left\{|x_{jk}|^{1-s} + |y_{jk}|^{1-s}\right\} \\ &+ \frac{4\left(\frac{3}{8}\right)^{\frac{1+s}{4}}\pi^{\frac{s}{2}}}{\Gamma\left(\frac{s}{2}\right)} \sum_{j,k\in\mathbb{Z}} |x_{jk}|^{\frac{1-s}{2}} \sum_{m\in\mathbb{N}} m^{\frac{s-1}{2}} K_{\frac{s-1}{2}}\left(\sqrt{\tfrac{3}{2}}\pi m|x_{jk}|\right) \\ &+ \frac{4\left(\frac{3}{8}\right)^{\frac{1+s}{4}}\pi^{\frac{s}{2}}}{\Gamma\left(\frac{s}{2}\right)} \sum_{j,k\in\mathbb{Z}} |y_{jk}|^{\frac{1-s}{2}} \sum_{m\in\mathbb{N}} (-1)^m m^{\frac{s-1}{2}} K_{\frac{s-1}{2}}\left(\sqrt{\tfrac{3}{2}}\pi m|y_{jk}|\right), \end{aligned} \tag{6.7.15}$$

with the definitions

$$\begin{aligned} x_{jk}^2 &= \left(j^2 + k^2 + jk\right), \\ y_{jk}^2 &= \left(j+\tfrac{1}{3}\right)^2 + \left(k+\tfrac{1}{3}\right)^2 + \left(j+\tfrac{1}{3}\right)\left(k+\tfrac{1}{3}\right). \end{aligned} \tag{6.7.16}$$

The sums containing Bessel functions are converging fast. The remaining problem lies in the slow converging double sums in this expression. For the first sum over x_{jk} we can apply Terras' expansion of the Epstein zeta function using the matrix

$$S_2^{fcc} = \frac{1}{2}\begin{pmatrix} 2 & 1 \\ 1 & 2 \end{pmatrix}, \quad \left(S_2^{fcc}\right)^{-1} = \frac{2}{3}\begin{pmatrix} 2 & -1 \\ -1 & 2 \end{pmatrix}. \tag{6.7.17}$$

This gives according to the definitions in (6.6.11) using $\sigma_{22} = 1$, $\sigma_{12} = \frac{1}{2}$ and $p = \frac{3}{4}$,

$$\begin{aligned} Z_{S_2}\left(\tfrac{s-1}{2}\right) &= \left(\tfrac{3}{4}\right)^{1-\frac{s}{2}}\pi^{\frac{1}{2}}\Gamma\left(\tfrac{s}{2}-1\right)\Gamma\left(\tfrac{s-1}{2}\right)^{-1}\zeta(s-2) + \zeta(s-1) \\ &+ 2\sqrt{3}\left(\tfrac{4}{3}\right)^{\frac{s}{4}}\pi^{\frac{s-1}{2}}\Gamma\left(\tfrac{s-1}{2}\right)^{-1} \sum_{j,k\in\mathbb{N}} (-1)^{jk}\left(jk^{-1}\right)^{\frac{s}{2}-1} K_{\frac{s}{2}-1}\left(\sqrt{3}\pi jk\right). \end{aligned} \tag{6.7.18}$$

We note that this double sum has been decomposed into a product of simple Dirichlet L-functions by Zucker and Robertson,[105] which we apply for second case. However, as Bessel functions are already used here, for numerical accuracy it does not matter which technique is applied.

The other double sum containing the y_{jk} terms requires some special attention. It is a summation on a two-dimensional hexagonal lattice and can therefore be

related to another summation given by Van der Hoff and Benson,[111]

$$\begin{aligned}\sum_{j,k\in\mathbb{Z}}|y_{jk}|^{-s} &= \sum_{j,k\in\mathbb{Z}}\left[\left(j+\tfrac{1}{3}\right)^2+\left(k+\tfrac{1}{3}\right)^2+\left(j+\tfrac{1}{3}\right)\left(k+\tfrac{1}{3}\right)\right]^{-\frac{s}{2}} \\ &= \frac{3^{\frac{s}{2}}-1}{2}\left\{\sum_{j,k\in\mathbb{Z}}{}'\left(j^2+3k^2\right)^{-\frac{s}{2}}+\sum_{j,k\in\mathbb{Z}}\left[\left(j+\tfrac{1}{2}\right)^2+3\left(k+\tfrac{1}{2}\right)^2\right]^{-\frac{s}{2}}\right\}.\end{aligned} \tag{6.7.19}$$

We use both Van der Hoff-Benson expansions (6.7.2) and (6.7.6) for these sums and obtain,[111]

$$\begin{aligned}\sum_{j,k\in\mathbb{Z}}|y_{jk}|^{-s} &= \left(3^{\frac{s}{2}}-1\right)\zeta(s)+2^{s-1}\sqrt{3}\left(1-3^{-\frac{s}{2}}\right)\pi^{1/2}\frac{\Gamma\left(\frac{s-1}{2}\right)}{\Gamma\left(\frac{s}{2}\right)}\zeta(s-1) \\ &\quad+\frac{4\left(3^{\frac{s}{2}}-1\right)\pi^{\frac{s}{2}}}{3^{\frac{s-1}{4}}\Gamma\left(\frac{s}{2}\right)}\sum_{m,k\in\mathbb{N}}\left(\frac{m}{k}\right)^{\frac{s-1}{2}}K_{\frac{s-1}{2}}\left(2\sqrt{3}\,\pi mk\right) \\ &\quad+\frac{2^{\frac{s+3}{2}}\left(3^{\frac{s}{2}}-1\right)\pi^{\frac{s}{2}}}{3^{\frac{s-1}{4}}\Gamma\left(\frac{s}{2}\right)}\sum_{m,k\in\mathbb{N}}(-1)^m\left(\frac{m}{(2k-1)}\right)^{\frac{s-1}{2}} \\ &\quad\times K_{\frac{s-1}{2}}\left(\sqrt{3}\pi m(2k-1)\right).\end{aligned} \tag{6.7.20}$$

Taking the case $j=k$ out of the double sums containing the Bessel functions, using permutation symmetry, and finally adding, sorting and combining some of the terms gives,

$$
\begin{aligned}
L_s^{\mathrm{hcp}} &= 2\left(\tfrac{3}{8}\right)^{\frac{s}{2}}\zeta(s) + \frac{\left(\frac{3}{8}\right)^{\frac{1}{2}}\pi^{1/2}\Gamma\left(\frac{s-1}{2}\right)}{\Gamma\left(\frac{s}{2}\right)}\left(1+3^{\frac{s-1}{2}}\right)\zeta(s-1) \\
&+ \frac{3\pi}{\sqrt{2}(s-2)}\left(1+2^{s-2}\right)\left(1+3^{\frac{1-s}{2}}\right)\zeta(s-2) \\
&+ \frac{2^{\frac{s-1}{2}}3^{\frac{s+2}{4}}\left(1+3^{\frac{1-s}{2}}\right)\pi^{\frac{s}{2}}}{\Gamma\left(\frac{s}{2}\right)}\sum_{j,k\in\mathbb{N}}(-1)^{jk}\left(jk^{-1}\right)^{\frac{s}{2}-1}K_{\frac{s}{2}-1}\left(\sqrt{3}\pi jk\right) \\
&+ \frac{2^{\frac{9-3s}{4}}\sqrt{3}\,\pi^{\frac{s}{2}}}{\Gamma\left(\frac{s}{2}\right)}\sum_{j,k\in\mathbb{N}}\left(jk^{-1}\right)^{\frac{s-1}{2}}K_{\frac{s-1}{2}}\left(\tfrac{3}{\sqrt{2}}\pi jk\right) \\
&+ \frac{2^{\frac{5-3s}{4}}\sqrt{3}\,\pi^{\frac{s}{2}}}{\Gamma\left(\frac{s}{2}\right)}\sum_{k\in\mathbb{Z}}\left|k+\tfrac{1}{3}\right|^{\frac{1-s}{2}}\sum_{j\in\mathbb{N}}(-1)^j j^{\frac{s-1}{2}}K_{\frac{s-1}{2}}\left(\tfrac{3}{\sqrt{2}}\pi j\left|k+\tfrac{1}{3}\right|\right) \\
&+ \frac{8\left(\frac{3}{8}\right)^{\frac{1+s}{4}}\pi^{\frac{s}{2}}}{\Gamma\left(\frac{s}{2}\right)}\sum_{j<k\in\mathbb{Z}}|x_{jk}|^{\frac{1-s}{2}}\sum_{m\in\mathbb{N}}m^{\frac{s-1}{2}}K_{\frac{s-1}{2}}\left(\sqrt{\tfrac{3}{2}}\pi m|x_{jk}|\right) \\
&+ \frac{8\left(\frac{3}{8}\right)^{\frac{1+s}{4}}\pi^{\frac{s}{2}}}{\Gamma\left(\frac{s}{2}\right)}\sum_{j<k\in\mathbb{Z}}|y_{jk}|^{\frac{1-s}{2}}\sum_{m\in\mathbb{N}}(-1)^m m^{\frac{s-1}{2}}K_{\frac{s-1}{2}}\left(\sqrt{\tfrac{3}{2}}\pi m|y_{jk}|\right).
\end{aligned}
\tag{6.7.21}
$$

This is a rather more complicated expression compared to the cubic cases.

Case 2

The first triple sum in (6.2.12) can be treated by Terras' decomposition of the Epstein zeta function. However, we treat all three sums in (6.2.12) here using the Van der Hoff–Benson expansion (6.7.1). We first rewrite (6.2.12) valid for either sign definitions,

$$
\begin{aligned}
L_s^{\mathrm{hcp}} &= \left(\frac{3}{8}\right)^{\frac{s}{2}}{\sum_{i,j,k\in\mathbb{Z}}}'\left[i^2+\tfrac{3}{8}\left(j^2+k^2\pm jk\right)\right]^{-\frac{s}{2}} \\
&+ \frac{1}{2}\left(\frac{3}{8}\right)^{\frac{s}{2}}\sum_{i,j,k\in\mathbb{Z}}\left[(i+\tfrac{1}{2})^2+\tfrac{1}{8}\left(j^2+k^2\pm jk\right)\right]^{-\frac{s}{2}} \\
&- \frac{1}{2}\left(\frac{3}{8}\right)^{\frac{s}{2}}\sum_{i,j,k\in\mathbb{Z}}\left[(i+\tfrac{1}{2})^2+\tfrac{3}{8}\left(j^2+k^2\pm jk\right)\right]^{-\frac{s}{2}},
\end{aligned}
\tag{6.7.22}
$$

and expand accordingly and reorder the terms,

$$
\begin{aligned}
L_s^{hcp} &= 2\left(\tfrac{3}{8}\right)^{\frac{s}{2}}\zeta(s) + \frac{\pi^{1/2}\Gamma\left(\frac{s-1}{2}\right)}{2^{\frac{5}{2}}\Gamma\left(\frac{s}{2}\right)}\left(\sqrt{3}+3^{\frac{s}{2}}\right)\sum_{j,k\in\mathbb{Z}}{}'\left\{|x_{jk}|^{1-s}\right\} \\
&+ \frac{2\left(\frac{3}{8}\right)^{\frac{1+s}{4}}\pi^{\frac{s}{2}}}{\Gamma\left(\frac{s}{2}\right)}\sum_{j,k\in\mathbb{Z}}{}'|x_{jk}|^{\frac{1-s}{2}}\sum_{m\in\mathbb{N}}\left\{2-(-1)^m\right\}m^{\frac{s-1}{2}}K_{\frac{s-1}{2}}\left(\sqrt{\tfrac{3}{2}}\pi m|x_{jk}|\right) \\
&+ \frac{3^{\frac{s}{2}}2^{\frac{1-3s}{4}}\pi^{\frac{s}{2}}}{\Gamma(\frac{s}{2})}\sum_{j,k\in\mathbb{Z}}{}'|x_{jk}|^{\frac{1-s}{2}}\sum_{m\in\mathbb{N}}(-1)^m m^{\frac{s-1}{2}}\,K_{\frac{s-1}{2}}\left(\frac{\pi}{\sqrt{2}}m|x_{jk}|\right),
\end{aligned}
\tag{6.7.23}
$$

with $x_{jk}^2 = \left(j^2+k^2-jk\right)$ (we conveniently choose the negative sign in front of jk). The double sum containing x_{jk} has been introduced already in (6.4.28). We finally get by taking care of the terms with $j=k$ in the last two sums containing Bessel functions,

$$
\begin{aligned}
L_s^{hcp} &= 2\left(\tfrac{3}{8}\right)^{\frac{s}{2}}\zeta(s) + \frac{3\sqrt{3}\pi^{1/2}\Gamma\left(\frac{s-1}{2}\right)}{2\sqrt{2}\Gamma\left(\frac{s}{2}\right)}\left(3^{\frac{1-s}{2}}+1\right) \\
&\quad\times\zeta(\tfrac{s-1}{2})\left\{\zeta\left(\tfrac{s-1}{2},\tfrac{1}{3}\right)-\zeta\left(\tfrac{s-1}{2},\tfrac{2}{3}\right)\right\} \\
&+ \frac{4\left(\frac{3}{8}\right)^{\frac{1+s}{4}}\pi^{\frac{s}{2}}}{\Gamma\left(\frac{s}{2}\right)}\sum_{m,j\in\mathbb{N}}\left\{2-(-1)^m\right\}\left(mj^{-1}\right)^{\frac{s-1}{2}}K_{\frac{s-1}{2}}\left(\sqrt{\tfrac{3}{2}}\pi mj\right) \\
&+ \frac{3^{\frac{s}{2}}2^{\frac{5-3s}{4}}\pi^{\frac{s}{2}}}{\Gamma(\frac{s}{2})}\sum_{m,j\in\mathbb{N}}(-1)^m\left(mj^{-1}\right)^{\frac{s-1}{2}}\,K_{\frac{s-1}{2}}\left(\frac{\pi}{\sqrt{2}}mj\right) \\
&+ \frac{4\left(\frac{3}{8}\right)^{\frac{1+s}{4}}\pi^{\frac{s}{2}}}{\Gamma\left(\frac{s}{2}\right)}\sum_{j<k\in\mathbb{Z}}|x_{jk}|^{\frac{1-s}{2}}\sum_{m\in\mathbb{N}}\left\{2-(-1)^m\right\}m^{\frac{s-1}{2}}K_{\frac{s-1}{2}}\left(\sqrt{\tfrac{3}{2}}\pi m|x_{jk}|\right) \\
&+ \frac{3^{\frac{s}{2}}2^{\frac{5-3s}{4}}\pi^{\frac{s}{2}}}{\Gamma(\frac{s}{2})}\sum_{j<k\in\mathbb{Z}}|x_{jk}|^{\frac{1-s}{2}}\sum_{m\in\mathbb{N}}(-1)^m m^{\frac{s-1}{2}}\,K_{\frac{s-1}{2}}\left(\frac{\pi}{\sqrt{2}}m|x_{jk}|\right).
\end{aligned}
\tag{6.7.24}
$$

This form is rather short and therefore perhaps more appealing to use than (6.7.21). We could use our number-theoretical tool we introduced in the previous chapter as applied before by Lennard-Jones, but the sums when programmed converge rather fast and can be evaluated to computer precision within seconds.

6.8 Analytical formulae for the special case $s = 4$

Here we only consider the special case of $s = 4$. More general formulae are given in the Appendix 6.D. For $s = 4$ we can use the following expansion (see

Appendices A and D),

$$\sum_{i\in\mathbb{Z}}\left[(i+a_p)^2+x^2\right]^{-2} = \frac{\pi}{2x^3}+\frac{\pi b_p e^{-\pi x}}{2x^3}h_p(\pi x) + \frac{\pi b_p e^{-\pi x}}{2x^2}\left\{\pi h_p(\pi x)-h_p^{(1)}(\pi x)\right\}, \tag{6.8.1}$$

with $b_1 = 1$ for $a_1 = 0$ and $b_2 = -1$ for $a_2 = \frac{1}{2}$, and $h_1(\pi x) = csch(\pi x)$, $h_2(\pi x) = sech(\pi x)$, $h_1^{(1)}(\pi x) = -\pi cosh(\pi x)csch^2(\pi x)$, and $h_2^{(1)}(\pi x) = -\pi tanh(\pi x)sech(\pi x)$. The relation between the a_p and b_p parameters are explained in Appendix 6.D.

6.8.1 The simple cubic case

We apply (6.8.1) for the simple cubic case, and choose $a_1 = 0$, $b_1 = 1$ and $x_{jk} = \left(j^2+k^2\right)^{1/2}$. We remember again as in the previous section that the case $x \neq 0$ was excluded by introducing an extra sum, and sum over the remaining two indices in (6.D.48) of the lattice sum. For n=4 we obtain after using some well-known relations between hyperbolic functions,

$$L_4^{sc} = {\sum_{k\in\mathbb{Z}}}' k^{-4} + \frac{\pi}{2}{\sum_{j,k\in\mathbb{Z}}}' x_{jk}^{-3} + \pi {\sum_{j,k\in\mathbb{Z}}}' x_{jk}^{-3}\left(e^{2\pi x_{jk}}-1\right)^{-1} + \frac{\pi^2}{2}{\sum_{j,k\in\mathbb{Z}}}' x_{jk}^{-2}csch^2(\pi x_{jk}). \tag{6.8.2}$$

This formula can also be found in Borwein et al.[26] For the other two sums we separate out the terms where either $j = 0$ or $k = 0$,

$$L_4^{sc} = 2\zeta(4)+2\pi\beta\left(\tfrac{3}{2}\right)\zeta\left(\tfrac{3}{2}\right)+4\pi\sum_{k\in\mathbb{N}}k^{-3}\left(e^{2\pi k}-1\right)^{-1}+2\pi^2\sum_{k\in\mathbb{N}}k^{-2}csch^2(\pi k) + 4\pi{\sum_{j,k\in\mathbb{N}}}' x_{jk}^{-3}\left(e^{2\pi x_{jk}}-1\right)^{-1}+2\pi^2{\sum_{j,k\in\mathbb{N}}}' x_{jk}^{-2}csch^2(\pi x_{jk}). \tag{6.8.3}$$

We use one of Ramanujan's identities,[144]

$$\sum_{k\in\mathbb{N}}k^{-3}\left(e^{2\pi k}-1\right)^{-1} = \frac{7\zeta(4)}{4\pi}-\frac{\zeta(3)}{2} = \frac{7\pi^3}{360}-\frac{\zeta(3)}{2}, \tag{6.8.4}$$

and the cosecant sum which we resolve from a comparison of our result here with that of Borwein et al.,[26]

$$\sum_{k\in\mathbb{N}}k^{-2}csch^2(\pi k) = \frac{4}{\pi^2}\zeta(2)\beta(2)-\frac{11\zeta(4)}{2\pi^2} = \frac{2\beta(2)}{3}-\frac{11\pi^2}{180}, \tag{6.8.5}$$

and finally obtain

$$L_4^{sc} = {\sum_{i,j,k\in\mathbb{Z}}}' \left(S_{ijk}^{sc}\right)^{-2} = 8\zeta(2)\beta(2) + 2\pi\left[\zeta\left(\tfrac{3}{2}\right)\beta\left(\tfrac{3}{2}\right) - \zeta(3)\right] - \frac{\pi^4}{45} + 4\pi \sum_{j,k\in\mathbb{N}} \left[x_{jk}^3\left(e^{2\pi x_{jk}} - 1\right)\right]^{-1} + 2\pi^2 \sum_{j,k\in\mathbb{N}} \frac{\mathrm{csch}^2\left(\pi x_{jk}\right)}{x_{jk}^2}, \tag{6.8.6}$$

with $\beta(2)$ being Catalan's constant. We note that the first three terms containing the Riemann zeta and Dirichlet beta functions already give 99.963% of the exact value. Further, the double sums are very fast converging and one has to sum only up to $N_{max} = 5$ to reach 10^{-15} accuracy in L_4^{sc}.

6.8.2 The body-centered cubic case

For the bcc case we take (6.2.7). We already treated the simple cubic system for $s = 4$. We now treat the second sum in (6.2.7) using $b_2 = -1$ and $a = \frac{1}{2}$ in our expansion (6.8.1),

$$\begin{aligned} L_4^{bcc} = \frac{9}{16}\Bigg\{ & 8\zeta(2)\beta(2) + 2\pi\left[\zeta\left(\tfrac{3}{2}\right)\beta\left(\tfrac{3}{2}\right) - \zeta(3)\right] \\ & - \frac{\pi^4}{45} + 4\pi \sum_{j,k\in\mathbb{N}} \left[x_{jk}^3\left(e^{2\pi x_{jk}} - 1\right)\right]^{-1} \\ & + 2\pi^2 \sum_{j,k\in\mathbb{N}} \frac{\mathrm{csch}^2\left(\pi x_{jk}\right)}{x_{jk}^2} + \frac{\pi}{2} \sum_{j,k\in\mathbb{Z}} y_{jk}^{-3} \\ & - \pi \sum_{j,k\in\mathbb{Z}} \left[y_{jk}^3\left(e^{2\pi y_{jk}} + 1\right)\right]^{-1} - \frac{\pi^2}{2} \sum_{j,k\in\mathbb{Z}} \frac{\mathrm{sech}^2(\pi y_{jk})}{y_{jk}^2} \Bigg\}, \end{aligned} \tag{6.8.7}$$

with $x_{jk} = +\sqrt{(j^2 + k^2)}$ and $y_{jk} = +\sqrt{(j+\frac{1}{2})^2 + (k+\frac{1}{2})^2}$. The expression contains fast converging sums except for the simple sum over y_{jk}^{-3}, which however has already been evaluated by Zucker,

$$\sum_{j,k\in\mathbb{Z}} \left((j+\tfrac{1}{2})^2 + (k+\tfrac{1}{2})^2\right)^{-s} = 4(2^s - 1)\zeta(s)\beta(s). \tag{6.8.8}$$

We finally get

$$\begin{aligned} L_4^{bcc} &= \frac{9}{2}\zeta(2)\beta(2) + \frac{9\sqrt{2}\pi}{4}\zeta\left(\tfrac{3}{2}\right)\beta\left(\tfrac{3}{2}\right) - \frac{9\pi}{8}\zeta(3) - \frac{\pi^4}{80} \\ &+ \frac{9\pi}{4}\sum_{j,k\in\mathbb{N}}\left[x_{jk}^3\left(e^{2\pi x_{jk}}-1\right)\right]^{-1} \\ &- \frac{9\pi}{16}\sum_{j,k\in\mathbb{Z}}\left[y_{jk}^3\left(e^{2\pi y_{jk}}+1\right)\right]^{-1} \\ &+ \frac{9\pi^2}{8}\sum_{j,k\in\mathbb{N}}\frac{\mathrm{csch}^2\left(\pi x_{jk}\right)}{x_{jk}^2} - \frac{9\pi^2}{32}\sum_{j,k\in\mathbb{Z}}\frac{\mathrm{sech}^2(\pi y_{jk})}{y_{jk}^2}. \end{aligned} \tag{6.8.9}$$

This could possibly be simplified further. However, all double sums are converging fast like in the simple cubic case.

6.8.3 The face-centered cubic case

For the face-centered cubic case we take (6.2.4) and expand in a similar fashion

$$\begin{aligned} L_4^{fcc} &= \frac{3}{4}{\sum_{i,j,k\in\mathbb{Z}}}'\left(i^2+\frac{j^2+k^2}{2}\right)^{-2} - \frac{1}{2}L_4^{sc} = \frac{3}{2}\zeta(4) + \frac{3\sqrt{2}\pi}{4}{\sum_{j,k\in\mathbb{Z}}}' x_{jk}^{-3} \\ &+ \frac{3\sqrt{2}\pi}{2}{\sum_{j,k\in\mathbb{Z}}}' x_{jk}^{-3}\left(e^{\sqrt{2}\pi x_{jk}}-1\right)^{-1} \\ &+ \frac{3\pi^2}{4}{\sum_{j,k\in\mathbb{Z}}}' x_{jk}^{-2}\mathrm{csch}^2\left(\tfrac{\pi}{\sqrt{2}}x_{jk}\right) - 4\zeta(2)\beta(2) \\ &- \pi\left[\zeta\left(\tfrac{3}{2}\right)\beta\left(\tfrac{3}{2}\right) - \zeta(3)\right] + \zeta(4) \\ &- 2\pi\sum_{j,k\in\mathbb{N}}\left[x_{jk}^3\left(e^{2\pi x_{jk}}-1\right)\right]^{-1} - \pi^2\sum_{j,k\in\mathbb{N}}\frac{\mathrm{csch}^2\left(\pi x_{jk}\right)}{x_{jk}^2}, \end{aligned} \tag{6.8.10}$$

with the same definition for x_{jk} as in the simple cubic case. We simplify as in the simple cubic case and use for the exponential expression the fact that $k = j$ leads again to (6.4.5) and to (6.8.5) for the hyperbolic function,

$$\begin{aligned} L_4^{fcc} &= \left(3\sqrt{2}-1\right)\pi\zeta\left(\tfrac{3}{2}\right)\beta\left(\tfrac{3}{2}\right) - \frac{\pi^2}{6}\beta(2) + \frac{\pi}{4}\zeta(3) + \frac{\pi^4}{90} \\ &+ 3\sqrt{2}\pi\sum_{j<k\in\mathbb{Z}}\left[x_{jk}^3\left(e^{\sqrt{2}\pi x_{jk}}-1\right)\right]^{-1} - 2\pi\sum_{j,k\in\mathbb{N}}\left[x_{jk}^3\left(e^{2\pi x_{jk}}-1\right)\right]^{-1} \\ &+ \frac{3\pi^2}{2}\sum_{j<k\in\mathbb{Z}}\frac{\mathrm{csch}^2\left(\frac{\pi}{\sqrt{2}}x_{jk}\right)}{x_{jk}^2} - \pi^2\sum_{j,k\in\mathbb{N}}\frac{\mathrm{csch}^2\left(\pi x_{jk}\right)}{x_{jk}^2}. \end{aligned} \tag{6.8.11}$$

6.8.4 The hexagonal close-packed case

For the hexagonal close-packed case we use (6.2.12) and consider the more general sum (6.2.13),

$$\begin{aligned} S_4^{hcp}(c) &= c^{-2} {\sum_{i,j,k\in\mathbb{Z}}}' \left(i^2 + \frac{j^2+k^2-jk}{c} \right)^{-2} \\ &= 2c^{-2}\zeta(4) + \frac{\pi}{2\sqrt{c}} {\sum_{j,k\in\mathbb{Z}}}' x_{jk}^{-3} + \frac{\pi}{\sqrt{c}} {\sum_{j,k\in\mathbb{Z}}}' x_{jk}^{-3} \left(e^{\frac{2\pi}{\sqrt{c}} x_{jk}} - 1 \right)^{-1} \\ &\quad + \frac{\pi^2}{2c} {\sum_{j,k\in\mathbb{Z}}}' x_{jk}^{-2} \mathrm{csch}^2 \left(\frac{\pi x_{jk}}{\sqrt{c}} \right), \end{aligned} \tag{6.8.12}$$

with $x_{jk} = \sqrt{(j^2+k^2-jk)}$. We now use (6.4.28) and get

$$\begin{aligned} S_4^{hcp}(c) &= 2c^{-2}\zeta(4) + \frac{\pi}{\sqrt{3c}} \zeta(\tfrac{3}{2}) \left\{ \zeta\left(\tfrac{3}{2}, \tfrac{1}{3}\right) - \zeta\left(\tfrac{3}{2}, \tfrac{2}{3}\right) \right\} \\ &\quad + \frac{\pi}{\sqrt{c}} {\sum_{j,k\in\mathbb{Z}}}' x_{jk}^{-3} \left(e^{\frac{2\pi}{\sqrt{c}} x_{jk}} - 1 \right)^{-1} + \frac{\pi^2}{2c} {\sum_{j,k\in\mathbb{Z}}}' x_{jk}^{-2} \mathrm{csch}^2 \left(\frac{\pi x_{jk}}{\sqrt{c}} \right). \end{aligned} \tag{6.8.13}$$

We now add the three terms in (6.2.12) and get,

$$\begin{aligned} L_4^{hcp} &= \sum_{i=1}^{4} a_i \, S_4^{hcp}(c_i) = \frac{9}{32}\zeta(4) + \frac{\sqrt{2}}{8} \left(1 + 3\sqrt{3} \right) \pi \zeta(\tfrac{3}{2}) \left\{ \zeta\left(\tfrac{3}{2}, \tfrac{1}{3}\right) - \zeta\left(\tfrac{3}{2}, \tfrac{2}{3}\right) \right\} \\ &\quad + \sum_{i=1}^{4} \frac{a_i \pi}{\sqrt{c_i}} {\sum_{j,k\in\mathbb{Z}}}' x_{jk}^{-3} \left(e^{\frac{2\pi}{\sqrt{c_i}} x_{jk}} - 1 \right)^{-1} + \sum_{i=1}^{4} \frac{a_i \pi^2}{2c_i} {\sum_{j,k\in\mathbb{Z}}}' x_{jk}^{-2} \mathrm{csch}^2 \left(\frac{\pi x_{jk}}{\sqrt{c_i}} \right), \end{aligned} \tag{6.8.14}$$

with $a_1 = \frac{3}{2}$, $a_2 = \frac{9}{2}$, $a_3 = -\frac{9}{2}$, $a_4 = -\frac{1}{2}$, $c_1 = \frac{8}{3}$, $c_2 = 2$, $c_3 = 8$, and $c_4 = \frac{2}{3}$. Again, this expressions could perhaps be further simplified, but the remaining sums are converging fast. In fact, we only have to sum over N_{max}=17 values to reach double precision accuracy.

6.9 Results: Lattice Sums for Integer Exponents

To compute the lattice sums for the sc, bcc, fcc and hcp structures and to test the many formulae introduced in this work, the computer program Jones.f was written (in FORTRAN) which is freely available from our website.[143] For the Hurwitz zeta function we use the Euler-Maclaurin summation formula to

obtain the expression[106]:

$$\zeta(s,x) = \sum_{k=1}^{n} (k+x)^{-s} + \frac{(n+x)^{1-s}}{s-1} - \tfrac{1}{2}(n+x)^{-s} + \sum_{j=1}^{\infty} B_{2j} \frac{s(s+1)\cdots(s+2j)}{(2j)!\,(n+x)^{s+2j+1}}, \tag{6.9.1}$$

where B_{2k} are the Bernoulli numbers, $x \in (0,1)$, and we chose $n < 9$ in our computer code. This routine was used for all other functions which can be expressed in terms of Hurwitz zeta functions. For the Bessel functions we used the algorithm published in Numerical Recipes.[145]

The computed lattice sums $L_s - L_\infty$ are listed in Table 7.1 to 15 digit accuracy for integer exponents $s \leq 30$. For this we used 128-bit arithmetic (quadruple precision) in the floating point arithmetic.

In Figure 6.3 the behavior of the sums for the cubic and hexagonal structures is shown on a logarithmic scale, this includes results for non-integer exponents in the range close to $s = 3$. It can be seen that the fcc and hcp graphs are so close as to be indistinguishable, the difference between the two at most is 10^{-3} which we show in Figure 6.3b. This is perhaps expected as both are close-packed structures with the same packing density for unit hard spheres. Further it is clear that $(L_s^{fcc} - L_s^{hcp}) \to 0$ for $s \to \infty$. Further we observe that while both the fcc and hcp curves have a singularity at $s = 3$, they seem to approach a constant value at that point, i.e., $\lim_{s\to 3^+}(L_n^{fcc} - L_n^{hcp}) \simeq -5.74 \times 10^{-4}$. For this case the analytical continuation to exponents $s < 3$ would be interesting. Further, the formulae given here may lead to interesting functional relationships which needs to be explored.

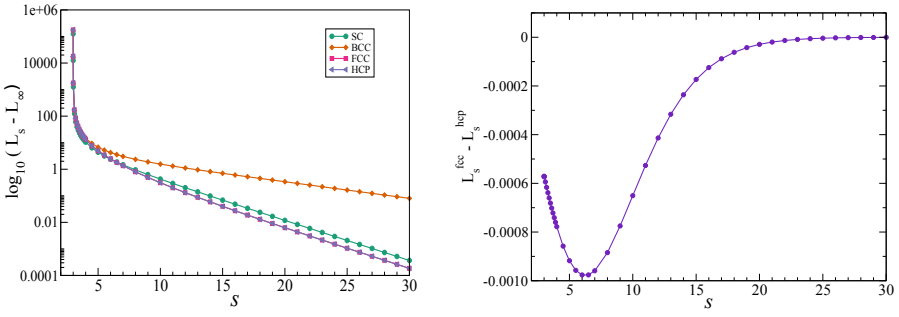

Figure 6.3 Lattice sums for the four lattices sc, bcc, fcc and hcp. a) $\log_{10}(L_s - L_\infty)$; b) $(L_s^{fcc} - L_s^{hcp})$.

n	$L_n^{\mathrm{sc}} - L_\infty^{\mathrm{sc}}$	$L_n^{\mathrm{bcc}} - L_\infty^{\mathrm{bcc}}$	$L_n^{\mathrm{fcc}} - L_\infty^{\mathrm{fcc}}$	$L_n^{\mathrm{hcp}} - L_\infty^{\mathrm{hcp}}$	$L_n^{\mathrm{hcp}} - L_n^{\mathrm{fcc}}$
4	1.05323159597617E+1	1.46387216437935E+1	1.33383043051302E+1	1.33390823380551E+1	7.78032924974526E-4
5	4.37752483084708E+0	6.75850937014712E+0	4.96751845837841E+0	4.96843634796979E+0	9.17889591383232E-4
6	2.40192397482754E+0	4.25366786729232E+0	2.45392104374447E+0	2.45489727784162E+0	9.76234097145690E-4
7	1.46705778091881E+0	3.05424347924446E+0	1.35938770074208E+0	1.36034677619555E+0	9.59075453468315E-4
8	9.45807927226370E-1	2.35519790840251E+0	8.01937231378133E-1	8.02821852809896E-1	8.84621431763331E-4
9	6.28859198886779E-1	1.89458965632112E+0	4.92546702137558E-1	4.93321725001782E-1	7.75022864223436E-4
10	4.26119102533089E-1	1.56440061535995E+0	3.11245665477406E-1	3.11896233818981E-1	6.50568341575253E-4
11	2.92294499234567E-1	1.31326253739910E+0	2.00920351277113E-1	2.01447099831955E-1	5.26748554841471E-4
12	2.02149045047519E-1	1.11418326807536E+0	1.31880196544580E-1	1.32293769098918E-1	4.13572554337918E-4
13	1.40599580021692E-1	9.51807318574715E-1	8.77263213520527E-2	8.80425502984390E-2	3.16228946386338E-4
14	9.81841257121521E-2	8.16770228485920E-1	5.89919443508593E-2	5.92282550682414E-2	2.36310717382134E-4
15	6.87642950388921E-2	7.02984559980926E-1	4.00240550990886E-2	4.01971443472233E-2	1.73089248134625E-4
16	4.82634695858417E-2	6.06254047544529E-1	2.73548440185703E-2	2.74794193038561E-2	1.24575285285802E-4
17	3.39293163672074E-2	5.23531250439298E-1	1.88094367104578E-2	1.88977196228595E-2	8.82829124017101E-5
18	2.38817078667148E-2	4.52503168608382E-1	1.29983096659596E-2	1.30600231774083E-2	6.17135114487303E-5
19	1.68254563317377E-2	3.91350791413118E-1	9.01960443932357E-3	9.06222411120950E-3	4.26196718859239E-5
20	1.18628308899457E-2	3.38604005679563E-1	6.28004132634266E-3	6.30915811465870E-3	2.91167883160407E-5
21	8.36875754668317E-3	2.93050370415294E-1	4.38480936230330E-3	4.40451008477321E-3	1.97007224699113E-5
22	5.90652613429112E-3	2.53675218084780E-1	3.06856932292989E-3	3.08178423329668E-3	1.32149103667949E-5
23	4.17024007074802E-3	2.19620534883649E-1	2.15149097471211E-3	2.16028673932262E-3	8.79576461050519E-6
24	2.94520818412950E-3	1.90155475483163E-1	1.51082493970707E-3	1.51663857704596E-3	5.81363733888953E-6
25	2.08052037491334E-3	1.64654351927331E-1	1.06227870924614E-3	1.06609714202720E-3	3.81843278106124E-6
26	1.46997249608606E-3	1.42579615920799E-1	7.47674897726916E-4	7.50168624485191E-4	2.49372675827520E-6
27	1.03875223830484E-3	1.23468315872789E-1	5.26690212160028E-4	5.28310428505144E-4	1.62021634511562E-6
28	7.34121070789493E-4	1.06921071038717E-1	3.71277553079702E-4	3.72325322411022E-4	1.04776933131979E-6
29	5.18879212211412E-4	9.25929383761218E-2	2.61871447419640E-4	2.62546150133902E-4	6.74702714262418E-7
30	3.66774897184039E-4	8.01857499061731E-2	1.84790059821197E-4	1.85222851788274E-4	4.32791967077113E-7

Table 6.2 Lattice sums (Lennard-Jones–Ingham coefficients) L_n with respect to the infinite limit (L_∞^{sc}=6, L_∞^{bcc}=8, L_∞^{fcc}=12, L_∞^{hcp}=12) for $n \in \mathbb{N}$ obtained from various expansion methods described in this paper.

6.10 Conclusions

For the four lattices sc, bcc, fcc and hcp we developed fast converging expansions to evaluate the corresponding lattice sums to computer precision. Especially the Terras and the Van der Hoff–Benson expansions are ideal methods for small exponents, while for larger exponents one can use direct summation techniques including symmetry, or the corresponding Dirichlet series. The methods outlined here can be used for lattices in higher dimensions which we currently explore. Analytical extensions are also possible through these expansions, which we did not touch in this paper. These lattice sums can be used to calculate solid-state structural properties like the cohesive energy, pressure and bulk modulus analytically if the ELJ form is taken for the 2-body interaction potential, which is the subject of a subsequent paper.

6.11 Appendix

A The Mellin transformation and theta function method in the evaluation of lattice sums

Here we introduce some of the methodology used in the next section for the evaluation of double sums like the ones which appear in (6.4.26). The Mellin transformation M is defined as,[61, 146]

$$[Mf](s) = \phi(s) = \int_0^\infty t^{s-1} f(t)\, dt\,, \tag{6.A.1}$$

and is particularly useful for treating lattice sums.[26, 61] In order to see this we choose the function $f(t) = e^{-pt}$ and get

$$[Mf](s) = \int_0^\infty t^{s-1} e^{-pt}\, dt = p^{-s}\Gamma(s)\,. \tag{6.A.2}$$

For $p = 1$ we get the integral representation of the gamma function. As an example, we apply this to the more general lattice sum as given in (6.7.1),

$$\sum_{i\in\mathbb{Z}} \left[(i+a)^2 + x^2\right]^{-s} \quad with \quad a \in [0,1)\,, \tag{6.A.3}$$

(we attend the case $a \to 0$ further below) and get

$$\sum_{i\in\mathbb{Z}} \left[(i+a)^2 + x^2\right]^{-s} = \Gamma(s)^{-1} \sum_{i\in\mathbb{Z}} \int_0^\infty t^{s-1} e^{-\left[(i+a)^2+x^2\right]t}\, dt\,. \tag{6.A.4}$$

We now use the Poisson summation formula applied to Gaussian functions,[111, 147]

$$\sum_{i\in\mathbb{Z}} e^{-(i+a)^2 t} = \sqrt{\frac{\pi}{t}} \sum_{k\in\mathbb{Z}} e^{-k^2\pi^2 t^{-1}} cos(2\pi k a)\,, \tag{6.A.5}$$

and the expansion in terms of Bessel functions (Hobson's integral),[148]

$$\int_0^\infty t^{s-1} e^{-x^2 t - k^2\pi^2 t^{-1}}\, dt = 2\left(\frac{|k|\pi}{|x|}\right)^s K_s\left(2|kx|\pi\right). \tag{6.A.6}$$

For treating the sum (6.A.5) and the Bessel function (6.A.6) we need to separate out the special case where $k = 0$,

$$\begin{aligned}\sum_{i\in\mathbb{Z}} \left[(i+a)^2 + x^2\right]^{-s} = {} & 2\pi^{\frac{1}{2}}\Gamma(s)^{-1} \sum_{k\in\mathbb{N}} \int_0^\infty t^{s-\frac{3}{2}} e^{-x^2 t - k^2\pi^2 t^{-1}} cos(2\pi k a)\, dt \\ & + \pi^{\frac{1}{2}}\Gamma(s)^{-1} \int_0^\infty t^{s-\frac{3}{2}} e^{-x^2 t}\, dt\,.\end{aligned} \tag{6.A.7}$$

We use the Bessel expansion (6.A.6) for the first integral while the second integral has a well-known expression,

$$\begin{aligned}\sum_{i\in\mathbb{Z}} \left[(i+a)^2 + x^2\right]^{-s} = {} & 4\pi^s\Gamma(s)^{-1} \sum_{k\in\mathbb{N}} \left(\frac{k}{|x|}\right)^{s-\frac{1}{2}} cos(2\pi k a)\, K_{s-\frac{1}{2}}\left(2\pi k|x|\right) \\ & + \pi^{\frac{1}{2}} \frac{\Gamma\left(s-\frac{1}{2}\right)}{\Gamma(s)} |x|^{1-2s}\,.\end{aligned} \tag{6.A.8}$$

For the special cases of $a = 0$ and $a = \frac{1}{2}$ we get (6.7.2) and (6.7.6) respectively. This is all we need to treat inverse powers of quadratic forms of the more general form

$$\sum_{i_1, i_2, \ldots \in\mathbb{Z}} \left[(i_1 + a_1)^2 + (i_2 + a_2)^2 + \ldots\right]^{-s}, \tag{6.A.9}$$

as the parameter x can be defined in terms of the other summation parameters in the lattice sums. This method is particularly useful, easy to use and can be applied to higher dimensions as well. Zucker and co-workers used the Mellin transformation intensively together with Jacobi's theta functions and relations between them to evaluate lattice sums.[26] We use this technique here to evaluate several double sums in Appendix 6.B.

Let us now consider the double sum

$$S(s) = {\sum_{m,n\in\mathbb{Z}}}' \left(am^2 + bn^2\right)^{-s}, \tag{6.A.10}$$

where the sum is over all integer values of m and n with the term $(m,n) = (0,0)$

omitted. Using (6.A.2) we get

$$S(s) = {\sum_{m,n\in\mathbb{Z}}}' \frac{1}{\Gamma(s)} \int_0^\infty u^{s-1} e^{-(am^2+bn^2)u}\, du = \frac{1}{\Gamma(s)} \int_0^\infty u^{s-1} {\sum_{m,n\in\mathbb{Z}}}' e^{-(am^2+bn^2)u}\, du\,. \tag{6.A.11}$$

Consider the sum in (6.A.11), and set $q = e^{-u}$. For many values of a and b the theta series can be written in the form

$${\sum_{m,n\in\mathbb{Z}}}' q^{am^2+bn^2} = \sum_{k,n\in\mathbb{N}} f_1(k)\, f_2(n)\, q^{kn} \tag{6.A.12}$$

for some functions $f_1(k)$ and $f_2(n)$. Using (6.A.12) in (6.A.11) we deduce

$$\begin{aligned} S(s) &= \frac{1}{\Gamma(s)} \int_0^\infty u^{s-1} \sum_{k,n\in\mathbb{N}} f_1(k)\, f_2(n)\, e^{-knu}\, du \\ &= {\sum_{m,n\in\mathbb{N}}}' \frac{f_1(k)\, f_2(n)}{(kn)^s} = \left(\sum_{k=1}^{\infty} \frac{f_1(k)}{k^s}\right)\left(\sum_{n=1}^{\infty} \frac{f_2(n)}{n^s}\right). \end{aligned} \tag{6.A.13}$$

For example when $a = b = 1$ for (6.A.12) we have by Jacobi's sum of two squares theorem [Ref.[132], p.177]

$${\sum_{m,n\in\mathbb{Z}}}' q^{m^2+n^2} = 4 \sum_{k,n\in\mathbb{N}} \sin\frac{\pi n}{2}\, q^{kn}\,, \tag{6.A.14}$$

and so $f_1(k) = 1$ and $f_2(n) = 4\sin\frac{\pi n}{2}$. It follows that

$${\sum_{m,n\in\mathbb{Z}}}' \left(m^2+n^2\right)^{-s} = 4\left(\sum_{k\in\mathbb{N}} \frac{1}{k^s}\right)\left(\sum_{n\in\mathbb{N}} \frac{\sin\frac{\pi n}{2}}{n^s}\right) \quad = 4\,\zeta(s)\,\beta(s)\,. \tag{6.A.15}$$

For other values of a and b, formulas of the type (C.4) can be found in the literature.[107] To evaluate the double sums $S_2(s,\frac{2}{9}), S_2(s,\frac{8}{9})$ and $S_2(s,\frac{8}{3})$ in (6.4.26) we use the results of Chan and Toh[109] to express the resulting series as linear combinations of Hurwitz zeta functions shown in the following section.

B Double sum relations

Here we present solutions for several double sums required in our lattice sum treatment. The first double sum shown in (6.4.21) is related to Zucker's Z_1-function defined in (6.4.5), and has already been decomposed in terms of Dirichlet L-series.[105] The relation between the two sums can be easily ob-

tained,

$$\begin{aligned}
&\sum_{i,j\in\mathbb{Z}}{}' (-1)^j \left(2i^2+j^2\right)^{-s} = \sum_{\substack{i,j\in\mathbb{Z}\\ j \text{ even}}}{}' \left(2i^2+j^2\right)^{-s} - \sum_{\substack{i,j\in\mathbb{Z}\\ j \text{ odd}}} \left(2i^2+j^2\right)^{-s} \\
&= 2\sum_{\substack{i,j\in\mathbb{Z}\\ j \text{ even}}}{}' \left(2i^2+j^2\right)^{-s} - \sum_{i,j\in\mathbb{Z}}{}' \left(2i^2+j^2\right)^{-s} = 2\sum_{i,j\in\mathbb{Z}}{}' \left(2i^2+(2j)^2\right)^{-s} - Z_1(s) \\
&= \left(2^{1-s}-1\right) Z_1(s)\,.
\end{aligned} \tag{6.B.16}$$

The second double sum appearing in the bcc case, (6.4.12), can be decomposed in a similar way,

$$\begin{aligned}
&\sum_{\substack{i,j\in\mathbb{Z}\\ i \text{ odd},\ j \text{ odd}}} \left(2i^2+j^2\right)^{-s} = \sum_{i,j\in\mathbb{Z}}{}' \left(2i^2+j^2\right)^{-s} - \sum_{\substack{i,j\in\mathbb{Z}\\ i \text{ even},\ j \text{ odd}}} \left(2i^2+j^2\right)^{-s} \\
&- \sum_{\substack{i,j\in\mathbb{Z}\\ i \text{ odd},\ j \text{ even}}} \left(2i^2+j^2\right)^{-s} - \sum_{\substack{i,j\in\mathbb{Z}\\ i,j \text{ even}}}{}' \left(2i^2+j^2\right)^{-s}\,.
\end{aligned} \tag{6.B.17}$$

The last sum which is easily derived is

$$\begin{aligned}
\sum_{\substack{i,j\in\mathbb{Z}\\ i,j \text{ even}}}{}' \left(2i^2+j^2\right)^{-s} &= \sum_{i,j\in\mathbb{Z}}{}' \left(2(2i)^2+(2j)^2\right)^{-s} \\
&= 2^{-2s}\sum_{i,j\in\mathbb{Z}}{}' \left(2i^2+j^2\right)^{-s} \\
&= 2^{-2s} Z_1(s)\,.
\end{aligned} \tag{6.B.18}$$

The second sum in (6.B.17) becomes

$$\begin{aligned}
&\sum_{\substack{i,j\in\mathbb{Z}\\ i \text{ even},\ j \text{ odd}}} \left(2i^2+j^2\right)^{-s} = \sum_{\substack{i,j\in\mathbb{Z}\\ i \text{ even}}}{}' \left(2i^2+j^2\right)^{-s} - \sum_{\substack{i,j\in\mathbb{Z}\\ i,j \text{ even}}}{}' \left(2i^2+j^2\right)^{-s} \\
&= \sum_{i,j\in\mathbb{Z}}{}' \left(8i^2+j^2\right)^{-s} - 2^{-2s} Z_1(s)\,.
\end{aligned} \tag{6.B.19}$$

Now, the unknown sum in (6.B.19) has been evaluated by Zucker and is related to the Z_1-function (6.4.5) and (6.4.15),[105]

$$\begin{aligned}
Z_3(s) = \sum_{i,j\in\mathbb{Z}}{}' \left(8i^2+j^2\right)^{-s} = 2^{-3s}\big[&\left(1-2^{-s}+2^{1-2s}\right)\zeta(s)\zeta\left(s;\tfrac{1}{8},\tfrac{3}{8};\tfrac{5}{8},\tfrac{7}{8}\right) \\
&+\beta(s)\zeta\left(s;\tfrac{1}{8},\tfrac{7}{8};\tfrac{3}{8},\tfrac{5}{8}\right),
\end{aligned}$$

where we are using the compact notation for sums of Hurwitz zeta functions given by (6.4.8).

The last sum to treat is

$$\begin{aligned}\sum_{\substack{i,j\in\mathbb{Z}\\ i \text{ odd},\ j \text{ even}}} \left(2i^2+j^2\right)^{-s} &= \sum_{\substack{i,j\in\mathbb{Z}\\ j \text{ even}}}{}' \left(2i^2+j^2\right)^{-s} - \sum_{\substack{i,j\in\mathbb{Z}\\ i \text{ even},\ j \text{ even}}}{}' \left(2i^2+j^2\right)^{-s} \\ &= 2^{-s}Z_1(s) - 2^{-2s}Z_1(s)\,.\end{aligned} \tag{6.B.20}$$

We now take all terms together and get

$$\begin{aligned}\sum_{\substack{i,j\in\mathbb{Z}\\ i \text{ odd},\ j \text{ odd}}} \left(2i^2+j^2\right)^{-s} &= \left(1-2^{-s}+2^{-2s}\right)Z_1(s) - Z_3(s) \\ &= \tfrac{1}{2}\left(1-2^{-s}\right)Z_1(s) - 2^{-3s}\beta(s)\zeta\left(s;\tfrac{1}{8},\tfrac{7}{8};\tfrac{3}{8},\tfrac{5}{8}\right)\,.\end{aligned} \tag{6.B.21}$$

The three double sums $S_2(s,\frac{8}{3})$, $S_2(s,\frac{2}{9})$ and $S_2(s,\frac{8}{9})$ in (6.4.26) can be decomposed using the results of Chan and Toh[109] and the method outlined in the previous section. For $S_2(s,\frac{8}{3})$ we obtain the following[109], where $\left(\frac{a}{n}\right)$ denotes the Kronecker symbol listed in Appendix 6.C,

$$\begin{aligned}&\sum_{m,n\in\mathbb{Z}}{}' \left(8m^2+3n^2\right)^{-s} \\ &= \frac{1}{2}\sum_{n\in\mathbb{N}}\left(\frac{4}{n}\right)n^{-s}\sum_{n\in\mathbb{N}}\left(\frac{-24}{n}\right)n^{-s} + \frac{\zeta(s)}{4^s}\sum_{n\in\mathbb{N}}\left(\frac{-24}{n}\right)n^{-s} \\ &- \frac{1}{2}\sum_{n\in\mathbb{N}}\left(\frac{-12}{n}\right)n^{-s}\sum_{n\in\mathbb{N}}\left(\frac{8}{n}\right)n^{-s} - \frac{1}{4^s}\sum_{n\in\mathbb{N}}\left(\frac{-3}{n}\right)n^{-s}\sum_{n\in\mathbb{N}}\left(\frac{8}{n}\right)n^{-s} \\ &- \frac{1}{2}\sum_{n\in\mathbb{N}}\left(\frac{-4}{n}\right)n^{-s}\sum_{n\in\mathbb{N}}\left(\frac{24}{n}\right)n^{-s} + \frac{1}{2}\sum_{n\in\mathbb{N}}\left(\frac{12}{n}\right)n^{-s}\sum_{n\in\mathbb{N}}\left(\frac{-8}{n}\right)n^{-s}\quad.\end{aligned} \tag{6.B.22}$$

Where possible terms in (6.B.22) can be decomposed into combinations of Hurwitz zeta functions by the notation outlined in (6.4.8),

$$
\begin{aligned}
&\sum_{m,n\in\mathbb{Z}}{}' \left(8m^2+3n^2\right)^{-s} \\
&\quad = \quad \frac{1}{2}\left(1-2^{-s}\right)\zeta\left(s\right)24^{-s}\zeta\left(s;\tfrac{1}{24},\tfrac{5}{24},\tfrac{7}{24},\tfrac{11}{24};\tfrac{13}{24},\tfrac{17}{24},\tfrac{19}{24},\tfrac{23}{24}\right) \\
&\quad + 96^{-s}\zeta\left(s\right)\zeta\left(s;\tfrac{1}{24},\tfrac{5}{24},\tfrac{7}{24},\tfrac{11}{24};\tfrac{13}{24},\tfrac{17}{24},\tfrac{19}{24},\tfrac{23}{24}\right) \\
&\quad - \frac{1}{2}48^{-s}\zeta\left(s;\tfrac{1}{6};\tfrac{5}{6}\right)\zeta\left(s;\tfrac{1}{8},\tfrac{7}{8};\tfrac{3}{8},\tfrac{5}{8}\right) \\
&\quad - 96^{-s}\zeta\left(s;\tfrac{1}{3};\tfrac{2}{3}\right)\zeta\left(s;\tfrac{1}{8},\tfrac{7}{8};\tfrac{3}{8},\tfrac{5}{8}\right) \\
&\quad - \frac{1}{2}96^{-s}\zeta\left(s;\tfrac{1}{4};\tfrac{3}{4}\right)\zeta\left(s;\tfrac{1}{24},\tfrac{5}{24},\tfrac{19}{24},\tfrac{23}{24};\tfrac{7}{24},\tfrac{11}{24},\tfrac{13}{24},\tfrac{17}{24}\right) \\
&\quad + \frac{1}{2}96^{-s}\zeta\left(s;\tfrac{1}{12},\tfrac{11}{12};\tfrac{5}{12},\tfrac{7}{12}\right)\zeta(s;\tfrac{1}{8},\tfrac{3}{8};\tfrac{5}{8},\tfrac{7}{8}) \quad .
\end{aligned}
\tag{6.B.23}
$$

For the sum $S_2(s,\frac{2}{9})$ we obtain[109],

$$
\begin{aligned}
\sum_{m,n\in\mathbb{Z}}{}' \left(2m^2+9n^2\right)^{-s} &= \sum_{n\in\mathbb{N}}\left(\frac{9}{n}\right)n^{-s}\sum_{n\in\mathbb{N}}\left(\frac{-72}{n}\right)n^{-s}+\frac{2\zeta\left(s\right)}{9^s}\sum_{n\in\mathbb{N}}\left(\frac{-8}{n}\right)n^{-s} \\
&\quad -\sum_{n\in\mathbb{N}}\left(\frac{-3}{n}\right)n^{-s}\sum_{n\in\mathbb{N}}\left(\frac{24}{n}\right)n^{-s}
\end{aligned}
\tag{6.B.24}
$$

and

$$
\begin{aligned}
\sum_{m,n\in\mathbb{Z}}{}' \left(2m^2+9n^2\right)^{-s} &= \zeta\left(s\right)2^{1-3s}3^{-2s}\zeta\left(s;\tfrac{1}{8},\tfrac{3}{8};\tfrac{5}{8},\tfrac{7}{8}\right) \\
&\quad -72^s\zeta\left(s;\tfrac{1}{3};\tfrac{2}{3}\right)\zeta\left(s;\tfrac{1}{24},\tfrac{5}{24},\tfrac{19}{24},\tfrac{23}{24};\tfrac{7}{24},\tfrac{11}{24},\tfrac{13}{24},\tfrac{17}{24}\right) \\
&\quad +72^{-s}\zeta(s;\tfrac{1}{3},\tfrac{2}{3};)\zeta\left(s;\tfrac{1}{24},\tfrac{11}{24},\tfrac{17}{24},\tfrac{19}{24};\tfrac{5}{24},\tfrac{7}{24},\tfrac{13}{24},\tfrac{23}{24}\right) .
\end{aligned}
\tag{6.B.25}
$$

For the sum $S_2(s,\frac{8}{9})$ we obtain [109],

$$
\begin{aligned}
&\sum_{m,n\in\mathbb{Z}}{}' \left(8m^2+9n^2\right)^{-s} \\
&\quad = \frac{1}{2}\sum_{n\in\mathbb{N}}\left(\frac{-72}{n}\right)n^{-s}\sum_{n\in\mathbb{N}}\left(\frac{36}{n}\right)n^{-s} + \frac{1}{9^s}\sum_{n\in\mathbb{N}}\left(\frac{-8}{n}\right)n^{-s}\sum_{n\in\mathbb{N}}\left(\frac{4}{n}\right)n^{-s} \\
&\quad + \frac{1}{4^s}\sum_{n\in\mathbb{N}}\left(\frac{-72}{n}\right)n^{-s}\sum_{n\in\mathbb{N}}\left(\frac{9}{n}\right)n^{-s} + \frac{2\zeta(s)}{36^s}\sum_{n\in\mathbb{N}}\left(\frac{-8}{n}\right)n^{-s} \\
&\quad - \frac{1}{2}\sum_{n\in\mathbb{N}}\left(\frac{24}{n}\right)n^{-s}\sum_{n\in\mathbb{N}}\left(\frac{-12}{n}\right)n^{-s} - \frac{1}{4^s}\sum_{n\in\mathbb{N}}\left(\frac{24}{n}\right)n^{-s}\sum_{n\in\mathbb{N}}\left(\frac{-3}{n}\right)n^{-s} \\
&\quad + \frac{1}{2}\sum_{n\in\mathbb{N}}\left(\frac{72}{n}\right)n^{-s}\sum_{n\in\mathbb{N}}\left(\frac{-36}{n}\right)n^{-s} + \frac{1}{9^s}\sum_{n\in\mathbb{N}}\left(\frac{8}{n}\right)n^{-s}\sum_{n\in\mathbb{N}}\left(\frac{-4}{n}\right)n^{-s} \\
&\quad - \frac{1}{2}\sum_{n\in\mathbb{N}}\left(\frac{-24}{n}\right)n^{-s}\sum_{n\in\mathbb{N}}\left(\frac{12}{n}\right)n^{-s}
\end{aligned}
\tag{6.B.26}
$$

and

$$
\begin{aligned}
&\sum_{m,n\in\mathbb{Z}}{}' \left(8m^2+9n^2\right)^{-s} \\
&\quad = 2^{-4s-1}3^{-2s}\zeta\left(s;\tfrac{1}{24},\tfrac{11}{24},\tfrac{17}{24},\tfrac{19}{24};\tfrac{5}{24},\tfrac{7}{24},\tfrac{13}{24},\tfrac{23}{24}\right)\zeta\left(s;\tfrac{1}{6},\tfrac{5}{6}\right) \\
&\quad + 72^{-s}\left(1-2^{-s}\right)\zeta(s)\zeta\left(s;\tfrac{1}{8},\tfrac{3}{8};\tfrac{5}{8},\tfrac{7}{8}\right) \\
&\quad + 3^{-2s}2^{-5s}\zeta\left(s;\tfrac{1}{24},\tfrac{11}{24},\tfrac{17}{24},\tfrac{19}{24};\tfrac{5}{24},\tfrac{7}{24},\tfrac{13}{24},\tfrac{23}{24}\right)\zeta\left(s;\tfrac{1}{3},\tfrac{2}{3}\right) \\
&\quad + 2^{1-5s}3^{-2s}\zeta(s)\zeta\left(s;\tfrac{1}{8},\tfrac{3}{8};\tfrac{5}{8},\tfrac{7}{8}\right) \\
&\quad - 2^{-4s-1}3^{-2s}\zeta\left(s;\tfrac{1}{24},\tfrac{5}{24},\tfrac{19}{24},\tfrac{23}{24};\tfrac{7}{24},\tfrac{11}{24},\tfrac{13}{24},\tfrac{17}{24}\right)\zeta\left(s;\tfrac{1}{6};\tfrac{5}{6}\right) \\
&\quad - 2^{-5s}3^{-2s}\zeta\left(s;\tfrac{1}{24},\tfrac{5}{24},\tfrac{19}{24},\tfrac{23}{24};\tfrac{7}{24},\tfrac{11}{24},\tfrac{13}{24},\tfrac{17}{24}\right)\zeta\left(s;\tfrac{1}{3};\tfrac{2}{3}\right) \\
&\quad + 2^{-5s-1}3^{-2s}\zeta\left(s;\tfrac{1}{24},\tfrac{7}{24},\tfrac{17}{24},\tfrac{23}{24};\tfrac{5}{24},\tfrac{11}{24},\tfrac{13}{24},\tfrac{19}{24}\right)\ \zeta\left(s;\tfrac{1}{12},\tfrac{5}{12};\tfrac{7}{12},\tfrac{11}{12}\right) \\
&\quad + 3^{-2s}2^{-5s}\zeta\left(s;\tfrac{1}{8},\tfrac{7}{8};\tfrac{3}{8},\tfrac{5}{8}\right)\zeta\left(s;\tfrac{1}{4};\tfrac{3}{4}\right) \\
&\quad - 2^{-5s-1}3^{-2s}\zeta\left(s;\tfrac{1}{24},\tfrac{5}{24},\tfrac{7}{24},\tfrac{11}{24};\tfrac{13}{24},\tfrac{17}{24},\tfrac{19}{24},\tfrac{23}{24}\right)\zeta\left(s;\tfrac{1}{12},\tfrac{11}{12};\tfrac{5}{12},\tfrac{7}{12}\right).
\end{aligned}
\tag{6.B.27}
$$

C Kronecker symbols

The definitions for Kronecker symbols used in (6.B.22, 6.B.24, 6.B.26) are shown in Table 6.3, where we omit the case $\left(\frac{a}{n}\right)=0$ if $n\equiv 0(\mathrm{mod}\,a)$. We

provide the following full example for $a = -3$ below.

$$\left(\frac{-3}{n}\right) = \begin{cases} 1 & \text{if } n \equiv 1 (\text{mod } 3) \\ -1 & \text{if } n \equiv 2 (\text{mod } 3) \\ 0 & \text{if } n \equiv 0 (\text{mod } 3) \end{cases} \tag{6.C.28}$$

The data in the first row of Table A.3 corresponds to 6.C.29. The results in Appendix 6.B involve series of the form $\sum_{n=1}^{\infty} \left(\frac{a}{n}\right) n^{-s}$ for various values of a. These series can be expressed in terms of Hurwitz zeta functions (12.3.5), (6.4.8). For example,

$$\sum_{n=1}^{\infty} \left(\frac{-12}{n}\right) n^{-s} = \frac{1}{6^s}\left[\zeta(s, \tfrac{1}{6}) - \zeta(s, \tfrac{5}{6})\right] = 6^{-s}\zeta(s; \tfrac{1}{6}; \tfrac{5}{6}). \tag{6.C.29}$$

a	$(\frac{a}{n})$
-3	1 if $n \equiv 1 (\text{mod } 3)$ -1 if $n \equiv 2 (\text{mod } 3)$
4	1 if n is odd
-4	1 if $n \equiv 1 (\text{mod } 4)$ -1 if $n \equiv 3 (\text{mod } 4)$
8	1 if $n \equiv 1, 7 (\text{mod } 8)$ -1 if $n \equiv 3, 5 (\text{mod } 8)$
-8	1 if $n \equiv 1, 3 (\text{mod } 8)$ -1 if $n \equiv 5, 7 (\text{mod } 8)$
9	1 if $n \equiv 1, 2 (\text{mod } 3)$
12	1 if $n \equiv 1, 11 (\text{mod } 12)$ -1 if $n \equiv 5, 7 (\text{mod } 12)$
-12	1 if $n \equiv 1 (\text{mod } 6)$ -1 if $n \equiv 5 (\text{mod } 6)$
24	1 if $n \equiv 1, 5, 19, 23 (\text{mod } 24)$ -1 if $n \equiv 7, 11, 13, 17 (\text{mod } 24)$
-24	1 if $n \equiv 1, 5, 7, 11 (\text{mod } 24)$ -1 if $n \equiv 13, 17, 19, 23 (\text{mod } 24)$
36	1 if $n \equiv 1, 5 (\text{mod } 6)$
-36	1 if $n \equiv 1, 5 (\text{mod } 12)$ -1 if $n \equiv 7, 11 (\text{mod } 12)$
72	1 if $n \equiv 1, 7, 17, 23 (\text{mod } 24)$ -1 if $n \equiv 5, 11, 13, 19 (\text{mod } 24)$
-72	1 if $n \equiv 1, 11, 17, 19 (\text{mod } 24)$ -1 if $n \equiv 5, 7, 13, 23 (\text{mod } 24)$

Table 6.3 Values of n for Kronecker symbols $\left(\frac{a}{n}\right)$. The value of $\left(\frac{a}{n}\right)$ is defined to be 0 for positive values of n not covered in this table.

D Expansion for half-integer Bessel functions

For even exponents in $s = 2n, n \in \mathbb{N}$ one can obtain simplified expressions for L_s terms of hyperbolic functions, which we outline here. For half-integer

a	b	x
-3	3	$\frac{1}{3}; \frac{2}{3}$
4	2	$\frac{1}{2}$
-4	4	$\frac{1}{4}; \frac{3}{4}$
8	8	$\frac{1}{8}, \frac{7}{8}, \frac{3}{8}, \frac{5}{8}$
-8	8	$\frac{1}{8}, \frac{3}{8}, \frac{5}{8}, \frac{7}{8}$
9	3	$\frac{1}{3}, \frac{2}{3}$
12	12	$\frac{1}{12}, \frac{11}{12}, \frac{5}{12}, \frac{7}{12}$
-12	6	$\frac{1}{6}; \frac{5}{6}$
24	24	$\frac{1}{24}, \frac{5}{24}, \frac{19}{24}, \frac{23}{24}; \frac{7}{24}, \frac{11}{24}, \frac{13}{24}, \frac{17}{24}$
-24	24	$\frac{1}{24}, \frac{5}{24}, \frac{7}{24}, \frac{11}{24}; \frac{13}{24}, \frac{17}{24}, \frac{19}{24}, \frac{23}{24}$
36	6	$\frac{1}{6}, \frac{5}{6}$
-36	12	$\frac{1}{12}, \frac{5}{12}; \frac{7}{12}, \frac{11}{12}$
72	24	$\frac{1}{24}, \frac{7}{24}, \frac{17}{24}, \frac{23}{24}; \frac{5}{24}, \frac{11}{24}, \frac{13}{24}, \frac{19}{24}$
-72	24	$\frac{1}{24}, \frac{11}{24}, \frac{17}{24}, \frac{19}{24}; \frac{5}{24}, \frac{7}{24}, \frac{13}{24}, \frac{23}{24}$

Table 6.4 Values of a,b and x for $\sum_{n=1}^{\infty}\left(\frac{a}{n}\right)n^{-s} = b^{-s}\zeta(s;x)$, see (6.4.8) .

Bessel functions we can use the well-known expression ($n \in \mathbb{N}$),

$$K_{n-\frac{1}{2}}(x) = \sqrt{\frac{\pi}{2x}}e^{-x}\sum_{k=0}^{n-1}\frac{(n-1+k)!}{k!(n-1-k)!(2x)^k}\,. \tag{6.D.30}$$

We note that integer Bessel functions $K_n(x)$ reduce to $K_0(x)$ and $K_1(x)$, that is we only have integral representations for the Bessel functions and the procedure which follows cannot be applied. Substituting this equation for the Bessel function in (6.7.1) gives

$$\begin{aligned} s_n(a) &= \sum_{i\in\mathbb{Z}}\left[(i+a)^2+x^2\right]^{-n} = \pi^{\frac{1}{2}}\frac{\Gamma\left(n-\frac{1}{2}\right)}{\Gamma(n)}x^{1-2n} \\ &+ \frac{2\pi^n}{x^n\Gamma(n)}\sum_{k=0}^{n-1}\frac{(n-1+k)!}{(4\pi)^k k!(n-1-k)!}x^{-k}\sum_{m\in\mathbb{N}}cos(2\pi ma)\,m^{n-k-1}\,e^{-2\pi mx}\,, \end{aligned} \tag{6.D.31}$$

with $a \in [0,1)$ and we only consider the case $x > 0$. We now turn our attention to the last sum, consider only the cases where $a = a_1 = 0$ or $a = a_2 = \frac{1}{2}$ (although if a is a rational number we can split the sum in terms containing prefactors from the cosine term, e.g., we could treat the case $a = \frac{1}{3}$ as well and rewrite the second sum as a derivative,

$$\begin{aligned} s_n(a) &= \frac{\pi^{\frac{1}{2}}\Gamma\left(n-\frac{1}{2}\right)}{\Gamma(n)}x^{1-2n} \\ &+ \frac{2\pi^n}{x^n\Gamma(n)}\sum_{k=0}^{n-1}\frac{(-2\pi)^{1+k-n}(n-1+k)!}{(4\pi)^k k!(n-1-k)!}x^{-k}\frac{d^{n-k-1}}{dx^{n-k-1}}\sum_{m\in\mathbb{N}}b_p^m\,e^{-2\pi mx}\,, \end{aligned} \tag{6.D.32}$$

with $b_1 = 1$ for $a_1 = 0$ and $b_2 = -1$ for $a_2 = \frac{1}{2}$. Now the last sum can be evaluated by using,[149]

$$\sum_{k\in\mathbb{N}} e^{-kx} = \frac{1}{e^x - 1} \quad \textit{and} \quad \sum_{k\in\mathbb{N}} (-1)^{k-1} e^{-kx} = \frac{1}{e^x + 1} \quad , \quad x > 0\,, \tag{6.D.33}$$

which follows by geometric series. We finally get

$$\begin{aligned} s_{p,n} &= \sum_{i\in\mathbb{Z}} \left[(i+a_p)^2 + x^2\right]^{-n} = \pi^{\frac{1}{2}} \frac{\Gamma\left(n-\frac{1}{2}\right)}{\Gamma(n)} x^{1-2n} \\ &+ \frac{2^{2-n}\pi b_p}{x^n \Gamma(n)} \sum_{k=0}^{n-1} \frac{(-1)^{n+k-1}(n+k-1)!}{2^k k!(n-k-1)!} x^{-k} \frac{d^{n-k-1}}{dx^{n-k-1}} \left(e^{2\pi x} - b_p\right)^{-1} . \end{aligned} \tag{6.D.34}$$

We invert the summation and use the known expressions for the gamma functions to get

$$\begin{aligned} s_{p,n} &= \sum_{i\in\mathbb{Z}} \left[(i+a_p)^2 + x^2\right]^{-n} = \frac{\pi(2n-3)!!}{2^{n-1}(n-1)! x^{2n-1}} \\ &+ \frac{2^{3-2n}\pi b_p}{x^{2n-1}(n-1)!} \sum_{k=0}^{n-1} \frac{(-1)^k 2^k (2n-k-2)!}{k!(n-k-1)!} x^k \frac{d^k}{dx^k} \left(e^{2\pi x} - b_p\right)^{-1} . \end{aligned} \tag{6.D.35}$$

We finally have to address differentiating the last term in the equation above. Differentiating an inverse function n-times leads to rather complicated expressions (Faà di Bruno's equation). A far easier approach to this derivative is to re-express the exponential in terms of a hyperbolic function,

$$\begin{aligned} \left(e^{2\pi x} - b_p\right)^{-1} = \frac{1}{2} e^{-\pi x} h_p(\pi x) \quad &\text{with} \quad h_1(x) = \operatorname{csch}(x) \\ &\text{and} \quad h_2(x) = \operatorname{sech}(x)\,, \end{aligned} \tag{6.D.36}$$

and to use the Leibniz' product rule,

$$\frac{d^k}{dx^k}\left(\frac{1}{2} e^{-\pi x} h_p(\pi x)\right) = \frac{1}{2} e^{-\pi x} \sum_{m=0}^{k} (-1)^{k-m} \pi^{k-m} \binom{k}{m} h_p^{(m)}(\pi x)\,. \tag{6.D.37}$$

We now combine (6.D.38) and (6.D.37) and finally get,

$$\begin{aligned} s_{p,n} &= \frac{\pi(2n-3)!!}{2^{n-1}(n-1)! x^{2n-1}} \\ &+ \frac{2^{2(1-n)}\pi b_p e^{-\pi x}}{x^{2n-1}(n-1)!} \sum_{k=0}^{n-1} \frac{(2\pi)^k (2n-k-2)!}{(n-k-1)!} x^k \sum_{m=0}^{k} \frac{(-1)^m \pi^{-m}}{m!(k-m)!} h_p^{(m)}(\pi x)\,. \end{aligned} \tag{6.D.38}$$

In fact we can rewrite this expression by introducing the Bessel numbers of the first kind[150] $B_{nk} = (-1)^{n-k}\, a_{nk}$ $(0 \le k \le n)$ with $a_{00} = 1$, $a_{n0} = 0$ $\forall n \in \mathbb{N}$

and

$$a_{nk} = \frac{(2n-k-1)!}{2^{n-k}(k-1)!(n-k)!} \quad for \quad 1 \le k \le n\,, \tag{6.D.39}$$

which gives

$$\begin{aligned} s_{p,n} &= \frac{\pi(2n-3)!!}{2^{n-1}(n-1)!x^{2n-1}} \\ &+ \frac{2^{1-n}\pi b_p e^{-\pi x}}{x^{2n-1}(n-1)!}\sum_{k=1}^{n}(-1)^{n-k}(\pi x)^{k-1}B_{n,k}\sum_{m=0}^{k-1}\binom{k-1}{m}\frac{(-1)^m}{\pi^m}h_p^{(m)}(\pi x)\,. \end{aligned} \tag{6.D.40}$$

We may also consider the alternating series to equation (6.D.31),

$$\begin{aligned} s_n^{alt}(a) &= \sum_{i\in\mathbb{Z}}(-1)^i\left[(i+a)^2+x^2\right]^{-n} \\ &= \sum_{i\in\mathbb{Z}}\left[(2i+a)^2+x^2\right]^{-n} - \sum_{i\in\mathbb{Z}}\left[(2i+1+a)^2+x^2\right]^{-n} \\ &= 2^{-2n}\sum_{i\in\mathbb{Z}}\left[\left(i+\frac{a}{2}\right)^2+\left(\frac{x}{2}\right)^2\right]^{-n} - 2^{-2n}\sum_{i\in\mathbb{Z}}\left[\left(i+\frac{a+1}{2}\right)^2+\left(\frac{x}{2}\right)^2\right]^{-n} \\ &= \frac{2^{-n+1}\pi^n}{x^n\Gamma(n)}\sum_{k=0}^{n-1}\frac{(n-1+k)!}{(4\pi)^k k!(n-1-k)!}\left(\frac{x}{2}\right)^{-k}\sum_{m\in\mathbb{N}}cos(\pi ma)\; m^{n-k-1}\; e^{-\pi mx} \\ &- \frac{2^{-n+1}\pi^n}{x^n\Gamma(n)}\sum_{k=0}^{n-1}\frac{(n-1+k)!}{(4\pi)^k k!(n-1-k)!}\left(\frac{x}{2}\right)^{-k} \\ &\quad \sum_{m\in\mathbb{N}}cos(\pi m(a+1))\; m^{n-k-1}\; e^{-\pi mx} \\ &= \frac{2^{-n+1}\pi^n}{x^n\Gamma(n)}\sum_{k=0}^{n-1}\frac{(n-1+k)!}{(2\pi)^k k!(n-1-k)!}x^{-k} \\ &\quad \sum_{m\in\mathbb{N}}\{1-(-1)^m\}cos(\pi ma)\; m^{n-k-1}\; e^{-\pi mx} \\ &= \frac{2^{-n+2}\pi^n}{x^n\Gamma(n)}\sum_{k=0}^{n-1}\frac{(n-1+k)!}{(2\pi)^k k!(n-1-k)!}x^{-k} \\ &\quad \sum_{m\in\mathbb{N}}cos((2m-1)\pi a)\; (2m-1)^{n-k-1}\; e^{-\pi(2m-1)x}\,, \end{aligned} \tag{6.D.41}$$

with $a \in [0,1)$ and $x > 0$. For the special case $a = 0$ we have the identity,

$$s_1^{alt}(0) = \sum_{i\in\mathbb{Z}}(-1)^i\left[i^2+x^2\right]^{-1} = \frac{\pi}{x}csch(\pi x)\,, \tag{6.D.42}$$

with $x > 0$. From this one can derive a more general formula for exponents $n > 0$ which we do not detail here.

What is left are the derivatives of the two hyperbolic functions

$h_p^{(j)}(x) = \dfrac{d^j}{dx^j} h_p(x)$. Here we adopt the approach by Wintucky and distinguish between even and odd orders in our derivative,[151]

$$\frac{d^{2m+q}}{dx^{2m+q}} \mathrm{csch}(x) = (-1)^q \mathrm{coth}^q(x) \sum_{k=0}^{m} [2(m-k)+q]!\, W_{2(m-k)+1,k}\, [\mathrm{csch}(x)]^{2(m-k)+1} \tag{6.D.43}$$

and

$$\frac{d^{2m+q}}{dx^{2m+q}} \mathrm{sech}(x) = (-1)^q \mathrm{tanh}^q(x) \sum_{k=0}^{m} [2(m-k)+q]!\, W_{2(m-k)+1,k}\, [\mathrm{sech}(x)]^{2(m-k)+1}\,, \tag{6.D.44}$$

with $m \in \mathbb{N}$ and $q \in \{0,1\}$.[c] The secant coefficients $W_{n,k}$ can be calculated according to the following formulae and recursive relations (only the odd integer ones are required here),

$$\begin{aligned} W_{2n+1,0} &= 1\,, \\ W_{2n+1,1} &= \sum_{k=0}^{n} (2k+1)^2 = \frac{4}{3}n^3 + 4n^2 + \frac{11}{3}n + 1\,, \\ W_{2n+1,k} &= (2n+1)^2\, W_{2n+1,k-1} + W_{2n-1,k}\,. \end{aligned} \tag{6.D.45}$$

We now consider the special cases $n = 2, 3$ and 4 for the non-alternating series and sort with respect to powers of x,

$$s_{p,2}(x) = \frac{\pi}{2x^3} + \frac{\pi b_p e^{-\pi x}}{2x^3} h_p(\pi x) + \frac{\pi b_p e^{-\pi x}}{2x^2} \left\{ \pi h_p(\pi x) - h_p^{(1)}(\pi x) \right\}, \tag{6.D.46}$$

$$\begin{aligned} s_{p,3}(x) = {} & \frac{3\pi}{8x^5} + \frac{3\pi b_p e^{-\pi x}}{8x^5} h_p(\pi x) + \frac{3\pi b_p e^{-\pi x}}{8x^4} \left\{ \pi h_p(\pi x) - h_p^{(1)}(\pi x) \right\} \\ & + \frac{\pi b_p e^{-\pi x}}{8x^3} \left\{ \pi^2 h_p(\pi x) - 2\pi h_p^{(1)}(\pi x) + h_p^{(2)}(\pi x) \right\}, \end{aligned} \tag{6.D.47}$$

$$\begin{aligned} s_{p,4}(x) = {} & B_1 \frac{5\pi}{16x^7} + \frac{5\pi b_p e^{-\pi x}}{16x^7} h_p(\pi x) + \frac{5\pi b_p e^{-\pi x}}{16x^6} \left\{ \pi h_p(\pi x) - h_p^{(1)}(\pi x) \right\} \\ & + \frac{\pi b_p e^{-\pi x}}{8x^5} \left\{ \pi^2 h_p(\pi x) - 2\pi h_p^{(1)}(\pi x) + h_p^{(2)}(\pi x) \right\} \\ & + \frac{\pi b_p e^{-\pi x}}{48x^4} \left\{ \pi^3 h_p(\pi x) - 3\pi^2 h_p^{(1)}(\pi x) + 3\pi h_p^{(2)}(\pi x) - h_p^{(3)}(\pi x) \right\}, \end{aligned} \tag{6.D.48}$$

with the derivatives $h_p^{(n)}$ as defined in (6.D.43) and (6.D.44). The first few

[c] There is a typographical error in Wintucky's equation (6.D.44), a tan function is printed instead of a tanh function.

$h_1^{(n)}(\pi x)$ and $h_2^{(n)}(\pi x)$ functions are defined as follows,

$$
\begin{aligned}
&h_1^{(0)}(\pi x) = \mathrm{c}sch(\pi x), h_1^{(1)}(\pi x) = -\pi \mathrm{c}oth(\pi x)\mathrm{c}sch(\pi x) = -\pi \mathrm{c}osh(\pi x)\mathrm{c}sch^2(\pi x)\,,\\
&h_1^{(2)}(\pi x) = \pi^2 \mathrm{c}sch^3(\pi x) + \pi^2 \mathrm{c}oth^2(\pi x)\mathrm{c}sch(\pi x) = 2\pi^2 \mathrm{c}sch^3(\pi x) + \pi^2 \mathrm{c}sch(\pi x)\,,\\
&h_1^{(3)}(\pi x) = -\pi^3 \mathrm{c}oth(\pi x)\mathrm{c}sch(\pi x)\left(6\mathrm{c}sch^2(\pi x) + 1\right)\,,\\
&h_2^{(0)}(\pi x) = \mathrm{s}ech(\pi x), h_2^{(1)}(\pi x) = -\pi \mathrm{t}anh(\pi x)\mathrm{s}ech(\pi x)\,,\\
&h_2^{(2)}(\pi x) = 2\pi^2 \mathrm{s}ech^3(\pi x) + \pi^2 \mathrm{s}ech(\pi x)\,,\\
&h_2^{(3)}(\pi x) = -\pi^3 \mathrm{t}anh(\pi x)\mathrm{s}ech(\pi x)\left(6\mathrm{s}ech^2(\pi x) + 1\right)\,.
\end{aligned}
\tag{6.D.49}
$$

Higher derivatives can easily be derived.

Acknowledgments

This paper is dedicated to Prof. I. J. Zucker (King's College London) on the occasion of his 85th birthday, who gave us the inspiration for this work. We thank Gaven Martin, Morten Piilebeht and Lukas F. Pašteka for many valuable comments. This work was supported by the Marsden Fund Council from Government funding, managed by the Royal Society of New Zealand (MAU1409), and by the Centre for Advanced Study at the Norwegian Academy of Science and Letters (Molecules in Extreme Environments Research Program).

7 Project 2 - Analytical Expressions for Vibrational Effects in Cubic and HCP Lattices[a]

7.1 Introduction

The (n,m) Lennard-Jones (LJ) potential[18, 81–84] is, beside the Morse potential [85], the most widely used interaction potential in the physical and biological sciences,[86–90]

$$V_{\mathrm{LJ}}(r) = \frac{nm}{n-m}\varepsilon\left[\frac{1}{n}\left(\frac{r_e}{r}\right)^n - \frac{1}{m}\left(\frac{r_e}{r}\right)^m\right] \tag{7.1.1}$$

with an equilibrium distance r_e and binding energy ε (taken as a positive value) between two interacting systems.

The story of how this interaction potential came to be commonly known today as the LJ potential started with Mie's 1903 discussion suggesting an equation of state containing a volume dependent term of the form $(AV^{-1} - BV^{-\nu/3})$ with $\nu > 3$.[15] Following this, in 1912 Grüneisen[3] published the exact formula for what became the well known (n,m) LJ potential, and in 1920 Krater also introduced a less general (2,1) potential which went unnoticed.[16] The Grüneisen (n,m) potential was modified by Born and Landé[17] in 1918 for ionic crystal and the same year Madelung introduced the lattice sum for ionic crystals today known as the Madelung constant.[7] It wasn't until 1924 after Lennard-Jones solved the equation of state analytically to derive the parameters based on experimental results, that the LJ (n,m) potential gained notoriety.[18] However the physical relevance of the long-rang dispersive term came much later in 1930 by London.[19] What is curious about the chronology is that Simon and Simpson used the Grüneisen potential in 1924 giving it a proper citation, and Lennard-Jones in his second paper also cited Simon and Simpsons paper in 1924 within a series of papers, but Grüneisen's paper was ignored.

[a] This chapter is composed of sections previously published in the article "The Lennard-Jones Potential Revisited: Analytical Expressions for Vibrational Effects in Cubic and Hexagonal Close-Packed Lattices"[152] and is reprinted by permission from the publisher ©2022 American Chemical Society. Some sections may have been modified to fit the style of this thesis.

To allow for a more accurate description of the interacting potential, the LJ potential has been generalized into an inverse power series of the form[48, 94]

$$V_{\mathrm{ELJ}}(r) = \sum_{n=1}^{n_{\max}} c_n r^{-s_n}, \tag{7.1.2}$$

with $c_n \in \mathbb{R}$ and $s_n \in \mathbb{R}_+$ (s_1=6 and s_2=12 for the (12,6) LJ potential). A boundary condition such that the minimum is positioned at a distance r_e with a potential depth ε $\sum_{n=1}^{n_{\max}} c_n r_e^{-s_n} = -\varepsilon$ with $\varepsilon > 0$. The coefficients c_n can be obtained from either experimental data or accurate quantum-theoretical calculations.[48, 153]. The advantage of the inverse power series compared to more complicated expressions like the Morse potential,[85] or accurate potential forms separating the long-range from the short-range region,[95–97] is that one can express analytically the volume dependent two-body (static) cohesive energy of certain lattices in terms of infinite lattice sums,

$$\begin{aligned} E_{\mathrm{ELJ}}(V) &= \lim_{N\to\infty} \frac{1}{N} \sum_{i<j}^{N} V_{\mathrm{ELJ}}(r_{ij}) = \frac{1}{2} \sum_{i=1}^{\infty} V_{\mathrm{ELJ}}(r_{0i}) \\ &= \frac{1}{2} \sum_{n=1}^{n_{\max}} c_n L_{s_n} r_0^{-s_n} = \frac{1}{2} \sum_{n=1}^{n_{\max}} f_L^{s_n/3} c_n L_{s_n} V^{-s_n/3}. \end{aligned} \tag{7.1.3}$$

Here, $n > m$ guarantees the existence of a minimum and $s_n > 3$ to guarantee convergence for the 3D bulk system.[48] In Eq.(7.1.3) r_0 is the nearest neighbor distance of the lattice $r_0 = \min\{r_{0i}\}$, with r_{0i} being the distance from one selected atom in the lattice to all other atoms i), and f_L is a lattice-specific parameter converting r_0 into the volume $V = f_L r_0^3$, i.e. $f_{\mathrm{sc}} = 1$, $f_{\mathrm{bcc}} = 4/(3\sqrt{3})$, $f_{\mathrm{fcc}} = f_{\mathrm{hcp}} = 1/\sqrt{2}$. We use the fact that for a cubic lattice the summation over all atoms i and j with distance r_{ij} simplifies to summing over all interactions from one selected atom placed at the origin to all other atoms i in the solid because of translational symmetry. Once basic lattice vectors are introduced to express the distances r_{0i} from the chosen atom to all other atoms in the lattice, the cohesive energy can be expressed in terms of three-dimensional lattice sums $L_s \in \mathbb{R}_+$ multiplied by inverse powers of the nearest neighbor distance r_0 as originally described by Lennard-Jones in 1924[6, 22] and analyzed in detail by Borwein et al.[26]

For example, the (n,m) LJ potential, and more specifically, the (12,6) LJ potential with coefficients $c_1 = \varepsilon r_e^{12}$ ($s_1 = 12$) and $c_2 = -2\varepsilon r_e^6$ ($s_2 = 6$), becomes (in atomic units),

$$\begin{aligned} E_{\mathrm{LJ}}(r_0) &= \frac{nm\varepsilon}{2(n-m)} \left[\frac{1}{n} L_n \left(\frac{r_e}{r_0} \right)^n - \frac{1}{m} L_m \left(\frac{r_e}{r_0} \right)^m \right] \\ &\overset{\substack{n=12 \\ m=6}}{=} \varepsilon \left(\frac{r_e}{r_0} \right)^6 \left[\frac{L_{12}}{2} \left(\frac{r_e}{r_0} \right)^6 - L_6 \right]. \end{aligned} \tag{7.1.4}$$

From Eq.(7.1.3) one easily obtains the corresponding analytical expressions for the volume dependent pressure P and the bulk modulus B of a lattice expressed in terms of lattice sums as,[48]

$$P_{\mathrm{ELJ}}(V) = -\frac{\partial E_{\mathrm{ELJ}}(V)}{\partial V} = \frac{1}{6V}\sum_{n=1}^{n_{\max}} s_n c_n L_{s_n} r_0^{-s_n} = \frac{1}{6}\sum_{n=1}^{n_{\max}} s_n f_L^{s_n/3} c_n L_{s_n} V^{-\frac{s_n}{3}-1}, \tag{7.1.5}$$

$$\begin{aligned} B_{\mathrm{ELJ}}(V) &= V\frac{\partial^2 E_{\mathrm{ELJ}}(V)}{\partial V^2} = \frac{1}{18V}\sum_{n=1}^{n_{\max}} s_n\left(s_n+3\right) c_n L_{s_n} r_0^{-s_n} \\ &= \frac{1}{18}\sum_{n=1}^{n_{\max}} s_n\left(s_n+3\right) f_L^{s_n/3} c_n L_{s_n} V^{-\frac{s_n}{3}-1}. \end{aligned} \tag{7.1.6}$$

These formulae clearly demonstrate the usefulness of an extended LJ potential as important solid-state properties can be calculated *analytically* to computer precision for any volume V or pressure P if the lattice sums are accurately known.

Working on the melting of argon, Herzfeld and Goeppert-Mayer pointed out as early as in 1934 that lattice vibrations increase the equilibrium lattice distance and must therefore be considered.[154] Corner[155] and Wallace[98] analyzed such lattice vibrational effects in more detail for the $(n,6)$ LJ potential, and through approximations derived an analytical formula for the zero-point vibrational energy of the fcc lattice. Later, Nijboer and deWette analyzed lattice vibrations in k-space for the dynamic matrix for a face-centered cubic crystal with a varying lattice constant.[156, 157] However, the corresponding lattice sums become rather complicated, and fast converging forms for the dynamic matrix for phonon dispersion are not available.

In this paper we derive exact analytical expressions for the zero-point vibrational energy and corresponding anharmonicity correction to the cohesive energy and the lattice (mode) Grüneisen parameter within the Einstein approximation.[158] That is, moving a single atom in the field of an ELJ potential, for the simple cubic (sc), body-centered cubic (bcc) or face centered cubic (fcc) lattices, including thermodynamic properties, and applying these formulae to various model systems for the rare gases from helium to the heaviest element in this group, oganesson. We also include in our discussion the more complicated hexagonal close-packed structure (hcp). As specific applications we focus on the high-pressure range of helium, and the fcc and hcp phase for argon which are energetically very close, and discuss the limitations of the Einstein model. For the Grüneisen parameter we investigate solid neon as an example where anharmonicity effects are large.

7.2 Methods

The total cohesive energy per atom, $E_{coh}(V)$, can be divided into static $E_{coh}^{stat}(V)$ and dynamic $E_{coh}^{\mathrm{dyn}}(V)$ contributions, the latter resulting from zero-point vibrational motion:

$$E_{coh}(V) = E_{coh}^{stat}(V) + E_{coh}^{\mathrm{dyn}}(V). \tag{7.2.1}$$

The total static contribution can be approximated within the many-body ansatz including two- and higher body contributions in the solid if the many-body expansion is converging fast.[55] We use translational symmetry to evaluate the most important two-body contribution through an ELJ potential, $E_{coh}^{stat}(V) \cong E_{\mathrm{ELJ}}(V)$, and for the dynamic part,

$$E_{coh}^{\mathrm{dyn}}(V) \cong E_{ELJ}^{ZPVE}(V) + E_{ELJ}^{\mathrm{AZPVE}}(V). \tag{7.2.2}$$

We apply the Einstein approximation for a vibrating atom in the interacting ELJ field of all other atoms. Here $E_{ELJ}^{ZPVE}(V)$ is the volume dependent zero-point vibrational energy (ZPVE) contribution within the harmonic oscillator approximation, and $E_{ELJ}^{\mathrm{AZPVE}}(V)$ is the corresponding anharmonicity correction (AZPVE). Although this treatment neglects important higher-body contributions and phonon dispersion, and for helium important quantum effects originating from the nuclear motion, analytical formulae derived in terms of Eq.(7.2.1) will provide us with some useful qualitative insight into solid-state properties. For a more accurate treatment which goes beyond this approximation see Ref.[51] for example, where J/mol accuracy has been achieved for the cohesive energy of solid argon.

7.3 Lattice sums

Lattice sums are of key importance in the work presented in this article, a field pioneered early on by Lennard-Jones.[6, 22] Any expression in inverse powers of distances for interacting atoms in a lattice can be uniquely described by a three-dimensional lattice sum L_s (if convergent). For the case of the cubic lattices sc, bcc and fcc we have,[26]

$$\sum_{i=1}^{\infty} r_i^{-s} = L_s r_0^{-s}, \tag{7.3.1}$$

where the sum runs over all lattice points i in three dimensions located at distances r_i from a selected atom is reduced to L_s multiplied by the nearest neighbor distance, r_0 to the power of s ($s > 3$ to ensure convergence of the lattice sum, otherwise appropriate expressions for the analytical continuation of conditionally convergent series have to be found as in the case for the Madelung

constant[63]).
Analytical expressions for lattice sums L_s (also called Lennard-Jones-Ingham parameters) have a long history[26, 159] and have been tabulated for a number of lattices with integer exponents ($s \in \mathbb{N}$) by several authors.[48, 65, 98, 99, 131, 160] Even for more complicated lattices such as hcp, expressions of the cohesive energy in terms of lattice sums have been formulated[160] based on the 1940 paper by Kane and Goeppert-Mayer.[24] For the lattices considered in this work we have the following lattice sums

$$L_s^{\mathrm{sc}} = {\sum_{i,j,k\in\mathbb{Z}}}' \left[i^2+j^2+k^2\right]^{-\frac{s}{2}}, \tag{7.3.2}$$

$$L_s^{\mathrm{bcc}} = {\sum_{i,j,k\in\mathbb{Z}}}' \left[i^2+j^2+k^2-\tfrac{2}{3}\left(ij+ik+jk\right)\right]^{-\frac{s}{2}}, \tag{7.3.3}$$

$$L_s^{\mathrm{fcc}} = {\sum_{i,j,k\in\mathbb{Z}}}' \left[i^2+j^2+k^2+ij+ik+jk\right]^{-\frac{s}{2}}, \tag{7.3.4}$$

$$\begin{aligned} L_s^{\mathrm{hcp}} = & {\sum_{i,j,k\in\mathbb{Z}}}' \left[i^2+j^2+ij+\tfrac{8}{3}k^2\right]^{-\frac{s}{2}} \\ & + \sum_{i,j,k\in\mathbb{Z}} \left[\left(i+\tfrac{1}{3}\right)^2+\left(j+\tfrac{1}{3}\right)^2+\left(i+\tfrac{1}{3}\right)\left(j+\tfrac{1}{3}\right)+\tfrac{8}{3}\left(k+\tfrac{1}{2}\right)^2\right]^{-\frac{s}{2}}. \end{aligned} \tag{7.3.5}$$

The notation $\sum'$ implies that singularities in the sum at zero are avoided. Alternative decompositions to these expressions can also be found.[160] In fact, these lattice sums are functions of quadratic forms generated by its Gram matrix $G_{ij} = \vec{b_i}^{\top}\vec{b_j}$, where $\vec{b_i}$ are the generating basis vectors of the lattice.[161] A program to calculate these usually slow convergent lattice sums through various algorithms leading to fast converging series for real exponents $s \in \mathbb{R}_+, s > 3$ is freely available from our website,[143] and the lattice sums required for the formulae presented here for the LJ potential are given in Table 7.1. L_{12}^{bcc}= 9.11418, L_6^{fcc}= 14.45392, L_{12}^{fcc}=12.13188, and L_6^{hcp}=14.45490, L_{12}^{hcp}=12.13229.[160]

We have for the limit $\lim_{s\to\infty} L_s = N_c$, where N_c is the number of nearest neighbors in the crystal (N_c=6 for sc, 8 for bcc, and 12 for fcc and hcp), also called the kissing number. The lattice sums (minus the kissing number for better comparison) are depicted in Figure 7.1.

7.4 Lattice vibrations for the cubic lattices

As we move an atom in the crystal field of all other atoms, we break translational symmetry. Hence we need to apply a 3D Taylor expansion first to find appropriate formulae for the harmonic and anharmonic contributions to

n	$L_n^{sc} - L_\infty^{sc}$	$L_n^{bcc} - L_\infty^{bcc}$	$L_n^{fcc} - L_\infty^{fcc}$	$L_n^{hcp} - L_\infty^{hcp}$
6	2.40192397482754	4.25366786729232	2.45392104374447	2.45489727784162
8	0.94580792722637	2.35519790840251	0.80193723137813	0.80282185280990
10	0.42611910253309	1.56440061535995	0.31124566547741	0.31189623381898
12	0.20214904504752	1.11418326807536	0.13188019654458	0.13229376909892
14	0.09818412571215	0.81677022848592	0.05899194435086	0.05922825506824
16	0.04826346958584	0.60625404754453	0.02735484401857	0.02747941930386

Table 7.1 Lennard-Jones lattice sums L_n with respect to the infinite limit (L_∞^{sc}=6, L_∞^{bcc}=8, L_∞^{fcc}=12, L_∞^{hcp}=12) for $n \in \mathbb{N}$ for the sc, bcc, fcc and hcp lattices. For a more detailed Table see Ref.[160].

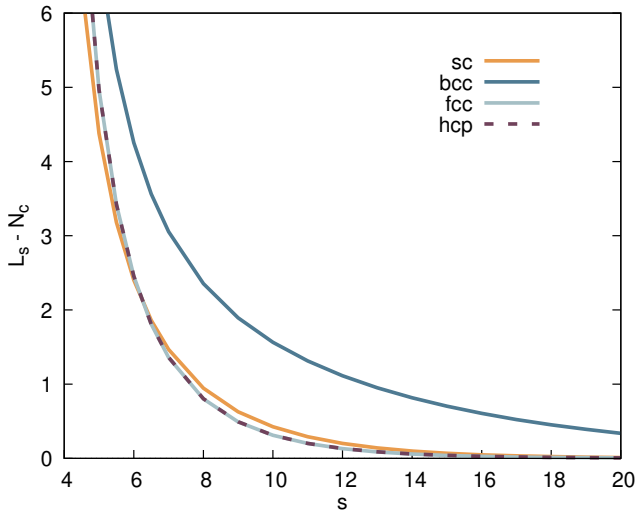

Figure 7.1 Lattice sums, L_s, minus the kissing number, $L_\infty = N_c$, of sc, bcc, fcc and hcp for a range of real exponents s. For details see Ref.[160]

the total energy, and introduce the lattice sums, Eq.(7.3.1), in a subsequent step. Within the Einstein (E) model each atom of mass M in the lattice is an independent 3D quantum harmonic oscillator,[158] i.e. all atoms oscillate with the same frequency ω_E, whereas in the Debye model the atoms are assumed to be oscillating with their own frequencies and modes. For the zero-point vibrational energy contribution within the Einstein model, which neglects the vibrational coupling with neighboring atoms, we obtain a simple analytical formula for the three cubic lattices sc, bcc and fcc analogous to the simple harmonic oscillator formula (atomic units are used throughout),

$$E_{\mathrm{ELJ}}^{\mathrm{ZPVE}} = \frac{1}{2\sqrt{M}}\left(F_{xx}^{\frac{1}{2}} + F_{yy}^{\frac{1}{2}} + F_{zz}^{\frac{1}{2}}\right) = \frac{1}{2r_0}\sqrt{\frac{3}{M}}\left[\sum_n s_n\left(s_n-1\right)c_n L_{s_n+2} r_0^{-s_n}\right]^{\frac{1}{2}} \tag{7.4.1}$$

where the second derivative matrix (F_{xy}) denotes the harmonic force field. To obtain this expression, a selected atom is moved in an external ELJ field created by all the other atoms. The derivatives of the total energy with respect to the cartesian coordinates of a moving atom in a crystal lattice up to fourth order, e.g. $F_{xyz...} = \partial^n E/\partial x \partial y \partial z ...$, are detailed in the appendix. For the cubic lattices the Euclidean coordinate system (x,y,z) is chosen parallel to the crystal axes such that (F_{xy}) is diagonal, and symmetry demands that $F_{xx} = F_{yy} = F_{zz} = tr(F)/3$. We mention that Corner also used a Taylor expression, but in his classical treatment for the vibrational movement, had to average over the angular part.[155]

The ZPVE for the (n,m) LJ potential, and more specifically, for the (12,6) LJ potential with coefficients $c_1 = \varepsilon r_e^{12}$ ($s_1 = 12$) and $c_2 = -2\varepsilon r_e^6$ ($s_2 = 6$) becomes (in atomic units),

$$\begin{aligned} E_{\mathrm{LJ}}^{\mathrm{ZPVE}}(r_0) = \frac{1}{2r_e}\sqrt{\frac{3\varepsilon}{M}}\sqrt{\frac{nm}{n-m}}\left(\frac{r_e}{r_0}\right)^{n+1} \\ \times\left[(n-1)L_{n+2} - (m-1)L_{m+2}\left(\frac{r_0}{r_e}\right)^{n-m}\right]^{\frac{1}{2}} \\ \overset{\substack{n=12\\ m=6}}{=} \frac{3}{r_e}\sqrt{\frac{\varepsilon}{M}}\left(\frac{r_e}{r_0}\right)^7\left[11L_{14} - 5L_8\left(\frac{r_0}{r_e}\right)^6\right]^{\frac{1}{2}}, \end{aligned} \tag{7.4.2}$$

This expression is identical to that of Corner for a $(n,6)$-LJ potential.[155] The (harmonic) Einstein frequency, $\omega_{\mathrm{E}} = 2E_{\mathrm{ELJ}}^{\mathrm{ZPVE}}/3$, therefore becomes

$$\omega_{\mathrm{E}} = \frac{1}{3\sqrt{M}}\left[3\,\mathrm{Tr}\,(F)\right]^{\frac{1}{2}} = \frac{1}{r_0\sqrt{3M}}\left[\sum_n s_n\,(s_n-1)\,c_n L_{s_n+2} r_0^{-s_n}\right]^{\frac{1}{2}}. \tag{7.4.3}$$

The anharmonicity correction is usually small and can be obtained from first-order perturbation theory. Since the 3rd order term in the Taylor expansion around the origin is parity odd and the corresponding matrix elements thus equals zero, the anharmonicity correction is given by the corresponding expectation value (in Dirac notation) of the 4th order term (see eq.(7.A.2) in the Appendix)

$$E^{\mathrm{AZPVE}} = \frac{1}{24}\sum_{i=1}^{\infty}\sum_{n>3} c_n \left\langle \phi_0^{\mathrm{E}}(\vec{r})\right| \left(\vec{r}\cdot\vec{\nabla}\right)^4 |\vec{r}-\vec{r}_i|^{-n}|_{\vec{0}} \left|\phi_0^{\mathrm{E}}(\vec{r})\right\rangle, \tag{7.4.4}$$

where the corresponding ground state harmonic oscillator (HO) solutions for a vibrating atom in 3D space is given by the Hartree product

$$\phi_0^{\mathrm{E}}(\vec{r}) = \phi_0^{\mathrm{HO}}(x,\omega_{\mathrm{E}})\,\phi_0^{\mathrm{HO}}(y,\omega_{\mathrm{E}})\,\phi_0^{\mathrm{HO}}(z,\omega_{\mathrm{E}}). \tag{7.4.5}$$

This is very much in the spirit of the perturbative treatment for anharmonicity effects of a vibrating diatomic molecule. In first-order perturbation theory we only have to consider two matrix elements in the Taylor expansion for the ground vibrational state (apart from permutations in x, y and z), $\left\langle \phi_0^{\mathrm{HO}}(x,\omega_{\mathrm{E}})\,|x^2|\,\phi_0^{\mathrm{HO}}(x,\omega_{\mathrm{E}})\right\rangle$ and $\left\langle \phi_0^{\mathrm{HO}}(x,\omega_{\mathrm{E}})\,|x^4|\,\phi_0^{\mathrm{HO}}(x,\omega_{\mathrm{E}})\right\rangle$, as all other quartic force constants with an odd number in one of the cartesian coordinates of the moving atom are zero due to crystal symmetry (and conveniently the cubic force field as well). The resulting anharmonic correction therefore becomes,

$$E^{\mathrm{AZPVE}} = \frac{3}{32M^2\omega_E^2}\left(F_{xxxx}+2F_{xxyy}\right). \tag{7.4.6}$$

By using the results from the appendix we obtain for an ELJ potential,

$$E_{\mathrm{ELJ}}^{\mathrm{AZPVE}}(r_0) = \frac{1}{32M^2\omega_E^2}\sum_n (s_n+2)(s_n+1)\,s_n(s_n-1)\,c_n L_{s_n+4} r_0^{-s_n-4} \tag{7.4.7}$$

and using Eq.(7.4.3),

$$E_{\mathrm{ELJ}}^{\mathrm{AZPVE}}(r_0) = \frac{3}{32Mr_0^2}\frac{\sum_n (s_n+2)(s_n+1)\,s_n(s_n-1)\,c_n L_{s_n+4} r_0^{-s_n}}{\sum_n s_n(s_n-1)\,c_n L_{s_n+2} r_0^{-s_n}}. \tag{7.4.8}$$

The AZPVE for the (n,m) LJ potential, and more specifically, the (12,6) LJ potential with coefficients c_1 and c_2 as defined above becomes (in atomic units),

$$\begin{aligned} &E_{\mathrm{LJ}}^{\mathrm{AZPVE}}(r_0) \\ &= \frac{3}{32Mr_0^2}\frac{(n+2)(n+1)(n-1)L_{n+4}r_e^{n-m} - (m+2)(m+1)(m-1)L_{m+4}r_0^{n-m}}{(n-1)L_{n+2}r_e^{n-m} - (m-1)L_{m+2}r_0^{n-m}} \\ &\underset{m=6}{\overset{n=12}{=}} \frac{21}{16M}\frac{20L_{10}r_0^6 - 143L_{16}r_e^6}{5L_8r_0^8 - 11L_{14}r_0^2r_e^6}. \end{aligned} \tag{7.4.9}$$

This shows that by using the Einstein model, compact analytical expressions can be obtained for the vibrational contributions for the ELJ potential. Since the quartic force-constants are all positive, the anharmonicity correction *increases* the zero-point vibrational energy in contrast to a diatomic molecule, where a non-zero (negative) cubic force constant becomes important in second-order perturbation, leading to a decrease in the vibrational levels and transitions.

By defining the following sums,

$$\begin{aligned}
A_L(r_0) &= r_0^{-2}\sum_n s_n\,(s_n-1)\,c_n L_{s_n+2} r_0^{-s_n},\\
B_L(r_0) &= r_0^{-2}\sum_n (s_n+2)\,s_n\,(s_n-1)\,c_n L_{s_n+2} r_0^{-s_n},\\
C_L(r_0) &= r_0^{-2}\sum_n (s_n+5)\,(s_n+2)\,s_n\,(s_n-1)\,c_n L_{s_n+2} r_0^{-s_n},\\
D_L(r_0) &= r_0^{-4}\sum_n (s_n+2)\,(s_n+1)\,s_n\,(s_n-1)\,c_n L_{s_n+4} r_0^{-s_n},\\
E_L(r_0) &= r_0^{-4}\sum_n (s_n+4)\,(s_n+2)\,(s_n+1)\,s_n\,(s_n-1)\,c_n L_{s_n+4} r_0^{-s_n},\\
F_L(r_0) &= r_0^{-4}\sum_n (s_n+7)\,(s_n+4)\,(s_n+2)\,(s_n+1)\,s_n\,(s_n-1)\,c_n L_{s_n+4} r_0^{-s_n},
\end{aligned} \tag{7.4.10}$$

the volume/nearest neighbour distance expression for the ZPVE and anharmonicity corrections become,

$$E_{\mathrm{ELJ}}^{\mathrm{ZPVE}}(r_0) = \frac{1}{2}\sqrt{\frac{3}{M}}A_L(r_0)^{\frac{1}{2}} \tag{7.4.11}$$

and

$$E_{\mathrm{ELJ}}^{\mathrm{AZPVE}}(r_0) = \frac{3}{32M}A_L(r_0)^{-1}D_L(r_0)\,. \tag{7.4.12}$$

Analytical expressions for the vibrational pressure and bulk modulus contributions for these cubic lattice can now be obtained. We get for the vibrational pressure,

$$P_{\mathrm{ELJ}}^{\mathrm{ZPVE}}(r_0) = \frac{1}{4V\sqrt{3M}}A_L(r_0)^{-\frac{1}{2}}B_L(r_0)\,, \tag{7.4.13}$$

$$P_{\mathrm{ELJ}}^{\mathrm{AZPVE}}(r_0) = \frac{1}{32VM}\left[A_L(r_0)^{-1}E_L(r_0) - A_L(r_0)^{-2}B_L(r_0)D_L(r_0)\right]\,, \tag{7.4.14}$$

and the bulk modulus,

$$B_{\mathrm{ELJ}}^{\mathrm{ZPVE}}(r_0) = \frac{1}{24V\sqrt{3M}}A_L(r_0)^{-\frac{1}{2}}\left[2C_L(r_0) - A_L(r_0)^{-1}B_L(r_0)^2\right]\,, \tag{7.4.15}$$

$$\begin{aligned}
B_{\mathrm{ELJ}}^{\mathrm{AZPVE}}(r_0) = \frac{1}{96VM}A_L(r_0)^{-1}\big\{&F_L(r_0) - A_L(r_0)^{-1}\left[2B_L(r_0)E_L(r_0) + C_L(r_0)D_L(r_0)\right]\\
&+ 2A_L(r_0)^{-2}D_L(r_0)B_L(r_0)^2\big\}\,.
\end{aligned} \tag{7.4.16}$$

7.5 Grüneisen parameter

An important parameter in the theory of the equation of state and thermal expansion of solids is the volume (or pressure) and temperature dependent Grüneisen parameter $\gamma(V,T)$, which describes the effect of changing the volume of a lattice on its vibrational properties.[162–165] At the microscopic level this parameter depends on the volume derivative of the phonon frequencies, and at T =0 K with wave vector $\vec{k}$ and band index j the dimensionless mode Grüneisen parameter becomes,

$$\gamma_{\vec{k},j}(V) = -\frac{\partial \ln \omega_{\vec{k},j}(V)}{\partial \ln V}\,. \tag{7.5.1}$$

For the Einstein approximation Eq.(7.5.1) simplifies to

$$\gamma_E(V) = -\frac{\partial \ln \omega_E(V)}{\partial \ln V}, \tag{7.5.2}$$

where we simply replaced the commonly used Debye frequency by the Einstein frequency. Using Eqs. (7.4.10), (7.4.11) and (7.4.13) we obtain the ELJ potential

$$\gamma^{\rm ELJ}_{E,h}(r_0) = -\frac{V}{E^{\rm ZPVE}_{\rm ELJ}(r_0)}\frac{\partial E^{\rm ZPVE}_{\rm ELJ}(r_0)}{\partial V} = V\frac{P^{\rm ZPVE}_{\rm ELJ}(r_0)}{E^{\rm ZPVE}_{\rm ELJ}(r_0)} = \frac{B_L(r_0)}{6A_L(r_0)}\,. \tag{7.5.3}$$

There is no mass dependence in $\gamma^{\rm ELJ}_E(r_0)$. The Grüneisen parameter for the (n,m) LJ potential, and more specifically, the (12,6) LJ potential with our coefficients c_1 and c_2 as defined above becomes (in atomic units),

$$\gamma^{\rm LJ}_{E,h}(r_0) = \frac{1}{6}\frac{(n+2)(n-1)L_{n+2}\left(\frac{r_e}{r_0}\right)^{n-m} - (m+2)(m-1)L_{m+2}}{(n-1)L_{n+2}\left(\frac{r_e}{r_0}\right)^{n-m} - (m-1)L_{m+2}} \tag{7.5.4}$$

$$\underset{m=6}{\overset{n=12}{=}} \quad \frac{77L_{14}r_e^6 - 20L_8r_0^6}{33L_{14}r_e^6 - 15L_8r_0^6} = \frac{77L_{14}V_e^2 - 20L_8V^2}{33L_{14}V_e^2 - 15L_8V^2}$$

where V_e is the volume at nearest neighbor distance $r_0 = r_e$. The simplicity of this analytical formula demonstrates the beauty of the Einstein model. In a similar way one can derive the anharmonicity contribution to the mode Grüneisen parameter by the substitution $E^{\rm ZPVE}_{\rm ELJ}(r_0) \to E^{\rm ZPVE}_{\rm ELJ}(r_0) + E^{\rm AZPVE}_{\rm ELJ}(r_0)$,

$$\gamma^{\rm ELJ}_{E,h+ah}(r_0) = V\frac{P^{\rm ZPVE}_{\rm ELJ}(r_0) + P^{\rm AZPVE}_{\rm ELJ}(r_0)}{E^{\rm ZPVE}_{\rm ELJ}(r_0) + E^{\rm ZPVE}_{\rm ELJ}(r_0)}\,, \tag{7.5.5}$$

leading to a more complicated mass-dependent expression.

A The hexagonal close-packed structure

Like fcc, the hcp lattice is a close-packed structure and often lies energetically very close to fcc. For the hard-sphere model the fcc and hcp packing densities are identical, as are any mixed fcc/hcp Barlow packings[166]. We remember that a cubic lattice is a lattice whose points lie at positions (n_1, n_2, n_3) in the Cartesian three-space, where n_i are integers. Unlike fcc however, the hcp lattice is not cubic and not a Bravais lattice, but instead belongs to the D_{6h} point group. Although it has inversion symmetry, symmetry breaking occurs in the force field resulting in a lifting of the degeneracy of the Einstein frequencies. Hence, we lose the high symmetry compared to the three cubic lattices. This results in a far more complicated expression for the hcp compared to the fcc lattice sum, i.e. compare Eqs.(7.3.2)-(7.3.4) with (7.3.5), which has been resolved in terms of fast converging series only very recently by our group[160]. The hcp lattice can be seen as a hexagonal Bravais lattice with lattice vectors $\vec{a}_1 = \frac{a}{2}\hat{x} - \frac{\sqrt{3}a}{2}\hat{y}$, $\vec{a}_2 = \frac{a}{2}\hat{x} + \frac{\sqrt{3}a}{2}\hat{y}$, $\vec{a}_3 = c\hat{z}$, but with two atoms located at positions $\vec{r}_1^{\top} = (0,0,0)$ and $\vec{r}_2^{\top} = (2/3, 1/3, 1/2)$. Since each atom is experiencing exactly the same field from all other surrounding atoms in the bulk system, we only need to consider the summation over the many-body contributions from the atom placed at the origin for the cohesive energy. This implies that both atoms give the same diagonal 3D force field and the same set of Einstein frequencies. However, from the lattice vectors and the atom located at the origin it is clear that the vibration parallel to the hexagonal plane (h) axis will differ from the vibrations perpendicular to it (c). Thus we get for the diagonal force constants $F_{xx} = F_{yy} \neq F_{zz}$ and the corresponding three Einstein frequencies $\omega_1^h = \omega_2^h \neq \omega_3^c$. Even so we have relations between the different force constant for the hcp lattice as detailed by Wallace,[98] unfortunately for the Einstein frequency we have a sum of square-root terms for the force constants. Therefore the relations found for the cubic lattices cannot be applied anymore for the hcp structure. Fortunately, it turns out that the difference $\Delta\omega = \omega_2^h - \omega_3^c$ is very small (of the order of 0.01 cm^{-1} for argon) such that we can safely set $F_{xx} \approx F_{zz}$ and obtain to a very good approximation for hcp the same expression as in (7.4.1) with the corresponding hcp lattice sums. This holds for very small volumes (high pressures) as confirmed by numerical calculations carried out with our program SAMBA.[167] The fact that Eq.(7.4.1) works is not surprising as we can use Corner's approximate treatment of vibrational motions applied to the hcp lattice.[155]

Analyzing the higher derivatives for the hcp force field we obtain the symmetry relations for the quartic force constants $F_{xxxx} = F_{yyyy} \neq F_{zzzz}$ and $F_{xxzz} = F_{yyzz} \neq F_{xxyy}$ as discussed in detail by Wallace.[98] Again we see to a good approximation that $F_{xxxx} \approx F_{zzzz}$, but see larger differences for the mixed contributions in

our numerical calculations. Fortunately, $F_{zzzz} \gg F_{xxzz}$ and therefore the AZPVE expression in Eq.(7.4.6) is applicable to a good approximation for the hcp lattice as well. For example, comparing both equations with numerical simulations for hcp argon at a volume set at 24 $\mathrm{cm}^3/\mathrm{mol}$ (nearest neighbor distance of 3.8341 Å close to the equilibrium distance), we obtain from numerical force field calculations the Einstein frequencies ω^h=33.152 and ω^c=33.141 cm^{-1} and the ZPVE and AZPVE corrections of 49.7230 and 1.7758 cm^{-1} respectively. This compares well with the ZPVE and AZPVE contributions from Eqs. (7.4.1) and (7.4.6) of 49.7230 and 1.7732 cm^{-1} respectively, where the latter small difference could come from numerical inaccuracies.

B Thermodynamics

The thermodynamics of the solid state using the LJ potential has been reviewed by Anderson containing many useful formulae.[168] The finite temperature contributions to the entropy and free energy may now also be expressed in terms of the lattice sums, using the expression for the Einstein frequency and the Boltzmann distribution. We start from the partition function for a single harmonic oscillator with frequency ω_i,

$$Z_i = \frac{e^{-\beta\omega_i/2}}{1-e^{-\beta\omega_i}}\,, \tag{7.5.6}$$

with $\beta = 1/k_BT$, T being the temperature and k_B the Boltzmann constant converting the units of Kelvin to the desired energy unit. From this we get the phonon free energy for N vibrating atoms, $F_{\mathrm{vib}} = -k_BT\ln Z$,

$$F_{\mathrm{vib}} = \frac{1}{2}\sum_i^{3N}\omega_i + \beta^{-1}\sum_i^{3N}\ln\left(1-e^{-\beta\omega_i}\right) \tag{7.5.7}$$

which contains the zero-point vibrational contribution and the phonon entropy $S = k_BT\partial\ln Z/\partial T + k_B\ln Z$,

$$S_{\mathrm{vib}} = k_B\sum_i^{3N}\left[\text{-}\ln\left(1-e^{-\beta\omega_i}\right) - \frac{\beta\omega_i}{1-e^{-\beta\omega_i}}\right]. \tag{7.5.8}$$

This expression trivially shows that for $T\to 0$ there is, aside the residual entropy, no entropy difference due to zero-point vibration between the lattices. For the Einstein approximation we obtain from Eq.(7.5.7) the relation,

$$F_{\mathrm{vib}} = \frac{3}{2}\omega_E + 3\beta^{-1}\ln\left(1-e^{-\beta\omega_E}\right) \tag{7.5.9}$$

and

$$S_{\mathrm{vib}} = 3k_B\left[\text{-}\ln\left(1-e^{-\beta\omega_E}\right) - \frac{\beta\omega_E}{1-e^{-\beta\omega_E}}\right]. \tag{7.5.10}$$

We obtain the following equation for the specific heat at constant volume ($F = E - TS$)

$$C_V = \left(\frac{\partial E}{\partial T}\right)_V = \frac{3}{4} k_B (\beta \omega_E)^2 \left[\frac{e^{\beta \omega_E}}{\left(e^{\beta \omega_E} - 1\right)^2}\right]. \tag{7.5.11}$$

7.6 Results and Discussion

In this section we apply our derived formulae for the LJ and ELJ potentials to the rare gas bulk phases of which the LJ potential already has a long history in the treatment of bulk systems.[47, 48, 169, 170] Beside the simplicity of this model, for which we shall highlight the limitations, especially for a quantum system such as bulk helium, it offers qualitative yet valuable insight into bulk properties. Furthermore, these analytical formulae serve as a first good initial estimate of how important vibrational effects are for bulk quantities such as the equation of state. They also point towards further improvements like inclusion of higher body forces, phonon dispersion and, in the case of helium, dynamic effects to achieve better agreement with experimental observations. It should be borne in mind, however, that the rare gas solids represent a special case as the many-body expansion of the interaction energy converges reasonably fast with increasing n-body force, even at higher pressures.[50, 51, 55, 171, 172] The results are collected in Table 7.2 and the potential curves used are shown and analyzed in Figures 7.2a-c.

A The equilibrium nearest neighbor distance and cohesive energy of the rare gas solids

From the condition $\partial E_{\mathrm{ELJ}}(r_0)/\partial r_0 = 0$ we derive the minimum nearest neighbor distance $r_0^{\min}$ of the atoms in the solid described by an ELJ potential. In the case of a general (n,m) LJ potential we obtain a simple relationship between the equilibrium distance r_e of the diatomic and the lattice $r_0^{\min}$ value,[48]

$$r_0^{\min} = \left(\frac{L_n}{L_m}\right)^{\frac{1}{n-m}} r_e\,. \tag{7.6.1}$$

As for $n > m$ we have $L_n < L_m$ for a specific lattice,[160] we have $r_0^{\min} < r_e$. The same inequality holds for the ELJ potentials for the rare gases as the values in Table 7.2 show and is due to the fact that the lattice summation introduces attractive forces originating from non-nearest neighbors causing a bond contraction compared to the diatomic.

Isotope	-ε	E^{stat}	E^{ZPVE}	E^{AZPVE}	r_e	r^{infl}	r_0^{min}	r_0^{ZPVE}	r_0^{infl}	r_0^{crit}
LJ										
^{3}He	-34.8	-299.8	462.3	153.2	2.9676	3.2901	2.8822	(3.3508)	3.1955	3.3508
^{4}He	-34.8	-299.8	401.3	115.4	2.9676	3.2901	2.8822	(3.3508)	3.1955	3.3508
^{20}Ne	-133.5	-1149.4	337.7	21.3	3.0895	3.4252	3.0006	3.1250	3.3267	3.4884
^{40}Ar	-453.2	-3902.5	361.4	7.2	3.7618	4.1706	3.6536	3.6975	4.0507	4.2476
^{84}Kr	-636.1	-5477.3	276.8	3.0	4.0158	4.4523	3.9003	3.9255	4.3242	4.5344
^{132}Xe	-894.0	-7697.1	240.9	1.6	4.3630	4.8372	4.2375	4.2543	4.6980	4.9264
^{222}Rn	-1282.2	-11040	219.2	0.9	4.4270	4.9081	4.2997	4.3104	4.7670	4.9986
^{294}Og	-2844.3	-24490	290.1	0.7	4.3290	4.7995	4.2045	4.2108	4.6614	4.8880
ELJ										
^{3}He	-34.9	-258.1	432.0	113.9	2.9676	3.2906	2.9112	(3.3530)	3.2322	3.3530
^{4}He	-34.9	-258.1	375.0	85.8	2.9676	3.2906	2.9112	(3.3530)	3.2322	3.3530
^{20}Ne	-132.2	-1040.7	328.7	17.8	3.0930	3.4167	3.0278	3.1538	3.3501	3.4768
^{40}Ar	-441.8	-3470.0	346.7	5.5	3.7782	4.1731	3.7004	3.7430	4.0958	4.2460
^{84}Kr	-636.1	-4683.6	266.6	2.2	4.0157	4.4381	3.9346	3.9584	4.3577	4.5156
^{132}Xe	-894.3	-6844.8	233.8	1.2	4.3616	4.8126	4.2782	4.2941	4.7309	4.8943
^{222}Rn	-1212.9	-9665.3	202.9	0.6	4.4407	4.9153	4.3420	4.3520	4.8235	5.0004
^{294}Og	-2853.6	-22482	258.1	0.4	4.3138	4.8259	4.1957	4.2011	4.7122	4.9256

Table 7.2 (12,6) LJ and ELJ properties for the fcc lattices of the rare gases at minimum energy. Binding energies -ε, cohesive energies E^{stat}, zero-point vibrational energies (ZPVE) E^{ZPVE} and anharmonicity corrections E^{AZPVE} in [μHa] at r_0^{min}. Equilibrium distances r_e of the diatomic, nearest neighbour distance of the solid r_0^{min}, ZPVE corrected nearest neighbour distance r_0^{ZPVE}, critical distance r_0^{crit} and inflection point r_0^{infl} in []. Atomic masses M used (in [amu]) are 3.016 and 4.003 for ^{3}He and ^{4}He respectively, 19.992 for ^{20}Ne, 39.962 for ^{40}Ar, 83.912 for ^{84}Kr, 131.904 for ^{132}Xe, 222.018 for ^{222}Rn and 294.0 for ^{294}Og. Binding energies and equilibrium distances for the (12,6) LJ potential are taken from Refs. [96, 173–175] The ELJ potential parameters are from: He (this work), Ne (Ref.[50]), Ar (Ref.[51]), Kr (Ref.[176]), Xe (Ref.[176]), Rn (Ref.[53]), Og (Ref.[54]).

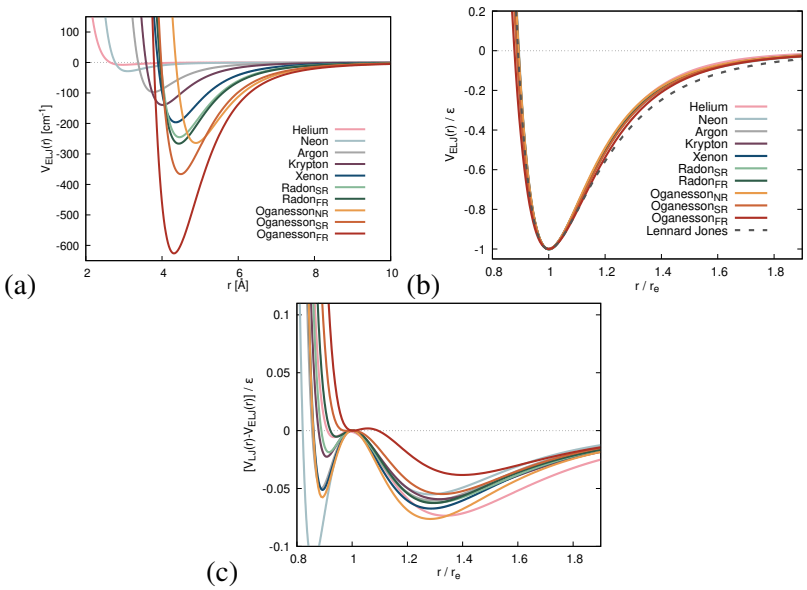

Figure 7.2 (a) ELJ potentials of the noble gases, including potentials of Rn and Og at different levels of relativistic theory (NR: non-relativistic, SR: scalar relativistic, FR: fully relativistic (X2C). (b) All potentials rescaled to a potential with $r_e = 1, \varepsilon = 1$. In grey the (12,6) LJ potential. (c) Difference between the LJ and ELJ potentials with $r_e = 1, \varepsilon = 1$, $\Delta V(r) = V_{\mathrm{LJ}}(r) - V_{\mathrm{ELJ}}(r)$

Using our analytical expressions we can determine the nearest neighbor distance for an ELJ potential including zero-point vibration. Table 7.2 shows that vibrational effects increase the nearest neighbor distance in the solid, $r_0^{\mathrm{ZPVE}} > r_0^{\mathrm{min}}$, as pointed out earlier by accurate ab-initio calculations.[51, 53, 54, 176, 177] For example, the total cohesive energy for a (12,6) LJ potential including harmonic vibrational contributions within the Einstein approximation from Eqs. (7.1.3) and (7.4.1) becomes,

$$\begin{aligned} E_{\mathrm{LJ}}^{\mathrm{T}}(r_0) &= E_{\mathrm{LJ}}^{\mathrm{coh}}(r_0) + E_{\mathrm{LJ}}^{\mathrm{ZPVE}}(r_0) \\ &= \frac{1}{2}\left(c_6 L_6 r_0^{-6} + c_{12} L_{12} r_0^{-12}\right) + \frac{3}{\sqrt{2M}} r_0^{-7}\left(5 c_6 L_8 r_0^{6} + 22 c_{12} L_{14}\right)^{\frac{1}{2}} . \end{aligned} \tag{7.6.2}$$

For the minimum $\partial E_{\mathrm{LJ}}^{\mathrm{T}}(r_0)/\partial r_0 = 0$ we get, after some algebraic manipulations, an 11th order polynomial in $x = r_0^2$,

$$a_0 + a_3 x^3 + a_5 x^5 + a_6 x^6 + a_8 x^8 + a_9 x^9 + a_{11} x^{11} = 0 \tag{7.6.3}$$

with coefficients

$$
\begin{aligned}
a_0 &= 44\varepsilon L_{12}^2 L_{14}, \\
a_3 &= -4\varepsilon r_e^{-6} L_{12}\left(22L_6L_{14} + 5L_8L_{12}\right), \\
a_5 &= -5929M^{-1} r_e^{-12} L_{14}^2, \\
a_6 &= 4\varepsilon r_e^{-12} L_6\left(11L_6L_{14} + 10L_8L_{12}\right), \\
a_8 &= 3080M^{-1} r_e^{-18} L_8 L_{14}, \\
a_9 &= -20\varepsilon r_e^{-18} L_6^2 L_8, \\
a_{11} &= -400M^{-1} r_e^{-24} L_8^2,
\end{aligned}
$$

the problem is then reduced to finding the zeros of the polynomial (7.6.3). There is no trivial solution except for $M \to \infty$, which yields just $r_0^{\min}$ for the minimum structure of the lattice and the polynomial has exactly one real solution. For a finite mass, the polynomial needs to be evaluated case by case. For all the rare gas solids, the polynomial has three real solutions and we find the second root to be the physical one. A similar expression can be obtained if the anharmonicity correction is added.

Using Eq. (7.6.1) for (7.1.4) we obtain a relationship for the cohesive energy at $r_0^{\min}$ in terms of the binding energy of the diatomic molecule and lattice sums,

$$
E_{\mathrm{LJ}}(r_0^{\min}) = \varepsilon \frac{nm}{2(n-m)} \left[\frac{L_n}{n} \left(\frac{L_m}{L_n} \right)^{\frac{n}{n-m}} - \frac{L_m}{m} \left(\frac{L_m}{L_n} \right)^{\frac{m}{n-m}} \right] \underset{m=6}{\overset{n=12}{=}} -\varepsilon \frac{L_6^2}{2L_{12}} \,. \tag{7.6.4}
$$

Figures 7.3a and b show trends in cohesive energy contributions and a comparison between the LJ and ELJ potentials along the row of the rare gas solids. For the fcc lattice we have $L_6^2/2L_{12}$=8.6102.[48] The ratios $-E_{\mathrm{ELJ}}(r_0^{\min})/\varepsilon$ for the ELJ potential as well as with respect to the experimental or best theoretical values for the rare gas lattices are shown in Figure 7.3b. There are two important messages we can deduce from this figure. First, the ELJ potential gives lower cohesive energies compared to the (12,6) LJ potential and the ratio $E_{\mathrm{ELJ}}/\varepsilon$ varies slightly between 7.36 (Kr) and 7.90 (Og) compared to the LJ ideal value of 8.6102. Second, if we take the best available cohesive energy values for the rare gases to obtain the ratio $E_{\mathrm{coh}}/\varepsilon$,[54, 177–180] we see that zero-point vibrational effects lead to larger deviations for the lighter rare gas elements and the three-body effects to larger deviations for the heavier ones.

Table 7.2 shows properties for the fcc phase of the rare gas solids obtained by using both a (12,6) LJ as well as an ELJ potential with the values for the

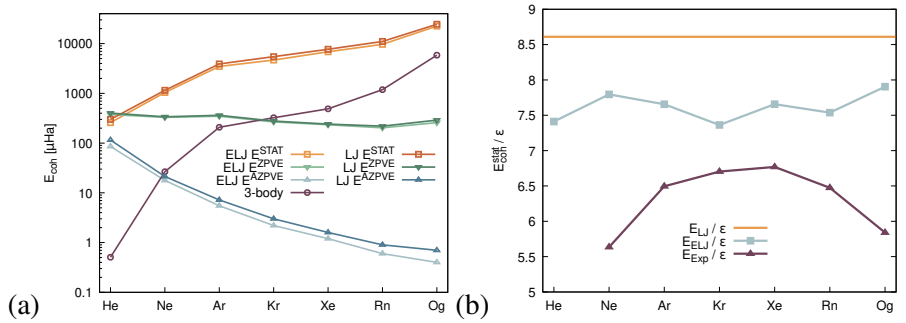

Figure 7.3 (a) Trends in cohesive energy contributions for E^{stat}, E^{ZPVE}, E^{AZPVE} and $E^{(3)}$ (in μHa) shown at a logarithmic scale for all the rare gases. The values in Table 7.2 were chosen, and for helium the ^{4}He isotope was selected. The three-body contribution $E^{(3)}$ was taken from Ref.[180] for Ne to Xe, and Ref.[54] for Rn and Og. For He the program Samba was used and the three-body potential of Cencek, Patkowski and Szalewicz was taken (Ref.[181]) at the equilibrium distance r_e for the dimer listed in Table 7.2. (b) Ratio between the two-body ELJ cohesive energy E_{ELJ} and the binding energy $-\varepsilon$ of the diatomic molecule (values taken from Table 7.2), and ratio for the best available cohesive energies [54, 177–180] E_{coh} and ε. The ideal LJ ratio is shown as a straight line.

lattice sums L_n published recently.[160] The corresponding potential curves are drawn in Figure 7.2a which show the very weak bonding for the lightest element, helium and the relatively strong bonding for the heaviest element in this group, oganesson. As can be seen from Figure 7.2a, the unusually large cohesive energy of the heaviest known element in the periodic table is due to relativistic effects,[54, 182, 183] which, despite the very large three-body contribution, results in a melting point above room temperature for oganesson [184].

Concerning vibrational effects, we obtain a slow decrease in the ZPVE with increasing mass, gradually becoming less important compared to the static part of the cohesive energy. Oganesson is exceptional, since the increase in the cohesive energy and decrease in the bond distance, both due to relativistic effects, lead to a larger vibrational contribution compared to radon despite the larger mass. [54] In contrast, anharmonicity effects diminish rather fast with increasing Z, see Figure 7.3. This can be understood from Eqs. (7.4.1) and (7.4.8): For the ZPVE we have $E^{\mathrm{ZPVE}}_{\mathrm{LJ/ELJ}} \propto r_0^{-1}\sqrt{\varepsilon/M}$. As ε, M and r_0 increase down the group in the periodic table we have a compensating effect and a small net decrease in the Einstein frequency. For the anharmonic contribution, however, we have $E^{\mathrm{AZPVE}}_{\mathrm{LJ/ELJ}} \propto r_0^{-2}M^{-1}$ leading to a much faster decrease in $E^{\mathrm{ZPVE}}_{\mathrm{LJ/ELJ}}$ with increasing mass and distance r_0^{min}.

To compare to experimental values we take solid argon as an example. The experimental nearest neighbor distance is 3.7560 Å[185] and the cohesive energy -2941(4) μHa[179], in good agreement with the ELJ values of $E_{\mathrm{ELJ}} + E_{\mathrm{ELJ}}^{\mathrm{ZPVE}} + E_{\mathrm{ELJ}}^{\mathrm{AZPVE}}$= -3118 μHa. If we take the optimized r_0^{AZPVE} distance instead, we obtain a similar value of 3134 μHa), but the (12,6) LJ potential with -3534 μHa clearly overestimates the cohesive energy. The remaining error for the ELJ potential lies mainly in the missing three-body effect. For a detailed analysis of the rare gas solids see Refs.[51, 53, 54, 176, 177]. For comparison, we include three-body contributions from the literature in Figure 7.3, which shows that these effects become increasingly important with increasing nuclear charge and polarizability of the rare gas atom [186].

Figure 7.2b compares the ELJ potentials by scaling both the equilibrium distance and the binding energy to unity. They all show a very similar functional form, the differences being barely visible on this graph. This suggests that, to a reasonable approximation, we can use the same analytical form for $\varepsilon^{-1}E_{\mathrm{ELJ}}(r/r_e)$, which needs to be further investigated for the solid state properties of the rare gases. Figure 7.2c shows the difference between these curves and the standard (12,6) LJ potential. We see that the LJ potential over-binds in the long-range, but becomes too repulsive in the short-range, which will have consequences for the pressure-volume and bulk modulus-volume equations of states as we shall see below. However, before we proceed with the discussion of three of the rare gas solids, helium, neon and argon, we shall briefly discuss the analytical expressions for the critical points for the LJ and the ELJ potentials, and their relevance for the solid state.

B Critical points for the extended Lennard-Jones potential energy curves

Multiple critical points, which in a strict mathematical sense are points on the function where the first or higher-order derivatives are equal to zero or where the function or derivative is discontinuous, for the ELJ potential can be identified. The first critical point is at the nearest neighbor distance r_0^{min} where the pressure is zero, $P = \partial E^{\mathrm{coh}}(r_0)/\partial r_0 = 0$. Expansion beyond the nearest neighbor distance into the region of negative pressure, $r > r_0^{\mathrm{min}}$, is achieved by adding thermal pressure through the Boltzmann term, which keeps the pressure positive. The negative pressure range has however been used, for example, to theoretically analyze the metal-to-nonmetal transition in expanded fluid mercury. [187]

A second critical point lies at the distance where $\partial^2 E^{\mathrm{coh}}(r_0)/\partial r_0^2 = 0$, referred

to as the cohesive energy inflection point

$$r_0^{\text{infl}} = \left[\frac{(n+1)L_n}{(m+1)L_m}\right]^{\frac{1}{n-m}} r_e = \left[\frac{(n+1)}{(m+1)}\right]^{\frac{1}{n-m}} r_0^{\min} = \left[\frac{L_n}{L_m}\right]^{\frac{1}{n-m}} r^{\text{infl}}, \quad (7.6.5)$$

where r^{infl} is the inflection point of the (12,6) LJ potential defined in Eq.(10.2.4). For the $(12,6)$ LJ potential we have $r_0^{\text{infl}} = 1.07679\, r_e = 1.10868\, r_0^{\min}$. The restoring forces decrease with increasing deviations from equilibrium and at the inflection point the bulk modulus becomes zero, indicating that the compressibility becomes infinitely high, alike a gas at very low pressure. Even though the lattice symmetry is maintained when moving along the cohesive energy curve, this hints that the inflection point can be used as a qualitative measure for symmetry breaking in the solid, resulting in a phase transition into the liquid or gas phase.[188, 189]

Symmetry breaking occurs when one or more atoms in the lattice or unit cell move to positions where the lattice symmetry is not conserved, in contrast to expansion or compression of all atoms simultaneously of which the energy is given by the cohesive energy curve for the specific lattice symmetry. A good example for symmetry breaking is the so-called Peierls distortion (Jahn-Teller effect).[190, 191] A local form of symmetry breaking happens when the Einstein frequency becomes zero and the square root in Eq. (7.4.1) or (7.4.2) vanishes. This form of symmetry breaking was already discussed qualitatively for helium in 1955 by Houton [169, 192] and occurs at a distance of

$$r_0^{\text{crit}} = \left[\frac{(n-1)}{(m-1)}\frac{L_{n+2}}{L_{m+2}}\right]^{\frac{1}{n-m}} r_e = \left[\frac{(n-1)}{(m-1)}\frac{L_{n+2}L_m}{L_{m+2}L_n}\right]^{\frac{1}{n-m}} r_0^{\min}. \quad (7.6.6)$$

For the $(12,6)$ LJ potential, $r_0^{\text{crit}} = 1.12912\, r_e = 1.16257\, r_0^{\min}$. Note that both Eq. (7.6.5) and (7.6.6) are not mass dependent. At expansion beyond r_0^{crit} a double minimum for the internal energy of the atom is formed, causing the atom to move away from the equilibrium distance and consequently the lattice locally distorts, breaking the symmetry of the bulk system. Yet, this simplified Einstein picture involves only the movement of one atom in the field of all other atoms which are kept at lattice symmetry points. If we allow all atoms in the solid to move, the point where symmetry breaks, r_0^{sb}, lies below this Einstein estimate, $r_0^{\text{sb}} < r_0^{\text{crit}}$, and perhaps also below the inflection point for which we have $r_0^{\text{infl}} < r_0^{\text{crit}}$.

We briefly consider the inflection point and critical distance for close-packed structures in one and two dimensions for a LJ potential as they serve as a good models for symmetry breaking effects in solids. The expressions for the cohesive energy in Eq.(7.1.4), the inflection point, Eq.(7.6.5), and critical

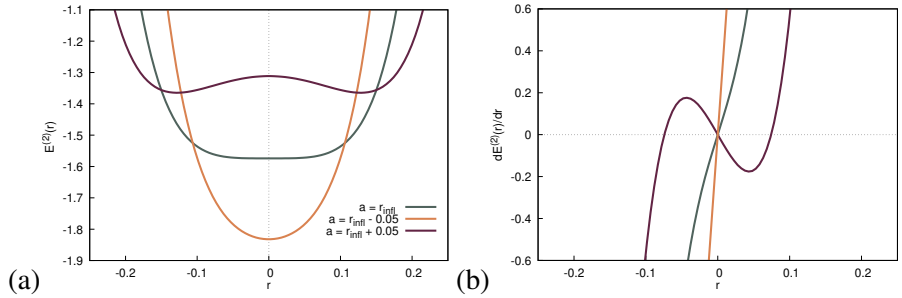

Figure 7.4 LJ potential experienced by an atom confined by two other atoms to the left and right and separated by a distance of $2a$ resulting in a total interaction energy of $E_{LJ}(r) = (r+a)^{-12} - 2(r+a)^{-6} + (r-a)^{-12} - 2(r-a)^{-6}$. The parameter used is (a) $a = r_{\text{infl}} + 0.05$, (b) $a = r_{\text{infl}}$, (c) $a = r_{\text{infl}} - 0.05$ (the inflection distance which is equal to the critical distance for a 1 dimensional chain). (b) Corresponding effective on-site forces.

distance, Eq (7.6.6), remain unchanged except that we have to substitute the 3D lattice sums L_n^{3D} for the corresponding 1D or 2D ones. For a one-dimensional chain, these are related to the well-known Riemann zeta function, i.e. $L_n^{1D} = 2\zeta(n)$ with the number of nearest neighbors $L_\infty^{1D} = 2$, thus for the (12,6) LJ potential we have $\zeta(6) = \pi^6/945$, $\zeta(8) = \pi^8/9450$, $\zeta(12) = 691\pi^{12}/638512875$ and $\zeta(14) = 2\pi^{14}/18243225$. We obtain $r_0^{1D,\text{infl}} = 1.10556 r_e$ and $r_0^{1D,\text{crit}} = 1.13967 r_e$. However, moving an atom in-between only two other atoms in one dimension, as shown in Figure 7.4a and b, results in the equality $r_0^{\text{crit}} = r^{\text{infl}}$.

For the two-dimensional case the close-packed arrangement is the hexagonal lattice (one layer of the 3D fcc lattice) for which we can derive the corresponding lattice sums in terms of Riemann $\zeta(x)$ and Hurwitz $h(x,y)$ functions[193] according to Zucker and Robertson[105],

$$L_n^{2D} = 3^{1-\frac{n}{2}} 2\zeta(\tfrac{n}{2}) \left[h(\tfrac{n}{2}, \tfrac{1}{3}) - h(\tfrac{n}{2}, \tfrac{2}{3})\right] . \tag{7.6.7}$$

There are six nearest neighbors and therefore $L_\infty^{2D} = 6$.[65, 160] We get $L_6^{2D} = 6.37705$, $L_{12}^{2D} = 6.01079$, $L_8^{2D} = 6.10578$ and $L_{14}^{2D} = 6.00382$. This leads to $r_0^{2D,\text{infl}} = 1.09781 r_e$ and $r_0^{2D,\text{crit}} = 1.13724 r_e$.

For the fourth, and final, critical point let us discuss the minimal mass needed to stabilize the solid. Let us start with the minimal mass needed to form a bond between two atoms. Within the Born-Oppenheimer approximation two atoms can form a chemical bond if the ZPVE is smaller than the binding energy, $E_{\text{ZPVE}} < \varepsilon$. This implies that, within the harmonic approximation for the

ground state vibrational energy level, we need

$$E_{\mathrm{ZPVE}} = \frac{6}{r_e}\sqrt{\frac{\varepsilon}{M}} < \varepsilon\,, \tag{7.6.8}$$

from which we deduct the critical mass,

$$M_{\mathrm{crit}}^{\mathrm{dimer}} = \frac{36}{\varepsilon r_e^2}\,. \tag{7.6.9}$$

In this simple picture, $M > M_{\mathrm{crit}}^{\mathrm{dimer}}$ is thus required to stabilize a diatomic molecule E_2. This is intuitive as a small binding energy requires a larger critical mass to stabilize a diatomic molecule within the Born-Oppenheimer approximation. Using the values for helium in Table 7.2 we obtain a critical mass of $M_{\mathrm{crit}}^{\mathrm{dimer}} = 17.9$ amu, which is far too high for any stable helium isotope. The harmonic ground state vibrational level lies above the diatomic He_2 potential curve,[194, 195] and only anharmonicity corrections, which are very large for this system due to the low mass and binding energy, together with an accurate treatment of the diatomic potential energy curve, can stabilize He_2 to such an extend that it can be observed at ultra-low temperatures.[196–199] Yet, the remaining dissociation energy is very small for He_2, [199] measured to be 5.58±0.49 nHa compared to the (uncorrected) binding energy shown in Table 7.2. In contrast, for Ne we obtain 4.3 amu well far below the mass of the most stable isotope of ^{20}Ne.

The same analysis may now be performed for the solid state, that is, we stabilize the solid described by a LJ potential if $E_{\mathrm{LJ}}^{\mathrm{ZPVE}} < -E_{\mathrm{LJ}}$ (remembering that $E_{\mathrm{LJ}}(r_0)$ was chosen to be negative in the attractive region). Within the Einstein approximation we obtain the following relation from the combination of Eqs. (7.1.4), (7.4.2) and (7.6.1),

$$M_{\mathrm{crit}} = \frac{36}{\varepsilon r_e^2} f_{\mathrm{solid}} \quad \text{with} \quad f_{\mathrm{solid}} = \frac{1}{L_6^3}\left(\frac{L_6}{L_{12}}\right)^{\frac{1}{3}} \left(11L_{14}L_6 - 5L_8L_{12}\right)\,. \tag{7.6.10}$$

This is identical to the result for the diatomic molecule except for the factor f_{solid}. Using the lattice sums from Ref.[160], we get for the different structures f_{bcc}=0.4298, f_{fcc}=0.4005 and f_{hcp}=0.4004. This reduces the helium critical mass to 7.17 amu for the fcc lattice compared to 17.9 amu for the diatomic. However, the atomic critical mass is still too large for solid helium, i.e., the 8-He isotope has a half-life of 119 ms. Additionally, anharmonicity effects destabilize the rare gas solid. Phonon dispersion[200] most likely reduces the destabilizing harmonic ZPVE compared to the Einstein approximation,[51] and quantum effects beyond the Born-Oppenheimer approximation also become important for the treatment of solid helium.[201]

Figures 7.5a and b show the cohesive energy of the (12,6) LJ potential with M below and with mass M above the critical mass respectively. If the mass M is small, as it is for ^{3}He or ^{4}He, the vibrating periodic lattice does not have a minimum, see Figure 7.5(a) where the potential curve for $E_{\mathrm{LJ}}(r) + E_{\mathrm{LJ}}^{\mathrm{ZPVE}}(r)$ abruptly ends when ω_{E} becomes imaginary. Hence, the r_0^{ZPVE} values for helium are set in parentheses as this is the point when the lattice optimization stops because of $\omega_E = 0$. Here the perturbative treatment for anharmonicity effects completely breaks down. At larger masses the minimum is retained, see Figure 7.5(b).

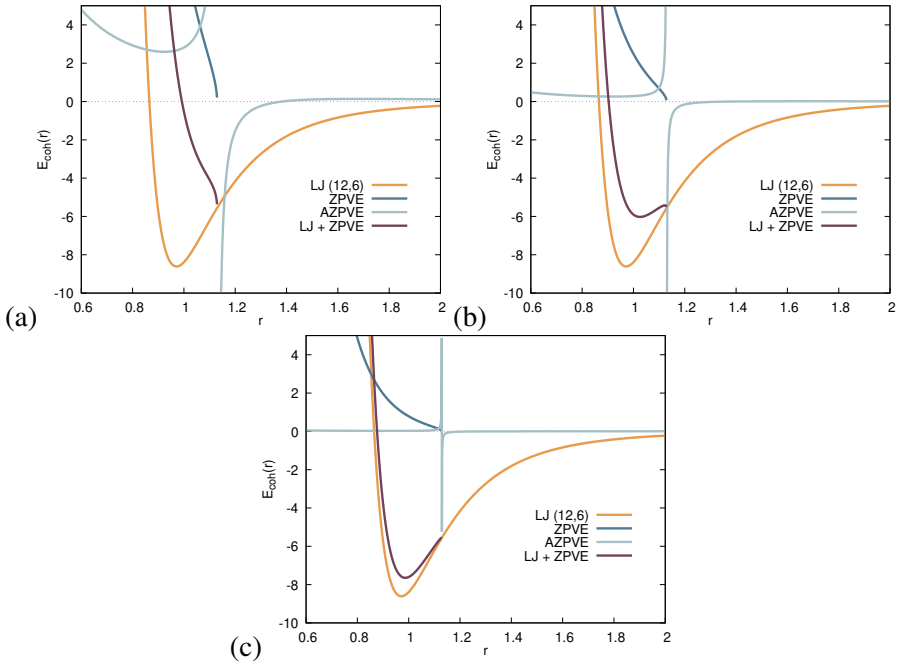

Figure 7.5 (Color online) Static and dynamic contributions (only the real part of the ZPVE is shown, the expression for the ZPVE becomes complex beyond the critical distance) to the total cohesive energy for the (12,6) LJ potential (ε and r_e set to unity), for the three different masses (a) $M = 10$ (b) $M = 100$ (c) $M = 1000$ according to Eq.(7.6.8).

Experimentally, it is known that under pressures of approximately 2.5 MPa helium is quite unusual as it solidifies to the hcp phase,[202, 203] and a hcp→fcc phase transition occurs at 1.1 GPa and 15K.[204] Helium at extreme conditions plays an important role within the science of planets and stars. [203, 205–207] We therefore discuss the validity of the (12,6) LJ model for the less critical helium high-pressure range in the following section.

C The equation of state for solid helium

Figures 7.6a-d show LJ $P(V)$- and $B(V)$ curves for solid helium for the three different observed phases fcc, hcp and bcc of ^{4}He in the pressure/volume range where this simple LJ Einstein model should work reasonably well.[208–211] To give a feeling for the volume range to be considered for bulk helium, the liquid state of ^{4}He at normal pressure has a density of 0.125 g/cm^3 corresponding to a very large volume of 32 cm^3/mol.[212] In contrast, solid helium has a density of 0.214 g/cm^3 at 6.7 GPa corresponding to a volume of 18.7 cm^3/mol and nearest neighbor distance of r_0=3.528 Å, which is larger then both the inflection point, r_0^{infl}, and critical distance, r_0^{crit}, see Table 7.2. This shows the limitation of the simple Einstein model for bulk helium.[213] Indeed, in this very low density range, zero-point vibrational energy effects dominate for both the pressure and the bulk modulus as can be seen from Figures 7.6a and 7.6b.

Solid helium shows giant plasticity and superfluid-like mass transport at large volumes and low temperatures[214, 215] (for a recent review see Beamish and Balibar[216]), and our 'static' model used here cannot accurately describe such phenomena. Moreover, at these large volumes perturbation theory used for the anharmonicity effects breaks down and one requires a full dynamic treatment, for example by using quantum Monte-Carlo simulations.[201, 203, 217] This can already be seen for the bulk moduli at volumes $V > 12$ cm^3/mol, where the LJ results start to deviate substantially from the experimental results, see Figure 7.6d. We therefore focus on the high pressure regime instead.

Grüneisen already pointed out in 1912 that the vibrational frequency increases with pressure[3] because the potential energy becomes increasingly repulsive. Our Einstein model shows that harmonic vibrational contributions to the pressure dominate down to volumes of 8 cm^3/mol. Below 8 cm^3/mol, the pressure contribution coming directly from the static cohesive energy (7.1.5) starts to dominate over vibrational effects. A similar behavior is observed for the bulk modulus. Here, anharmonicity effects become even more important in the low density range. As helium represents a special case within the rare gas elements, [169] for the heavier rare gases this picture changes significantly because of the increasing mass.[50, 177, 180]

We can determine the point at which the vibrational pressure becomes less important than the pressure created by the repulsive wall of the potential energy curve for a LJ potential, that is $P_{\mathrm{LJ}}^{\mathrm{ZPVE}}(V) = P_{\mathrm{LJ}}(V)$ at a specific volume, which we denote as V_{H}. For a (12,6) LJ potential we get a simple relation from Eqs. (7.1.5) and (7.4.13),

$$f\,(V_{\mathrm{H}}/V_e) = \varepsilon r_e^2 M\,, \tag{7.6.11}$$

where $f(x)$ is an algebraic function containing only the lattice sums for a spe-

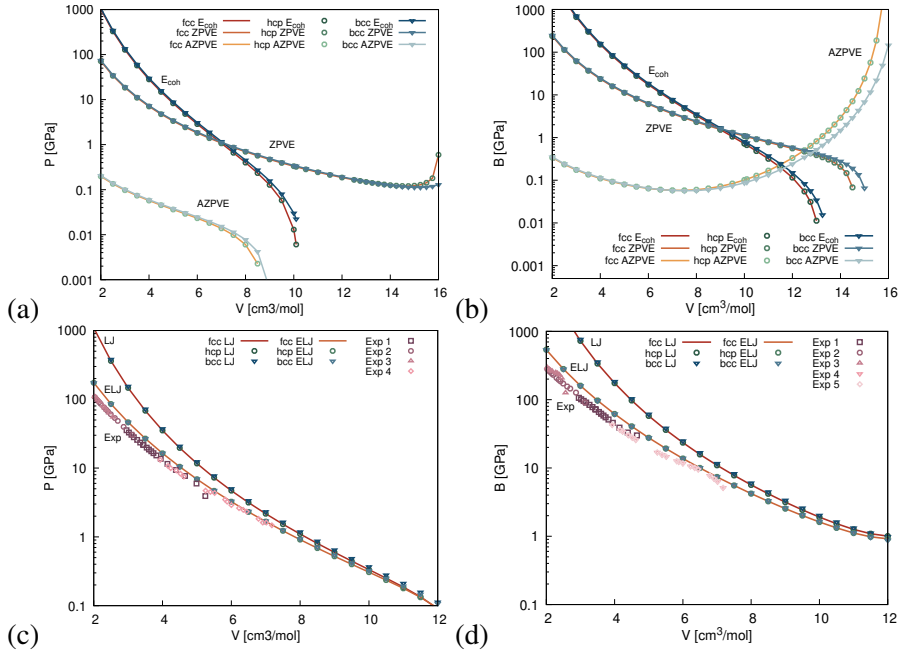

Figure 7.6 (Color online) Pressure $P(V)$ and bulk modulus $B(V)$ curves for the fcc, hcp and bcc phases of solid helium derived from the analytical formulae presented in this paper (logarithmic scale is used for P and B). (a) (12-6) LJ $P(V)$-diagram for the different pressure contributions to the static cohesive energies $P_{\rm LJ}$, harmonic zero-point vibrational $P_{\rm LJ}^{\rm ZPVE}$ and anharmonic contributions $P_{\rm LJ}^{\rm AZPVE}$ within the Einstein approximation. (b) Same as (a) but for the bulk modulus $B(V)$. (c) Total pressure $P = P_{\rm ELJ}^{\rm stat} + P_{\rm ELJ}^{\rm ZPVE} + P_{\rm ELJ}^{\rm AZPVE}$ for the LJ and ELJ potentials in comparison to experimental data from Refs.[218–220]. Exp1: T=15K, pressure gauge (PG): $SrB_4O_7:Sm^{2+}$; Exp2: T=297K, PG: W; Exp3: T=297K, PG: ruby; Exp4: T=300K, PG: ruby. (d) Exp1-Exp3 as (c) for the bulk modulus $B(V)$. Exp5: extrapolated to T=0K , isochor cell, from Ref.[221]. For the conversion of pressure units we used 1 a.u. = 2.94210157×10^4 GPa. For hcp we took the ideal $c/a = \sqrt{8/3}$ ratio as lattice distortions are small even at higher pressures.[222]

cific lattice,

$$f(x) = \left(\frac{L_6}{L_{12}}\right)^{\frac{1}{3}} \frac{x^4\left(77L_{14} - 20L_8x^2\right)^2}{4\left(L_{12} - L_6x^2\right)^2\left(11L_{14} - 5L_8x^2\right)}\,. \tag{7.6.12}$$

The left- and right-hand side of Eq. (7.6.11) are dimensionless (either use atomic units for calculating $\varepsilon r_e^2 M$ or divide this expression by $\hbar^2$). As the pressure from the cohesive energy is zero at the minimum distance, the validity range is $x = V_{\rm H}/V_e \ll 1$. In any case, from the data in Table 7.2 we get

$\varepsilon r_e^2 M = 8.048$ for ^{4}He and $\varepsilon r_e^2 M = 6.065$ for ^{3}He corresponding to a volume ratio of $V_H/V_e = 0.647$ and $V_H/V_e = 0.624$ for the fcc lattice respectively (for comparison for ^{20}Ne we have $V_H/V_e = 0.829$ and for ^{40}Ar 0.886, much closer to the minimum value $V = V^{\min}/V_e = (r_0^{\min}/r_e)^3 = 0.916$). This demonstrates the importance of vibrational effects for ^{4}He and ^{3}He in the low to medium pressure range because of their low mass.

The question now arises how well this (12,6) LJ model works. As already mentioned, in the low density range one requires a more complete quantum picture not considered here.[200, 201, 203, 223] In the high density range we can compare to experimental data from Dewaele [218] as shown in Figure 7.6c and d (when bulk experimental moduli were not available, a polynomial fit to the observed $P(V)$ data was used to obtain $B(V)$). The data show that the LJ $P(V)$ curve (containing all terms within the Einstein approximation) deviates substantially from the experimentally obtained values,[218] and increasingly so with decreasing volume. These large deviations in the high pressure range are mostly due to the incorrect repulsive form of the (12,6) LJ potential as has been pointed out before.[224, 225] Of course, one can always modify the repulsive term in the LJ potential.[226, 227]

More accurate two-body potentials $V^{(2)}(r)$ are known for all the rare gases up to oganesson,[96, 170, 173–175, 228–230] and there are already a number of theoretical studies for the $P(V)$ curves of solid helium.[231, 232] To further investigate the failure of the LJ potential in the high pressure range we fitted a recently published potential energy curve $V^{(2)}_{\rm PCJS}$ by Przybytek, Cencek, Jeziorski, and Szalewicz (PCJS) for the helium dimer,[230] who included adiabatic, relativistic as well as QED effects in their coupled-cluster treatment, to an ELJ potential. We used a least-squares fit procedure introducing distance dependent weights $\omega(r)$ to take care of the very small and large energy values in the long- and short-range of the potential energy curve respectively,

$$\frac{\partial}{\partial c_m}\int_{r_c}^{\infty} dr\ \omega(r)\left[\sum_{n=1}^{N} c_n r^{-s_n} - V^{(2)}_{\rm CS}(r)\right]^2 = 0\,, \qquad (7.6.13)$$

which leads to a set of N linear equations for the coefficients c_n ($m = 1,...,N$),

$$\sum_{n=1}^{N} c_n \int_{r_c}^{\infty} dr\ \omega(r) r^{-(s_n+s_m)} = \int_{r_c}^{\infty} dr\ \omega(r) r^{-s_m} V^{(2)}_{\rm PCJS}(r)\,. \qquad (7.6.14)$$

We applied a numerical integration scheme, a weighting function of $\omega(r) = 1 - e^{-ar}$ with $a = 0.89$, and set r_c to the lowest possible value of 2.1 a.u. to obtain a good fit over the whole distance range. The resulting ELJ potential yields an equilibrium distance of $r_e = 5.6080$ a.u., an inflection point $r^{\rm infl}$ at 6.2183 a.u. and a binding energy of ε =-348.746 μHa compared to the PCJS potential of 5.6080 a.u, 6.2089 a.u. and -348.236 μHa respectively. This should

give accurate two-body pressures up to about 1 TPa. We fixed the parameter $c_1 = -C_6$ and $c_2 = -C_8$ to the Van der Waals coefficients given in Ref.[230] to correctly describe the long-range, and chose $c_N > 0$ to correctly describe the repulsive short-range. The obtained parameters c_n are listed in Table 7.3.

Table 7.3 Potential parameters for the He dimer obtained from a least-squares fit to the analytical form of Szalewicz and co-workers[230]. All potential parameters are given in atomic units.

n	s_n	c_n	n	s_n	c_n
1	6	-1.4618550565137	2	8	-14.1208183897247
3	9	13997.975339736	4	10	-304327.625470953
5	11	2441586.03190761	6	12	-8163337.07262287
7	13	3390456.21241699	7	14	51324186.4628455
9	15	-118039510.368528	10	16	-31496186.3299036
11	17	456234485.18761	12	18	-639488529.764361
13	19	296722948.860609			

Figure 7.7 shows the deviations $[V^{(2)}_{\rm ELJ}(r) - V^{(2)}_{\rm PCJS}(r)]^{(n)}$ up to the second derivatives ($n = 2$). As can be seen, the error in the energy is of the order of a few μHa which is acceptable and the error in the first and second derivatives increase by an order of magnitude each. A test calculation with our program SAMBA[167] ensured that in the distance range $r > 2.1$ a.u. ($V > 0.6$ cm^3/mol for the fcc structure) the energy, pressure and bulk moduli are in very good agreement with the results from the PCJS potential. For example, the two-body cohesive energy, pressure and bulk modulus at a small volume of $V = 1$ cm^3/mol for the ELJ and PCJS potential (the latter obtained numerically and given in parentheses) are P =1.2187 (1.2183) TPa and B =3.221 (3.227) TPa.

To compare with experimental $P(V,T)$ and $B(V,T)$ data, one has to include the increase in pressure and bulk modulus due to finite temperature effects. For this we use the Einstein approximation (7.5.9) to obtain the thermal phonon pressure ($\beta = 1/k_B T$),

$$P_{th}(V,T) = -3\frac{\partial \omega_E(V)}{\partial V}\left[e^{\beta\omega_E(V)} - 1\right]^{-1} = 2P_{\rm ZPVE}\left[e^{\beta\omega_E(V)} - 1\right]^{-1} \quad (7.6.15)$$

and similar for the bulk modulus,

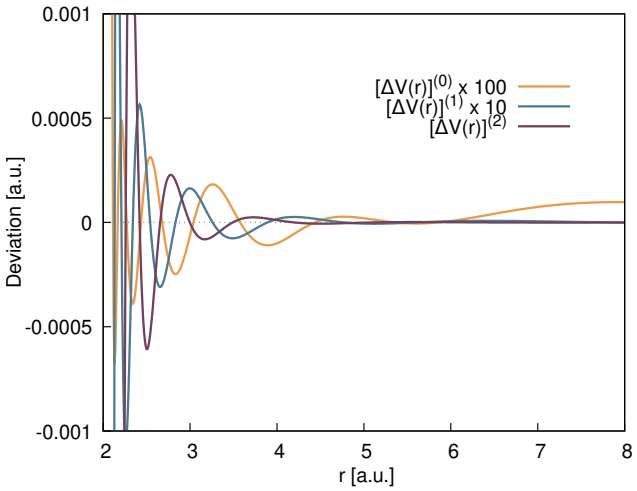

Figure 7.7 (Color online) Deviations between the ELJ and the PCJS potential, $[V^{(2)}_{\mathrm{ELJ}}(r) - V^{(2)}_{\mathrm{PCJS}}(r)]^{(n)}$, up to second order in the derivatives ($n \leq 2$).

$$B_{th}(V,T) = B_{th1}(V,T) + B_{th2}(V,T) \tag{7.6.16}$$

$$= 2B_{\mathrm{ZPVE}}(V)\left[e^{\beta\omega_E(V)} - 1\right]^{-1} - \frac{4}{3}P^2_{\mathrm{ZPVE}}(V)\,\beta V e^{\beta\omega_E(V)}\left[e^{\beta\omega_E(V)} - 1\right]^{-2}. \tag{7.6.17}$$

For an LJ or ELJ potential we have analytical expressions for both terms through Eqs. (7.4.3), (7.4.13) and (7.4.15). These equations show that $P_{th} \propto P_{\mathrm{ZPVE}}, T, \omega_E^{-1}$ and $B_{th} \propto B_{\mathrm{ZPVE}}, P^2_{\mathrm{ZPVE}}, T, \omega_E^{-1}$. Different formulae for thermal contributions are available from the Debye model which requires the Debye frequency and the Grüneisen parameter.[233] Using our two formulae we obtain for the ELJ potential at T =297 K and $V = 2\mathrm{cm}^3$/mol a thermal pressure component of P_{th}= 0.21 GPa and bulk modulus of B_{th}= -0.69 GPa (B_{th1}= 0.36 GPa, and B_{th2}= -1.05 GPa). These are relatively small compared to the measured values of about P =110 GPa and B =290 GPa at that volume.[218] We find that the B_{th2} term in Eq.(7.6.16) dominates leading to a negative thermal contribution to the bulk modulus, in agreement with the values provided by Zha, Mao and Hemley.[233] These authors also noted relatively small values for the thermal pressure. The reason for this lies in the small ^{4}He mass resulting in a large Einstein frequency ω_E and small thermal contribution. It explains why the experimental temperature differences for the pressure and bulk modulus between 15 and 297 K are barely visible in Figures 7.6c and d. As shown for neon, the thermal contributions become far more important

in the low-pressure regime.[50] We therefore neglect temperature effects for ^{4}He in our discussion because the neglect of higher-body terms contains much larger errors compared to the thermal contributions.
While the qualitative LJ picture shown in Figures 7.6a and b remains the same for the ELJ potential, the pressure and bulk moduli are a fraction smaller and much closer to the experimental values, that is because the ELJ potential describes the repulsive wall correctly in contrast to the (12,6) LJ potential. Further improvement requires the inclusion of phonon dispersion and, more importantly, higher N-body terms in the interaction potential[207, 225] which become attractive in the short-range.[201, 203, 223, 228, 234–237] For higher n-body forces analytical formulae in terms of lattice sums are unfortunately not available. Moreover, the most accurate three-body potential obtained from ab-initio data by Cencek, Patkowski, and Szalewicz (CPS)[238] is only valid for internuclear distances of $r > 3.5$ a.u. ($V > 2.8$ cm^3/mol for the fcc structure), and to add to this, the different three-body potentials available[234, 238–240] lead to quite different results in the short range. Nevertheless, in the valid volume range we calculate a total pressure including three-body effects with the ELJ two-body and CPS three-body potential of 27.3 GPa at V=2.954 cm^3/mol compared to the experimental value of 35.5 GPa.[218] This underestimation of the pressure at small volumes was also noted by Chang and Boninsegni.[241] Bulk moduli calculations by Barnes and Hinde show that three-body interactions become very important in the short-range.[236] How important the three-body, and higher order, contributions are to the vibrational pressure are topics to be further investigated.

7.7 The difference in Lennard-Jones cohesive energies between the bcc, fcc and hcp phases

The almost energetically degenerate fcc and hcp phases for the rare gases have been a matter of long standing debate.[98, 242–246] We therefore discuss the difference in cohesive energies between the different phases for a (n,m) LJ potential in more detail.
Using Eqs. (7.1.4) and (7.6.1) we obtain for the cohesive energy at the minimum nearest neighbor distance,

$$E_{\mathrm{LJ}}(r_0^{\min}) = \frac{\varepsilon}{2(n-m)}\left[mL_n\left(\frac{L_m}{L_n}\right)^{\frac{n}{n-m}} - nL_m\left(\frac{L_m}{L_n}\right)^{\frac{m}{n-m}}\right] \quad , \quad m<n\,. \tag{7.7.1}$$

Similar to the minimum neighbor distance which is directly related to the equilibrium distance of the dimer, (see Eq.(7.6.1)), the cohesive energy is only dependent on the binding energy ε of the diatomic and the ratios between LJI coefficients. From this we derive the relative difference in cohesive energies

$\Delta_{\mathrm{P1,P2}}$ between the two phases P1 and P2,

$$\Delta_{\mathrm{P1,P2}}(n,m) = 1 - \frac{E_{\mathrm{LJ}}^{\mathrm{P2}}\left(r_0^{\mathrm{P2}}\right)}{E_{\mathrm{LJ}}^{\mathrm{P1}}\left(r_0^{\mathrm{P1}}\right)} = 1 - \frac{mL_n^{\mathrm{P2}}\left(\frac{L_m^{\mathrm{P2}}}{L_n^{\mathrm{P2}}}\right)^{\frac{n}{n-m}} - nL_m^{\mathrm{P2}}\left(\frac{L_m^{\mathrm{P2}}}{L_n^{\mathrm{P2}}}\right)^{\frac{m}{n-m}}}{mL_n^{\mathrm{P1}}\left(\frac{L_m^{\mathrm{P1}}}{L_n^{\mathrm{P1}}}\right)^{\frac{n}{n-m}} - nL_m^{\mathrm{P1}}\left(\frac{L_m^{\mathrm{P1}}}{L_n^{\mathrm{P1}}}\right)^{\frac{m}{n-m}}} . \tag{7.7.2}$$

For the (12,6) LJ potential this simplifies to,

$$\Delta_{\mathrm{P1,P2}}(12,6) = 1 - \frac{L_{12}^{\mathrm{P1}}\left(L_6^{\mathrm{P2}}\right)^2}{L_{12}^{\mathrm{P2}}\left(L_6^{\mathrm{P1}}\right)^2} \tag{7.7.3}$$

and we obtain $\Delta_{\mathrm{fcc/hcp}}(12,6) = -1.00994 \times 10^{-4}$ and $\Delta_{\mathrm{bcc/hcp}}(12,6) = -4.53763 \times 10^{-2}$ using the lattice sums from Ref.[160]. We see that such a potential prefers the hcp structure as correctly analyzed by Kihara and Koba,[242] although fcc is very close in energy.[51, 225, 247] For a general (n,m) LJ potential allowing for real exponents, one has to introduce unphysical soft potentials of low (n,m) values with $n < 5.7$ to stabilize the fcc structure through two-body forces alone as the Figures 7.8a-d show. The figures also show that hcp is preferred over bcc through a range of (n,m) values.

The preference for hcp over fcc can easily be explained. Looking at shells of atoms around one arbitrarily-chosen central atom, we find the same numbers of atoms in the first and second shell for the fcc and hcp lattice. Differences only start from the third shell onwards, hcp has two extra atoms at a distance of $\sqrt{8/3}r_0$ that are not present in the fcc structure. Therefore, at a distance of $\sqrt{8/3}r_0$, the fcc cluster contains 18 atoms while the hcp has already 20 atoms. The third fcc shell is found at a much larger distance of $\sqrt{3}r_0$ with an additional 24 atoms.[127, 245]. This is reflected in the lattice sums, as we obtain the inequality

$$\Delta L_s^{\mathrm{fcc/hcp}} = L_s^{\mathrm{fcc}} - L_s^{\mathrm{hcp}} < 0\,, \tag{7.7.4}$$

over whole range of real values of $n \in \mathbb{R}_+, n \geq 3$ (also allowing for the singularity at $n = 3$).[160] In fact, $\Delta L_n^{\mathrm{fcc/hcp}}$ has a minimum at n=6.2448 with $\Delta L_s^{\mathrm{fcc/hcp}}$=-0.00097845 with maximum preference for the hcp structure, which is close to the dispersive $n = 6$ term. As the r^{-6} term is the dominant interaction for the first few nearest neighboring shells, this situation does not change if we adopt a more accurate two-body potential.[51] This explains that for a simple LJ potential, without inclusion of zero-point vibrational effects, hcp is preferred over the fcc lattice contrary to what is known from experiment.[48] The only exception we find for ultra-soft LJ potentials with small (n,m) values close to the singularity of the lattice sum at $n = 3$. Here counting shells further

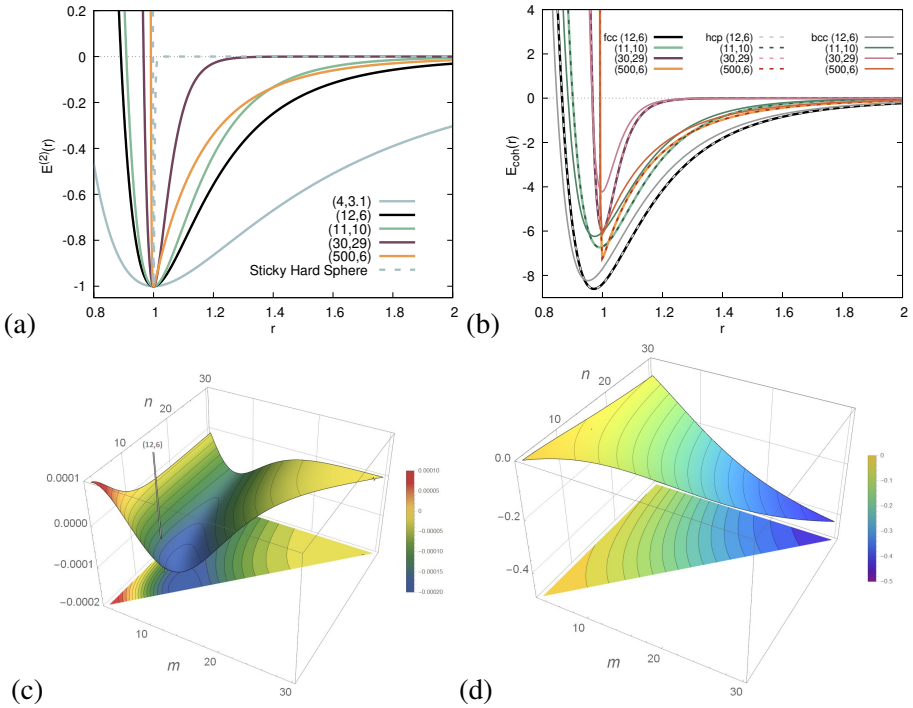

Figure 7.8 (Color online) (a) The interaction potential and (b) the cohesive energy for a range of n and m values of the (n,m) LJ potentials. Relative difference in cohesive energies (c) $\Delta_{\text{hcp}}^{\text{fcc}}(n,m)$ between the fcc and hcp phase and (d) $\Delta_{\text{hcp}}^{\text{bcc}}(n,m)$ between the bcc and hcp phase, for different choices of $(n,m) \in \mathbb{R}_{+}^{2}, n > m > 3$ of the LJ potential.

away becomes important.

A special case of the (n,m) LJ potential is the Sticky Hard Sphere (SHS) potential

$$V_{\text{SHS}}(r) = \begin{cases} \infty, & r < r_e \\ -\varepsilon, & r = r_e \\ 0, & r > r_e \end{cases} \tag{7.7.5}$$

which is reached in the limit $n \to \infty, m \to \infty, n > m$, depicted with the blue dashed line in Figure (7.8)a. The SHS potential does not distinguish between the fcc or hcp phases, i.e. they are energetically degenerate, since both phases have, within this limit, the same packing density, representing the densest possible packings of spheres. In fact, combinations of fcc and hcp layers, so-called Barlow packings also belong to the most dense sphere packings.[166] However, such packings have not been observed experimentally, which remains an unresolved problem in the theory of lattice packings.[248] A SHS potential with long-range dispersion can be constructed by using the $(n,6)$ LJ potential

with a very large n value, depicted with the orange line in Figures (7.8)a and b.[249, 250] In this case the cohesive energy is given by,[250]

$$\lim_{n\to\infty} E_{\mathrm{LJ}}(r_0) = -\varepsilon \frac{L_m}{2} \left(\frac{r_e}{r_0}\right)^m . \tag{7.7.6}$$

A The difference between the fcc and hcp phase for solid argon under pressure

In the previous section the difference in cohesive energy between the fcc, hcp and bcc at zero Kelvin was discussed. To compare these phases under pressure, the enthalpy has to be considered instead. The difference in enthalpies between hcp and fcc at constant pressure P at zero Kelvin is,

$$\begin{aligned} \Delta H_{\mathrm{hcp/fcc}}(P) &= \Delta E_{\mathrm{hcp/fcc}}(P) + P\Delta V_{\mathrm{hcp/fcc}}(P) \\ &= E_{\mathrm{hcp}}[V_{\mathrm{hcp}}(P)] - E_{\mathrm{fcc}}[V_{\mathrm{fcc}}(P)] + P\{V_{\mathrm{hcp}}(P) - V_{\mathrm{fcc}}(P)\} \end{aligned} \tag{7.7.7}$$

which will be used to determine if the hcp phase persists into the high pressure region for a LJ potential. Here $E = E^{\mathrm{coh}} + E^{\mathrm{ZPVE}} + E^{\mathrm{AZPVE}}$. For a (12,6) LJ potential relation between pressure and volume is given by Eq.(7.1.5),

$$P(V) = 2\varepsilon r_e^6 \left(r_e^6 V^{-5} - 2L_6 V^{-3}\right) + P^{\mathrm{ZPVE}}(V) + P^{\mathrm{AZPVE}}(V) . \tag{7.7.8}$$

Even if we neglect vibrational effects, for converting the pressure into volume one has to solve a fifth-order polynomial equation $ax^5 + bx^3 + c = 0$, which according to the Abel-Ruffini theorem has no general analytical solution. If we add vibrational effects both equations become more demanding and we have to get the volume from the pressure through more complicated algebraic equations, which can only be solved by numerical methods. We therefore calculate the volume V from a given pressure P by a two-point interpolation between (P_1, V_1) and (P_2, V_2) using an exponential ansatz,

$$P(V) = Ae^{-aV} \quad \text{with} \quad A = P_1 e^{\ln\left(\frac{P_2}{P_1}\right)\frac{V_1}{V1-V2}} \quad \text{and} \quad a = \frac{\ln\left(\frac{P_2}{P_2}\right)}{V_1 - V_2} . \tag{7.7.9}$$

This results in an iterative process for the volume determination,

$$V_1^{(n+1)} = V_1^{(n)} + \frac{\ln\left[P/P_1^{(n)}\right]}{\ln\left[P_2^{(n)}/P_1^{(n)}\right]} \left[V_2^{(n)} - V_1^{(n)}\right] , \tag{7.7.10}$$

with $V_2^{(n)} = f_n V_1^{(n)}$ with $f_n = 1 \pm \varepsilon$ and $\varepsilon \to 0$ for $n \to \infty$ ($P_2^{(n)}$ follows from $V_2^{(n)}$). In general, choosing $f_{n+1} = f_n/a$ ($a = 5.0$ for example) only five iterations are required to reach computer precision for the volume $V_1^{(n)} \to V$ at

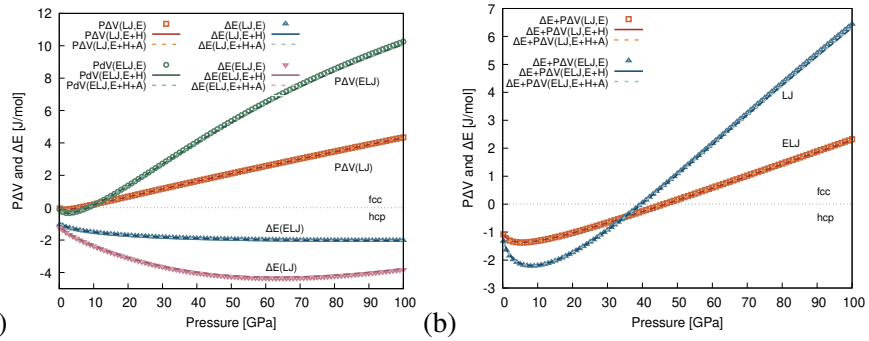

Figure 7.9 Enthalpy difference $\Delta H_{\text{fcc/hcp}}(P)$ between fcc and hcp against the pressure P for the LJ and the ELJ potential. Negative values implies that the hcp phase is more stable. (a) lower two curves are $\Delta E_{\text{hcp/fcc}}(P)$ plots, upper two curves $P\Delta V_{\text{hcp/fcc}}$ plots. (b) $\Delta E_{\text{hcp/fcc}}(P) + \Delta E_{\text{hcp/fcc}}(P)$. The individual contributions are cohesive energy expression used only (E), Eqs.(7.1.3) and (7.1.5), harmonic ZPVE added to the cohesive energy expression (H), Eqs.(7.1.3), (7.1.5), (7.4.1) and (7.4.13), and finally anharmonicity corrections added (A), Eqs.(7.1.3), (7.1.5), (7.4.1), (7.4.8), (7.4.13) and (7.4.14).

a given pressure P. This procedure works well as long as the curve behaves exponential, i.e., in the region where the pressure becomes negative a second-order polynomial fit for $P(V)$ is preferred. We now apply this to the fcc and hcp phase of solid argon at high pressures. The individual contributions for $\Delta H_{\text{fcc/hcp}}(P)$ up to pressures of 100 GPa are shown in Figures 7.9a and b.
The differences in enthalpies between the fcc and hcp phase are very small (see Figure 7.9a) (in the J/mol range), and this small difference persists up to very high pressures. We also see that at high pressures the $P\Delta V_{\text{hcp/fcc}}(P)$ starts to dominate over the $\Delta E_{\text{hcp/fcc}}(P)$ term. The almost linear behavior of the $P\Delta V_{\text{hcp/fcc}}(P)$ comes from an almost constant value of the volume difference, e.g. $\Delta V_{\text{hcp/fcc}}(P) \approx$1.85-1.95$\times 10^{-5}$ cm^3/mol in the high pressure range for the LJ potential. Within this model, the hcp phase is preferred at low pressures, while the fcc phase becomes more stable at pressures between 40-50 GPa, Figure 7.9b. This is in agreement with Stillinger's analysis[5] who predicts an hcp$\rightarrow$fcc transition for the LJ potential for Ar at a volume ratio of $V/V^{\min} = 0.537$. This is also the case for the more accurate ELJ potential which we used from Ref.[171]. However, this is contrary to experimental findings where a fcc phase is observed at standard conditions,[185, 251] and a subsequent fcc-to-hcp phase transition occurs at high pressures. In fact, Errandonea et al. observed a broad fcc-to-hcp transition in room temperature X-ray studies extending from 49.6 GPa to an estimated 300 GPa. At the highest pressure of 114 GPa, they determined a ratio of 0.3 for the amount of hcp to fcc.[252]

We showed recently that the fcc phase is stabilized by phonon dispersion at 0 K.[51] As phonon contributions play a lesser role at increased pressures, one can speculate that three- and higher body contributions must be responsible for the phase change to hcp at higher pressures.[253] From a theoretical point of view, to simulate a phase transition with such small enthalpy differences remains a major challenge. If experimental data fitted to many-body potentials, based for example on the embedded atom model, one can obtain more accurate results.[254]

B The Mode Grüneisen Parameter for the Rare Gas Solids

Grüneisen stated in 1912 that the parameter $\gamma(V,T)$ is almost independent of volume and temperature and expected to have the same value for elements of similar structure and interaction potential.[3] An estimate was given by considering nearest neigbor interactions only, (see Ref.[255]) which gives the value of γ =3.17 for a (12,6) LJ potential,

$$\gamma = \frac{n+m+1}{6}\,. \tag{7.7.11}$$

Indeed, the value varies very little for the rare gases from about 2.5 to 2.7,[256, 257] but deviates substantially from Grüneisen's original estimate. In the following we only consider the volume dependent mode Grüneisen parameter, for a discussion on the temperature dependence for the solid and liquid rare gas phases we refer the reader to Refs.[258–261].

The Einstein approximation within the LJ model provides a more rigorous insight into the constant value of the mode Grüneisen's parameter for the noble gasses. If we substitute Eq.(7.6.1) into (7.5.4) we get for the mode Grüneisen parameter at distance $r_0 = r_0^{\min}$,

$$\begin{aligned}\gamma_E^{\mathrm{LJ}}(r_0^{\min}) &= \frac{1}{6}\frac{(n+2)(n-1)L_{n+2}L_m-(m+2)(m-1)L_{m+2}L_n}{(n-1)L_{n+2}L_m-(m-1)L_{m+2}L_n}\\ &\underset{m=6}{\overset{n=12}{=}}\quad \frac{77L_{14}L_6-20L_8L_{12}}{33L_{14}L_6-15L_8L_{12}}\end{aligned} \tag{7.7.12}$$

This displays that the mode Grüneisen parameter only depends on the type of lattice through their lattice sums. The corresponding values are shown in Table 7.4.

The LJ γ_E value for the fcc lattice is considerably below the value estimated by Grüneisen which demonstrates that the summation over the whole lattice is important. Moreover, the γ_E values vary only slightly between the different lattices, and the difference between fcc and hcp is miniscule. Table 7.4 also

Table 7.4 Dimensionless mode Grüneisen parameter γ for the four different lattices sc, bcc, fcc and hcp. The LJ values listed are from Eq.(7.7.12) (the LJ value for the simple cubic structure is 2.951916). For the harmonic (h) and anharmonic part (ah) we used Eqs.(7.5.3) and (7.5.5). For He we used the optimized lattice distance $r_0^{\min}$ without vibrational effects included as inclusion of ZPVE contributions causes symmetry breaking of the lattice.

Atom	r_0(bcc)	γ_E(bcc)	r_0(fcc)	γ_E(fcc)	r_0(hcp)	γ_E(hcp)
LJ	$(\frac{L_{12}}{L_6})^{\frac{1}{6}} r_e$	2.991928	$(\frac{L_{12}}{L_6})^{\frac{1}{6}} r_e$	3.014083	$(\frac{L_{12}}{L_6})^{\frac{1}{6}} r_e$	3.014102
ELJ(h)						
He	2.84847	3.035488	2.91126	2.767544	2.91123	2.767651
Ne	3.09254	4.076591	3.15380	3.457913	3.15376	3.457846
Ar	3.66546	3.312865	3.74303	2.971256	3.74298	2.971366
Kr	3.87459	3.171161	3.95843	2.857477	3.95839	2.857453
Xe	4.20349	3.170670	4.29406	2.851391	4.29401	2.851350
Rn	4.25436	2.921074	4.35199	2.632502	4.35193	2.632446
Og	4.09982	2.557463	4.20118	2.332987	4.20112	2.333014
ELJ(h+ah)						
^{4}He	2.84847	1.889964	2.91126	2.030678	2.91123	2.030698
^{20}Ne	3.08478	3.068178	3.14609	2.962300	3.14605	2.962298
^{40}Ar	3.66501	3.163060	3.74258	2.886474	3.74254	2.886454
^{84}Kr	3.87447	3.102133	3.95831	2.817675	3.95827	2.817654
^{132}Xe	4.20344	3.127559	4.29400	2.826453	4.29396	2.826419
^{222}Rn	4.25434	2.901018	4.35198	2.621050	4.35192	2.621010
^{294}Og	4.09982	2.549471	4.20118	2.328094	4.20112	2.328116

contains ELJ results for the rare gases for both the harmonic and anharmonic approximation at the optimized nearest neighbor distances. These values show that anharmonicity effects play a major role especially for He and Ne.

Table 7.5 shows the mode Grüneisen parameter for the fcc lattice at the experimentally determined nearest neighbor distance in comparison with experimental γ-values. Considering that phonon dispersion and higher body effects are neglected, our results are in reasonable agreement with experiment. Previous calculations using the Debye model are also in good agreement with experiment.[259, 262]

Figure 7.10 demonstrates the behavior of γ_E for neon over a range of volumes. It shows that, around V/V_e the ELJ and LJ curves are close, but major deviations are observed in the high-pressure regime. Equation (7.5.4)

Atom	$r_0^{\text{exp.}}$	$\gamma_E(h)$	$\gamma_E(h+ah)$	γ_E(exp.)
^{20}Ne	3.15681±0.00006	3.4757	2.9866	2.51±0.03
^{40}Ar	3.74779±0.00006	2.9869	2.9011	2.7±0.1
^{84}Kr	3.99223±0.00007	2.9592	2.9126	2.67±0.07
^{132}Xe	4.3358±0.0004	2.9754	2.9453	2.5±0.1

Table 7.5 Dimensionless mode Grüneisen parameter γ_E for the fcc lattice at the experimental nearest neighbor distances[251, 263–265] for Ne, Ar, Kr and Xe. Experimental γ-values are from Refs.[256, 257].

gives for the high-pressure limit at $\gamma_E(V/V_e = 0) = (n+2)/6$ and the point of singularity $\gamma_E(V/V_e) = \infty$ happens at r_0^{crit}, Eq.(7.6.6), when the denominator in Eq.(7.5.4) becomes zero. While this behavior has been addressed before,[266, 267] the Einstein approximation provides an analytical explanation.

We observe that in the high-pressure region anharmonicity effects are small, but become important around the equilibrium distance. At distances close to r_0^{crit} the perturbative treatment for anharmonicity effects fails. In this region the mode Grüneisen parameter becomes very sensitive to volume changes, which will be especially important for the liquid phase (for a discussion on liquid helium see for example de Souza et al.[268]).

7.8 Conclusion

We derived analytical formulae for the vibrational contributions to the pressure and bulk modulus within the Einstein model, which give us qualitative, yet deep insight into many bulk properties such as the mode Grüneisen parameter. The rare gases served as a good starting point to estimate harmonic and anharmonic vibrational contributions to solids. While the LJ potential may be inadequate to model interactions in solids over a large $P(V)$ range, the ELJ potential provides analytical formulae for vibrational effects within the Einstein approximation that are capable for accurately describing two-body interactions over a large volume range.

There are many open questions in this field. It would be desirable to find approximate analytical formula for the dynamic matrix for an ELJ potential to include phonon dispersion, as well as for the three-body potential such as the Axilrod-Teller-Muto expression[186, 270] or similar expressions which work in the high pressure range. One could, for example, extend the work by Nijboer and deWette[156, 157] and use the Terras expansion of quadratic forms

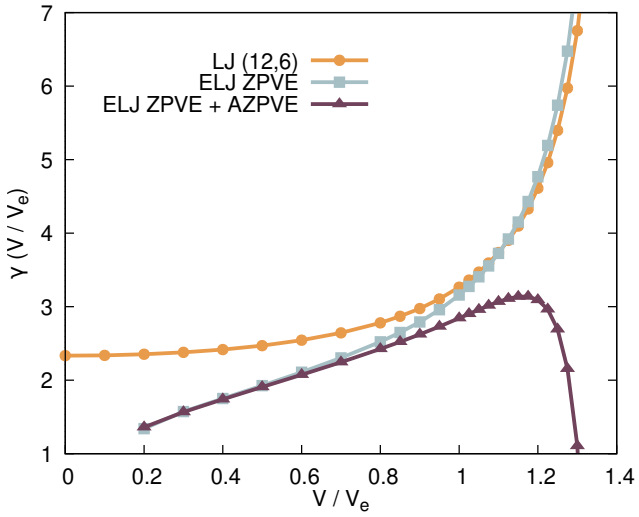

Figure 7.10 Grüneisen parameter $\gamma(V/V_e)$ as a function of volume for the LJ potential and for the ELJ of Ne (harmonic and anharmonic). For r_e we used the experimentally derived equilibrium distance of 3.094 ± 0.001 Å[269] for Ne_2 resulting in a volume for solid neon of $V_e = 12.612$ cm^3/mol.

in terms of Bessel functions.[112] Our group is currently trying to resolve these long-standing issues. Specifically, the fcc/hcp phases are very close in energy for the rare gases and the correct treatment of phase diagrams requires phonon dispersion and inclusion of at least three-body forces or even beyond. Especially for helium at high pressures such effects become crucial to correctly predict the $P(V,T)$ and $B(V,T)$ surfaces and phases. Moreover, for helium at low pressures one requires a more accurate quantum treatment.[201, 271]

7.9 Appendix

A Derivatives of the Extended Lennard-Jones potential in the crystal field

In order to describe the vibrational motion in a lattice within the Einstein approximation (E), we express the two-body energy of the vibrating atom at position $\vec{r}_A$ in the ELJ field of all other (fixed) atoms $i \in \mathbb{N}$ positioned at $\vec{r}_i = (x_i, y_i, z_i)^\top$ as

$$E(\vec{r}_A) = \sum_{i=1}^{\infty} \sum_{n>3} c_n |\vec{r}_A - \vec{r}_i|^{-n}. \tag{7.A.1}$$

with, $|\vec{r}_A - \vec{r}_i| = [(x_A - x_i)^2 + (y_A - y_i)^2 + (z_A - z_i)^2]^{\frac{1}{2}}$ the distance between the central vibrating atom and the other atoms i. This extends the work of Corner[155] and Wallace[98, 272, 273] to the terms in the ELJ potential.

A Taylor expansion in three dimensions around the minimum $\vec{r}_A = \vec{r}_0$ of the moving atom is defined by,

$$E(\vec{r}_0 + \vec{r}) = \sum_{m=0}^{\infty} \frac{1}{m!} \left(\vec{r} \cdot \vec{\nabla}\right)^m E(\vec{r}_0) \,. \tag{7.A.2}$$

and the expression is understood that the derivative of $E(\vec{r})$ has to be taken first and then evaluated at point $\vec{r}_0$ and $\left(\vec{r} \cdot \vec{\nabla}\right)^m$ is defined through the multinomial theorem. We conveniently put the vibrating atom at the origin, $\vec{r}_0 = \vec{0}$. The zero-order term just gives the cohesive energy of the crystal, and the second-order term is the expression for a harmonic oscillator in three dimensions. All derivatives in cartesian coordinates up to 4th order with respect to the atom moving around the origin may now be derived

$$F_x = \left.\frac{\partial E}{\partial x}\right|_{\vec{0}} = \sum_{i,n} n c_n x_i r_i^{-n-2} \tag{7.A.3}$$

$$F_{xy} = \left.\frac{\partial^2 E}{\partial x \partial y}\right|_{\vec{0}} = \sum_{i,n} n(n+2)\, c_n x_i y_i r_i^{-n-4} \,, \tag{7.A.4}$$

$$F_{xx} = \left.\frac{\partial^2 E}{\partial x^2}\right|_{\vec{0}} = \sum_{i,n} n c_n r_i^{-n-4} \left[(n+2)\, x_i^2 - r_i^2\right] \,, \tag{7.A.5}$$

$$F_{xxx} = \left.\frac{\partial^3 E}{\partial x^3}\right|_{\vec{0}} = \sum_{i,n} n(n+2)\, c_n x_i r_i^{-n-6} \left[(n+4)\, x_i^2 - 3 r_i^2\right] \,, \tag{7.A.6}$$

$$F_{xxy} = \left.\frac{\partial^3 E}{\partial x^2 \partial y}\right|_{\vec{0}} = \sum_{i,n} n(n+2)\, c_n y_i r_i^{-n-6} \left[(n+4)\, x_i^2 - r_i^2\right] \,, \tag{7.A.7}$$

$$F_{xyz} = \left.\frac{\partial^3 E}{\partial x \partial y \partial z}\right|_{\vec{0}} = \sum_{i,n} n(n+2)(n+4)\, c_n x_i y_i z_i r_i^{-n-6} \,, \tag{7.A.8}$$

$$F_{xxxx} = \left.\frac{\partial^4 E}{\partial x^4}\right|_{\vec{0}} = \sum_{i,n} n(n+2)\, c_n r_i^{-n-8} \left[3 r_i^4 - 6(n+4)\, x_i^2 r_i^2 + (n+4)(n+6)\, x_i^4\right] \,, \tag{7.A.9}$$

$$F_{xxxy} = \left.\frac{\partial^4 E}{\partial x^3 \partial y}\right|_{\vec{0}} = \sum_{i,n} n(n+2)(n+4)\, c_n x_i y_i r_i^{-n-8} \left[(n+6)\, x_i^2 - 3 r_i^2\right] \,, \tag{7.A.10}$$

$$F_{xxyy} = \left.\frac{\partial^4 E}{\partial x^2 \partial y^2}\right|_{\vec{0}}$$
$$= \sum_{i,n} n\,(n+2)\,c_n r_i^{-n-8}\left[r_i^4 - (n+4)\left(x_i^2+y_i^2\right)r_i^2 + (n+4)\,(n+6)\,x_i^2 y_i^2\right], \tag{7.A.11}$$

(7.A.12)

$$F_{xxyz} = \left.\frac{\partial^4 E}{\partial x^2 \partial y \partial z}\right|_{\vec{0}} = \sum_{i,n} n\,(n+2)\,(n+4)\,c_n y_i z_i r_i^{-n-8}\left[(n+6)\,x_i^2 - r_i^2\right]. \tag{7.A.13}$$

From Eq.(7.A.5), we derive the Laplacian ΔE with respect to our vibrating atom,

$$\Delta E|_{\vec{0}} = (F_{xx}+F_{yy}+F_{zz})\,|_{\vec{0}} = \mathrm{Tr}\{F\}|_{\vec{0}} = \sum_{i,n} n\,(n-1)\,c_n r_i^{-n-2} \tag{7.A.14}$$

The cubic lattices sc, bcc and fcc belong to the local O_h point group. If we rotate the orthogonal coordinate system such that F is diagonal[b] we have $F_{xx} = F_{yy} = F_{zz}$ because of O_h symmetry (not for hcp as already mentioned).[98] Thus we obtain

$$F_{xx}^{\mathrm{c}}|_{\vec{0}} = \frac{1}{3}\Delta E|_{\vec{0}} = \frac{1}{3}\sum_{i,n} n\,(n-1)\,c_n r_i^{-n-2}, \tag{7.A.15}$$

where (c) stands for one of the cubic lattices. In this case we obtain also simple relationships for the quartic force constants; $F_{xxyy}^{\mathrm{c}} = F_{yyzz}^{\mathrm{c}} = F_{xxzz}^{\mathrm{c}}$ and $F_{xxxx}^{\mathrm{c}} = F_{yyyy}^{\mathrm{c}} = F_{zzzz}^{\mathrm{c}}$.[98] Further we have $F_{xxxy}^{\mathrm{c}} = F_{xxyz}^{\mathrm{c}} = 0$. Because O_h contains inversion symmetry we also have $F_{x^i y^j z^k}^{\mathrm{c}} = 0$ for any odd combination $(i+j+k)$, for example $F_x^{\mathrm{c}} = 0$, $F_{xxx}^{\mathrm{c}} = 0$, $F_{xyy}^{\mathrm{c}} = 0$, and $F_{xyz}^{\mathrm{c}} = 0$. Thus, all odd derivatives vanish and for these lattices we only have to consider the quartic force constants for the anharmonicity correction (see below). Using these symmetry relations we can further simplify the two important (non-zero) quartic force constants for the cubic lattices,

$$F_{xxxx}^{\mathrm{c}}|_{\vec{0}} = \frac{1}{3}\left(F_{xxxx}+F_{yyyy}+F_{xxxx}\right)|_{\vec{0}} \tag{7.A.16}$$

and

$$F_{xxyy}^{\mathrm{c}}|_{\vec{0}} = \frac{1}{3}\left(F_{xxyy}+F_{xxzz}+F_{yyzz}\right)|_{\vec{0}}. \tag{7.A.17}$$

[b] This normal coordinate system is identical to the orthogonal coordinate system commonly used for the cubic Bravais lattices.

which gives

$$F^{\mathrm{c}}_{xxxx}|_{\vec{0}} = \frac{1}{3}\sum_{i,n} n\,(n+2)\,c_n r_i^{-n-8}\left[(n+4)\,(n+6)\left(x_i^4+y_i^4+z_i^4\right)-3\,(2n+5)\,r_i^4\right] \tag{7.A.18}$$

and

$$F^{\mathrm{c}}_{xxyy}|_{\vec{0}} = \frac{1}{3}\sum_{i,n} n\,(n+2)\,c_n r_i^{-n-8}\left[(n+4)\,(n+6)\,\left(x_i^2y_i^2+y_i^2z_i^2+x_i^2z_i^2\right)\right.$$
$$\left.-\,(2n+5)\,r_i^4\right]\,.$$

No further simplification is possible. However, we can combine Eqs.(7.A.18) and (A) and we obtain

$$F^{\mathrm{c}}_{xxxx}|_{\vec{0}} + 2F^{\mathrm{c}}_{xxyy}|_{\vec{0}} = \frac{1}{3}\sum_{i,n}(n+2)\,(n+1)\,n\,(n-1)\,c_n r_i^{-n-4}\,. \tag{7.A.19}$$

8 Project 3 - The Cuboidal Lattices and their Lattice Sums [a]

8.1 Introduction

Lattice sums have a long history in solid-state physics and discrete mathematics.[275] They connect lattices to observables such as the equation of state for a bulk system using interacting potentials between the lattice points (atoms or molecules) in three-dimensional space.[2, 3, 5, 276] Most notable cases for such interactions are the Lennard-Jones [6] and the Coulomb potential, leading in the latter case, for example, to the famous Madelung constant derived as early as in 1918.[7] For such potentials the corresponding lattice sums become functions of quadratic forms $\vec{i}^{\top} G\vec{i}$ with $\vec{i} \in \mathbb{Z}^3$, i.e. the expression $\vec{i}^{\top} G\vec{i}$ is the quadratic form associated with the lattice $\mathscr{L}$ (or simply, the associated quadratic form).[8]
In the general case of a n-dimensional lattice ($\vec{i} \in \mathbb{Z}^n$), G is a positive definite, real and symmetric $(n \times n)$ matrix called the Gram matrix of the lattice $\mathscr{L}$, defined by its basis (or lattice) vectors $\{\vec{b}_i\}$ through $G = BB^{\top}$. $B = (\vec{b}_1, ..., \vec{b}_n)^{\top}$ is called the generator matrix (B not necessarily positive definite). Lattice sums represent often conditionally convergent series [277], and the theory of converting them into fast converging series has become an intense research field over the past 50 years.[275]
Concerning the Gram matrix G or generator matrix we introduce a few important definitions required in this work.[123] Two generator matrices B_1 and B_2 are equivalent if $B_2 = cUB_1\mathscr{O}$, c a non-zero real number, $\mathscr{O}$ a real orthogonal matrix ($\mathscr{O}\mathscr{O}^{\top} = 1$) with $\det(\mathscr{O}) = \pm 1$ describing rotation, reflection or rotoreflection of the lattice, and U a matrix containing integers with $\det U = 1$ describing for example permutations of the basis vectors. Given two equivalent generator matrices B_1 and B_2, the corresponding Gram matrices are related by

$$G_2 = B_2 B_2^{\top} = cUB_1\mathscr{O}\left(cUB_1\mathscr{O}\right)^{\top} = c^2 UB_1\mathscr{O}\mathscr{O}^{\top}B_1^{\top}U^{\top} = c^2 UG_1U^{\top}.$$

The minimum distance $d_{\min}$ in a lattice $\mathscr{L}$ is defined by

$$d_{\min}(\mathscr{L}) = \min\{d(\vec{v}_1;\vec{v}_2) | \vec{v}_1, \vec{v}_2 \in \mathscr{L}; \vec{v}_1 \neq \vec{v}_2\}$$

[a] This chapter is composed of sections previously published in the article *The Cuboidal Lattices and their Lattice Sums*[274] and is reprinted by permission from the publisher ©2022 arXiv.org open-access. Some sections may have been modified to fit the style of this thesis.

where $d(\vec{v}_1;\vec{v}_2) = |\vec{v}_1 - \vec{v}_2|$ is the Euclidean distance. In terms of the Gram matrix this is equivalent to

$$d_{\min} = \min\{+\sqrt{\vec{i}^\top G\vec{i}} \mid \vec{i} \in \mathbb{Z}^3 \backslash (0,0,0)^\top\}.$$

The minimal norm is related to the minimum distance by $\mu = d_{\min}^2$. Dividing G by μ assures that $d_{\min} = 1$ used in most lattice sum applications.[8] For dense sphere packings the radius of a sphere ρ is simply $\rho = d_{\min}/2$. The packing density Δ_L and the center density δ_L of a three-dimensional lattice are given by

$$\Delta_{\mathscr{L}} = \frac{4\pi}{3}\delta_{\mathscr{L}} = \frac{4\pi}{3}\frac{\rho^3}{\mathrm{vol}(\mathscr{L})} = \frac{4\pi}{3}\frac{\rho^3}{|\det(B)|} = \frac{4\pi}{3}\frac{\rho^3}{\sqrt{\det(G)}}.$$

The kissing number for dense sphere packings is defined by

$$\mathrm{kiss}(\mathscr{L}) = \#\{v \in \mathscr{L} \mid |v| = d_{\min}(\mathscr{L})\}.$$

In this work we discuss cuboidal lattices and their lattice sums. We first present the characteristics of cuboidal lattices $\mathscr{L}(A)$ dependent on a single parameter A. In what follows we decompose the corresponding lattice sum into two lattice sums, where one is related to a scaled cubic lattice and the other to a scaled Madelung constant. We evaluate these lattice sums in two ways using theta functions. We discuss these lattice sums including their analytical continuations and provide a more complete analysis for the lattice sum difference between f.c.c. (face centred cubic) and h.c.p. (hexagonal close packing).

8.2 The cuboidal lattices

Following Conway and Sloane (cite: Sec.3 duals) we consider the lattice generated by the vectors: $(\pm u, \pm v, 0)^\top$ and $(0, \pm v, \pm v)^\top$,
where u and v are non-zero real numbers. To make it specific, take the basis vectors

$$\vec{b}_1 = (u,v,0)^\top, \quad \vec{b}_2 = (u,0,v)^\top, \quad \vec{b}_3 = (0,v,v)^\top. \tag{8..1}$$

Then the generator matrix B is given by

$$B = \begin{pmatrix} u & v & 0 \\ u & 0 & v \\ 0 & v & v \end{pmatrix}$$

which has determinant $-2uv^2$.

The Gram matrix is

$$G = BB^{\top} = \begin{pmatrix} u^2+v^2 & u^2 & v^2 \\ u^2 & u^2+v^2 & v^2 \\ v^2 & v^2 & 2v^2 \end{pmatrix} = v^2 \begin{pmatrix} 1+A & A & 1 \\ A & 1+A & 1 \\ 1 & 1 & 2 \end{pmatrix} \quad (8..2)$$

where $A = u^2/v^2$ and G is positive definite for $A > 0$. Conway and Sloane use $\sigma = u/v$, so $A = \sigma^2$.[278] The most important cases, in decreasing numerical order, are:

1. $A = 1$: the face-centred cubic (f.c.c.) lattice;
2. $A = 1/\sqrt{2}$: the mean centred-cuboidal (m.c.c.) lattice;
3. $A = 1/2$: the body-centred cubic (b.c.c.) lattice;
4. $A = 1/3$: the axial centred-cuboidal (a.c.c.) lattice.

The f.c.c. and b.c.c. lattices are well known. The corresponding Gram matrices for the f.c.c. and b.c.c lattices are identical to the ones shown in our previous paper on lattice sums.[8] The m.c.c. and a.c.c. lattices occur in [278] and [279]. The m.c.c. lattice is the densest isodual lattice in three-dimensional space.

The quadratic form associated with the lattice is

$$\begin{aligned} g(i,j,k) &= (i,j,k)\,G(i,j,k)^{\top} \\ &= (u^2+v^2)i^2 + (u^2+v^2)j^2 + 2v^2k^2 + 2u^2ij + 2v^2ik + 2v^2jk \\ &= u^2(i^2+j^2) + v^2(j+k)^2 + v^2(i+k)^2 \\ &= v^2\left(A(i+j)^2 + (j+k)^2 + (i+k)^2\right). \end{aligned} \quad (8..3)$$

It is easy to check that

$$\min_{\substack{i,j,k\in\mathbb{Z} \\ (i,j,k)\neq(0,0,0)}} \{A(i+j)^2 + (j+k)^2 + (i+k)^2\} = \begin{cases} 4A & \text{if } 0 < A < 1/3, \\ A+1 & \text{if } 1/3 \le A \le 1, \\ 2 & \text{if } A > 1. \end{cases} \quad (8..4)$$

It follows from (8..3) and (8..4) that the minimum distance is given by

$$d_{\min} = \min_{\substack{i,j,k\in\mathbb{Z} \\ (i,j,k)\neq(0,0,0)}} \sqrt{g(i,j,k)} = \begin{cases} 2v\sqrt{A} & \text{if } 0 < A < 1/3, \\ v\sqrt{A+1} & \text{if } 1/3 \le A \le 1, \\ v\sqrt{2} & \text{if } A > 1. \end{cases} \quad (8..5)$$

We rescale to make the minimum distance 1 by defining

$$g(A;i,j,k) = \frac{g(i,j,k)}{(d_{\min})^2}$$
$$= \begin{cases} \dfrac{1}{4A}\left(A(i+j)^2+(j+k)^2+(i+k)^2\right) & \text{if } 0<A<1/3, \\ \dfrac{1}{A+1}\left(A(i+j)^2+(j+k)^2+(i+k)^2\right) & \text{if } 1/3\le A\le 1, \\ \dfrac{1}{2}\left(A(i+j)^2+(j+k)^2+(i+k)^2\right) & \text{if } A>1. \end{cases}$$

The examples we are interested are in (f.c.c., m.c.c., b.c.c., a.c.c.) all satisfy $1/3 \le A \le 1$. Because of its practical interest, this is the only case we will study, and from here on (unless otherwise mentioned) we will always assume $1/3 \le A \le 1$ in which case we have

$$g(A;i,j,k) = \frac{1}{A+1}\left(A(i+j)^2+(j+k)^2+(i+k)^2\right), \tag{8..6}$$

corresponding to the rescaled Gram matrix

$$G(A) := \frac{1}{(d_{\min})^2}\,G = \frac{1}{A+1}\begin{pmatrix} 1+A & A & 1 \\ A & 1+A & 1 \\ 1 & 1 & 2 \end{pmatrix}. \tag{8..7}$$

The packing density is calculated as

$$\Delta_{\mathscr{L}} = \frac{4\pi}{3}\frac{\rho^3}{\sqrt{\det(G)}}$$

where $\rho = d_{\min}/2$ and

$$\det(G) = (\det(B))^2 = 4u^2v^4 = 4Av^6.$$

It follows that

$$\Delta_{\mathscr{L}} = \frac{\pi}{12\sqrt{A}}\left(\frac{d_{\min}}{v}\right)^3.$$

On using the formula for $d_{\min}$ in (8..5) we obtain the formula for the packing

density, given by

$$\Delta_{\mathscr{L}} = \begin{cases} \dfrac{2\pi A}{3} & \text{if } 0 < A < 1/3, \\ \dfrac{\pi}{12}\sqrt{\dfrac{(A+1)^3}{A}} & \text{if } 1/3 \le A \le 1, \\ \dfrac{\pi}{6}\sqrt{\dfrac{2}{A}} & \text{if } A > 1. \end{cases}$$

Figure 1 shows a graph of the packing density as a function of the parameter A. Further information is recorded in Table 8.1. In the main region of interest $1/3 \le A \le 1$, we have

$$\Delta_{\mathscr{L}} = \frac{\pi}{12}\sqrt{\frac{(A+1)^3}{A}} \tag{8..8}$$

and so

$$\frac{\mathrm{d}\Delta_{\mathscr{L}}}{\mathrm{d}A} = \frac{\pi}{12}\left(A - \frac{1}{2}\right)\sqrt{\frac{A+1}{A^3}}. \tag{8..9}$$

It follows that on the interval $1/3 \le A \le 1$, the packing density has a maximum of $\pi\sqrt{2}/6 \approx 0.74048$ at $A = 1$ corresponding to f.c.c., and a minimum of $\pi\sqrt{3}/8 \approx 0.68017$ at $A = 1/2$ corresponding to b.c.c.
It is also interesting to note that as $A \to \infty$ the limiting case of the lattice is the two-dimensional square close packing with minimal distance 1 and kissing number 4; while in the other extreme case the limit as $A \to 0$ gives the one-dimensional lattice with minimal distance 1 and kissing number 2. These cases are briefly analysed in Appendix B.

Table 8.1 Kissing number, packing density $\Delta_{\mathscr{L}}$ and integer combinations $\vec{i}_n$ for the lattice associated with the Gram matrix G defined in (8..2). The values in the table depend only on A and are independent of v.

Region	A	$\mathrm{kiss}(\mathscr{L})$	$\Delta_{\mathscr{L}}$	integer combinations[a]
I	$(0, \frac{1}{3})$	2	$\frac{2\pi A}{3}$	$\vec{i}_1, \vec{i}_2$
a.c.c.	$\frac{1}{3}$	10	$\frac{2\pi}{9}$	$\vec{i}_1, \ldots, \vec{i}_{10}$
II	$(\frac{1}{3}, 1)$	8	$\frac{\pi}{12}\sqrt{\frac{(A+1)^3}{A}}$	$\vec{i}_3, \ldots, \vec{i}_{10}$
f.c.c.	1	12	$\frac{\pi\sqrt{2}}{6}$	$\vec{i}_3, \ldots, \vec{i}_{14}$
III	$(1, \infty)$	4	$\frac{\pi}{6}\sqrt{\frac{2}{A}}$	$\vec{i}_{11}, \ldots, \vec{i}_{14}$

[a] The integer combinations $\vec{i}$ which determine $d_{\min}$ in (8..5) for the different regions are as follows: $\vec{i}_1^{\,\mathrm{I}} = (-1,-1,1)$, $\vec{i}_2^{\,\mathrm{I}} = (1,1,-1)$, $\vec{i}_3^{\,\mathrm{II}} = (-1,0,0)$, $\vec{i}_4^{\,\mathrm{II}} = (-1,0,1)$, $\vec{i}_5^{\,\mathrm{II}} = (0,-1,0)$, $\vec{i}_6^{\,\mathrm{II}} = (0,-1,1)$, $\vec{i}_7^{\,\mathrm{II}} = (0,1,-1)$, $\vec{i}_8^{\,\mathrm{II}} = (0,1,0)$, $\vec{i}_9^{\,\mathrm{II}} = (1,0,-1)$, $\vec{i}_{10}^{\,\mathrm{II}} = (1,0,0)$, $\vec{i}_{11}^{\,\mathrm{III}} = (-1,1,0)$, $\vec{i}_{12}^{\,\mathrm{III}} = (0,0,-1)$, $\vec{i}_{13}^{\,\mathrm{III}} = (0,0,1)$, $\vec{i}_{14}^{\,\mathrm{III}} = (1,-1,0)$.

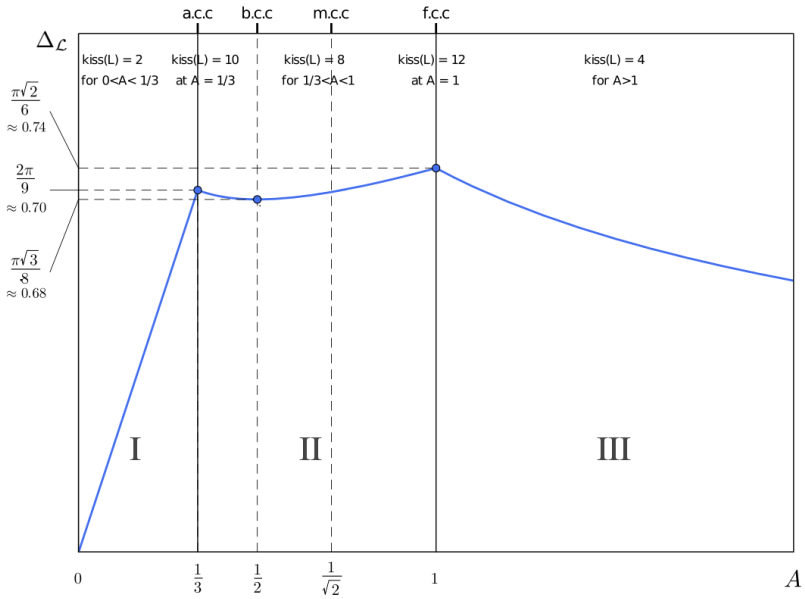

Figure 8.1 Graph of the packing density $\Delta_{\mathscr{L}}$ versus A. The regions I, II and III are ordering to the different kissing numbers. Explicit formulas are given in Table 8.1. The location of the f.c.c., m.c.c., b.c.c. and a.c.c. lattices are indicated on the graph.

Given a positive definite quadratic form $g(i,j,k)$, the corresponding theta series is defined for $|q| < 1$ by

$$\theta_g(q) = \sum_{i=-\infty}^{\infty} \sum_{j=-\infty}^{\infty} \sum_{k=-\infty}^{\infty} q^{g(i,j,k)}.$$

For the quadratic form in (8..6) the theta series is

$$\theta(A;q) = \sum_{i=-\infty}^{\infty} \sum_{j=-\infty}^{\infty} \sum_{k=-\infty}^{\infty} q^{(A(i+j)^2+(j+k)^2+(i+k)^2)/(A+1)} \quad \text{where } 1/3 \le A \le 1.$$

The first few terms in the theta series for f.c.c., m.c.c., b.c.c. and a.c.c. as far

as q^9 are given respectively by

$$\begin{aligned}
\theta(1;q) &= 1+12q+6q^2+24q^3+12q^4+24q^5 \\
&\quad +8q^6+48q^7+6q^8+36q^9+\cdots, \\
\theta(\frac{1}{\sqrt{2}};q) &= 1+8q+4q^{4-2\sqrt{2}}+2q^{4\sqrt{2}-4}+4q^{8-4\sqrt{2}}+8q^{2\sqrt{2}}+16q^{-4\sqrt{2}+9} \\
&\quad +8q^4+8q^{8\sqrt{2}-7}+4q^{16-8\sqrt{2}}+8q^{-8\sqrt{2}+17}+8q^{20-10\sqrt{2}} \\
&\quad +8q^{-4\sqrt{2}+12}+2q^{16\sqrt{2}-16}+16q^{4\sqrt{2}+1} \\
&\quad +16q^{-6\sqrt{2}+16}+8q^{14\sqrt{2}-12}+16q^{-12\sqrt{2}+25} \\
&\quad +8q^{-8+12\sqrt{2}}+8q^9+\cdots, \\
\theta(\frac{1}{2};q) &= 1+8q+6q^{4/3}+12q^{8/3}+8q^4+24q^{11/3}+6q^{16/3} \\
&\quad +24q^{19/3}+24q^{20/3}+24q^8+32q^9+\cdots, \\
\theta(\frac{1}{3};q) &= 1+10q+4q^{3/2}+8q^{5/2}+12q^3+26q^4+8q^{11/2}+20q^6+32q^7 \\
&\quad +8q^{15/2}+16q^{17/2}+10q^9+\cdots.
\end{aligned}$$

Since the quadratic form $g(A;i,j,k)$ has been normalised to make the minimum distance 1, the kissing number occurs in each theta series as the coefficient of q. That is, we have kiss(f.c.c.) = 12, kiss(m.c.c.) = 8, kiss(b.c.c.) = 8 and kiss(a.c.c.) = 10.
We introduce the following lattice sum important in solid state theory,[275]

$$L(A;s)=\sum_{i,j,k}{}'\left(\frac{1}{g(A;i,j,k)}\right)^s=\sum_{i,j,k}{}'\left(\frac{A+1}{A(i+j)^2+(j+k)^2+(i+k)^2}\right)^s \tag{8..10}$$

where $1/3\le A\le 1$. Here and throughout this work, a prime on the summation symbol will denote that the sum ranges over all integer values except for the term when all of the summation indices are simultaneously zero. Thus, the sums in (8..10) are over all integer values of i, j and k except for the term $(i,j,k)=(0,0,0)$ which is omitted. This lattice sum smoothly connects four different well known lattices, i.e., when $A=1$, $1/\sqrt{2}$, $1/2$ or $1/3$ we obtain the expressions for the lattices f.c.c, m.c.c., b.c.c. and a.c.c. respectively (face-centred cubic, mean centred-cuboidal, body-centred cubic, and axial centred cuboidal). In these cases, we also write

$$\begin{aligned}
L_3^{\mathrm{FCC}}(s) &= L(1;s), \\
L_3^{\mathrm{MCC}}(s) &= L(1/\sqrt{2};s), \\
L_3^{\mathrm{BCC}}(s) &= L(1/2;s), \\
\text{and}\quad L_3(s) &= L(1/3;s).
\end{aligned}$$

We conclude this section by reconciling the Gram matrix G in (8..2) with two matrices given by Conway and Sloane.[278] Let

$$U_1 = \begin{pmatrix} 1 & 0 & 0 \\ -1 & 0 & 1 \\ 0 & -1 & 0 \end{pmatrix} \quad \text{and} \quad U_2 = \begin{pmatrix} 1 & 1 & -1 \\ 1 & 0 & 0 \\ 0 & 1 & 0 \end{pmatrix}$$

and consider the equivalent matrices G_1 and G_2 defined by

$$G_1 = U_1 G U_1^\top = \begin{pmatrix} u^2+v^2 & -u^2 & -u^2 \\ -u^2 & u^2+v^2 & u^2-v^2 \\ -u^2 & u^2-v^2 & u^2+v^2 \end{pmatrix} \tag{8..11}$$

and

$$G_2 = U_2 G U_2^\top = \begin{pmatrix} 4u^2 & 2u^2 & 2u^2 \\ 2u^2 & u^2+v^2 & u^2 \\ 2u^2 & u^2 & u^2+v^2 \end{pmatrix}. \tag{8..12}$$

When $u = 1/\sqrt{2}$ and $v = 1/\sqrt[4]{2}$, the matrix G_1 in (8..11) is the Gram matrix for the m.c.c lattice given by Conway and Sloane [122]. Moreover, when $u = \sqrt{1/3}$ and $v = \sqrt{2/3}$, the matrix G_1 leads to another well-known quadratic form for the b.c.c. lattice, e.g., see [[58]]. When $u = 1$, $v = \sqrt{3}$, the matrix G_2 in (8..12) is the Gram matrix for the a.c.c. lattice given in [p. 378][122]. Since $\det U_1 = \det U_2 = 1$ it follows that

$$\det G_1 = \det G_2 = \det G = (\det B)^2 = 4u^2v^4 = 4v^6 A.$$

The corresponding quadratic forms g_1 and g_2 are defined by

$$\begin{aligned} g_1(i,j,k) &= (i,j,k)\, G_1 (i,j,k)^\top \\ &= (u^2+v^2)i^2 + (u^2+v^2)j^2 + (u^2+v^2)k^2 - 2u^2 ij - 2u^2 ik + 2(u^2-v^2)jk \end{aligned}$$

and

$$\begin{aligned} g_2(i,j,k) &= (i,j,k)\, G_2 (i,j,k)^\top \\ &= 4u^2 i^2 + (u^2+v^2)j^2 + (u^2+v^2)k^2 + 4u^2 ij + 4u^2 ik + 2u^2 jk. \end{aligned}$$

They are related to the quadratic form g in (8..3) by

$$g_1(i,j,k) = g\left((i,j,k)U_1\right) = g(i-j,-k,j) \tag{8..13}$$

and

$$g_2(i,j,k) = g\left((i,j,k)U_2\right) = g(i+j,i+k,-i).$$

8.3 A minimum property of the lattice sum $L(A;s)$

In the previous section — see (8..8) and (8..9) — it was noted that on the interval $1/3 \le A \le 1$, the packing density function $\Delta_{\mathscr{L}}$ has a minimum value when $A = 1/2$. The next result shows that provided $s > 3/2$, the corresponding lattice sum $L(A;s)$ also attains a minimum at the same value $A = 1/2$.

A Theorem

Let $L(A;s)$ be the lattice defined by (8..10), that is,

$$L(A;s) = \sum_{i,j,k}{}' \left(\frac{1}{g(A;i,j,k)} \right)^s = \sum_{i,j,k}{}' \left(\frac{A+1}{A(i+j)^2 + (j+k)^2 + (i+k)^2} \right)^s$$

where $s > 3/2$ and $1/3 \le A \le 1$. Then

$$\frac{\partial}{\partial A} L(A;s)\bigg|_{A=1/2} = 0 \quad \text{and} \quad \frac{\partial^2}{\partial A^2} L(A;s)\bigg|_{A=1/2} > 0.$$

B proof

By definition we have

$$L(A;s) = \sum_{I,J,K}{}' \left(\frac{1}{g(A;I,J,K)} \right)^s$$

where

$$g(A;I,J,K) = \frac{1}{A+1} \left(A(I+J)^2 + (J+K)^2 + (I+K)^2 \right).$$

Now make the change of variables given by (8..13), namely

$$(I,J,K) = (i-j,-k,j).$$

This is a bijection since

$$(i,j,k) = (I+K,K,-J),$$

and it follows that

$$\begin{aligned} L(A;s) &= \sum_{i,j,k}{}' \left(\frac{1}{g(A;i-j,-k,j)} \right)^s \\ &= \sum_{i,j,k}{}' \frac{1}{\left(i^2+j^2+k^2 - 2(ij+ik)\left(\frac{A}{A+1}\right) + 2jk\left(\frac{A-1}{A+1}\right)\right)^s}. \end{aligned}$$

By direct calculation, the derivative is given by

$$\frac{\partial}{\partial A}L(A;s) = \frac{2s}{(A+1)^2}\sum_{i,j,k}{}' \frac{ij+ik-2jk}{\left(i^2+j^2+k^2-2(ij+ik)\left(\frac{A}{A+1}\right)+2jk\left(\frac{A-1}{A+1}\right)\right)^{s+1}}. \tag{8.B.1}$$

Setting $A = 1/2$ gives

$$\left.\frac{\partial}{\partial A}L(A;s)\right|_{A=1/2} = \frac{8s}{9}\sum_{i,j,k}{}' \frac{ij+ik-2jk}{\left(i^2+j^2+k^2-\frac{2}{3}(ij+ik+jk)\right)^{s+1}}. \tag{8.B.2}$$

Switching i and j gives

$$\left.\frac{\partial}{\partial A}L(A;s)\right|_{A=1/2} = \frac{8s}{9}\sum_{i,j,k}{}' \frac{ij+jk-2ik}{\left(i^2+j^2+k^2-\frac{2}{3}(ij+ik+jk)\right)^{s+1}}, \tag{8.B.3}$$

while switching i and k in (8.B.2) gives

$$\left.\frac{\partial}{\partial A}L(A;s)\right|_{A=1/2} = \frac{8s}{9}\sum_{i,j,k}{}' \frac{jk+ik-2ij}{\left(i^2+j^2+k^2-\frac{2}{3}(ij+ik+jk)\right)^{s+1}}. \tag{8.B.4}$$

On adding (8.B.2), (8.B.3) and (8.B.4) and noting that

$$(ij+ik-2jk)+(ij+jk-2ik)+(jk+ik-2ij) = 0$$

it follows that

$$\left.\frac{\partial}{\partial A}L(A;s)\right|_{A=1/2} = 0.$$

Next, taking the derivative of (8.B.1) gives

$$\begin{aligned}\frac{\partial^2}{\partial A^2}L(A;s) = {} & \frac{-4s}{(A+1)^3}\sum_{i,j,k}{}' \frac{ij+ik-2jk}{\left(i^2+j^2+k^2-2(ij+ik)\left(\frac{A}{A+1}\right)+2jk\left(\frac{A-1}{A+1}\right)\right)^{s+1}} \\ & + \frac{4s(s+1)}{(A+1)^4}\sum_{i,j,k}{}' \frac{(ij+ik-2jk)^2}{\left(i^2+j^2+k^2-2(ij+ik)\left(\frac{A}{A+1}\right)+2jk\left(\frac{A-1}{A+1}\right)\right)^{s+2}}.\end{aligned}$$

When $A = 1/2$ the first sum is zero by the calculations in the first part of the proof. Therefore,

$$\left.\frac{\partial^2}{\partial A^2}L(A;s)\right|_{A=1/2} = \frac{64s(s+1)}{81}\sum_{i,j,k}{}' \frac{(jk+ik-2ij)^2}{\left(i^2+j^2+k^2-\frac{2}{3}(ij+ik+jk)\right)^{s+2}}.$$

The term $(jk+ik-2ij)^2$ in the numerator is non-negative and not always zero. The denominator is always positive because the quadratic form is positive

definite. It follows that

$$\frac{\partial^2}{\partial A^2} L(A;s)\bigg|_{A=1/2} > 0$$

as required.

The calculations above are valid provided term-by-term differentiation of the series is allowed. All of the series encountered above converge absolutely and uniformly on compact subsets of the region $\mathrm{Re}(s) > 3/2$. On restricting s to real values, the conclusion about positivity is valid for $s > 3/2$.

A consequence of Theorem A is that for any fixed value $s > 3/2$, the lattice sum $L(A;s)$ attains a minimum when $A = 1/2$. Graphs of $y = L(A;s)$ to illustrate this minimum property are shown in Fig. 2. In the limiting case $s \to \infty$ we have

$$L(A;\infty) = \lim_{s\to\infty} L(A;s) = \mathrm{kiss}(\mathscr{L}) = \begin{cases} 10 & \text{if } A = 1/3, \\ 8 & \text{if } 1/3 < A < 1, \\ 12 & \text{if } A = 1. \end{cases}$$

This graph is also shown in Fig.8.2.

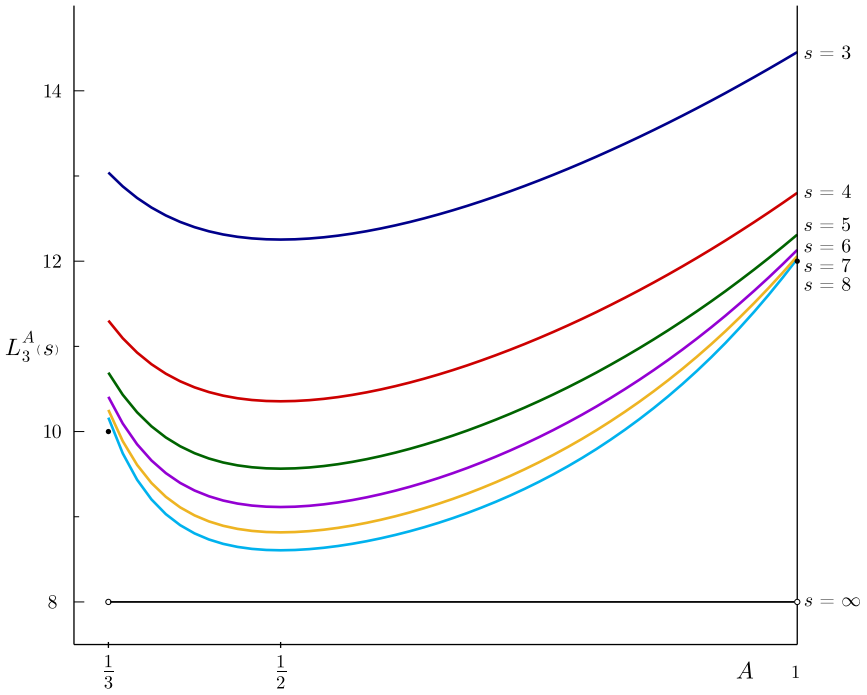

Figure 8.2 Graph of $L(A;s)$ versus A for various values of s

8.4 Evaluation of the sum $L(A;s)$

We now turn to the evaluation of $L(A;s)$. Our objectives are to find formulas that are both simple and computationally efficient. The formulas we obtain can be used to show that $L(A;s)$ can be analytically continued to complex values of s, with a simple pole at $s = 3/2$ and no other singularities.

One method of evaluating the sum $L(A;s)$ is to use the Terras decomposition. This was done for f.c.c. and b.c.c.[8] and can in principle also be used for $L(A;s)$. Here we use an easier method that also works the whole parameter range $1/3 \le A \le 1$ and hence gives the lattice sum for all four lattices f.c.c., m.c.c., b.c.c. and a.c.c. In fact, the advantage here is that we obtain two formulas which not only can be used as checks, but also contain different information about their analytic continuation.

We begin by writing the lattice sum in the form

$$\begin{aligned} L(A;s) &= {\sum_{i,j,k}}' \left(\frac{A+1}{A(i+j)^2+(j+k)^2+(i+k)^2} \right)^s \\ &= {\sum_{\substack{I,J,K \\ I+J+K \text{ even}}}}' \left(\frac{A+1}{AI^2+J^2+K^2} \right)^s \\ &= \frac{(A+1)^s}{2} {\sum_{i,j,k}}' \frac{1+(-1)^{i+j+k}}{(Ai^2+j^2+k^2)^s}. \end{aligned} \tag{8..1}$$

Therefore, we evaluate the sums

$$T_1(A;A;s) := {\sum_{i,j,k}}' \frac{1}{(Ai^2+j^2+k^2)^s} \tag{8..2}$$

and

$$T_2(A;s) := {\sum_{i,j,k}}' \frac{(-1)^{i+j+k}}{(Ai^2+j^2+k^2)^s}. \tag{8..3}$$

By (8..1), (8..2) and (8..3), the required lattice sum is given by

$$L(A;s) = \frac{(A+1)^s}{2} \left(T_1(A;s) + T_2(A;s) \right). \tag{8..4}$$

A The sum $T_1(A;s)$

We shall consider two ways for handling the sum in (8..2). The first is to separate the terms ording to whether $i = 0$ or $i \neq 0$, which gives rise to

$$T_1(A;s) = f(s) + 2F(s) \tag{8.A.5}$$

where

$$f(s) = \sum_{j,k}{}' \frac{1}{(j^2+k^2)^s}$$

and

$$F(s) = \sum_{i=1}^{\infty} \sum_{j=-\infty}^{\infty} \sum_{k=-\infty}^{\infty} \frac{1}{(Ai^2+j^2+k^2)^s}.$$

This is the starting point of the approach taken by Selberg and Chowla [[124][Section 7]]. Another way is to separate the terms ording to whether $(j,k) = (0,0)$ or $(j,k) \neq (0,0)$ and write

$$T_1(A;s) = 2g(s) + G(s) \tag{8.A.6}$$

where

$$g(s) = \sum_{i=1}^{\infty} \frac{1}{(Ai^2)^s}$$

and

$$G(s) = \sum_{j,k}{}' \sum_{i=-\infty}^{\infty} \frac{1}{(Ai^2+j^2+k^2)^s}.$$

The series $F(s)$, $g(s)$ and $G(s)$ also depend on A. For simplicity we omit the parameter A from the notation and just write $F(s)$, $g(s)$ and $G(s)$ in place of $F(A;s)$, $g(A;s)$ and $G(A;s)$, respectively.

We will now analyse (8.A.5); the corresponding analysis for (8.A.6) will be given in Section B. By the well-known result (12.A.17) we have

$$f(s) = \sum_{j,k}{}' \frac{1}{(j^2+k^2)^s} = 4\zeta(s)L_{-4}(s)$$

where

$$\zeta(s) = \sum_{n=1}^{\infty} \frac{1}{n^s}$$

is the Riemann zeta function, and

$$L_{-4}(s) = \sum_{n=1}^{\infty} \frac{\sin\frac{n\pi}{2}}{n^s} = \frac{1}{1^s} - \frac{1}{3^s} + \frac{1}{5^s} - \frac{1}{7^s} + \cdots.$$

is the Dirichlet beta series. It remains to analyse $F(s)$. By the integral formula for the gamma function (12.A.2) we have

$$\pi^{-s}\Gamma(s)F(s) = \int_0^\infty x^{s-1}\sum_{i=1}^\infty e^{-\pi Axi^2}\sum_{j=-\infty}^\infty\sum_{k=-\infty}^\infty e^{-\pi x(j^2+k^2)}\,\mathrm{d}x$$
$$= \int_0^\infty x^{s-1}\sum_{i=1}^\infty e^{-\pi Axi^2}\left(\sum_{j=-\infty}^\infty e^{-\pi xj^2}\right)^2\,\mathrm{d}x.$$

Now apply the modular transformation for theta functions (12.A.10) to obtain

$$\pi^{-s}\Gamma(s)F(s) = \int_0^\infty x^{s-1}\sum_{i=1}^\infty e^{-\pi Axi^2}\left(\frac{1}{\sqrt{x}}\sum_{j=-\infty}^\infty e^{-\pi j^2/x}\right)^2\,\mathrm{d}x$$
$$= \int_0^\infty x^{s-2}\sum_{i=1}^\infty e^{-\pi Axi^2}\sum_{N=0}^\infty r_2(N)e^{-\pi N/x}\,\mathrm{d}x$$

where $r_2(N)$ is the number of representations of N as a sum of two squares, e.g., see (12.A.11). Now separate out the $N=0$ term and evaluate the resulting integrals. We find that

$$\pi^{-s}\Gamma(s)F(s) = \sum_{i=1}^\infty\int_0^\infty x^{s-2}e^{-\pi Axi^2}\,\mathrm{d}x + \sum_{i=1}^\infty\sum_{N=1}^\infty r_2(N)\int_0^\infty x^{s-2}e^{-\pi Axi^2-\pi N/x}\,\mathrm{d}x$$
$$= \frac{\Gamma(s-1)\zeta(2s-2)}{A^{s-1}\pi^{s-1}} + 2\sum_{i=1}^\infty\sum_{N=1}^\infty r_2(N)\left(\frac{N}{Ai^2}\right)^{(s-1)/2}$$
$$\times K_{s-1}\left(2\pi i\sqrt{AN}\right)$$

where we have used the formula (12.A.3) for the K-Bessel function. On using all of the above back in (8.A.5) we obtain

$$\sum_{i,j,k}{}' \frac{1}{(Ai^2+j^2+k^2)^s} = 4\zeta(s)L_{-4}(s) + \frac{2\pi}{(s-1)}\frac{\zeta(2s-2)}{A^{s-1}}$$
$$+ \frac{4\pi^s}{\Gamma(s)}A^{(1-s)/2}\sum_{i=1}^\infty\sum_{N=1}^\infty r_2(N)\left(\frac{N}{i^2}\right)^{(s-1)/2}K_{s-1}\left(2\pi i\sqrt{AN}\right). \qquad (8.A.7)$$

This is essentially Selberg and Chowla's formula (45) [124]. They write it in a slightly different form in terms of a sum over the divisors of N to minimise the number of Bessel function evaluations. We will leave it as it is for simplicity.

B A second formula for the sum $T_1(A;s)$

This time we split the terms ording as in (8.A.6) and start with

$$T_1(A;s) = 2g(s) + G(s) \qquad (8.B.8)$$

where

$$g(s) = \sum_{i=1}^{\infty} \frac{1}{(Ai^2)^s} = A^{-s}\,\zeta(2s)$$

and

$$G(s) = \sum_{j,k}{}' \sum_{i=-\infty}^{\infty} \frac{1}{(Ai^2+j^2+k^2)^s}.$$

Now apply the integral formula for the gamma function (12.A.2) and then the modular transformation for the theta function (12.A.7) to obtain

$$\begin{aligned}\pi^{-s}\Gamma(s)G(s) &= \int_0^{\infty} x^{s-1} \sum_{j,k}{}' e^{-\pi(j^2+k^2)x} \sum_{i=-\infty}^{\infty} e^{-\pi i^2 Ax}\,\mathrm{d}x \\ &= \frac{1}{\sqrt{A}} \int_0^{\infty} x^{s-3/2} \sum_{j,k}{}' e^{-\pi(j^2+k^2)x} \sum_{i=-\infty}^{\infty} e^{-\pi i^2/Ax}\,\mathrm{d}x.\end{aligned}$$

Separate the $i=0$ term, to get

$$\begin{aligned}\pi^{-s}\Gamma(s)G(s) &= \frac{1}{\sqrt{A}} \int_0^{\infty} x^{s-3/2} \sum_{j,k}{}' e^{-\pi(j^2+k^2)x}\,\mathrm{d}x \\ &\quad + \frac{2}{\sqrt{A}} \int_0^{\infty} x^{s-3/2} \sum_{j,k}{}' e^{-\pi(j^2+k^2)x} \sum_{i=1}^{\infty} e^{-\pi i^2/Ax}\,\mathrm{d}x.\end{aligned}$$

The first integral can be evaluated in terms of the gamma function by (12.A.2), while the second integral can be expressed in terms of the modified Bessel function by (12.A.3). The result is

$$\begin{aligned}\pi^{-s}\Gamma(s)G(s) &= \frac{\Gamma\left(s-\frac{1}{2}\right)}{\sqrt{A}\,\pi^{s-\frac{1}{2}}} \sum_{j,k}{}' \frac{1}{(j^2+k^2)^{s-\frac{1}{2}}} \\ &\quad + \frac{4}{A^{\frac{s}{2}+\frac{1}{4}}} \sum_{j,k}{}' \sum_{i=1}^{\infty} \left(\frac{i}{\sqrt{j^2+k^2}}\right)^{s-\frac{1}{2}} K_{s-\frac{1}{2}}\left(2\pi i\sqrt{\frac{j^2+k^2}{A}}\right) \\ &= \frac{4}{\sqrt{A}}\,\pi^{-(s-\frac{1}{2})}\,\Gamma\left(s-\frac{1}{2}\right)\,\zeta\left(s-\frac{1}{2}\right)\,L_{-4}\left(s-\frac{1}{2}\right) \\ &\quad + \frac{4}{A^{\frac{s}{2}+\frac{1}{4}}} \sum_{N=1}^{\infty} \sum_{i=1}^{\infty} r_2(N) \left(\frac{i}{\sqrt{N}}\right)^{s-\frac{1}{2}} K_{s-\frac{1}{2}}\left(2\pi i\sqrt{\frac{N}{A}}\right).\end{aligned}$$

On using all of the above back in (8.B.8) we obtain

$$\begin{aligned}
&\sum_{i,j,k}{}' \frac{1}{(Ai^2+j^2+k^2)^s} \\
&= 2A^{-s}\zeta(2s) + 4\sqrt{\frac{\pi}{A}}\frac{\Gamma\left(s-\frac{1}{2}\right)}{\Gamma(s)}\zeta\left(s-\frac{1}{2}\right)L_{-4}\left(s-\frac{1}{2}\right) \\
&\quad + \frac{4}{A^{\frac{s}{2}+\frac{1}{4}}}\frac{\pi^s}{\Gamma(s)}\sum_{N=1}^{\infty}\sum_{i=1}^{\infty} r_2(N)\left(\frac{i}{\sqrt{N}}\right)^{s-\frac{1}{2}} K_{s-\frac{1}{2}}\left(2\pi i\sqrt{\frac{N}{A}}\right). \qquad \text{(8.B.9)}
\end{aligned}$$

The terms in (9.A.4) involve K_{s-1} Bessel functions whereas $K_{s-1/2}$ Bessel functions occur in (8.B.9). That is because each application of the theta function transformation formula lowers the subscript in the resulting Bessel function by $1/2$, due to the creation of a $x^{-1/2}$ factor in the integral. The theta function transformation formula is used twice (i.e., the formula is squared) in the derivation of (9.A.4) and only once in the derivation of (8.B.9).

Each of (9.A.4) and (8.B.9) turns out to have its own advantages, as will be seen in Sections D and C.

C The alternating sum $T_2(A;s)$

The analysis in the previous sections can be modified to handle the alternating series (8..3) which has the term $(-1)^{i+j+k}$ in the numerator, as follows. Separating the terms ording to whether $i=0$ or $i\neq 0$ gives

$$T_2(A;s) = h(s) + 2H(S) \qquad \text{(8.C.10)}$$

where

$$h(s) = \sum_{j,k}{}' \frac{(-1)^{j+k}}{(j^2+k^2)^s}$$

and

$$H(s) = \sum_{i=1}^{\infty}\sum_{j=-\infty}^{\infty}\sum_{k=-\infty}^{\infty}\frac{(-1)^{i+j+k}}{(Ai^2+j^2+k^2)^s}.$$

By a known result (8.B.21), we have

$$h(s) = -4(1-2^{1-s})\zeta(s)L_{-4}(s).$$

Next, by the integral formula for the gamma function (12.A.2) we have

$$\begin{aligned}\pi^{-s}\Gamma(s)H(s) &= \int_0^\infty x^{s-1}\sum_{i=1}^{\infty}(-1)^i e^{-\pi Axi^2}\sum_{j=-\infty}^{\infty}\sum_{k=-\infty}^{\infty}(-1)^{j+k}e^{-\pi x(j^2+k^2)}\,\mathrm{d}x\\ &= \int_0^\infty x^{s-1}\sum_{i=1}^{\infty}(-1)^i e^{-\pi Axi^2}\left(\sum_{j=-\infty}^{\infty}(-1)^j e^{-\pi xj^2}\right)^2\,\mathrm{d}x.\end{aligned}$$

Now apply the modular transformation for theta functions to obtain

$$\pi^{-s}\Gamma(s)H(s) = \int_0^\infty x^{s-1}\sum_{i=1}^{\infty}(-1)^i e^{-\pi Axi^2}\left(\frac{1}{\sqrt{x}}\sum_{j=-\infty}^{\infty}e^{-\pi(j+\frac{1}{2})^2/x}\right)^2\,\mathrm{d}x.$$

By formula (8.A.14) this can be expressed as

$$\begin{aligned}\pi^{-s}\Gamma(s)H(s) &= \int_0^\infty x^{s-2}\sum_{i=1}^{\infty}(-1)^i e^{-\pi Axi^2}\sum_{N=0}^{\infty}r_2(4N+1)e^{-\pi(4N+1)/2x}\,\mathrm{d}x\\ &= \sum_{i=1}^{\infty}\sum_{N=0}^{\infty}(-1)^i r_2(4N+1)\int_0^\infty x^{s-2}e^{-\pi Axi^2-\pi(4N+1)/2x}\,\mathrm{d}x.\end{aligned}$$

The integral can be expressed in terms of Bessel functions by (12.A.3) to give

$$\begin{aligned}\pi^{-s}\Gamma(s)H(s) = 2\sum_{i=1}^{\infty}\sum_{N=0}^{\infty}(-1)^i r_2(4N+1)&\left(\frac{2N+\frac{1}{2}}{Ai^2}\right)^{(s-1)/2}\\ &\times K_{s-1}\left(2\pi i\sqrt{A(2N+\frac{1}{2})}\right).\end{aligned}$$

On using all of the above back in (8.C.10) we obtain

$$\begin{aligned}&\sum_{i,j,k}{}' \frac{(-1)^{i+j+k}}{(Ai^2+j^2+k^2)^s}\\ &= -4(1-2^{1-s})\zeta(s)L_{-4}(s)\\ &+\frac{4\pi^s}{\Gamma(s)}A^{(1-s)/2}\sum_{i=1}^{\infty}\sum_{N=0}^{\infty}(-1)^i r_2(4N+1)\left(\frac{2N+\frac{1}{2}}{i^2}\right)^{(s-1)/2}\\ &\qquad\times K_{s-1}\left(2\pi i\sqrt{A(2N+\frac{1}{2})}\right).\end{aligned}\tag{8.C.11}$$

D A second formula for the alternating sum $T_2(A;s)$

This time we separate the terms ording to whether $(j,k)=(0,0)$ or $(j,k)\neq(0,0)$ and write

$$T_2(A;s)=2\sum_{i=1}^{\infty}\frac{(-1)^i}{(Ai^2)^s}+J(s) \tag{8.D.12}$$

where

$$J(s)=\sum_{j,k}{}'\sum_{i=-\infty}^{\infty}\frac{(-1)^{i+j+k}}{(Ai^2+j^2+k^2)^s}.$$

By (8.B.30) we have

$$2\sum_{i=1}^{\infty}\frac{(-1)^i}{(Ai^2)^s}=-2A^{-s}(1-2^{1-2s})\zeta(2s).$$

It remains to analyse the sum for $J(s)$. By the integral formula for the gamma function (12.A.2) we have

$$\pi^{-s}\Gamma(s)J(s)=\int_0^{\infty}x^{s-1}\sum_{j,k}{}'(-1)^{j+j}e^{-\pi(j^2+k^2)x}\sum_{i=-\infty}^{\infty}(-1)^i e^{-\pi i^2Ax}\,\mathrm{d}x.$$

Now apply the modular transformation (12.A.9) to obtain

$$\pi^{-s}\Gamma(s)J(s)=\frac{1}{\sqrt{A}}\int_0^{\infty}x^{s-3/2}\sum_{j,k}{}'(-1)^{j+k}e^{-\pi(j^2+k^2)x}\sum_{i=-\infty}^{\infty}e^{-\pi(i+\frac{1}{2})^2/Ax}\,\mathrm{d}x.$$

Now put $N=j^2+k^2$ and use

$$\sum_{i=-\infty}^{\infty}e^{-\pi(i+\frac{1}{2})^2/Ax}=2\sum_{i=0}^{\infty}e^{-\pi(i+\frac{1}{2})^2/Ax}=2\sum_{i=1}^{\infty}e^{-\pi(i-\frac{1}{2})^2/Ax}$$

to deduce

$$\pi^{-s}\Gamma(s)J(s)=\frac{2}{\sqrt{A}}\sum_{N=1}^{\infty}\sum_{i=1}^{\infty}(-1)^N r_2(N)\int_0^{\infty}x^{s-3/2}\,e^{-\pi Nx-\pi(i-\frac{1}{2})^2/Ax}\,\mathrm{d}x.$$

The integral can be evaluated in terms of the modified Bessel function by (12.A.3) to give

$$\pi^{-s}\Gamma(s)J(s)=\frac{4}{A^{\frac{s}{2}+\frac{1}{4}}}\sum_{N=1}^{\infty}\sum_{i=1}^{\infty}(-1)^N r_2(N)\left(\frac{i-\frac{1}{2}}{\sqrt{N}}\right)^{s-\frac{1}{2}}K_{s-\frac{1}{2}}\left(2\pi(i-\frac{1}{2})\sqrt{\frac{N}{A}}\right).$$

It follows that

$$\begin{aligned}
&\sum_{i,j,k}{}' \ \frac{(-1)^{i+j+k}}{(Ai^2+j^2+k^2)^s} \\
&= -2A^{-s}(1-2^{1-2s})\zeta(2s) \\
&\quad + \frac{4}{A^{\frac{s}{2}+\frac{1}{4}}}\frac{\pi^s}{\Gamma(s)}\sum_{N=1}^{\infty}\sum_{i=1}^{\infty}(-1)^N r_2(N)\left(\frac{i-\frac{1}{2}}{\sqrt{N}}\right)^{s-\frac{1}{2}} K_{s-\frac{1}{2}}\left(2\pi(i-\frac{1}{2})\sqrt{\frac{N}{A}}\right).
\end{aligned} \tag{8.D.13}$$

E Two formulas for $L(A;s)$

On substituting the results of (9.A.4) and (8.C.11) back into (8..4) we obtain a formula for $L(A;s)$ in terms of K_{s-1} Bessel functions:

$$\begin{aligned}
L(A;s) &= 4\left(\frac{A+1}{2}\right)^s \zeta(s)L_{-4}(s) + \frac{\pi A}{s-1}\left(1+\frac{1}{A}\right)^s \zeta(2s-2) \\
&\quad + \frac{2\pi^s\sqrt{A}}{\Gamma(s)}\left(\sqrt{A}+\frac{1}{\sqrt{A}}\right)^s \sum_{i=1}^{\infty}\sum_{N=1}^{\infty} r_2(N)\left(\frac{N}{i^2}\right)^{(s-1)/2} K_{s-1}\left(2\pi i\sqrt{AN}\right) \\
&\quad + \frac{2\pi^s\sqrt{A}}{\Gamma(s)}\left(\sqrt{A}+\frac{1}{\sqrt{A}}\right)^s \sum_{i=1}^{\infty}\sum_{N=0}^{\infty}(-1)^i r_2(4N+1) \\
&\qquad \times \left(\frac{2N+\frac{1}{2}}{i^2}\right)^{(s-1)/2} K_{s-1}\left(2\pi i\sqrt{A(2N+\frac{1}{2})}\right).
\end{aligned} \tag{8.E.14}$$

On the other hand, if the results of (8.B.9) and (8.D.13) are used in (8..4), the resulting formula for $L(A;s)$ involves $K_{s-1/2}$ Bessel functions:

$$\begin{aligned}
L(A;s) &= 2\left(\frac{A+1}{4A}\right)^s \zeta(2s) \\
&\quad + 2\sqrt{\frac{\pi}{A}}(A+1)^s \frac{\Gamma\left(s-\frac{1}{2}\right)}{\Gamma(s)}\zeta\left(s-\frac{1}{2}\right) L_{-4}\left(s-\frac{1}{2}\right) \\
&\quad + \frac{2}{A^{1/4}}\left(\sqrt{A}+\frac{1}{\sqrt{A}}\right)^s \frac{\pi^s}{\Gamma(s)}\sum_{N=1}^{\infty}\sum_{i=1}^{\infty} N^{(1-2s)/4} r_2(N) \\
&\qquad \times \left\{ i^{s-\frac{1}{2}} K_{s-\frac{1}{2}}\left(2\pi i\sqrt{\frac{N}{A}}\right) + (-1)^N\left(i-\frac{1}{2}\right)^{s-\frac{1}{2}} \right. \\
&\qquad\quad \left. \times K_{s-\frac{1}{2}}\left(2\pi(i-\frac{1}{2})\sqrt{\frac{N}{A}}\right)\right\}.
\end{aligned} \tag{8.E.15}$$

The formulas (8.E.14) and (8.E.15) can be used as checks against each other. Moreover, the formulas offer different information about special values of the lattice sum, as will be seen in Section 8.6.

8.5 Hexagonal close packing

Because of its importance in solid state chemistry and physics, we give a similar analysis of the lattice sum for the hexagonal close packed structure given by[280]

$$L_3^{\mathrm{HCP}}(s) = S_1(s) + S_2(s)$$

where

$$S_1(s) = \sum_{i,j,k}{}' \frac{1}{(i^2+ij+j^2+\frac{8}{3}k^2)^s}$$

and

$$S_2(s) = \sum_{i,j,k} \frac{1}{((i+\frac{1}{3})^2+(i+\frac{1}{3})(j+\frac{1}{3})+(j+\frac{1}{3})^2+\frac{8}{3}(k+\frac{1}{2})^2)^s}.$$

As before, the prime on the sum for $S_1(s)$ indicates that the summation is over all integers except for the term corresponding to $i=j=k=0$ which is omitted. The sum for $S_2(s)$ is over all integer values of i, j and k. We shall analyse $S_1(s)$ and $S_2(s)$ one at a time.

A The sum $S_1(s)$

Break the sum for $S_1(s)$ into two, ording to whether $k=0$ or $k\neq 0$. This gives

$$S_1(s) = f(s) + 2F(s) \tag{8.A.1}$$

where

$$f(s) = \sum_{i,j}{}' \frac{1}{(i^2+ij+j^2)^s}$$

and

$$F(s) = \sum_{k=1}^{\infty}\sum_{i,j} \frac{1}{(i^2+ij+j^2+\frac{8}{3}k^2)^s}.$$

By (12.A.24) we have

$$f(s) = 6\zeta(s)L_{-3}(s)$$

where

$$L_{-3}(s) = \sum_{k=1}^{\infty}\left(\frac{\sin(2k\pi/3)}{\sin(2\pi/3)}\right)\frac{1}{k^s} = \frac{1}{1^s} - \frac{1}{2^s} + \frac{1}{4^s} - \frac{1}{5^s} + \cdots.$$

It remains to calculate $F(s)$. Applying the gamma function integral (8.12.A.2) followed by the theta function transformation formula (8.12.A.12), we obtain

$$\begin{aligned}(2\pi)^{-s}\Gamma(s)F(s) &= \int_0^\infty x^{s-1}\sum_{k=1}^{\infty} e^{-16\pi k^2 x/3}\sum_{i,j} e^{-2\pi(i^2+ij+j^2)x}\,\mathrm{d}x \\ &= \frac{1}{\sqrt{3}}\int_0^\infty x^{s-2}\sum_{k=1}^{\infty} e^{-16\pi k^2 x/3}\sum_{i,j} e^{-2\pi(i^2+ij+j^2)/3x}\,\mathrm{d}x.\end{aligned}$$

Now separate out the $i=j=0$ term and evaluate the resulting integrals. The result is

$$\begin{aligned}(2\pi)^{-s}\Gamma(s)F(s) &= \frac{1}{\sqrt{3}}\sum_{k=-\infty}^{\infty}\int_0^\infty x^{s-2}e^{-16\pi k^2 x/3}\,\mathrm{d}x \\ &\quad + \frac{1}{\sqrt{3}}\sum_{k=-\infty}^{\infty}{\sum_{i,j}}'\int_0^\infty x^{s-2}e^{-16\pi k^2 x/3-2\pi(i^2+ij+j^2)/3x}\,\mathrm{d}x \\ &= \frac{1}{\sqrt{3}}\left(\frac{3}{16\pi}\right)^{s-1}\Gamma(s-1)\zeta(2s-2) \\ &\quad + \frac{2}{\sqrt{3}}\sum_{k=1}^{\infty}{\sum_{i,j}}'\left(\frac{i^2+ij+j^2}{8k^2}\right)^{(s-1)/2} \\ &\qquad \times K_{s-1}\left(\frac{8\pi k}{3}\sqrt{2(i^2+ij+j^2)}\right).\end{aligned}$$

It follows that

$$\begin{aligned}S_1(s) &= 6\zeta(s)L_{-3}(s) + \frac{4\pi}{\sqrt{3}}\left(\frac{3}{8}\right)^{s-1}\left(\frac{1}{s-1}\right)\zeta(2s-2) \\ &\quad + \frac{8}{\sqrt{3}}\frac{\pi^s}{\Gamma(s)}\sum_{k=1}^{\infty}{\sum_{i,j}}'\left(\frac{i^2+ij+j^2}{2k^2}\right)^{(s-1)/2} K_{s-1}\left(\frac{8\pi k}{3}\sqrt{2(i^2+ij+j^2)}\right) \\ &= 6\zeta(s)L_{-3}(s) + \frac{4\pi}{\sqrt{3}}\left(\frac{3}{8}\right)^{s-1}\left(\frac{1}{s-1}\right)\zeta(2s-2) \\ &\quad + \frac{8}{\sqrt{3}}\frac{\pi^s}{\Gamma(s)}\sum_{k=1}^{\infty}\sum_{N=1}^{\infty}u_2(N)\left(\frac{N}{2k^2}\right)^{(s-1)/2} K_{s-1}\left(\frac{8\pi k}{3}\sqrt{2N}\right) \qquad (8.\mathrm{A}.2)\end{aligned}$$

where $u_2(N)$ is the number of representations of N by the form i^2+ij+j^2.

B A second formula for the sum $S_1(s)$

A different formula for $S_1(s)$ can be obtained by separating the terms in the series ording to whether $i = j = 0$ or i and j are not both zero. This gives

$$S_1(s) = 2\left(\frac{3}{8}\right)^s \sum_{k=1}^{\infty} \frac{1}{k^{2s}} + G(s)$$

where

$$G(s) = \sum_{i,j}{}' \sum_{k=-\infty}^{\infty} \frac{1}{(i^2+ij+j^2+\frac{8}{3}k^2)^s}.$$

Applying the gamma function integral (8.12.A.2) followed by the theta function transformation formula (8.12.A.7), we obtain

$$\begin{aligned}\pi^{-s}\Gamma(s)G(s) &= \int_0^{\infty} x^{s-1} \sum_{i,j}{}' e^{-\pi(i^2+ij+j^2)x} \sum_{k=-\infty}^{\infty} e^{-8\pi k^2 x/3}\,\mathrm{d}x \\ &= \sqrt{\frac{3}{8}} \int_0^{\infty} x^{s-\frac{3}{2}} \sum_{i,j}{}' e^{-\pi(i^2+ij+j^2)x} \sum_{k=-\infty}^{\infty} e^{-3\pi k^2/8x}\,\mathrm{d}x.\end{aligned}$$

Now separate out the $k = 0$ term and evaluate the resulting integrals. The result is

$$\begin{aligned}&\pi^{-s}\Gamma(s)G(s) \\ &= \sqrt{\frac{3}{8}} \int_0^{\infty} x^{s-\frac{3}{2}} \sum_{i,j}{}' e^{-\pi(i^2+ij+j^2)x}\,\mathrm{d}x \\ &\quad + 2\sqrt{\frac{3}{8}} \int_0^{\infty} x^{s-\frac{3}{2}} \sum_{i,j}{}' e^{-\pi(i^2+ij+j^2)x} \sum_{k=1}^{\infty} e^{-3\pi k^2/8x}\,\mathrm{d}x \\ &= \sqrt{\frac{3}{8}}\,\pi^{-(s-\frac{1}{2})}\,\Gamma(s-\frac{1}{2}) \sum_{i,j}{}' \frac{1}{(i^2+ij+j^2)^{s-1/2}} \\ &\quad + 4\left(\frac{3}{8}\right)^{(2s+1)/4} \sum_{i,j}{}' \sum_{k=1}^{\infty} \left(\frac{k^2}{i^2+ij+j^2}\right)^{(2s-1)/4} K_{s-\frac{1}{2}}\left(\sqrt{\frac{3}{2}}\,\pi k\sqrt{i^2+ij+j^2}\right).\end{aligned}$$

The first sum can be evaluated in terms of the Riemann zeta function and the L_{-3} function by (8.12.A.24). In the second sum, we again use the notation $u_2(N)$ for the number of representations of N by the form i^2+ij+j^2. The result is

$$\begin{aligned}\pi^{-s}\Gamma(s)G(s) = \sqrt{\frac{27}{2}}\,\pi^{-(s-\frac{1}{2})}\,\Gamma\left(s-\frac{1}{2}\right)\zeta\left(s-\frac{1}{2}\right)L_{-3}\left(s-\frac{1}{2}\right) \\ + 4\left(\frac{3}{8}\right)^{(2s+1)/4} \sum_{N=1}^{\infty}\sum_{k=1}^{\infty} u_2(N)\left(\frac{k^2}{N}\right)^{(2s-1)/4} K_{s-\frac{1}{2}}\left(\pi k\sqrt{\frac{3N}{2}}\right).\end{aligned}$$

It follows that

$$S_1(s) = 2\left(\frac{3}{8}\right)^s \zeta(2s) + \sqrt{\frac{27\pi}{2}}\,\frac{\Gamma(s-\frac{1}{2})}{\Gamma(s)}\,\zeta\left(s-\frac{1}{2}\right)L_{-3}\left(s-\frac{1}{2}\right) + \frac{4\pi^s}{\Gamma(s)}\left(\frac{3}{8}\right)^{(2s+1)/4}\sum_{N=1}^{\infty}\sum_{k=1}^{\infty}u_2(N)\left(\frac{k^2}{N}\right)^{(2s-1)/4}K_{s-\frac{1}{2}}\left(\pi k\sqrt{\frac{3N}{2}}\right). \tag{8.B.3}$$

C The sum $S_2(s)$

The analysis in this case is a little simpler because the summation is over all integers i, j and k. We apply the gamma function integral (8.12.A.2) to write

$$\begin{aligned} S_2(s) &= \sum_{i,j,k}\frac{1}{((i+\frac{1}{3})^2+(i+\frac{1}{3})(j+\frac{1}{3})+(j+\frac{1}{3})^2+\frac{8}{3}(k+\frac{1}{2})^2)^s} \\ &= \frac{(2\pi)^s}{\Gamma(s)}\int_0^\infty x^{s-1}\sum_{k=-\infty}^{\infty}e^{-16\pi(k+\frac{1}{2})^2x/3} \\ &\qquad\times\sum_{i,j=-\infty}^{\infty}e^{-2\pi((i+\frac{1}{3})^2+(i+\frac{1}{3})(j+\frac{1}{3})+(j+\frac{1}{3})^2)x}\,\mathrm{d}x. \end{aligned} \tag{8.C.4}$$

Now make use of the transformation formula (8.12.A.13) to deduce

$$\begin{aligned} S_2(s) = \frac{(2\pi)^s}{\Gamma(s)}\int_0^\infty x^{s-1}&\left(2\sum_{k=0}^{\infty}e^{-16\pi(k+\frac{1}{2})^2x/3}\right) \\ &\times\left(\frac{1}{x\sqrt{3}}\sum_{i,j=-\infty}^{\infty}\omega^{i-j}e^{-2\pi(i^2+ij+j^2)/3x}\right)\mathrm{d}x \end{aligned}$$

where $\omega = e^{2\pi i/3}$ is a primitive cube root of 1. Now separate the term $i=j=0$ to deduce

$$\begin{aligned} S_2(s) = &\frac{(2\pi)^s}{\Gamma(s)}\frac{2}{\sqrt{3}}\int_0^\infty x^{s-2}\sum_{k=0}^{\infty}e^{-16\pi(k+\frac{1}{2})^2x/3}\,\mathrm{d}x \\ &+\frac{(2\pi)^s}{\Gamma(s)}\frac{2}{\sqrt{3}}\int_0^\infty x^{s-2}\sum_{k=0}^{\infty}e^{-16\pi(k+\frac{1}{2})^2x/3}\sum_{N=1}^{\infty}\omega^N u_2(N)\,e^{-2\pi N/3x}\,\mathrm{d}x \end{aligned}$$

where $u_2(N)$ is the number of representations of N by the form i^2+ij+j^2, as

before. On evaluating the integrals using (8.12.A.2) and (8.12.A.3) we obtain

$$S_2(s) = \frac{4\pi}{\sqrt{3}}\left(\frac{3}{8}\right)^{s-1}\left(\frac{1}{s-1}\right)\sum_{k=0}^{\infty}\frac{1}{(k+\frac{1}{2})^{2s-2}} + \frac{8}{\sqrt{3}}\frac{\pi^s}{\Gamma(s)}\sum_{k=0}^{\infty}\sum_{N=1}^{\infty}\omega^N u_2(N)\left(\frac{N}{2(k+\frac{1}{2})^2}\right)^{(s-1)/2} \times K_{s-1}\left(\frac{8\pi\left(k+\frac{1}{2}\right)}{3}\sqrt{2N}\right).$$

The first sum can be evaluated in terms of the Riemann zeta function by using (8.12.A.23). The ω^N term can be handled by using

$$\omega^N = \cos\frac{2\pi N}{3} + i\sin\frac{2\pi N}{3}$$

along with the fact that $S_2(s)$ is real valued when s is real. It follows that

$$S_2(s) = \frac{4\pi}{\sqrt{3}}\left(\frac{3}{8}\right)^{s-1}(2^{2s-2}-1)\left(\frac{1}{s-1}\right)\zeta(2s-2) + \frac{8}{\sqrt{3}}\frac{\pi^s}{\Gamma(s)}\sum_{k=0}^{\infty}\sum_{N=1}^{\infty}\cos\frac{2\pi N}{3}u_2(N)\left(\frac{N}{2(k+\frac{1}{2})^2}\right)^{(s-1)/2} \times K_{s-1}\left(\frac{8\pi\left(k+\frac{1}{2}\right)}{3}\sqrt{2N}\right). \tag{8.C.5}$$

D A second formula for the sum $S_2(s)$

We introduce the abbreviation

$$Y_{i,j} = \left(i+\frac{1}{3}\right)^2 + \left(i+\frac{1}{3}\right)\left(j+\frac{1}{3}\right) + \left(j+\frac{1}{3}\right)^2$$

to write (12.3.18) in the form

$$S_2(s) = \frac{(2\pi)^s}{\Gamma(s)}\int_0^{\infty} x^{s-1}\sum_{i,j=-\infty}^{\infty} e^{-2\pi Y_{i,j}x}\sum_{k=-\infty}^{\infty} e^{-16\pi(k+\frac{1}{2})^2x/3}\,\mathrm{d}x.$$

This time we apply the transformation formula (12.A.9) to the sum over k to obtain

$$S_2(s) = \frac{\sqrt{3}}{4}\frac{(2\pi)^s}{\Gamma(s)}\int_0^{\infty} x^{s-3/2}\sum_{i,j=-\infty}^{\infty} e^{-2\pi Y_{i,j}x}\sum_{k=-\infty}^{\infty}(-1)^k e^{-3\pi k^2/16x}\,\mathrm{d}x.$$

Now separate the terms ordering to whether $k = 0$ or $k \neq 0$ and evaluate the resulting integrals by (8.12.A.2) and (8.12.A.3). The result is

$$S_2(s) = \sqrt{\frac{3\pi}{8}}\,\frac{\Gamma(s-\frac{1}{2})}{\Gamma(s)} \sum_{i,j=-\infty}^{\infty} \frac{1}{Y_{ij}^{s-1/2}} + \frac{4\pi^s}{\Gamma(s)} \left(\frac{3}{8}\right)^{(2s+1)/4} \sum_{k=1}^{\infty} (-1)^k \sum_{i,j=-\infty}^{\infty} \left(\frac{k}{\sqrt{Y_{ij}}}\right)^{s-\frac{1}{2}} K_{s-\frac{1}{2}}\left(\pi k\sqrt{3Y_{i,j}/2}\right).$$

The first sum can be handled by (8.12.A.25) to give

$$\sum_{i,j=-\infty}^{\infty} \frac{1}{Y_{ij}^{s-1/2}} = 3(3^{s-1/2}-1)\zeta\left(s-\frac{1}{2}\right) L_{-3}\left(s-\frac{1}{2}\right).$$

For the other sum, observe that

$$3Y_{i,j} = 3i^2 + 3ij + 3j^2 + 3i + 3j + 1,$$

that is to say $3Y_{i,j}$ is a positive integer and $3Y_{i,j} \equiv 1 \pmod 3$. Therefore we set $3Y_{i,j} = 3N+1$ and use (8.12.A.16) to deduce that the number of solutions of

$$3i^2 + 3ij + 3j^2 + 3i + 3j + 1 = 3N + 1$$

is equal to $\frac{1}{2}u_2(3N+1)$. Taking all of the above into account, we finally obtain

$$S_2(s) = \sqrt{\frac{27\pi}{8}}\,\frac{\Gamma(s-\frac{1}{2})}{\Gamma(s)}\,(3^{s-1/2}-1)\,\zeta\left(s-\frac{1}{2}\right) L_{-3}\left(s-\frac{1}{2}\right) + \frac{2\pi^s}{\Gamma(s)} \left(\frac{3}{8}\right)^{(2s+1)/4} \sum_{k=1}^{\infty}\sum_{N=0}^{\infty} (-1)^k u_2(3N+1) \times \left(\frac{k}{\sqrt{N+\frac{1}{3}}}\right)^{s-\frac{1}{2}} K_{s-\frac{1}{2}}\left(\pi k\sqrt{\frac{3N+1}{2}}\right). \qquad (8.D.6)$$

E The lattice sum for hexagonal close packing

On adding the results for $S_1(s)$ and $S_2(s)$ in (8.A.2) and (8.C.5) we obtain

$$\begin{aligned} L_3^{\mathrm{HCP}}(s) = {} & 6\zeta(s)L_{-3}(s) + \frac{4\pi}{\sqrt{3}}\left(\frac{3}{2}\right)^{s-1}\left(\frac{1}{s-1}\right)\zeta(2s-2) \\ & + \frac{8}{\sqrt{3}}\frac{\pi^s}{\Gamma(s)}\sum_{k=1}^{\infty}\sum_{N=1}^{\infty}u_2(N)\left(\frac{N}{2k^2}\right)^{(s-1)/2}K_{s-1}\left(\frac{8\pi k}{3}\sqrt{2N}\right) \\ & + \frac{8}{\sqrt{3}}\frac{\pi^s}{\Gamma(s)}\sum_{k=0}^{\infty}\sum_{N=1}^{\infty}\cos\frac{2\pi N}{3}\,u_2(N) \\ & \qquad \times\left(\frac{N}{2(k+\frac{1}{2})^2}\right)^{(s-1)/2}K_{s-1}\left(\frac{8\pi\left(k+\frac{1}{2}\right)}{3}\sqrt{2N}\right). \end{aligned} \tag{8.E.7}$$

On the other hand, if we add the results of (8.B.3) and (8.D.6) we obtain

$$\begin{aligned} L_3^{\mathrm{HCP}}(s) = {} & 2\left(\frac{3}{8}\right)^{s}\zeta(2s) + \sqrt{\frac{27\pi}{8}}\,\frac{\Gamma(s-\frac{1}{2})}{\Gamma(s)}\,(3^{s-1/2}+1)\,\zeta\left(s-\frac{1}{2}\right)L_{-3}\left(s-\frac{1}{2}\right) \\ & + \frac{4\pi^s}{\Gamma(s)}\left(\frac{3}{8}\right)^{(2s+1)/4}\sum_{N=1}^{\infty}\sum_{k=1}^{\infty}u_2(N)\left(\frac{k}{\sqrt{N}}\right)^{s-1/2}K_{s-\frac{1}{2}}\left(\pi k\sqrt{\frac{3N}{2}}\right) \\ & + \frac{2\pi^s}{\Gamma(s)}\left(\frac{3}{8}\right)^{(2s+1)/4}\sum_{k=1}^{\infty}\sum_{N=0}^{\infty}(-1)^k u_2(3N+1) \\ & \qquad \times\left(\frac{k}{\sqrt{N+\frac{1}{3}}}\right)^{s-\frac{1}{2}}K_{s-\frac{1}{2}}\left(\pi k\sqrt{\frac{3N+1}{2}}\right) \end{aligned} \tag{8.E.8}$$

8.6 Analytic continuations of the lattice sums $L(A;s)$ and $L_3^{\mathrm{HCP}}(s)$

We will now show that the lattice sums $L(A;s)$ and $L_3^{\mathrm{HCP}}(s)$ can be continued analytically to the whole s-plane, and that the resulting functions have a single simple pole at $s = 3/2$ and no other singularities. We do this in steps. First, in Section 8.6.A we show that the lattice sums each have a simple pole at $s = 3/2$ and determine the residue. Then, in Section 8.6.B we show that the analytic continuations obtained are valid for the whole s-plane and there are no other singularities. Finally, in Sections 8.6.C–E, values of the analytic continuations at the points $s = 1/2$ and $s = 1, 0, -1, -2, \ldots$ are computed. In particular, the evaluation of $T_2(A;s)$ at $s = 1/2$ in the case $A = 1$ gives the Madelung constant, e.g., see [277], [1, pp. xiii, 39–51], [281].

A Behaviour of the lattice sums at $s = 3/2$

We start by showing that $L(A;s)$ has a simple pole at $s = 3/2$ and determine the residue. In the formula (8.E.14), all of the terms are analytic at $s = 3/2$ except for the term involving $\zeta(2s-2)$. It follows that

$$\begin{aligned}\lim_{s\to 3/2}(s-3/2)L(A;s) &= \lim_{s\to 3/2}(s-3/2)\frac{\pi A}{s-1}\left(1+\frac{1}{A}\right)^s\zeta(2s-2)\\ &= 2\pi A\left(1+\frac{1}{A}\right)^{3/2}\lim_{s\to 3/2}(s-3/2)\zeta(2s-2)\\ &= \frac{2\pi}{\sqrt{A}}(A+1)^{3/2}\times\frac{1}{2}\lim_{u\to 1}(u-1)\zeta(u)\\ &= \frac{\pi}{\sqrt{A}}(A+1)^{3/2}\end{aligned}$$

where (8.12.A.19) was used in the last step of the calculation. It follows further that $L(A;s)$ has a simple pole at $s = 3/2$ and the residue is given by

$$\mathrm{Res}(L(A;s),3/2) = \frac{\pi}{\sqrt{A}}(A+1)^{3/2}.$$

By (8..8) this is just 12 times the packing density, i.e.,

$$\mathrm{Res}(L(A;s),3/2) = 12\Delta_{\mathscr{L}}.$$

For example, taking $A = 1$ gives

$$\mathrm{Res}(L_3^{\mathrm{FCC}}(s),3/2) = 2\sqrt{2}\,\pi \tag{8.A.1}$$

while taking $A = 1/2$ gives

$$\mathrm{Res}(L_3^{\mathrm{BCC}}(s),3/2) = 3\sqrt{3}\,\pi/2.$$

Laurent's theorem implies there is an expansion of the form

$$L(A;s) = \frac{c_{-1}}{s-3/2} + c_0 + \sum_{n=1}^{\infty} c_n(s-3/2)^n \tag{8.A.2}$$

where

$$c_{-1} = \mathrm{Res}(L(A;s),3/2) = \frac{\pi}{\sqrt{A}}(A+1)^{3/2}$$

and the coefficients c_0, c_1, $c_2,\ldots$ depend on A but not on s. To calculate c_0, start with the fact that

$$\lim_{s\to 3/2}\left(\frac{\pi A}{s-1}\left(1+\frac{1}{A}\right)^s\zeta(2s-2) - \frac{c_{-1}}{s-3/2}\right)$$

$$= \frac{\pi}{\sqrt{A}}(A+1)^{3/2}\left(2\gamma - 2 + \log\left(1+\frac{1}{A}\right)\right)$$

where $\gamma = 0.57721\,56649\,01532\,86060\cdots$ is Euler's constant. Then use (8.E.14) and (8.12.A.5) to deduce

$$\begin{aligned}
c_0 &= \lim_{s\to 3/2}\left(L(A;s) - \frac{c_{-1}}{s-3/2}\right)\\
&= \sqrt{2}(A+1)^{3/2}\,\zeta\left(\frac{3}{2}\right)L_{-4}\left(\frac{3}{2}\right)\\
&\quad + \frac{\pi}{\sqrt{A}}(A+1)^{3/2}\left(2\gamma - 2 + \log\left(1+\frac{1}{A}\right)\right)\\
&\quad + \frac{2\pi}{\sqrt{A}}(A+1)^{3/2}\sum_{k=1}^{\infty}\sum_{N=1}^{\infty}\frac{1}{k}\,r_2(N)\exp\left(-2\pi k\sqrt{AN}\right)\\
&\quad + \frac{2\pi}{\sqrt{A}}(A+1)^{3/2}\sum_{k=1}^{\infty}\sum_{N=0}^{\infty}\frac{(-1)^k}{k}\,r_2(4N+1)\exp\left(-2\pi k\sqrt{A\left(2N+\frac{1}{2}\right)}\right).
\end{aligned}$$

Interchanging the order of summation and evaluating the sum over k gives

$$\begin{aligned}
c_0 &= \sqrt{2}(A+1)^{3/2}\,\zeta\left(\frac{3}{2}\right)L_{-4}\left(\frac{3}{2}\right)\\
&\quad + \frac{\pi}{\sqrt{A}}(A+1)^{3/2}\left(2\gamma - 2 + \log\left(1+\frac{1}{A}\right)\right)\\
&\quad - \frac{2\pi}{\sqrt{A}}(A+1)^{3/2}\sum_{N=1}^{\infty}r_2(N)\log\left(1-e^{-2\pi\sqrt{AN}}\right)\\
&\quad - \frac{2\pi}{\sqrt{A}}(A+1)^{3/2}\sum_{N=0}^{\infty}r_2(4N+1)\log\left(1+e^{-\pi\sqrt{2A(4N+1)}}\right).
\end{aligned}$$

Numerical evaluation in the case $A=1$ gives

$$c_0|_{A=1} = 6.98405\,25503\,22247\,93406\cdots. \tag{8.A.3}$$

A similar analysis can be given for $L_3^{\mathrm{HCP}}(s)$ using (8.E.7). We omit the details of the calculations as they are similar to the above. The end result is a Laurent expansion of the form

$$L_3^{\mathrm{HCP}}(s) = \frac{d_{-1}}{s-3/2} + d_0 + \sum_{n=1}^{\infty} d_n (s-3/2)^n \tag{8.A.4}$$

where

$$d_{-1} = \mathrm{Res}(L_3^{\mathrm{HCP}}(s), 3/2) = 2\sqrt{2}\pi \tag{8.A.5}$$

and

$$\begin{aligned}
d_0 &= 6\zeta\left(\frac{3}{2}\right)L_{-3}\left(\frac{3}{2}\right) + 2\sqrt{2}\,\pi\left(2\gamma-2+\log\frac{3}{2}\right)\\
&\quad + 2\sqrt{2}\pi\sum_{k=1}^{\infty}\sum_{N=1}^{\infty}\frac{1}{k}\,u_2(N)\exp\left(-\frac{8}{3}\pi k\sqrt{2N}\right)\\
&\quad + 2\sqrt{2}\pi\sum_{k=0}^{\infty}\sum_{N=1}^{\infty}\frac{\cos\left(\frac{2\pi N}{3}\right)}{(k+\frac{1}{2})}\,u_2(N)\exp\left(-\frac{8}{3}\pi\left(k+\frac{1}{2}\right)\sqrt{2N}\right)\\
&= 6\zeta\left(\frac{3}{2}\right)L_{-3}\left(\frac{3}{2}\right) + 2\sqrt{2}\,\pi\left(2\gamma-2+\log\frac{3}{2}\right)\\
&\quad - 2\sqrt{2}\pi\sum_{N=1}^{\infty}u_2(N)\log\left(1-e^{-\frac{8}{3}\pi\sqrt{2N}}\right)\\
&\quad + 2\sqrt{2}\pi\sum_{N=1}^{\infty}\cos\left(\frac{2\pi N}{3}\right)u_2(N)\log\left(\frac{1+e^{-\frac{4}{3}\pi\sqrt{2N}}}{1-e^{-\frac{4}{3}\pi\sqrt{2N}}}\right)\\
&= 6.98462\ 37414\ 38416\ 61307\ \cdots. \qquad (8.A.6)
\end{aligned}$$

In particular, the pole of $L_3^{\mathrm{HCP}}(s)$ at $s=3/2$ is simple. By (8.A.1) and (8.A.5) we have

$$\mathrm{Res}(L_3^{\mathrm{HCP}}(s),3/2) = \mathrm{Res}(L_3^{\mathrm{FCC}}(s),3/2).$$

It follows that the difference $L_3^{\mathrm{FCC}}(s)-L_3^{\mathrm{HCP}}(s)$ has a removable singularity at $s=3/2$ and from the Laurent expansions we deduce that

$$\lim_{s\to\frac{3}{2}}\left(L_3^{\mathrm{FCC}}(s)-L_3^{\mathrm{HCP}}(s)\right) = c_0|_{A=1}-d_0.$$

Using the numerical values from (8.A.3) and (8.A.6) we obtain

$$\lim_{s\to\frac{3}{2}}\left(L_3^{\mathrm{FCC}}(s)-L_3^{\mathrm{HCP}}(s)\right) = -0.00057\ 11911\ 16168\ 67901\cdots.$$

This gives the value at the left hand end of the graph in [8, Fig. 3]. The value $s=3/2$ used here corresponds to taking $s=3$ in [8] because of the different way the exponents are used in the definitions.

B Analyticity of the lattice sums at other values of s

By (8.12.A.6), the double series of Bessel functions in (8.E.14) converges absolutely and uniformly on compact subsets of the s-plane and therefore represents an entire function of s. It follows that $L(A;s)$ has an analytic continuation to a meromorphic function which is analytic except possibly at the singularities of the terms

$$4\left(\frac{A+1}{2}\right)^{s}\zeta(s)L_{-4}(s) \qquad (8.B.7)$$

and

$$\frac{\pi A}{s-1}\left(1+\frac{1}{A}\right)^s \zeta(2s-2). \tag{8.B.8}$$

The function in (8.B.7) is analytic except at $s=1$ due to the pole of $\zeta(s)$, as the function $L_{-4}(s)$ and the exponential function are both entire. The function in (8.B.8) is analytic except at $s=1$ and $s=3/2$. We studied the singularity at $s=3/2$ in the previous section, so this leaves only the point $s=1$. Using (8.12.A.19) and the values of $\zeta(0)$ and $L_{-4}(1)$ in (8.12.A.21) and 8.B.27 we find that

$$4\left(\frac{A+1}{2}\right)^s \zeta(s)L_{-4}(s) = \frac{(A+1)\pi}{2(s-1)} + O(1) \quad \text{as } s \to 1$$

and

$$\frac{\pi A}{s-1}\left(1+\frac{1}{A}\right)^s \zeta(2s-2) = -\frac{(A+1)\pi}{2(s-1)} + O(1) \quad \text{as } s \to 1.$$

It follows that the sum of the functions in (8.B.7) and (8.B.8) has a removable singularity at $s=1$ and so $L(A;s)$ is also analytic at $s=1$. The analyticity at $s=1$ can also be seen directly from the alternative formula for $L(A;s)$ in (8.E.15).

In conclusion, it has been shown that $L(A;s)$ has an analytic continuation to a meromorphic function of s which has a simple pole at $s=3/2$ and no other singularities. Because $L(A;s)$ has only one singularity, namely $s=3/2$, the Laurent expansion (8.A.2) is valid in the annulus $0<|s-3/2|<\infty$, i.e., for all $s\neq 3/2$.

In a similar way, (8.E.7) and (8.E.8) can be used to show that $L_3^{\mathrm{HCP}}(s)$ also has an analytic continuation to a meromorphic function of s which has a simple pole at $s=3/2$ and no other singularities. The Laurent expansion (8.A.4) converges for all $s\neq 3/2$.

By the theory of complex variables, the analytic continuation, if one exists, is unique, e.g., see [282, p. 147, Th. 1]. Therefore analytic continuation formulas can be used to assign values to divergent series. For example, the Madelung constant is defined by

$$M = \sum_{i,j,k}{}' \quad \frac{(-1)^{i+j+k}}{(i^2+j^2+k^2)^s}\bigg|_{s=1/2}. \tag{8.B.9}$$

This is interpreted as being the value of the analytic continuation of the series at $s=1/2$, because

$$\sum_{i,j,k}{}' \quad \frac{(-1)^{i+j+k}}{(i^2+j^2+k^2)^s}$$

obviously diverges if $s=1/2$. From now on, we shall use the expression "the value of a series at a point s" to mean "the value of the analytic continuation of the series at the point s".

C Values at $s = 1/2$ and the Madelung constant

On putting $s = 1/2$ in (8.C.11) we obtain an analytic expression for the value of

$$M(A) = \sum_{i,j,k}{}' \quad \frac{(-1)^{i+j+k}}{(Ai^2+j^2+k^2)^s}\bigg|_{s=1/2}$$

which specialises to the Madelung constant in the case $A = 1$. We have

$$M(A) = -4(1-2^{1-s})\zeta(s)L_{-4}(s)\bigg|_{s=1/2} + \frac{4\pi^s}{\Gamma(s)}A^{(1-s)/2}\sum_{i=1}^{\infty}\sum_{N=0}^{\infty}(-1)^i r_2(4N+1)\left(\frac{2N+\frac{1}{2}}{i^2}\right)^{(s-1)/2} \times K_{s-1}\left(2\pi i\sqrt{A(2N+\frac{1}{2})}\right)\bigg|_{s=1/2}.$$

Now use (8.12.A.4) and (8.12.A.5) to express the Bessel functions in terms of exponential functions. The result simplifies to

$$M(A) = 4(\sqrt{2}-1)\zeta\left(\frac{1}{2}\right)L_{-4}\left(\frac{1}{2}\right) + 2\sum_{i=1}^{\infty}\sum_{N=0}^{\infty}(-1)^i\frac{r_2(4N+1)}{\sqrt{2N+\frac{1}{2}}}e^{-2\pi i\sqrt{A(2N+1/2)}}.$$

On interchanging the order of summation and summing the geometric series, we obtain

$$M(A) = 4(\sqrt{2}-1)\zeta\left(\frac{1}{2}\right)L_{-4}\left(\frac{1}{2}\right) - 2\sqrt{2}\sum_{N=0}^{\infty}\frac{r_2(4N+1)}{\sqrt{4N+1}}\left(\frac{1}{e^{\pi\sqrt{2A(4N+1)}}+1}\right).$$

When $A = 1$ this gives the Madelung constant defined by (8.B.9). Numerical evaluation gives

$$M = M(1) = -1.74756\,45946\,33182\,19063\cdots \tag{8.C.10}$$

which is in agreement with [275, p. xiii] (apart from the minus sign which we have corrected here) and matches the value of $d(1)$ in [275, pp 39–51].

In a similar way, starting from (8.9.A.4) and using (8.12.A.5) and (8.12.A.21)

we obtain

$$\begin{aligned}
&\sum_{i,j,k}{}' \quad \frac{1}{(Ai^2+j^2+k^2)^s}\bigg|_{s=1/2} \\
&= 4\zeta\left(\frac{1}{2}\right)L_{-4}\left(\frac{1}{2}\right)+\frac{\pi\sqrt{A}}{3}+2\sum_{i=1}^{\infty}\sum_{N=1}^{\infty}\frac{r_2(N)}{\sqrt{N}}\,e^{-2\pi i\sqrt{AN}} \\
&= 4\zeta\left(\frac{1}{2}\right)L_{-4}\left(\frac{1}{2}\right)+\frac{\pi\sqrt{A}}{3}+2\sum_{N=1}^{\infty}\frac{r_2(N)}{\sqrt{N}}\left(\frac{1}{e^{2\pi\sqrt{AN}}-1}\right). \qquad (8.C.11)
\end{aligned}$$

Numerical evaluation in the case $A=1$ gives

$$\sum_{i,j,k}{}' \quad \frac{1}{(i^2+j^2+k^2)^s}\bigg|_{s=1/2} = -2.83729\,74794\,80619\,47666\cdots. \qquad (8.C.12)$$

Now, from (8..4) we have

$$L_3^{\mathrm{FCC}}(1/2)=\frac{1}{\sqrt{2}}\sum_{i,j,k}{}'\frac{1}{(i^2+j^2+k^2)^s}\bigg|_{s=1/2}+\frac{1}{\sqrt{2}}\sum_{i,j,k}{}'\frac{(-1)^{i+j+k}}{(i^2+j^2+k^2)^s}\bigg|_{s=1/2}.$$

Hence, using the values from (8.C.10) and (8.C.12) we obtain

$$L_3^{\mathrm{FCC}}(1/2) = -3.24198\,70634\,10888\,39428\cdots.$$

We also record the result

$$\begin{aligned}
L_3^{\mathrm{HCP}}(1/2) &= 6\zeta\left(\frac{1}{2}\right)L_{-3}\left(\frac{1}{2}\right)+\frac{2\sqrt{2}\pi}{9}+2\sum_{N=1}^{\infty}\frac{u_2(N)}{\sqrt{N}}\left(\frac{1}{e^{8\pi\sqrt{2N}/3}-1}\right) \\
&\quad +2\sum_{N=1}^{\infty}\cos\left(\frac{2\pi N}{3}\right)\frac{u_2(N)}{\sqrt{N}}\left(\frac{1}{e^{4\pi\sqrt{2N}/3}-e^{-4\pi\sqrt{2N}/3}}\right) \\
&= -3.24185\,86150\,75732\,86473\cdots
\end{aligned}$$

which is obtained in the same way, starting from (8.E.7).

D The value at $s=1$

It was noted above that (8.E.14), which involves K_{s-1} Bessel functions, contains terms with singularities at $s=1$ and therefore is not suitable for calculations at that value of s. Instead we can use (8.E.15), which involves $K_{s-1/2}$ Bessel functions. As in the previous section, two steps are involved. First, the the $K_{1/2}$ Bessel functions can be expressed in terms of the exponential function by (8.12.A.5). Then, the double sum can be reduced to a single sum by geometric series. We omit the details and just record the final results and corresponding numerical values.

From (8.B.9) we have

$$\sum_{i,j,k}{}' \left. \frac{1}{(Ai^2+j^2+k^2)^s} \right|_{s=1}$$
$$= \frac{\pi^2}{3A} + \frac{4\pi}{\sqrt{A}}\zeta\left(\frac{1}{2}\right)L_{-4}\left(\frac{1}{2}\right) + \frac{2\pi}{\sqrt{A}}\sum_{N=1}^{\infty}\frac{r_2(N)}{\sqrt{N}}\left(\frac{1}{e^{2\pi\sqrt{N/A}}-1}\right) \quad (8.D.13)$$

while (8.D.13) gives

$$\sum_{i,j,k}{}' \left. \frac{(-1)^{i+j+k}}{(Ai^2+j^2+k^2)^s} \right|_{s=1}$$
$$= \frac{-\pi^2}{6A} + \frac{2\pi}{\sqrt{A}}\sum_{N=1}^{\infty}(-1)^N\frac{r_2(N)}{\sqrt{N}}\left(\frac{1}{e^{\pi\sqrt{N/A}}-e^{-\pi\sqrt{N/A}}}\right).$$

Then (8..4) can be used to write down the value of $L(A;s)$.

For example, when $A=1$ the above formulas give

$$\sum_{i,j,k}{}' \left. \frac{1}{(i^2+j^2+k^2)^s} \right|_{s=1} = -8.91363\ 29175\ 85151\ 27268\cdots \quad (8.D.14)$$

and

$$\sum_{i,j,k}{}' \left. \frac{(-1)^{i+j+k}}{(i^2+j^2+k^2)^s} \right|_{s=1} = -2.51935\ 61520\ 89445\ 31334\cdots.$$

Then taking $A=1$ and $s=1$ in (8..4) gives

$$L_3^{\mathrm{FCC}}(1) = \sum_{i,j,k}{}' \left. \frac{1}{(i^2+j^2+k^2)^s} \right|_{s=1} + \sum_{i,j,k}{}' \left. \frac{(-1)^{i+j+k}}{(i^2+j^2+k^2)^s} \right|_{s=1}$$
$$= -11.43298\ 90696\ 74596\ 58602\cdots.$$

For h.c.p., the formula (8.E.7) cannot be used to evaluate $L_3^{\mathrm{HCP}}(1)$ because two of the terms have cancelling singularities at $s=1$. Therefore we take $s=1$

in (8.E.8) instead to obtain

$$\begin{aligned} L_3^{\mathrm{HCP}}(1) &= \frac{\pi^2}{8} + \pi\sqrt{\frac{27}{8}}\,(\sqrt{3}+1)\,\zeta\left(\frac{1}{2}\right) L_{-3}\left(\frac{1}{2}\right) \\ &\quad + \pi\sqrt{\frac{3}{2}}\sum_{N=1}^{\infty}\frac{u_2(N)}{\sqrt{N}}\left(\frac{1}{e^{\pi\sqrt{3N/2}}-1}\right) \\ &\quad - \frac{3\pi}{\sqrt{8}}\sum_{N=0}^{\infty}\frac{u_2(3N+1)}{\sqrt{3N+1}}\left(\frac{1}{e^{\pi\sqrt{(3N+1)/2}}+1}\right) \\ &= -11.43265\ 30014\ 95285\ 63572\cdots. \end{aligned}$$

We end this section by noting a connection between two of the values in the above analysis. By setting $A = 1$ in each of (8.C.11) and (8.D.13) we obtain the remarkable result

$$\sum_{i,j,k}{}' \quad \frac{1}{(i^2+j^2+k^2)^s}\bigg|_{s=1} = \pi \sum_{i,j,k}{}' \quad \frac{1}{(i^2+j^2+k^2)^s}\bigg|_{s=1/2}. \tag{8.D.15}$$

This is consistent with [275, p. 46 (1.3.44)] and is the special case $s = 1$ of the functional equation

$$\pi^{-s}\Gamma(s)T_1(1;s) = \pi^{-(\frac{3}{2}-s)}\Gamma\left(\frac{3}{2}-s\right)T_1\left(1;\frac{3}{2}-s\right). \tag{8.D.16}$$

This functional equation can be deduced from the two formulas for $T_1(A;s)$ in (8.9.A.4) and (8.B.9), as follows. Replace s with $\frac{3}{2}-s$ in (8.9.A.4), then multiply by $\pi^{s-\frac{3}{2}}\Gamma(\frac{3}{2}-s)$ and set $A = 1$ to get

$$\begin{aligned} &\pi^{s-\frac{3}{2}}\Gamma\left(\frac{3}{2}-s\right)T_1\left(1;\frac{3}{2}-s\right) \\ &= 4\pi^{s-\frac{3}{2}}\Gamma\left(\frac{3}{2}-s\right)\zeta\left(\frac{3}{2}-s\right)L_{-4}\left(\frac{3}{2}-s\right) + 2\pi^{s-\frac{1}{2}}\Gamma\left(\frac{1}{2}-s\right)\zeta(1-2s) \\ &\quad + 4\sum_{i=1}^{\infty}\sum_{N=1}^{\infty} r_2(N)\left(\frac{N}{i^2}\right)^{(\frac{1}{2}-s)/2} K_{\frac{1}{2}-s}\left(2\pi i\sqrt{N}\right), \end{aligned}$$

where we have used the functional equation for the gamma function in the form

$$\Gamma(3/2-s) = (1/2-s)\Gamma(1/2-s)$$

to obtain the second term on the right hand side. Now apply the functional

equations (8.12.A.4),(8.12.A.20) and (8.B.25) to deduce

$$\begin{aligned}
&\pi^{-(\frac{3}{2}-s)}\Gamma\left(\frac{3}{2}-s\right)T_1\left(1;\frac{3}{2}-s\right)\\
&=4\pi^{\frac{1}{2}-s}\Gamma\left(s-\frac{1}{2}\right)\zeta\left(s-\frac{1}{2}\right)L_{-4}\left(s-\frac{1}{2}\right)+2\pi^{-s}\Gamma(s)\zeta(2s)\\
&\quad+4\sum_{i=1}^{\infty}\sum_{N=1}^{\infty}r_2(N)\left(\frac{i}{\sqrt{N}}\right)^{s-\frac{1}{2}}K_{s-\frac{1}{2}}\left(2\pi i\sqrt{N}\right).
\end{aligned}$$

The functional equation (8.D.16) follows from this by using (8.B.9). In addition to providing another proof of the functional equation, the calculation above also demonstrates the interconnection between the formulas (8.9.A.4) and (8.B.9). Further functional equations of this type are considered in [275, p. 46].

E Values at $s = 0, -1, -2, -3, \ldots$

Recall from (8.E.14) that

$$\begin{aligned}
L(A;s)&=4\left(\frac{A+1}{2}\right)^s\zeta(s)L_{-4}(s)+\frac{\pi A}{s-1}\left(1+\frac{1}{A}\right)^s\zeta(2s-2)\\
&\quad+\frac{2\pi^s\sqrt{A}}{\Gamma(s)}\left(\sqrt{A}+\frac{1}{\sqrt{A}}\right)^s\sum_{i=1}^{\infty}\sum_{N=1}^{\infty}r_2(N)\left(\frac{N}{i^2}\right)^{(s-1)/2}K_{s-1}\left(2\pi i\sqrt{AN}\right)\\
&\quad+\frac{2\pi^s\sqrt{A}}{\Gamma(s)}\left(\sqrt{A}+\frac{1}{\sqrt{A}}\right)^s\sum_{i=1}^{\infty}\sum_{N=0}^{\infty}(-1)^i r_2(4N+1)\\
&\qquad\times\left(\frac{2N+\frac{1}{2}}{i^2}\right)^{(s-1)/2}K_{s-1}\left(2\pi i\sqrt{A(2N+\frac{1}{2})}\right).
\end{aligned}$$

On using the values $\zeta(0)=-\frac{1}{2}$, $\zeta(-2)=0$, $L_{-4}(0)=\frac{1}{2}$ and the limiting value

$$\lim_{s\to 0}\frac{1}{\Gamma(s)}=0$$

we readily obtain the result

$$L(A;0)=-1.$$

Moreover, since

$$\zeta(-2)=\zeta(-4)=\zeta(-6)=\cdots=0,$$

$$L_{-4}(-1)=L_{-4}(-3)=\zeta(-5)=\cdots=0,$$

and

$$\lim_{s\to N}\frac{1}{\Gamma(s)}=0 \quad \text{if } N=0,-1,-2,\cdots$$

it follows that

$$L(A;-1)=L(A;-2)=L(A;-3)=\cdots=0.$$

In a similar way, it can be shown using (8.E.7) that

$$L_3^{\mathrm{HCP}}(0)=-1$$

and

$$L_3^{\mathrm{HCP}}(-1)=L_3^{\mathrm{HCP}}(-2)=L_3^{\mathrm{HCP}}(-3)=\cdots=0.$$

8.7 Graphs

The formulas (8.E.14), (8.E.15), (8.E.7) and (8.E.8) have been used to produce the following graphs of $y = L_3^{\mathrm{FCC}}(s)$ on the intervals $-10 < s < 10$ and $-7 < s < 0$ in Figure 8.4. The graph of $y = L_3^{\mathrm{HCP}}(s)$ has a similar appearance, and so to allow a comparison the difference

$$y = L_3^{\mathrm{HCP}}(s) - L_3^{\mathrm{FCC}}(s)$$

is plotted using a finer vertical scale in Figure 8.5.

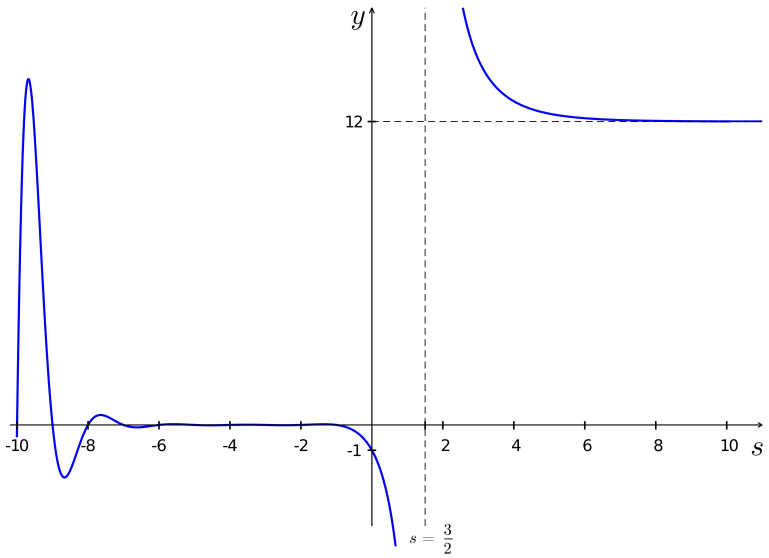

Figure 8.3 Graph of $y = L_3^{\mathrm{FCC}}(s)$ for $-10 < s < 10$.

The graphs appear to suggest the following:

Conjecture:

$$L_3^{\mathrm{HCP}}(s) > L_3^{\mathrm{FCC}}(s) > 0 \quad \text{for} \quad s \in \cdots \cup (-6,-5) \cup (-4,-3) \cup (-2,-1) \cup (3/2,\infty)$$

$$L_3^{\mathrm{HCP}}(s) < L_3^{\mathrm{FCC}}(s) < 0 \quad \text{for} \quad s \in \cdots \cup (-5,-4) \cup (-3,-2) \cup (-1,0)$$

and

$$-1 > L_3^{\mathrm{HCP}}(s) > L_3^{\mathrm{FCC}}(s) \quad \text{for} \quad s \in (0,3/2).$$

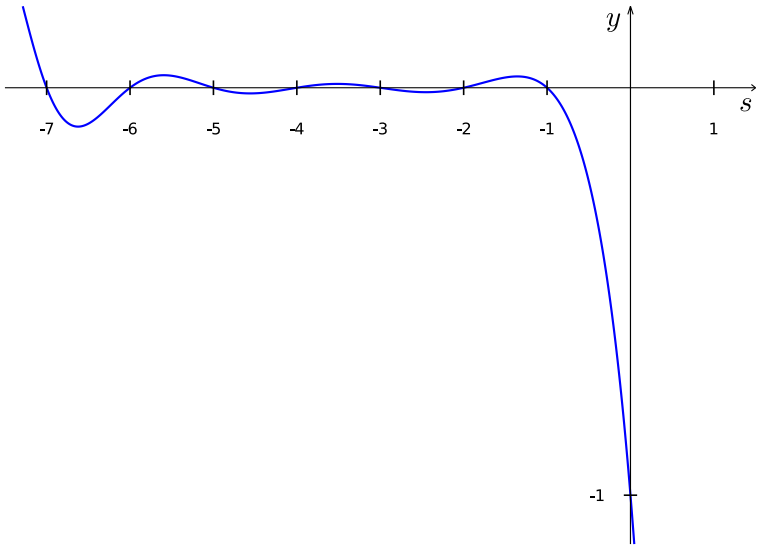

Figure 8.4 Graph of $y = L_3^{\mathrm{FCC}}(s)$ for $-7 < s < 0$.

8.8 Appendix

A Formulas for special functions

Many results for special functions and analytic number theory have been used in this work. For clarity and ease of use, they are stated here along with references.

The gamma function

The gamma function may be defined for $s > 0$ by

$$\Gamma(s) = \int_0^\infty t^{s-1} e^{-t} \, \mathrm{d}t. \tag{8.A.1}$$

By the change of variable $t = wx$ this can be rewritten in the useful form

$$\frac{1}{w^s} = \frac{1}{\Gamma(s)} \int_0^\infty x^{s-1} e^{-wx} \, \mathrm{d}x. \tag{8.A.2}$$

See [283, (1.1.18)].

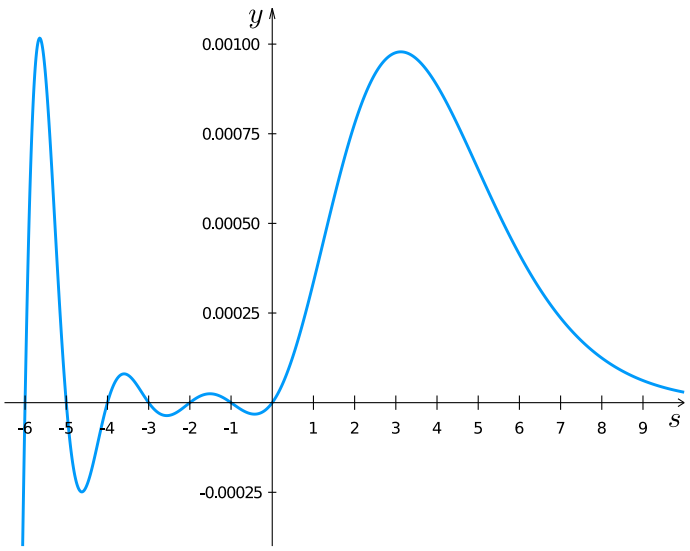

Figure 8.5 Graph of $y = L_3^{\mathrm{HCP}}(s) - L_3^{\mathrm{FCC}}(s)$.

The modified Bessel function

The following integral may be evaluated in terms of the modified Bessel function:

$$\int_0^\infty x^{s-1} e^{-ax-b/x} \mathrm{d}x = 2\left(\frac{b}{a}\right)^{s/2} K_s(2\sqrt{ab}). \tag{8.A.3}$$

By the change of variable $x = u^{-1}$ it can be shown that

$$K_s(z) = K_{-s}(z). \tag{8.A.4}$$

When $s = 1/2$ the modified Bessel function reduces to an elementary function:

$$K_{1/2}(z) = \sqrt{\frac{\pi}{2z}}\, e^{-z}. \tag{8.A.5}$$

The asymptotic formula holds:

$$K_s(z) \sim \sqrt{\frac{\pi}{2z}}\, e^{-z} \quad \text{as} \quad z \to \infty, \quad (|\arg z| < 3\pi/2). \tag{8.A.6}$$

For all of these properties, see [283, pp. 223, 237] or [110, pp. 233–248].

Characters

For an integer n, let $\chi_{-4}(n)$ and $\chi_{-3}(n)$ be defined by

$$\chi_{-4}(n) = \sin(\pi n/2) = \begin{cases} 1 & \text{if } n \equiv 1 \pmod 4, \\ -1 & \text{if } n \equiv 3 \pmod 4, \\ 0 & \text{otherwise} \end{cases} \tag{8.A.7}$$

and

$$\chi_{-3}(n) = \frac{\sin(2\pi n/3)}{\sin(2\pi/3)} = \begin{cases} 1 & \text{if } n \equiv 1 \pmod 3, \\ -1 & \text{if } n \equiv 2 \pmod 3, \\ 0 & \text{otherwise.} \end{cases} \tag{8.A.8}$$

Theta functions

The transformation formula for theta functions is [283, p. 119], [275, (2.2.5)]:

$$\sum_{n=-\infty}^{\infty} e^{-\pi n^2 t + 2\pi i n a} = \frac{1}{\sqrt{t}} \sum_{n=-\infty}^{\infty} e^{-\pi (n+a)^2/t}, \quad \text{assuming } \mathrm{Re}(t) > 0. \tag{8.A.9}$$

We will need the special cases $a = 0$ and $a = 1/2$, which are

$$\sum_{n=-\infty}^{\infty} e^{-\pi n^2 t} = \frac{1}{\sqrt{t}} \sum_{n=-\infty}^{\infty} e^{-\pi n^2/t} \tag{8.A.10}$$

and

$$\sum_{n=-\infty}^{\infty} (-1)^n e^{-\pi n^2 t} = \frac{1}{\sqrt{t}} \sum_{n=-\infty}^{\infty} e^{-\pi (n+\frac{1}{2})^2/t} \tag{8.A.11}$$

respectively. The sum of two squares formula is [78, (3.111)]

$$\left(\sum_{j=-\infty}^{\infty} q^{j^2} \right)^2 = \sum_{j=-\infty}^{\infty} \sum_{k=-\infty}^{\infty} q^{j^2+k^2} = \sum_{N=0}^{\infty} r_2(N) q^N \tag{8.A.12}$$

where

$$r_2(N) = \#\left\{ j^2 + k^2 = N \right\} = \begin{cases} 1 & \text{if } N = 0, \\ 4 \sum_{d \mid N} \chi_{-4}(d) & \text{if } N \geq 1, \end{cases} \tag{8.A.13}$$

the sum being is over the positive divisors d of N. For example,

$$\begin{aligned} r_2(18) &= 4\left(\chi_{-4}(1)+\chi_{-4}(2)+\chi_{-4}(3)+\chi_{-4}(6)+\chi_{-4}(9)+\chi_{-4}(18)\right) \\ &= 4\left(1+0-1+0+1+0\right) = 4. \end{aligned}$$

By [78, (3.15) and (3.111)] we also have

$$\left(\sum_{j=-\infty}^{\infty} q^{(j+\frac{1}{2})^2}\right)^2 = \sum_{N=0}^{\infty} r_2(4N+1)q^{(4N+1)/2}. \tag{8.A.14}$$

B The cubic theta function

The cubic analogues of the transformation formula are [275, (2.2)], [284, Cor. 5.19]

$$\sum_{j=-\infty}^{\infty}\sum_{k=-\infty}^{\infty} e^{-2\pi(j^2+jk+k^2)t} = \frac{1}{\sqrt{3}}\sum_{j=-\infty}^{\infty}\sum_{k=-\infty}^{\infty} e^{-2\pi(j^2+jk+k^2)/3t} \tag{8.B.15}$$

and

$$\begin{aligned} &\sum_{j=-\infty}^{\infty}\sum_{k=-\infty}^{\infty} e^{-2\pi((j+\frac{1}{3})^2+(j+\frac{1}{3})(k+\frac{1}{3})+(k+\frac{1}{3})^2)t} \\ &\qquad = \frac{1}{\sqrt{3}}\sum_{j=-\infty}^{\infty}\sum_{k=-\infty}^{\infty} \omega^{j-k} e^{-2\pi(j^2+jk+k^2)/3t} \end{aligned} \tag{8.B.16}$$

where $\omega = \exp(2\pi i/3)$ is a primitive cube root of unity. The analogue of the sum of two squares result is [78, (3.124)]

$$\sum_{j=-\infty}^{\infty}\sum_{k=-\infty}^{\infty} q^{j^2+jk+k^2} = \sum_{N=0}^{\infty} u_2(N)q^N \tag{8.B.17}$$

where

$$u_2(N) = \#\left\{j^2+jk+k^2 = N\right\} = \begin{cases} 1 & \text{if } N=0, \\ 6\displaystyle\sum_{d|N}\chi_{-3}(d) & \text{if } N\geq 1, \end{cases} \tag{8.B.18}$$

where the sum is again over the positive divisors d of N. By [78, (3.18) and (3.124)] we also have

$$\sum_{j=-\infty}^{\infty}\sum_{k=-\infty}^{\infty} q^{(j+\frac{1}{3})^2+(j+\frac{1}{3})(k+\frac{1}{3})+(k+\frac{1}{3})^2} = \frac{1}{2}\sum_{N=0}^{\infty} u_2(3N+1)q^{N+\frac{1}{3}} \tag{8.B.19}$$

which is the analogue of (8.A.14).

The Riemann zeta function and L functions

The definitions are:

$$\zeta(s) = \sum_{j=1}^{\infty} \frac{1}{j^s} \tag{8.B.20}$$

$$L_{-4}(s) = \sum_{j=1}^{\infty} \frac{\chi_{-4}(j)}{j^s} = 1 - \frac{1}{3^s} + \frac{1}{5^s} - \frac{1}{7^s} + \cdots . \tag{8.B.21}$$

$$L_{-3}(s) = \sum_{j=1}^{\infty} \frac{\chi_{-3}(j)}{j^s} = 1 - \frac{1}{2^s} + \frac{1}{4^s} - \frac{1}{5^s} + \frac{1}{7^s} - \frac{1}{8^s} + \cdots . \tag{8.B.22}$$

The function $\zeta(s)$ is the Riemann zeta function. It has a pole of order 1 at $s = 1$, and in fact

$$\lim_{s\to 1}(s-1)\zeta(s) = 1. \tag{8.B.23}$$

This is a consequence of [283, (1.3.2)]. See also [110, p. 58].
We will require the functional equations

$$\pi^{-s/2}\Gamma(s/2)\zeta(s) = \pi^{-(1-s)/2}\Gamma((1-s)/2)\zeta(1-s) \tag{8.B.24}$$

and

$$\pi^{-s}\Gamma(s)\,\zeta(s)L_{-4}(s) = \pi^{-(1-s)}\Gamma(1-s)\,\zeta(1-s)L_{-4}(1-s) \tag{8.B.25}$$

and the special values

$$\begin{aligned} \zeta(2) = \frac{\pi^2}{6}, \quad \zeta(0) = -\frac{1}{2}, \quad \zeta(-1) = -\frac{1}{12}, \\ \zeta(-2) = \zeta(-4) = \zeta(-6) = \cdots = 0, \end{aligned} \tag{8.B.26}$$

$$L_{-4}(1) = \frac{\pi}{4}, \quad L_{-4}(0) = \frac{1}{2}, \quad L_{-4}(-1) = L_{-4}(-3) = L_{-4}(-5) = \cdots = 0, \tag{8.B.27}$$

and

$$L_{-3}(1) = \frac{\pi\sqrt{3}}{9}, \quad L_{-3}(0) = \frac{1}{3}, \quad L_{-3}(-1) = L_{-3}(-3) = L_{-3}(-5) = \cdots = 0. \tag{8.B.28}$$

See [285, Ch. 12] or [286]. Other results used are

$$\sum_{j=0}^{\infty} \frac{1}{(j+\frac{1}{2})^s} = (2^s-1)\zeta(s) \tag{8.B.29}$$

$$\sum_{j=1}^{\infty} \frac{(-1)^j}{j^s} = -(1-2^{1-s})\zeta(s) \tag{8.B.30}$$

$$\sum_{j,k}{}' \frac{1}{(j^2+k^2)^s} = 4\zeta(s)L_{-4}(s) \tag{8.B.31}$$

$$\sum_{j,k}{}' \frac{(-1)^{j+k}}{(j^2+k^2)^s} = -4(1-2^{1-s})\zeta(s)L_{-4}(s). \tag{8.B.32}$$

$$\sum_{i,j}{}' \frac{1}{(i^2+ij+j^2)^s} = 6\zeta(s)L_{-3}(s) \tag{8.B.33}$$

$$\sum_{i,j} \frac{1}{((i+\frac{1}{3})^2+(i+\frac{1}{3})(j+\frac{1}{3})+(j+\frac{1}{3})^2)^s} = 3(3^s-1)\zeta(s)L_{-3}(s). \tag{8.B.34}$$

The identities (12.A.23) and (8.B.30) follow from the definition of $\zeta(s)$ by series rearrangements. For (8.B.31), (8.B.32) and (12.A.24), see (1.4.14), (1.7.5) and (1.4.16), respectively, of [1]. The identity (B.0.15) can be obtained by the method of Mellin transforms, e.g., see [58, Appendix A], starting with [78, (3.36)].

C Behaviour as $A \to 0^+$ and $A \to +\infty$

We briefly consider the behaviour of the lattices in the limiting cases $A \to 0^+$ and $A \to +\infty$. Some of the basis vectors become infinite in the limit, leaving a sublattice of lower dimension. We discuss each case $A \to 0^+$ and $A \to +\infty$ both in terms of theta functions and then in terms of the basis vectors.

First, consider the limit $A \to 0^+$. In the interval $0 < A < 1/3$ the theta function is

$$\begin{aligned}\theta(A;q) &= \sum_{i=-\infty}^{\infty}\sum_{j=-\infty}^{\infty}\sum_{k=-\infty}^{\infty} q^{g(A;i,j,k)} \\ &= \sum_{i=-\infty}^{\infty}\sum_{j=-\infty}^{\infty}\sum_{k=-\infty}^{\infty} q^{(A(i+j)^2+(j+k)^2+(i+k)^2)/4A}.\end{aligned}$$

As $A \to 0^+$ we have

$$q^{(j+k)^2/4A} \to 0 \quad \text{and} \quad q^{(i+k)^2/4A} \to 0$$

unless $j=-k$ and $i=-k$, respectively. Hence,

$$\begin{aligned}\lim_{A\to 0^+}\theta(A;q) &= \lim_{A\to 0^+}\sum_{k=-\infty}^{\infty}\left(\sum_{i=-k}\sum_{j=-k} q^{(A(i+j)^2+(j+k)^2+(i+k)^2)/4A}\right)\\ &= \lim_{A\to 0^+}\sum_{k=-\infty}^{\infty} q^{A(-k-k)^2/4A}\\ &= \sum_{k=-\infty}^{\infty} q^{k^2}.\end{aligned}$$

This corresponds to the one-dimensional lattice with minimal distance 1. The kissing number is 2, which is in agreement with the other lattices in the range $0<A<1/3$, as indicated in Table 8.1. In terms of the basis vectors, from (8..1) we have

$$b_1=\left(\frac{1}{2},\frac{1}{2\sqrt{A}},0\right)^\top, b_2=\left(\frac{1}{2},0,\frac{1}{2\sqrt{A}}\right)^\top, b_3=\left(0,\frac{1}{2\sqrt{A}},\frac{1}{2\sqrt{A}}\right)^\top.$$

The only linear combinations $v=ib_1+jb_2+kb_3$ (for $i,j,k\in\mathbf{Z}$) that remain finite in the limit $A\to 0^+$ occur when $i=-k$, $j=-k$ in which case we obtain

$$v=-kb_1-kb_2+kb_3=-k(1,0,0)^\top.$$

That is, the limiting lattice is just the one-dimensional lattice consisting of integer multiples of $(1,0,0)^\top$.
Now consider the limit $A\to+\infty$. For $A>1$ the theta function is

$$\begin{aligned}\theta(A;q) &= \sum_{i=-\infty}^{\infty}\sum_{j=-\infty}^{\infty}\sum_{k=-\infty}^{\infty} q^{g(A;i,j,k)}\\ &= \sum_{i=-\infty}^{\infty}\sum_{j=-\infty}^{\infty}\sum_{k=-\infty}^{\infty} q^{(A(i+j)^2+(j+k)^2+(i+k)^2)/2}.\end{aligned}$$

Since $q^{A(i+j)^2/2}\to 0$ as $A\to+\infty$ unless $i=-j$, it follows that

$$\begin{aligned}\lim_{A\to+\infty}\theta(A;q) &= \sum_{j=-\infty}^{\infty}\sum_{k=-\infty}^{\infty}\left(\sum_{i=-j} q^{(A(i+j)^2+(j+k)^2+(i+k)^2)/2}\right)\\ &= \sum_{j=-\infty}^{\infty}\sum_{k=-\infty}^{\infty} q^{((j+k)^2+(-j+k)^2)/2}\\ &= \sum_{j=-\infty}^{\infty}\sum_{k=-\infty}^{\infty} q^{j^2+k^2}.\end{aligned}$$

This is the theta series for the two-dimensional square close packing lattice

with minimal distance 1. The kissing number is 4, in agreement with other values in the range $A > 1$ given by Table 8.1. In terms of the basis vectors, from (8..1) we have

$$b_1 = \frac{1}{\sqrt{2}}(\sqrt{A},1,0)^\top, \quad b_2 = \frac{1}{\sqrt{2}}(\sqrt{A},0,1)^\top, \quad b_3 = \frac{1}{\sqrt{2}}(0,1,1)^\top.$$

The only linear combinations $v = ib_1 + jb_2 + kb_3$ (for $i, j, k \in \mathbf{Z}$) that remain finite in the limit $A \to +\infty$ occur when $i = -j$, in which case we obtain

$$v = -jb_1 + jb_2 + kb_3 = \frac{1}{\sqrt{2}}\left[j(0,-1,1)^\top + k(0,1,1)^\top\right].$$

This is isomorphic to the two-dimensional square close packing lattice with minimal distance 1, rotated from the coordinate axes by 45 degrees.

9 Project 4 results - Instability of the Body-Centered Cubic Lattice within the Sticky Hard Sphere and Lennard-Jones Model obtained from Exact Lattice Summations[a]

9.1 Introduction

The stability of different bulk phases and their possible connections through distortions and rearrangements in phase transitions remain an open and challenging field in solid-state physics [288]. Solid-to-solid phase transitions are commonly modeled by computer intensive molecular dynamic or Monte-Carlo simulations at finite temperatures and pressures [289, 290], or by various algorithms to find phase transition paths on a Born-Oppenheimer hypersurface [291]. For example, the relative stability of the fcc versus the hexagonal close packing (hcp) and possible transition mechanisms between these two phases for the rare gas elements has been a matter of a long-standing controversy [5, 51, 246, 292–296]. While fcc has a higher excess entropy compared to hcp by a rather small difference (for the hard sphere model it is 0.00115 ± 0.00004 k_B per sphere [292]), the energetic stability of the fcc over the hcp phase for the rare gas solid argon (at low temperatures and pressures) is due to quantum effects (phonon dispersion) [51, 295]. Similarly, the transformation between the bcc$\leftrightarrow$fcc phases and their relative stabilities have been the subject of many discussions [297, 298] as the exact martensitic type of transformation path for a solid, such as in iron-based materials, or in clusters, is still being debated [299–302].

It is commonly believed that strong repulsive forces favor close-packed arrangements such as fcc or hcp, whereas soft repulsion favors less dense packed

[a]This chapter is composed of sections previously published in the article "Instability of the body-centered cubic lattice within the sticky hard sphere and Lennard-Jones model obtained from exact lattice summations"[287] and is reprinted by permission from the publisher ©2022 American Physical Society. Some sections may have been modified to fit the style of this thesis.

structures such as bcc [303–306]. Laird showed that the bcc phase is unstable within the hard-sphere model [307], while Hoover et al. and later Agrawi and Kofke showed that soft repulsive potentials of the form ar^{-n} with small n values are required to stabilize the bcc phase [303, 308]. Very recently Ono and Ito used phonon dispersion curves to show that soft Lennard-Jones (LJ) forces are required to turn the bcc phase into a minimum [309]. However, as minima can be very shallow on an energy hypersurface, one requires accurate numerical or analytical methods to determine if the bcc phase represents a (metastable) minimum for a two-body potential or not. Moreover, the bcc phase was absent in recent LJ lattice dynamic simulations of Travesset [293]. Inverse power law potentials such as the LJ potential have the advantage that properties such as the cohesive energy can be evaluated analytically through lattice sums [26, 160]. If a single path through a lattice parameter can be found [291] describing smoothly the bcc↔fcc transition (not necessarily a minimum energy path), one gains valuable insight into the stability of the bcc phase.
Conway and Sloane introduced the isodual mean-centered cuboidal lattice (mcc) which can be seen as an average between the bcc and the fcc lattice [310]. They introduced lattice vectors depending on two parameters connecting the bcc, mcc and fcc lattices. Recently we were able to find fast converging lattice sums for these cuboidal lattices derived from their corresponding Gram matrices and quadratic forms using a single parameter [311]. These lattice sums, which can be evaluated to computer precision, will be introduced in the next section and applied to analyse the energy profile of the bcc lattice distortion into the fcc densest packing using LJ and SHS interaction potentials. For more realistic two-body forces we apply extended LJ potentials (ELJ) [48, 296] for Ar_2 and Cr_2, and briefly discuss Li_2.

9.2 Method

Lattice vectors for the unit cell of a cuboidal lattice depending on a single parameter A are defined by

$$\vec{b}_1^{\top}(A) = (1,0,0) \quad , \quad \vec{b}_2^{\top}(A) = \left(\frac{A}{A+1}, \frac{\sqrt{2A+1}}{A+1}, 0\right), \tag{9.2.1}$$
$$\vec{b}_3^{\top}(A) = \left(\frac{1}{A+1}, \frac{1}{(A+1)\sqrt{2A+1}}, \sqrt{\frac{4A}{(A+1)(2A+1)}}\right).$$

The corresponding Gram matrix for the quadratic form is given by the scalar product between these lattice vectors,

$$G_{ij}(A) = \langle \vec{b}_i(A), \vec{b}_j(A) \rangle = \frac{1}{A+1} \begin{pmatrix} A+1 & A & 1 \\ A & A+1 & 1 \\ 1 & 1 & 2 \end{pmatrix}. \tag{9.2.2}$$

The cuboidal lattices are defined in the range $A \in [\frac{1}{3}, 1]$ [311], and for the special values of $A = \frac{1}{3}$, $A = \frac{1}{2}$, $A = \frac{1}{\sqrt{2}}$, and $A = 1$ lattice vectors for the acc (axial centered cuboidal [310]), bcc, mcc and fcc lattices are obtained, with number of nearest neighbors of 10, 8, 8 and 12 respectively. This sets the minimal distance between two lattice points to 1 for the range $A \in [\frac{1}{3}, 1]$, which ensures that the lattice deformation is compatible with the hard sphere model. The volume spanned by these three vectors is

$$V(A) = \sqrt{\det G(A)} = 2A^{1/2}(A+1)^{-3/2} \tag{9.2.3}$$

with a maximum volume at the bcc structure ($A = \frac{1}{2}$). The lattices with the corresponding lattice vectors (12.7.1) are shown in Figure 9.1.

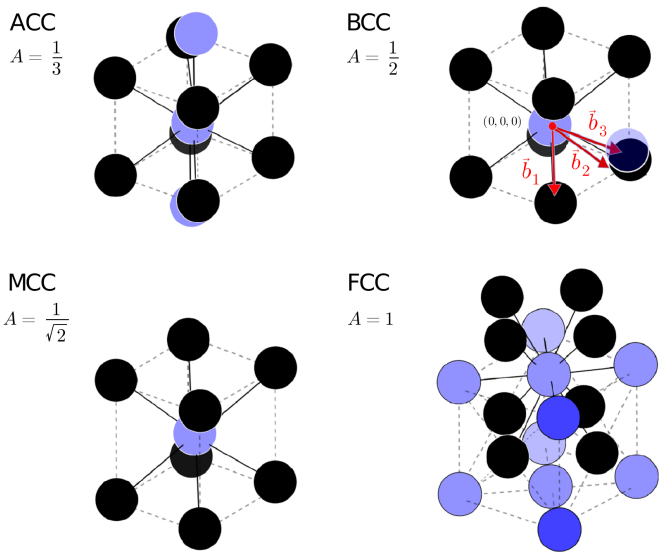

Figure 9.1 The four lattices acc, bcc, mcc and fcc along the cuboidal transition path. The corresponding primitive cell basis vectors according to Eq.(12.7.1) are shown for the bcc lattice. For the fcc lattice the lighter colored atoms moving towards the central atom (0,0,0) become nearest neighbors, with the overall cuboidal fcc structure displayed.

The choice of the basis vectors (12.7.1) has the advantage that only $\vec{b}_2$ and $\vec{b}_3$ move in this 3D lattice transformation. The length of $\vec{b}_1$ and $\vec{b}_2$ is 1 for all A values considered, and the angle between $\vec{b}_1$ and $\vec{b}_3$ is the same as between $\vec{b}_2$ and $\vec{b}_3$. From the Gram matrix one obtains the atomic packing fraction or packing density [161] for the cuboidal lattices, [311]

$$\rho(A) = \frac{\pi}{12}\sqrt{\frac{(A+1)^3}{A}} \,. \tag{9.2.4}$$

This yields the well known values for fcc ($\rho(1) = \frac{\pi\sqrt{2}}{6}$) and bcc ($\rho(\frac{1}{2}) = \frac{\pi\sqrt{3}}{8}$). In fact, from this formula we deduce that bcc is the least packed arrangement of all the cuboidal lattices considered here.

Using an (a,b) LJ potential in its most general form [3, 6]

$$V_{\mathrm{LJ}}(r,a,b) = \frac{ab}{a-b}\varepsilon\left[\frac{1}{a}\left(\frac{r_e}{r}\right)^a - \frac{1}{b}\left(\frac{r_e}{r}\right)^b\right], \tag{9.2.5}$$

where r_e is the minimum (equilibrium) distance, $\varepsilon > 0$ is the dissociation energy and $a > b > 3$ are real numbers, we obtain an analytical expression for the cohesive energy in terms of lattice sums $L(a,A)$ and the nearest neighbor distance R in the lattice [160],

$$E_{\mathrm{LJ}}(R,a,b,A) = \frac{ab\varepsilon}{2(a-b)}\left[\frac{1}{a}L(a,A)\left(\frac{r_e}{R}\right)^a - \frac{1}{b}L(b,A)\left(\frac{r_e}{R}\right)^b\right]. \tag{9.2.6}$$

Here, $b > 3$ is required to avoid the singularity in $L(b,A)$ at $b = 3$ [48] (although these lattice sums can be analytically continued [26, 63, 311]). The lattice sums $L(a,A)$ are defined through their corresponding quadratic forms $\vec{i}^{\top} G\vec{i}$, $\vec{i} \in \mathbb{Z}^3$ by [161]

$$L(a,A) = \sum_{\vec{i}\in\mathbb{Z}^3}{}' \left(\frac{1}{\vec{i}^{\top} G\vec{i}}\right)^{a/2} = \sum_{i,j,k}{}' \left(\frac{A+1}{A(i+j)^2+(j+k)^2+(i+k)^2}\right)^{a/2}, \tag{9.2.7}$$

where the prime symbol indicates that the term corresponding to $\vec{i}^{\top} = (0,0,0)$ is omitted in the summation. For small values of a, these triple sums are slowly convergent and one needs to find expansions in terms of fast converging series to obtain computer precision [26]. A number of methods to achieve this have recently been introduced by our group [160, 311]. A program to evaluate these lattice sums including the cuboidal lattices considered here is freely available from our website [143]. For this work we use either the Terras decomposition of the Epstein zeta function [112, 160] or the decomposition in terms of Jacobi θ functions and integral transforms to produce series expansions in terms of Bessel functions [160, 311]. More details are given in Appendix 9.A.

The SHS model can easily be obtained in the limit of $a \to \infty$ of the LJ potential [250], and the cohesive energy given by the expression

$$E_{\mathrm{SHS}}(R,b,A) = \lim_{a\to\infty} E_{\mathrm{LJ}}(R,a,b,A) = -\frac{\varepsilon}{2}L(b,A)\left(\frac{r_e}{R}\right)^b, \tag{9.2.8}$$

with $R \geq r_e$. This gives a direct relation between the SHS energy of the solid and the corresponding lattice sum.

It is convenient to introduce dimensionless units, i.e., $R^* = R/r_e$ and $E^* = E/\varepsilon$. The minimum nearest neighbor distance for a cuboidal lattice can be found

from (10.2.5),

$$R^*_{\min}(a,b,A) = \left[\frac{L(a,A)}{L(b,A)}\right]^{\frac{1}{a-b}}. \tag{9.2.9}$$

For the SHS model this reduces to $R^*_{\min} = 1$. The cohesive energy at minimum becomes

$$E^*(R^*_{\min},a,b,A) = -\frac{1}{2}\left[\frac{L(b,A)^a}{L(a,A)^b}\right]^{\frac{1}{a-b}}, \tag{9.2.10}$$

and for the SHS model we attain $E^*(R^*_{\min} = 1;b,A) = -L(b,A)/2$. Finally, a more realistic two-body potential is used, where lattice sum techniques can still be applied. This requirement is fulfilled by the ELJ potential, which is an inverse power series expansion in terms of the distance R,

$$E_{\mathrm{ELJ}}(R,c_n,A) = \frac{1}{2}\sum_{n=1}^{n_{\max}} c_n L(a_n,A) R^{-a_n}, \tag{9.2.11}$$

with $\sum_n c_n = -\varepsilon$ and $a_n > 3$ [48, 296].

9.3 Results and Discussion

Starting with the discussion of the SHS model, the difference in cohesive energies between the A-dependent cuboidal lattices and the fcc lattice ($A = 1$) as a function of the two parameters b and A,

$$\Delta E^*(b,A) = \frac{1}{2}\left[L(b,A=1) - L(b,A)\right] \tag{9.3.1}$$

at $R^*_{\min} = 1.0$, is shown in Figure 9.2. It is evident that the SHS model predicts a maximum in energy at the bcc structure. In fact, it was proved recently that $\partial L(b,A)/\partial A = 0$ and $\partial^2 L(b,A)/\partial A^2 > 0$ at $A = \frac{1}{2}$ (bcc) for all $b \in (3,\infty)$ [311]. The path chosen along the A parameter may not represent the true minimum energy path for the bcc→fcc phase transition, but what matters here is that it is clearly downhill energetically towards the fcc structure. As a result, the bcc lattice is unstable with respect to distortion to fcc within the SHS model. There is also the opposite path towards the acc crystal ($A = \frac{1}{3}$), which has to our knowledge not been observed in nature. Figure 9.2 shows that for low b values, $\Delta E^*(b,A)$ starts to increase again (at lower exponents $\Delta E^*(b,A) \to \infty$ for $b \to 3$). The most stable bcc lattice is observed at $\Delta E^*(b = 5.49363406\ldots,\frac{1}{2}) = 1.090510595\ldots$, with a b value close to the exponent $b = 6$ used for dispersive type of forces [19].

As the SHS model clearly has its limitations, we turn to the more accurate

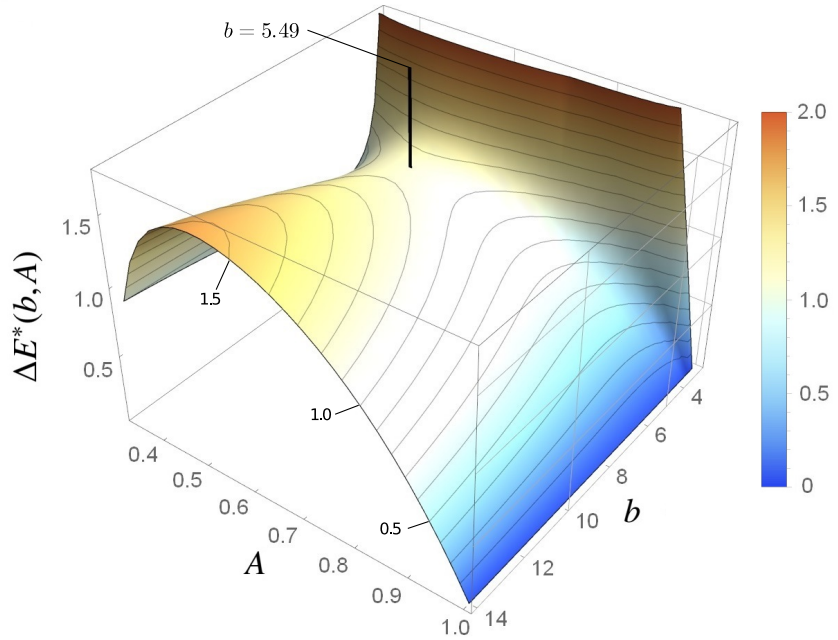

Figure 9.2 Difference in cohesive energies $\Delta E^*(b,A) = \frac{1}{2}(L(b,A=1)-L(b,A))$ between the cuboidal lattices and fcc for various exponents b and lattice parameter A of the SHS model. Contour interval chosen is 0.1. The vertical black line at $b = 5.493634$ shows the point of least instability for the bcc lattice.

(a,b) LJ potential, i.e., we introduce softer repulsive walls into the SHS model. This will also remove the discontinuity in the $\Delta E^*(a,b,A)$ curve at the fcc point ($A = 1$). Due to the attractive long-range lattice forces, the minimum distance between two neighboring lattice points in Eq.(9.2.9) is $R^*_{\min}(a,b,A) < 1$, provided that $a > b > 3$ for a finite (a,b) combination. Figure 9.3 shows that $R^*_{\min}(a,b,A)$ does not vary much with changing A for a fixed (a,b) combination. The minimum distance for the (12,6) LJ potential is $R^*_{\min}(12,6,\frac{1}{2})$=0.951864819 for the bcc lattice compared to $R^*_{\min}(12,6,1.0)$=0.9712336910 for fcc. For large a values the minimum bcc nearest neighbor distance $R^*_{\min}$ turns into a very shallow maximum and finally approaches the SHS limit of $R^*_{\min}$ =1.0. From Eq.(9.2.9) and $\partial L(b,A)/\partial A$=0 at $A = \frac{1}{2}$ [311] it follows that $\partial R^*_{\min}(a,b,A)/\partial A = 0$ at $A = \frac{1}{2}$, and the bcc point remains a critical point for all (a,b) values in the allowed range.

Shorter distances are usually associated with greater stability of the lattice. This is however not the case for the bcc compared to the fcc lattice as Figure 9.4 shows. In fact, the bcc lattice is *not* a stable lattice compared to fcc, i.e.

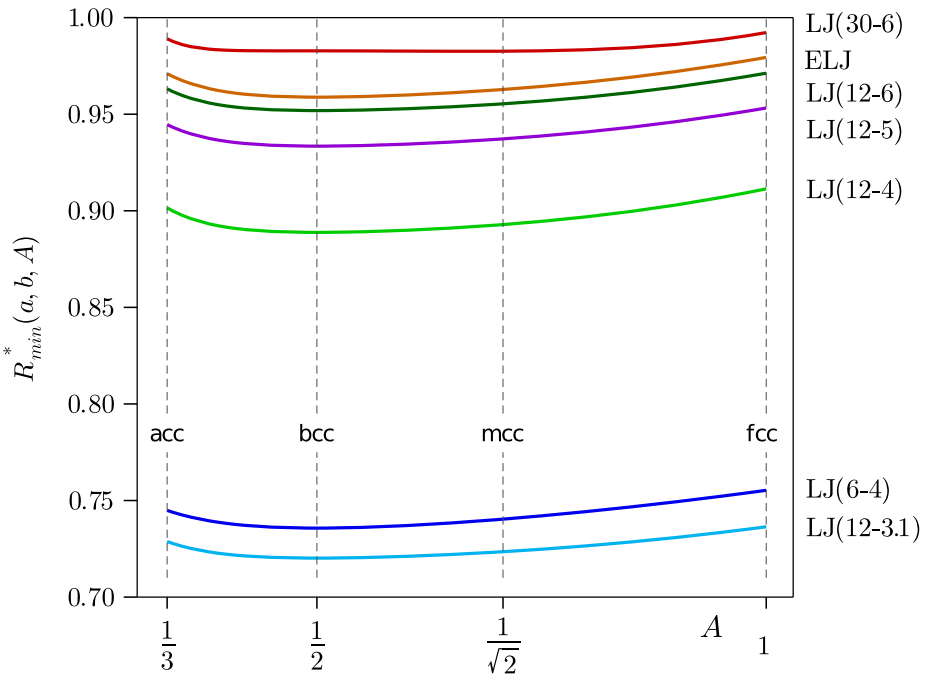

Figure 9.3 Minimum distance $R^*_{\rm min}(a,b,A)$ for various (a,b) LJ potentials and for the ELJ potential for argon (taken from Ref.[51]) dependent on the lattice parameter A.

$\Delta E^*_{\rm bcc,fcc}(a,b) = E^*(R^*_{\rm min,bcc},a,b,\frac{1}{2}) - E^*(R^*_{\rm min,fcc},a,b,1) > 0$ for all $a > b > 3$. The bcc lattice will continuously distort by lowering the energy toward the most densely packed fcc lattice, except for a very small (a,b) range where the bcc phase becomes metastable. In this case, the minimum at $A < \frac{1}{2}$ shifts toward the bcc structure, see Figure 9.5.

The (a,b) phase transition line from the unstable to the metastable bcc lattice is approximately described by the polynomial $a_{\rm PT} = -6.3829845 \times 10^{-4} b_{\rm PT}^3 + 3.8186745 \times 10^{-2} b_{\rm PT}^2 - 1.3466248 b_{\rm PT} + 1.1373783 \times 10^1$ with $a_{\rm PT} > b_{\rm PT} \in (3, 5.25673]$ (see Appendix 9.B), and we see an almost linear behavior as shown as a yellow line in the left lower corner of Figure 9.5. This also explains why Ono and Ito obtained imaginary phonon frequencies for some low (a,b) combinations [309] (their results have to be taken with some care as the r^{-3} potential used leads to a singularity in the cohesive energy). In fact, the bcc structure becomes metastable if and only if $L(a,A)\partial^2 L(a,A)/\partial A^2 < L(b,A)\partial^2 L(b,A)/\partial A^2$ for $A = \frac{1}{2}$ and $a > b > 3$ (see Appendix 9..B). However, these minima appear at energies $\Delta E^*_{\rm bcc,fcc}(a,b) > 0.2$ ($a < 7.660388$) for rather unphysical potentials, with low ΔE^* values only if $a \approx b$. As an example, for a (4,3.1) LJ potential the bcc

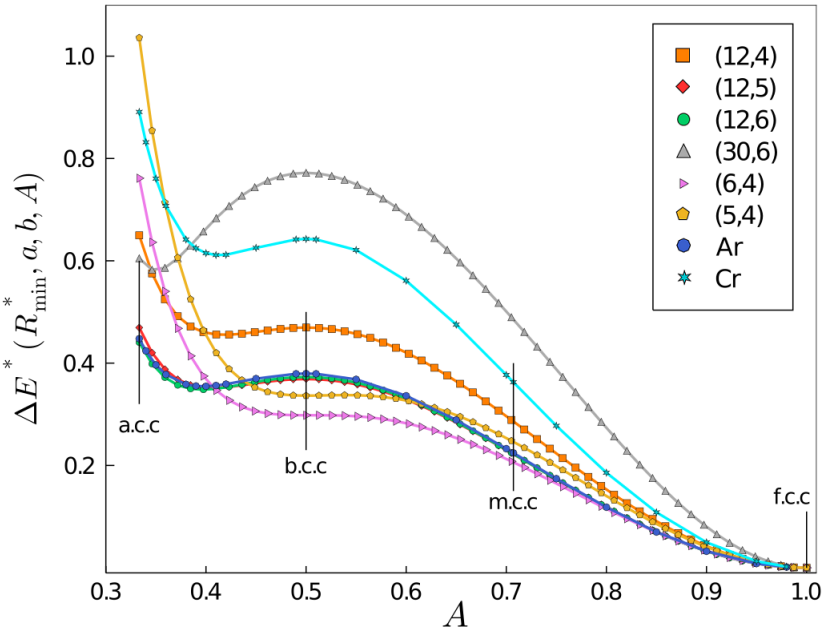

Figure 9.4 Cohesive energy differences $\Delta E^*(R^*_{\min},a,b,A) = E^*(R^*_{\min},a,b,A) - E^*(R^*_{\min},a,b;A=1)$ for the (a,b) LJ potential dependent on the lattice parameter A, and for the two ELJ potentials of argon and chromium (see appendix 9.C).

structure is a minimum at $\Delta E^*_{\text{bcc,fcc}} = 170.2$ with an activation barrier of $\Delta E^{*\#} = 12.2$ situated at $A = 0.6$ on the path toward the distortion to the fcc structure. As $\partial L(b,A)/\partial A = 0$ at $A = \frac{1}{2}$ [311] we obtain $\partial E^*(R^*_{\min},a,b,A)/\partial A = 0$ at $A = \frac{1}{2}$ (see appendix 9.B), and the bcc structure remains a critical point for all (a,b) combinations. Moreover, if the exponent a responsible for the repulsive wall increases, we approach the limit of the SHS potential with much higher energies compared to the LJ potential.

By applying an inverse power law potential for the repulsive wall (opposed to the long-range part in the SHS model) in Monte Carlo simulations, Agrawal and Kofke also showed that the bcc phase is unstable [303]. An interesting point of this bcc→fcc phase transition is that the Einstein frequency ω_E, obtained analytically in terms of lattice sums from a single atom moving in the field of all other atoms [296], remains positive, $\omega_E(a,b,A) > 0$, for all $A \in [\frac{1}{3},1]$ and $a > b > 3$ (see Appendix 9.C). As a consequence, a single atom is locked and more than one atom has to move simultaneously along the bcc→fcc path similar to a Zener or Bain martensitic transformation [301, 312]. As Figure 9.4 shows, the distortion along the A parameter away from bcc can also occur towards a metastable lattice with $A < \frac{1}{2}$ and higher packing

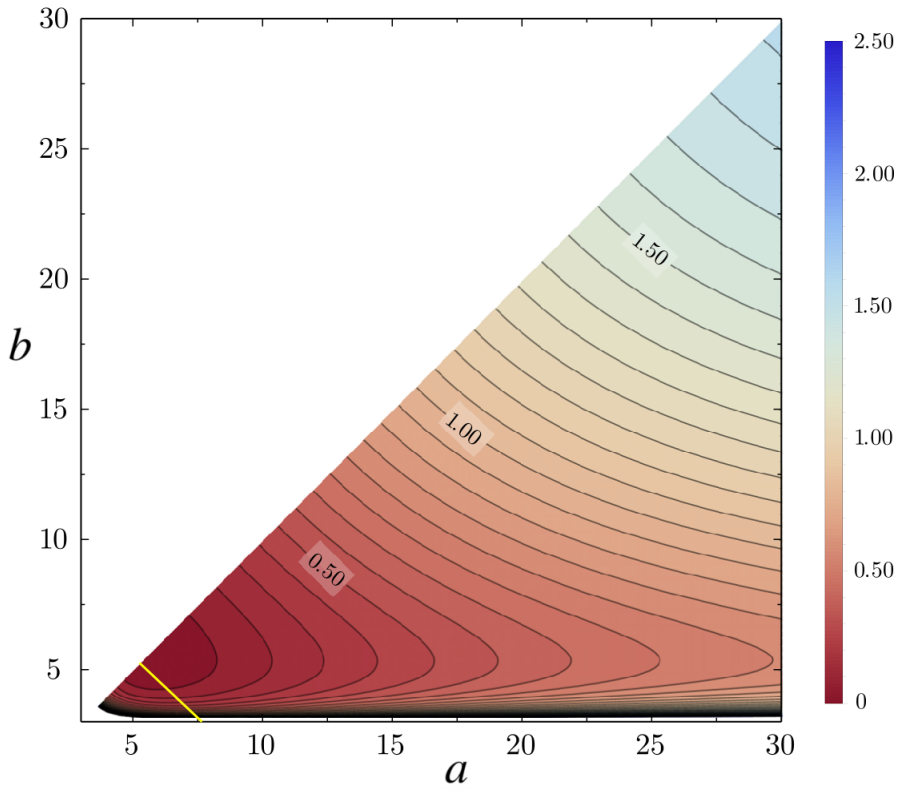

Figure 9.5 Energy difference $\Delta E^*_{\mathrm{bcc,fcc}}(a,b) = E^*(R^*_{\mathrm{min,bcc}},a,b,\frac{1}{2}) - E^*(R^*_{\mathrm{min,fcc}},a,b,1)$ between the bcc and fcc lattice for the (a,b) LJ potential. Contour interval chosen is 0.0625. The almost linear (yellow) curve in the lower left corner of the plot describes the phase transition line to a metastable bcc state.

density. Using a (12,6) LJ potential the metastable minimum sits at a lattice with $A = 0.3962483\ldots$ and packing density $\rho = 0.6861655\ldots$, a cuboidal lattice in-between bcc and acc. Finally, the mcc lattice is just a lattice along the energetic downward path towards fcc as it is for the SHS model.

The question remains as to why low temperature bcc lattices are observed in nature given their instability, large volume and small bulk modulus within the cuboidal structures. It is clear that two-body forces favor dense packings with the largest kissing number for an atom, that is fcc or hcp. The answer therefore lies in the failure of the two-body potential to correctly describe the interactions in the crystal, i.e., neglecting important higher than two-body interactions (and perhaps quantum effects for quantum solids such as helium). It is well known that the many-body expansion is only slowly convergent for metallic systems [55, 313]. due to higher than two-body forces.

To see if the form of the LJ potential limits our conclusion, a more accurate ELJ two-body potential is taken, derived from relativistic coupled cluster theory for argon [51, 314]. As in the case for the (12,6) LJ potential, the ELJ potential has a minimum $R^*_{\min}(A)$ value at the bcc structure (see Appendix 9.D). More importantly, the $E^*_{\mathrm{ELJ}}(A)$ curve does not change substantially in shape and is only slightly shifted compared to the (12,6) LJ potential, as shown in Figure 9.4. This is perhaps expected from the comparison between the two potentials, and from the fact that for the fcc structure $E^*(R^*_{\min}, 1.0) = 7.8532$ [296] for the ELJ potential and close to $E^*(R^*_{\min}, 12, 6, 1.0) = -L_6^2/(2L_{12}) = 8.6102$ for the (12,6) LJ potential (exp. $E^* = 6.4951$ using the data from Ref.[179]).

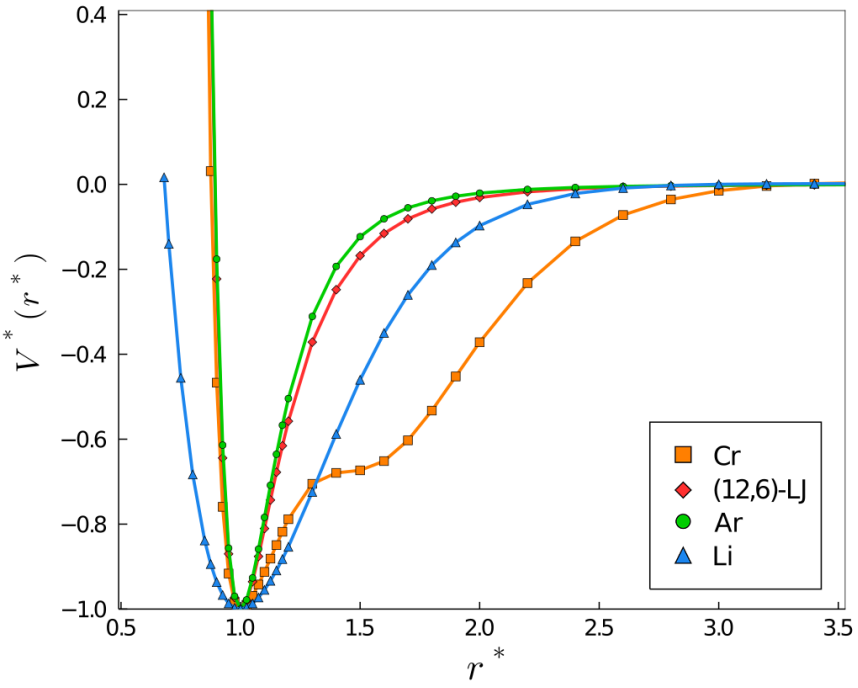

Figure 9.6 Potential energy curves $V^*(r^*)$ (in dimensionless units) for a (12-6) LJ potential, and for Ar_2, Li_2 and Cr_2 (see Appendix 9.C).

To underscore our argument even further the unusual potential energy curve for Cr_2 is considered. Here we use experimental potential values of Casey and Leopold [315], but attenuated for the long range dispersion using the C_6 coefficient of Roos and co-workers [316], and finally fitted to an extended Lennard Jones potential potential (see Appendix 9.D). This potential curve, shown in Figure 9.6, is extremely broad and has a large dip in the medium distance range $r \in [1.3, 1.7]r_e$, and therefore deviates substantially from a

typical potential energy curve such as LJ or Morse [317]. As it turns out, this potential leads to far too small distances and far too large cohesive energies for the solid state. However, the chromium $\Delta E^*(R^*_{\min}, a, b, A)$ curve in Figure 9.4 shows that bcc remains a transition state along the distortion parameter A in line with all the other two-body potentials.

We also looked at lithium, which adopts a bcc structure at normal conditions. Lithium has an extremely broad potential energy curve (see Figure 9.6) even in the repulsive region [318], which leads surprisingly to a collapse of the crystal to a very small nearest neighbor distance (see Appendix 9.D). It is clear that N-body forces describing correctly the confinement of the atoms in the solid state become very important here, i.e., the N-body expansion is not converging smoothly with increasing N for metals such as lithium or chromium [55]. One may argue that a broad potential energy curve such as for Li_2 gives lower exponents for a LJ potential energy curves typical for metallic systems. It should be pointed out however, that the long range has to be correctly described and potential curves containing terms of $r^{-n}, n \leq 3$ in the interaction between atoms in the solid lead to divergent series (if not analytically continued). Moreover, the correct description for the cuboidal transformation for lithium,[302] for example by ab-initio or density functional theory, requires the inclusion of vibrational and thermal effects, which is currently a subject of our investigating.

9.4 Conclusion

From exact lattice summations we were able to derive cohesive energies within the SHS and LJ models analytically, and compute them as Bessel function expansions to computer precision. Both potentials result in an unstable bcc phase distorting toward the fcc phase or toward a phase in-between acc and bcc. The metastable bcc phase for an (a,b) LJ potential occurs for unphysical potentials with very low (a,b) values. The situation does not change if accurate two-body potentials are used such as for argon or chromium, the latter known to crystallize in the bcc phase. As a result, the bcc phase (at low temperatures and pressures) is stabilized only by higher than two-body forces, which have to be large enough to compete with the fcc (or hcp) structure. High pressures will most likely destabilize the bcc phase in this simple model, which we are currently exploring. The mcc lattice unknown in nature and introduced by Conway and Sloane [310] is merely a point on an energetic bcc→fcc downhill path. How well effective two-body potentials [319, 320], which incorporate many-body terms, will work for the bcc problem remains to be seen.

9.5 Appendix

A Lattice Sums and Their Derivatives

The Gram matrix G in Eq.(9.2.2) leads to the following lattice sum,

$$L(a,A) = L(2s,A) = \mathscr{L}(s,A) = {\sum_{\vec{i}\in\mathbb{Z}^3}}' \left(\vec{i}^{\top} G \vec{i}\right)^{-s} \tag{9.A.1}$$
$$= {\sum_{i,j,k\in\mathbb{Z}}}' \left(\frac{A+1}{A(i+j)^2+(j+k)^2+(i+k)^2}\right)^s,$$

with the prime indicating that the term with $\vec{i}^{\top} = (0,0,0)$ is not included, and $A \in [\frac{1}{3},1]$ for the cuboidal lattices considered here. These sums are important for inverse power law potentials such as the LJ potential [311]. Here the exponent s is set to $s = \frac{a}{2}$ for simplicity compared to the main paper. The lattice sums for the acc, bcc, mcc, and fcc lattices are obtained for the values $A = \frac{1}{3}$, $A = \frac{1}{2}$, $A = \frac{1}{\sqrt{2}}$, and $A = 1$, respectively. We split the lattice sum into two sums according to Ref.[311],

$$\mathscr{L}(s,A) = \frac{(A+1)^s}{2}\left[S_1(s,A)+S_2(s,A)\right] \tag{9.A.2}$$
$$\text{with} \quad S_1(s,A) = {\sum_{i,j,k\in\mathbb{Z}}}' (Ai^2+j^2+k^2)^{-s}$$
$$\text{and} \quad S_2(s,A) = {\sum_{i,j,k\in\mathbb{Z}}}' (-1)^{i+j+k}(Ai^2+j^2+k^2)^{-s}.$$

For the special case of $A = 1$, the sum $S_1(1,s)$ represents the lattice sum for the simple cubic (sc) lattice, and the alternating sum $S_2(1,s)$ is known as the Madelung constant when $s = \frac{1}{2}$ [7]. In the following, we only consider $s > \frac{3}{2}$, keeping in mind that the lattice sums are valid for all $s \in \mathbb{R}$ through analytical continuation and that $S_1(s,A)$ (and therefore $\mathscr{L}(s,A)$) has a singularity at $s = \frac{3}{2}$.

The two lattice sums can be expanded in terms of modified Bessel functions of the second kind $K_s(x)$ [311],

$$S_1(s,A) = a_1(s) + a_2(s)A^{1-s}$$
$$+ a_3(s)A^{(1-s)/2}\sum_{i=1}^{\infty}\sum_{N=1}^{\infty} c_{iN}(s)K_{s-1}\left(d_{iN}(s)\sqrt{A}\right) \tag{9.A.3}$$

$$S_2(s,A) = b_1(s) + a_3(s)A^{(1-s)/2}\sum_{i=1}^{\infty}\sum_{N=0}^{\infty} p_{iN}(s)K_{s-1}\left(q_{iN}(s)\sqrt{A}\right), \tag{9.A.4}$$

with the following coefficients

$$\begin{aligned}
&a_1(s) = 4\zeta(s)\beta(s) \quad , \quad a_2(s) = \frac{2\pi}{(s-1)}\zeta(2s-2) \\
&a_3(s) = \frac{4\pi^s}{\Gamma(s)} \quad , \quad b_1(s) = -4(1-2^{1-s})\zeta(s)\beta(s) \\
&c_{iN}(s) = r_2(N)\left(i^{-2}N\right)^{(s-1)/2} \quad , \quad d_{iN}(s) = 2\pi i\sqrt{N} \\
&p_{iN}(s) = (-1)^i r_2(4N+1)\left(\frac{4N+1}{2i^2}\right)^{(s-1)/2} \\
&q_{iN}(s) = \pi i\sqrt{8N+2}\,.
\end{aligned} \tag{9.A.5}$$

$\zeta(s)$ is the Riemann zeta function, $\beta(s)$ the Dirichlet beta function, and $r_2(N)$ the number of representations of number N as a sum of two squares.

We are interested in the first and second derivatives, $\partial_A\mathscr{L}(s,A) := \partial\mathscr{L}(s,A)/\partial A$ and $\partial_A^2\mathscr{L}(s,A) := \partial^2\mathscr{L}(s,A)/\partial A^2$, of the lattice sums. It was already proven directly from (9.A.2) that $\partial_A\mathscr{L}(s,A)|_{A=1/2} = 0$ and $\partial_A^2\mathscr{L}(s,A)|_{A=1/2} > 0$ if $s > \frac{3}{2}$ [311]. We therefore derive from Eq.(9.A.2) the following expressions,

$$\partial_A\mathscr{L}(s,A) = \frac{s}{A+1}\mathscr{L}(s,A) + \frac{(A+1)^s}{2}\left[\partial_A S_1(s,A) + \partial_A S_2(s,A)\right] \tag{9.A.6}$$

and

$$\begin{aligned}
\partial_A^2\mathscr{L}(s,A) = &-\frac{s(s+1)}{(A+1)^2}\mathscr{L}(s,A) + \frac{2s}{A+1}\partial_A\mathscr{L}(s,A) \\
&+\frac{(A+1)^s}{2}\left[\partial_A^2 S_1(s,A) + \partial_A^2 S_2(s,A)\right]\,.
\end{aligned} \tag{9.A.7}$$

The derivatives $\partial_A S_1(s,A)$, $\partial_A S_2(s,A)$, $\partial_A^2 S_1(s,A)$ and $\partial_A^2 S_2(s,A)$ are evaluated from the Bessel function expansions (9.A.3) and (9.A.4). For this, the following relations are required,

$$K_s(x) = K_{s+2}(x) - \frac{2(s+1)}{x}K_{s+1}(x) \tag{9.A.8}$$

$$\begin{aligned}
\partial_x K_s(x) &= \frac{s}{x}K_s(x) - K_{s+1} = -\frac{s}{x}K_s(x) - K_{s-1} \\
&= -\frac{1}{2}\left[K_{s-1}(x) + K_{s+1}(x)\right]\,.
\end{aligned} \tag{9.A.9}$$

After some algebraic manipulations the following expressions are obtained

$$\partial_A S_1(s,A) = -(s-1)a_2(s)A^{-s} - \frac{a_3(s)}{2}A^{-\frac{s}{2}}\sum_{i=1}^{\infty}\sum_{N=1}^{\infty} c_{iN}(s)d_{iN}(s)K_s\left(d_{iN}(s)\sqrt{A}\right) \tag{9.A.10}$$

$$\partial_A S_2(s,A) = - \frac{a_3(s)}{2}A^{-\frac{s}{2}}\sum_{i=1}^{\infty}\sum_{N=0}^{\infty} p_{iN}(s)q_{iN}(s)K_s\left(q_{iN}(s)\sqrt{A}\right) \tag{9.A.11}$$

$$\partial_A^2 S_1(s,A) = s(s-1)a_2(s)A^{-s-1} + \frac{a_3(s)}{4}A^{-\frac{s+1}{2}}\sum_{i=1}^{\infty}\sum_{N=1}^{\infty} c_{iN}(s)d_{iN}^2(s)K_{s+1}\left(d_{iN}(s)\sqrt{A}\right) \tag{9.A.12}$$

$$\partial_A^2 S_2(s,A) = \frac{a_3(s)}{4}A^{-\frac{s+1}{2}}\sum_{i=1}^{\infty}\sum_{N=0}^{\infty} p_{iN}(s)q_{iN}^2(s)K_{s+1}\left(q_{iN}(s)\sqrt{A}\right). \tag{9.A.13}$$

The Bessel function sums are fast converging, therefore making the evaluation of lattice sums and their derivatives to computer precision attainable within less than a second on a modern laptop computer [143].

B Critical Points for the bcc structure

For the following, we set a to $2s$, making the lattice sum $L(a,A) = L(2s,A)$, which is more convenient for the LJ potential. Figure 9.7 shows the lattice sums and their second derivative for $A = \frac{1}{2}$ (bcc lattice) as a function of the exponent a. It is clear that $\partial_A^2 L(A,a)|_{A=\frac{1}{2}}$ has a peculiar form with a minimum at $a = 5.52534$ and a maximum at $a = 12.57676$, this becomes important in the discussion of the bcc stability for Lennard-Jones systems detailed below. However, it is illustrative to evaluate the minimum distance derivatives $\partial_A^n R^*_{\min}(a,b,A)$ for $A = \frac{1}{2}$ and $n = 1,2$ (using dimensionless quantities as discussed in the main paper).

The first derivative of $R^*_{\min}(a,b,A)$ defined in Eq.9.A.6 for $a > b > 3$ is given by

$$\partial_A R^*_{\min}(a,b,A) = \frac{R^*_{\min}(a,b,A)}{a-b}\left(\frac{\partial_A L(a,A)}{L(a,A)} - \frac{\partial_A L(b,A)}{L(b,A)}\right), \tag{9.B.14}$$

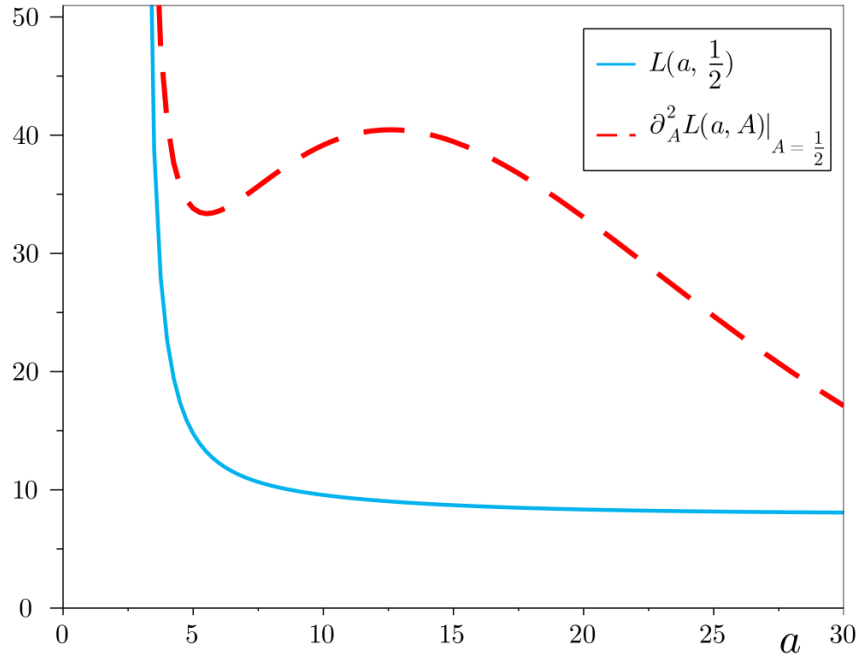

Figure 9.7 Lattice sums $L(a,\frac{1}{2})$ and $\partial_A^2 L(a,A)|_{A=\frac{1}{2}}$ (bcc lattice) as a function of the exponent a. Note that $\partial_A L(a,A)|_{A=\frac{1}{2}} = 0$ for all a values.

which for the bcc lattice ($A=\frac{1}{2}$) is zero because $\partial^A L(a,A)|_{A=\frac{1}{2}} = 0$ identically for all values of $a > 3$ [311]. The second derivative evaluated at $A=\frac{1}{2}$ is given by

$$\partial_A^2 R^*_{\min}(a,b,A)|_{A=\frac{1}{2}} = \left[\frac{R^*_{\min}(a,b,A)}{a-b}\left(\frac{\partial_A^2 L(a,A)}{L(a,A)} - \frac{\partial_A^2 L(b,A)}{L(b,A)}\right)\right]_{A=1/2}. \tag{9.B.15}$$

Evaluating the expression in parentheses in (9.B.15) shows that $R^*_{\min}(a,b,A)$ has a minimum at $A=\frac{1}{2}$ if $a < 14.17598$. For values $a > 14.17598$ we have a certain range of b values where $R^*_{\min}(a,b,A)$ becomes a shallow maximum as is the case for the (30,6) LJ potential shown in Figure 9.3.

In a similar way we evaluate the cohesive energy for an (a,b) LJ potential at

$R^*_{\min}(a,b,A)$,

$$E^*(R^*_{\min},a,b,A) = \frac{1}{2(a-b)}\left[bL(a,A)\left(\frac{L(b,A)}{L(a,A)}\right)^{\frac{a}{a-b}} - aL(b,A)\left(\frac{L(b,A)}{L(a,A)}\right)^{\frac{b}{a-b}}\right] = -\frac{1}{2}\left[\frac{L(b,A)^{1/b}}{L(a,A)^{1/a}}\right]^{\frac{ab}{a-b}}. \tag{9.B.16}$$

The first and second derivatives are evaluated as,

$$\partial_A E^*(R^*_{\min},a,b,A) = E^*(R^*_{\min},a,b,A)\frac{ab}{(a-b)}\left[\frac{1}{b}\frac{\partial_A L(b,A)}{L(b,A)} - \frac{1}{a}\frac{\partial_A L(a,A)}{L(a,A)}\right] \tag{9.B.17}$$

and

$$\partial_A^2 E^*(R^*_{\min},a,b,A) = \frac{\{\partial_A E^*(R^*_{\min},a,b,A)\}^2}{E^*(R^*_{\min},a,b,A)} + \frac{ab}{a-b}E^*(R^*_{\min},a,b,A)\left[\frac{1}{b}\frac{\partial_A^2 L(b,A)}{L(b,A)} - \frac{1}{a}\frac{\partial_A^2 L(a,A)}{L(a,A)} - \frac{1}{b}\frac{\{\partial_A L(b,A)\}^2}{L(b,A)^2} + \frac{1}{a}\frac{\{\partial_A L(a,A)\}^2}{L(a,A)^2}\right]. \tag{9.B.18}$$

The first derivative is zero for the bcc lattice ($A=\frac{1}{2}$) because $\partial^A L(a,A)|_{A=\frac{1}{2}} = 0$ as mentioned above. This makes the bcc point strictly an extremum along the A coordinate for any (a,b) combination of the LJ potential. The second derivative evaluated at $A=\frac{1}{2}$ gives

$$\partial_A^2 E^*(R^*_{\min},a,b,A)|_{A=\frac{1}{2}} = \frac{ab}{a-b}E^*(R^*_{\min},a,b,\tfrac{1}{2})\left[\frac{1}{b}\frac{\partial_A^2 L(b,A)|_{A=\frac{1}{2}}}{L(b,\frac{1}{2})} - \frac{1}{a}\frac{\partial_A^2 L(a,A)|_{A=\frac{1}{2}}}{L(a,\frac{1}{2})}\right]. \tag{9.B.19}$$

Hence, the bcc instability can be a maximum or a (metastable) minimum depending on the sign of the expression in the square brackets. The transition to a metastable phase occurs at

$$\frac{\partial_A^2 L(b,A)|_{A=\frac{1}{2}}}{bL(b,\frac{1}{2})} = \frac{\partial_A^2 L(a,A)|_{A=\frac{1}{2}}}{aL(a,\frac{1}{2})}, \tag{9.B.20}$$

with $b < a$. For the singularity at $a = 3$ we get from computation,

$$\lim_{a\to 3} \frac{\partial_A^2 L(a,A)|_{A=\frac{1}{2}}}{aL(a,\frac{1}{2})} = \frac{4}{9}, \tag{9.B.21}$$

which is shown on Figure 9.8. This can be proven using a Laurent expansion around the simple pole at $a = 3$ [311],

$$L(A;s) = \frac{2c_{-1}(A)}{a-3} + c_0(A) + \sum_{n=1}^{\infty} 2^{-n} c_n(A)(a-3)^n \tag{9.B.22}$$

with

$$c_{-1}(A) = \pi\sqrt{\frac{(A+1)^3}{A}} \quad \text{and} \quad \partial_A^2 c_{-1}(A) = \frac{3\pi}{4A^2\sqrt{A(A+1)}}. \tag{9.B.23}$$

This gives

$$\frac{\partial_A^2 L(a,A)}{L(a,A)} = \frac{\partial_A^2 c_{-1}(A)}{c_{-1}(A)} + \mathcal{O}(a-3) = \frac{3}{4A^2(A+1)^2} + \mathcal{O}(a-3) \tag{9.B.24}$$

which results in (11.3.1) for $a = 3$ and $A = \frac{1}{2}$.
From this limit it is clear that a metastable minimum can only exist if $a < a_{\mathrm{MS}} = 7.66039$, but with a limited range of small b values evident from (9.B.20) and Figure 9.8. The maximum of the curve shown in Figure 9.8 is at $a_{\max}$=5.25673, for which all $b < a < a_{\max}$ values result in a metastable state. We note that the curve in Figure 9.8 is almost (but not quite) symmetric around the maximum. This makes the phase transition line from the unstable to the metastable bcc phase almost linear in the (a,b) plane.

C Einstein Frequency

We consider the Einstein frequency of a single atom of mass M moving in the field of other atoms (in atomic units) for an (a,b) LJ potential [296],

$$\begin{aligned}\omega_E(R,a,b,A) = &\frac{1}{3r_e}\sqrt{\frac{3\varepsilon}{M}}\sqrt{\frac{ab}{a-b}}\left(\frac{r_e}{R}\right)^{\frac{a}{2}+1} \\ &\times\left[(a-1)L(a+2,A) - (b-1)L(b+2,A)\left(\frac{R}{r_e}\right)^{a-b}\right]^{\frac{1}{2}}.\end{aligned} \tag{9.C.25}$$

It is clear that $\omega_E(R)$ describes the instability of lattice by moving a single atom as opposed to a collective movement of several atoms in the lattice. However, at $R_{\min}$ we always arrive at $\omega_E(R_{\min}) > 0$ for a finite mass M. To prove this

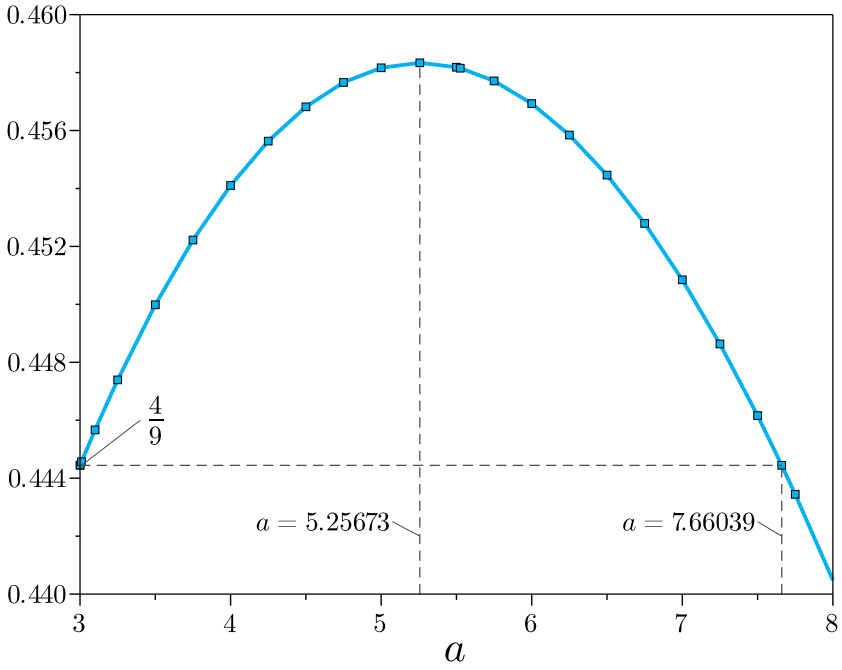

Figure 9.8

we have to show that the term in the square brackets stays positive at $R_{\min}$ for a fixed A value, that is

$$\frac{L(a+2,A)}{L(b+2,A)} > \frac{(b-1)L(a,A)}{(a-1)L(b,A)}. \tag{9.C.26}$$

As $a > b$ it suffices to show that

$$\frac{L(a+2,A)}{L(b+2,A)} \geq \frac{L(a,A)}{L(b,A)},$$

or more generally

$$\frac{L(b,A)}{L(b+h,A)} \geq \frac{L(a,A)}{L(a+h,A)} \tag{9.C.27}$$

for any $h > 0$ and $a > b > 3$. The proof goes a follows.

A function $g(x)$ is said to be logarithmically convex on an interval if $g(x) > 0$ and $\log g(x)$ is convex on the interval. It can be shown that the sum of logarithmically convex functions is logarithmically convex, e.g., see [321, p. 19]. It follows that the lattice sum $L(x,A)$ is a logarithmically convex function of x because it is a sum of terms of the form n^{-x}, each of which is logarithmically convex.

Now suppose that $f(x)$ is a convex function, and x_1, $x_2 > 0$. By applying the definition of convexity to the interval $[0, x_1 + x_2]$ we have

$$f(x_1) \leq \frac{x_2}{x_1+x_2} f(0) + \frac{x_1}{x_1+x_2} f(x_1+x_2),$$

while interchanging x_1 and x_2 gives

$$f(x_2) \leq \frac{x_1}{x_1+x_2} f(0) + \frac{x_2}{x_1+x_2} f(x_1+x_2).$$

Adding the inequalities gives

$$f(x_1) + f(x_2) \leq f(0) + f(x_1+x_2). \tag{9.C.28}$$

Incidentally, it can be shown from this using mathematical induction that

$$f(x_1) + f(x_2) + \cdots + f(x_n) \leq (n-1) f(0) + f(x_1 + x_2 + \cdots + x_n),$$

a result known as Petrović's inequality, e.g., see [322, p. 22], [323]. We shall only require the case $n = 2$ as given by (9.C.28).

Suppose $a > b$, $h > 0$, and $g(x)$ is a convex function for $x \geq b$. Let $f(x) = g(x+b)$ and take $x_1 = h$ and $x_2 = a - b$. Then Petrović's inequality (9.C.28) gives

$$f(h) + f(a-b) \leq f(0) + f(a-b+h).$$

This implies

$$g(b+h) + g(a) \leq g(a+h) + g(b)$$

which is equivalent to

$$g(b+h) - g(b) \leq g(a+h) - g(a).$$

It follows that if $G(x)$ is logarithmically convex, then

$$\log G(b+h) - \log G(b) \leq \log G(a+h) - \log G(a).$$

This can be rearranged to give

$$\frac{G(b+h)}{G(b)} \leq \frac{G(a+h)}{G(a)},$$

which is exactly the inequality we seek for the lattice sums.

D Extended Lennard-Jones Potentials for Li_2, Ar_2 and Cr_2

The extended Lennard-Jones potential is defined by

$$V_{\mathrm{ELJ}}(r,c_n) = \sum_{n=1}^{n_{\max}} c_n r^{-a_n} \quad \text{with} \quad \sum_{n=1}^{n_{\max}} c_n r_e^{-a_n} = -D_e\,. \tag{9.D.29}$$

It then follows that the cohesive energy for an extended Lennard-Jones potential becomes,

$$E_{\mathrm{ELJ}}(R,c_n,A) = \frac{1}{2}\sum_{n=1}^{n_{\max}} c_n L(a_n,A) R^{-a_n} \tag{9.D.30}$$

with R being the nearest neighbor distance in the solid. The corresponding parameters for the potential energy curves in reduced units, $V^*(r^*)$, for Ar_2, Li_2 and Cr_2 are listed in Table 1. For Ar_2 the extended LJ potential from Ref.[51] has been converted to dimensionless units for this work ($r^* = r/r_e$, $V^*(r) = V^*(r)/D_e$, from which follows that $r^*_{\min} = 1$ and $V^*_{\min} = -1$).

For Cr_2 we took the potential curve from experimental data of Casey and Leopold, who obtained the potential energy curve $V(r)$ from vibrational data through the RKR method [315]. This potential curve only describes the medium range of the potential energy curve. We therefore attenuated the long range by matching the last point $R_{\max}$ =3.35 Å to a $-C_6/r^{-6}$ dispersion curve. Finally, the points are used to fit an inverse power potential (extended Lennard-Jones) to the potential energy curve fixing the Van der Waals coefficient to C_6 =800 a.u. according to Roos and co-workers [316]. Because of the peculiar shape of the Cr_2 potential energy curve the fit was rather difficult to achieve, but is accurate enough (R^2=0.9984) for the discussion of the bcc instability. The potential energy curve for Cr_2 was then converted to dimensionless units. For the ELJ form we obtain E^* =24.0 and 23.3 for the fcc and bcc structures respectively. These values are unusually large, but perhaps not surprising given the broad potential energy curve of Cr_2. In fact, using the original potential energy curve we obtain a nearest neighbor distance for bcc chromium of $R_{\min}$ = 1.479 Å, just above the hard sphere radius of the diatomic potential energy curve with σ = 1.467 Å, and a cohesive energy E_{coh} = 33.6 eV. This is in stark disagreement with the experimental values of $R_{\min}$ = 2.52 Å and E_{coh} = 4.1 eV [324]. It clearly demonstrates that the direct use of potential curves from the free unconfined diatomic is not useful to describe the solid state of metals as the many-body expansion is not converging fast and smoothly.

We briefly discuss lithium. For Li_2 we used the Rydberg-Klein-Rees (RKR) potential curve of Barakat et al. [318] and fixed the Van der Waals coefficient C_6 =1408 a.u. [325]. For the fit to an extended LJ potential we obtained with

Table 9.1 Potential parameters for the Ar, Li and Cr dimers obtained from a least-squares fit to the (a) analytical form of Cybulski and Toczyłowski for Ar_2 [51, 314], (b) exp. determined potential of Barakat et al. [318], and (c) exp. determined potential of Casey and Leopold [315] as described in detail in the text. Dimensionless units are used. For Li_2 and Cr_2 the potential parameters are only valid for the region $V^*(r^*) < 0$.

n	a_n	c_n	n	a_n	c_n
Ar					
1	6	-2.112319339	2	8	7.126409258
3	10	-21.30053312	3	12	24.42390886
5	14	-10.89025935	6	16	1.752793693
Li					
1	6	-2.185099402	2	8	1588.743093
3	9	-13096.66094	4	10	44937.24250
5	11	-85547.67477	6	12	100055.5130
7	13	-74450.14624	8	14	35150.12854
9	15	-10264.39581	10	16	1744.182010
11	17	25.87885791	12	18	-237.6273332
13	19	114.6392978	14	20	-18.63705649
Cr					
1	6	-15.20122639	2	8	13471.86476
3	9	-124591.4050	4	10	464698.3696
5	11	-888076.6787	6	12	854878.9650
7	13	-190568.3900	8	14	-441981.1016
9	15	487340.5171	10	16	-209652.8384
11	17	34494.89857	12	18	0.000016589

an R^2 value of 0.99997, but only by including terms up to $1/r^{20}$. However, the situation here is even worse compared to chromium as the Li_2 potential energy curve is so broad in both the repulsive and attractive region that crystal optimizations entered the repulsive wall well below the hard-sphere radius of $\sigma = 1.822$ Å, where our extended LJ potential is not accurate anymore. In general, a fit to an extended LJ form works reasonably well for the whole distance region if it deviates not too much from an ideal (a,b)-LJ potential, which is certainly not the case for Li_2. In fact, if we optimize the exponents a,b for the LJ potential we get $a \approx b < 3$ left of the singularity at $b = 3$ and therefore an unphysical result. Using the far more accurate extended Morse potential by LeRoy and co-workers [326], which correctly describes the repulsive region, we obtain from crystal optimizations [167] a nearest neighbor distance of $R_{\min} = 0.21$ Å and a cohesive energy of $E_{\text{coh}} = 9.2 \times 10^3$ eV for bcc lithium. This can be best described as a collapse of the crystal to

small internuclear distances with large overbinding, and clearly demonstrates that many-body forces in a confined bulk system cannot be neglected.

10 Project 5 - Cuboidal bcc to fcc Transformation of Lennard-Jones Phases under High Pressure derived from Exact Lattice Summations[a]

10.1 Introduction

Within the periodic table of elements, only oxygen, fluorine and polonium exhibit simple cubic (sc) structure, similarily the body-centered cubic (bcc) phase is adapted by only a few elements, namely the group 1 elements, barium and radium, group 5 and 6 transition metals, as well as by manganese, iron and europium [328–330]. Intuitively this can be explained from the fact that two-body interactions between atoms tend to maximize the number of nearest neighbors (the so-called coordination or kissing number N) in a crystal, favoring the closed packed fcc ($N = 12$) or hcp crystal structures ($N = 12$) over the bcc ($N = 8$) or simple cubic (sc) ($N = 6$) lattice. From this simplified picture we expect that closed packed structures with maximum packing density are preferred at higher pressures. This is indeed observed in most cases [331–333], although many counterexamples are known [334, 335]. On the other hand, it is well known that Landau theory favors the bcc phase near the melting line at finite pressures [297]. Here, high-temperature phases also depend on the phonon dispersion and resulting thermal/entropic effects especially for atoms with low masses, which makes crystal structure predictions rather more complicated and challenging [302, 336]. Therefore, John Maddox famous quote in 1988 comes at no surprise: *One of the continuing scandals in the physical sciences is that it remains impossible to predict the structure of even the simplest crystalline solids from a knowledge of their composition*.[337] In other words, chemical intuition is often insufficient to correctly predict the crystal structure for an atomic or molecular system at specific pressures and temperatures.
Simulations of phase transitions for the solid state are known to be notoriously

[a]This chapter is composed of sections previously published in the article "Cuboidal bcc to fcc Transformation of Lennard-Jones Phases under High Pressure Derived from Exact Lattice Summations"[327] and is reprinted by permission from the publisher ©2022 American Chemical Society. Some sections may have been modified to fit the style of this thesis.

difficult to perform[291, 330], as often large supercells are required in molecular dynamic simulations and defects or dislocations may be involved as well. Reliable predictions for the stability of certain phases also critically depend on the chosen interaction potential or the accuracy of the quantum chemical method applied [338]. The (a,b) Lennard-Jones (LJ) potential [3, 6, 82]

$$\phi_{=LJ}(r) = \varepsilon \frac{ab}{a-b}\left[\frac{1}{a}\left(\frac{r_e}{r}\right)^a - \frac{1}{b}\left(\frac{r_e}{r}\right)^b\right], \tag{10.1.1}$$

($a > b > 3$ with a,b real numbers) is perhaps the most widely used and simplest interaction potential in the simulation of phase transitions [293, 295, 309, 339–341]. Here, ε is the binding energy, r the internuclear distance and r_e the equilibrium distance for a diatomic interaction. A selection of LJ potentials for different (a,b) parameters are shown in Figure 10.1. For the (12,6) LJ potential the phase diagram is well known, with fcc and hcp (and associated Barlow structures between these two phases) being energetically quasi-degenerate, resulting in many controversies (see for example Refs. [171, 296]), and bcc appearing as a phase near the melting point.[5, 244, 293, 296, 340]

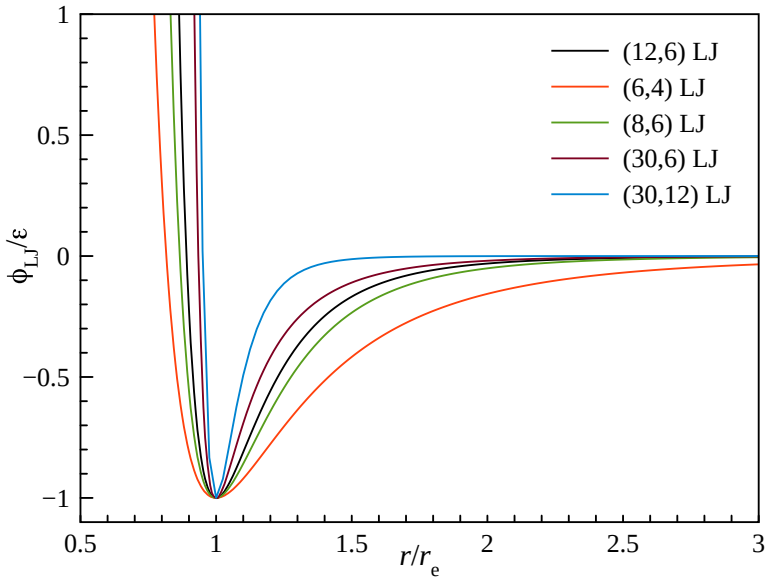

Figure 10.1 Lennard-Jones potentials for a selection of parameters (a,b).

On the mathematical side, the crystallization problem and stability of certain periodic lattices has been the subject of intense discussion for quite some time. The crystallization conjecture states that most of the ground states of physical interacting systems are periodic lattices [342]. This is not a particularly strong

conjecture, however, the occurrence of periodic lattices in nature is still an unresolved problem even for simple pairwise interactions [140].
In 1924, Lennard-Jones introduced so-called lattice sums for the sc, bcc and fcc lattices [6, 22] which was extended later by Herzfeld and Goeppert-Mayer [154] to the hcp lattice. These lattice sums arise from quadratic forms and Gram matrices constructed from lattice vectors of a Bravais lattice (note that hcp is a multi-lattice consisting of a superposition of two shifted Bravais lattices), and for inverse power law potentials such as Lennard-Jones they belong to the class of Epstein zeta functions [342]. When these lattice sums are expanded in terms of Bessel functions, one derives fast converging series from the originally slow converging (or conditionally converging) sums[26, 131, 160, 311]. Lattice sums have the advantage that bulk properties such as the cohesive energy, pressure and bulk modulus can be determined analytically to computer precision,[296] and useful relations can therefore be obtained, for example for the stability of the bcc phase. Here we demonstrated very recently that (in the low temperature, pressure, and high mass limit) the LJ potential leads to an unstable bcc phase. Or at rather low (unphysical) combinations of values for the exponents (a,b) in eq.(10.1.1), leads to a metastable phase with the fcc phase always being lower in energy compared to the bcc phase [343]. The bcc$\rightarrow$fcc transition path for a (12,6) LJ potential is smooth and downhill and can be described by a single lattice parameter only. Moreover, the phase line to metastability was determined to high precision for the valid (a,b) parameter range of a LJ potential [343].
Most mathematical studies are concerned with the stability of crystals at constant density [140, 344, 345]. In this work we want to shed light on the bcc stability at finite pressures P by using exact lattice summations for pairwise Lennard-Jones interactions based on lattice vectors describing a primitive cuboidal cell, which gives rise to lattice sums and to a free energy expression for a general (a,b) LJ potential. We are particularly interested in the phase transition from the unstable to the metastable bcc phase in order to predict the high-pressure limit in terms of the LJ exponents (a,b). The transition path chosen is identical to a Bain distortion for a cuboidal cell [301, 312, 346].
In the next section we derive and describe in detail the equations used in the determination of the LJ Helmholtz free energy dependent on the pressure P and cuboidal distortion parameter A. This is followed by a general discussion where we show that the instability of the bcc phase propagates into the high-pressure regime. Finally we predict the high-pressure limit ($P \rightarrow \infty$) for the onset of the metastable bcc phase with respect to the (a,b) parameter range.

10.2 Method

For the exact evaluation of the pressure dependent free energy and transformation path for the bcc$\leftrightarrow$fcc transition we introduce the following lattice vectors

describing the primitive cell of a body-centered tetragonal (bct) lattice [311],

$$b_1^\top(A) = R(1,0,0) \quad , \quad b_2^\top(A) = R\left(\frac{A}{A+1}, \frac{\sqrt{2A+1}}{A+1}, 0\right), \qquad (10.2.1)$$
$$b_3^\top(A) = R\left(\frac{1}{A+1}, \frac{1}{(A+1)\sqrt{2A+1}}, \sqrt{\frac{4A}{(A+1)(2A+1)}}\right).$$

Beside the usually slow varying nearest neighbor distance R in the solid, these lattice vectors are dependent on a single parameter A smoothly connecting the bcc ($A = \frac{1}{2}$) with the fcc ($A = 1$) lattice along a (martensitic) Bain-type transformation path [343].

These lattice vectors can be derived from an earlier paper of Conway and Sloane who introduced the mean centered cubic ($A = 1/\sqrt{2}$) lattice as an average between the bcc ($A = 1/2$) and the fcc lattice ($A = 1$) [310, 311], or directly from the conventional bct cell (space group $I4/mmm$) with lattice constants $a_1 = a_2$ and a_3 ($\alpha_1 = \alpha_2 = \alpha_3 = 90^o$) through the relations

$$a_1 = R\sqrt{\frac{2}{A+1}} \quad , \quad a_3 = 2R\sqrt{\frac{A}{A+1}} \qquad (10.2.2)$$

The cuboidal lattice is shown in Figure 10.2 for the special case of a bcc cell.

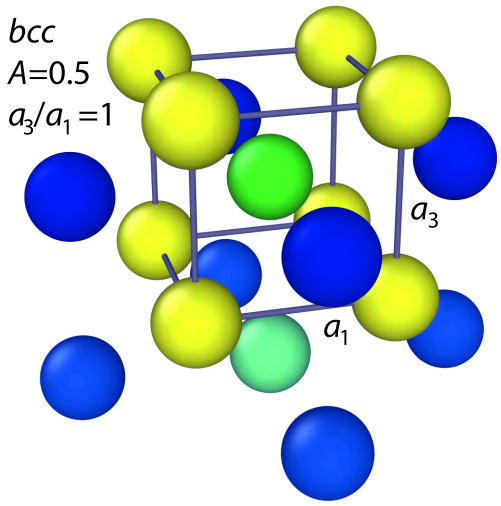

Figure 10.2 The bct lattice ($a_1 = a_2, a_3, \alpha_1 = \alpha_2 = \alpha_3 = 90^o$) shown for the special case of $A = 1/2, a_3/a_1 = 1$. The 8 yellow atoms define the conventional bct cell with lattice parameter ($a_1 = a_2, a_3$). The 8 blue, 4 lower yellow and 2 green atoms define the conventional fcc cell.

The lattice vectors defined in (12.7.1) lead to the following Gram matrix $G(A)$ [310, 311],

$$G(A) = B^{\top}(A)B(A) = \frac{1}{A+1}\begin{pmatrix} A+1 & A & 1 \\ A & A+1 & 1 \\ 1 & 1 & 2 \end{pmatrix}. \tag{10.2.3}$$

where $B(A)$ is the (3×3) matrix containing the lattice basis vectors b_i for the unit distance ($R=1$).

If we introduce dimensionless units, i.e. $\phi^*_{\mathrm{LJ}}(r^*,a,b) = \phi_{\mathrm{LJ}}(r/r_e,a,b)/\varepsilon$, the (a,b)-LJ potential in its most general form becomes

$$\phi^*_{\mathrm{LJ}}(r^*,a,b) = \frac{ab}{a-b}\left[\frac{1}{a}r^{*-a} - \frac{1}{b}r^{*-b}\right], \tag{10.2.4}$$

This sets the equilibrium distance to r^*=1 and the potential energy to $\phi^*_{\mathrm{LJ}}(r^*=1,a,b) = -1$. Here, $a,b \in \mathbb{R}_+$ are real numbers and we require $a > b > 3$ to avoid divergencies for the lattice summations [311]. The analytical expression for the cohesive energy in terms of lattice sums $L(a,A)$ and nearest neighbor distance $R^* = R/r_e$ for a lattice defined by the lattice vectors (12.7.1) then becomes [160],

$$E^*_{\mathrm{LJ}}(R^*,a,b,A) = \frac{ab}{2(a-b)}\left[\frac{1}{a}L(a,A)R^{*-a} - \frac{1}{b}L(b,A)R^{*-b}\right]. \tag{10.2.5}$$

Vibrational effects are neglected in this work (high mass limit, $M\to\infty$). The lattice sums $L(a,A)$ introduced by Lennard-Jones and co-workers can be evaluated to computer precision by various expansion techniques leading to fast converging series [160, 311]. The volume can be defined through the Gram matrix (10.2.3) [311],

$$V^*(A,R^*) = R^{*3}\mathrm{det}B(A) = R^{*3}\sqrt{\mathrm{det}G(A)} = 2R^{*3}A^{1/2}(A+1)^{-3/2} \tag{10.2.6}$$

In a similar way we define the pressure P^* and bulk modulus B^* in dimensionless units,

$$\begin{aligned} P^*(R^*,a,b,A) &= -\frac{\partial E^*_{\mathrm{LJ}}(R^*,a,b,A)}{\partial V^*(R^*,A)} \\ &= \frac{ab}{6(a-b)V(R^*,A)^*}\left[L(a,A)R^{*-a} - L(b,A)R^{*-b}\right], \end{aligned} \tag{10.2.7}$$

$$B^*(R^*,a,b,A) = V^*(R^*,A)\frac{\partial^2 E^*_{\rm LJ}(R^*,a,b,A)}{\partial V^*(R^*,A)^2}$$
$$= \frac{ab}{18(a-b)V(R^*,A)^*}\left[L(a,A)(a+3)R^{*-a} - L(b,A)(b+3)R^{*-b}\right]. \quad (10.2.8)$$

For the Helmholtz free energy for fixed values of a,b,A we have

$$F^*(P^*,V^*) = E^*_{\rm LJ}(V^*) + P^*V^*$$
$$= \frac{ab}{2(a-b)}\left[\frac{3+a}{3a}L(a,A)R^{*-a} - \frac{3+b}{3b}L(b,A)R^{*-b}\right], \quad (10.2.9)$$

and we need to obtain the volume V^* for a fixed pressure P^*. This requires to obtain the zero of the function,

$$f(P^*,R^*,a,b,A) = \frac{6(a-b)\sqrt{\det G(A)}}{abL(a,A)}P^*R^{*(a+3)} + \frac{L(b,A)}{L(a,A)}R^{*(a-b)} - 1 \quad (10.2.10)$$

derived from eq.(10.2.7). The Newton-Raphson procedure is used to obtain R^* iteratively for fixed values of P^*,A,a,b,

$$R^*_{n+1}(P^*) = R^*_n(P^*) - \frac{f(P^*,R^*)}{\partial f(P^*,R^*)/\partial R^*(P^*)} \quad (10.2.11)$$

and we reach convergence if $|R^*_{n+1} - R^*_n| < 10^{-14}$. The lattice sums $L(a,A)$ are obtained from fast converging Bessel function expansions introduced previously [160, 311].

For the critical point analysis of the bcc structure ($A = 1/2$) we require the derivatives at $A = 1/2$. In our previous work we showed that $\partial L(a,A)/\partial A|_{A=1/2} = 0$ and $\partial^2 L(a,A)/\partial A^2|_{A=1/2} > 0$ [160]. From this one follows $\partial E^*(A)/\partial A|_{A=1/2} = 0$ and $\partial F^*(A)/\partial A|_{A=1/2} = 0$ for any a,b combination at zero pressure. To answer the question if when $A = 1/2$ (corresponding to bcc) on the A-dependent stability line remains an extremum for any pressure P^* and a,b combination we evaluate the first and second derivatives at constant pressure P^*. For this the function at a specific pressure P^* and fixed a,b is defined,

$$g(P^*,R^*,A) = \frac{ab}{2(a-b)}\left[c_1 L(a,A)R^*(P^*,A)^{-a} - c_2 L(b,A)R^*(P^*,A)^{-b}\right]. \quad (10.2.12)$$

With coefficients $c^E_1 = 1/a$ and $c^E_2 = 1/b$ if g describes the internal energy E^*,

and $c_1^F = (3+a)/(3a)$ and $c_2^F = (3+b)/(3b)$ if g describes the Helmholtz free energy F^*. Here $R^*(P^*,A)$ at constant pressure becomes dependent on the lattice parameter A. The following derivatives are obtained (using $\partial L(a,A)/\partial A|_{A=1/2} = 0$),

$$\left.\frac{\partial g(P^*,R^*,A)}{\partial A}\right|_{A=1/2} = -\frac{ab}{2(a-b)}\left.\frac{\partial R^*(P^*,A)}{\partial A}\right|_{A=1/2} \times \left[ac_1 L(a,A)R^*(P^*,A)^{-a-1} - bc_2 L(b,A)R^*(P^*,A)^{-b-1}\right], \tag{10.2.13}$$

and

$$\left.\frac{\partial^2 g(P^*,R^*,A)}{\partial A^2}\right|_{A=1/2} = -\frac{ab}{2(a-b)}\left\{g_1(R^*,A=\tfrac{1}{2}) + g_2(R^*,A=\tfrac{1}{2}) + g_3(R^*,A=\tfrac{1}{2})\right\} \tag{10.2.14}$$

with

$$g_1(R^*,A=\tfrac{1}{2}) = \frac{ab}{2(a-b)}\left\{\left.\frac{\partial^2 L(a,A)}{\partial A^2}\right|_{A=1/2} ac_1 R^*(P^*,A)^{-a} - \left.\frac{\partial^2 L(b,A)}{\partial A^2}\right|_{A=1/2} bc_2 R^*(P^*,A)^{-b}\right\} \tag{10.2.15}$$

$$g_2(R^*,A=\tfrac{1}{2}) = -\frac{ab}{2(a-b)}\left.\frac{\partial^2 R^*(P^*,A)}{\partial A^2}\right|_{A=1/2} \times \left\{ac_1 L(a,A)R^*(P^*,A)^{-a-1} - bc_2 L(b,A)R^*(P^*,A)^{-b-1}\right\} \tag{10.2.16}$$

$$g_3(R^*,A=\tfrac{1}{2}) = \frac{ab}{2(a-b)}\left.\left(\frac{\partial R^*(P^*,A)}{\partial A}\right)^2\right|_{A=1/2} \times \left\{a(a+1)c_1 L(a,A)R^*(P^*,A)^{-a-2} - b(b+1)c_2 L(b,A)R^*(P^*,A)^{-b-2}\right\}. \tag{10.2.17}$$

The lattices sums and their derivatives are obtained analytically while the $\partial R^*(P*,A,a,b)/\partial A$ and $\partial^2 R^*(P*,A,a,b)/\partial A^2$ are treated numerically through a five-point central numerical differentiation. We find that at any pressure $P^* \geq 0$, $\partial R^*(P^*,A)/\partial A = 0$ at $A = 1/2$, which implies that for eq.(12.C.2) $\partial g(P^*,R^*,A)/\partial A = 0|_{A=1/2}$, and the corresponding term in eq.(10.2.17) can therefore be deleted. We point out that these formulae contain no approximations beside the neglect of vibrational and temperature effects. As the lattice summations used here give exact expressions for the

energy, and the lattice sums and neighbor distances at given pressure P^* can be obtained to computer precision.
To assess the pressure range required for this work we mention that for high pressures in the TPa range one obtains volume compressions down to $V/V_0 = 1/3$ where V_0 is the crystal volume at zero pressure [347]. This relates to a smallest nearest neighbor distance of about $R^* = 0.7$. We therefore decided to choose a pressure range of $P^* \in [0, 10^6]$ for our calculations. To relate this to real systems we may consider, for example, the bond distance and dissociation energy of argon ($r_e = 3.757$ Å, $\varepsilon = 1.191$ J/mol)[348] and use the pressure relationship $P = \varepsilon P^*/r_e^3$. For $P^* = 10^6$ we get ca. 34 TPa for a LJ potential. The range for the lattice parameter A was chosen to be $A \in [\frac{1}{3}, 1]$ (see Ref.[311] for details), describing a Bain transformation from the axially centered cubic lattice acc ($A = \frac{1}{3},\ a_3/a_1 = \frac{2}{3}$) to the fcc lattice ($A = 1,\ a_3/a_1 = \sqrt{2}$) through the bcc ($A = 1/2,\ a_3/a_1 = 1$) and mcc ($A = 1/\sqrt{2},\ a_3/a_1 = 2^{1/4}$) lattices. The Bain transformation is a diffusionless movement of atoms in a lattice starting from bcc by compression parallel to the a_3-axis and simultaneous expansion of the (a_1, a_2) plane.[301, 349]

10.3 Results and Discussion

The following graphs in Figures 10.3-10.5 show 2D and 3D plots of the form,

$$\Delta f^*(\log_{10}P^*, A) = f^*(\log_{10}P^*, A) - f^*(\log_{10}P^*, A = 1.0) \qquad (10.3.1)$$

relative to the most stable fcc structure, that is $\Delta f^*(\log_{10}P^*, A = 1.0) = 0$, for every pressure P^* for the properties $f^* = V^*, P^*V^*, E^*, and F^*$ for a number of selected (a, b) combinations of the LJ potential. For the large range of pressures we chose a logarithmic scale, as we also did for some of the Δf plots for better clarity because of the underlying exponential behavior. The corresponding LJ potentials are shown in Figure 10.1.

The A-dependent volume for the different cuboidal structures is defined in eq.(10.2.6). For the same R^* values we can easily derive from this equation that the bcc ($A = 1/2$) structure has a larger volume compared to the fcc ($A = 1$) structure. In fact it is a maximum along the A dependent line at zero pressure [343]. For the standard (12,6) LJ potential shown in Figure 10.3(a) or 10.5(a), there is a small minimum for $\Delta V^*(A)$ visible towards the acc structure ($A = \frac{1}{3}$). The volume difference between the bcc and fcc structures diminishes at higher pressures as one expects. If multiplied by the corresponding pressure (Figure 10.3b) we see that the $\Delta PV^*(P^*, A)$ looks rather smooth and increasing from fcc (which is zero by definition) to bcc. This increase is substantial at higher pressures and will add to the instability of the bcc phase. The rather small volume change with respect to the lattice parameter A shows that the choice of the

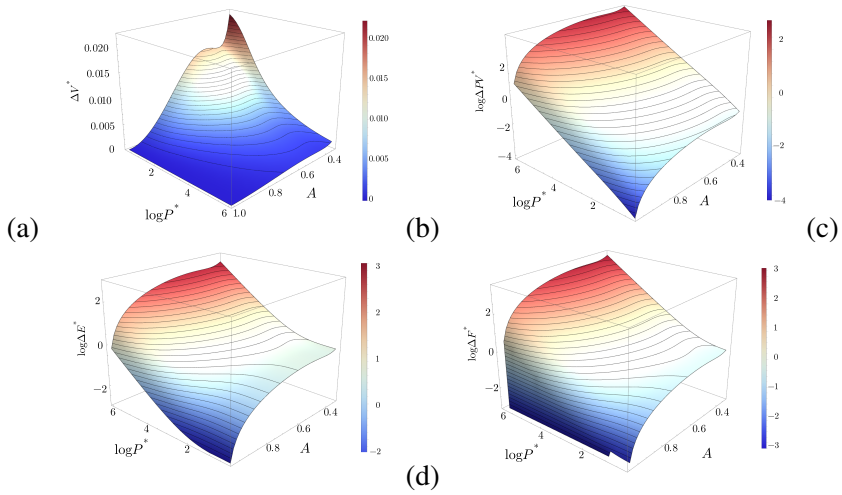

Figure 10.3 (a) $\Delta V^*(\log_{10}P^*,A)$, (b) $\log_{10}\Delta PV^*(\log_{10}P^*,A)$, (c) $\log_{10}\Delta E^*(\log_{10}P^*,A)$, and (d) $\log_{10}\Delta F^*(\log_{10}P^*,A)$ hypersurfaces for the $(12,6)$ LJ potential. For (a) we reversed the $\log_{10}P^*$ axis for better visibility.

parameter space (A,R) or (A,V) is rather better suited compared to the usually chosen lattice parameters (a_1,a_3) for the Bain transformation.

Figure 10.3(c) shows the internal energy - pressure plot for the different cuboidal lattices. Again we observe a successive destabilization of the bcc structure with increasing pressure. Adding both the internal energy and pressure-volume term, which are both energetically destabilizing for the bcc phase compared to the fcc phase, we clearly see that the bcc phase is unstable at all pressures, see Figure 10.3d. The instability increases substantially with increasing pressures. The plots also indicate that the acc and mcc lattices as discussed by Conway and Sloane [310] are not stable in terms of a (12,6) LJ potential [311] (beside a smaller metastable minimum at $A < 1/2$).. In order to stabilize such exotic crystal structures one requires other bonding conditions than simply described by a two-body potential such as Lennard-Jones.

Changing the parameter space for the LJ potential, in Figure 10.4 we show $\Delta F^*(\log_{10}P^*,A)$ for different combinations of (a,b) values. Topologically they look very similar, but for the $(6,4)$-LJ potential a metastable minimum is observed occurring at the bcc structure ($A = 1/2$) persisting into the high pressure regime, see Figure 10.5(b). Although the differences in the free energy ΔF^* between the bcc and the fcc structures become quite large at higher pressures, it is clear that harder potentials lead to larger differences in ΔF^* as one expects.

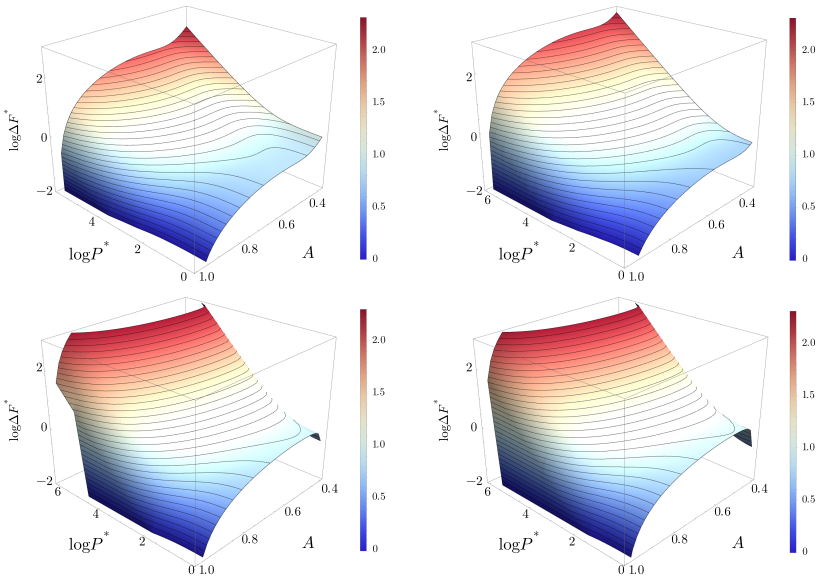

Figure 10.4 $\log_{10}\Delta F^*(\log_{10}P^*,A)$ 3D plots for the $(6,4)$, $(8,6)$, $(30,6)$ and $(30,12)$ LJ potential.

The second derivative of the internal energy $\partial^2 E^*(A)/\partial A^2|_{A=1/2}$ and the Helmholtz free energy $\partial^2 F^*(A)/\partial A^2|_{A=1/2}$ can change sign for the bcc structure from the metastable to the unstable phase depending on the combination of the a,b values. The boundary between the two phases at $\partial^2 E^*(A)/\partial A^2|_{A=1/2}=0$ is shown in Figure 10.6 for different pressures P^*. This first-order phase transition boundary line shifts at higher pressures to a larger set of possible (a,b) values. At $P^*=0$ the phase transition line is almost linear, and at the $P* \to \infty$ we predict a constant boundary for the phase transition with a value of $a=7.6603891$ (notice that $b<a$). The boundary line can be approximated by a polynomial and for few selected values of P^* the polynomial coefficients are collected in Table 10.1.
Finally a brief discussion in regard to the differences in bulk moduli between the cuboidal and the fcc structures is accompanied by Figure 10.7. We show that ΔB^* is at a minimum for the bcc structure (see also Figure 10.8), this difference gets smaller with increasing pressure. At values of $(a,b)=(30,6)$ for the LJ potential when the repulsive wall becomes harder, we see a change in the topology with the structures towards acc having smaller ΔB values.

c_i	$P^* = 0$	$P^* = 10^3$	$P^* = 10^6$	$P^* = 10^9$	$P^* = 10^{12}$	$P^* = \infty$
c_0	$+1.1373783 \times 10^1$	$+2.050791 \times 10^2$	$+1.492989 \times 10^1$	-3.508933×10^0	-9.441552×10^0	7.660389×10^0
c_1	-1.3466248×10^0	-2.628550×10^2	-8.542681×10^0	$+1.541380 \times 10^1$	$+2.318545 \times 10^1$	-
c_2	$+3.8186745 \times 10^{-2}$	$+1.448482 \times 10^2$	$+4.038010 \times 10^0$	-8.736197×10^0	-1.289675×10^1	-
c_3	$-6.3829845 \times 10^{-4}$	-4.227390×10^1	-9.729635×10^{-1}	$+2.605382 \times 10^0$	$+3.770280 \times 10^0$	-
c_4	-	$+6.886016 \times 10^0$	$+1.236268 \times 10^{-1}$	-4.318079×10^{-1}	-6.116289×10^{-1}	-
c_5	-	-5.937885×10^{-1}	-7.547246×10^{-3}	$+3.779518 \times 10^{-2}$	$+5.228404 \times 10^{-2}$	-
c_6	-	$+2.116745 \times 10^{-2}$	$+1.463303 \times 10^{-4}$	-1.370930×10^{-3}	$+1.844032 \times 10^{-3}$	-
rms	2.292×10^{-4}	1.985×10^{-3}	1.793×10^{-3}	7.941×10^{-4}	1.440×10^{-3}	-

Table 10.1 Polynomial coefficients for the phase transition boundary line $a(b) = \sum_n c_n(P^*)b^n$ and root mean squares error (rms) for the polynomial fit.

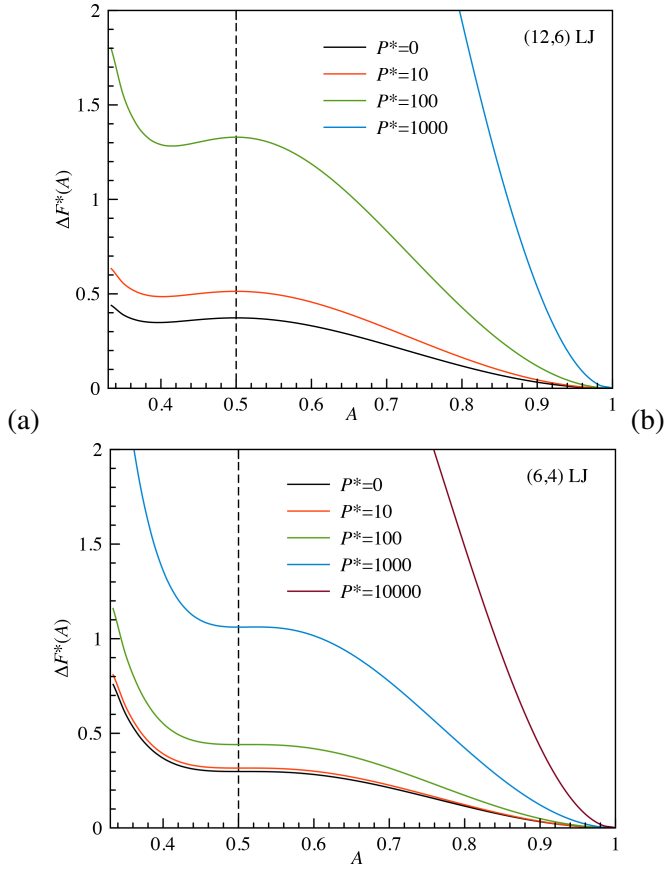

Figure 10.5 $\Delta F^*(P^*,A)$ plots for the (a) (12,6) and (b) (6,4) LJ potentials for a selection of P^* values. The bcc phase at $A = \frac{1}{2}$ is shown as a vertical dashed line.

10.4 Conclusions

We demonstrated that the bcc phase becomes energetically increasingly unstable at higher pressures for a (12,6) LJ potential. For low values of the Lennard-Jones exponents (a,b) the bcc phase becomes metastable along the Bain phase transition path. The (a,b) phase transition line to metastability shifts with increasing pressure with the high pressure limit $P \to \infty$ predicted at exponent $a = 7.6603891$ for the repulsive wall.

One cannot exclude other transformation paths which are energetically downhill toward fcc. However, our findings are in line with Ono and Ito who also showed from phonon dispersion curves at zero pressure that soft Lennard-Jones (LJ) forces are required to turn the bcc phase into a

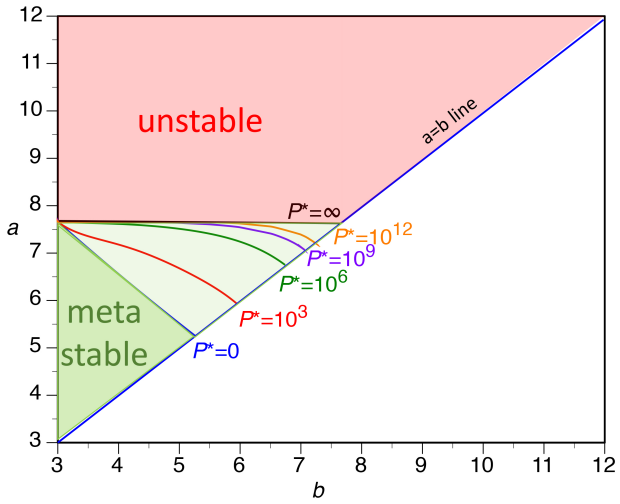

Figure 10.6 bcc first-order phase transition lines at different pressures P^* between the unstable (red) and the metastable (green) bcc phase for different combinations of (a,b) LJ exponents $(a > b)$. The black linear horizontal line at $a = 7.6603891$ represents the predicted high-pressure limit ($P^* \to \infty$). The light green area of metastability is accessible only at finite pressures $P^* > 0$.

minimum.[309] It would also be desirable to perform a more careful analysis along the Bain path in terms of the Born-Huang criterium [159] for mechanical stability (for a recent discussion see refs.[350, 351]). Here, one needs to investigate if lattice sums can be efficiently used for obtaining elastic constants, similar to the bulk modulus derived through lattice sums [296]. Nevertheless, above the (a,b) stability line, the instability of the bcc LJ phase at pressures $P^* > 0$ has been demonstrated in our work.

Naturally, one also wants to include temperature effects from vibrations. This, however, will introduce two more parameters to the (P,A) parameter space, that is the mass M and temperature T, which we intend to explore in our future work. Moreover, as the importance of zero-point vibrational effects diminish with increasing pressure, two-body effects in general may not be sufficient to stabilize the bcc phase at low temperatures [296]. For example, in lithium one observes a bcc→fcc transition at higher pressures [352]. However, the interaction between atoms is rarely well described by two-body interactions alone (lithium being a prime example here), and it would be interesting to see the interplay between two- and higher body effects [345].

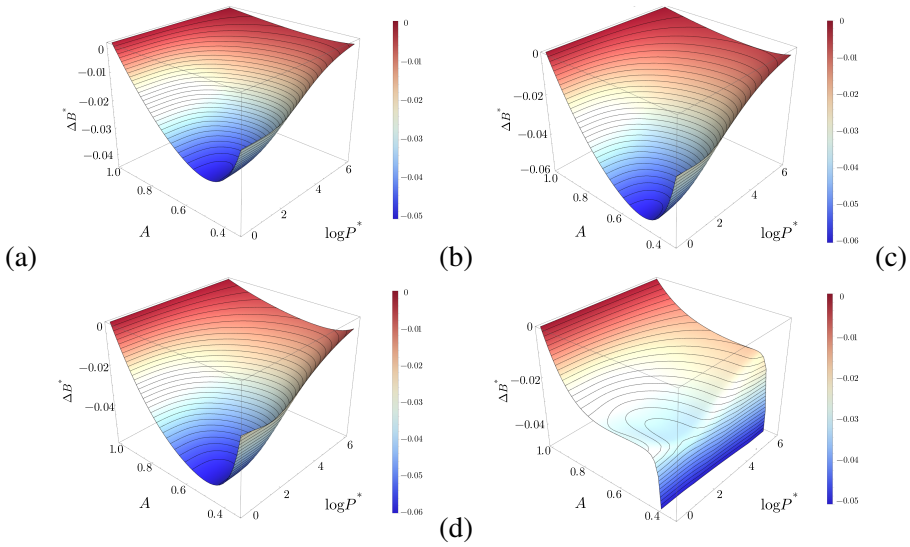

Figure 10.7 $\Delta B^*(\log_{10}P^*, A)$ 3D plots for the $(6,4)$, $(8,6)$, $(12,6)$ and $(30,6)$ LJ potential.

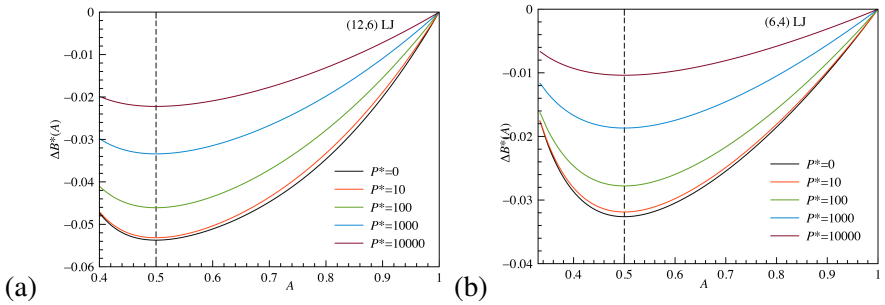

Figure 10.8 $\Delta B^*(P^*, A)$ plots for the (12,6) and (6,4) LJ potentials for a selection of P^* values. The bcc phase at $A = \frac{1}{2}$ is shown as a vertical dashed line.

10.5 Cover Page

The cover page for ACS Journal - Journal of Physical Chemistry C - May 26, 2022, Volume 126, Number 20, in which this paper is published can be seen in Appendix C.

11 Project 6 results - The Madelung Constant in N Dimensions

11.1 Introduction

The classical lattice energy E_{lat} of an ionic crystal M^+X^- can be obtained from lattice summations of Coulomb interacting point charges and is usually presented by the Born-Lande form [353, 354]

$$E_{lat} = -\frac{N_A Z^2 e^2}{4\pi\varepsilon_0 R_0} M_{lat}\left(1-n^{-1}\right), \tag{11.1.1}$$

where M_{lat} is the Madelung constant for a specific lattice [7], N_A is Avogadro's constant, and n is the Born exponent which corrects for the repulsion energy $V = aR^{-n}, a > 0$ at nearest neighbor distance R_0, Z is the ionic charge (+1 in the ideal case), e and ε_0 are the elementary charge and vacuum permittivity respectively. Values for Z^2M and n have been tabulated for different crystals in the past [355]. For a simple cubic lattice with alternating charges in the crystal the Madelung constant (or function) $M(s) \equiv M_{sc}(s)$ is given by the 3D alternating lattice sum

$$M(s) = {\sum_{i,j,k\in\mathbb{Z}}}' \frac{(-1)^{i+j+k}}{(i^2+j^2+k^2)^s} \quad , \tag{11.1.2}$$

where the summation is over all integer values, the prime behind the sum indicates that $i = j = k = 0$ is omitted, $s \in \mathbb{R}$, and $s = \frac{1}{2}$ is chosen for a Coulomb-type of interaction. This sum is absolutely convergent for $s > \frac{3}{2}$, but only conditionally convergent for smaller s-values [62, 63]. The problem with conditionally convergent series is that the Riemann Series Theorem states that one can converge to any desired value or even diverge by a suitable rearrangement of the terms in the series. This problem is well known for the Madelung constant ($s = \frac{1}{2}$) and has been documented and analyzed in great detail by Borwein et al [26, 63, 65] and Crandall et al [42, 64]. For example, one has to sum over expanding cubes and not spheres to arrive at the correct result of $M(\frac{1}{2}) = -1.747\,564\,594\,633\,182\,\ldots$ [64].

It is currently not known if the Madelung constant can be expressed in terms of standard functions. The closest formula one can get is the one for $s = \frac{1}{2}$

recently derived by Tyagi [356] following an approach by Crandall [64],

$$M\left(\tfrac{1}{2}\right) = -\frac{1}{8} - \frac{\ln 2}{4\pi} - \frac{4\pi}{3} + \frac{1}{2\sqrt{2}} + \frac{\Gamma\left(\frac{1}{8}\right)\Gamma\left(\frac{3}{8}\right)}{\pi^{3/2}\sqrt{2}} - 2\sum_{k\in\mathbb{N}} \frac{(-1)^k r_3(k)}{\sqrt{k}\left[e^{8\pi\sqrt{k}}-1\right]} \tag{11.1.3}$$

which is correct to 10 significant figures if the sum is neglected (for more recent work and improvement of Tyagi's formula see Zucker [357]). Moreover, the sum converges relatively fast. Here $r_3(k)$ is the number of representations of k as a sum of three squares.

There are many expansions available leading to an accurate determination of the Madelung constant [64]. Perhaps the most prominent formulas are the ones by Benson-Mackenzie [27, 68]

$$M\left(\tfrac{1}{2}\right) = -12\pi \sum_{i,j\in\mathbb{N}} sech^2\left[\frac{\pi}{2}\sqrt{(2i-1)^2+(2j-1)^2}\right] \tag{11.1.4}$$

and by Hautot [69] (in modified form by Crandall [64])

$$M\left(\tfrac{1}{2}\right) = -\frac{\pi}{2} + 3\sum_{i,j\in\mathbb{Z}}{}' \quad \frac{(-1)^i cosech\left(\pi\sqrt{i^2+j^2}\right)}{\sqrt{i^2+j^2}} \tag{11.1.5}$$

The Madelung constant can easily be extended to a N dimensional series ($N>0$),

$$M_N(s) = \sum_{i_1,\ldots,i_N\in\mathbb{Z}}{}' \frac{(-1)^{i_1+\cdots+i_N}}{(i_1^2+i_2^2+\cdots+i_N^2)^s} = \sum_{\vec{i}\in\mathbb{Z}^N\setminus\{\vec{0}\}} \frac{(-1)^{\vec{i}\cdot\vec{1}}}{|\vec{i}|^{2s}} \quad , \tag{11.1.6}$$

and the prime after the sum denotes that the term corresponding to $i_1 = i_2 = \cdots = i_N = 0$ is omitted (in the shorter notation on the right $\vec{1} = (1,1,\ldots,1)^\top$). The sum is absolutely convergent for exponents $s > \frac{N}{2}$. The Madelung series is as a special case of the more general Epstein zeta function [117].

Zucker has found analytical expressions in terms of standard functions for even dimensions up to $N = 8$ [107],

$$M_1(s) = -2\eta(2s) \tag{11.1.7}$$
$$M_2(s) = -4\beta(s)\eta(s) \tag{11.1.8}$$
$$M_4(s) = -8\eta(s-1)\eta(s) \tag{11.1.9}$$
$$M_6(s) = -16\eta(s-2)\beta(s) + 4\eta(s)\beta(s-2) \tag{11.1.10}$$
$$M_8(s) = -16\eta(s-3)\zeta(s) \tag{11.1.11}$$

Here $\eta(s)$ is the Dirichlet eta function, $\beta(s)$ the Dirichlet beta function, and

$\zeta(s)$ the Riemann zeta function [107]. These standard functions are defined in the Appendix A together with their analytical continuations to the whole range of real (or complex) numbers, $s \in \mathbb{R}(\mathbb{C})$.

By analogy with the three-dimensional case, an N-dimensional lattice can easily be constructed from its N linearly independent basis lattice vectors (or transformations of it). Higher dimensional lattices and their properties have been catalogued (up to certain dimensions) by Nebe and Sloane [358]. The simple cubic N-dimensional lattice can be drawn as an infinite graph with atoms (vertices) and edges connecting the nearest neighbor atoms (adjacent vertices). If we walk around the edges we alternate the charges (+/- sign or red/blue color of the vertices in the graph) in the ionic lattice corresponding to the alternating series for the Madelung constant. We can also derive the lattice from tiling the N-dimensional space with N-cubes by implying translational symmetry. Figure 11.1 shows the graphs for such N-cubes up to $N = 5$ together with the alternating color scheme. We notice that for dimensions $N > 3$ the graphs are not planar anymore. The number of nearest neighbor vertices for an N-dimensional cubic lattice is $2N$ and corresponds to the limit,

$$\lim_{s\to\infty} M_N(s) = -2N \quad . \tag{11.1.12}$$

For example, Crandall reports $M_3(50) = -5.999\,999\,999\,999\,989\,341\ldots$ [64].

A general and relatively fast converging series expansion for the N-dimensional Madelung constant has been elusive for a very long time. For example, a recent suggestion was made by Mamode to use the Hadamard finite part of the integral representation of the underlying potential (e.g. a Coulomb potential) within the N-dimensional crystal [359], but computations are quite involved and results presented were only up to three dimensions. For the N-dimensional case one can explore expansions known for example for the Epstein zeta function [42, 112, 121] or similar techniques [160]. In this work, we introduce a general formula for the N-dimensional Madelung constant for a simple cubic crystal in terms of a fast convergent Bessel function expansion allowing for analytical continuation, which gives deep insight into the functional behavior of the N-dimensional Madelung constant. The derivation is given in the next section. The convergence of $M_N(s)$ with increasing dimension N is discussed in detail in the results section.

11.2 Theory

In this section we derive two useful expansions for the N-dimensional Madelung constant. Consider $M_{N+1}(s)$ and change the last summation index

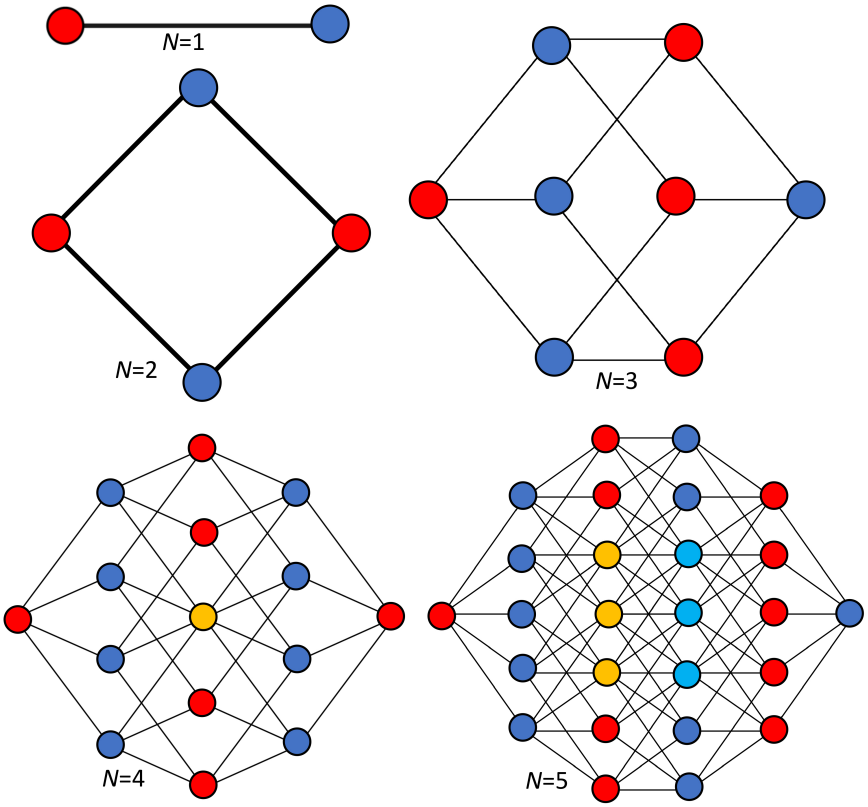

Figure 11.1 Graphs derived from orthogonal 2D projections of N-cubes ($1 \leq N \leq 5$) showing the alternating colors for the vertices (± 1 charges for the atoms). Starting with the 4-cube (tesseract) the orthogonal projection shows vertices overlapping and we use lighter colors to highlight the two overlapping vertices (orange for two red vertices and light blue for the two blue vertices).

to k, and write

$$M_{N+1}(s) = \sum_{\substack{i_1,\ldots,i_N \in \mathbb{Z} \\ k \in \mathbb{Z}}}{}' \frac{(-1)^{i_1+\cdots+i_N+k}}{(i_1^2+i_2^2+\cdots+i_N^2+k^2)^s}. \tag{11.2.1}$$

Now separate the sum into the two cases $k = 0$ and $k \neq 0$ to get

$$M_{N+1}(s) = M_N(s) + 2F(s) \tag{11.2.2}$$

where

$$F(s)=\sum_{k\in\mathbb{N}}\left(\sum_{i_1,\ldots,i_N\in\mathbb{Z}}\frac{(-1)^{i_1+\cdots+i_N+k}}{(i_1^2+i_2^2+\cdots+i_N^2+k^2)^s}\right). \tag{11.2.3}$$

By the gamma function integral in the form ($\mathbb{R}_+=\{x\in\mathbb{R}\mid x\geq 0\}$)

$$\frac{1}{z^s}=\frac{1}{\Gamma(s)}\int_{\mathbb{R}_+}t^{s-1}e^{-zt}\,\mathrm{d}t \tag{11.2.4}$$

we have

$$\begin{aligned}\pi^{-s}\Gamma(s)F(s)&=\int_{\mathbb{R}_+}t^{s-1}\left(\sum_{k\in\mathbb{N}}(-1)^k e^{-\pi k^2 t}\right)\\&\quad\times\left(\sum_{i_1,\ldots,i_N\in\mathbb{Z}}(-1)^{i_1+\cdots+i_N}e^{-\pi(i_1^2+\cdots+i_N^2)t}\right)\mathrm{d}t\\&=\int_{\mathbb{R}_+}t^{s-1}\left(\sum_{k\in\mathbb{N}}(-1)^k e^{-\pi k^2 t}\right)\left(\sum_{j\in\mathbb{Z}}(-1)^j e^{-\pi j^2 t}\right)^N\mathrm{d}t.\end{aligned} \tag{11.2.5}$$

By using the modular transformation for the theta function [79],

$$\sum_{n\in\mathbb{Z}}e^{-\pi n^2 t+2\pi i n a}=\frac{1}{\sqrt{t}}\sum_{n\in\mathbb{Z}}e^{-\pi(n+a)^2/t} \tag{11.2.6}$$

we get

$$\pi^{-s}\Gamma(s)F(s)=\int_{\mathbb{R}_+}t^{s-1}\left(\sum_{k\in\mathbb{N}}(-1)^k e^{-\pi k^2 t}\right)\left(\frac{1}{\sqrt{t}}\sum_{j\in\mathbb{Z}}e^{-\pi(j+\frac{1}{2})^2/t}\right)^N\mathrm{d}t. \tag{11.2.7}$$

This can be rearranged further to give

$$\begin{aligned}\pi^{-s}\Gamma(s)F(s)&=\int_{\mathbb{R}_+}t^{s-1-\frac{N}{2}}\left(\sum_{k\in\mathbb{N}}(-1)^k e^{-\pi k^2 t}\right)\\&\quad\times\left(\sum_{m\in\mathbb{N}_0}r_N^{\mathrm{odd}}(8m+N)\,e^{-\pi(8m+N)/4t}\right)\mathrm{d}t\end{aligned} \tag{11.2.8}$$

where $\mathbb{N}_0$ denotes the natural numbers including zero, and $r_N^{\mathrm{odd}}(m)$ is the number of representations of m as a sum of N odd squares. That is, $r_N^{\mathrm{odd}}(m)$ is the

number of solutions of

$$(2j_1+1)^2+(2j_2+1)^2+\cdots+(2j_N+1)^2=m \tag{11.2.9}$$

in integers. The integral in (11.2.8) can be evaluated in terms of Bessel functions by means of the formula

$$\int_{\mathbb{R}_+} t^{\nu-1}e^{-at-b/t}\mathrm{d}t = 2\left(\frac{b}{a}\right)^{\nu/2}K_\nu(2\sqrt{ab}). \tag{11.2.10}$$

to give

$$\begin{aligned}\pi^{-s}\Gamma(s)F(s) = 2\sum_{k\in\mathbb{N}}\sum_{m\in\mathbb{N}_0}(-1)^k r_N^{\mathrm{odd}}(8m+N)\left(\frac{8m+N}{4k^2}\right)^{(2s-N)/4} \\ \times K_{s-N/2}\left(\pi k\sqrt{8m+N}\right)\ .\end{aligned} \tag{11.2.11}$$

On using this result back in (11.2.1) we obtain the recursion relation for the Madelung constant in terms of the dimension N,

$$\begin{aligned}M_{N+1}(s) &= M_N(s)+\frac{4\pi^s}{\Gamma(s)}\sum_{k\in\mathbb{N}}\sum_{m\in\mathbb{N}_0}(-1)^k r_N^{\mathrm{odd}}(8m+N)\left(\frac{8m+N}{4k^2}\right)^{(2s-N)/4} \\ &\qquad\times K_{s-N/2}\left(\pi k\sqrt{8m+N}\right) \\ &= M_N(s)+\sum_{m\in\mathbb{N}_0} r_N^{\mathrm{odd}}(8m+N)c_{s,N}(m)\end{aligned} \tag{11.2.12}$$

with

$$c_{s,N}(m)=\frac{4\pi^s}{\Gamma(s)}\sum_{k\in\mathbb{N}}(-1)^k\left(\frac{8m+N}{4k^2}\right)^{(2s-N)/4}K_{s-N/2}\left(\pi k\sqrt{8m+N}\right)\ . \tag{11.2.13}$$

For fixed N, the term $r_N^{\mathrm{odd}}(8m+N)$ can become very large for larger m and N values, but is more than compensated by the exponentially decreasing Bessel function, which we discuss in detail in the next section. The $r_N^{\mathrm{odd}}(m)$ values can be determined recursively which is described in the Appendix.

While the recursion relation (11.2.12) is useful if the Madelung constant of lower dimension is known, we seek for a second formula where the recursion relation has been resolved. Here, we proceed as above and separate the sum for $M_{N+1}(s)$ into two cases according to whether $i_1=i_2=\cdots=i_N=0$ or i_1,

$i_2, \ldots, i_N$ are not all zero. This gives

$$M_{N+1}(s) = 2\sum_{k\in\mathbb{N}} \frac{(-1)^k}{k^{2s}} + g(s) \tag{11.2.14}$$

where

$$g(s) = \sum_{k\in\mathbb{Z}} \left({\sum_{i_1,\ldots,i_N\in\mathbb{Z}}}' \frac{(-1)^{i_1+\cdots+i_N+k}}{(i_1^2+i_2^2+\cdots+i_N^2+k^2)^s} \right).$$

Applying the integral formula for the gamma function and then the modular transformation for the theta function we obtain

$$\pi^{-s}\Gamma(s)g(s) = \int_{\mathbb{R}_+} t^{s-1} {\sum_{i_1,\ldots,i_N\in\mathbb{Z}}}' (-1)^{i_1+\cdots+i_N} e^{-\pi(i_1^2+\cdots+i_N^2)t} \sum_{k\in\mathbb{Z}} (-1)^k e^{-\pi k^2 t}\,\mathrm{d}t \tag{11.2.15}$$

$$= \int_{\mathbb{R}_+} t^{s-3/2} {\sum_{i_1,\ldots,i_N\in\mathbb{Z}}}' (-1)^{i_1+\cdots+i_N} e^{-\pi(i_1^2+\cdots+i_N^2)t} \sum_{k\in\mathbb{Z}} e^{-\pi(k+\frac{1}{2})^2/t}\,\mathrm{d}t$$

$$= 2\int_{\mathbb{R}_+} t^{s-3/2} {\sum_{i_1,\ldots,i_N\in\mathbb{Z}}}' (-1)^{i_1+\cdots+i_N} e^{-\pi(i_1^2+\cdots+i_N^2)t} \sum_{k\in\mathbb{N}} e^{-\pi(k-\frac{1}{2})^2/t}\,\mathrm{d}t,$$

where the last step follows by noting

$$\sum_{k\in\mathbb{Z}} e^{-\pi(k+\frac{1}{2})^2/t} = 2\sum_{k\in\mathbb{N}_0} e^{-\pi(k+\frac{1}{2})^2/t} = 2\sum_{k\in\mathbb{N}} e^{-\pi(k-\frac{1}{2})^2/t}. \tag{11.2.16}$$

In terms of the modified Bessel function this becomes, by (11.2.10),

$$\pi^{-s}\Gamma(s)g(s) = 4 {\sum_{i_1,\ldots,i_N\in\mathbb{Z}}}' \sum_{k\in\mathbb{N}} (-1)^{i_1+\cdots+i_N} \left(\frac{k-\frac{1}{2}}{\sqrt{i_1^2+\cdots+i_N^2}} \right)^{s-\frac{1}{2}}$$
$$\times K_{s-\frac{1}{2}}\left(2\pi(k-\frac{1}{2})\sqrt{i_1^2+\cdots+i_N^2} \right) \tag{11.2.17}$$

$$= 4\sum_{m\in\mathbb{N}}\sum_{k\in\mathbb{N}} (-1)^m r_N(m) \left(\frac{k-\frac{1}{2}}{\sqrt{m}} \right)^{s-\frac{1}{2}} K_{s-\frac{1}{2}}\left(2\pi(k-\frac{1}{2})\sqrt{m} \right).$$

On using this back in (11.2.14) we obtain

$$M_{N+1}(s) = -2\eta(2s) + \frac{4\pi^s}{\Gamma(s)} \sum_{m\in\mathbb{N}} (-1)^m r_N(m) \sum_{k\in\mathbb{N}} \left(\frac{k-\frac{1}{2}}{\sqrt{m}} \right)^{s-\frac{1}{2}}$$
$$\times K_{s-\frac{1}{2}}\left(\pi(2k-1)\sqrt{m} \right). \tag{11.2.18}$$

For the case of $N = 0$ the sum of the right-hand side is zero ($r_0(m) = 0$) and

we have $M_1(s) = -2\eta(2s)$ in agreement with Zucker's formula (11.1.7). We can conveniently write the sum in the form,

$$M_{N+1}(s) = -2\eta(2s) + \sum_{m\in\mathbb{N}} (-1)^m r_N(m) c_s(m) \tag{11.2.19}$$

with

$$c_s(m) = \frac{4\pi^s}{\Gamma(s)} m^{\frac{1-2s}{4}} \sum_{k\in\mathbb{N}} \left(k-\frac{1}{2}\right)^{s-\frac{1}{2}} K_{s-\frac{1}{2}}\left(\pi(2k-1)\sqrt{m}\right) \tag{11.2.20}$$

Note that the coefficients $c_s(m)$ are independent of the dimension N. The sum in (11.2.20) converges fast because of the exponential asymptotic decay of the Bessel function. The more problematic part is the convergence with respect to the first sum (see Eq.11.2.19) over m as we shall see.

As a special case we evaluate $M_N(1/2)$. Letting $s \to 1/2$ in (11.2.18) gives a formula for the $N+1$ dimensional Madelung constant

$$M_{N+1}(1/2) = -2\ln 2 + 4 \sum_{m\in\mathbb{N}} \sum_{k\in\mathbb{N}} (-1)^m r_N(m) K_0\left(\pi(2k-1)\sqrt{m}\right) \tag{11.2.21}$$

where $r_N(m)$ is the number of representations of m as a sum of N squares. The coefficient $c_{1/2}(m)$ becomes

$$c_{1/2}(m) = 4 \sum_{k\in\mathbb{N}} K_0\left(\pi(2k-1)\sqrt{m}\right) = 2\int_{\mathbb{R}_+} \frac{1}{\sinh(\pi\sqrt{m}\cosh t)}\, \mathrm{d}t. \tag{11.2.22}$$

where the integral is obtained using the formula [110]

$$K_0(z) = \int_{\mathbb{R}_+} e^{-z\ cosh(t)}\, \mathrm{d}t. \tag{11.2.23}$$

and summing the resulting geometric series. For example, taking $N = 2$ gives

$$M_3(1/2) = -2\ln 2 + 4 \sum_{m\in\mathbb{N}} \sum_{k\in\mathbb{N}} (-1)^m r_2(m) K_0\left(\pi(2k-1)\sqrt{m}\right) \tag{11.2.24}$$

On the other hand, using (11.2.12) and Zucker's equation (11.1.7) we get

$$M_3(1/2) = -4\beta(1/2)\eta(1/2) + 4 \sum_{k\in\mathbb{N}} \sum_{m\in\mathbb{N}_0} (-1)^k r_2^{\mathrm{odd}}(8m+2) \times \left(\frac{2k^2}{4m+1}\right)^{1/4} K_{1/2}\left(\pi k\sqrt{8m+2}\right) \tag{11.2.25}$$

m	$c_{1/2}(m)$	$r_2(m)$	$r_3(m)$	$r_4(m)$	$r_6(m)$	$r_8(m)$	$r_{10}(m)$
1	$1.18165052269629\times10^{-1}$	4	6	8	12	16	20
2	$2.72719460116136\times10^{-2}$	4	12	24	60	112	180
3	$9.11805054978030\times10^{-3}$	0	8	32	160	448	960
4	$3.66634491506766\times10^{-3}$	4	6	24	252	1136	3380
5	$1.65469973003050\times10^{-3}$	8	24	48	312	2016	8424
6	$8.09716792986126\times10^{-4}$	0	24	96	544	3136	16320
7	$4.21007519555378\times10^{-4}$	0	0	64	960	5504	28800
8	$2.29579583843101\times10^{-4}$	4	12	24	1020	9328	52020
9	$1.30128289377942\times10^{-4}$	4	30	104	876	12112	88660
10	$7.61717027007281\times10^{-5}$	8	24	144	1560	14112	129064
11	$4.58237287636094\times10^{-5}$	0	24	96	2400	21312	175680
12	$2.82249344482993\times10^{-5}$	0	8	96	2080	31808	262080
13	$1.77472886511553\times10^{-5}$	8	24	112	2040	35168	386920
14	$1.13644088647490\times10^{-5}$	0	48	192	3264	38528	489600
15	$7.39644406563549\times10^{-6}$	0	0	192	4160	56448	600960
16	$4.88482197748104\times10^{-6}$	4	6	24	4092	74864	840500
17	$3.26906868046647\times10^{-6}$	8	48	144	3480	78624	1137960
18	$2.21430457563634\times10^{-6}$	4	36	312	4380	84784	1330420
19	$1.51652113308388\times10^{-6}$	0	24	160	7200	109760	1563840
20	$1.04924116314272\times10^{-6}$	8	24	144	6552	143136	2050344
40	$2.62596820286192\times10^{-9}$	8	24	144	26520	1175328	32826664
60	$2.73153353546195\times10^{-11}$	0	0	576	54080	4007808	164062080
80	$5.89549945570033\times10^{-13}$	8	24	144	106392	9432864	525104424
100	$2.02339226243198\times10^{-14}$	12	30	744	164052	17893136	1282320348
120	$9.64273816463316\times10^{-16}$	0	48	576	213824	32909184	2625594240
140	$5.88915444967014\times10^{-17}$	0	48	1152	324480	49238784	4921862400
160	$4.37540432127918\times10^{-18}$	8	24	144	425880	75493152	8402122024
180	$3.81438178722105\times10^{-19}$	8	72	1872	478296	108353952	13297454504
200	$3.80087523208009\times10^{-20}$	12	84	744	664020	146925328	20513309148

Table 11.1 Coefficients $c_{1/2}(m)$ for exponent $s = 1/2$ and representations $r_N(m)$ for a number of m and N values.

11.3 Results

The coefficients $c_{1/2}(m)$ are listed in Table 11.1 together with few selected $r_N(m)$ values. The Madelung constants $M_N(s)$ for selected s values up to dimension $N = 20$ are listed in Table 11.2 and are depicted in Figures 11.2 and 11.3. The coefficients $c_s(M)$ are all positive for $s > 0$, which implies through (11.2.12) that $M_N(s) > M_{N+1}(s)$ for $s > 0$. For $N = 3$ and $s = 1/2$ the Madelung constant is readily evaluated to computer precision (summing $1 \leq m \leq 117$ to reach 14 significant digits (we chose $1 \leq k \leq 200$) as $M_3(1/2) = -1.74756459463318$ in agreement with the known value of Madelung's constant [64]. For larger exponents the series converges much faster, i.e. for $M_3(6)$ (Table 11.2) we need to sum only over $1 \leq m \leq 51$ to reach convergence to 14 significant digits behind the decimal point. Note that we used backwards summation as small numbers add up. We also checked our values for the even dimensions up to $N = 8$ with the values obtained from the analytical function in (11.1.7) by Zucker [107], and they are in perfect agreement.

N	m_{max}	$M_N(1/2)$	$M_N(3/2)$	$M_N(3)$	$M_N(6)$
1	0	-1.38629436111989	-1.80308535473939	-1.97110218259487	-1.99951537028771
2	101	-1.61554262671282	-2.64588653230643	-3.49418521170288	-3.93702124248001
3	117	-1.74756459463318	-3.23862476605177	-4.78844371389142	-5.82302778890550
4	135	-1.83939908404504	-3.70269117771204	-5.93191305089188	-7.66458960508610
5	158	-1.90933781561876	-4.08665230978501	-6.96536812867633	-9.46689838517490
6	184	-1.96555703900907	-4.41541406455743	-7.91367677818339	-11.2339815395894
7	212	-2.01240598979798	- 4.70360905429867	-8.79344454973204	-12.9690759046272
8	240	-2.05246682726927	-4.96062369646463	-9.61645522527675	-14.6748510064791
9	268	-2.08739431267374	-5.19286448579961	-10.3914475289766	-16.3535526240382
10	302	-2.11831050138482	-5.40491155391300	-11.1251231380028	-18.0071001619883
11	338	-2.14601010324383	-5.60015959755479	-11.8227595210275	-19.6371554488071
12	375	-2.17107583567180	-5.78119850773166	-12.4886029215377	-21.2451729486919
13	415	-2.19394722663803	-5.95005160868701	-13.1261312983588	-22.8324373927323
14	458	-2.21496368855843	-6.10833126513306	-13.7382364790321	-24.4000926119446
15	504	-2.23439258374969	-6.25734417113144	-14.3273540620924	-25.9491640475311
16	552	-2.25244813503955	-6.39816474499813	-14.8955583649474	-27.4805766108785
17	603	-2.26930453765447	-6.53168761111553	-15.4446333073194	-28.9951690545215
18	657	-2.28510527781503	-6.65866596401893	-15.9761263123420	-30.4937056794534
19	714	-2.29996989965861	-6.77974015828765	-16.4913899618245	-31.9768859775816
20	773	-2.31399901326838	-6.89545937988985	-16.9916146519184	-33.4453526516541

Table 11.2 Calculated Madelung constants $M_N(s)$ up to dimension N =20 for selected s values. The last digit has not been rounded. m_{max} is the maximum integer value in the sum over m in Eq.(11.2.19), where the remainder $R_{(m_{max}+1)} < 10^{-14}$ for $M_N(1/2)$.

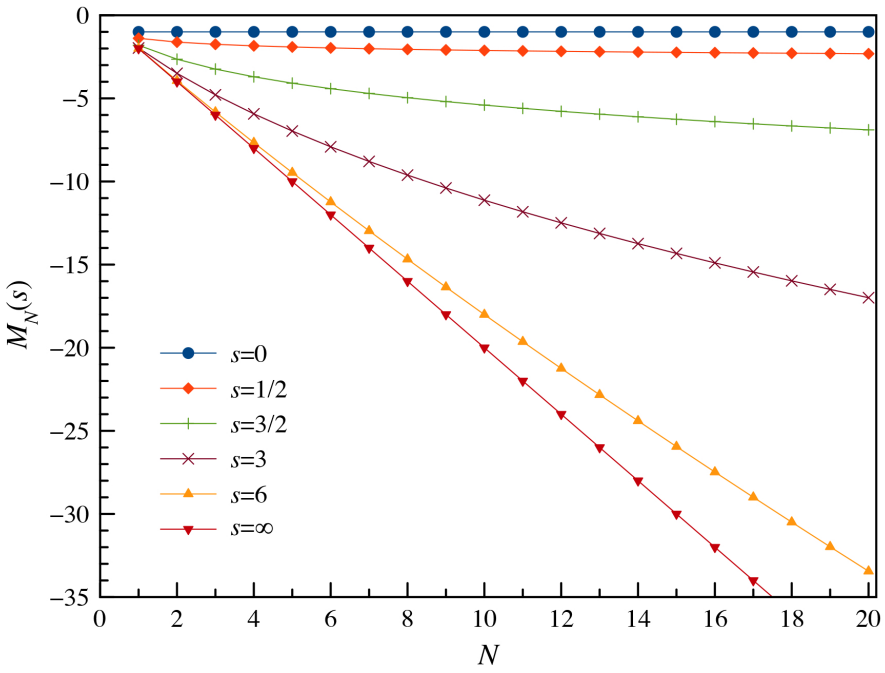

Figure 11.2 Madelung constants, $M_N(s)$, as a function of the dimension N.

To discuss the convergence behavior of the series (11.2.19) we observe that the coefficients $c_{1/2}(m)$ are rapidly decreasing with increasing m. However, at the same time the $r_N(m)$ values increase also rapidly with increasing m (and increasing N) shown in Figure 11.4. The asymptotic behavior of the Bessel functions is well known, i.e.they decrease exponentially with increasing m, $K_s(x) \sim (\pi/2x)^{\frac{1}{2}} e^{-x}$. On the other hand, the sum of squares representation increases polynomially for fixed N [360–362], e.g. we know from Ramanujan's work that $r_{2N}(m) = \mathcal{O}(m^N)$ (derived from Eq.(14) in Ref.[363]). This is also seen in the logarithmic behavior of $log_{10} r_N(m)$ in Figure 11.4. This implies that the Madelung series expansion in terms of Bessel functions is converging, but very slowly for higher dimensions because of a very large dimensional prefactor. This can clearly seen from the m_{max} values for $M_N(1/2)$ in Table 11.2. For $M_N(s), s \geq 1/2$ we approximately have $m_{max} \leq nint(1.16N^2 + 11.5N + 73)$, where n*int* represents the nearest integer function.

Perhaps more problematic is the appearance of large numbers due to the $r_N(m)$ values in the sum over m in Eq.(11.2.19) where one reaches soon the limit with double precision arithmetic at large N values. This is clearly seen in Figure 11.5 for the case of dimension 16 and $s = 1/2$ which shows for the

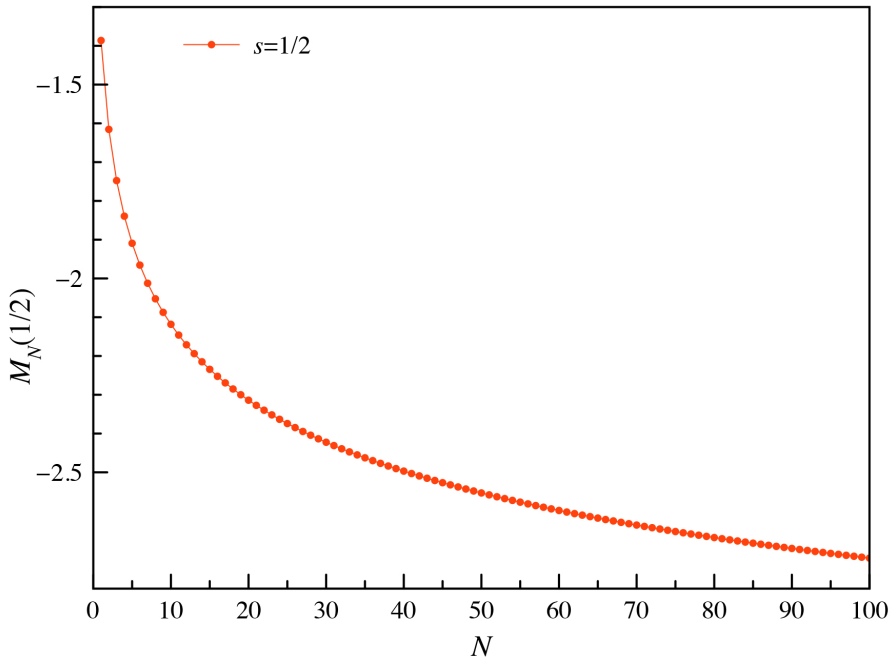

Figure 11.3 Madelung constants, $M_N(1/2)$, as a function of the dimension N up to $N = 100$.

individual terms a strong oscillating behavior and polynomial increase up to rather large values around $m = 14$ followed by an exponential decay. For higher dimensions this maximum shifts to higher m values before the exponential decay sets in. However, if we add pairs of positive and negative terms in the oscillating series to obtain new coefficients $b(2m) = a(2m) + a(2m-1)$, we experience a far smoother and better convergence behavior.

By using the recursive formula (11.2.12) instead we obtain much fast convergence as we reach the exponential decay far earlier because of the argument $8m+N$ in the Bessel function, see Figure 11.6. Here we avoid such large values and the strong oscillating behavior as the sign change appears in the summation over k in .(11.2.19) rather than in (11.2.12). Hence, for accuracy reasons Eq.(11.2.12) is preferred, and we used this equation instead for the values in Table 11.2.

Concerning the analytical continuation all standard functions used including the Bessel function, gamma function and the Dirichlet eta function can be analytically continued (see Appendix) as shown in Figure 11.7. Moreover, the

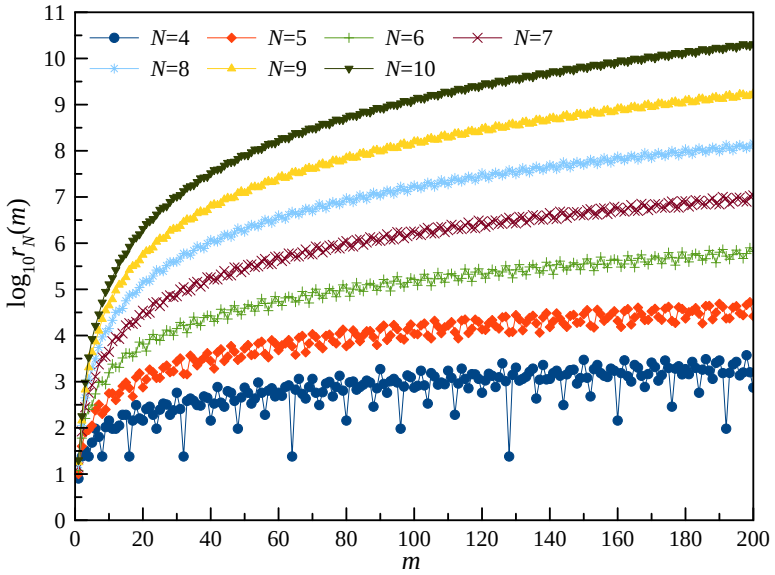

Figure 11.4 Representations for number of squares, $r_N(m)$, for dimensions $N = 4 - 10$.

Madelung constants $M_N(s)$ are all smooth functions without any singularities for all $s \in \mathbb{R}$. For example, from Zucker's formula of $M_8(s) = -16\eta(s-3)\zeta(s)$ we see that for $s = 1$ we have $\zeta(1) = \infty$ and $\eta(-2) = 0$. However, it can easily be shown that the product of the two functions gives a finite value for $s = 1$.

Equations (11.2.12) and (11.2.18) allow for some interesting analysis. The gamma function $\Gamma(x)$ has poles at $x = 0, -1, -2, \ldots$ for which the Bessel sum in (11.2.12) and (11.2.18) vanishes. In this case we get

$$M_N(s) = -2\eta(2s) \quad if\ s = 0, -1, -2, \ldots \tag{11.3.1}$$

which is independent of the dimension N. This implies that all Madelung curves cross at these critical points. Moreover, from the Dirichlet eta function we know that $\eta(2s) = 0$ for $s = -1, -2, \ldots$. This behavior is nicely seen in Figure 11.7. Comparing with Zucker's formulas we see that this is easily fulfilled for the specific dimensions given. Concerning the usual Madelung constant at $s = 1/2$ we see that they lie close to the crossing point at $s = 0$ which explains their rather slow decrease with increasing dimension N.
Zucker was able to evaluate the Madelung series analytically for even dimensions up to $N = 8$ [107] based on previous work of Glasser [364, 365]. He

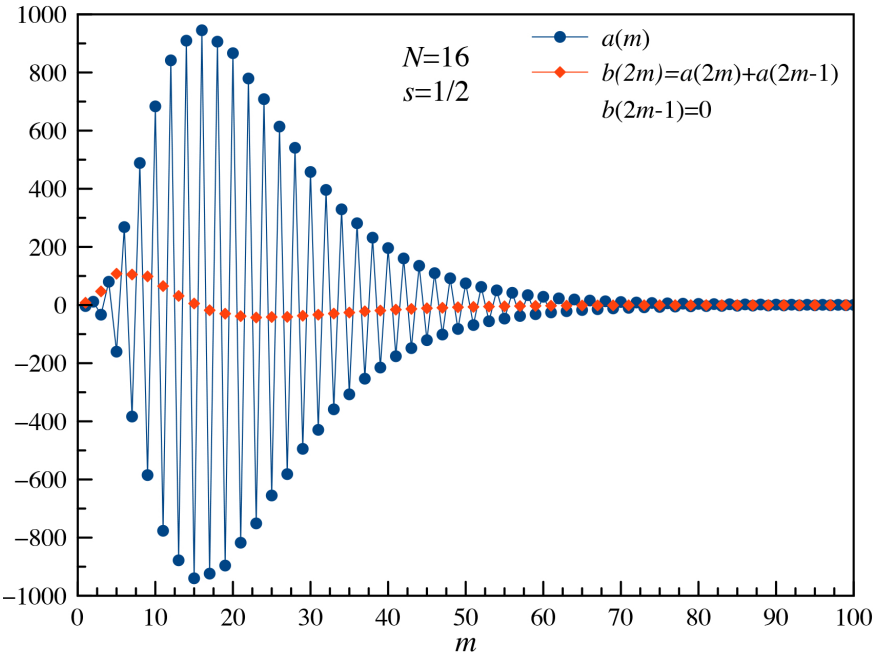

Figure 11.5 Convergence behaviour for for the Madelung constant with $s = 1/2$ and $N = 16$. Shown are the coefficients $a(m) = (-1)^m r_{15}(m) c_s(m)$ of Eq.(11.2.19) (in blue) and the corresponding coefficients by adding the odd and even terms, $b(2m) = a(2m) + a(2m-1)$ (in red). The sum of these values converge against the Bessel sum value of -0.866153773918593.

further conjectured that $M_3(s)$ may be expressed in terms of a yet unknown Dirichlet series (for a recent analysis of lattice sums arising from the Poisson equation see Ref.[366]). Of considerable help for future investigations will be the condition that $M_N(0) = -1$ and $M_N(-n) = 0$ for all $n \in \mathbb{N}$. At these critical points we have the following properties

$$\begin{aligned}
&\zeta(0) = -\frac{1}{2} \quad , \quad \zeta(-2n) = 0 \quad , \quad \zeta(-n) = (-1)^n \frac{B_{n+1}}{n+1} \\
&\eta(0) = \frac{1}{2} \quad , \quad \eta(-2n) = 0 \quad , \quad \eta(-n) = \frac{\left(2^{n+1}-1\right)}{n+1} B_{n+1} \\
&\beta(0) = \frac{1}{2} \quad , \quad \beta(-2n+1) = 0 \quad , \quad \beta(-n) = \frac{E_n}{2}
\end{aligned} \tag{11.3.2}$$

where B_n and E_n are the Bernoulli and Euler numbers respectively [79]. For example, from Zucker's formulas (11.1.10) and (11.1.11) we follow immediately that $M_6(0) = E_2 = -1$ and $M_8(0) = 2(2^4 - 1)B_4 = -1$. Further, because of $\lim_{s\to\infty} \eta(s) = 1$, $\lim_{s\to\infty} \beta(s) = 1$, $\lim_{s\to\infty} \zeta(s) = 1$ we see that the coeffi-

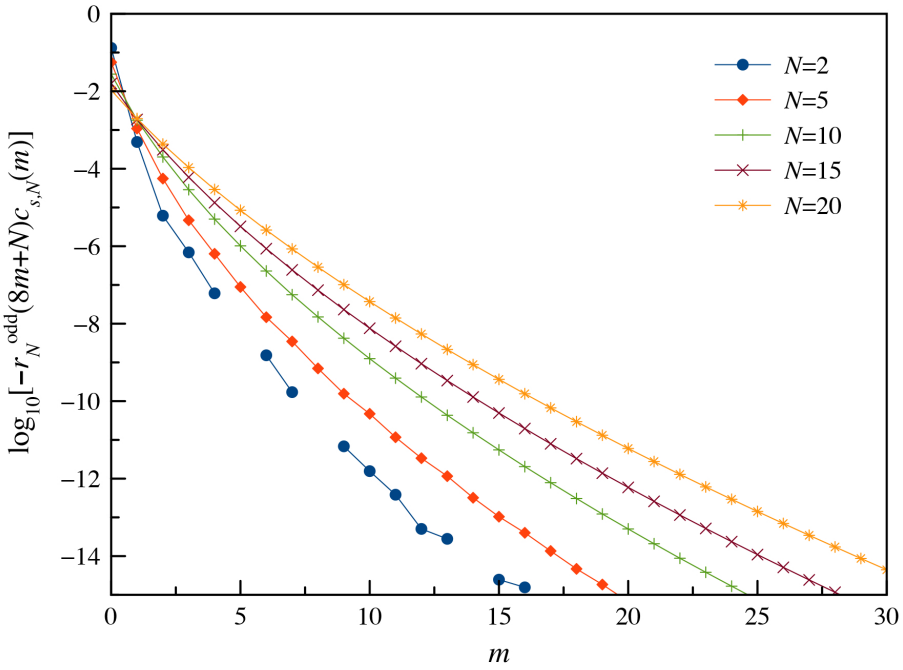

Figure 11.6 Convergence behaviour for the Madelung constants with $s = 1/2$. Shown are the numbers $log_{10}[-d(m)]$ with the coefficients $d(m) = r_N^{odd}(8m+N)c_{s,N}(m)$ from Eq.(11.2.12). For $N = 2$ the missing points have zero value for $r_N^{odd}(8m+N)$.

cients in front of the functions in eqs.(11.1.7)-(11.1.11) add up to exactly $-2N$. It is, however, incorrect to assume that analytical formulas in terms of these standard functions can be obtained for higher even dimensions. For a detailed discussion we refer to Appendix B. In this sense, our expansions in terms of Bessel functions is perhaps the closest general form for a fast convergent series we can get for the N-dimensional Madelung constant.

11.4 Conclusions

We presented fast convergent expressions for the Madelung constant in terms of Bessel function expansions which allow for an asymptotic exponential decay of the series. Even for higher dimensions the Madelung constants can be evaluated efficiently and accurately through the recursive expression or by using computer algebra to work with the generating functions. The number of representations of the N sum of squares can also be efficiently handled through recursive relations. The Madelung constants and their analytical continuations

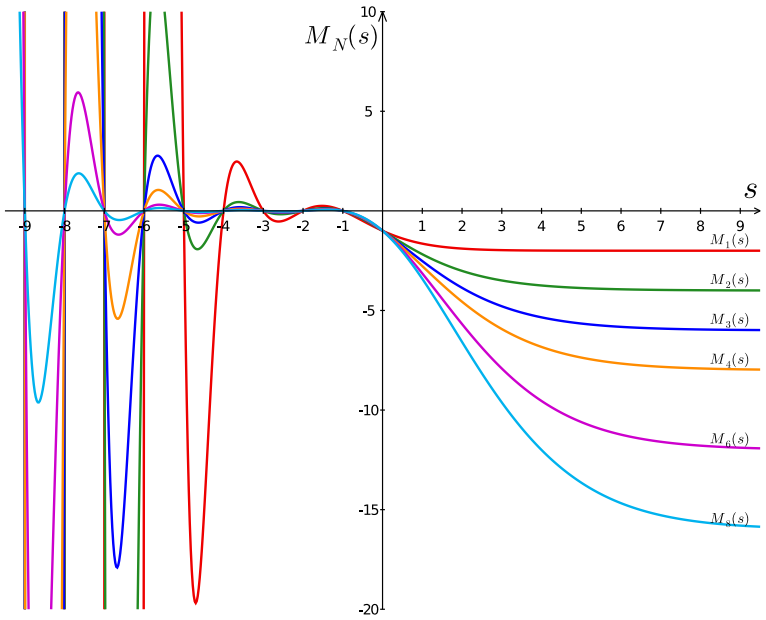

Figure 11.7 The Madelung constant $M_1(s), M_2(s), M_3(s), M_4(s), M_6(s)$ and $M_8(s)$ for $s \in [-9,9]$.

can be calculated easily by standard mathematical software packages to any precision. These numbers may be useful for future explorations of analytical formulas in higher dimensions. For $s \geq 1/2$ a Fortran program with double precision accuracy is available from our CTCP website [143].

11.5 Appendix

A Special Functions

We give a brief overview over the special functions used in this work. More details can be found in the book by Andrews [79]. The Dirichlet (or L-) series (Riemann zeta, Dirichlet eta, and Dirichlet beta functions) are defined as

$$\zeta(s) = \sum_{i \in \mathbb{N}} i^{-s}, \tag{11.A.1}$$

$$\eta(s) = \sum_{i \in \mathbb{N}} (-1)^{i-1} i^{-s} = \left(1 - 2^{1-s}\right) \zeta(s). \tag{11.A.2}$$

$$\beta(s) = \sum_{i \in \mathbb{N}} (-1)^{i+1} (2i-1)^{-s}. \tag{11.A.3}$$

Their analytic continuations to L-functions into the negative real part (or the whole complex plane) are given by [364]

$$\eta(-s) = s(2-2^{-s})\pi^{-s-1}sin(\tfrac{\pi}{2}s)\Gamma(s)\zeta(s+1)\,. \tag{11.A.4}$$

$$\beta(1-s) = \left(\frac{\pi}{2}\right)^{-s} sin(\tfrac{\pi}{2}s)\Gamma(s)\beta(s)\,. \tag{11.A.5}$$

$$\zeta(-s) = -2^{-s}\pi^{-s-1}\left(\frac{\pi}{2}\right)^{-s} sin(\tfrac{\pi}{2}s)\Gamma(s+1)\zeta(s+1)\,. \tag{11.A.6}$$

Here, the gamma function is usually defined for real positive numbers as

$$\Gamma(s) = \int_{\mathbb{R}_+} x^{s-1}e^{-x}dx\,. \tag{11.A.7}$$

and when $s = n \in \mathbb{N}$ we have $\Gamma(n) = (n-1)!$. The gamma function on the whole real axis is then defined as the analytic continuation of this integral function to a meromorphic function by the simple recursion relation $\Gamma(x) = \Gamma(x+1)/x$ with $1/\Gamma(-n) = 0$ for $n \in \mathbb{N}_0$ [367].
The modified Bessel function of the second kind is defined as

$$K_\nu(x) = \frac{1}{2}\int_{\mathbb{R}_+} u^{\nu-1}exp\left\{-x\left(u+u^{-1}\right)/2\right\}du\,, \tag{11.A.8}$$

The higher-order Bessel functions can be successively reduced to lower order Bessel functions by

$$K_\nu(x) = \frac{2(\nu-1)}{x}K_{\nu-1}(x) + K_{\nu-2}(x)\,, \tag{11.A.9}$$

and we use the symmetry $K_{-\nu}(x) = K_\nu(x)$ for its analytical continuation.
The representations of the sum of squares is obtained from the recursive formula

$$r_{N+1}(m) = r_N(m) + 2\sum_{\substack{i\in\mathbb{N}\\ m-i^2\geq 0}} r_N(m-i^2) \tag{11.A.10}$$

keeping in mind that $r_N(0) = 1$. Eq.(11.A.10) can easily be derived from its generating function,

$$\sum_{m\in\mathbb{N}_0} r_N(m) = \left(\sum_{k\in\mathbb{Z}} q^{k^2}\right)^N. \tag{11.A.11}$$

In a similar fashion one obtains a recursive formula for the sum of odd squares,

$$r^{odd}_{N+1}(m) = 2\sum_{\substack{i\in\mathbb{N}\\ m-(2i-1)^2>0}} r^{odd}_N(m-(2i-1)^2) \tag{11.A.12}$$

keeping in mind that $r^{odd}_N(0) = 0$ and we do not include this term in our sum-

mation. For completeness we mention that the sum of even squares is trivially related to the sum of squares by $r_N^{even}(4m) = r_N(m)$ and $r_N^{even}(m) = 0$ if m is not divisible by 4.

B Why Zucker's analytical formulas do not continue into higher dimensions

Zucker's formulas (11.1.7)-(11.1.11) are equivalent to Jacobi's formulas for sums of 2, 4, 6 and 8 squares (e.g., see [132] pp. 177, 202, 238):

$$\left(\sum_{j\in\mathbb{Z}}(-1)^j q^{j^2}\right)^2 = 1-4\sum_{n\in\mathbb{N}}\chi_4(n)\frac{q^n}{1+q^n}, \tag{11.B.13}$$

$$\left(\sum_{j\in\mathbb{Z}}(-1)^j q^{j^2}\right)^4 = 1+8\sum_{j\in\mathbb{N}}\frac{j(-q)^j}{1+q^j}, \tag{11.B.14}$$

$$\left(\sum_{j\in\mathbb{Z}}(-1)^j q^{j^2}\right)^6 = 1+4\sum_{j\in\mathbb{N}}\chi_4(j)\frac{j^2q^j}{1+q^j}+16\sum_{j\in\mathbb{N}}\frac{j^2(-q)^j}{1+q^{2j}}, \tag{11.B.15}$$

$$\left(\sum_{j\in\mathbb{Z}}(-1)^j q^{j^2}\right)^8 = 1+16\sum_{j\in\mathbb{N}}\frac{j^3(-q)^j}{1-q^j}, \tag{11.B.16}$$

respectively, where

$$\chi_4(n) = \sin\frac{n\pi}{2} = \begin{cases} 1 & \text{if } n\equiv 1 \pmod 4,\\ -1 & \text{if } n\equiv 3 \pmod 4,\\ 0 & \text{otherwise.}\end{cases} \tag{11.B.17}$$

For example, the formula (11.B.16) can be written in the form

$$\sum_{i_1,i_2,\ldots,i_8\in\mathbb{Z}}{}' (-1)^{i_1+i_2+\cdots+i_8}\, q^{i_1^2+i_2^2+\cdots+i_8^2} = 16\sum_{j\in\mathbb{N}}\sum_{k\in\mathbb{N}} j^3(-1)^j q^{jk}. \tag{11.B.18}$$

Put $q = e^{-u}$, multiply both sides by u^{s-1} and integrate, to obtain

$$\sum_{i_1,i_2,\ldots,i_8\in\mathbb{Z}}{}' (-1)^{i_1+i_2+\cdots+i_8}\int_{\mathbb{R}_+} u^{s-1}e^{-u(i_1^2+i_2^2+\cdots+i_8^2)}\mathrm{d}u = 16\sum_{j\in\mathbb{N}}\sum_{k\in\mathbb{N}} j^3(-1)^j\int_{\mathbb{R}_+} u^{s-1}e^{-ujk}\mathrm{d}u. \tag{11.B.19}$$

The integrals can be evaluated using Eq.(11.A.7) to give

$$\sum_{i_1,i_2,\ldots,i_8\in\mathbb{Z}}{}' \frac{(-1)^{i_1+i_2+\cdots+i_8}}{(i_1^2+i_2^2+\cdots+i_8^2)^s} = 16\sum_{j\in\mathbb{N}}\sum_{k\in\mathbb{N}}\frac{j^3(-1)^j}{(jk)^s}, \tag{11.B.20}$$

where the common factor $\Gamma(s)$ has been cancelled from each side. In other words, we have obtained

$$\begin{aligned} M_8(s) &= 16\left(\sum_{j\in\mathbb{N}}\frac{j^3(-1)^j}{j^s}\right)\left(\sum_{k\in\mathbb{N}}\frac{1}{k^s}\right) \\ &= -16\left(\sum_{j\in\mathbb{N}}\frac{(-1)^{j-1}}{j^{s-3}}\right)\left(\sum_{k\in\mathbb{N}}\frac{1}{k^s}\right) \\ &= -16\eta(s-3)\zeta(s). \end{aligned} \tag{11.B.21}$$

Thus we have obtained Zucker's formula (11.1.11) from the sum of squares formula (11.B.16).

The process is reversible, so (11.1.11) is equivalent to (11.B.16).

By similar calculations, each of Zucker's formulas (11.1.8)–(11.1.11) is equivalent to the respective formula in (11.B.13)–(11.B.16).

By analogy with $M_8(s)$ in Eq.(11.1.11), it is tempting to speculate that there might be expressions for $M_{10}(s)$ and $M_{12}(s)$ as finite sums of the forms

$$M_{10}(s) = \sum_i f_i(s-4)g_i(s) \quad \textit{and} \quad M_{12}(s) = \sum_i F_i(s-5)G_i(s) \tag{11.B.22}$$

for certain L-functions $f_i(s)$, $g_i(s)$, $F_i(s)$ and $G_i(s)$. However this is unlikely to be true for reasons that we shall now explain.

There are formulas for sums of 10, 12, 14, ... squares that are similar to Jacobi's (11.B.13)–(11.B.16), but they involve other more complicated terms called cusp forms [368]. Glaisher found the formulas for 10, 12, 14, 16 and 18 squares, and a general formula for any even number of squares was obtained by Ramanujan. The formulas for sums of 10 and 12 squares are

$$\left(\sum_{j\in\mathbb{Z}}(-1)^j q^{j^2}\right)^{10} = 1 - \frac{4}{5}\sum_{j\in\mathbb{N}}\frac{\chi_4(j)j^4q^j}{1+q^j} + \frac{64}{5}\sum_{j\in\mathbb{N}}\frac{j^4(-q)^j}{1+q^{2j}} - \frac{32}{5}E_{10}(q) \tag{11.B.23}$$

and

$$\left(\sum_{j\in\mathbb{Z}}(-1)^j q^{j^2}\right)^{12} = 1+8\sum_{j\in\mathbb{N}}\frac{j^5(-q)^j}{1+q^j} - 16E_{12}(q) \tag{11.B.24}$$

where

$$E_{10}(q) = q\prod_{j\in\mathbb{N}}\frac{(1-q^{2j})^{14}}{(1-q^j)^4} \quad \text{and} \quad E_{12}(q) = q\prod_{j\in\mathbb{N}}(1-q^{2j})^{12}. \tag{11.B.25}$$

For a statement of the general formula, see [132] (p. 214). A proof of the general formula and references to other proofs can be found in Ref.[369].

There is no simple formula for the coefficients in the expansions of $E_{10}(q)$ or $E_{12}(q)$, but they satisfy some remarkable properties. For example, if we write

$$E_{12}(q) = \sum_{n\in\mathbb{N}} e_{12}(n)q^n \tag{11.B.26}$$

then it is known that

$$e_{12}(mn) = e_{12}(m)e_{12}(n) \tag{11.B.27}$$

if m and n are relatively prime. For prime powers, there is the three-term recurrence

$$e_{12}(p^{\lambda+1}) = e_{12}(p)e_{12}(p^\lambda) - p^5 e_{12}(p^{\lambda-1}). \tag{11.B.28}$$

Furthermore, Ramanujan proved that

$$|e_{12}(n)| = O(n^{3+\varepsilon}) \quad \text{as } n\to\infty \tag{11.B.29}$$

and conjectured that

$$|e_{12}(n)| \le n^{5/2}d(n) \tag{11.B.30}$$

where $d(n)$ is the number of divisors of n. In fact Ramanujan had a conjecture for a sum of $2k$ squares ($k \ge 5$), and that conjecture was proved by Deligne about 50 years later (as part of work for which he subsequently received the Fields medal).

To complete the example for the 12-dimensional lattice, if we put $q = e^{-u}$ in (11.B.24), multiply by u^{s-1} and integrate, the result is

$$M_{12}(s) = -8\eta(s-5)\eta(s) - 16\sum_{n\in\mathbb{N}}\frac{e_{12}(n)}{n^s}, \tag{11.B.31}$$

where the coefficients $e_{12}(n)$ are as above. It was known to Ramanujan that

the Dirichlet series can be factored, and hence we obtain the formula

$$M_{12}(s) = -8\eta(s-5)\eta(s) - 16\prod_p \frac{1}{\left(1 - \frac{e_{12}(p)}{p^s} + \frac{1}{p^{2s-5}}\right)} \qquad (11.B.32)$$

where the product is over the odd prime values of p. The first few values are as follows: $e_{12}(3) = -12, e_{12}(5) = 54, e_{12}(7) = -88, e_{12}(11) = 540, e_{12}(13) = -418, e_{12}(17) = 594, e_{12}(19) = 836, e_{12}(23) = -4104, e_{12}(29) = -594$.

The formula (11.B.32) is the analogue of Zucker's formulas for the 12-dimensional lattice. Similar formulas can be given for sums of $2k$ squares for any positive integer k. The number of cusp forms is $\lfloor (k-1)/4 \rfloor$. In particular, there are no cusp forms for $1 \le k \le 4$ corresponding to Zucker's formulas for the lattice sums in 2, 4, 6 or 8 dimensions; there is one cusp form for $5 \le k \le 8$ corresponding to the lattice sums in 10, 12, 14 or 16 dimensions; and there are two cusp forms for $9 \le k \le 12$ corresponding to the lattice sums in 18, 20, 22 or 24 dimensions.

As a consequence of Ramanujan's conjectures and Deligne's proofs, we now know that the number of representations of N as a sum of an even number $2k$ squares is given by a dominant term that involves a sum of the $(k-1)$th powers of the divisors of N, plus a correction term (the coefficient in a cusp form) that is roughly the square root in magnitude of the dominant term. When the number of squares is 2, 4, 6 or 8 there is no cusp form, and the divisor sum formula is exact, and that is the reason the formulas of Zucker exist. When the number of squares is 10, 12, 14, ..., there is an increasing number of cusp forms, and there is no easy formula for the coefficients in their power series expansions. That is the reason why Zucker's formulas stop at 8 dimensions, and why there are no similar formulas for dimensions 10, 12, 14, ...

12 Project 7 - The Lattice Sum for a Hexagonal Close Packed Structure and its Dependence on the c/a Ratio of the Hexagonal Cell Parameters[a]

12.1 Introduction

The hexagonal close packed structure (hcp) shown in Figure 12.1 with a packing sequence of $(AB)_\infty$ is made up of hexagonal layers in three dimensions and has the same packing density ($\rho = \pi/3\sqrt{2}$) as the face-centered cubic structure (fcc) with a stacking sequence of $(ABC)_\infty$. It has only recently been proven by Hales that the fcc packing density cannot be surpassed (Kepler's original conjecture [370]) and therefore is optimal.[371] Of course, any Barlow packing, which are mixtures of hcp and fcc stacking sequences, such as ABABCABAB..., is also optimal, and there are infinitely many.[166, 372–374]

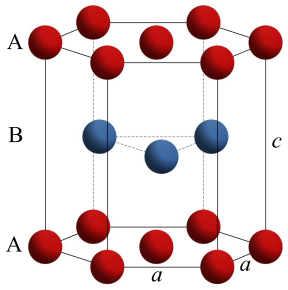

Figure 12.1 The hcp structure with ABABAB... sequence (layers A in red and B in blue) of hexagonal close-packed layers, and corresponding cell parameters a and c. The ratio $c/a = \sqrt{8/3}$ leads to the optimal hcp lattice with 12 kissing spheres around a central atom.

In 1924, Lennard-Jones and Ingham used an inverse power law potential of the

[a]This chapter is composed of sections from unpublished results. Some sections may have been modified to fit the style of this thesis.

form

$$V_{\mathrm{LJ}}(r) = \frac{\varepsilon nm}{n-m}\left[\frac{1}{n}\left(\frac{r_e}{r}\right)^n - \frac{1}{m}\left(\frac{r_e}{r}\right)^m\right], \tag{12.1.1}$$

for $n > m$ ($n, m \in \mathbb{R}$ and $n, m > 3$) and lattice sums L_n in order to obtain estimates for the cohesive energies for the simple cubic (sc), body-centered cubic (bcc) and face-centered cubic (fcc) lattices, given by [6, 22],

$$E_{\mathrm{LJ}}^{\mathrm{coh}}(R) = \frac{\varepsilon nm}{2(n-m)}\left[\frac{L_n}{n}\left(\frac{r_e}{R}\right)^n - \frac{L_m}{m}\left(\frac{r_e}{R}\right)^m\right]. \tag{12.1.2}$$

In the above equation, r_e is the minimum distance for the LJ potential, R represents the nearest neighbor distance r_{NN} or a lattice constant for the solid, and ε is the dissociation energy between two atoms. The potential form in (12.1.1) would later come to be commonly known as the Lennard-Jones potential and become one of the most widely used two body potentials. The lattice sums for the cubic lattices are infinite sums in terms of quadratic forms involving the (3×3) Gram matrix G,

$$L_n = \sum_{\vec{i} \in \mathbb{Z}^3 \setminus \vec{0}} \left(\vec{i}^{\top} G \vec{i}\right)^{-n/2}. \tag{12.1.3}$$

The components of G are defined by the scalar products of three lattice vectors $\vec{b}_i$ defining the Bravais lattice in question (setting the nearest neighbour distance to one), i.e. $(G_{ij}) = (\vec{b}_i^{\top} \vec{b}_j)$. For example, in the simple cubic lattice, G becomes the identity matrix. Such lattice sum expressions can easily be extended to higher dimensions ($N > 3$), and in principle to other type of potentials, although expressions for L_n can become rather more complicated functions of the underlying lattice.[26, 375] A nice example here is the Madelung constant for dimensions up to $N = 4$ and even dimensions $N = 6$ and 8.[26, 107] The series (12.1.3) converges for $n > 3$ and diverges otherwise.

There are many different methods to convert the usually slow convergent lattice sums for inverse power potentials into fast converging series for which a detailed account is given by Borwein et al.[26] This allows analytical continuation into the region ($n < 3$ or the cubic lattices) where such series shown in (12.1.3) diverges. Some of these methods have recently be used to produce fast converging series [311] in analogy to Lennard-Jones' early attempts.[6, 22]

In 1940, Kane and Goeppert-Mayer evaluated the lattice sum for the ideal hcp structure [24]. Although they did not provide an explicit formula for the lattice sum in their paper (which was given later by Bell and Zucker [70]), their values obtained from direct summation plus estimate of the remainder

for L_n where $n = 6$, 8, 10 and 12 were accurate to four decimal places. They stated that "*for the hexagonal crystal, the method used by Lennard-Jones could not easily be adopted, so we have used a more tedious and less elegant method* " [24], which was by direct summation [48]. Borwein et al. decomposed the hcp lattice in terms of four different lattice sums containing quadratic functions, but did not provide an efficient method for evaluating them.[26]

In a recent paper[160] we introduced lattice sums for cubic lattices and the hcp structure followed by various expansion methods using Bessel functions. The derived expansions for the hcp lattice were all restricted to the ideal ratio of $c/a = \sqrt{8/3}$ and were in some cases rather cumbersome. Here we introduce new and more efficient fast converging expressions for the lattices sums of the hcp structure with an arbitrary c/a ratio. We analyze the lattice in detail for the Lennard-Jones potential defined in (12.1.1), and look for possible symmetry breaking effects where the kissing number (number of touching spheres around a central atom in a lattice) of the 12 equidistant atoms from the central atom is lowered. Here we mention that recently a second metastable minimum was found in solid-state calculations using an extended Lennard-Jones potential and direct lattice summations [376], and we will show that an analytical treatment using exact lattice summations, leads not only to the same metastable minimum but gives insight in why such a minimum exists. Moreover, we discuss the relationship with the fcc lattice in terms of lattice sums.

12.2 The Lattice Sum for the hcp structure

If only a simple hexagonal lattice is considered, the basis vectors for the hexagonal Bravais lattice are given by the following lattice vectors,

$$\vec{b}_1^{\top} = a\,(1,0,0)\,, \quad \vec{b}_2^{\top} = a\left(\frac{1}{2},\frac{\sqrt{3}}{2},0\right), \quad \vec{b}_3^{\top} = c\,(0,0,1)\,. \tag{12.2.1}$$

This leads to the following positive definite symmetric Gram matrix

$$(G_{ij}) = \left(\vec{b}_i^{\top}\vec{b}_j\right) = a^2 \begin{pmatrix} 1 & \frac{1}{2} & 0 \\ \frac{1}{2} & 1 & 0 \\ 0 & 0 & \frac{c^2}{a^2} \end{pmatrix}, \tag{12.2.2}$$

with $\det(G) = \frac{3}{4}a^4c^2 > 0$. From an arbitrarily chosen atom at the origin, all points in the hexagonal lattice are described by

$$\vec{r}_{ijk} = i\vec{b}_1 + j\vec{b}_2 + k\vec{b}_3 \,. \tag{12.2.3}$$

Their distances to the origin are given by the quadratic form

$$r_{ijk} = \left(\vec{v}^{\top} G \vec{v}\right)^{\frac{1}{2}} = a\left(i^2 + ij + j^2 + \frac{c^2}{a^2}k^2\right)^{\frac{1}{2}} , \tag{12.2.4}$$

with $\vec{v}^{\top} = (i, j, k) \in \mathbb{Z}^3$ and $i, j, k \in \mathbb{Z}$ ($i = j = k = 0$ excluded). The volume of the unit cell is determined through the Gram matrix

$$V(a,c) = \sqrt{\det G} = \frac{\sqrt{3}}{2} a^2 c \tag{12.2.5}$$

The nearest neighbor distance is given by

$$r_{\mathrm{NN}} = \min\{r_{ijk}\} = \min\{a, c\} \,. \tag{12.2.6}$$

For the following we define the parameter $\gamma = c/a > 0$ and set arbitrarily $a = 1$. This leads to the following lattice sum for potentials $\sim r^{-n}$ such as the Lennard-Jones potential,

$$L^A(s,\gamma) = {\sum_{i,j,k\in\mathbb{Z}}}' \left(i^2 + ij + j^2 + \gamma^2 k^2\right)^{-s} \tag{12.2.7}$$

with $s = n/2$. The prime on the sum indicates that the summation is over all integers except for the term corresponding to $i = j = k = 0$. We note here that these lattice sums can be seen as special cases of the Epstein zeta function.[117] A peculiarity of this lattice sum is that $\lim_{s\to\infty} L^A(s,\gamma) = \infty$ for $\gamma < 1$, and one has to take special care of large s values in this small γ region.

The hcp structure is a multi-lattice characterised by two nested hexagonal Bravais lattices with one layer shifted by a vector of $\vec{v}_s^{\top} = a\left(\frac{1}{2}, \frac{1}{2\sqrt{3}}, \frac{c}{2a}\right)$ with respect to the lattice vectors given in (12.2.1), so that the position of any atom in the B layers is given by

$$\vec{r}^{\,\mathrm{AB}}_{ijk} = i\vec{b}_1 + j\vec{b}_2 + k\vec{b}_3 + \vec{v}_s \,, \tag{12.2.8}$$

with $\vec{b}_1, \vec{b}_2$ and $\vec{b}_3$ as in (12.2.1). The shift vector can easily be derived from the fact that an atom in the B layer sits above the centroid of a triangle of neigboring lattice points in the A layer. The corresponding lattice sum for the distances from the origin in the A-layer to all points in the B-layers can now

easily be obtained and is given by [160]

$$L^B(s,\gamma)=\sum_{i,j,k\in\mathbb{Z}}\left[\left(i+\tfrac{1}{3}\right)^2+\left(j+\tfrac{1}{3}\right)^2+\left(i+\tfrac{1}{3}\right)\left(j+\tfrac{1}{3}\right)+\gamma^2\left(k+\tfrac{1}{2}\right)^2\right]^{-s}, \tag{12.2.9}$$

where we have set $a=1$. The lattice sum $L^B(s,\gamma)$ is not a quadratic form but instead a quadratic function, which is therefore more difficult to evaluate through techniques such as the Terras decomposition. [112, 160] One way is to decompose $L^B(s,\gamma)$ into a sum of four lattice sums that involve quadratic forms; see Appendix D. Another way is to work with (12.2.9) directly and employ the theory of cubic theta functions, as we will see in section 12.3, where two different formulas are obtained. Again, one has to take care of large s values for small values of γ as we have $\lim_{s\to\infty}L^B(s,\gamma)=\infty$ for $\gamma<\sqrt{\frac{8}{3}}$.

Taking both AB layers into account the lattice sum for the hexagonal close packed structure is given by

$$L^{\mathrm{hcp}}(s,\gamma)=L^A(s,\gamma)+L^B(s,\gamma). \tag{12.2.10}$$

For the minimum distance r_{NN} in an hcp lattice we have to consider an additional case of $i=j=k=0$ in the lattice sum in (12.2.9),

$$r_{\mathrm{NN}}=\min\left\{a,c,\sqrt{\frac{a^2}{3}+\frac{c^2}{4}}\right\}=a\min\left\{1,\gamma,\sqrt{\frac{1}{3}+\frac{1}{4}\gamma^2}\right\}. \tag{12.2.11}$$

For the hcp structure with ideal value of $\gamma_{\mathrm{hcp}}=\sqrt{\frac{8}{3}}$ the kissing number defined by the number of minimum distances is $\kappa=12$.

Given the above properties, it is shown by Figure 12.2, that $r_{\mathrm{NN}}=c$ for $\gamma\in(0,\frac{2}{3}]$ corresponding to region I, $r_{\mathrm{NN}}=\sqrt{\frac{a^2}{3}+\frac{c^2}{4}}$ for $\gamma\in(\frac{2}{3},\sqrt{\frac{8}{3}})$ to region II and $r_{\mathrm{NN}}=a$ for $\gamma\in[\sqrt{\frac{8}{3}},\infty)$ to region III. For hard unit spheres there is a requirement that $r_{\mathrm{NN}}\geq 1$. Setting $a=1$ for the densest packing of unit spheres in a hexagonal sheet, we obtain the condition that $\gamma\geq\sqrt{8/3}$, otherwise one requires $a>1$. Hence, the densest packing of unit spheres is achieved at $\gamma_{\mathrm{hcp}}=\sqrt{8/3}$. This results in a hcp unit cell volume of $V=\sqrt{2}$ for $a=1$. As there are two atoms in the unit cell the volume per atom (or sphere) according to (12.2.5) of $V_{\mathrm{hcp}}(1,\sqrt{8/3})/2=1/\sqrt{2}$. Taking the sphere radius of $\frac{1}{2}$, this results in a packing density of

$$\rho=\frac{V_{\mathrm{sphere}}}{V_{\mathrm{hcp}}}=\frac{4\pi}{3}\left(\frac{1}{2}\right)^3\sqrt{2}=\frac{\pi}{3\sqrt{2}}=0.74048048969... \tag{12.2.12}$$

identical to that of the fcc lattice.

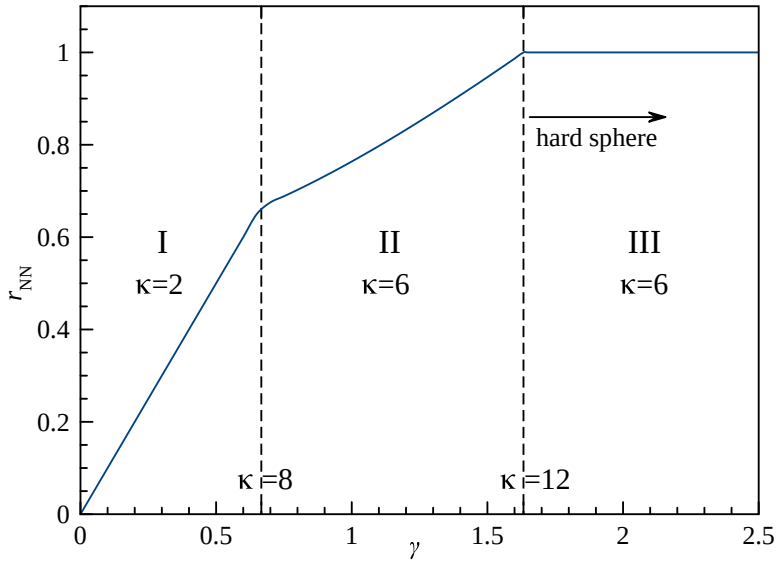

Figure 12.2 Minimum distance r_{NN} according to Eq. (12.2.11) for $a = 1$. The kissing number κ for the three regions and at the two boundaries are shown. The vertical dashed lines are at $\gamma = \frac{2}{3}$ and $\sqrt{\frac{8}{3}}$ where we have an increased kissing number.

12.3 Bessel Function Expansions of the hcp Lattice Sum

In the following we analyse $L^A(s)$ and $L^B(s)$ one at a time (we omit the argument γ for better clarity). We obtain two different Bessel function expansions which have poles at different s values (except for $s = 3/2$) and thus can be used to check against each other. In the proofs we will frequently refer to formulas for special functions given by (12.A.1)–(12.A.25) in Appendix A.

A The lattice sum $L^A(s)$

We break the sum for $L^A(s)$ into two, according to whether $k = 0$ or $k \neq 0$. This gives

$$L^A(s) = f(s) + 2F(s) \tag{12.3.1}$$

where

$$f(s) = {\sum_{i,j\in\mathbb{Z}}}'(i^2+ij+j^2)^{-s} \tag{12.3.2}$$

and

$$F(s) = \sum_{k\in\mathbb{N}}\sum_{i,j\in\mathbb{Z}}(i^2+ij+j^2+\gamma^2k^2)^{-s}, \tag{12.3.3}$$

with $\mathbb{N}$ defined as the set of positive integers, and $\mathbb{N}_0$ includes the zero. The function $f(s)$ has been evaluated before [26, 105],

$$f(s) = 6\zeta(s)L_{-3}(s) = 3^{1-s}2\zeta(s)\left[\zeta(s,\tfrac{1}{3}) - \zeta(s,\tfrac{2}{3})\right] \tag{12.3.4}$$

where $\zeta(s,x)$ is the Hurwitz zeta function

$$\zeta(s,x) = \sum_{i\in\mathbb{N}_0}(i+x)^{-s}, \tag{12.3.5}$$

where $\zeta(s) = \zeta(s,1)$ is the Riemann zeta function, and L_{-3} is the L-function defined by

$$L_{-3}(s) = \sum_{k\in\mathbb{N}}\frac{\sin(2k\pi/3)}{\sin(2\pi/3)}\frac{1}{k^s} = \frac{1}{1^s} - \frac{1}{2^s} + \frac{1}{4^s} - \frac{1}{5^s} + \cdots. \tag{12.3.6}$$

It remains to calculate $F(s)$. Applying the gamma function integral shown in (12.A.2),

$$\frac{1}{w^s} = \frac{1}{\Gamma(s)}\int_0^\infty x^{s-1}e^{-wx}\,\mathrm{d}x \tag{12.3.7}$$

followed by the cubic analogue of the theta function transformation formula, (12.A.12), we obtain

$$\begin{aligned}(2\pi)^{-s}\Gamma(s)F(s) &= \int_0^\infty x^{s-1}\sum_{k\in\mathbb{N}}e^{-2\pi\gamma^2k^2x}\sum_{i,j\in\mathbb{Z}}e^{-2\pi(i^2+ij+j^2)x}\,\mathrm{d}x \qquad (12.3.8)\\ &= \frac{1}{\sqrt{3}}\int_0^\infty x^{s-2}\sum_{k\in\mathbb{N}}e^{-2\pi\gamma^2k^2x}\sum_{i,j\in\mathbb{Z}}e^{-2\pi(i^2+ij+j^2)/3x}\,\mathrm{d}x.\end{aligned}$$

Now separating out the $i=j=0$ term and evaluate the resulting integrals using the following expression for the modified Bessel functions of the second kind shown in (12.A.3)

$$\int_0^\infty x^{s-1}e^{-ax-b/x}\mathrm{d}x = 2\left(\frac{b}{a}\right)^{s/2}K_s(2\sqrt{ab}), \tag{12.3.9}$$

we get

$$\begin{aligned}(2\pi)^{-s}\Gamma(s)F(s) &= \frac{1}{\sqrt{3}}\sum_{k\in\mathbb{N}}\int_0^\infty x^{s-2}e^{-2\pi\gamma^2k^2x}\,\mathrm{d}x \\ &\quad + \frac{1}{\sqrt{3}}\sum_{k\in\mathbb{N}}\sum_{i,j\in\mathbb{Z}}{}'\int_0^\infty x^{s-2}e^{-2\pi\gamma^2k^2x-2\pi(i^2+ij+j^2)/3x}\,\mathrm{d}x \\ &= \frac{\left(2\pi\gamma^2\right)^{1-s}}{\sqrt{3}}\Gamma(s-1)\zeta(2s-2) \\ &\quad + \frac{2}{\sqrt{3}}\sum_{k\in\mathbb{N}}\sum_{i,j}{}'\left(\frac{i^2+ij+j^2}{3\gamma^2k^2}\right)^{(s-1)/2} \\ &\qquad \times K_{s-1}\left(\frac{4\pi}{\sqrt{3}}\gamma k\sqrt{i^2+ij+j^2}\right). \end{aligned} \tag{12.3.10}$$

It follows that

$$\begin{aligned}L^A(s) &= 6\zeta(s)L_{-3}(s) + \frac{4\pi}{\sqrt{3}(s-1)}\gamma^{2-2s}\zeta(2s-2) \\ &\quad + \frac{4}{\sqrt{3}}\frac{(2\pi)^s}{\Gamma(s)}\sum_{k\in\mathbb{N}}\sum_{i,jk\in\mathbb{Z}}{}'\left(\frac{i^2+ij+j^2}{3\gamma^2k^2}\right)^{(s-1)/2} \\ &\qquad \times K_{s-1}\left(\frac{4\pi}{\sqrt{3}}\gamma k\sqrt{(i^2+ij+j^2)}\right) \\ &= 6\zeta(s)L_{-3}(s) + \frac{4\pi}{\sqrt{3}(s-1)}\gamma^{2-2s}\zeta(2s-2) \\ &\quad + \frac{4}{\sqrt{3}}\frac{(2\pi)^s}{\Gamma(s)}\sum_{k\in\mathbb{N}}\sum_{N\in\mathbb{N}}u_2(N)\left(\frac{N}{3\gamma^2k^2}\right)^{(s-1)/2}K_{s-1}\left(\frac{4\pi}{\sqrt{3}}\gamma k\sqrt{N}\right)\end{aligned} \tag{12.3.11}$$

where $u_2(N)$ is the number of representations of N by the form i^2+ij+j^2.

B A second formula for the lattice sum $L^A(s)$

A different formula for $L^A(s)$ can be obtained by separating the terms in the series (12.2.7) according to whether $i=j=0$ or i and j are not both zero. This gives

$$L^A(s) = 2\gamma^{-2s}\zeta(2s) + G(s) \tag{12.3.12}$$

where

$$G(s) = \sum_{i,j\in\mathbb{Z}}{}'\sum_{k\in\mathbb{Z}}(i^2+ij+j^2+\gamma^2k^2)^{-s}. \tag{12.3.13}$$

Applying the gamma function integral (12.A.2) followed by the theta function transformation formula (12.A.8) for the k summation, we obtain

$$\pi^{-s}\Gamma(s)G(s) = \int_0^\infty x^{s-1} {\sum_{i,j\in\mathbb{Z}}}' e^{-\pi(i^2+ij+j^2)x} \sum_{k\in\mathbb{Z}} e^{-\pi\gamma^2k^2x}\,\mathrm{d}x \tag{12.3.14}$$
$$= \gamma^{-1}\int_0^\infty x^{s-\frac{3}{2}} {\sum_{i,j\in\mathbb{Z}}}' e^{-\pi(i^2+ij+j^2)x} \sum_{k\in\mathbb{Z}} e^{-\pi k^2/(\gamma^2x)}\,\mathrm{d}x\,.$$

Now separate out the $k=0$ term and evaluate the resulting integrals. The result is

$$\begin{aligned}\pi^{-s}\Gamma(s)G(s) &= \gamma^{-1}\int_0^\infty x^{s-\frac{3}{2}} {\sum_{i,j\in\mathbb{Z}}}' e^{-\pi(i^2+ij+j^2)x}\,\mathrm{d}x \\ &\quad + 2\gamma^{-1}\int_0^\infty x^{s-\frac{3}{2}} {\sum_{i,j\in\mathbb{Z}}}' e^{-\pi(i^2+ij+j^2)x} \sum_{k\in\mathbb{N}} e^{-\pi k^2/(\gamma^2x)}\,\mathrm{d}x \\ &= \gamma^{-1}\,\pi^{-(s-\frac{1}{2})}\,\Gamma\left(s-\tfrac{1}{2}\right) {\sum_{i,j\in\mathbb{Z}}}' (i^2+ij+j^2)^{-s+\frac{1}{2}} \\ &\quad + 4\gamma^{-(2s+1)/2} {\sum_{i,j\in\mathbb{Z}}}' \sum_{k\in\mathbb{N}} \left(\frac{k^2}{i^2+ij+j^2}\right)^{(2s-1)/4} \\ &\qquad \times K_{s-\frac{1}{2}}\left(\frac{2\pi k}{\gamma}\sqrt{i^2+ij+j^2}\right).\end{aligned} \tag{12.3.15}$$

The first sum can be evaluated in terms of the Riemann zeta function and the L_{-3} function by (12.A.24). In the second sum, we again use the notation $u_2(N)$ for the number of representations of N by the form i^2+ij+j^2. The result is

$$\begin{aligned}\pi^{-s}\Gamma(s)G(s) &= 6\,\pi^{-(s-\frac{1}{2})}\,\gamma^{-1}\Gamma(s-\tfrac{1}{2})\zeta(s-\tfrac{1}{2})L_{-3}(s-\tfrac{1}{2}) \\ &\quad + 4\gamma^{-(2s+1)/2} \sum_{N\in\mathbb{N}}\sum_{k\in\mathbb{N}} u_2(N)\left(\frac{k^2}{N}\right)^{(2s-1)/4} K_{s-\frac{1}{2}}\left(\frac{2\pi k}{\gamma}\sqrt{N}\right).\end{aligned} \tag{12.3.16}$$

It follows that

$$\begin{aligned}L^A(s) &= 2\gamma^{-2s}\zeta(2s) + 6\sqrt{\pi}\gamma^{-1}\,\frac{\Gamma(s-\frac{1}{2})}{\Gamma(s)}\,\zeta(s-\tfrac{1}{2})L_{-3}(s-\tfrac{1}{2}) \\ &\quad + \frac{4\pi^s}{\Gamma(s)}\,\gamma^{-(2s+1)/2} \sum_{N\in\mathbb{N}}\sum_{k\in\mathbb{N}} u_2(N)\left(\frac{k^2}{N}\right)^{(2s-1)/4} K_{s-\frac{1}{2}}\left(\frac{2\pi k}{\gamma}\sqrt{N}\right).\end{aligned} \tag{12.3.17}$$

C The lattice sum $L^B(s)$

We apply the gamma function integral (12.A.2) for (12.2.9) to write

$$L^B(s) = \frac{(2\pi)^s}{\Gamma(s)} \int_0^\infty x^{s-1} \sum_{k\in\mathbb{Z}} e^{-2\pi\gamma^2(k+\frac{1}{2})^2 x} \times \sum_{i,j\in\mathbb{Z}} e^{-2\pi\{(i+\frac{1}{3})^2+(i+\frac{1}{3})(j+\frac{1}{3})+(j+\frac{1}{3})^2\}x}\,\mathrm{d}x\,. \tag{12.3.18}$$

Now make use of the transformation formula (12.A.13) to deduce

$$L^B(s) = \frac{(2\pi)^s}{\Gamma(s)} \int_0^\infty x^{s-1} \left(2\sum_{k\in\mathbb{N}_0} e^{-2\pi\gamma^2(k+\frac{1}{2})^2 x}\right) \times \left(\frac{1}{x\sqrt{3}} \sum_{i,j\in\mathbb{Z}} \omega^{i-j} e^{-2\pi(i^2+ij+j^2)/3x}\right) \mathrm{d}x \tag{12.3.19}$$

where $\omega = \exp(2\pi i/3)$ is a primitive cube root of 1. Now separate the term $i = j = 0$ to deduce

$$L^B(s) = \frac{(2\pi)^s}{\Gamma(s)} \frac{2}{\sqrt{3}} \int_0^\infty x^{s-2} \sum_{k\in\mathbb{N}_0} e^{-2\pi\gamma^2(k+\frac{1}{2})^2 x}\,\mathrm{d}x \tag{12.3.20}$$

$$+ \frac{(2\pi)^s}{\Gamma(s)} \frac{2}{\sqrt{3}} \int_0^\infty x^{s-2} \sum_{k\in\mathbb{N}_0} e^{-2\pi\gamma^2(k+\frac{1}{2})^2 x} \times \sum_{N\in\mathbb{N}_0} \cos\left(\frac{2\pi N}{3}\right) u_2(N)\, e^{-2\pi N/3x}\,\mathrm{d}x \tag{12.3.21}$$

where $u_2(N)$ is the number of representations of N by the form $i^2 + ij + j^2$, as before. Here we used Euler's formula, $e^{i\theta} = \cos\theta + i\sin\theta$ and retain only the real part as $L^B(s)$ is real. On evaluating the integrals using (12.A.2) and (12.A.3) we obtain

$$L^B(s) = \frac{4\pi}{\sqrt{3}(s-1)} \gamma^{-2s+2} \sum_{k\in\mathbb{N}_0} \frac{1}{(k+\frac{1}{2})^{2s-2}} + \frac{4}{\sqrt{3}} \frac{(2\pi)^s}{\Gamma(s)} \sum_{k\in\mathbb{N}_0} \sum_{N\in\mathbb{N}} \cos\left(\frac{2\pi N}{3}\right) u_2(N) \left(\frac{N}{3\gamma^2(k+\frac{1}{2})^2}\right)^{(s-1)/2} \times K_{s-1}\left(\frac{4\pi}{\sqrt{3}}\gamma\left(k+\tfrac{1}{2}\right)\sqrt{N}\right). \tag{12.3.22}$$

The first sum can be evaluated in terms of the Riemann zeta function by using (12.A.23) to give

$$L^B(s) = \frac{4\pi}{\sqrt{3}(s-1)}\gamma^{-2s+2}(2^{2s-2}-1)\zeta(2s-2) + \frac{4}{\sqrt{3}}\frac{(2\pi)^s}{\Gamma(s)}\sum_{k\in\mathbb{N}_0}\sum_{N\in\mathbb{N}}\cos\left(\frac{2\pi N}{3}\right)u_2(N)\left(\frac{N}{3\gamma^2(k+\frac{1}{2})^2}\right)^{(s-1)/2} \times K_{s-1}\left(\frac{4\pi}{\sqrt{3}}\gamma\left(k+\tfrac{1}{2}\right)\sqrt{N}\right). \tag{12.3.23}$$

D A second formula for the sum $L^B(s)$

We introduce the abbreviation

$$Y_{ij} = \left(i+\tfrac{1}{3}\right)^2 + \left(i+\tfrac{1}{3}\right)\left(j+\tfrac{1}{3}\right) + \left(j+\tfrac{1}{3}\right)^2 \tag{12.3.24}$$

to write (12.3.18) in the form

$$L^B(s) = \frac{(2\pi)^s}{\Gamma(s)}\int_0^\infty x^{s-1}\sum_{i,j\in\mathbb{Z}} e^{-2\pi Y_{ij}x}\sum_{k\in\mathbb{Z}} e^{-2\pi\gamma^2(k+\frac{1}{2})^2 x}\,\mathrm{d}x\,. \tag{12.3.25}$$

This time we apply the transformation formula (12.A.9) to the sum over k to obtain

$$L^B(s) = \frac{(2\pi)^s}{\sqrt{2}\Gamma(s)}\gamma^{-1}\int_0^\infty x^{s-3/2}\sum_{i,j\in\mathbb{Z}} e^{-2\pi Y_{ij}x}\sum_{k\in\mathbb{Z}}(-1)^k e^{-\pi k^2/(2\gamma^2 x)}\,\mathrm{d}x\,. \tag{12.3.26}$$

Now separate the terms according to whether $k=0$ or $k\neq 0$ and evaluate the resulting integrals by (12.A.2) and (12.A.3). The result is

$$L^B(s) = \frac{\sqrt{\pi}\Gamma(s-\frac{1}{2})}{\gamma\Gamma(s)}\sum_{i,j\in\mathbb{Z}} Y_{ij}^{1/2-s} + \frac{4\pi^s}{\Gamma(s)}\gamma^{-(2s+1)/2}\sum_{k\in\mathbb{N}}(-1)^k\sum_{i,j\in\mathbb{Z}}\left(\frac{k}{\sqrt{Y_{ij}}}\right)^{s-\frac{1}{2}} K_{s-\frac{1}{2}}\left(2\pi\frac{k}{\gamma}\sqrt{Y_{ij}}\right). \tag{12.3.27}$$

The first sum can be handled by (12.A.25) to give

$$\sum_{i,j\in\mathbb{Z}} Y_{ij}^{1/2-s} = 3(3^{s-1/2}-1)\zeta\left(s-\tfrac{1}{2}\right)L_{-3}\left(s-\tfrac{1}{2}\right). \tag{12.3.28}$$

For the other sum, observe that $3Y_{ij} = 3i^2+3ij+3j^2+3i+3j+1$, that is to say $3Y_{ij}$ is a positive integer and $3Y_{ij}\equiv 1 \pmod 3$. Therefore we set $3Y_{ij} = 3N+1$

and use (12.A.16) to deduce that the number of solutions of $3i^2+3ij+3j^2+3i+3j+1=3N+1$ is equal to $\frac{1}{2}u_2(3N+1)$, and we get

$$L^B(s)=\frac{3\sqrt{\pi}\,\Gamma(s-\frac{1}{2})}{\gamma\Gamma(s)}\left(3^{s-1/2}-1\right)\zeta\left(s-\tfrac{1}{2}\right)L_{-3}\left(s-\tfrac{1}{2}\right)$$
$$+\frac{2\pi^s}{\Gamma(s)}\gamma^{-(2s+1)/2}\sum_{k\in\mathbb{N}}(-1)^k\sum_{N\in\mathbb{N}_0}u_2(3N+1)\left(\frac{k}{\sqrt{N+\frac{1}{3}}}\right)^{s-\frac{1}{2}}$$
$$\times K_{s-\frac{1}{2}}\left(2\pi\frac{k}{\gamma}\sqrt{N+\tfrac{1}{3}}\right). \tag{12.3.29}$$

E Adding $L^A(s)$ and $L^B(s)$

On adding the results for $L^A(s)$ and $L^B(s)$ in (12.3.11) and (12.3.23) we obtain

$$L^{\mathrm{hcp}}(s,\gamma)=6\zeta(s)L_{-3}(s)+\frac{4\pi}{\sqrt{3}(s-1)}\left(\frac{\gamma}{2}\right)^{2-2s}\zeta(2s-2)$$
$$+\frac{4}{\sqrt{3}}\frac{(2\pi)^s}{\Gamma(s)}\sum_{k\in\mathbb{N}}\sum_{N\in\mathbb{N}}u_2(N)\left(\frac{N}{3\gamma^2k^2}\right)^{(s-1)/2}K_{s-1}\left(\frac{4\pi}{\sqrt{3}}\gamma k\sqrt{N}\right)$$
$$+\frac{4}{\sqrt{3}}\frac{(2\pi)^s}{\Gamma(s)}\sum_{k\in\mathbb{N}_0}\sum_{N\in\mathbb{N}}\cos\left(\frac{2\pi N}{3}\right)u_2(N)\left(\frac{N}{3\gamma^2(k+\frac{1}{2})^2}\right)^{(s-1)/2}$$
$$\times K_{s-1}\left(\frac{4\pi}{\sqrt{3}}\gamma\left(k+\tfrac{1}{2}\right)\sqrt{N}\right). \tag{12.3.30}$$

On the other hand, if we add the results of (12.3.17) and (12.3.29) we obtain

$$L^{\mathrm{hcp}}(s,\gamma)=2\gamma^{-2s}\zeta(2s)+\frac{3\sqrt{\pi}\,\Gamma(s-\frac{1}{2})}{\gamma\Gamma(s)}\left(3^{s-1/2}+1\right)\zeta\left(s-\tfrac{1}{2}\right)L_{-3}\left(s-\tfrac{1}{2}\right)$$
$$+\frac{4\pi^s}{\Gamma(s)}\gamma^{-(2s+1)/2}\sum_{N\in\mathbb{N}}\sum_{k\in\mathbb{N}}u_2(N)\left(\frac{k}{\sqrt{N}}\right)^{(2s-1)/2}K_{s-\frac{1}{2}}\left(\frac{2\pi k}{\gamma}\sqrt{N}\right)$$
$$+\frac{2\pi^s}{\Gamma(s)}\gamma^{-(2s+1)/2}\sum_{k\in\mathbb{N}}(-1)^k\sum_{N\in\mathbb{N}_0}u_2(3N+1)\left(\frac{k}{\sqrt{N+\frac{1}{3}}}\right)^{s-\frac{1}{2}}$$
$$\times K_{s-\frac{1}{2}}\left(2\pi\frac{k}{\gamma}\sqrt{N+\tfrac{1}{3}}\right). \tag{12.3.31}$$

Equation (12.3.31) is numerically more stable for small values of γ as the argument in the Bessel function $K_{s-\frac{1}{2}}(x)$ becomes larger and therefore further away from the singularity at $x=0$, while (12.3.30) is better suited for larger

values of γ. The lattice sums as a function of γ for different s values are shown in Figure 12.3, and the corresponding values of $L^{\rm hcp}(s,\gamma)$ (including the first and second derivatives) for the ideal ratio of $\gamma_{\rm hcp} = \sqrt{\frac{8}{3}}$ and selected s-values are collected in Table 12.1.

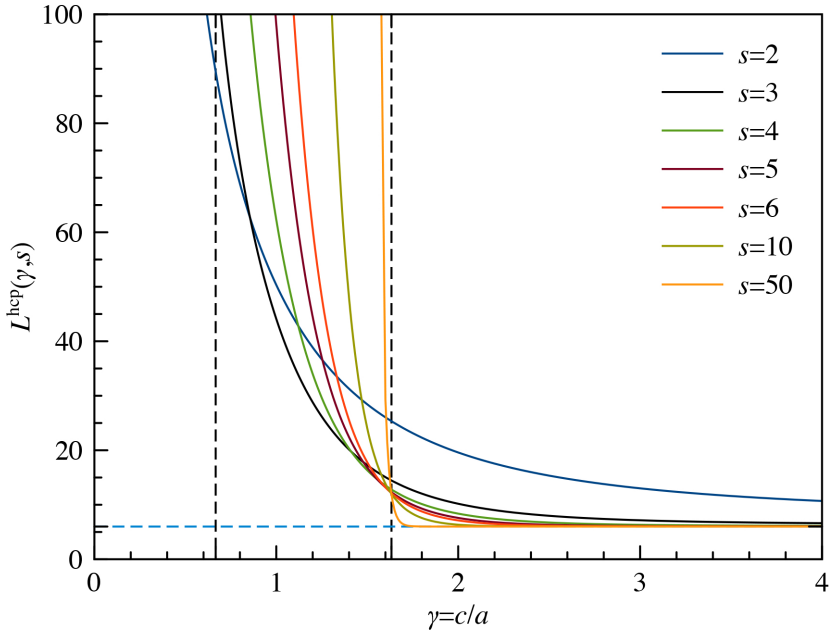

Figure 12.3 Lattice sums $L^{\rm hcp}(s,\gamma)$ as a function of γ for various s values. The vertical dashed lines are at $\gamma = \frac{2}{3}$ and $\sqrt{\frac{8}{3}}$ as in Figure 12.2, and the horizontal dashed line represents $\lim_{\gamma,s\to\infty} L^{\rm hcp}(s,\gamma) = 6$. The curve for s=50 is close to the hard-sphere limit of $s = \infty$.

We obtain the following limits for all values of $s > \frac{3}{2}$,

$$\lim_{\gamma\to\infty} L^{\rm hcp}(s,\gamma) \to 6\zeta(s)L_{-3}(s) \quad \text{and} \quad \lim_{\gamma\to 0} L^{\rm hcp}(s,\gamma) \to \infty\,. \qquad (12.3.32)$$

The first limit reflects the fact that the limiting case $\gamma\to\infty$ corresponds to a single 2D hexagonal lattice with $L_2^{\rm hcp}(s) = 6\zeta(s)L_{-3}(s)$ being the corresponding lattice sum (see Eq.(47) in Ref.[296]). Moreover, as mentioned before we have $\lim_{s\to\infty} L^{\rm hcp}(s,\gamma) = \infty$ for $\gamma < \sqrt{\frac{8}{3}}$, and for larger values of s direct summation using the original lattice sum (12.2.10) is to be preferred, e.g., for $s = 50$ and $\gamma = \gamma_{\rm hcp} = \sqrt{\frac{8}{3}}$ we obtain $L^{\rm hcp}(s,\gamma) = L^{\rm hcp}(50,\sqrt{\frac{8}{3}}) = 12.000000000000$, corresponding to the kissing number for an ideal hcp lattice.

s	$L^{\mathrm{hcp}}(s,\gamma)$	$\partial L^{\mathrm{hcp}}(s,\gamma)/\partial\gamma$	$\partial^2 L^{\mathrm{hcp}}(s,\gamma)/\partial\gamma^2$
2	25.339082338055	-20.695008216087	34.645562350540
3	14.454897277842	-17.711026910386	45.197828381987
4	12.802821852810	-20.913971214589	71.283006314719
5	12.311896233819	-25.136976828849	106.83160316772
6	12.132293769099	-29.721546123728	151.03829753868
7	12.059228255068	-34.464287703815	203.59375072251
8	12.027479419304	-39.282788797012	264.34146680290
9	12.013060023177	-44.139430042060	333.19696813736
10	12.006309158115	-49.015864608041	410.11367485711

Table 12.1 Values for $L^{\mathrm{hcp}}(s,\gamma)$ at the ideal ratio of $c/a = \gamma_{\mathrm{hcp}} = \sqrt{\frac{8}{3}}$ for selected $s = n/2$. The first and second derivatives with respect to γ are reported as well (see appendix 12.D for details).

12.4 The Lennard-Jones cohesive energy for the hcp structure with varying c/a ratio

The cohesive energy for the hcp structure for a general (n,m) LJ potential expressed in terms of lattice sums is given by

$$E_{\mathrm{LJ}}^{\mathrm{coh}}(n,m,a,\gamma) = \frac{\varepsilon nm}{2(n-m)}\left[\frac{L^{\mathrm{hcp}}(\frac{n}{2},\gamma)}{n}\left(\frac{r_e}{a}\right)^n - \frac{L^{\mathrm{hcp}}(\frac{m}{2},\gamma)}{m}\left(\frac{r_e}{a}\right)^m\right]. \tag{12.4.1}$$

The definitions for the lattice sums $L^{\mathrm{hcp}}(s,\gamma)$ are taken from eqs. (12.3.30) and (12.3.31) with $\gamma = c/a$. In order to discuss the behavior for the LJ potential with varying c/a ratio we calculate the minimum cohesive energy with respect to the lattice parameter a for fixed γ. For this we follow the procedure in Ref.[343] and get,

$$R^*_{\mathrm{min}}(\gamma) = \frac{a_{\mathrm{min}}(\gamma)}{r_e} = \left(\frac{L^{\mathrm{hcp}}(\frac{n}{2},\gamma)}{L^{\mathrm{hcp}}(\frac{m}{2},\gamma)}\right)^{\frac{1}{n-m}}, \tag{12.4.2}$$

and the * indicates reduced (or dimensionless) units are used. The cohesive energy can now be evaluated at R^*_{min},

$$E^*_{nm}(\gamma) = E_{\mathrm{LJ}}^{\mathrm{coh}}(n,m,R^*_{\mathrm{min}}(\gamma),\gamma)/\varepsilon = -\frac{1}{2}\left[\frac{L^{\mathrm{hcp}}(\frac{m}{2},\gamma)^n}{L^{\mathrm{hcp}}(\frac{n}{2},\gamma)^m}\right]^{\frac{1}{n-m}}. \tag{12.4.3}$$

The function $E^*_{nm}(\gamma)$ is shown in Figure 12.4 for various (n,m) combinations of the LJ potential. For the (12,6) LJ potential we see a metastable minimum

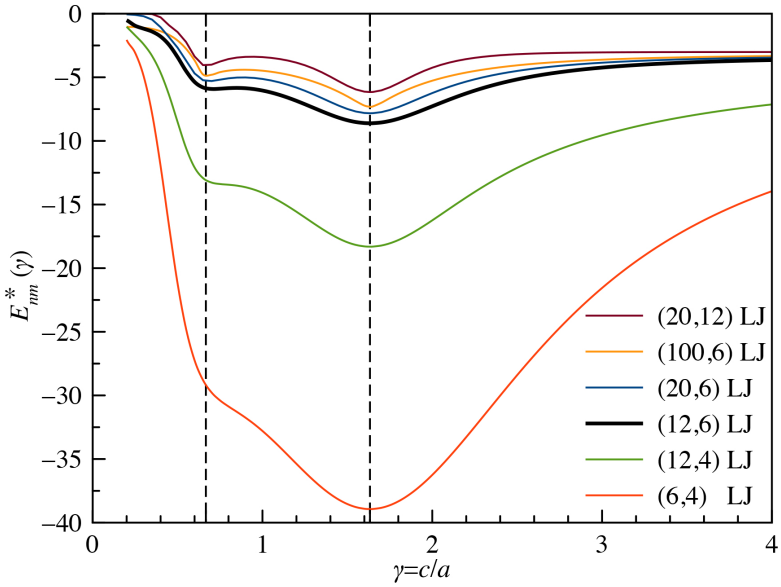

Figure 12.4 $E^*_{nm}(\gamma)$ as a function of $\gamma = \sqrt{\frac{c}{a}}$ for a number of (n,m) combinations for the LJ potential. The vertical dashed lines are at $\gamma = \frac{2}{3}$ and $\sqrt{\frac{8}{3}}$ as in Figure 12.2. Note that the exponents n,m are multiplied by 2 compared to the s exponent used in the previous sections.

around $\gamma = 2/3$, γ=0.710188 for the (12,6) LJ potential with an energy difference to the global minimum of $\Delta E^* = 2.691401$. The metastable minimum becomes more pronounced for harder potentials and disappears for very soft potentials. Concerning the maximum, for the (12,6) LJ potential it sits at γ=0.848360 with an activation barrier of ΔE^*= 0.084494 from the metastable minimum to the more stable minimum around $\gamma_{\text{hcp}} = \sqrt{\frac{8}{3}}$. Data for the metastable minimum for some other (n,m) combinations of the LJ potential are collected in Table 12.2.

The question why a second minimum appears around $\gamma = \frac{2}{3}$ needs to be addressed. This is at the boundary between regions I and II shown in Figure 12.2 where the kissing number is increased to $\kappa = 8$ due to the fact that beside the six surrounding atoms from the A-layer of an atom in the B-layer, we have two more touching spheres above and below from other C-layers with an underlying elongated triangular bipyramid (or dipyramid). In region I, the minimum distance is determined by the lattice constant c. In this case the atoms in the two A-layers shown in Figure 12.1 come in direct neighborhood and start to interact more strongly. In order to avoid strong repulsive forces we have to make space for the C-layer in the middle position by increasing the lattice constant a. As an atom in layer C sits exactly in the centroid of a triangle spanned by neighboring atoms in the A-layer, we consider a trigonal pyramid of unit spheres with edge length $e = 1$ and height $h = c = \frac{1}{2}$. This gives for the nearest neighbor distances in the A-layer $a = \frac{3}{2}$, and therefore a ration of $\gamma = c/a = \frac{2}{3}$. Such a lattice is best described by linear chains along the c axis with atoms from the A-layers and shifted by c/a atoms from the C-layers (notice that in the region $\gamma < \frac{2}{3}$ we have $\kappa = 2$). As the kissing number is $\kappa = 8$ at the boundary (see Figure 12.2), we expect that the minimum occurs at higher energies compared to the one around $\gamma_{\text{hcp}} = \sqrt{\frac{8}{3}}$.

n	m	$\gamma_{\text{min}}^{\text{meta}}$	γ_{max}	ΔE_{nm}^*	$\Delta E_{nm}^{*\ \#}$
12	6	0.710188	0.848360	2.691402	0.08449406
20	6	0.683350	0.883096	2.519636	0.29600569
20	12	0.668678	0.935797	2.073051	0.70435894

Table 12.2 $\gamma_{\text{min}}^{\text{meta}}$ for the metastable minimum and corresponding energy difference ΔE_{nm}^* to the global minimum around $\gamma_{\text{hcp}} = \sqrt{\frac{8}{3}}$, and γ_{max} between the two minima and corresponding energy difference $\Delta E_{nm}^{*\ \#}$ to the metastable minimum for three selected (n,m) combinations of the LJ potential. Note that the exponents n,m are multiplied by 2 compared to the s exponent used in the previous sections.

In regard to the global minimum, there is no reason for the LJ potential to have the minimum exactly at $\gamma_{\rm hcp} = \sqrt{\frac{8}{3}}$ as the first derivatives $\partial_\gamma E^*_{nm}(\gamma_{\rm hcp})$ in Table 12.1 show for various (n,m) combinations. Indeed, it was already shown by Howard [377] by direct lattice summations over 450 shells around a central atom that the minimum occurs at 99.986% of the ideal hcp value for the (12,6) LJ potential. To obtain more detailed information if $\gamma_{\rm min}$ is greater or lower than $\gamma_{\rm hcp}$ we used a Newton-Raphson procedure as described in Appendix 12.D. The dividing line between the two regions of $\gamma < \sqrt{\frac{8}{3}}$ and $\gamma > \sqrt{\frac{8}{3}}$ is shown in Figure 12.5. Only for very soft potentials (low n and m values) the minimum comes at values $\gamma_{\rm min} > \gamma_{\rm hcp}$. For the common (12,6) LJ potential, $\gamma_{\rm min} = 1.6327633 < \gamma_{\rm hcp}$. However, the deviations δ_{nm} defined by $\gamma_{\rm min} = \sqrt{\frac{8}{3}} + \delta_{nm}$ are very small, and so are the energy differences between the minimum and the ideal hcp structure, see Table **??**. To give a real example we take argon with a dissociation energy of $\varepsilon = 1191$ J/mol for the dimer.[348] The change due to the deviation from the ideal c/a ratio is therefore $\Delta E_{nm} = \Delta E^*_{nm}\varepsilon = -8.661 \times 10^{-4}$ J/mol. This value is far smaller than the accuracy which can be achieved in any solid-state calculation.[51] Accordingly, for the deviation $\delta_{nm} = 7.701 \times 10^{-4}$ we use the equilibrium distance of 3.3502 Å of Azis [348] and obtain a slight difference in the atomic distance between the pair of 6 neighboring atoms. Such a small deviation is perhaps within experimental reach.

When considering the hard sphere limit with an attractive a^{-n} potential in (12.4.1), we present the (100,6) LJ potential (s=50 and 3 respectively in our earlier definition) in Figure 12.5 as best candidate, as it is still numerically manageable despite the large exponent of m=100. Here the deviation δ_{nm} listed in Table 12.3 is indeed very small. The curve shows a rather peculiar behavior around $\gamma = \sqrt{\frac{8}{3}}$ going steeply towards infinity for $\gamma_{\rm hcp} \leq \sqrt{\frac{8}{3}}$. For an infinite repulsive wall the minimum sits at exactly $\gamma_{\rm hcp} = \sqrt{\frac{8}{3}}$ as one expects. For values of $\gamma < \sqrt{\frac{8}{3}}$ and $m < \infty$ we enter a steep repulsive wall where the atoms in the hexagonal closed packed sheets need to give space for the next layer.

12.5 Analytic continuation of the lattice sum $L^{\rm hcp}(s)$

We show that the lattice sum $L^{\rm hcp}(s)$ can be continued analytically to the whole s-plane, and that the resulting functions have a single simple pole at $s = 3/2$ and no other singularities. We start by determining the residue of $L^{\rm hcp}(s)$ at $s = 3/2$. In the formula (12.3.30), all of the terms are analytic at $s = 3/2$ except for the term involving $\zeta(2s-2)$, which has a simple pole there. Therefore, the

n	m	$E^*_{nm}(\gamma_{\min})$	δ_{nm}	ΔE^*_{nm}	$\partial_\gamma E^*_{nm}(\gamma_{\rm hcp})$
12	6	-8.611070	-2.298569×10^{-4}	-7.272348×10^{-7}	6.327613×10^{-3}
6	4	-38.932531	3.077860×10^{-4}	-2.121345×10^{-6}	-1.378463×10^{-2}
12	4	-18.309854	-8.758790×10^{-5}	-1.526585×10^{-7}	3.485817×10^{-3}
20	6	-7.825827	-1.404378×10^{-4}	-3.993197×10^{-7}	5.686712×10^{-3}
20	12	-6.161877	-6.980408×10^{-5}	-1.518888×10^{-7}	4.351831×10^{-3}
100	6	-7.313826	-2.186397×10^{-5}	-2.082085×10^{-7}	4.013898×10^{-3}

Table 12.3 $\partial_\gamma E^*_{nm}(\gamma_{\rm hcp})$, $\delta_{nm} = \gamma_{\min} - \sqrt{\frac{8}{3}}$ and $\Delta E^*_{nm} = E^*_{nm}(\gamma_{\min}) - E^*_{nm}(\gamma_{\rm hcp})$ for various (n,m) Lennard-Jones potentials. Note that the exponents n,m are multiplied by 2 compared to the s exponent used in the previous sections.

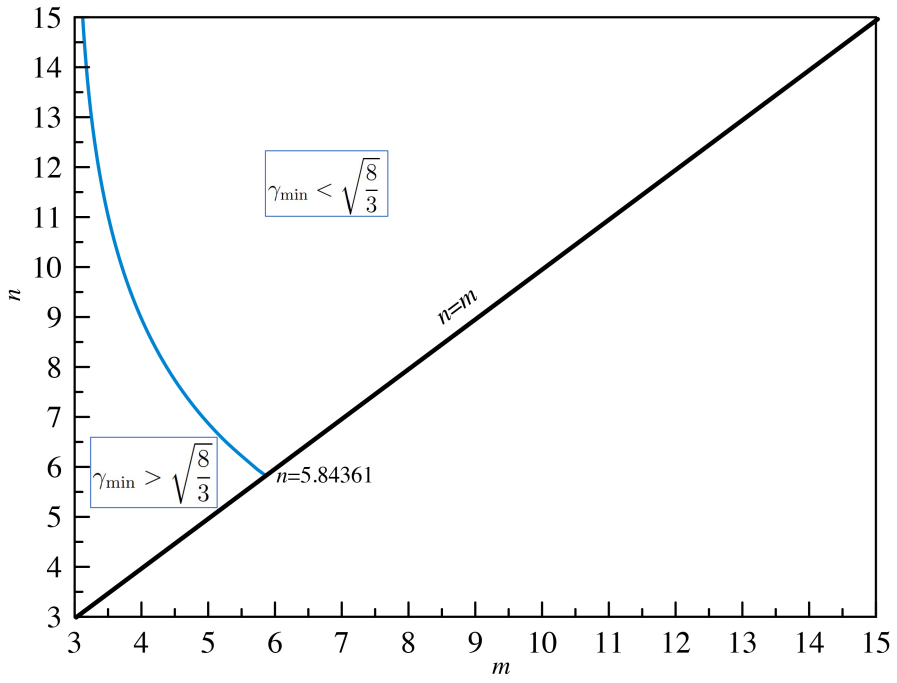

Figure 12.5 Dividing (n,m) areas $(n > m)$ of regions where $\gamma_{\min} > \gamma_{\rm hcp}$ and $\gamma_{\min} < \gamma_{\rm hcp}$. Note that the dividing line intersects with the $n = m$ line at n =5.84361 and approaches $m = 3$ for $n \to \infty$.

Laurent series for $L^{\mathrm{hcp}}(\gamma,s)$ around the pole at $s=3/2$ is of the form,

$$L^{\mathrm{hcp}}(s,\gamma)=\frac{d_{-1}}{s-3/2}+d_0+\sum_{n\in\mathbb{N}}d_n(s-3/2)^n \tag{12.5.1}$$

where

$$d_{-1}=\mathrm{Res}(L^{\mathrm{hcp}}(s),3/2)=\frac{8\pi}{\gamma\sqrt{3}} \tag{12.5.2}$$

and

$$\begin{aligned}d_0(\gamma)=6\zeta(3/2)L_{-3}(3/2)\;+\;&\frac{16\pi}{\gamma\sqrt{3}}\left(\gamma_0+\ln(2/\gamma)-1\right)\\&+\frac{4}{\sqrt{3}}\frac{(2\pi)^{3/2}}{\Gamma(3/2)}\sum_{k\in\mathbb{N}}\sum_{N\in\mathbb{N}}u_2(N)\left(\frac{N}{3\gamma^2k^2}\right)^{1/4}K_{1/2}\left(\frac{4\pi}{\sqrt{3}}\gamma k\sqrt{N}\right)\\&+\frac{4}{\sqrt{3}}\frac{(2\pi)^{3/2}}{\Gamma(3/2)}\sum_{k\in\mathbb{N}_0}\sum_{N\in\mathbb{N}}\cos\left(\frac{2\pi N}{3}\right)u_2(N)\left(\frac{N}{3\gamma^2(k+\frac{1}{2})^2}\right)^{1/4}\\&\qquad\times K_{1/2}\left(\frac{4\pi}{\sqrt{3}}\gamma\left(k+\tfrac{1}{2}\right)\sqrt{N}\right).\end{aligned} \tag{12.5.3}$$

$\gamma_0=0.57721566490153286...$ is the Euler-Mascheroni constant. The derivation of the residue and the second term in equation (12.5.3) is given in Appendix B. Using well known relations for the Bessel function $K_{1/2}(x)=\sqrt{\pi/2x}\,e^{-x}$ we obtain

$$\begin{aligned}d_0(\gamma)=6\zeta(3/2)L_{-3}(3/2)\;+\;&\frac{16\pi}{\gamma\sqrt{3}}\left(\gamma_0+\ln(2/\gamma)-1\right)\\&+\frac{8\pi}{\gamma\sqrt{3}}\sum_{k\in\mathbb{N}}\sum_{N\in\mathbb{N}}\frac{1}{k}u_2(N)\exp\left(-\frac{4\pi}{\sqrt{3}}\gamma k\sqrt{N}\right)\\&+\frac{8\pi}{\gamma\sqrt{3}}\sum_{k\in\mathbb{N}_0}\sum_{N\in\mathbb{N}}\frac{\cos\left(\frac{2\pi N}{3}\right)}{(k+\frac{1}{2})}u_2(N)\exp\left(-\frac{4\pi}{\sqrt{3}}\gamma\left(k+\tfrac{1}{2}\right)\sqrt{N}\right)\\=6\zeta(3/2)L_{-3}(3/2)\;+\;&\frac{16\pi}{\gamma\sqrt{3}}\left(\gamma_0+\ln(2/\gamma)-1\right)\\&-\frac{8\pi}{\gamma\sqrt{3}}\sum_{N=1}^{\infty}u_2(N)\ln\left(1-e^{-\frac{4\pi}{\sqrt{3}}\gamma k\sqrt{N}}\right)\\&+\frac{8\pi}{\gamma\sqrt{3}}\sum_{N\in\mathbb{N}}\cos\left(\frac{2\pi N}{3}\right)u_2(N)\ln\left(\frac{1+e^{-\frac{2\pi}{\sqrt{3}}\gamma k\sqrt{N}}}{1-e^{-\frac{2\pi}{\sqrt{3}}\gamma k\sqrt{N}}}\right).\end{aligned} \tag{12.5.4}$$

Here we use the series expansion for the logarithm

$$\ln(1+x) = \sum_{k\in\mathbb{N}} \frac{(-1)^{k+1}}{k} x^k \quad \text{or} \quad \ln(1-x) = -\sum_{k\in\mathbb{N}} \frac{1}{k} x^k, \tag{12.5.5}$$

substituting $x \to e^{-x}$. For the special value of $\gamma_{\text{hcp}} = \sqrt{8/3}$ we have

$$d_0(\sqrt{8/3}) = 6.98462\ 37414\ 38416\ 61307\ \cdots. \tag{12.5.6}$$

Concerning the analytical continuation to the left of the simple pole, $s < 3/2$, by (12.A.6) the double series of Bessel functions in (12.3.30) converges absolutely and uniformly on compact subsets of the s-plane and therefore represents an entire function of s. It follows that L^{hcp} has an analytic continuation to a meromorphic function. Moreover, the Laurent expansion (12.5.1) converges for all $s \neq 3/2$. Further inspection reveals that the only problematic case in (12.3.30) is for $s = 1$ because of the two terms having cancelling singularities. Therefore we take $s = 1$ in the second formula (12.3.31) instead to obtain

$$\begin{aligned} L^{\text{hcp}}(1) = {} & \frac{\pi^2}{3\gamma^2} + \frac{3\pi}{\gamma}\,(\sqrt{3}+1)\,\zeta\,(1/2)\,L_{-3}\,(1/2) \\ & + \frac{2\pi}{\gamma} \sum_{N\in\mathbb{N}} \frac{u_2(N)}{\sqrt{N}} \left(\exp\left\{ \left(\tfrac{2\pi\sqrt{N}}{\gamma} \right) \right\} - 1 \right)^{-1} \\ & - \frac{\pi}{\gamma} \sum_{N\in\mathbb{N}_0}^{\infty} \frac{u_2(3N+1)}{\sqrt{N+\frac{1}{3}}} \left(\exp\left\{ \left(\tfrac{2\pi\sqrt{N+\frac{1}{3}}}{\gamma} \right) \right\} - 1 \right)^{-1}, \end{aligned} \tag{12.5.7}$$

where we have used (12.A.5) for the modified Bessel function of the second kind, and used a geometric series to evaluated the sum over k. For the special value of $\gamma_{\text{hcp}} = \sqrt{8/3}$ we have

$$L^{\text{hcp}}(1, \gamma = \sqrt{8/3}) = -11.43265\ 30014\ 95285\ 63572 \cdots. \tag{12.5.8}$$

We also record the result

$$\begin{aligned} L^{\text{hcp}}(1/2) = {} & 6\zeta(1/2)L_{-3}(1/2) + \frac{\pi\gamma}{3\sqrt{3}} \\ & + 2\sum_{N=1}^{\infty} \frac{u_2(N)}{\sqrt{N}} \left(\exp\left(\frac{4\pi}{\sqrt{3}} \gamma\sqrt{N} \right) - 1 \right)^{-1} \\ & + 2\sum_{N=1}^{\infty} \cos\left(\frac{2\pi N}{3} \right) \frac{u_2(N)}{\sqrt{N}} \\ & \qquad \times \left(\exp\left(\frac{2\pi}{\sqrt{3}} \gamma\sqrt{N} \right) - \exp\left(-\frac{2\pi}{\sqrt{3}} \gamma\sqrt{N} \right) \right)^{-1}, \end{aligned}$$

which is obtained in the same way, starting from (12.3.30) and using the symmetry for the Bessel function, $K_{-s}(x) = K_s(x)$. We obtain using $\gamma = \sqrt{8/3}$,

$$L^{\mathrm{hcp}}(1/2, \gamma = \sqrt{8/3}) = -3.24185\ 86150\ 75732\ 86473\cdots \tag{12.5.9}$$

Finally, using (12.3.31) we observe that $L^{\mathrm{hcp}}(0) = 2\zeta(0) = -1$ for all $\gamma > 0$. A graph of the function $y = L^{\mathrm{hcp}}(s)$ is shown in Figure 12.6 for the case $\gamma_{\mathrm{hcp}} = \sqrt{8/3}$. We see that the curve has zeros at $s = -1, -2, -3, \ldots$ as we have $\Gamma(s) \to \infty$ for $s \in -\mathbb{N}_0$, and the Bessel terms vanish in both equations (12.3.30) and (12.3.31). Taking (12.3.31), the only remaining term for $n \in \mathbb{N}$ is $2\gamma^{-2s}\zeta(2s)$, and $\zeta(s)$ has zeros exactly at $s = -2, -4, -6, \ldots$

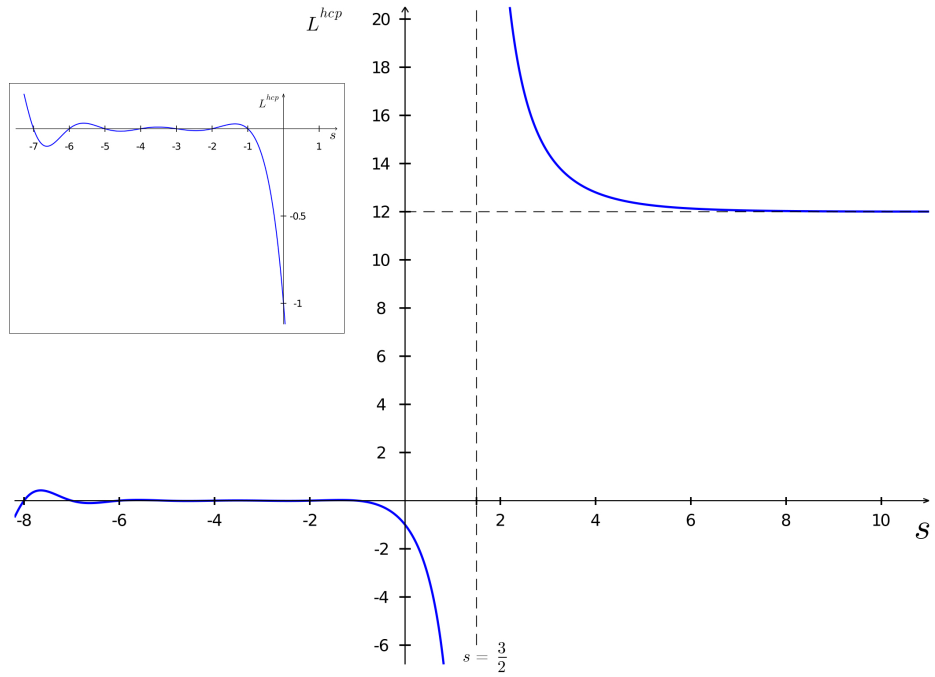

Figure 12.6 Graphs of $L^{\mathrm{hcp}}(s)$ for $-10 < s < 10$ (inlet shows the region $-7 < s < 0$).

12.6 Can analytical continuation be used for the Kratzer potential?

It is well known that for the Madelung constant analytical continuation can be used where the underlying series is only conditionally convergent [64]. The (2,1) LJ potential is known as the Kratzer potential. Introduced in 1920 it

has the form [16] and in analagous to the Lennard-Jones potential shown in (12.1.1) with $n = 2$ and $m = 1$,

$$V_{\text{Kratzer}}(r)/\varepsilon = \left[\left(\frac{r_e}{r}\right)^2 - 2\left(\frac{r_e}{r}\right)\right] . \tag{12.6.1}$$

The Kratzer potential has a Coulomb like behavior in the long range and a harmonic repulsive behavior in the short range. It is a very soft potential compared to the usual (12,6) LJ potential and could in principle be useful for example for metallic interaction. The question arises if we can use Eq.(12.1.2) which requires lattice sums to the left of the singularity at $s=\frac{3}{2}$ where $L_3^{\text{hcp}}(s=1) < 0$ for $s \in (0, \frac{3}{2})$. It is sufficient to consider the ideal hcp lattice only ($\gamma_{\text{hcp}} = \sqrt{8/3}$). By taking $n = 2$ and $m = 1$ in (12.4.1), the Kratzer potential dependent on the lattice constant a then becomes,

$$E^{\text{coh}}_{\text{Kratzer}}(a,\gamma)/\varepsilon = \frac{r_e^2}{2a^2}L^{hcp}(1,\gamma) - \frac{r_e}{a}L^{hcp}(\tfrac{1}{2},\gamma) , \tag{12.6.2}$$

for which the required lattice sums are given in eqs.(12.3.30) and (12.3.31).

The Kratzer potential together with the cohesive energy is shown in Figure 12.7. The cohesive energy has a maximum and not a minimum as it should be. The distance and energy can be obtained from (12.4.2) and (12.4.3),

$$\begin{aligned} R^*_{\text{min}} &= \frac{L\left(1,\sqrt{\frac{8}{3}}\right)}{L\left(\frac{1}{2},\sqrt{\frac{8}{3}}\right)} = \frac{-11.432653001495}{-3.241858615076} \\ &= 3.526573598346 \end{aligned} \tag{12.6.3}$$

$$E^*(R^*_{\text{min}}) = E^{\text{coh}}_{\text{Kratzer}}(R^*_{\text{min}})/\varepsilon = -\frac{L(s=\frac{1}{2})^2}{2L(s=1)} = +0.45963\ldots . \tag{12.6.4}$$

Even if only positive lattice sums are taken to obtain a proper cohesive energy curve with a minimum instead of a maximum, the nearest neighbor distance increases from the dimer to the solid state contrary to the (6,12) LJ potential. This clearly demonstrates that the Kratzer potential gives non-physical results for the solid state as the exponents lie left to the pole at $s=\frac{3}{2}$ producing negative lattice sums in the required region. Even if absolute values of $L^{\text{hcp}}(s)$ are used instead to invert the shape and produce a minimum, it would lack physical justification. The situation does not change if we choose $n < 3$ and $m > 3$ for a (n,m) LJ potential. As there is no alternative to an analytic continuation, the Kratzer potential cannot be used for the solid state in contrast, for example, to the Madelung constant. The main difference here is that the Madelung constant is a smooth function over the whole range of real exponents containing no

singularities.[378]

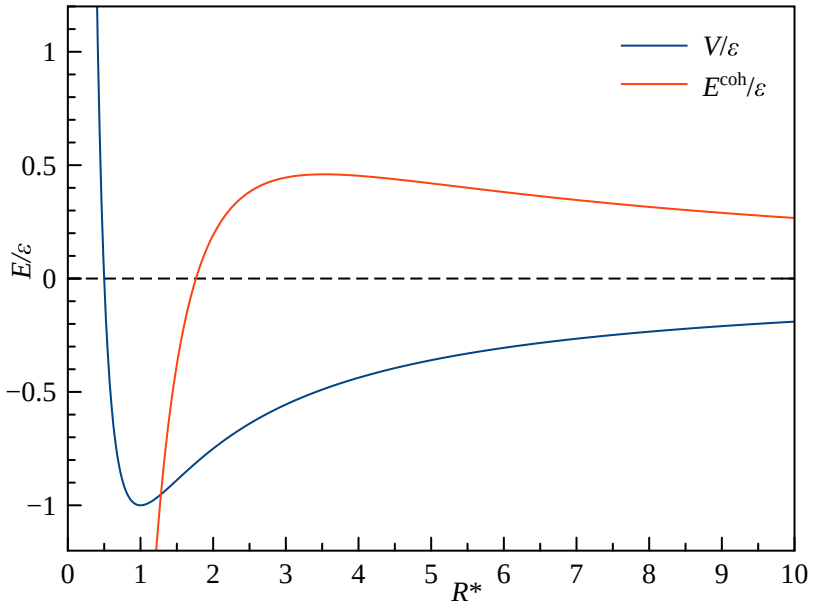

Figure 12.7 Kratzer potential for $V_{\mathrm{Kratzer}}(R^*)/\varepsilon$ with $R^* = r/r_e$ and for the cohesive energy $E^{\mathrm{coh}}_{\mathrm{Kratzer}}(R^*)/\varepsilon$ with $R^* = a/r_e$ where a is the hcp lattice constant and $c/a = \gamma = \sqrt{8/3}$.

12.7 Relation between the hcp structure and the cuboidal lattices

We recently introduced lattice sums for cubic lattices by introducing the following basis vectors [311]

$$b_1^{\top}(A) = (1,0,0) \quad , \quad b_2^{\top}(A) = \left(\frac{A}{A+1}, \frac{\sqrt{2A+1}}{A+1}, 0\right), \qquad (12.7.1)$$

$$b_3^{\top}(A) = \left(\frac{1}{A+1}, \frac{1}{(A+1)\sqrt{2A+1}}, \sqrt{\frac{4A}{(A+1)(2A+1)}}\right).$$

Where $A = 1/2$ defines the body-centred cubic (bcc) lattice and $A = 1$ the face-centred cubic (fcc) lattice. The packing density has been obtained as [311]

$$\rho(A) = \frac{\pi}{12}\sqrt{\frac{(A+1)^3}{A}}\,. \tag{12.7.2}$$

We can compare this to the hcp lattice with $\gamma \geq \sqrt{8/3}$ derived from the volume (12.2.5),

$$\rho(\gamma) = \frac{2\pi}{3\gamma\sqrt{3}}\,. \tag{12.7.3}$$

As the validity range for hard-sphere packing is $\gamma \in \left[\sqrt{8/3},\infty\right)$ we see that the largest packing density is achieved by the ideal value of $\gamma = \sqrt{8/3}$. Comparing both densities, hcp has the same packing density as the cuboidal lattices for

$$\gamma = \sqrt{\frac{8}{3}}\,f(A) \quad \text{with} \quad f(A) = \sqrt{\frac{8(A+1)^3}{A}}\,. \tag{12.7.4}$$

Again, for $A = 1$ (fcc) we see that the packing density is identical to the ideal hcp structure. For $A = 1/2$ (bcc) $f(A) = 1.08866...$, that is the hcp structure has the same packing density compared to bcc if we increase the c/a ratio by approximately 8.9%.

The corresponding lattice sum for the cuboidal lattice was already given in Ref.[379]

$$\begin{aligned} L^{\mathrm{cub}}(s,A) = {} & 4\left(\frac{A+1}{2}\right)^s \zeta(s) L_{-4}(s) + \frac{\pi A}{s-1}\left(1+\frac{1}{A}\right)^s \zeta(2s-2) \\ & + \frac{2\pi^s\sqrt{A}}{\Gamma(s)}\left(\sqrt{A}+\frac{1}{\sqrt{A}}\right)^s \sum_{i=1}^{\infty}\sum_{N=1}^{\infty} r_2(N)\left(\frac{N}{i^2}\right)^{(s-1)/2} \\ & \qquad \times K_{s-1}\left(2\pi i\sqrt{AN}\right) \\ & + \frac{2\pi^s\sqrt{A}}{\Gamma(s)}\left(\sqrt{A}+\frac{1}{\sqrt{A}}\right)^s \sum_{i=1}^{\infty}\sum_{N=0}^{\infty} (-1)^i r_2(4N+1) \\ & \qquad \times \left(\frac{2N+\frac{1}{2}}{i^2}\right)^{(s-1)/2} K_{s-1}\left(2\pi i\sqrt{A(2N+\frac{1}{2})}\right), \end{aligned} \tag{12.7.5}$$

where the L_{-4} function is defined in the appendix. $L^{\mathrm{cub}}(A;s)$ has a simple pole

at $s = 3/2$ and the residue is given by

$$\mathrm{Res}(L^{\mathrm{cub}}(A;s),3/2) = \frac{\pi}{\sqrt{A}}(A+1)^{3/2}. \tag{12.7.6}$$

It follows that the difference between the two lattice sums, cuboidal and hcp, the singularity is removed if

$$\begin{aligned}\mathrm{Res}(L^{\mathrm{cub}}(s,A),3/2) - \mathrm{Res}(L^{\mathrm{hcp}}(s,\gamma),3/2) &= d_{-1}^{\mathrm{cub}} - d_{-1}^{\mathrm{hcp}} \\ &= \frac{\pi}{\sqrt{A}}(A+1)^{3/2} - \frac{8\pi}{\gamma\sqrt{3}} = 0\,.\end{aligned} \tag{12.7.7}$$

This gives the condition in (12.7.4). Hence we follow that the singularity at $s = 3/2$ is removed for the difference between the cuboidal lattices and the hcp structure if they have the same packing density. Notice, that in removing the singularity we do not just have to consider hard spheres and only need the condition in (12.7.4) that $\gamma > 0$.
Evaluating the coefficient for d_0^{cub} given in Ref.[379] and using (12.5.6) we obtain

$$\lim_{s\to\frac{3}{2}}\left\{L^{\mathrm{cub}}(s,A=1) - L^{\mathrm{hcp}}(s,\gamma=\sqrt{8/3})\right\} = -0.00057\,11911\,16168\,67901\cdots. \tag{12.7.8}$$

The difference between the two function $L^{\mathrm{cub}}(s,A=1) - L^{\mathrm{hcp}}(s,\gamma=\sqrt{8/3})$ is shown in Figure 12.8. What is evident is that the difference in lattice sums between fcc and hcp is very small which is reflected in the fact that both phases often coexist for real compounds. The graph also appears to suggest the following for the relation between the ideal hcp and fcc structures:

$$\begin{aligned}&L^{\mathrm{hcp}}(s) > L^{\mathrm{fcc}}(s) > 0 \\ &\qquad \text{for} \quad s \in \cdots \cup (-6,-5) \cup (-4,-3) \cup (-2,-1) \cup (3/2,\infty) \\ &L^{\mathrm{hcp}}(s) < L^{\mathrm{fcc}}(s) < 0 \\ &\qquad \text{for} \quad s \in \cdots \cup (-5,-4) \cup (-3,-2) \cup (-1,0) \\ &-1 > L^{\mathrm{hcp}}(s) > L^{\mathrm{fcc}}(s) \quad \text{for} \quad s \in (0,3/2)\end{aligned}$$

12.8 Conclusions

We presented an efficient and fast convergent expansion for the multi-lattice hcp with variable c/a ratio. We demonstrated that the series can be analytically continued, albeit while mathematically sound the physical relevance has to be questioned at least for LJ type of potentials. We also showed that a metastable minimum appears for the (12,6) LJ potential at $\gamma = 0.71$, close to $\gamma = \frac{2}{3}$ where

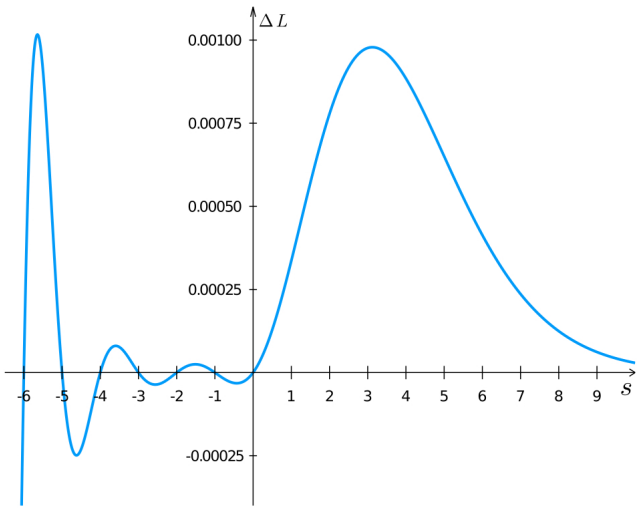

Figure 12.8 Graph of $L^{\mathrm{hcp}}(s) - L^{\mathrm{fcc}}(s)$.

the kissing number is $\kappa = 8$, and showed its dependence on the choice of exponents $(n.m)$. For the minimum close to the ideal c/a ratio of $\gamma_{\mathrm{hcp}} = \sqrt{\frac{8}{3}}$ we discussed the slight symmetry breaking for $(n.m)$ Lennard-Jones potentials where the sign of $\delta_{nm} = \gamma_{\min} - \sqrt{\frac{8}{3}}$ depends on the parameter range (n,m). This symmetry breaking will be dependent upon changing the pressure and temperature,[222, 380] which is currently under investigation. As a final remark, we mention that many-body forces in real bulk systems can stabilize the minimum around $\gamma = \sqrt{\frac{8}{3}}$ as this is well known, for example, for metallic systems [381]. The program for calculating lattice sums is freely available from our website [143].

12.9 Appendix

A Formulas for special functions

Many results for special functions and analytic number theory have been used in this work. For clarity and ease of use, they are stated here along with references if not given in the books by Andrews, Askey and R. Roy [382] or Temme [110].

The gamma function

The gamma function may be defined for $s > 0$ by

$$\Gamma(s) = \int_0^\infty t^{s-1} e^{-t} \, \mathrm{d}t \; . \tag{12.A.1}$$

By the change of variable $t = wx$ this can be rewritten in the useful form

$$\frac{1}{w^s} = \frac{1}{\Gamma(s)} \int_0^\infty x^{s-1} e^{-wx} \, \mathrm{d}x \; . \tag{12.A.2}$$

The modified Bessel function

The following integral may be evaluated in terms of the modified Bessel function:

$$\int_0^\infty x^{s-1} e^{-ax-b/x} \mathrm{d}x = 2 \left(\frac{b}{a} \right)^{s/2} K_s(2\sqrt{ab}) \; . \tag{12.A.3}$$

By the change of variable $x = u^{-1}$ it can be shown that

$$K_s(z) = K_{-s}(z) \; . \tag{12.A.4}$$

When $s = 1/2$ the modified Bessel function reduces to an elementary function:

$$K_{1/2}(z) = \sqrt{\frac{\pi}{2z}} \, e^{-z} \; . \tag{12.A.5}$$

The asymptotic formula holds:

$$K_s(z) \sim \sqrt{\frac{\pi}{2z}} \, e^{-z} \quad \text{as} \quad z \to \infty, \quad (\, |\arg z| < 3\pi/2) \; . \tag{12.A.6}$$

Theta functions

The transformation formula for theta functions is [382, 383]:

$$\sum_{n \in \mathbb{Z}} e^{-\pi n^2 t + 2\pi i n a} = \frac{1}{\sqrt{t}} \sum_{n \in \mathbb{Z}} e^{-\pi (n+a)^2 / t}, \quad \text{assuming } \mathrm{Re}(t) > 0 \quad . \tag{12.A.7}$$

We will need the special cases $a = 0$ and $a = 1/2$, which are

$$\sum_{n \in \mathbb{Z}} e^{-\pi n^2 t} = \frac{1}{\sqrt{t}} \sum_{n \in \mathbb{Z}} e^{-\pi n^2 / t} \tag{12.A.8}$$

and

$$\sum_{n \in \mathbb{Z}} (-1)^n e^{-\pi n^2 t} = \frac{1}{\sqrt{t}} \sum_{n \in \mathbb{Z}} e^{-\pi (n+\frac{1}{2})^2 / t} \tag{12.A.9}$$

respectively. The sum of two squares formula is [132]

$$\left(\sum_{j\in\mathbb{Z}} q^{j^2}\right)^2 = \sum_{j,k\in\mathbb{Z}} q^{j^2+k^2} = \sum_{N\in\mathbb{N}_0} r_2(N) q^N \tag{12.A.10}$$

where

$$r_2(N) = \#\left\{j^2+k^2 = N\right\} = \begin{cases} 1 & \text{if } N = 0\,, \\ 4\sum_{d|N} \chi_{-4}(d) & \text{if } N \geq 1\,, \end{cases} \tag{12.A.11}$$

the sum being is over the positive divisors d of N. For example,

$$\begin{aligned} r_2(18) &= 4\left(\chi_{-4}(1)+\chi_{-4}(2)+\chi_{-4}(3)+\chi_{-4}(6)+\chi_{-4}(9)+\chi_{-4}(18)\right) \\ &= 4\left(1+0-1+0+1+0\right) = 4. \end{aligned}$$

The cubic analogues of the transformation formula are[383, 384]

$$\sum_{j,k\in\mathbb{Z}} e^{-2\pi(j^2+jk+k^2)t} = \frac{1}{t\sqrt{3}} \sum_{j,k\in\mathbb{Z}} e^{-2\pi(j^2+jk+k^2)/3t} \tag{12.A.12}$$

and

$$\sum_{j,k\in\mathbb{Z}} e^{-2\pi((j+\frac{1}{3})^2+(j+\frac{1}{3})(k+\frac{1}{3})+(k+\frac{1}{3})^2)t} = \frac{1}{t\sqrt{3}} \sum_{j,k\in\mathbb{Z}} \omega^{j-k} e^{-2\pi(j^2+jk+k^2)/3t} \tag{12.A.13}$$

where $\omega = \exp\left(2\pi\sqrt{-1}/3\right)$ is a primitive cube root of unity. The analogue of the sum of two squares result is [132]

$$\sum_{j,k\in\mathbb{Z}} q^{j^2+jk+k^2} = \sum_{N\in\mathbb{N}_0} u_2(N) q^N \tag{12.A.14}$$

where

$$u_2(N) = \#\left\{j^2+jk+k^2 = N\right\} = \begin{cases} 1 & \text{if } N = 0, \\ 6\sum_{d|N} \chi_{-3}(d) & \text{if } N \geq 1, \end{cases} \tag{12.A.15}$$

where the sum is again over the positive divisors d of N. By Ref.[78] we also have

$$\sum_{j,k\in\mathbb{Z}} q^{(j+\frac{1}{3})^2+(j+\frac{1}{3})(k+\frac{1}{3})+(k+\frac{1}{3})^2} = \frac{1}{2} \sum_{N\in\mathbb{N}_0} u_2(3N+1) q^{N+\frac{1}{3}}\,. \tag{12.A.16}$$

The Riemann zeta function and L functions

The definitions are:

$$\zeta(s) = \sum_{j\in\mathbb{N}} \frac{1}{j^s} \tag{12.A.17}$$

$$L_{-3}(s) = \sum_{j\in\mathbb{N}} \frac{\chi_{-3}(j)}{j^s} = 1 - \frac{1}{2^s} + \frac{1}{4^s} - \frac{1}{5^s} + \frac{1}{7^s} - \frac{1}{8^s} + \cdots . \tag{12.A.18}$$

The function $\zeta(s)$ is the Riemann zeta function. It has a pole of order 1 at $s = 1$, and in fact[110, 382]

$$\lim_{s\to 1}(s-1)\zeta(s) = 1 . \tag{12.A.19}$$

We will require the functional equations

$$\pi^{-s/2}\Gamma(s/2)\zeta(s) = \pi^{-(1-s)/2}\Gamma((1-s)/2)\zeta(1-s) \tag{12.A.20}$$

and the special values

$$\zeta(2) = \frac{\pi^2}{6}, \quad \zeta(0) = -\frac{1}{2}, \quad \zeta(-1) = -\frac{1}{12}, \quad \zeta(-2n) = 0 \quad \text{for} \quad n \in \mathbb{N}, \tag{12.A.21}$$

and

$$L_{-3}(1) = \frac{\pi\sqrt{3}}{9}, \quad L_{-3}(0) = \frac{1}{3}, \quad L_{-3}(-2n+1) = 0 \quad \text{for} \quad n \in \mathbb{N}. \tag{12.A.22}$$

For details see Refs.[105, 285].

Other results used are

$$\sum_{j\in\mathbb{N}_0}^{\infty} \frac{1}{(j+\frac{1}{2})^s} = (2^s - 1)\zeta(s) \tag{12.A.23}$$

$$\sum_{i,j\in\mathbb{Z}}{}' \frac{1}{(i^2+ij+j^2)^s} = 6\zeta(s)L_{-3}(s) \tag{12.A.24}$$

$$\sum_{i,j\in\mathbb{Z}} \frac{1}{((i+\frac{1}{3})^2+(i+\frac{1}{3})(j+\frac{1}{3})+(j+\frac{1}{3})^2)^s} = 3(3^s-1)\zeta(s)L_{-3}(s) . \tag{12.A.25}$$

The identity (12.A.23) follows from the definition of $\zeta(s)$ by series rearrangements. For (12.A.24), see (1.4.16) of Ref.[275]. The identity (12.A.25) can be obtained by the method of Mellin transforms [26, 78, 382].

B Laurent expansion

Laurent's theorem implies there is an expansion of the form,

$$L^{\rm hcp}(s,\gamma) = \frac{d_{-1}}{s-3/2} + d_0 + \sum_{n=1}^{\infty} d_n (s-3/2)^n \,, \tag{12.B.1}$$

where we get for (12.3.30) the residue (12.5.2). This follows from

$$\begin{aligned} \lim_{s\to 3/2}(s-3/2)L^{\rm hcp}(s) &= \lim_{s\to 3/2}(s-3/2)\frac{4\pi}{\sqrt{3}(s-1)}\left(\frac{\gamma}{2}\right)^{2-2s}\zeta(2s-2) \\ &= \frac{16\pi}{\gamma\sqrt{3}}\lim_{s\to 3/2}(s-3/2)\zeta(2s-2) = \frac{8\pi}{\gamma\sqrt{3}}\lim_{u\to 1}(u-1)\zeta(u) = \frac{8\pi}{\gamma\sqrt{3}}\,, \end{aligned} \tag{12.B.2}$$

where (12.A.19) was used in the last step of the calculation. To get the coefficient d_0 in (12.3.30) we need to consider the following limit

$$w = \lim_{s\to 3/2}\left\{\frac{4\pi}{\sqrt{3}(s-1)}\left(\frac{\gamma}{2}\right)^{2-2s}\zeta(2s-1) - \frac{8\pi}{\gamma\sqrt{3}(s-\frac{3}{2})}\right\}. \tag{12.B.3}$$

Substituting $s=(t+3)/2$ and using the Laurent expansion for the Riemann zeta function,

$$\begin{aligned} w &= \lim_{t\to 0}\left\{\frac{8\pi}{\sqrt{3}(t+1)}\left(\frac{2}{\gamma}\right)^{t+1}\left[t^{-1}+\gamma_0-\gamma_1 t+...\right] - \frac{16\pi}{\gamma t\sqrt{3}}\right\} \\ &= \lim_{t\to 0}\frac{f(t)-f(0)}{t} \;+\; \frac{16\pi}{\gamma\sqrt{3}}\gamma_0 = f'(t)|_0 \;+\; \frac{16\pi}{\gamma\sqrt{3}}\gamma_0 \end{aligned} \tag{12.B.4}$$

where

$$f(t) = \frac{8\pi}{\sqrt{3}}\frac{1}{(t+1)}\left(\frac{2}{\gamma}\right)^{t+1} \tag{12.B.5}$$

and $\gamma_0 = 0.57721\,56649\,01532\,86060\cdots$ is Euler's constant. It is easy to verify that

$$f'(t) = -\frac{8\pi}{\sqrt{3}(t+1)^2}\left(\frac{2}{\gamma}\right)^{t+1} + \frac{8\pi}{\sqrt{3}(t+1)}\left(\frac{2}{\gamma}\right)^{t+1}\ln\left(\frac{2}{\gamma}\right). \tag{12.B.6}$$

We finally obtain

$$w = \frac{16\pi}{\gamma\sqrt{3}}\left\{\gamma_0 + \ln\left(\frac{2}{\gamma}\right) - 1\right\}. \tag{12.B.7}$$

C Minimum of Lennard-Jones potentials near $\gamma = \sqrt{\frac{8}{3}}$

The iterative Newton–Raphson algorithm [385] can be used to determine $\gamma_{\min}$ to the required accuracy

$$\gamma_{i+1} = \gamma_i - \frac{\partial_\gamma E^*_{nm}(\gamma_i)}{\partial^2_\gamma E^*_{nm}(\gamma_i)}\,, \tag{12.C.1}$$

starting with $\gamma_1 = \sqrt{\frac{8}{3}}$. Only few iterations are required to achieve convergence to computer accuracy. The required derivatives for $E^*_{nm}(\gamma)$ can be easily derived

$$\begin{aligned}
\partial_\gamma E^*_{nm}(\gamma) &= \frac{1}{2(n-m)} \left\{ m \left(\frac{L(\frac{m}{2},\gamma)}{L(\frac{n}{2},\gamma)} \right)^{\frac{n}{n-m}} \partial_\gamma L(\tfrac{n}{2},\gamma) \right. \\
&\qquad \left. -n \left(\frac{L(\frac{m}{2},\gamma)}{L(\frac{n}{2},\gamma)} \right)^{\frac{m}{n-m}} \partial_\gamma L(\tfrac{m}{2},\gamma) \right\} \\
\partial^2_\gamma E^*_{nm}(\gamma) &= \frac{nm}{2(n-m)^2} \left[L(\tfrac{n}{2},\gamma)\partial_\gamma L(\tfrac{m}{2},\gamma) + L(\tfrac{m}{2},\gamma)\partial_\gamma L(\tfrac{n}{2},\gamma) \right] \\
&\quad \times \left[\frac{\partial_\gamma L(\frac{n}{2},\gamma)}{L^2(\frac{n}{2},\gamma)} \left(\frac{L(\frac{m}{2},\gamma)}{L(\frac{n}{2},\gamma)} \right)^{\frac{m}{n-m}} - \frac{\partial_\gamma L(\frac{m}{2},\gamma)}{L^2(\frac{m}{2},\gamma)} \left(\frac{L(\frac{m}{2},\gamma)}{L(\frac{n}{2},\gamma)} \right)^{\frac{n}{n-m}} \right] \\
&\quad + \frac{m}{2(n-m)} \left(\frac{L(\frac{m}{2},\gamma)}{L(\frac{n}{2},\gamma)} \right)^{\frac{m}{n-m}} \partial^2_\gamma L(\tfrac{n}{2},\gamma) \\
&\quad - \frac{n}{2(n-m)} \left(\frac{L(\frac{m}{2},\gamma)}{L(\frac{n}{2},\gamma)} \right)^{\frac{m}{n-m}} \partial^2_\gamma L(\tfrac{m}{2},\gamma)\,,
\end{aligned} \tag{12.C.2}$$

leading to the simple condition for the minimum through the first derivative

$$nL(\tfrac{n}{2},\gamma)\partial_\gamma L(\tfrac{m}{2},\gamma) - mL(\tfrac{m}{2},\gamma)\partial_\gamma L(\tfrac{n}{2},\gamma) = 0\,. \tag{12.C.3}$$

For (12.C.2) we require the derivatives $\partial_\gamma L(s,\gamma)$ and $\partial^2_\gamma L(s,\gamma)$, which involves derivatives of the Bessel function $K_s(a\gamma)$. We only need the first derivative as we can use the two formulae,

$$\begin{aligned}
\partial_x K_{s-1}(x) &= -K_s(x) + \frac{(s-1)}{x} K_{s-1}(x) \\
\partial_x K_s(x) &= -K_{s-1}(x) - \frac{s}{x} K_s(x)\,.
\end{aligned} \tag{12.C.4}$$

We rewrite Eq.(12.3.30) in the following short-hand notation,

$$L(s,\gamma) = A_s + B_s\gamma^{2-2s} + C_s\gamma^{1-s}\sum_{k,N\in\mathbb{N}}\{d_{skN}K_{s-1}(w_{kN}\gamma) + f_{skN}K_{s-1}(v_{kN}\gamma)\} \tag{12.C.5}$$

with the coefficients

$$\begin{aligned}
A_s &= 6\zeta(s)L_{-3}(s) \quad , \quad B_s = \frac{4^s\pi}{\sqrt{3}(s-1)}\zeta(2s-2) \quad , \quad C_s = \frac{4}{\sqrt{3}}\frac{(2\pi)^s}{\Gamma(s)} \\
d_{skN} &= u_2(N)\left(\frac{N}{3k^2}\right)^{(s-1)/2} \quad , \\
f_{skN} &= \cos\left(\frac{2\pi N}{3}\right)u_2(N)\left(\frac{N}{3(k-\frac{1}{2})^2}\right)^{(s-1)/2} \\
w_{kN} &= \frac{4\pi}{\sqrt{3}}k\sqrt{N} \quad , \quad v_{kN} = \frac{4\pi}{\sqrt{3}}\left(k-\tfrac{1}{2}\right)\sqrt{N}\,.
\end{aligned} \tag{12.C.6}$$

The lattice sum derivatives are derived as,

$$\begin{aligned}
\partial_\gamma L(s,\gamma) = 2(1-s)B_s\gamma^{1-2s} - C_s\gamma^{1-s} \\
\times\sum_{k,N\in\mathbb{N}}\{d_{skN}w_{kN}K_s(w_{kN}\gamma) + f_{skN}v_{kN}K_s(v_{kN}\gamma)\}
\end{aligned} \tag{12.C.7}$$

and

$$\begin{aligned}
\partial_\gamma^2 L(s,\gamma) &= (2s-1)(2s-2)B_s\gamma^{-2s} \\
&+ C_s\gamma^{1-s}\sum_{k,N\in\mathbb{N}}\left\{d_{skN}w_{kN}^2K_{s-1}(w_{kN}\gamma) + f_{skN}v_{kN}^2K_{s-1}(v_{kN}\gamma)\right\} \\
&+ C_s(2s-1)\gamma^{-s}\sum_{k,N\in\mathbb{N}}\{d_{skN}w_{kN}K_s(w_{kN}\gamma) + f_{skN}v_{kN}K_s(v_{kN}\gamma)\}\,.
\end{aligned} \tag{12.C.8}$$

We note that Eq.(12.C.9) is converging very fast in our case and only few iterations are required. For example, starting with $\gamma_1 = \sqrt{\frac{8}{3}}$ we get after the first iteration $\gamma_2 = 1.6327632935$ very close to the converged result of $\gamma_2 = 1.6327633049$.

Finally, calculating the (m,n) combination $(n,m\in\mathbb{R})$ reaching the ideal $\gamma_{\rm hcp} = \sqrt{\frac{8}{3}}$ value (see Figure 12.5), we use again the Newton-Raphson method in the following form

$$m_{i+1} = m_i - \frac{\partial_\gamma E^*_{nm}(\gamma_{\rm hcp})}{\partial_m\partial_\gamma E^*_{nm}(\gamma_{\rm hcp})}\,, \tag{12.C.9}$$

for a fixed n value where $\partial_\gamma E^*_{nm}(\gamma_{\rm hcp})$ is obtained from (12.C.8) and the derivative with respect to m in the denominator is obtained numerically through a two-point formula.

D The hcp lattice sum expressed in quadratic forms

In order to show that the lattice sum (12.2.9) can be decomposed into four sums containing pure quadratic forms, we start with the double sum $g_1(s,a)$ defined by

$$g_1(s,a) = \sum_{i,j\in\mathbb{Z}} ((3i+1)^2 + (3i+1)(3j+1) + (3j+1)^2 + a^2)^{-s} \qquad (12.D.1)$$

where a and s are real numbers and $s > 1$. We will need the following alternative expression for $g_1(s,a)$.

Lemma D.1 *The following identity holds:*

$$g_1(s,a) = \frac{1}{2}\left(\sum_{i,j\in\mathbb{Z}}{}' (3i^2+9ij+9j^2+a^2)^{-s} - \sum_{i,j\in\mathbb{Z}}{}' (9i^2+9ij+9j^2+a^2)^{-s} \right) \qquad (12.D.2)$$

where the primes indicate that the terms corresponding to $(i,j) = (0,0)$ are omitted from the summations if $a = 0$.

Proof. First, let us consider the case $a \neq 0$. For $r \in \{0,1,2\}$ let $g_r(s,a)$ be defined by

$$g_r(s,a) = \sum_{i,j\in\mathbb{Z}} ((3i+r)^2 + (3i+r)(3j+r) + (3j+r)^2 + a^2)^{-s} \qquad (12.D.3)$$

and observe that this definition is consistent with (12.D.1) when $r = 1$. Then

$$g_0(s,a) + g_1(s,a) + g_2(s,a) = \sum_{\substack{i,j\in\mathbb{Z} \\ i-j\equiv 0 \pmod 3}} (i^2 + ij + j^2 + a^2)^{-s}$$

where the sum is over all integers i and j satisfying the given congruence. Since $i-j$ is a multiple of 3, put $i = j+3k$ to get

$$\begin{aligned} g_0(s,a) + g_1(s,a) + g_2(s,a) &= \sum_{j,k\in\mathbb{Z}} ((j+3k)^2 + (j+3k)j + j^2 + a^2)^{-s} \\ &= \sum_{j,k\in\mathbb{Z}} (3j^2 + 9jk + 9k^2 + a^2)^{-s}. \end{aligned} \qquad (12.D.4)$$

Next, by replacing the summation indices i and j in the definition (12.D.1) with $-i-1$ and $-j-1$, respectively, we readily find that $g_1(s;a) = g_2(s;a)$.

Hence, (12.D.4) may be written as

$$g_1(s,a) = \frac{1}{2}\left(\sum_{i,j\in\mathbb{Z}} (3i^2+9ij+9j^2+a^2)^{-s} - g_0(s;a)\right)$$
$$= \frac{1}{2}\left(\sum_{i,j\in\mathbb{Z}} (3i^2+9ij+9j^2+a^2)^{-s} - \sum_{i,j\in\mathbb{Z}} (9i^2+9ij+9j^2+a^2)^{-s}\right). \tag{12.D.5}$$

This proves the result in the case $a \neq 0$.
On separating out the terms corresponding to $(i,j) = (0,0)$ from each of the series in (12.D.5), we obtain

$$g_1(s,a) = \frac{1}{2}\left(\frac{1}{a^{2s}} + \sum_{i,j\in\mathbb{Z}}{}' (3i^2+9ij+9j^2+a^2)^{-s}\right)$$
$$- \frac{1}{2}\left(\frac{1}{a^{2s}} + \sum_{i,j\in\mathbb{Z}}{}' (9i^2+9ij+9j^2+a^2)^{-s}\right)$$
$$= \frac{1}{2}\sum_{i,j\in\mathbb{Z}}{}' (3i^2+9ij+9j^2+a^2)^{-s} - \frac{1}{2}\sum_{i,j\in\mathbb{Z}}{}' (9i^2+9ij+9j^2+a^2)^{-s}.$$

This has been obtained under the assumption $a \neq 0$. Now take the limit as $a \to 0$ on each side to complete the proof. This completes the proof of Lemma (D.1)
We will now show that the triple sum $L^B(s,\gamma)$ in (12.2.9) can be evaluated in terms of the sums $L(s,\gamma)$ and $M(s,\gamma)$ defined by

$$L(s,\gamma) = \sum_{i,j,k\in\mathbb{Z}}{}' (i^2+ij+j^2+\gamma^2k^2)^{-s}, \tag{12.D.6}$$

and

$$M(s,\gamma) = \sum_{i,j,k\in\mathbb{Z}}{}' \left(\frac{i^2}{3}+ij+j^2+\gamma^2k^2\right)^{-s}, \tag{12.D.7}$$

where the primes indicate that the terms corresponding to $(i,j,k) = (0,0,0)$ are omitted from the summations.

Theorem D.2 *The following evaluation holds:*

$$L^B(s,\gamma) = \frac{1}{2}\left[M\left(s,\frac{\gamma}{2}\right) - L\left(s,\frac{\gamma}{2}\right) - M(s,\gamma) + L(s,\gamma)\right]. \tag{12.D.8}$$

Proof. Let

$$L^C(s,\gamma) = \sum_{i,j,k\in\mathbb{Z}} \left((i+\tfrac{1}{3})^2 + (i+\tfrac{1}{3})(j+\tfrac{1}{3}) + (j+\tfrac{1}{3})^2 + \gamma^2k^2\right)^{-s}. \tag{12.D.9}$$

Clearly,

$$\begin{aligned} L^B(s,\gamma)+L^C(s,\gamma) &= \sum_{i,j,k\in\mathbb{Z}} ((i+\frac{1}{3})^2+(i+\tfrac{1}{3})(j+\tfrac{1}{3})+(j+\tfrac{1}{3})^2+\gamma^2(\tfrac{k}{2})^2)^{-s} \\ &= L^C\left(s;\frac{\gamma}{2}\right) \end{aligned}$$

and therefore

$$L^B(s,\gamma) = L^C\left(s,\frac{\gamma}{2}\right) - L^C(s,\gamma). \tag{12.D.10}$$

We now turn to the evaluation of $L^C(s,\gamma)$. By the definition (12.D.9) we have

$$\begin{aligned} L^C(s,\gamma) &= \sum_{k\in\mathbb{Z}} \left(\sum_{i,j\in\mathbb{Z}} ((i+\tfrac{1}{3})^2+(i+\tfrac{1}{3})(j+\frac{1}{3})+(j+\tfrac{1}{3})^2+\gamma^2k^2)^{-s} \right) \\ &= 3^{2s} \sum_{k\in\mathbb{Z}} \left(\sum_{i,j\in\mathbb{Z}} ((3i+1)^2+(3i+1)(3j+1)+(3j+1)^2+9\gamma^2k^2)^{-s} \right) \\ &= 3^{2s} \sum_{k\in\mathbb{Z}} g_1(s;3\gamma k) \end{aligned}$$

where in the last step we used the definition of g_1 from (12.D.1). Now apply Lemma D.1 to get

$$\begin{aligned} L^C(s,\gamma) &= 3^{2s} \sum_{k\in\mathbb{Z}} \left(\frac{1}{2} \sum_{k\in\mathbb{Z}} (3i^2+9ij+9j^2+9\gamma^2k^2)^{-s} \right. \\ &\qquad \left. -\frac{1}{2} \sum_{k\in\mathbb{Z}} (9i^2+9ij+9j^2+9\gamma^2k^2)^{-s} \right) \\ &= \frac{1}{2}\left(M(s,\gamma)-L(s;\gamma)\right). \end{aligned} \tag{12.D.11}$$

On using (12.D.11) in (12.D.10) we complete the proof of Theorem (D.2).
Adding both lattice sums (12.2.7) and (12.2.9) and using (12.D.8) we get

$$\begin{aligned} L^{\mathrm{hcp}}(s,\gamma) &= L^A(s,\gamma)+L^B(s,\gamma) \\ &= \frac{1}{2}\left[M\left(s,\frac{\gamma}{2}\right)-L\left(s,\frac{\gamma}{2}\right)-M\left(s,\gamma\right)+3L(s,\gamma)\right]. \end{aligned} \tag{12.D.12}$$

One can easily check that the associated Gram matrices to these two lattice sums M and L are positive definite and one can use, for example, the Van der Hoff-Benson-Houtot [111, 136, 160] or the Terras expansion [112] to express them in terms of standard functions and Bessel function expansion terms. Table 12.4 contains the lattice sums for a few selected values of s and γ. We note that the decomposition into quadratic forms is numerically less stable at higher

s and smaller γ values as large terms cancel out in the sum (12.D.12).

term	$s=2$	$s=3$	$s=6$
$\gamma=\sqrt{\frac{8}{3}}$			
$L_A(s,\gamma)$	12.187035832908817	6.9286599267897087	6.0208613527770725
$L_B(s,\gamma)$	13.152046505146327	7.5262373510519094	6.1114324163218541
$L_A(s,\gamma)+L_B(s,\gamma)$	25.339082338055150	14.454897277841617	12.132293769098926
$+\frac{1}{2}M\left(s,\frac{\gamma}{2}\right)$	61.566637885614639	99.388534652974585	2208.3785419040942
$-\frac{1}{2}L\left(s,\frac{\gamma}{2}\right)$	-13.094897505088104	-8.4240358782104963	-14.684205942268090
$-\frac{1}{2}M(s,\gamma)$	-41.413211791834620	-86.902591387107066	-2190.5933342218777
$+\frac{3}{2}L(s,\gamma)$	18.280553749363229	10.392989890184563	9.0312920291656038
Sum(M,L)	25.339082338055142	14.454897277841578	12.132293769114119
$\gamma=\frac{2}{3}$			
$L_A(s,\gamma)$	227.33369931200846	1507.1847446374013	1063157.5188371434
$L_B(s,\gamma)$	109.06159263354647	174.00606910065562	8036.0292167961597
$L_A(s,\gamma)+L_B(s,\gamma)$	336.39529194555502	1681.1908137380569	1071193.5480539501
$+\frac{1}{2}M\left(s,\frac{\gamma}{2}\right)$	1672.8769558418203	47837.699032123222	2177323887.1934562
$-\frac{1}{2}L\left(s,\frac{\gamma}{2}\right)$	-1454.6882390304756	-47489.056422016118	-2177318026.8192515
$-\frac{1}{2}M(s,\gamma)$	-222.79399165372277	-928.23250403133125	-534574.05138774007
$+\frac{3}{2}L(s,\gamma)$	341.00054896801259	2260.7771169561056	1594736.2782562445
Sum(M,L)	336.39527412563450	1681.1872230318791	1066022.6010731400
$\gamma=2$			
$L_A(s,\gamma)$	10.694752688165460	6.6212978506634972	6.0112376723424239
$L_B(s,\gamma)$	8.8968902346685326	3.5631812795615505	1.1145428205070376
$L_A(s,\gamma)+L_B(s,\gamma)$	19.591642922833991	10.184479130225048	7.1257804928494615
$+\frac{1}{2}M\left(s,\frac{\gamma}{2}\right)$	52.602679315049684	91.967422008460545	2192.7895136662119
$-\frac{1}{2}L\left(s,\frac{\gamma}{2}\right)$	-9.8776390781413106	-5.2724042151945429	-4.1012852765432157
$-\frac{1}{2}M(s,\gamma)$	-39.175526346322584	-86.442485439036091	-2190.5793044050806
$+\frac{3}{2}L(s,\gamma)$	16.042129032248191	9.9319467759952484	9.0168565085136336
Sum(M,L)	19.591642922833977	10.184479130225162	7.1257804931014519

Table 12.4 Values for $L_A(s,\gamma)$ and $L_B(s,\gamma)$ using eqs. (12.3.11) and (12.3.23), and for the four different lattice sums using eqs. (12.D.6) and (12.D.7) for three different c/a ratios and for some selected $s=n/2$. For the entry Sum(M,L) Eq. (12.D.12) is used. For the lattices sums $M(s,x)$ and $L(s,x)$ the Terras decomposition was used. The last digit is not rounded.

Part IV

Conclusion

13 Summary & Conclusion

Throughout this thesis various projects on lattice sums were worked on that produced seven papers starting from re-exploring direct summation methods for lattice sums to applications of lattice sums in solid-state physics. As a point of first call, building upon the work of the early 20^{th} century on lattice sums, direct summation was investigated with the added tools from arbitrary precision floating point software techniques from modern computers and some number theoretical techniques not used by the original pioneers on that topic. This motivated the investigation into alternative methods that expressed lattice sums as fast converging series or reduced the problem in dimension allowing various mathematical techniques to be employed. At a minimum, this allowed evaluations for up to a desired numerical precision e.g., at least to double precision floating point, to be used further down the line in applications in solid-state physics such as for properties on elemental rare gas solids. More importantly, finding lattice sums for common cubic lattices and hexagonal structures in terms of fast converging functions or in terms of simple functions using number theoretical techniques provided also deep insight into the behaviour of these sums including their analytical continuations.

Along the total energy curve corresponding to a Bain phase transition pathway from acc to fcc using a single lattice parameter A and the lattice sums from Project 4, we were able to show that the bcc phase remains energetically unstable at higher pressures. Fast converging lattice sums were used in the calculation of ground state cohesive energy curves that gave insight into the stability of lattices under varying conditions, and were additionally applied to calculate basic solid-state properties like the pressure or the bulk modulus as volume derivatives of the cohesive energy in Project 5. These calculations exposed the meta-stability of the bcc lattice at low values of a and b in the (a,b) LJ potential and found that the bcc lattice decreases in stability with increasing pressure, which suggests that to stabilize these types of crystal structures one requires other bonding conditions in addition to a simple two-body potential such as the Lennard-Jones.

Following the work done on cubic lattice sums in Projects 1,3 and 4, and the application of the results of their fast converging expressions we moved to the lattice sum for the hexagonal close packed structure. Continuing the work

done by Lennard-Jones and Ingham as well as Kane and Goeppert-Mayer, in Project 7 an efficient and fast converging expansion was presented for the hexagonal close packed multi-lattice with a variable c/a ratio for the first time. This was a significantly new sum to that of the hcp lattice sum that was worked on in Project 1 and evaluated using the Van der Hoff–Benson and Terras methods. This allowed us to analytically examine the behaviour of a Lennard-Jones potential as a function of the c/a ratio, however the use (if any) in terms of its physical relevance for a simple LJ potential is yet to be investigated. We observed the occurrence of a slight symmetry breaking effect and the appearance of a second metastable minimum using the (12,6) Lennard-Jones potential in contrast to the hard-sphere model with an ideal ratio of $c/a = \sqrt{8/3}$ exhibiting 12 kissing spheres around a central atom. Similarly to the stability of the cubic system, we remark that with respect to the hcp structure, many-body forces in real bulk systems can stabilize the minimum around $\gamma = \sqrt{\frac{8}{3}}$. In this respect, a continuation of this thesis would be to find efficient fast converging series for many-body potentials such as the 3-body Axilrod-Teller-Muto potential

Part V

Appendix

A Appendix

A.1 Tables

Table A.1 Number of representations $r_3^{\mathscr{L}}(n)$ for the sc, bcc, fcc and hcp structures (sequences A005875, A004013, A004015 and A004012 in Sloane's database[75]), see (2.6.1).

n	$r_3^{\mathrm{sc}}(n)$	$r_3^{\mathrm{bcc}}(n)$	$r_3^{\mathrm{fcc}}(n)$	$r_3^{\mathrm{hcp}}(n)$
0	1	1	1	1
1	6	0	12	0
2	12	0	6	0
3	8	8	24	12
4	6	6	12	0
5	24	0	24	0
6	24	0	8	6
7	0	0	48	0
8	12	12	6	2
9	30	0	36	18
10	24	0	24	0
11	24	24	24	12
12	8	8	24	6
13	24	0	72	0
14	48	0	0	0
15	0	0	48	12
16	6	6	12	0
17	48	0	48	12
18	36	0	30	6
19	24	24	72	6
20	24	24	24	12
21	48	0	48	24
22	24	0	24	6
23	0	0	48	0
24	24	24	8	0
25	30	0	84	12
26	72	0	24	0
27	32	32	96	12
28	0	0	48	0
29	72	0	24	24
30	48	0	0	12
31	0	0	96	12
32	12	12	6	2
33	48	0	96	12
34	48	0	48	6
35	48	48	48	24
36	30	30	36	6
37	24	0	120	12
38	72	0	24	0
39	0	0	48	24
40	24	24	24	0
41	96	0	48	12
42	48	0	48	0

a	$(\frac{a}{n})$
-3	1 if $n \equiv 1 \pmod 3$ -1 if $n \equiv 2 \pmod 3$
4	1 if n is odd
-4	1 if $n \equiv 1 \pmod 4$ -1 if $n \equiv 3 \pmod 4$
8	1 if $n \equiv 1,7 \pmod 8$ -1 if $n \equiv 3,5 \pmod 8$
-8	1 if $n \equiv 1,3 \pmod 8$ -1 if $n \equiv 5,7 \pmod 8$
9	1 if $n \equiv 1,2 \pmod 3$
12	1 if $n \equiv 1,11 \pmod{12}$ -1 if $n \equiv 5,7 \pmod{12}$
-12	1 if $n \equiv 1 \pmod 6$ -1 if $n \equiv 5 \pmod 6$
24	1 if $n \equiv 1,5,19,23 \pmod{24}$ -1 if $n \equiv 7,11,13,17 \pmod{24}$
-24	1 if $n \equiv 1,5,7,11 \pmod{24}$ -1 if $n \equiv 13,17,19,23 \pmod{24}$
36	1 if $n \equiv 1,5 \pmod 6$
-36	1 if $n \equiv 1,5 \pmod{12}$ -1 if $n \equiv 7,11 \pmod{12}$
72	1 if $n \equiv 1,7,17,23 \pmod{24}$ -1 if $n \equiv 5,11,13,19 \pmod{24}$
-72	1 if $n \equiv 1,11,17,19 \pmod{24}$ -1 if $n \equiv 5,7,13,23 \pmod{24}$

Table A.2 Values of n for Kronecker symbols $\left(\frac{a}{n}\right)$. The value of $\left(\frac{a}{n}\right)$ is defined to be 0 for other residue classes modulo n not covered in this table.

a	b	x
-3	3	$\frac{1}{3}; \frac{2}{3}$
4	2	$\frac{1}{2}$
-4	4	$\frac{1}{4}; \frac{3}{4}$
8	8	$\frac{1}{8}, \frac{7}{8}, \frac{3}{8}, \frac{5}{8}$
-8	8	$\frac{1}{8}, \frac{3}{8}, \frac{5}{8}, \frac{7}{8}$
9	3	$\frac{1}{3}, \frac{2}{3}$
12	12	$\frac{1}{12}, \frac{11}{12}, \frac{5}{12}, \frac{7}{12}$
-12	6	$\frac{1}{6}; \frac{5}{6}$
24	24	$\frac{1}{24}, \frac{5}{24}, \frac{19}{24}, \frac{23}{24}; \frac{7}{24}, \frac{11}{24}, \frac{13}{24}, \frac{17}{24}$
-24	24	$\frac{1}{24}, \frac{5}{24}, \frac{7}{24}, \frac{11}{24}; \frac{13}{24}, \frac{17}{24}, \frac{19}{24}, \frac{23}{24}$
36	6	$\frac{1}{6}, \frac{5}{6}$
-36	12	$\frac{1}{12}, \frac{5}{12}; \frac{7}{12}, \frac{11}{12}$
72	24	$\frac{1}{24}, \frac{7}{24}, \frac{17}{24}, \frac{23}{24}; \frac{5}{24}, \frac{11}{24}, \frac{13}{24}, \frac{19}{24}$
-72	24	$\frac{1}{24}, \frac{11}{24}, \frac{17}{24}, \frac{19}{24}; \frac{5}{24}, \frac{7}{24}, \frac{13}{24}, \frac{23}{24}$

Table A.3 Values of a,b and x for $\displaystyle\sum_{n=1}^{\infty} \left(\frac{a}{n}\right) n^{-s} = b^{-s}\zeta(s;x)$, see (6.4.8) .

n	$L_n^{\mathrm{sc}} - L_\infty^{\mathrm{sc}}$	$L_n^{\mathrm{bcc}} - L_\infty^{\mathrm{bcc}}$	$L_n^{\mathrm{fcc}} - L_\infty^{\mathrm{fcc}}$	$L_n^{\mathrm{hcp}} - L_\infty^{\mathrm{hcp}}$	$L_n^{\mathrm{hcp}} - L_n^{\mathrm{fcc}}$
4	1.05323159597617E+1	1.46387216437935E+1	1.33383043051302E+1	1.33390823380551E+1	7.78032924974526E-4
5	4.37752483084708E+0	6.75850937014712E+0	4.96751845837841E+0	4.96843634796979E+0	9.17889591383232E-4
6	2.40192397482754E+0	4.25366786729232E+0	2.45392104374447E+0	2.45489727784162E+0	9.76234097145690E-4
7	1.46705778091881E+0	3.05424347924446E+0	1.35938770074208E+0	1.36034677619555E+0	9.59075453468315E-4
8	9.45807927226370E-1	2.35519790840251E+0	8.01937231378133E-1	8.02821852809896E-1	8.84621431763331E-4
9	6.28859198886779E-1	1.89458965632112E+0	4.92546702137558E-1	4.93321725001782E-1	7.75022864223436E-4
10	4.26119102533089E-1	1.56440061535995E+0	3.11245665477406E-1	3.11896233818981E-1	6.50568341575253E-4
11	2.92294499234567E-1	1.31326253739910E+0	2.00920351277113E-1	2.01447099831955E-1	5.26748554841471E-4
12	2.02149045047519E-1	1.11418326807536E+0	1.31880196544580E-1	1.32293769098918E-1	4.13572554337918E-4
13	1.40599580021692E-1	9.51807318574715E-1	8.77263213520527E-2	8.80425502984390E-2	3.16228946386338E-4
14	9.81841257121521E-2	8.16770228485920E-1	5.89919443508593E-2	5.92282550682414E-2	2.36310717382134E-4
15	6.87642950388921E-2	7.02984559980926E-1	4.00240550990886E-2	4.01971443472233E-2	1.73089248134625E-4
16	4.82634695858417E-2	6.06254047544529E-1	2.73548440185703E-2	2.74794193038561E-2	1.24575285285802E-4
17	3.39293163672074E-2	5.23531250439298E-1	1.88094367104578E-2	1.88977196228595E-2	8.82829124017101E-5
18	2.38817078667148E-2	4.52503168608382E-1	1.29983096659596E-2	1.30600231774083E-2	6.17135114487303E-5
19	1.68254563317377E-2	3.91350791413118E-1	9.01960443932357E-3	9.06222411120950E-3	4.26196718859239E-5
20	1.18628308899457E-2	3.38604005679563E-1	6.28004132634266E-3	6.30915811465870E-3	2.91167883160407E-5
21	8.36875754668317E-3	2.93050370415294E-1	4.38480936230330E-3	4.40451008477321E-3	1.97007224699113E-5
22	5.90652613429112E-3	2.53675218084780E-1	3.06856932292989E-3	3.08178423329668E-3	1.32149103667949E-5
23	4.17024007074802E-3	2.19620534883649E-1	2.15149097471211E-3	2.16028673932262E-3	8.79576461050519E-6
24	2.94520818412950E-3	1.90155475483163E-1	1.51082493970707E-3	1.51663857704596E-3	5.81363733888953E-6
25	2.08052037491334E-3	1.64654351927331E-1	1.06227870924614E-3	1.06609714202720E-3	3.81843278106124E-6
26	1.46997249608606E-3	1.42579615920799E-1	7.47674897726916E-4	7.50168624485191E-4	2.49372675827520E-6
27	1.03875223830484E-3	1.23468315872789E-1	5.26690212160028E-4	5.28310428505144E-4	1.62021634511562E-6
28	7.34121070789493E-4	1.06921071038717E-1	3.71277553079702E-4	3.72325322411022E-4	1.04776933131979E-6
29	5.18879212211412E-4	9.25929383761218E-2	2.61871447419640E-4	2.62546150133902E-4	6.74702714262418E-7
30	3.66774897184039E-4	8.01857499061731E-2	1.84790059821197E-4	1.85222851788274E-4	4.32791967077113E-7

Table A.4 Lattice sums (Lennard-Jones–Ingham coefficients) L_n with respect to the infinite limit (L_∞^{sc}=6, L_∞^{bcc}=8, L_∞^{fcc}=12, L_∞^{hcp}=12) for $n \in \mathbb{N}$ obtained from various expansion methods described in this paper.

B Special functions

A The Riemann zeta function and L functions

The definitions are:

$$\zeta(s) = \sum_{j=1}^{\infty} \frac{1}{j^s} \tag{B.0.1}$$

$$L_{-4}(s) = \sum_{j=1}^{\infty} \frac{\chi_{-4}(j)}{j^s} = 1 - \frac{1}{3^s} + \frac{1}{5^s} - \frac{1}{7^s} + \cdots. \tag{B.0.2}$$

$$L_{-3}(s) = \sum_{j=1}^{\infty} \frac{\chi_{-3}(j)}{j^s} = 1 - \frac{1}{2^s} + \frac{1}{4^s} - \frac{1}{5^s} + \frac{1}{7^s} - \frac{1}{8^s} + \cdots. \tag{B.0.3}$$

The function $\zeta(s)$ is the Riemann zeta function. It has a pole of order 1 at $s = 1$, and in fact

$$\lim_{s\to 1}(s-1)\zeta(s) = 1. \tag{B.0.4}$$

This is a consequence of [283, (1.3.2)]. See also [110, p. 58].

We will require the functional equations

$$\pi^{-s/2}\Gamma(s/2)\zeta(s) = \pi^{-(1-s)/2}\Gamma((1-s)/2)\zeta(1-s) \tag{B.0.5}$$

and

$$\pi^{-s}\Gamma(s)\,\zeta(s)L_{-4}(s) = \pi^{-(1-s)}\Gamma(1-s)\,\zeta(1-s)L_{-4}(1-s) \tag{B.0.6}$$

and the special values

$$\begin{aligned} &\zeta(2) = \frac{\pi^2}{6}, \quad \zeta(0) = -\frac{1}{2}, \quad \zeta(-1) = -\frac{1}{12}, \\ &\zeta(-2) = \zeta(-4) = \zeta(-6) = \cdots = 0, \end{aligned} \tag{B.0.7}$$

$$L_{-4}(1) = \frac{\pi}{4}, \quad L_{-4}(0) = \frac{1}{2}, \quad L_{-4}(-1) = L_{-4}(-3) = L_{-4}(-5) = \cdots = 0, \tag{B.0.8}$$

and

$$L_{-3}(1) = \frac{\pi\sqrt{3}}{9}, \quad L_{-3}(0) = \frac{1}{3}, \quad L_{-3}(-1) = L_{-3}(-3) = L_{-3}(-5) = \cdots = 0. \tag{B.0.9}$$

See [285, Ch. 12] or [286]. Other results used are

$$\sum_{j=0}^{\infty} \frac{1}{(j+\frac{1}{2})^s} = (2^s - 1)\zeta(s) \tag{B.0.10}$$

$$\sum_{j=1}^{\infty} \frac{(-1)^j}{j^s} = -(1 - 2^{1-s})\zeta(s) \tag{B.0.11}$$

$$\sum_{j,k}{}' \frac{1}{(j^2+k^2)^s} = 4\zeta(s)L_{-4}(s) \tag{B.0.12}$$

$$\sum_{j,k}{}' \frac{(-1)^{j+k}}{(j^2+k^2)^s} = -4(1 - 2^{1-s})\zeta(s)L_{-4}(s). \tag{B.0.13}$$

$$\sum_{i,j}{}' \frac{1}{(i^2+ij+j^2)^s} = 6\zeta(s)L_{-3}(s) \tag{B.0.14}$$

$$\sum_{i,j} \frac{1}{((i+\frac{1}{3})^2 + (i+\frac{1}{3})(j+\frac{1}{3}) + (j+\frac{1}{3})^2)^s} = 3(3^s - 1)\zeta(s)L_{-3}(s). \tag{B.0.15}$$

The identities (B.0.10) and (B.0.11) follow from the definition of $\zeta(s)$ by series rearrangements. For (B.0.12), (B.0.13) and (B.0.14), see (1.4.14), (1.7.5) and (1.4.16), respectively, of [1]. The identity (B.0.15) can be obtained by the method of Mellin transforms, e.g., see [58, Appendix A], starting with [78, (3.36)].

C Cover Page

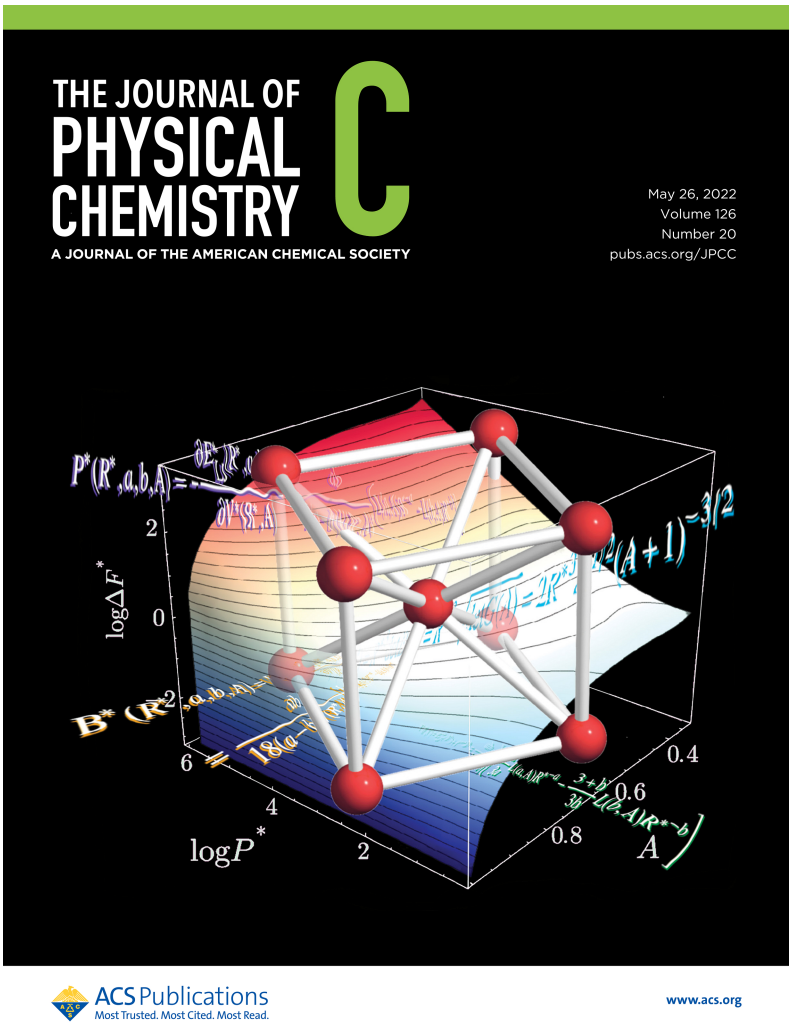

Figure C.1 Cover page for ACS Journal - Journal of Physical Chemistry C - May 26, 2022, Volume 126, Number 20.

References

[1] J. M. Borwein, M. Glasser, R. McPhedran, J. Wan, and I. Zucker, *Lattice sums then and now*, 150 (Cambridge University Press, 2013).

[2] R. Furth, en, Proc. R. Soc. Lond. **183**, 87 (1944).

[3] E. Grüneisen, **344**, 257 (1912).

[4] P. Schwerdtfeger, A. Burrows, and O. R. Smits, J. Phys. Chem. A **125**, _eprint: https://doi.org/10.1021/acs.jpca.1c00012, 3037 (2021).

[5] F. H. Stillinger, **115**, 5208 (2001).

[6] J. E. Jones and A. E. Ingham, **107**, 636 (1925).

[7] E. Madelung, Phys. Z **19**, 32 (1918).

[8] A. Burrows, P. Schwerdtfeger, and E. Pahl, Publisher: unpublished results (2020).

[9] P. Appell, Acta Math. **4**, 313 (1884).

[10] W. H. Bragg and W. L. Bragg, Proceedings of the Royal Society of London. Series A, Containing Papers of a Mathematical and Physical Character **88**, 428 (1913).

[11] W. H. Bragg, Proceedings of the Royal Society of London. Series A, Containing Papers of a Mathematical and Physical Character **89**, 246 (1913).

[12] M. Born, *Dynamik Der Kristallgitter* (1916).

[13] E. Madelung, Phys. Z **19**, 32 (1918).

[14] P. P. Ewald, de, Ann. Phys. **369**, 253 (1921).

[15] G. Mie, **316**, 657 (1903).

[16] A. Kratzer, **3**, 289 (1920).

[17] M. Born and A. Landé, Verh. Deut. Phys. Ges. **20**, 21o (1918).

[18] J. E. Jones, **106**, 441 (1924).

[19] F. London, **63**, 245 (1930).

[20] O. Emersleben, Phys. Zeit **24**, 73 (1923).

[21] O. Emersleben, Phys. Z **24**, 97 (1923).

[22] J. E. Jones, **106**, 709 (1924).

[23] J. E. Jones and A. E. Ingham, PRSLA **107**, 636 (1925).

[24] G. Kane and M. Goeppert-Mayer, **8**, 642 (1940).

[25] L. L. Foldy, **17**, 4889 (1978).

[26] J. M. Borwein, M. Glasser, R. McPhedran, J. Wan, and I. Zucker, *Lattice sums then and now*, 150 (Cambridge University Press, 2013).

[27] J. Mackenzie, Can. J. Phys. **35**, 500 (1957).

[28] G. C. Benson, Canadian Journal of Physics **34**, 888 (1956).

[29] B. M. E. van der Hoff and G. C. Benson, Canadian Journal of Physics **31**, 1087 (1953).

[30] G. C. Benson, H. Schreiber, and D. Patterson, Canadian Journal of Physics, 10.1139/p56-031 (1956).

[31] O. Emersleben, de, Math. Nachr. **44**, 205 (1970).

[32] M. L. Glasser, Journal of Mathematical Physics **14**, 409 (1973).

[33] M. L. Glasser, Journal of Mathematical Physics **14**, 701 (1973).

[34] M. L. Glasser, Journal of Mathematical Physics **15**, 188 (1974).

[35] M. L. Glasser, Journal of Mathematical Physics **16**, 1237 (1975).

[36] A. N. Chaba and R. K. Pathria, J. Phys. A Math. Gen. **9**, 1411 (1976).

[37] A. N. Chaba and R. K. Pathria, J. Phys. A Math. Gen. **9**, 1801 (1976).

[38] A. N. Chaba and R. K. Pathria, J. Phys. A Math. Gen. **10**, 1823 (1977).

[39] I. Zucker and M. Robertson, Journal of Physics A: Mathematical and General **9**, 1215 (1976).

[40] A. A. Terras, Trans. Am. Math. Soc. **183**, 477 (1973).

[41] A. Hautot, Journal of Mathematical Physics **15**, 1722 (1974).

[42] R. E. Crandall and J. P. Buhler, J.Phys. A: Math. Gen. **20**, 5497 (1987).

[43] H. S. M. Coxeter, *Regular polytopes* (Methuen, Pitman, Macmillan, Dover, 1973).

[44] S. R. D. L. Lynch and J. D. Doll, J. Chem. Phys. **95**, 3506 (1991).

[45] J. P. K. Doye, D. J. Wales, and M. A. Miller, J. Chem. Phys. **109**, 8143 (1998).

[46] J. A. P. J. M. Dumore and L. T. Tjoan, Physica Amsterdam **18**, 307 (1952).

[47] G. L. Pollack, Rev. Mod. Phys. **36**, 748 (1964).

[48] P. Schwerdtfeger, N. Gaston, R. P. Krawczyk, R. Tonner, and G. E. Moyano, Phys. Rev. B **73**, 064112 (2006).

[49] G. E. Moyano, P. Schwerdtfeger, and K. Rosciszewski, Phys. Rev. B **75**, 024101 (2007).

[50] P. Schwerdtfeger and A. Hermann, Phys. Rev. B **80**, 064106-1 (2009).

[51] P. Schwerdtfeger, R. Tonner, G. E. Moyano, and E. Pahl, **55**, 12200 (2016).

[52] P. Schwerdtfeger, K. G. Steenbergen, and E. Pahl, **95**, 214116 (2017).

[53] O. R. Smits, P. Jerabek, E. Pahl, and P. Schwerdtfeger, **57**, 9961 (2018).

[54] P. Jerabek, O. R. Smits, J.-M. Mewes, K. A. Peterson, and P. Schwerdtfeger, **123**, 4201 (2019).

[55] A. Hermann, R. P. Krawczyk, M. Lein, P. Schwerdtfeger, I. P. Hamilton, and J. J. P. Stewart, Phys. Rev. A **76**, 013202 (2007).

[56] I. J. Zucker, Journal of Physics A: Mathematical, Nuclear and General **7**, 1568 (1974).

[57] J. H. Conway and N. J. A. Sloane, *Sphere packings, lattices and groups*, Vol. 290 (Springer, New York, 2013).

[58] A. Burrows, S. Cooper, E. Pahl, and P. Schwerdtfeger, Journal of Mathematical Physics **61**, 10.1063/5.0021159 (2020).

[59] K. L. Fields, Acta Crystallographica Section A **36**, 194 (1980).

[60] P. Epstein, Math. Ann. **56**, 615 (1903).

[61] I. J. Zucker, **8**, 1734 (1975).

[62] O. Emersleben, Mathematische Nachrichten **4**, 468 (1950).

[63] D. Borwein, J. Borwein, and C. Pinner, Trans. Am. Math. Soc. **350**, 3131 (1998).

[64] R. E. Crandall, Exper. Math. **8**, 367 (1999).

[65] D. Borwein, J. M. Borwein, and K. F. Taylor, **26**, 2999 (1985).

[66] O. Emersleben, Mathematische Nachrichten **4**, Publisher: WILEY-VCH Verlag, 468 (1950).

[67] D. Borwein, J. M. Borwein, and K. F. Taylor, Journal of Mathematical Physics **26**, 2999 (1985).

[68] G. Benson, Can. J. Phys. **34**, 888 (1956).

[69] A. Hautot, Journal of Physics A: Mathematical and General **8**, 853 (1975).

[70] R. Bell and I. Zucker, M L Klein and J A Venebles (New York: Academic) (1976).

[71] A. Burrows, S. Cooper, E. Pahl, and P. Schwerdtfeger, Journal of Mathematical Physics **61**, 10.1063/5.0021159 (2020).

[72] G. H. Hardy, Quart. J. Math **46**, 1 (1915).

[73] G. H. Hardy and E. M. Wright, *An introduction to the theory of numbers* (Oxford University Press, 1979).

[74] N. J. A. Sloane and S. Plouffe, *The encyclopedia of integer sequences* (Academic Press, 1995).

[75] N. J. A. Sloane, *The on-line encyclopedia of integer solutions* (available at https://oeis.org/, 2016).

[76] P. T. Bateman, Transactions of the American Mathematical Society **71**, 70 (1951).

[77] S. Cooper, J. Number Theory **103**, 135 (2003).

[78] S. Cooper, *Ramanujan's theta functions* (Springer, Berlin, 2017).

[79] G. Andrews, *Special functions* (Cambridge University Press, Cambridge, UK New York, NY, USA, 1999).

[80] J. M. Borwein and P. B. Borwein, Transactions of the American Mathematical Society **323**, 691 (1991).

[81] J. E. Jones, Proc. R. Soc. Lond. A **106**, 463 (1924).

[82] F. Simon and C. Simson, **25**, 160 (1924).

[83] J. E. Lennard-Jones, Proc. Phys. Soc. **43**, 461 (1931).

[84] J. Lennard-Jones, Physica **4**, 941 (1937).

[85] P. M. Morse, Phys. Rev. **34**, 57 (1929).

[86] J. Wang, R. M. Wolf, J. W. Caldwell, P. A. Kollman, and D. A. Case, J. Comput. Chem. **25**, 1157 (2004).

[87] N. Gnan, T. B. Schrøder, U. R. Pedersen, N. P. Bailey, and J. C. Dyre, JCP **131**, _eprint: https://doi.org/10.1063/1.3265957, 234504 (2009).

[88] D. E. Albrechtsen, A. E. Olsen, U. R. Pedersen, T. B. Schrøder, and J. C. Dyre, Phys. Rev. B **90**, 094106 (2014).

[89] S. Stephan, M. Thol, J. Vrabec, and H. Hasse, **59**, PMID: 31609113, 4248 (2019).

[90] S. Stephan, J. Staubach, and H. Hasse, Fluid Phase Equilibria **523**, 112772 (2020).

[91] J. E. Jones, PRSLA **106**, The Royal Society, 441 (1924).

[92] J. E. Jones, Proc. R. Soc. Lond. A **106**, 463 (1924).

[93] J. E. Lennard-Jones, Proc. Phys. Soc. **43**, 461 (1931).

[94] M. Born and R. D. Misra, Math. Proc. Cambridge Phil. Soc. **36**, 466 (1940).

[95] K. T. Tang and J. P. Toennies, **80**, 3726 (1984).

[96] B. Jäger, R. Hellmann, E. Bich, and E. Vogel, Mol. Phys. **107**, 2181 (2009).

[97] K. Patkowski and K. Szalewicz, J. Chem. Phys. **133**, 094304-1 (2010).

[98] D. C. Wallace and J. L. Patrick, Phys. Rev. **137**, A152 (1965).

[99] M. Stein, Comp. Phys. Commun. **221**, 273 (2017).

[100] I. C. Society, *Ieee standard for floating-point arithmetic* (IEEE-SA Standards Board, 2008).

[101] ANSI/ISO, *American national standard for programming languages - c* (ANSI/ISO, 1990), section 6.1.2.5.

[102] F. Johansson, IEEE Transactions on Computers **66**, 1281 (2017).

[103] G. H. Hardy, Mess. Math **49**, 86 (1920).

[104] J. M. Borwein and P. B. Borwein, *Pi and the agm: a study in analytic number theory and computational complexity, cms monographs and advanced books in mathematics* (John Wiley, Hoboken, NJ, 1987).

[105] I. J. Zucker and M. M. Robertson, J. Phys. A: Math. General **8**, 874 (1975).

[106] I. S. Gradshteyn and I. M. Ryzhik, *Table of integrals, series, and products* (Academic press, Cambridge, Massachusetts, 2014).

[107] I. J. Zucker, Journal of Physics A: Mathematical, Nuclear and General **7**, 1568 (1974).

[108] A. Fletcher, J. C. P. Miller, L. Rosenhead, and L. J. Comrie, *An index of mathematical tables*, Vol. 1 (Blackwell, 1962).

[109] H. H. Chan and P. C. Toh, Acta Arithmetica **169**, 331 (2015).

[110] N. Temme, *Special functions : an introduction to the classical functions of mathematical physics* (John Wiley & Sons, New York, 1996).

[111] B. M. E. van der Hoff and G. C. Benson, Canadian Journal of Physics **31**, 1087 (1953).

[112] A. A. Terras, Trans. Am. Math. Soc. **183**, 477 (1973).

[113] O. Emersleben, Mathematische Nachrichten **4**, 468 (1950).

[114] O. Emersleben, Zeitschrift für Physik **127**, 588 (1950).

[115] O. Emersleben, Z. Physikalische Chem. **199**, 170 (1952).

[116] G. Hamel and O. Emersleben, Mathematische Nachrichten **9**, 221 (1953).

[117] P. Epstein, Math. Ann. **56**, 615 (1903).

[118] P. Bateman and E. Grosswald, Acta Arithmetica **4**, 365 (1964).

[119] A. Selberg and S. Chowla, J. Reine Angew. Math. **227**, 87 (1967).

[120] L. Glasser, K. T. Kohl, C. Koutschan, V. H. Moll, and A. Straub, Scientia. Series A. Mathematical Sciences. New Series **22**, 129 (2012).

[121] R. E. Crandall, manuscript, at http:== www. perfsci. com (1998).

[122] J. Conway and N. Sloane, J. Number Theory **48**, Publisher: Elsevier, 373 (1994).

[123] J. H. Conway and N. J. A. Sloane, *Sphere packings, lattices and groups*, Vol. 290 (Springer, New York, 2013).

[124] A. Selberg and S. Chowla, J. Reine Angew. Math. **227**, 87 (1967).

[125] G. Nebe. and N. Sloane, *A catalogue of lattices*, (2022) `http : / / www . math . rwth - aachen . de / ~Gabriele . Nebe / LATTICES/` (visited on 06/01/2022).

[126] S. D. Galbraith, *Mathematics of public key cryptography* (Cambridge University Press, 2012).

[127] J. H. Conway, C. Goodman-Strauss, and N. Sloane, Current Developments in Mathematics **1999**, 37 (1999).

[128] M. Born, **7**, 124 (1921).

[129] F. Hund, **34**, 833 (1925).

[130] F. Hund, **94**, 11 (1935).

[131] M. Glasser and I. Zucker, Theoretical chemistry: Advances and perspectives **5**, 67 (1980).

[132] S. Cooper, *Ramanujan's theta functions* (Springer, Berlin, 2017).

[133] E. Grosswald, *Representations of integers as sums of squares* (Springer Science, New York, 2012).

[134] S. Cooper and H. Y. Lam, Indian J. Math **44**, 21 (2002).

[135] G. C. Benson, Canadian Journal of Physics **34**, 888 (1956).

[136] A. Hautot, Journal of Mathematical Physics **15**, 1722 (1974).

[137] M. P. Tosi, in , Vol. 16, edited by F. Seitz and D. Turnbull, Solid State Physics (Academic Press, 1964), pp. 1–120.

[138] P. Jerabek, O. Smits, E. Pahl, and P. Schwerdtfeger, Mol. Phys. **116**, 1 (2018).

[139] X. Blanc and M. Lewin, arXiv preprint arXiv:1504.01153 (2015).

[140] L. Bétermin, Analysis Math. Phys. **9**, 403 (2019).

[141] V. Ennola, Mathematical Proceedings of the Cambridge Philosophical Society **60**, 855 (1964).

[142] A. Burrows, P. Schwerdtfeger, and E. Pahl, (2020).

[143] P. Schwerdtfeger and A. Burrows, *Program Jones - A Fortran Program for sc, bcc, fcc and hcp Lattice Sums, Massey University, Auckland*, 2021.

[144] S. Plouffe, *Identities inspired from Ramanujan's Notebooks II*, 1998.

[145] W. H. Press, S. A. Teukolsky, W. T. Vetterling, and B. P. Flannery, *Fortran numerical recipes*, 2nd ed., Vol. 1: Fortran 77 (Cambridge University Press, Cambridge, 1992).

[146] J. Bertrand, P. Bertrand, and J.-P. Ovarlez, in (Chapter 11, 2nd ed., CRC Press LLC, Boca Raton, 2000, 2000).

[147] E. T. Whittaker and G. N. Watson, *A course of modern analysis* (Cambridge University Press, 1996).

[148] G. N. Watson, *A treatise on the theory of bessel functions* (Cambridge University Press, 1995).

[149] A. Dieckmann, in (Universität Bonn, 2000).

[150] S. L. Yang and Z. K. Qiao, in Journal of mathematical research and exposition, Vol. 31 (2011), pp. 627–636.

[151] E. G. Wintucky, *Nasa tn d-6403* (National Aeronautics and Space Administration, 1971).

[152] P. Schwerdtfeger, A. Burrows, and O. R. Smits, J. Phys. Chem. A **125**, 3037 (2021).

[153] E. Pahl, D. Figgen, C. Thierfelder, K. A. Peterson, F. Calvo, and P. Schwerdtfeger, J. Chem. Phys. **132**, 114301-1 (2010).

[154] K. F. Herzfeld and M. G. Mayer, Phys. Rev. **46**, 995 (1934).

[155] J. Corner, Trans. Faraday Soc. **35**, 711 (1939).

[156] B. Nijboer and F. D. Wette, Phys. Lett. **17**, 256 (1965).

[157] F. De Wette, L. Fowler, and B. Nijboer, Physica **54**, 292 (1971).

[158] A. Einstein, Ann. Phys. **327**, 180 (1907).

[159] M. Born and K. Huang, *Dynamical theory of crystal lattices* (Oxford University Press, 1998).

[160] A. Burrows, S. Cooper, E. Pahl, and P. Schwerdtfeger, J. Math. Phys. **61**, 123503 (2020).

[161] J. H. Conway and N. J. A. Sloane, *Sphere packings, lattices and groups*, Vol. 290 (Springer, New York, 2013).

[162] T. Barron, The London, Edinburgh, and Dublin Philosophical Magazine and Journal of Science **46**, 720 (1955).

[163] J.-P. Poirier, *Introduction to the physics of the earth's interior - 2nd ed.* (Cambridge University Press, 2000).

[164] F. D. Stacey and J. H. Hodgkinson, Phys. Earth Planet. Interiors **286**, 42 (2019).

[165] O. L. Anderson, Geophys. J. Int. **143**, 279 (2000).

[166] W. Barlow, Nature **29**, 205 (1883).

[167] P. Schwerdtfeger, *Program SAMBA - A Fortran Program for optimizing and analyzing solid state structures by the use of a many-body expansion in terms of interaction potentials, Massey University*, 2020.

[168] D. L. Anderson, *Theory of the earth* (Blackwell scientific publications, 1989).

[169] G. Horton, *Rare gas solids*, Vol. 1 (Academic, New York, 1976).

[170] M. H. Kalos, M. A. Lee, P. A. Whitlock, and G. V. Chester, Phys. Rev. B **24**, 115 (1981).

[171] E. Pahl, F. Calvo, L. Koči, and P. Schwerdtfeger, Angew. Chem. Int. Ed. **47**, 8207 (2008).

[172] J. Wiebke, E. Pahl, and P. Schwerdtfeger, Angew. Chem. Int. Ed. **52**, 13202 (2013).

[173] W. Cencek, M. Przybytek, J. Komasa, J. B. Mehl, B. Jeziorski, and K. Szalewicz, **136**, 224303, `http://dx.doi.org/10.1063/1.4712218` (2012).

[174] E. Bich, R. Hellmann, and E. Vogel, Mol. Phys. **106**, 1107 (2008).

[175] A. Shee, S. Knecht, and T. Saue, **17**, 10978 (2015).

[176] O. R. Smits, P. Jerabek, E. Pahl, and P. Schwerdtfeger, Phys. Rev. B **101**, 104103 (2020).

[177] K. Ro ściszewski, B. Paulus, P. Fulde, and H. Stoll, Phys. Rev. B **60**, 7905 (1999).

[178] G. T. McConville, J. Chem. Phys. **60**, 4093 (1974).

[179] L. A. Schwalbe, R. K. Crawford, H. H. Chen, and R. A. Aziz, J. Chem. Phys. **66**, 4493 (1977).

[180] K. Ro ściszewski, B. Paulus, P. Fulde, and H. Stoll, Phys. Rev. B **62**, 5482 (2000).

[181] W. Cencek, K. Patkowski, and K. Szalewicz, en, J. Chem. Phys. **131**, 064105 (2009).

[182] S. A. Giuliani, Z. Matheson, W. Nazarewicz, E. Olsen, P.-G. Reinhard, J. Sadhukhan, B. Schuetrumpf, N. Schunck, and P. Schwerdtfeger, Rev. Mod. Phys. **91**, 011001 (2019).

[183] P. Schwerdtfeger, O. R. Smits, and P. Pyykkö, Nature Rev. Chem., 1 (2020).

[184] O. R. Smits, J.-M. Mewes, P. Jerabek, and P. Schwerdtfeger, **59**, 23636 (2020).

[185] C. S. Barrett and L. Meyer, **41**, 1078 (1964).

[186] B. M. Axilrod and E. Teller, J. Chem. Phys. **11**, 299 (1943).

[187] G. Kresse and J. Hafner, Phys. Rev. B **55**, 7539 (1997).

[188] R. M. Cotterill and J. L. Tallon, Faraday Discussions of the Chemical Society **69**, 241 (1980).

[189] J. L. Tallon, Nature **432**, 658 (1989).

[190] R. E. Peierls, *Quantum theory of solids* (Clarendon Press, Oxford, 1996).

[191] D. Kartoon, U. Argaman, and G. Makov, Phys. Rev. B **98**, 165429 (2018).

[192] D. Hooton, The London, Edinburgh, and Dublin Philosophical Magazine and Journal of Science **46**, 422 (1955).

[193] M. W. Coffey, J. Comput. Appl. Math. **216**, 297 (2008).

[194] J. Q. W. Lo and B. D. Shizgal, **41**, 185103 (2008).

[195] W. Cencek, M. Przybytek, J. Komasa, J. B. Mehl, B. Jeziorski, and K. Szalewicz, **136**, 224303 (2012).

[196] F. Luo, G. C. McBane, G. Kim, C. F. Giese, and W. R. Gentry, **98**, 3564 (1993).

[197] W. Schöllkopf and J. P. Toennies, Science **266**, 1345 (1994).

[198] R. E. Grisenti, W. Schöllkopf, J. P. Toennies, G. C. Hegerfeldt, T. Köhler, and M. Stoll, Phys. Rev. Lett. **85**, 2284 (2000).

[199] S. Zeller, M. Kunitski, J. Voigtsberger, A. Kalinin, A. Schottelius, C. Schober, M. Waitz, H. Sann, A. Hartung, T. Bauer, M. Pitzer, F. Trinter, C. Goihl, C. Janke, M. Richter, G. Kastirke, M. Weller, A. Czasch, M. Kitzler, M. Braune, R. E. Grisenti, W. Schöllkopf, L. P. H. Schmidt, M. S. Schöffler, J. B. Williams, T. Jahnke, and R. Dörner, **113**, 14651 (2016).

[200] J. Eckert, W. Thomlinson, and G. Shirane, Phys. Rev. B **16**, 1057 (1977).

[201] D. M. Ceperley, Rev. Mod. Phys. **67**, 279 (1995).

[202] F. Simon and C. Swenson, Nature **165**, 829 (1950).

[203] J. M. McMahon, M. A. Morales, C. Pierleoni, and D. M. Ceperley, Rev. Mod. Phys. **84**, 1607 (2012).

[204] J. S. Dugdale and F. E. Simon, Proc. Roy. Soc. Lond. A, Math. Phys. Sci. **218**, 291 (1953).

[205] D. Saumon and T. Guillot, Astrophys. J. **609**, 1170 (2004).

[206] L. Stixrude and R. Jeanloz, **105**, 11071 (2008).

[207] S. A. Khairallah and B. Militzer, Phys. Rev. Lett. **101**, 106407 (2008).

[208] D. O. Edwards and R. C. Pandorf, Phys. Rev. **140**, A816 (1965).

[209] D. O. Edwards and R. C. Pandorf, Phys. Rev. **144**, 143 (1966).

[210] B. L. Holian, W. D. Gwinn, A. C. Luntz, and B. J. Alder, **59**, 5444 (1973).

[211] D. A. Young, A. K. McMahan, and M. Ross, Phys. Rev. B **24**, 5119 (1981).

[212] D. R. Lide, *Crc handbook of chemistry and physics (86th ed.)* Vol. 85 (CRC press, Boca Radon (FL), 2004).

[213] D. G. Henshaw, Phys. Rev. **109**, 328 (1958).

[214] B. Hunt, E. Pratt, V. Gadagkar, M. Yamashita, A. V. Balatsky, and J. C. Davis, Science **324**, 632 (2009).

[215] E. J. Landinez Borda, W. Cai, and M. de Koning, Phys. Rev. Lett. **117**, 045301 (2016).

[216] J. Beamish and S. Balibar, Rev. Mod. Phys. **92**, 045002 (2020).

[217] C. Cazorla and J. Boronat, Phys. Rev. B **92**, 224113 (2015).

[218] A. Dewaele, Personal Communication, August 31, 2020, LaboratoireMatière en Conditions Extrêmes, Université Paris-Saclay, CEA Bruyères-le-Châtel, France, 2020.

[219] H. K. Mao, R. J. Hemley, Y. Wu, A. P. Jephcoat, L. W. Finger, C. S. Zha, and W. A. Bassett, Phys. Rev. Lett. **60**, 2649 (1988).

[220] P. Loubeyre, R. LeToullec, J. P. Pinceaux, H. K. Mao, J. Hu, and R. J. Hemley, Phys. Rev. Lett. **71**, 2272 (1993).

[221] A. Driessen, E. van der Poll, and I. F. Silvera, Phys. Rev. B **33**, 3269 (1986).

[222] Y. A. Freiman, S. M. Tretyak, A. Grechnev, A. F. Goncharov, J. S. Tse, D. Errandonea, H.-k. Mao, and R. J. Hemley, Phys. Rev. B **80**, 094112 (2009).

[223] D. M. Ceperley and B. J. Alder, Phys. Rev. B **36**, 2092 (1987).

[224] A. Polian and M. Grimsditch, Europhys. Lett. (EPL) **2**, 849 (1986).

[225] P. Loubeyre, Phys. Rev. Lett. **58**, 1857 (1987).

[226] M. Ross, The Journal of Chemical Physics **73**, 4445 (1980).

[227] R. J. Sadus, **153**, 214509 (2020).

[228] M. Ross and D. A. Young, Phys. Lett. A **118**, 463 (1986).

[229] R. A. Aziz and M. J. Slaman, **94**, 8047 (1991).

[230] M. Przybytek, W. Cencek, B. Jeziorski, and K. Szalewicz, Phys. Rev. Lett. **119**, 123401 (2017).

[231] S. Moroni, F. Pederiva, S. Fantoni, and M. Boninsegni, Phys. Rev. Lett. **84**, 2650 (2000).

[232] C. P. Herrero, J. Phys.: Cond. Mat. **18**, 3469 (2006).

[233] C.-S. Zha, H.-k. Mao, and R. J. Hemley, Phys. Rev. B **70**, 174107 (2004).

[234] M. J. Cohen and J. N. Murrell, Chem. Phys. Lett. **260**, 371 (1996).

[235] O. Syshchenko, J. Day, and J. Beamish, Phys. Rev. Lett. **104**, 195301 (2010).

[236] A. L. Barnes and R. J. Hinde, **147**, 114504 (2017).

[237] Z. G. Cheng and J. Beamish, Phys. Rev. Lett. **121**, 225304 (2018).

[238] W. Cencek, M. Jeziorska, O. Akin-Ojo, and K. Szalewicz, J. Phys. Chem. A **111**, 11311 (2007).

[239] C. A. Parish and C. E. Dykstra, **101**, 7618 (1994).

[240] L. Wang and R. J. Sadus, **125**, 144509 (2006).

[241] S.-Y. Chang and M. Boninsegni, **115**, 2629 (2001).

[242] T. Kihara and S. Koba, J. Phys. Soc. Jap. **7**, 348 (1952).

[243] K. Niebel and J. Venables, Proc. Roy. Soc. Lond. A: Math., Phys. Eng. Sci. **336**, 365 (1974).

[244] B. W. van de Waal, Phys. Rev. Lett. **67**, 3263 (1991).

[245] G. J. Ackland and A. P. Jones, Phys. Rev. B **73**, 054104 (2006).

[246] N. V. Krainyukova, R. E. Boltnev, E. P. Bernard, V. V. Khmelenko, D. M. Lee, and V. Kiryukhin, **109**, 245505 (2012).

[247] P. Loubeyre, Phys. Rev. B **37**, 5432 (1988).

[248] J. H. Conway and N. J. A. Sloane, Discrete & Computational Geometry **13**, 383 (1995).

[249] R. J. Baxter, **49**, 2770 (1968).

[250] L. Trombach, R. S. Hoy, D. J. Wales, and P. Schwerdtfeger, Phys. Rev. E **97**, 043309 (2018).

[251] O. G. Peterson, D. N. Batchelder, and R. O. Simmons, Phys. Rev. **150**, 703 (1966).

[252] D. Errandonea, R. Boehler, S. Japel, M. Mezouar, and L. R. Benedetti, Phys. Rev. B **73**, 092106 (2006).

[253] E. Troitskaya, E. Pilipenko, and I. I. Gorbenko, Physics of the Solid State **61**, 30 (2019).

[254] E. Pechenik, I. Kelson, and G. Makov, Phys. Rev. B **78**, 134109 (2008).

[255] W. F. Sherman, J. Phys. C: Solid State Phys. **15**, 9 (1982).

[256] C. R. Tilford and C. A. Swenson, Phys. Rev. B **5**, 719 (1972).

[257] R. Fugate and C. Swenson, J. Low Temp. Phys. **10**, 317 (1973).

[258] C. Feldman, J. L. Feldman, G. K. Horton, and M. L. Klein, Proc. Phys. Soc. **90**, 1182 (1967).

[259] J. B. Lurie, J. Low Temp. Phys. **10**, 751 (1973).

[260] J. C. Holste, Digital Repository@ Iowa State University, http://lib. dr. iastate. edu/ (1973).

[261] P. Mausbach, A. Köster, G. Rutkai, M. Thol, and J. Vrabec, **144**, 244505 (2016).

[262] N. Gupta and R. Gupta, Can. J. Phys. **47**, 617 (1969).

[263] D. N. Batchelder, D. L. Losee, and R. O. Simmons, Phys. Rev. **173**, 873 (1968).

[264] D. L. Losee and R. O. Simmons, Phys. Rev. **172**, 944 (1968).

[265] D. R. Sears and H. P. Klug, **37**, 3002 (1962).

[266] A. I. Karasevskii and W. B. Holzapfel, Phys. Rev. B **67**, 224301 (2003).

[267] W. Holzapfel, High Pressure Research **25**, 187 (2005).

[268] M. de Souza, P. Menegasso, R. Paupitz, A. Seridonio, and R. E. Lagos, Europ. J. Phys. **37**, 055105 (2016).

[269] A. Wüest and F. Merkt, J. Chem. Phys. **118**, 8807 (2003).

[270] Y. Muto, Proc. Phys. Math. Soc. Japan **17**, 629 (1943).

[271] R. Nomura and Y. Okuda, Rev. Mod. Phys. **92**, 041003 (2020).

[272] D. C. Wallace, Phys. Rev. **131**, 2046 (1963).

[273] D. C. Wallace, Phys. Rev. **133**, A153 (1964).

[274] A. Burrows, S. Cooper, and P. Schwerdtfeger, *The Cuboidal Lattices and their Lattice Sums*, _eprint: 2105.08922, 2021.

[275] J. M. Borwein, M. Glasser, R. McPhedran, J. Wan, and I. Zucker, *Lattice sums then and now*, 150 (Cambridge University Press, 2013).

[276] P. Schwerdtfeger, A. Burrows, and O. R. Smits, The Journal of Physical Chemistry A **125**, Publisher: American Chemical Society, 3037 (2021).

[277] D. Borwein, J. M. Borwein, and C. Pinner, en, Trans. Am. Math. Soc. **350**, 3131 (1998).

[278] J. Conway and N. Sloane, J. Number Theory **48**, Publisher: Elsevier, 373 (1994).

[279] J. H. Conway and N. J. A. Sloane, 10.48550/ARXIV.MATH/0701080 (2007).

[280] G. Kane and M. Goeppert-Mayer, JCP **8**, 642 (1940).

[281] E. Madelung, Phys. Z **19**, 32 (1918).

[282] N. Levinson and R. M. Redheffer, *Complex variables* (Holden-Day, 1970).

[283] G. E. Andrews, R. Askey, and R. Roy, *Special functions* (Cambridge University Press, Jan. 1999).

[284] S. Cooper, en, J. Comput. Appl. Math. **160**, 77 (2003).

[285] T. M. Apostol, *Introduction to analytic number theory* (Springer, 1976).

[286] I. J. Zucker and M. M. Robertson, J. Phys. A: Math. General **8**, 874 (1975).

[287] A. Burrows, S. Cooper, and P. Schwerdtfeger, Phys. Rev. E **104**, 035306 (2021).

[288] D. A. Young, *Phase diagrams of the elements* (UC Press, Berkeley, 1991).

[289] K. Binder, J. Comput. Phys. **59**, 1 (1985).

[290] H. Gomez, M. Bures, and A. Moure, Phil. Trans. A, Math. Phys. Eng. Sci. **377**, 20180203 (2019).

[291] K. J. Caspersen and E. A. Carter, **102**, 6738 (2005).

[292] S.-C. Mau and D. A. Huse, Phys. Rev. E **59**, 4396 (1999).

[293] A. Travesset, **141**, 164501 (2014).

[294] B. Li, G. Qian, A. R. Oganov, S. E. Boulfelfel, and R. Faller, **146**, 214502 (2017).

[295] H. Wiebe, T. L. Underwood, and G. J. Ackland, **153**, 074502 (2020).

[296] P. Schwerdtfeger, A. Burrows, and O. R. Smits, J. Phys. Chem. A **125**, PMID: 33787272, 3037 (2021).

[297] S. Alexander and J. McTague, Phys. Rev. Lett. **41**, 702 (1978).

[298] W. Klein, Phys. Rev. E **64**, 056110 (2001).

[299] T. Kraft, P. M. Marcus, M. Methfessel, and M. Scheffler, Phys. Rev. B **48**, 5886 (1993).

[300] G. Rollmann, M. E. Gruner, A. Hucht, R. Meyer, P. Entel, M. L. Tiago, and J. R. Chelikowsky, Phys. Rev. Lett. **99**, 083402 (2007).

[301] C. Cayron, Acta Materialia **96**, 189 (2015).

[302] G. J. Ackland, M. Dunuwille, M. Martinez-Canales, I. Loa, R. Zhang, S. Sinogeikin, W. Cai, and S. Deemyad, Science **356**, 1254 (2017).

[303] R. Agrawal and D. A. Kofke, Phys. Rev. Lett. **74**, 122 (1995).

[304] S. Prestipino, F. Saija, and P. V. Giaquinta, **123**, 144110 (2005).

[305] C. N. Likos, B. M. Mladek, D. Gottwald, and G. Kahl, **126**, 224502 (2007).

[306] A. S. Bharadwaj and Y. Singh, Phys. Rev. E **95**, 032120 (2017).

[307] B. B. Laird, **97**, 2699 (1992).

[308] W. G. Hoover, D. A. Young, and R. Grover, **56**, 2207 (1972).

[309] S. Ono and T. Ito, Phys. Rev. B **103**, 075406 (2021).

[310] J. Conway and N. Sloane, J. Number Theory **48**, 373 (1994).

[311] A. Burrows, S. Cooper, and P. Schwerdtfeger, *The cuboidal lattices and their lattice sums*, 2021.

[312] J. Rifkin, Phil. Mag. A **49**, L31 (1984).

[313] I. G. Kaplan, J. Hernández-Cobos, I. Ortega-Blake, and O. Novaro, Phys. Rev. A **53**, 2493 (1996).

[314] S. M. Cybulski and R. R. Toczyłowski, J. Chem. Phys. **111**, 10520 (1999).

[315] S. M. Casey and D. G. Leopold, J. Phys. Chem. **97**, 816 (1993).

[316] Z. Pavlovi ć, B. O. Roos, R. Côté, and H. R. Sadeghpour, Phys. Rev. A **69**, 030701 (2004).

[317] S. Vancoillie, P. Å. Malmqvist, and V. Veryazov, J. Chem. Theory Comput. **12**, 1647 (2016).

[318] B. Barakat, R. Bacis, F. Carrot, S. Churassy, P. Crozet, F. Martin, and J. Verges, Chem. Phys. **102**, 215 (1986).

[319] R. A. Johnson, Phys. Rev. B **37**, 3924 (1988).

[320] J. M. Holender, Phys. Rev. B **41**, 8054 (1990).

[321] A. W. Roberts and D. E. Varberg, *Convex functions* (Academic Press, New York, London, 1973).

[322] D. S. Mitrinović and P. M. Vasić, *Analytic inequalities* (Springer-Verlag, New York–Berlin, 1970).

[323] M. Petrović, Publications de l'Institut Mathématique Belgrade **1**, 149 (1932).

[324] C. Kittel, P. McEuen, and P. McEuen, *Introduction to solid state physics*, Vol. 8 (Wiley New York, 1996).

[325] T. Gould and T. Bučko, Journal of Chemical Theory and Computation **12**, PMID: 27304856, 3603 (2016).

[326] R. J. L. Roy, C. C. Haugen, J. Tao, and H. Li, Mol. Phys. **109**, 435 (2011).

[327] P. Schwerdtfeger and A. Burrows, The Journal of Physical Chemistry C, `10.1021/acs.jpcc.2c01255` (2022).

[328] D. Pettifor, Journal of Physics C: Solid State Physics **3**, 367 (1970).

[329] N. N. Greenwood and A. Earnshaw, *Chemistry of the elements* (Elsevier, Amsterdam, 2012).

[330] A. Togo and I. Tanaka, Phys. Rev. B **87**, 184104 (2013).

[331] S. Carlesi, A. Franchini, V. Bortolani, and S. Martinelli, Phys. Rev. B **59**, 11716 (1999).

[332] M. Hanfland, I. Loa, and K. Syassen, Phys. Rev. B **65**, 184109 (2002).

[333] Y. Xie, Y. M. Ma, T. Cui, Y. Li, J. Qiu, and G. T. Zou, New J. Phys. **10**, 063022 (2008).

[334] A. O. E. Animalu, Phys. Rev. **161**, 445 (1967).

[335] A. L. Kutepov and S. G. Kutepova, Phys. Rev. B **67**, 132102 (2003).

[336] S. M. Woodley and R. Catlow, Nature Materials **7**, 937 (2008).

[337] J. Maddox, Nature **335**, 201 (1988).

[338] M. J. Tambe, N. Bonini, and N. Marzari, Phys. Rev. B **77**, 172102 (2008).

[339] J.-P. Hansen and L. Verlet, Phys. Rev. **184**, 151 (1969).

[340] Y. Choi, T. Ree, and F. H. Ree, **99**, 9917 (1993).

[341] A. Hajibabaei and K. S. Kim, Phys. Rev. E **99**, 022145 (2019).

[342] M. Lewin and X. Blanc, EMS Surveys Math. Sci. **2**, 255 (2015).

[343] A. Burrows, S. Cooper, and P. Schwerdtfeger, *Instability of the body-centered cubic lattice within the sticky hard sphere and lennard-jones model obtained from exact lattice summations*, unpublished results, Massey University, 2021.

[344] A. Süt ő, Phys. Rev. B **74**, 104117 (2006).

[345] L. Flatley and F. Theil, Archive for Rational Mechanics and Analysis **218**, 363 (2015).

[346] F. Milstein, H. E. Fang, and J. Marschall, Phil. Mag. A **70**, 621 (1994).

[347] A. C. Mitchell, W. J. Nellis, J. A. Moriarty, R. A. Heinle, N. C. Holmes, R. E. Tipton, and G. W. Repp, Journal of Applied Physics **69**, 2981 (1991).

[348] R. A. Aziz, J. Chem. Phys. **99**, 4518 (1993).

[349] K. Koumatos and A. Muehlemann, Proc. Royal Soc. A: Math., Phys. Eng. Sci. **472**, 20150865 (2016).

[350] F. Mouhat and F. ç.-X. Coudert, Phys. Rev. B **90**, 224104 (2014).

[351] Z. Liu, H. Li, C. Fan, and W. Luo, Europ. J. Mech. A, Solids **65**, 30 (2017).

[352] B. Olinger and J. W. Shaner, Science **219**, 1071 (1983).

[353] M. Born and A. Lande, Verhandl. d. dtsch. Phys. Ges. **20**, 210 (1918).

[354] M. Born and A. Lande, Ber. Preuss. Akad. Wiss. Berlin **45**, 1048 (1918).

[355] D. Quane, J. Chem. Ed. **47**, 396 (1970).

[356] S. Tyagi, Prog. Theoret. Phys. **114**, 517 (2005).

[357] J. J. Zucker, in (2013).

[358] G. Nebe and N. J. Sloane, Published electronically at http://www. research. att. com/njas/lattices (2012).

[359] M. Mamode, J. Math. Chem. **55**, 734 (2017).

[360] G. Hardy, Trans. Am. Math. Soc. **21**, 255 (1920).

[361] R. A. Rankin, Am. J. Math. **87**, 857 (1965).

[362] J. Holley-Reid and J. Rouse, arXiv preprint arXiv:1910.01001 (2019).

[363] K. Ramachandra, Hardy-Ramanujan J. **10**, 9 (1987).

[364] M. L. Glasser, J. Math. Phys. **14**, 409 (1973).

[365] M. L. Glasser, Journal of Mathematical Physics **14**, 701 (1973).

[366] D. H. Bailey, J. M. Borwein, R. E. Crandall, and I. J. Zucker, J. Phys. A: Math. Theoret. **46**, 115201 (2013).

[367] E. Artin, *The gamma function* (Courier Dover Publications, New York, 2015).

[368] T. M. Apostol, *Modular functions and dirichlet series in number theory* (Springer-Verlag New York, 1976).

[369] S. Cooper, Contem. Math. **291**, 115 (2001).

[370] T. C. Hales, "Historical overview of the Kepler conjecture", in *The Kepler Conjecture: the Hales-Ferguson Proof*, edited by J. C. Lagarias (Springer New York, New York, NY, 2011), pp. 65–82.

[371] T. C. Hales, Annals of mathematics **162**, 1065 (2005).

[372] P. Krishna, D. Pandey, and C. A. Taylor, *Close-packed structures* (International Union of Crystallography, Chester, UK, 1981).

[373] C. H. Loach and G. J. Ackland, Phys. Rev. Lett. **119**, 205701 (2017).

[374] G. Osang, H. Edelsbrunner, and M. Saadatfar, Soft Matter **17**, 9107 (2021).

[375] R. E. Crandall and J. F. Delord, Journal of Physics A: Mathematical and General **20**, 2279 (1987).

[376] E. Florez, O. Smits, J.-M. Mewes, P. Jerabek, and P. Schwerdtfeger, *From the gas phase to the solid state: the chemical bonding in the superheavy element flerovium*, unpublished results, Massey University, 2022.

[377] R. Howard, Phys. Lett. A **32**, 37 (1970).

[378] A. Burrows, S. Cooper, and P. Schwerdtfeger, (2022).

[379] A. Burrows, S. Cooper, and P. Schwerdtfeger, *The Cuboidal Lattices and their Lattice Sums*, _eprint: 2105.08922, 2021.

[380] A. Dewaele, A. D. Rosa, N. Guignot, D. Andrault, J. E. F. S. Rodrigues, and G. Garbarino, Scientific Reports **11**, 15192 (2021).

[381] U. Häussermann and S. I. Simak, Phys. Rev. B **64**, 245114 (2001).

[382] G. E. Andrews, R. Askey, and R. Roy, *Special functions*, Vol. 71 (Cambridge university press, Cambridge, 1999).

[383] J. M. Borwein and P. B. Borwein, Transactions of the American Mathematical Society **323**, 691 (1991).

[384] S. Cooper, Journal of computational and applied mathematics **160**, 77 (2003).

[385] G. Hämmerlin and K.-H. Hoffmann, *Numerical mathematics* (Springer Science & Business Media, Berlin, 2012).

MASSEY UNIVERSITY
GRADUATE RESEARCH SCHOOL

STATEMENT OF CONTRIBUTION
DOCTORATE WITH PUBLICATIONS/MANUSCRIPTS

We, the candidate and the candidate's Primary Supervisor, certify that all co-authors have consented to their work being included in the thesis and they have accepted the candidate's contribution as indicated below in the *Statement of Originality*.

Name of candidate:	Antony Burrows
Name/title of Primary Supervisor:	Prof. Dr. Peter Schwerdtfeger
Name of Research Output and full reference:	
A Burrows, S Cooper, E Pahl and P Schwerdtfeger, Analytical methods for fast converging lattice sums for cubic and hexagonal close-packed lattices", J. Math. Phys. 61, 123503 (2020)	
In which Chapter is the Manuscript /Published work:	6
Please indicate:	
• The percentage of the manuscript/Published Work that was contributed by the candidate:	33%
and	
• Describe the contribution that the candidate has made to the Manuscript/Published Work:	
Derived formulas under supervision of both supervisors, did the programming and analysis, helped in writing the paper, contributed to all figures.	
For manuscripts intended for publication please indicate target journal:	
Candidate's Signature:	Antony Burrows Digitally signed by Antony Burrows Date: 2022.05.27 17:10:14 +12'00'
Date:	31/05/2022
Primary Supervisor's Signature:	PeterSchwerdtfeger Digitally signed by PeterSchwerdtfeger Date: 2022.06.01 09:53:18 +12'00'
Date:	31/05/2022

(This form should appear at the end of each thesis chapter/section/appendix submitted as a manuscript/ publication or collected as an appendix at the end of the thesis)

MASSEY UNIVERSITY
GRADUATE RESEARCH SCHOOL

STATEMENT OF CONTRIBUTION
DOCTORATE WITH PUBLICATIONS/MANUSCRIPTS

We, the candidate and the candidate's Primary Supervisor, certify that all co-authors have consented to their work being included in the thesis and they have accepted the candidate's contribution as indicated below in the *Statement of Originality*.

Name of candidate:	Antony Burrows
Name/title of Primary Supervisor:	Prof. Dr. Peter Schwerdtfeger
Name of Research Output and full reference: P Schwerdtfeger, A Burrows, and O R. Smits, "The Lennard-Jones Potential Revisited: Analytical Expressions for Vibrational Effects in Cubic and Hexagonal Close-Packed Lattices", J. Phys. Chem. A 2021, 125, 14, 3037–3057	
In which Chapter is the Manuscript /Published work:	7
Please indicate:	
• The percentage of the manuscript/Published Work that was contributed by the candidate:	40%
and	
• Describe the contribution that the candidate has made to the Manuscript/Published Work:	
Derived formulas under supervision of both supervisors, did the programming and analysis, helped in writing the paper, contributed to all figures.	
For manuscripts intended for publication please indicate target journal:	
Candidate's Signature:	Antony Burrows Digitally signed by Antony Burrows Date: 2022.05.27 17:19:00 +12'00'
Date:	31/05/2022
Primary Supervisor's Signature:	PeterSchwerdtfeger Digitally signed by PeterSchwerdtfeger Date: 2022.06.01 09:50:41 +12'00'
Date:	31/05/2022

(This form should appear at the end of each thesis chapter/section/appendix submitted as a manuscript/ publication or collected as an appendix at the end of the thesis)

MASSEY UNIVERSITY
GRADUATE RESEARCH SCHOOL

STATEMENT OF CONTRIBUTION
DOCTORATE WITH PUBLICATIONS/MANUSCRIPTS

We, the candidate and the candidate's Primary Supervisor, certify that all co-authors have consented to their work being included in the thesis and they have accepted the candidate's contribution as indicated below in the *Statement of Originality*.

Name of candidate:	Antony Burrows
Name/title of Primary Supervisor:	Prof. Dr. Peter Schwerdtfeger
Name of Research Output and full reference:	
A Burrows, S Cooper, P Schwerdtfeger, "The Cuboidal Lattices and their Lattice Sums", arXiv:2105.08922v1	
In which Chapter is the Manuscript /Published work:	8
Please indicate:	
• The percentage of the manuscript/Published Work that was contributed by the candidate:	50%
and	
• Describe the contribution that the candidate has made to the Manuscript/Published Work:	
Derived formulas under supervision of both supervisors, did the programming and analysis, helped in writing the paper, contributed to all figures.	
For manuscripts intended for publication please indicate target journal:	
Journal of Chemical Physics	
Candidate's Signature:	Antony Burrows Digitally signed by Antony Burrows Date: 2022.05.28 13:11:05 +12'00'
Date:	31/05/2022
Primary Supervisor's Signature:	PeterSchwerdtfeger Digitally signed by PeterSchwerdtfeger Date: 2022.06.01 09:49:15 +12'00'
Date:	31/05/2022

(This form should appear at the end of each thesis chapter/section/appendix submitted as a manuscript/ publication or collected as an appendix at the end of the thesis)

MASSEY UNIVERSITY
GRADUATE RESEARCH SCHOOL

STATEMENT OF CONTRIBUTION
DOCTORATE WITH PUBLICATIONS/MANUSCRIPTS

We, the candidate and the candidate's Primary Supervisor, certify that all co-authors have consented to their work being included in the thesis and they have accepted the candidate's contribution as indicated below in the *Statement of Originality*.

Name of candidate:	Antony Burrows
Name/title of Primary Supervisor:	Prof. Dr. Peter Schwerdtfeger
Name of Research Output and full reference: A Burrows, S Cooper, and P Schwerdtfeger , "Instability of the body-centered cubic lattice within the sticky hard sphere and Lennard-Jones model obtained from exact lattice summations", Phys. Rev. E 104, 035306 - Published 22 September 2021	
In which Chapter is the Manuscript /Published work:	9
Please indicate:	
• The percentage of the manuscript/Published Work that was contributed by the candidate:	50%
and	
• Describe the contribution that the candidate has made to the Manuscript/Published Work:	
Derived formulas under supervision of both supervisors, did the programming and analysis, helped in writing the paper, contributed to all figures.	
For manuscripts intended for publication please indicate target journal:	
Candidate's Signature:	Antony Burrows Digitally signed by Antony Burrows Date: 2022.05.28 14:02:10 +12'00'
Date:	31/05/2022
Primary Supervisor's Signature:	PeterSchwerdtfeger Digitally signed by PeterSchwerdtfeger Date: 2022.06.01 09:47:38 +12'00'
Date:	31/05/2022

(This form should appear at the end of each thesis chapter/section/appendix submitted as a manuscript/ publication or collected as an appendix at the end of the thesis)

MASSEY UNIVERSITY
GRADUATE RESEARCH SCHOOL

STATEMENT OF CONTRIBUTION
DOCTORATE WITH PUBLICATIONS/MANUSCRIPTS

We, the candidate and the candidate's Primary Supervisor, certify that all co-authors have consented to their work being included in the thesis and they have accepted the candidate's contribution as indicated below in the *Statement of Originality*.

Name of candidate:	Antony Burrows
Name/title of Primary Supervisor:	Prof. Dr. Peter Schwerdtfeger
Name of Research Output and full reference: P Schwerdtfeger and A Burrows, "Cuboidal bcc to fcc Transformation of Lennard-Jones Phases under High Pressure Derived from Exact Lattice Summations", J. Phys. Chem. C 2022, 126, 20, 8874–8882	
In which Chapter is the Manuscript /Published work:	10
Please indicate:	
• The percentage of the manuscript/Published Work that was contributed by the candidate:	50%
and	
• Describe the contribution that the candidate has made to the Manuscript/Published Work:	
Derived formulas under supervision of both supervisors, did the programming and analysis, helped in writing the paper, designed and made all figures.	
For manuscripts intended for publication please indicate target journal:	
Candidate's Signature:	Antony Burrows Digitally signed by Antony Burrows Date: 2022.05.28 14:07:45 +12'00'
Date:	31/05/2022
Primary Supervisor's Signature:	PeterSchwerdtfeger Digitally signed by PeterSchwerdtfeger Date: 2022.06.01 09:45:41 +12'00'
Date:	31/05/2022

(This form should appear at the end of each thesis chapter/section/appendix submitted as a manuscript/ publication or collected as an appendix at the end of the thesis)

MASSEY UNIVERSITY
GRADUATE RESEARCH SCHOOL

STATEMENT OF CONTRIBUTION
DOCTORATE WITH PUBLICATIONS/MANUSCRIPTS

We, the candidate and the candidate's Primary Supervisor, certify that all co-authors have consented to their work being included in the thesis and they have accepted the candidate's contribution as indicated below in the *Statement of Originality*.

Name of candidate:	Antony Burrows
Name/title of Primary Supervisor:	Prof. Dr. Peter Schwerdtfeger
Name of Research Output and full reference:	
A Burrows, S Cooper, P Schwerdtfeger, "The Madelung Constant in N-Dimensions", Journal TDB, arXiv:2202.01392	
In which Chapter is the Manuscript /Published work:	11
Please indicate:	
• The percentage of the manuscript/Published Work that was contributed by the candidate:	40%
and	
• Describe the contribution that the candidate has made to the Manuscript/Published Work:	
Derived formulas under supervision of both supervisors, did the programming and analysis, helped in writing the paper, contributed to the figures.	
For manuscripts intended for publication please indicate target journal:	
Proceedings of the Royal Society A: Mathematical and Physical Sciences	
Candidate's Signature:	Antony Burrows Digitally signed by Antony Burrows Date: 2022.05.31 20:01:06 +12'00'
Date:	31/05/2022
Primary Supervisor's Signature:	PeterSchwerdtfeger Digitally signed by PeterSchwerdtfeger Date: 2022.06.01 09:41:52 +12'00'
Date:	31/05/2022

(This form should appear at the end of each thesis chapter/section/appendix submitted as a manuscript/ publication or collected as an appendix at the end of the thesis)

MASSEY UNIVERSITY
GRADUATE RESEARCH SCHOOL

STATEMENT OF CONTRIBUTION
DOCTORATE WITH PUBLICATIONS/MANUSCRIPTS

We, the candidate and the candidate's Primary Supervisor, certify that all co-authors have consented to their work being included in the thesis and they have accepted the candidate's contribution as indicated below in the *Statement of Originality*.

Name of candidate:	Antony Burrows
Name/title of Primary Supervisor:	Prof. Dr. Peter Schwerdtfeger
Name of Research Output and full reference:	
A Burrows, S Cooper, P Schwerdtfeger, "The Lattice Sum for a Hexagonal Close Packed Structure and its Dependence on the c/a Ratio of the Hexagonal Cell Parameters", Journal TBD	
In which Chapter is the Manuscript /Published work:	12
Please indicate:	
• The percentage of the manuscript/Published Work that was contributed by the candidate:	40%
and	
• Describe the contribution that the candidate has made to the Manuscript/Published Work:	
Derived formulas under supervision of both supervisors, did the programming and analysis, helped in writing the paper, contributed to the figures.	
For manuscripts intended for publication please indicate target journal:	
Journal of Chemical Physics	
Candidate's Signature:	Antony Burrows Digitally signed by Antony Burrows Date: 2022.05.31 20:08:42 +12'00'
Date:	31/05/2022
Primary Supervisor's Signature:	PeterSchwerdtfeger Digitally signed by PeterSchwerdtfeger Date: 2022.06.01 09:43:16 +12'00'
Date:	31/05/2022

(This form should appear at the end of each thesis chapter/section/appendix submitted as a manuscript/ publication or collected as an appendix at the end of the thesis)